frontiers | Research Topics

Insights in Vaccines and Molecular Therapeutics 2021

Edited by
Denise L. Doolan, Lee Mark Wetzler and Fabio Bagnoli

Published in
Frontiers in Immunology

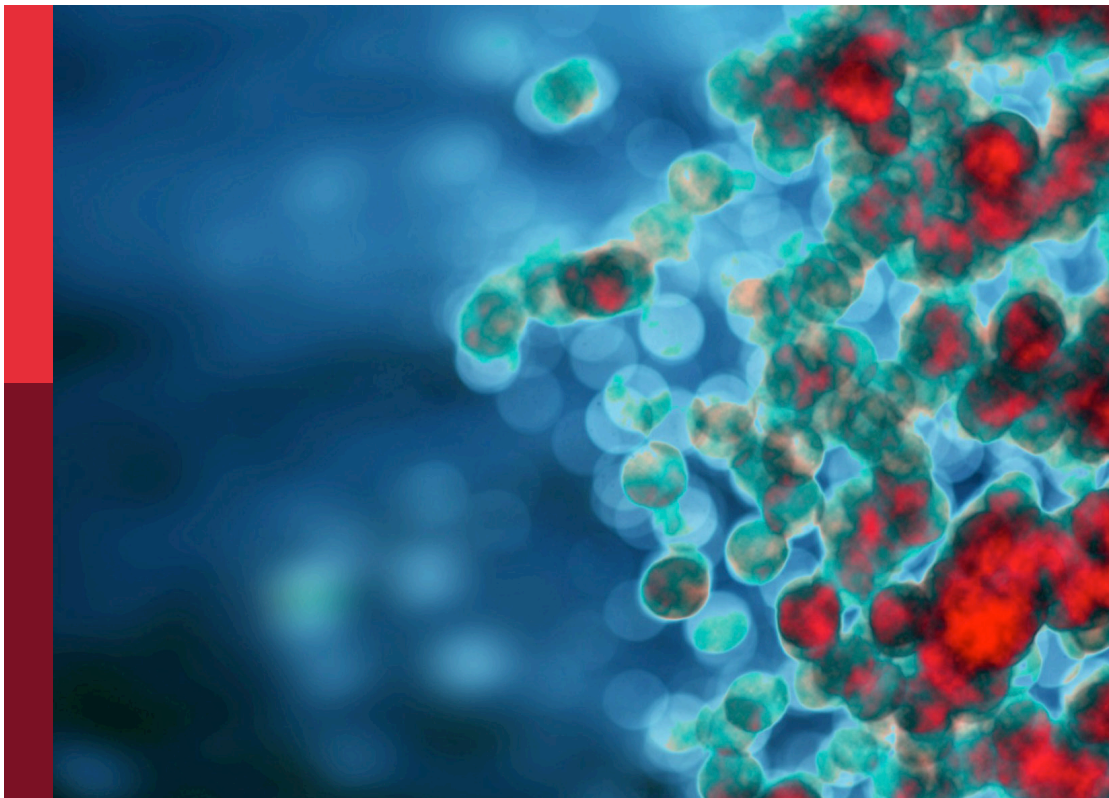

ISSN 1664-8714
ISBN 978-2-8325-2446-6
DOI 10.3389/978-2-8325-2446-6

About Frontiers

Frontiers is more than just an open access publisher of scholarly articles: it is a pioneering approach to the world of academia, radically improving the way scholarly research is managed. The grand vision of Frontiers is a world where all people have an equal opportunity to seek, share and generate knowledge. Frontiers provides immediate and permanent online open access to all its publications, but this alone is not enough to realize our grand goals.

Frontiers journal series

The Frontiers journal series is a multi-tier and interdisciplinary set of open-access, online journals, promising a paradigm shift from the current review, selection and dissemination processes in academic publishing. All Frontiers journals are driven by researchers for researchers; therefore, they constitute a service to the scholarly community. At the same time, the *Frontiers journal series* operates on a revolutionary invention, the tiered publishing system, initially addressing specific communities of scholars, and gradually climbing up to broader public understanding, thus serving the interests of the lay society, too.

Dedication to quality

Each Frontiers article is a landmark of the highest quality, thanks to genuinely collaborative interactions between authors and review editors, who include some of the world's best academicians. Research must be certified by peers before entering a stream of knowledge that may eventually reach the public - and shape society; therefore, Frontiers only applies the most rigorous and unbiased reviews. Frontiers revolutionizes research publishing by freely delivering the most outstanding research, evaluated with no bias from both the academic and social point of view. By applying the most advanced information technologies, Frontiers is catapulting scholarly publishing into a new generation.

What are Frontiers Research Topics?

Frontiers Research Topics are very popular trademarks of the *Frontiers journals series*: they are collections of at least ten articles, all centered on a particular subject. With their unique mix of varied contributions from Original Research to Review Articles, Frontiers Research Topics unify the most influential researchers, the latest key findings and historical advances in a hot research area.

Find out more on how to host your own Frontiers Research Topic or contribute to one as an author by contacting the Frontiers editorial office: frontiersin.org/about/contact

Insights in vaccines and molecular therapeutics: 2021

Topic editors

Denise L. Doolan — James Cook University, Australia
Lee Mark Wetzler — Boston University, United States
Fabio Bagnoli — GlaxoSmithKline, Italy

Citation

Doolan, D. L., Wetzler, L. M., Bagnoli, F., eds. (2023). *Insights in vaccines and molecular therapeutics: 2021*. Lausanne: Frontiers Media SA.
doi: 10.3389/978-2-8325-2446-6

Table of contents

05 Extracellular Vesicles as a New Promising Therapy in HIV Infection
Maria A. Navarrete-Muñoz, Carlos Llorens, José M. Benito and Norma Rallón

16 Breast Cancer Vaccines: Disappointing or Promising?
Si-Yuan Zhu and Ke-Da Yu

31 Antibody-Mediated Inhibition of Insulin-Degrading Enzyme Improves Insulin Activity in a Diabetic Mouse Model
Ofir Fursht, Mirit Liran, Yuval Nash, Vijay Krishna Medala, Dor Ini, Tabitha Grace Royal, Guy Goldsmith, Limor Nahary, Itai Benhar and Dan Frenkel

43 CRISPR/Cas9 Approach to Generate an Auxotrophic BCG Strain for Unmarked Expression of LTAK63 Adjuvant: A Tuberculosis Vaccine Candidate
Luana Moraes, Monalisa Martins Trentini, Dimitrios Fousteris, Silas Fernandes Eto, Ana Marisa Chudzinski-Tavassi, Luciana Cezar de Cerqueira Leite and Alex Issamu Kanno

53 Early-Life Antibiotic Exposure Associated With Varicella Occurrence and Breakthrough Infections: Evidence From Nationwide Pre-Vaccination and Post-Vaccination Cohorts
Teng-Li Lin, Yi-Hsuan Fan, Yi-Ling Chang, Hsiu J. Ho, Li-Lin Liang, Yi-Ju Chen and Chun-Ying Wu

62 Advances in Pathogenesis, Progression, Potential Targets and Targeted Therapeutic Strategies in SARS-CoV-2-Induced COVID-19
Hong Zhou, Wei-Jian Ni, Wei Huang, Zhen Wang, Ming Cai and Yan-Cai Sun

91 Bomidin: An Optimized Antimicrobial Peptide With Broad Antiviral Activity Against Enveloped Viruses
Rongrong Liu, Ziyu Liu, Haoran Peng, Yunhua Lv, Yunan Feng, Junjun Kang, Naining Lu, Ruixue Ma, Shiyuan Hou, Wenjie Sun, Qikang Ying, Fang Wang, Qikang Gao, Ping Zhao, Cheng Zhu, Yixing Wang and Xingan Wu

103 Meta-Analysis of Human Antibodies Against *Plasmodium falciparum* Variable Surface and Merozoite Stage Antigens
Eizo Takashima, Bernard N. Kanoi, Hikaru Nagaoka, Masayuki Morita, Ifra Hassan, Nirianne M. Q. Palacpac, Thomas G. Egwang, Toshihiro Horii, Jesse Gitaka and Takafumi Tsuboi

114 The Cross-Protective Immunity Landscape Among Different SARS-CoV-2 Variant RBDs
Wenqiang Sun, Lihong He, Huicong Lou, Wenhui Fan, Limin Yang, Gong Cheng, Wenjun Liu and Lei Sun

122 MIR4435-2HG Is a Potential Pan-Cancer Biomarker for Diagnosis and Prognosis
Chenming Zhong, Zijun Xie, Ling-hui Zeng, Chunhui Yuan and Shiwei Duan

141 Inactivated vaccine Covaxin/BBV152: A systematic review
Tousief Irshad Ahmed, Saqib Rishi, Summaiya Irshad, Jyoti Aggarwal, Karan Happa and Sheikh Mansoor

frontiers in Immunology

MINI REVIEW
published: 04 January 2022
doi: 10.3389/fimmu.2021.811471

Extracellular Vesicles as a New Promising Therapy in HIV Infection

Maria A. Navarrete-Muñoz[1,2,3], *Carlos Llorens*[3], *José M. Benito*[1,2*†] *and Norma Rallón*[1,2*†]

[1] HIV and Viral Hepatitis Research Laboratory, Instituto de Investigación Sanitaria Fundación Jiménez Díaz (IIS-FJD), Universidad Autónoma de Madrid (UAM), Madrid, Spain, [2] Hospital Universitario Rey Juan Carlos, Móstoles, Spain, [3] Biotechvana, Madrid Scientific Park Foundation, Madrid, Spain

Combination antiretroviral therapy (cART) effectively blocks HIV replication but cannot completely eliminate HIV from the body mainly due to establishment of a viral reservoir. To date, clinical strategies designed to replace cART for life and alternatively to eliminate the HIV reservoir have failed. The reduced expression of viral antigens in the latently infected cells is one of the main reasons behind the failure of the strategies to purge the HIV reservoir. This situation has forced the scientific community to search alternative therapeutic strategies to control HIV infection. In this regard, recent findings have pointed out extracellular vesicles as therapeutic agents with enormous potential to control HIV infection. This review focuses on their role as pro-viral and anti-viral factors, as well as their potential therapeutic applications.

Keywords: intercellular communication, extracellular vesicles (EVs), HIV infection, immunopathogenesis, clinical application, EVs as therapeutic agents for HIV, EVs as latency reversal agents

OPEN ACCESS

Edited by:
Denise L. Doolan, James Cook University, Australia

Reviewed by:
Matthias Clauss, Indiana University Bloomington, United States

****Correspondence:***
José M. Benito
jbenito1@hotmail.com; jose.benito@fjd.es
Norma Rallón
normaibon@yahoo.com; norma.rallon@fjd.es

†ORCID
José M. Benito
orcid.org/0000-0002-7172-049X
Norma Rallón
orcid.org/0000-0002-4643-247X

Specialty section:
This article was submitted to Vaccines and Molecular Therapeutics, a section of the journal Frontiers in Immunology

Received: *08 November 2021*
Accepted: *15 December 2021*
Published: *04 January 2022*

Citation:
Navarrete-Muñoz MA, Llorens C, Benito JM and Rallón N (2022) Extracellular Vesicles as a New Promising Therapy in HIV Infection. Front. Immunol. 12:811471. doi: 10.3389/fimmu.2021.811471

INTRODUCTION

Global HIV statistics indicate that around 37.7 million people are living with HIV infection with 1.5 million people newly infected in 2020 (1). Combination antiretroviral therapy (cART) has successfully decreased the associated mortality and consequently it has improved life expectancy (2). The cART can effectively block viral replication reducing plasma viremia to undetectable levels (3). However, cART is not able to completely restore immunological functions (4) and to reduce immune hyperactivation and persistent chronic systemic inflammation caused by HIV (5) which is associated with higher risk of developing cancer, as well as cardiovascular, metabolic, and bone disorders (6–9).

In addition, the cumulative toxicity of cART regimens remains a concern in people living with HIV (10–13). This toxicity added to the obligation of lifelong treatment prompted the research on different strategies with the aim to replace cART for life. These strategies include: a) the reduction of number of target cells available for the virus by CCR5-deficient bone marrow transplant (14–16); b) cART administration very early after primary (17) or acute (18) HIV infection to achieve post-treatment control after drug interruption; c) immunotherapies to delay HIV reactivation by blocking reactivation events (19); d) therapeutic HIV vaccines generated to boost the magnitude, breadth and functionality of HIV-specific immune response (20, 21). However, these strategies have not achieved the expected success, even for the strategy aimed at reducing available CCR5-cells, which is not feasible for the whole HIV^+ population, it was only successful in only two exceptional patients (14, 15). Thus, it is necessary to focus research on alternative solutions. In this regard, EVs

and their observed role in HIV restriction at multiples levels (22–29) lead to consider the potential application of these vesicles in the treatment of HIV infection in order to replace cART treatment.

Moreover, cART cannot completely eliminate the virus from the body, and viral load rapidly re-emergences after 2-8 weeks of cART interruption (30, 31). Establishment of a viral reservoir, very early after acute infection, has been proposed as the main reason for viral rebound and consequently as the main obstacle for HIV eradication. Different types of HIV reservoir have been described. First, the cellular HIV reservoir, formed by specific cells, in a latent state, with HIV-DNA integrated into their genome (32), being the virus invisible to the action of the immune system and of the cART. Second, the anatomical reservoirs, which are sites where the cART and/or the effector cells of the immune system cannot access allowing HIV replication for long periods of time (33).

Several therapeutic strategies specifically designed to eliminate HIV reservoir have been developed with limited success to date. Within them, the most widely explored strategy is the shock and kill approach (34). The goal of this strategy is to eliminate the HIV reservoir, either by cART or immune system, after reactivating it by using latency reversal agents -LRAs-. Despite of the promising results, this strategy has not achieved the expected results (35, 36). The "shock" phase fails to completely reactivate the reservoir, with only <1% of proviruses being reactivated after maximum *in vitro* activation (37). Moreover, this strategy does not discriminate between replication-competent and defective proviruses, and the response to LRAs is widely variable among patients due to the heterogeneous nature of the cellular and anatomical reservoirs and other features such as virus-integration sites and patient-specific aspects (38). Therefore, the search for strategies that can effectively target the HIV reservoir remain open. In this sense, recent findings have pointed out extracellular vesicles (EVs) as potential therapeutic tools to attack HIV infection given their pivotal role in mediating important cell-to-cell communication mechanisms (39).

In this Review, we focus on the understanding how extracellular vesicles mediate intercellular communication in HIV infection, its role as pro-viral and anti-viral factors and its tremendous potential as therapeutic agents to control HIV infection (blocking HIV infectivity and/or reactivating the HIV reservoir).

INTERCELLULAR COMMUNICATION MEDIATED BY EVs IN HIV INFECTION

Exosomes are membranous EVs of around 40-100 nm, released by many types of cells into the extracellular environment, found in several biological fluids such as blood, urine, semen and breast milk. Most studies use the term "exosomes" to refer to circulating vesicles. However, circulating vesicles are composed of exosomes and microvesicles, and the isolation techniques used do not allow a complete discrimination between them (40). Tetraspanins such as CD63, CD9, and CD81 are normally used as EVs-specific markers. Other proteins, such as Alix and Tsg101 are involved in their biogenesis. It is important to note that HIV virions and exosomes/microvesicles share many features including biophysical and molecular properties, biogenesis and uptake mechanisms. Indeed, Alix and Tsg101 proteins play important roles in the budding of HIV from the host cell (41).

Similarities found between HIV virions and exosomes/microvesicles lead to the so-called "Trojan Exosome Hypothesis", first proposed by Gould et al. (42). According to this hypothesis, HIV and other retroviruses will take advantage of the host cell exosomal biogenesis machinery for their own benefit. This hypothesis has implications for the virus-host interactions at several levels. The most obvious implication is that the hijacking by HIV of exosomal biogenesis machinery will lead to alternative ways for virus spreading and infection of new target cells, different from the classic direct budding from the plasma membrane (42). Also, the similarity between exosomes and viral biogenesis implies that several viral products can be incorporated into exosomes as several studies have reported (43–48). Full-length unspliced HIV RNA (43), several miRNAs such as the trans-activating response (TAR) element (44–46) and different viral proteins (47, 48) have all been found carried by exosomes of different origin. This ability of HIV to package its own products into exosomes has relevant implications not only for viral spreading but also for viral pathogenesis. In this regard, several studies point to Nef protein as especially relevant in different EVs-mediated mechanisms of viral pathogenesis. First, Nef can promote HIV infection by reducing the expression of CD4 in exosomes and thus neutralizing the ability of CD4-bearing exosomas to act as decoys (49). Second, HIV-infected macrophages can transfer Nef to B cells altering the virus-specific Ig-class switching in lymphoid follicles (50). Virus-specific T-cell responses are also affected by Nef through its modulating effect on both TCR-signalling and cytoskeleton reorganization in T cells. This effect of Nef is dependent on the hijacking of endosomal traffic of protein tyrosine kinase Lck (essential for TCR signaling) and the GTPase Rac1 (essential for cytoskeleton reorganization) (51). Lastly, Nef carried by exosomes has also been involved in promoting chronic inflammation through its effect on lipid rafts formation (reducing the activation of the GTPase Cdc42 and increasing the activation of NLRP3 inflammasome) (52).

In contrast, EVs may contribute to an anti-viral response by delivering HIV restriction factors to nearby cells or by presenting viral antigens (53, 54). Moreover, cell-to-cell communication by EVs could play an important role in the reactivation of the latent HIV (55–60), something of utmost relevance in the search for strategies aimed at eliminating the reservoir.

PRO-VIRAL EFFECTS OF EVs IN HIV INFECTION

As has been mentioned, EVs can promote HIV infection (**Figure 1**). HIV-RNA (43), and the HIV proteins Nef (61),

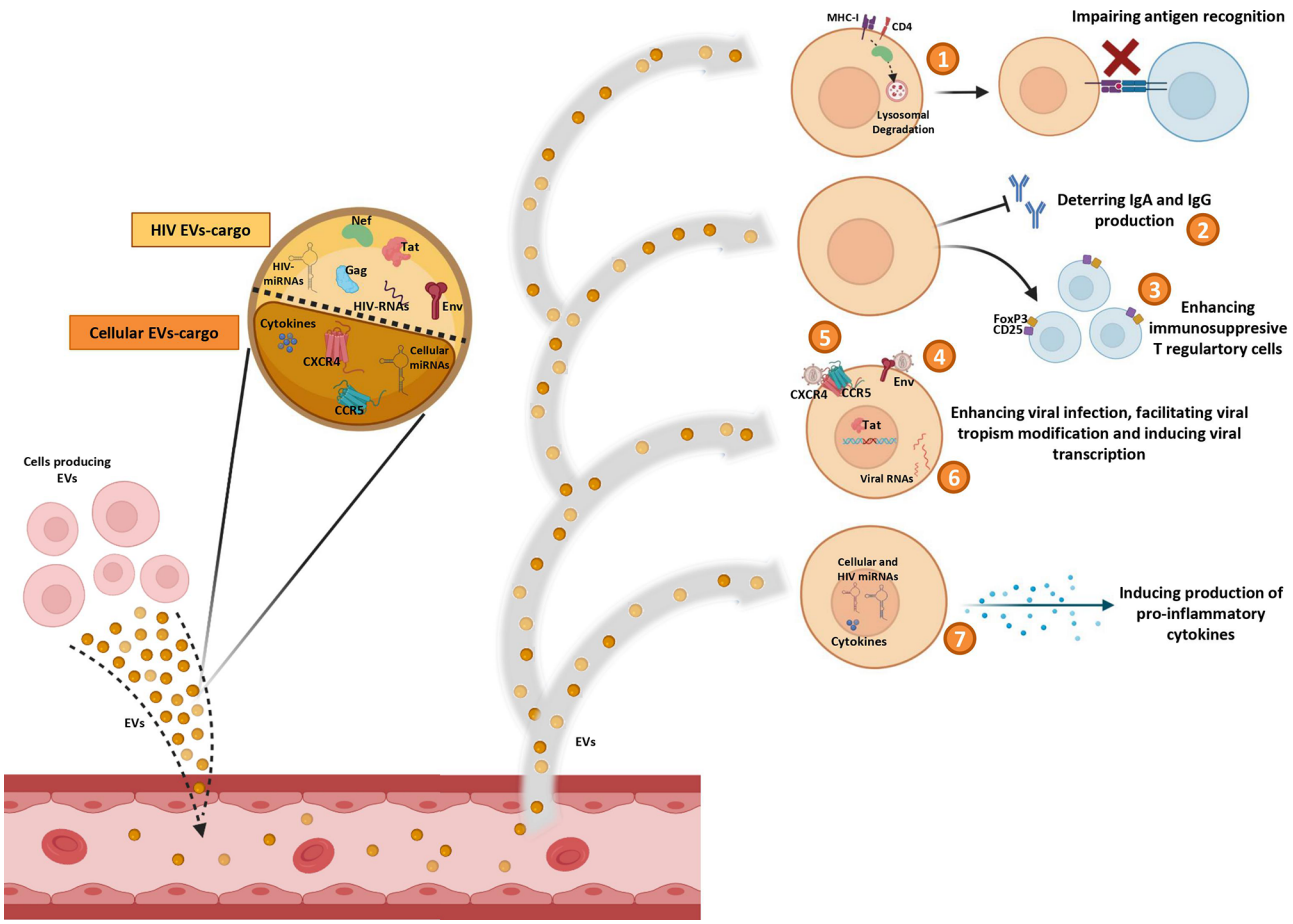

FIGURE 1 | *Pro-HIV actions of factors carried by extracelular vesicles (EVs).* Figure shows Evs produced by different cell sources and released into circulation containing cellular and viral factors that trigger pro-viral effects on target cells: 1) impairing antigen recognition by MHC-I and CD4 lysosomal degradation; 2) deterring IgA and IgG production by B cells; 3) enhancing immunosuppresive T regulatory cells; 4) promoting viral infection by fusing to the target cells with Env protein; 5) facilitating viral tropism modification; 6) activating viral promoter to induce HIV replication; 7) inducing production of pro-inflammatory cytokines.

Gag, Tat (62), and Env (63) have been observed into EVs from cell culture supernatants. Nef protein can interact with cellular trafficking pathways and induce lysosomal degradation of MHC-I (64, 65) and CD4 (64, 66), disrupting the viral antigen recognition by immune system (67). Moreover, an inhibitory effect of Nef on the adaptive immune response, by deterring the IgA and IgG production in B lymphocytes, has also been described in EVs derived from macrophages of HIV-infected subjects (50). Tat protein acts activating viral promoter to induce HIV replication (62). Gag (62) and Env (63) proteins participate in infection enhancement. EVs released by HIV-infected cells contain Env protein gp120 suggesting that this protein secreted in EVs may promote the virus to attach and fuse to the target cells and facilitate HIV infection (63).

Some HIV-miRNAs have been also observed in EVs from serum of HIV-infected patients and from infected cells culture (44–46). These miRNAs are involved in cytokine production (44–46) and in apoptosis downregulation (44). In general, it seems that EVs can impair the immune response by enhancing immunosuppressive $Foxp3^{+}CD4^{+}CD25^{+}$ T regulatory cells (68). Furthermore, EVs can act as inducers of the inflammatory state that contributes to HIV disease pathogenesis. Different studies have reported several molecules associated to development of inflammation into EVs, such as: TNFα (69, 70), IFNg (71), IL-12p40, sIL-6R, sTNF-RI, GRO (69), MCP-1, RANTES (72), IL-1α (70, 71), CXCL10 (70), viral Nef protein (that triggers TNF-α release) (73), viral miRNAs (45, 46), and cellular miRNAs (miR-10a-5p, miR-21-5p, miR-27b-3p, miR-122-5p, miR-146a-5p, miR-423-5p) (74). In addition, EVs derived from plasma of HIV subjects increase activation of monocytes/macrophages eliciting the production of inflammatory cytokines (IL-6, IL1-β and TNF-α) by these cells (75).

Interestingly, *in vitro* studies with EVs derived from cell lines culture supernatants (76) and from human peripheral blood mononuclear cells (PBMCs) (76) or platelets (77) of healthy donors, have revealed that virus can be able to use EVs to transfer CCR5 and CXCR4 HIV entry co-receptors to cells in order to facilitate the modification of the viral tropism increasing the

number of susceptible target cells (76, 77). However, this ability of EVs to transfer HIV coreceptors between cells could be exploited to combat HIV by engineering exosomes carrying defective correceptors with the aim to prevent HIV transmission, as is the case for the natural delta32-deleted version of host CCR5 (78).

ANTI-VIRAL EFFECTS OF EVs IN HIV INFECTION

Several anti-HIV effects of EVs have been described, such as the presence of MHC-II molecules as part of EVs cargo, a fact that reveals the potential ability of these vesicles to present viral antigens and induce T cells response (54). Tumne et al. revealed that EVs secreted by CD8 + T cells display a potent non-cytotoxic antiretroviral activity that specifically inhibits HIV transcription (79).

Some studies have assessed the capacity of EVs to transfer known restriction factors that can inhibit HIV infection in target cells (**Figure 2**). One of these factors is APOBEC3G (A3G - human cytidine deaminase that can cause hypermutation of the viral genome at the retrotranscription step) that has been found into EVs that potently restrict replication of HIV in recipient cells under *in vitro* conditions (80). Moreover, A3G and Tetherin (an interferon-induced protein whose expression blocks the

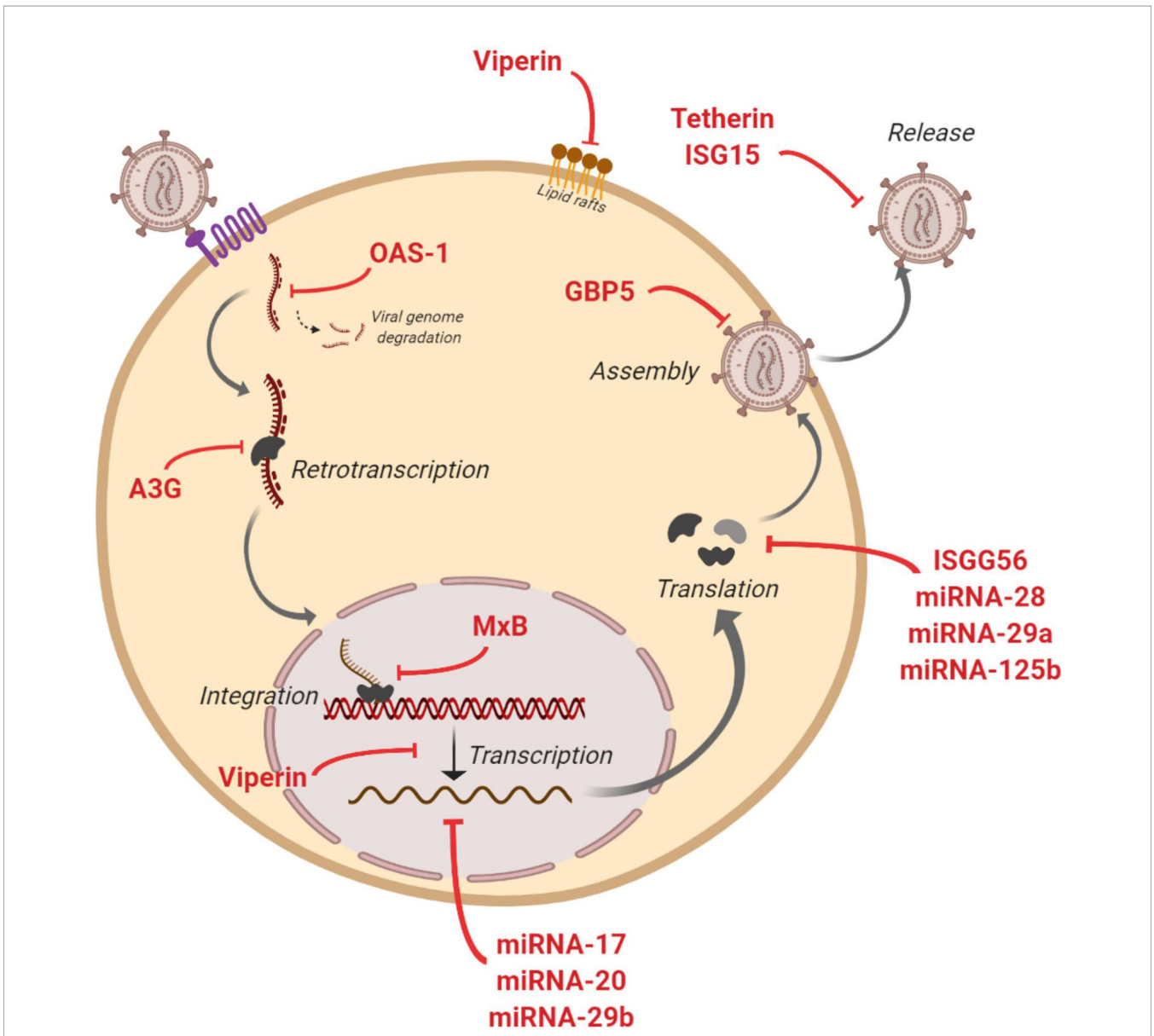

FIGURE 2 | *Anti-HIV actions of factors contained in extracelular vesicles (EVs).* Figure shows inhibitory actions (red lines) at multiples steps of HIV replicative cycle by IFN-stimulated genes and restriction miRNAs carried by EVs.

release of HIV), have also been found into EVs derived from human semen (22). At level of mRNA of cellular restriction factors, Tetherin and A3G expression could be induced by EVs. An *in vitro* study showed that EVs from intestinal epithelial cells culture transport antiviral factors at mRNA and protein levels to macrophages, increasing the expression of antiviral IFN-stimulated genes (ISGs) and cellular HIV restriction factors, including Tetherin and A3G, that restricts HIV replication in macrophages (23).

The presence of IFN-stimulated genes ISG15, ISG56, MxB, OAS-1, GBP5, and Viperin with anti-HIV activity has also been reported in EVs (23, 24). These genes code for proteins with diverse functions aimed at blocking HIV: ISG15 protein inhibits virions release; ISG56 restricts viral protein translation; MxB reduces viral DNA integration; OAS-1 activates RNAsa-L to degrade viral genome; GBP5 interferes in the Env protein incorporation to generated virions; and Viperin disturbs lipid rafts and impairs viral replication (**Figure 2**). Moreover, different miRNAs with a protective action against HIV have been found in EVs such as miRNA-17, miRNA-20, miRNA-28, miRNA-29a, miRNA29b and miRNA-125b (23). These anti-HIV miRNAs could regulate HIV expression by directly targeting the virus or by an indirect effect targeting cellular transcription factors. Thus, HIV virus is inhibited at multiple steps of its viral cycle (**Figure 2**). A very recent study has shown that EVs released from human TLR3-activated cervical epithelial cells contain antiviral factors such as multiple IFN-stimulated genes and HIV restriction miRNAs that were able to restrict HIV replication in macrophages in culture. These results suggest that this antiviral mechanism could participate in the innate immunity against HIV infection, and thus a EVs-based delivery system could be considered as a preventive strategy to protect the female reproductive tract against HIV sexual transmission (25).

Concerning the effect of EVs from body fluids, several studies suggest the presence of inhibitory components in semen-derived EVs that can mitigate HIV replication and sexual transmission. EVs derived from semen of healthy donors contain mRNA of Tetherin and A3G that could inhibit HIV infection of various cell types by potentially impairing reverse transcriptase activity (22). Also, these Evs blocked the spread of HIV from vaginal epithelial cells to other cells by restricting cell-to-cell transmission (26). HIV post-entry inhibitory effect of EVs derived from semen of healthy subjects has been proposed by Welch JL et al., in an *in vitro* study in which these EVs blocked HIV proviral transcription by repressing NF-kβ, RNA polymerase II, and Tat recruitment to the LTR region, and thus blocking transcription, initiation, and elongation (27). A recent study enrolling HIV-negative, HIV-infected cART-naïve and HIV-infected cART-treated participants observed that EVs derived from semen inhibited HIV replication *in vitro* independently of donor HIV-infection status (28). In addition, EVs derived from semen of healthy subjects downregulated HIV-induced proinflammatory cytokine production while preserved lymphocyte activation state (81).

EVs from other body fluids have also shown anti-HIV effects. EVs isolated from vaginal fluid could block HIV *in vitro* at post-entry steps, most likely by halving the reverse transcription and the integration processes (29). In EVs derived from breast milk of healthy donors has been shown an *in vitro* protective role. These EVs may bind to monocyte-derived dendritic cells *via* DC-SIGN, a common receptor used by HIV, and consequently, inhibit infection and viral transfer to CD4+ T cells (82).

All this evidence the potential application of these extracellular vesicles in the treatment of HIV infection as a novel and alternative solution to cART for life. EVs can be used as therapeutical agents either by taking advantage of their own natural cargo or by devising ways to engineering their content with different therapeutic agents ranging from anti-HIV drugs to immunomodulating factors. Since EVs function as natural transporters of different molecules between cells and play a pivotal role in intercellular communication, it is expected that they should be the ideal way of delivering different biomolecules to the desired target cells (83). Compared to more traditional approaches of drug delivering including liposome-based or cell-based therapy, EVs offer several advantages such as easier manipulation, long half-life, and higher biocompatibility (84). The feasibility to use EVs as delivery systems has been demonstrated in several studies reporting the use of exosomes as carriers of biomolecules to different types of cells (85, 86). Moreover, recent studies have suggested the potential of EVs as drug delivery systems for treatment of human viral diseases (87, 88). In the setting of HIV infection, the therapeutic potential of EVs is supported by clinical data emerging from other human diseases, especially from the field of cancer (89). Although EVs-based clinical trials for treating HIV have not yet been developed, different approaches have been proposed including the loading of EVs with small molecules with anti-HIV activity (84) and with HIV proteins to generate anti-HIV immune responses (90, 91).

ROLE OF EVs IN HIV RESERVOIR REACTIVATION

To date, none of clinical trials using LRAs have reached a significant and persistent reduction of the HIV reservoir. Therefore, an alternative strategy is necessary to efficiently reactivate the transcription of latent HIV as a necessary step to purge the reservoir by the combined action of cART, blocking the released virus, and of the host immune system, destroying productively infected cells (**Figure 3A**). Several studies have found that EVs can reactivate latent HIV infection through different mechanisms (55–60) (**Figure 3B**) as outlined below:

i) Viral transcripts are increased in HIV infected cells when these cells are exposed to purified EVs derived from uninfected cells culture (58). Barclay et al, showed that EVs from uninfected cells culture increased the amount of RNA polymerase II loading onto the HIV promoter, and also increased Cdk9 binding to the transcriptional complex in order to enhance RNA polymerase elongation. In a more recent study, it has been observed that EVs from uninfected cells culture contained activated c-Src (proto-oncogene tyrosine-protein kinase Src) that can trigger the PI3K/

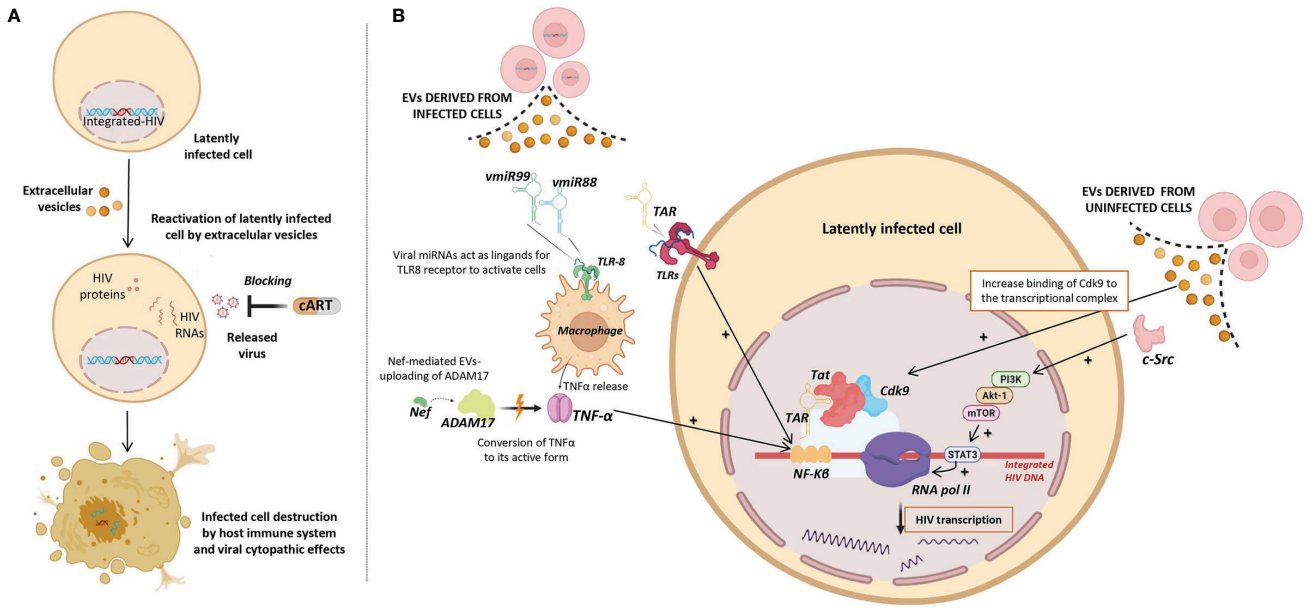

FIGURE 3 | *Role of Extracellular vesicles in HIV reservoir reactivation (EVs).* **(A)** Potential use of EVs as latency reversing agents (LRAs) to reactivate latently HIV infected cells. Reactivated infected cells produce viral antigens and can be destroyed either by viral cytopathic effects and/or by the host immune system, while released virus can be blocked by combination antiretroviral therapy (cART). **(B)** Different viral factors carried by EVs released from infected cells (left) and EVs released from uninfected cells (right) that could be involved in the induction of HIV transcription and consequently reactivation of HIV latency. Different molecular pathways involved in induction of HIV transcription are shown. Up-regulating actions are represented by black positive arrows.

AKT-1/mTOR signaling cascade, resulting in the activation of the transcription inducer STAT3, promoting the loading of RNA polymerase II onto the HIV promoter and allowing the reactivation of latent HIV (92). As consequence, larger amounts of viral transcripts were available to be packaged into new EVs and to be exported to uninfected cells.

ii) Tat, a known transactivator of viral transcription, has been detected in EVs isolated from urine of HIV infected patients (93). Tang et al. studied the role of EVs-delivered Tat in the reactivation of viral replication in latently-infected cells (55). For this purpose, the authors engineered human cellular EVs expressing activated Tat protein and they found that EVs-delivered Tat increased the potency of a selected LRA by over 30-fold, measured as change in HIV mRNA expression.

iii) EVs derived from infected cells have also been shown to contain HIV miRNAs that regulate viral and host gene expression (44–46). The most frequent miRNA found in serum EVs of HIV-infected patients is the trans-activation response element (TAR), which down-regulates apoptosis and enhances susceptibility to infection (44). A direct role of TAR in cytokine gene expression has been described by Sampey et al. (46), that observed increased levels of IL-6 and TNF-β in co-cultures of macrophages with EVs derived from HIV *in vitro* infected cells. They suggested that the underlying mechanism by which TAR increases the expression of these cytokines involves the activation of the NF-kβ pathway through the binding of TAR to the TLRs and PKR kinase. Interestingly, NF-kβ regulates the transcriptional activity of the long terminal repeat (LTR) region and therefore, enhances transcription of the HIV genome (94).

iv) Other viral miRNAs such as vmiR88 and vmiR99 have also been observed packaged into EVs derived from serum of HIV-infected patients (45). Bernard et al. found that vmiR88 and vmiR99 could act as ligands for TLR8 signaling that promotes macrophage TNFα release, a cytokine with a pivotal role in the chronic immune activation. TNFα is a pleiotropic protein with several roles in HIV pathogenesis, among them the induction of the nuclear factors binding to the NF-kβ in the LTR, resulting in an increase of HIV RNA expression (95). Interestingly, immature TNFα is converted into its active form by ADAM17, a disintegrin and metalloprotease present in EVs derived from *in vitro* HIV infected cells culture, with a relevant function in the HIV replication in resting CD4+ T cells (60). The packaging of ADAM17 has been observed only in EVs that also contain viral Nef protein. Arenaccio et al. showed that Nef seems to induce the uploading of active ADAM17 in EVs, highlighting the importance of Nef in the mechanism of latent HIV reactivation (60). Reactivation of latent HIV was not observed when Nef was absent or defective (59). Similarly, HIV reactivation was abolished when an inhibitor of the pro-TNFα-processing ADAM17 enzyme or neutralizing antibodies of TNFα were present (59).

All this highlight the relevant role of extracellular vesicles in the reactivation of the latent HIV and its potential application as an innovative and promising strategy aimed at eliminating the reservoir. Some of the studies mentioned above suggest that EVs could be engineered to carry different molecules to act as latency reversing agents. More specifically, the studies of Tan et al. (55), Arenaccio et al. (59) and Barclay et al. (92) clearly demonstrate in

in vitro systems the ability of EVs to induce HIV transcription and thus reservoir reactivation. These studies are a proof of concept of the potential use of EVs in reservoir reactivation and further studies in the near future are warranted to test the feasibility of this approach in the *in vivo* situation.

CONCLUSIONS AND FUTURE PERSPECTIVES

The study of EVs in HIV pathogenesis is an emerging field with enormous therapeutic potential to achieve HIV remission. In the current scenario, EVs engineering is possible, with the aim of manipulating their cargo in order to deliver selected molecules to the target cells. Use of EVs for HIV therapeutic purposes may range from modulating immune response, through anti-HIV factors delivery to target cells, in order to block HIV infectivity and control infection, to activating the viral reservoir with the aim to its elimination by either viral cytopathic effects and/or by the host immune system. However, further *in vivo* studies are urgently needed to ascertain the role of EVs in HIV infection and its application at the clinical level.

SEARCH STRATEGY AND SELECTION CRITERIA

Relevant scientific literature was surveyed to review evidence and prepare the manuscript. We searched PubMed for English language papers published until October 2021. Search terms included: "HIV infection", "Exosomes and HIV", "Extracellular vesicles and HIV", "Intercellular communication in HIV infection", "Exosomes and HIV inhibition", "Extracellular vesicles and HIV inhibition", "Proviral effects of Extracellular vesicles in HIV infection", "Antiviral effects of Extracellular vesicles in HIV infection", "Toxicity ART and HIV", "Alternative strategy to ART HIV", "Strategies HIV functional cure", "HIV reservoir", "Exosomes and HIV reservoir", "Extracellular vesicles and HIV reservoir" and "Role of Extracellular vesicles in HIV reservoir reactivation" Authors screened abstracts for relevance and reviewed full-text articles deemed relevant to the topics address in the manuscript.

AUTHOR CONTRIBUTIONS

All authors have participated in the preparation of the manuscript with contributions to draft the manuscript or providing revisions to content. All authors reviewed and approved the final version of the manuscript.

FUNDING

This work has been partially funded by the Spanish Directorate General for Research and Technological Comunidad de Madrid fund [grant: IND2018/BMD9651] and the Spanish Carlos III Institute of Health-ISCIII and FEDER fund [grant: PI19/01237]. M-NM is a predoctoral student funded by grant IND2018/BMD9651. NR is supported by the Miguel Servet program funded by the Spanish Health Institute Carlos III [grant: CPII19/00025].

REFERENCES

1. UNAIDS. *Global Aids Update*. Geneva, Switzerland : Joint United Nations Programme on HIV/AIDS (UNAIDS) (2020).
2. Mocroft A, Ledergerber B, Katlama C, Kirk O, Reiss P, d'Arminio Monforte A, et al. Decline in the AIDS and Death Rates in the EuroSIDA Study: An Observational Study. *Lancet* (2003) 362:22–9. doi: 10.1016/s0140-6736(03)13802-0
3. Perelson AS, Essunger P, Cao Y, Vesanen M, Hurley A, Saksela K, et al. Decay Characteristics of HIV-1-Infected Compartments During Combination Therapy. *Nature* (1997) 387:188–91. doi: 10.1038/387188a0
4. Kelley CF, Kitchen CM, Hunt PW, Rodriguez B, Hecht FM, Kitahata M, et al. Incomplete Peripheral $CD4^+$ Cell Count Restoration in Hiv-Infected Patients Receiving Long-Term Antiretroviral Treatment. *Clin Infect Dis* (2009) 48:787–94. doi: 10.1086/597093
5. Wada NI, Jacobson LP, Margolick JB, Crabb Breen E, Macatangay B, Penugonda S, et al. The Effect of HAART-Induced HIV Suppression on Circulating Markers of Inflammation and Immune Activation. *AIDS* (2015) 29(4):463–71. doi: 10.1097/QAD.0000000000000545
6. Nasi M, De Biasi S, Gibellini L, Bianchini E, Pecorini S, Bacca V, et al. Ageing and Inflammation in Patients With HIV Infection. *Clin Exp Immunol* (2017) 187(1):44–52. doi: 10.1111/cei.12814
7. Funderburg NT, Mehta NN. Lipid Abnormalities and Inflammation in HIV Infection. *Curr HIV/AIDS Rep* (2016) 13(4):218–25. doi: 10.1007/s11904-016-0321-0
8. Vos AG, Idris NS, Barth RE, Klipstein-Grobusch K, Grobbee DE. Pro-Inflammatory Markers in Relation to Cardiovascular Disease in HIV Infection. A Systematic Review. *PloS One* (2016) 11(1):e0147484. doi: 10.1371/journal.pone.0147484
9. D'Abramo A, Zingaropoli MA, Oliva A, D'Agostino C, Moghazi SA, De Luca G, et al. Higher Levels of Osteoprotegerin and Immune Activation/Immunosenescence Markers Are Correlated With Concomitant Bone and Endovascular Damage in HIV-Suppressed Patients. *PloS One* (2016) 11(2):e0149601. doi: 10.1371/journal.pone.0149601
10. Borges ÁH, Hoy J, Florence E, Sedlacek D, Stellbrink HJ, Uzdaviniene V, et al. Antiretrovirals, Fractures, and Osteonecrosis in a Large International HIV Cohort. *Clin Infect Dis* (2017) 64(10):1413–21. doi: 10.1093/cid/cix167
11. Scherzer R, Estrella M, Li Y, Choi AI, Deeks SG, Grunfeld C, et al. Association of Tenofovir Exposure With Kidney Disease Risk in HIV Infection. *AIDS* (2012) 26(7):867–75. doi: 10.1097/QAD.0b013e328351f68f
12. Ma Q, Vaida F, Wong J, Sanders CA, Kao Y, Croteau D, et al. Long-Term Efavirenz Use Is Associated With Worse Neurocognitive Functioning in HIV-Infected Patients. *J Neurovirol* (2016) 22(2):170–8. doi: 10.1007/s13365-015-0382-7
13. Friis-Møller N, Sabin CA, Weber R, d'Arminio Monforte A, El-Sadr WM, Reiss P, et al. Combination Antiretroviral Therapy and the Risk of Myocardial Infarction. *N Engl J Med* (2003) 349(21):1993–2003. doi: 10.1056/NEJMoa030218
14. Hütter G, Nowak D, Mossner M, Ganepola S, Müssig A, Allers K, et al. Long-Term Control of HIV by CCR5 Delta32/Delta32 Stem-Cell Transplantation. *N Engl J Med* (2009) 360(7):692–8. doi: 10.1056/NEJMoa0802905
15. Gupta RK, Abdul-Jawad S, McCoy LE, Mok HP, Peppa D, Salgado M, et al. HIV-1 Remission Following CCR5Δ32/Δ32 Haematopoietic Stem-Cell Transplantation. *Nature* (2019) 568(7751):244–8. doi: 10.1038/s41586-019-1027-4

16. Ding J, Liu Y, Lai Y. Knowledge From London and Berlin: Finding Threads to a Functional HIV Cure. *Front Immunol* (2021) 12:688747. doi: 10.3389/fimmu.2021.688747
17. Sáez-Cirión A, Bacchus C, Hocqueloux L, Avettand-Fenoel V, Girault I, Lecuroux C, et al. Post-Treatment HIV-1 Controllers With a Long-Term Virological Remission After the Interruption of Early Initiated Antiretroviral Therapy ANRS VISCONTI Study. *PloS Pathog* (2013) 9:e1003211. doi: 10.1371/journal.ppat.1003211
18. Kaufmann D, Lichterfeld M, Altfeld M, Addo MM, Johnston MN, Lee PK, et al. Limited Durability of Viral Control Following Treated Acute HIV Infection. *PloS Med* (2004) 1(2):e36. doi: 10.1371/journal.pmed.0010036
19. Barouch DH, Whitney JB, Moldt B, Klein F, Oliveira TY, Liu J, et al. Therapeutic Efficacy of Potent Neutralizing HIV-1-Specific Monoclonal Antibodies in SHIV-Infected Rhesus Monkeys. *Nature* (2014) 503:224–8. doi: 10.1038/nature12744
20. Mothe B, Climent N, Plana M, Rosàs M, Jiménez JL, Muñoz-Fernández MA, et al. Safety and Immunogenicity of a Modified Vaccinia Ankara-Based HIV-1 Vaccine (MVA-B) in HIV-1-Infected Patients Alone or in Combination With a Drug to Reactivate Latent HIV-1. *J Antimicrob Chemother* (2015) 70 (6):1833–42. doi: 10.1093/jac/dkv046
21. Hargrave A, Mustafa AS, Hanif A, Tunio JH, Hanif SNM. Current Status of HIV-1 Vaccines. *Vaccines (Basel)* (2021) 9(9):1026. doi: 10.3390/vaccines9091026
22. Madison MN, Roller RJ, Okeoma CM. Human Semen Contains Exosomes With Potent Anti-HIV-1 Activity. *Retrovirology* (2014) 11:102. doi: 10.1186/s12977-014-0102-z
23. Guo L, Xu XQ, Zhou L, Wang X, Li JL, Liu JB, et al. Human Intestinal Epithelial Cells Release Antiviral Factors That Inhibit HIV Infection of Macrophages. *Front Immunol* (2018) 9:247. doi: 10.3389/fimmu.2018.00247
24. Sun L, Wang X, Zhou Y, Ho WZ, Li JL. Exosomes Contribute to the Transmission of Anti-HIV Activity From TLR3-Activated Brain Microvascular Endothelial Cells to Macrophages. *Antiviral Res* (2016) 134:167–71. doi: 10.1016/j.antiviral.2016.07.013
25. Xu X, Zhang B, Guo L, Liu L, Meng FZ, Wang X, et al. Exosomes Transport Anti-Human Immunodeficiency Virus Factors From Human Cervical Epithelial Cells to Macrophages. *J Innate Immun* (2021) 3:1–11. doi: 10.1159/000514886
26. Madison MN, Jones PH, Okeoma CM. Exosomes in Human Semen Restrict HIV-1 Transmission by Vaginal Cells and Block Intravaginal Replication of LP-BM5 Murine AIDS Virus Complex. *Virology* (2015) 482:189–201. doi: 10.1016/j.virol.2015.03.040
27. Welch JL, Kaddour H, Schlievert PM, Stapleton JT, Okeoma CM. Semen Exosomes Promote Transcriptional Silencing of HIV-1 by Disrupting NF-κb/Sp1/Tat Circuitry. *J Virol* (2018) 92(21):e00731–18. doi: 10.1128/JVI.00731-18
28. Welch JL, Kaddour H, Winchester L, Fletcher CV, Stapleton JT, Okeoma CM. Semen Extracellular Vesicles From HIV-1-Infected Individuals Inhibit HIV-1 Replication *In Vitro*, and Extracellular Vesicles Carry Antiretroviral Drugs In Vivo. *J Acquir Immune Defic Syndr* (2020) 83(1):90–8. doi: 10.1097/QAI.0000000000002233
29. Smith JA, Daniel R. Human Vaginal Fluid Contains Exosomes That Have an Inhibitory Effect on an Early Step of the HIV-1 Life Cycle. *AIDS* (2016) 30 (17):2611–6. doi: 10.1097/QAD.0000000000001236
30. Calin R, Hamimi C, Lambert-Niclot S, Carcelain G, Bellet J, Assoumou L, et al. Treatment Interruption in Chronically HIV-Infected Patients With an Ultralow HIV Reservoir. *AIDS* (2016) 30(5):761–9. doi: 10.1097/QAD.0000000000000987
31. Chun TW, Davey RT, Engel D, Lane HC, Fauci AS. Re-Emergence of HIV After Stopping Therapy. *Nature* (1999) 401:874–5. doi: 10.1038/44755
32. Finzi D, Hermankova M, Pierson T, Carruth LM, Buck C, Chaisson RE, et al. Identification of a Reservoir for HIV-1 in Patients on Highly Active Antiretroviral Therapy. *Science* (1997) 278:1295. doi: 10.1126/science.278.5341.1295
33. Barton K, Winckelmann A, Palmer S. HIV-1 Reservoirs During Suppressive Therapy. *Trends Microbiol* (2016) 24:345–55. doi: 10.1016/j.tim.2016.01.006
34. Deeks SG. HIV: Shock and Kill. *Nature* (2012) 487(7408):439–40. doi: 10.1038/487439a
35. Archin NM, Kirchherr JL, Sung JA, Clutton G, Sholtis K, Xu Y, et al. Interval Dosing With the HDAC Inhibitor Vorinostat Effectively Reverses HIV Latency. *J Clin Invest* (2017) 127(8):3126–35. doi: 10.1172/JCI92684
36. Elliott JH, Wightman F, Solomon A, Ghneim K, Ahlers J, Cameronet MJ, et al. Activation of HIV Transcription With Short-Course Vorinostat in HIV-Infected Patients on Suppressive Antiretroviral Therapy. *PloS Pathog* (2014) 10(10):e1004473. doi: 10.1371/journal.ppat.1004473
37. Ho Y-C, Shan L, Hosmane NN, Wang J, Laskey SB, Rosenbloom DIS, et al. Replication-Competent Non-Induced Proviruses in the Latent Reservoir Increase Barrier to HIV-1 Cure. *Cell* (2013) 155(3):540–51. doi: 10.1016/j.cell.2013.09.020
38. Ait-Ammar A, Kula A, Darcis G, Verdikt R, De Wit S, Gautier V, et al. Current Status of Latency Reversing Agents Facing the Heterogeneity of HIV-1 Cellular and Tissue Reservoirs. *Front Microbiol* (2020) 24:3060. doi: 10.3389/fmicb.2019.03060
39. Pang S-W, Teow S-Y. Emerging Therapeutic Roles of Exosomes in HIV-1 Infection. *Exosomes* (2020) 7:147–78. doi: 10.1016/B978-0-12-816053-4.00007-9
40. Raposo G, Stoorvogel W. Extracellular Vesicles: Exosomes, Microvesicles, and Friends. *J Cell Biol* (2013) 200(4):373–83. doi: 10.1083/jcb.201211138
41. Usami Y, Popov S, Popova E, Inoue M, Weissenhorn W, Gottlinge HG. The ESCRT Pathway and HIV-1 Budding. *Biochem Soc Trans* (2009) 37:181–4. doi: 10.1042/BST0370181
42. Gould SJ, Booth AM, Hildreth JE. The Trojan Exosome Hypothesis. *Proc Natl Acad Sci USA* (2003) 100:10592–7. doi: 10.1073/pnas.1831413100
43. Columba Cabezas S, Federico M. Sequences Within RNA Coding for HIV-1 Gag P17 Are Efficiently Targeted to Exosomes. *Cell Microbiol* (2013) 15:412–29. doi: 10.1111/cmi.12046
44. Narayanan A, Iordanskiy S, Das R, Van Duyne R, Santos S, Jaworski E, et al. Exosomes Derived From HIV-1-Infected Cells Contain Trans-Activation Response Element RNA. *J Biol Chem* (2013) 288:20014–33. doi: 10.1074/jbc.M112.438895
45. Bernard MA, Zhao H, Yue SC, Anandaiah A, Tachado SD. Novel HIV-1 miRNAs Stimulate TNFalpha Release in Human Macrophages *via* TLR8 Signaling Pathway. *PloS One* (2014) 9:e106006. doi: 10.1371/journal.pone.0106006
46. Sampey GC, Saifuddin M, Schwab A, Barclay R, Punya S, Chung MC, et al. Exosomes From HIV-1-Infected Cells Stimulate Production of Pro-Inflammatory Cytokines Through Trans-Activating Response (TAR) RNA. *J Biol Chem* (2016) 291(3):1251–66. doi: 10.1074/jbc.M115.662171
47. Fang Y, Wu N, Gan X, Morrell JC, Gouldet SJ. Higher-Order Oligomerization Targets Plasma Membrane Proteins and HIV Gag to Exosomes. *PloS Biol* (2007) 5(6):e158. doi: 10.1371/journal.pbio.0050158
48. Lenassi M, Cagney G, Liao M, Vaupotic T, Bartholomeeusen K, Cheng Y, et al. HIV Nef Is Secreted in Exosomes and Triggers Apoptosis in Bystander CD4+ T Cells. *Traffic* (2010) 11(1):110–22. doi: 10.1111/j.1600-0854.2009.01006.x
49. de Carvalho JV, de Castro RO, da Silva EZ, Silveira PP, da Silva-Januario ME, Arruda E, et al. Nef Neutralizes the Ability of Exosomes From CD4+ T Cells to Act as Decoys During HIV-1 Infection. *PloS One* (2014) 9(11):e113691. doi: 10.1371/journal.pone.0113691
50. Xu W, Santini PA, Sullivan JS, He JS, Shan M, Ball SC, et al. HIV-1 Evades Virus-Specific IgG2 and IgA Responses by Targeting Systemic and Intestinal B Cells *via* Long-Range Intercellular Conduits. *Nat Immunol* (2009) 10 (9):1008–17. doi: 10.1038/ni.1753
51. Del Río-Iñiguez I, Vázquez-Chávez E, Cuche C, Bartolo VD, Bouchet J, Alcover A. HIV-1 Nef Hijacks Lck and Rac1 Endosomal Traffic To Dually Modulate Signaling-Mediated and Actin Cytoskeleton-Mediated T Cell Functions. *J Immunol* (2018) 201(9):2624–40. doi: 10.4049/jimmunol.1800372
52. Mukhamedova N, Hoang A, Dragoljevic D, Dubrovsky L, Pushkarsky T, Low H, et al. Exosomes Containing HIV Protein Nef Reorganize Lipid Rafts Potentiating Inflammatory Response in Bystander Cells. *PloS Pathog* (2019) 15(7):e1007907. doi: 10.1371/journal.ppat.1007907
53. Admyre C, Johansson SM, Paulie S, Gabrielsson S. Direct Exosome Stimulation of Peripheral Human T Cells Detected by ELISPOT. *Eur J Immunol* (2006) 36:1772–81. doi: 10.1002/eji.200535615
54. Raposo G, Nijman HW, Stoorvogel W, Liejendekker R, Harding CV, Melief CJ, et al. B Lymphocytes Secrete Antigen-Presenting Vesicles. *J Exp Med* (1996) 183:1161–72. doi: 10.1084/jem.183.3.1161
55. Tang X, Lu H, Dooner M, Chapman S, Quesenberry PJ, Ramratnam B. Exosomal Tat Protein Activates Latent HIV-1 in Primary, Resting CD4+ T Lymphocytes. *JCI Insight* (2018) 3(7):95676. doi: 10.1172/jci.insight.95676

56. Hong X, Schouest B, Xu H. Effects of Exosome on the Activation of CD4+ T Cells in Rhesus Macaques: A Potential Application for HIV Latency Reactivation. *Sci Rep* (2017) 7(1):15611. doi: 10.1038/s41598-017-15961-x
57. Chiozzini C, Arenaccio C, Olivetta E, Anticoli S, Manfredi F, Ferrantelli F, et al. Trans-Dissemination of Exosomes From HIV-1-Infected Cells Fosters Both HIV-1 Trans-Infection in Resting CD4+ T Lymphocytes and Reactivation of the HIV-1 Reservoir. *Arch Virol* (2017) 162(9):2565–77. doi: 10.1007/s00705-017-3391-4
58. Barclay RA, Schwab A, DeMarino C, Akpamagbo Y, Lepene B, Kassaye S, et al. Exosomes From Uninfected Cells Activate Transcription of Latent HIV-1. *J Biol Chem* (2017) 292(28):11682–701. doi: 10.1074/jbc.M117.793521
59. Arenaccio C, Anticoli S, Manfredi F, Chiozzini C, Olivetta E, Federico M. Latent HIV-1 Is Activated by Exosomes From Cells Infected With Either Replication-Competent or Defective HIV-1. *Retrovirology* (2015) 12:87. doi: 10.1186/s12977-015-0216-y
60. Arenaccio C, Chiozzini C, Columba-Cabezas S, Manfredi F, Affabris E, Baur A, et al. Exosomes From Human Immunodeficiency Virus Type 1 (HIV-1)-Infected Cells License Quiescent CD4+ T Lymphocytes to Replicate HIV-1 Through a Nef- and ADAM17-Dependent Mechanism. *J Virol* (2014) 88 (19):11529–39. doi: 10.1128/JVI.01712-14
61. McNamara RP, Costantini LM, Myers TA, Schouest B, Maness NJ, Griffith JD, et al. Nef Secretion Into Extracellular Vesicles or Exosomes Is Conserved Across Human and Simian Immunodeficiency Viruses. *mBio* (2018) 9(1): e02344–17. doi: 10.1128/mBio.02344-17
62. Kadiu I, Narayanasamy P, Dash PK, Zhang W, Gendelman HE. Biochemical and Biologic Characterization of Exosomes and Microvesicles as Facilitators of HIV-1 Infection in Macrophages. *J Immunol* (2012) 189(2):744–54. doi: 10.4049/jimmunol.1102244
63. Arakelyan A, Fitzgerald W, Zicari S, Vanpouille C, Margolis L. Extracellular Vesicles Carry HIV Env and Facilitate Hiv Infection of Human Lymphoid Tissue. *Sci Rep* (2017) 7(1):1695. doi: 10.1038/s41598-017-01739-8
64. Schaefer MR, Wonderlich ER, Roeth JF, Leonard JA, Collins KL. HIV-1 Nef Targets MHC-I and CD4 for Degradation *via* a Final Common β-COP-Dependent Pathway in T Cells. *PloS Pathog* (2008) 4:e1000131. doi: 10.1371/journal.ppat.1000131
65. Lubben NB, Sahlender DA, Motley AM, Lehner PJ, Benaroch P, Margaret S, et al. HIV-1 Nef-Induced Down-Regulation of MHC Class I Requires AP-1 and Clathrin But Not PACS-1 and is Impeded by AP-2. *Mol Biol Cell* (2007) 18:3351–65. doi: 10.1091/mbc.e07-03-0218
66. Da Silva LL, Sougrat R, Burgos PV, Janvier K, Mattera R, Bonifacino JS. Human Immunodeficiency Virus Type 1 Nef Protein Targets CD4 to the Multivesicular Body Pathway. *J Virol* (2009) 83:6578–90. doi: 10.1128/JVI.00548-09
67. Wonderlich ER, Leonard JA, Collins KL. HIV Immune Evasion Disruption of Antigen Presentation by the HIV Nef Protein. *Adv Virus Res* (2011) 80:103–27. doi: 10.1016/B978-0-12-385987-7.00005-1
68. Admyre C, Johansson SM, Rahman Qazi K, Filén JJ, Lahesmaa R, Norman M, et al. Exosomes With Immune Modulatory Features Are Present in Human Breast Milk. *J Immunol* (2007) 179:1969–78. doi: 10.4049/jimmunol.179.3.1969
69. Lee JH, Schierer S, Blume K, Dindorf J, Wittki S, Xiang W, et al. HIV-Nef and ADAM17-Containing Plasma Extracellular Vesicles Induce and Correlate With Immune Pathogenesis in Chronic HIV Infection. *EBioMedicine* (2016) 6:103–13. doi: 10.1016/j.ebiom.2016.03.004
70. Konadu KA, Huang MB, Roth W, Armstrong W, Powell M, Villinger F, et al. Isolation of Exosomes From the Plasma of HIV-1 Positive Individuals. *J Vis Exp* (2016) 107):1–9. doi: 10.3791/53495
71. Falasca K, Lanuti P, Ucciferri C, Pieragostino D, Concetta Cufaro M, Bologna G, et al. Circulating Extracellular Vesicles as New Inflammation Marker in HIV Infection. *AIDS* (2021) 35(4):595–604. doi: 10.1097/QAD.0000000000002794
72. Kodidela S, Ranjit S, Sinha N, McArthur C, Kumar A, Kumar S. Cytokine Profiling of Exosomes Derived From the Plasma of HIV-Infected Alcohol Drinkers and Cigarette Smokers. *PloS One* (2018) 13(7):e0201144. doi: 10.1371/journal.pone.0201144
73. Ostalecki C, Wittki S, Lee JH, Geist MM, Tibroni N, Harrer T, et al. HIV Nef- and Notch1-Dependent Endocytosis of ADAM17 Induces Vesicular TNF Secretion in Chronic HIV Infection. *EBioMedicine* (2016) 13:294–304. doi: 10.1016/j.ebiom.2016.10.027
74. Chettimada S, Lorenz DR, Misra V, Wolinsky SM, Gabuzda D. Small RNA Sequencing of Extracellular Vesicles Identifies Circulating miRNAs Related to Inflammation and Oxidative Stress in HIV Patients. *BMC Immunol* (2020) 21 (1):57. doi: 10.1186/s12865-020-00386-5
75. Duette G, Pereyra PP, Rubione J, Perez PS, Landay AL, Crowe SM, et al. Induction of HIF-1α by HIV-1 Infection in CD4+ T Cells Promotes Viral Replication and Drives Extracellular Vesicle-Mediated Inflammation. *mBio* (2018) 9(5):e00757–18. doi: 10.1128/mBio.00757-18
76. Mack M, Kleinschmidt A, Bruhl H, Klier C, Nelson PJ, Cihak J, et al. Transfer of the Chemokine Receptor CCR5 Between Cells by Membrane-Derived Microparticles: A Mechanism for Cellular Human Immunodeficiency Virus 1 Infection. *Nat Med* (2000) 6:769–75. doi: 10.1038/77498
77. Rozmyslowicz T, Majka M, Kijowski J, Murphy SL, Conover DO, Poncz M, et al. Platelet- and Megakaryocyte-Derived Microparticles Transfer CXCR4 Receptor to CXCR4-Null Cells and Make Them Susceptible to Infection by X4-HIV. *AIDS* (2003) 17:33–42. doi: 10.1097/00002030-200301030-00006
78. Dean M, Carrington M, Winkler C, Huttley GA, Smith MW, Allikmets R, et al. Genetic Restriction of HIV-1 Infection and Progression to AIDS by a Deletion Allele of the CKR5 Structural Gene. Hemophilia Growth and Development Study, Multicenter AIDS Cohort Study, Multicenter Hemophilia Cohort Study, San Francisco City Cohort, ALIVE Study. *Science* (1996) 273(5283):1856–62. doi: 10.1126/science.273.5283.1856
79. Tumne A, Prasad VS, Chen Y, Stolz DB, Saha K, Ratner DM, et al. Noncytotoxic Suppression of Human Immunodeficiency Virus Type 1 Transcription by Exosomes Secreted From CD8+ T Cells. *J Virol* (2009) 83 (9):4354–64. doi: 10.1128/JVI.02629-08
80. Khatua AK, Taylor HE, Hildreth JE, Popik W, et al. Exosomes Packaging APOBEC3G Confer Human Immunodeficiency Virus Resistance to Recipient Cells. *J Virol* (2009) 83(2):512–21. doi: 10.1128/JVI.01658-08
81. Welch JL, Kaufman TM, Stapleton JT, Okeoma CM. Semen Exosomes Inhibit HIV Infection and HIV-Induced Proinflammatory Cytokine Production Independent of the Activation State of Primary Lymphocytes. *FEBS Lett* (2020) 594(4):695–709. doi: 10.1002/1873-3468.13653
82. Näslund TI, Paquin-Proulx D, Paredes PT, Valhov E, Sandberg JK, Gabrielsson S. Exosomes From Breast Milk Inhibit HIV-1 Infection of Dendritic Cells and Subsequent Viral Transfer to CD4+ T Cells. *AIDS* (2014) 28(2):171–80. doi: 10.1097/QAD.0000000000000159
83. Antimisiaris SG, Mourtas S, Marazioti A. Exosomes and Exosome-Inspired Vesicles for Targeted Drug Delivery. *Pharmaceutics* (2018) 10(4):218. doi: 10.3390/pharmaceutics10040218
84. Qiu Y, Ma J, Zeng Y. Therapeutic Potential of Anti-HIV RNA-Loaded Exosomes. *BioMed Environ Sci* (2018) 31(3):215–26. doi: 10.3967/bes2018.027
85. Wahlgren J, De L Karlson T, Brisslert M, Sani FV, Telemo E, Sunnerhagen P, et al. Plasma Exosomes Can Deliver Exogenous Short Interfering RNA to Monocytes and Lymphocytes. *Nucleic Acids Res* (2012) 40(17):e130. doi: 10.1093/nar/gks463
86. O'Loughlin AJ, Mäger I, de Jong OG, Varela MA, Schiffelers RM, El Andaloussi S, et al. Functional Delivery of Lipid-Conjugated siRNA by Extracellular Vesicles. *Mol Ther* (2017) 25(7):1580–7. doi: 10.1016/j.ymthe.2017.03.021
87. Kumar S, Zhi K, Mukherji A, Gerth K. Repurposing Antiviral Protease Inhibitors Using Extracellular Vesicles for Potential Therapy of COVID-19. *Viruses* (2020) 12(5):486. doi: 10.3390/v12050486
88. Pinky, Gupta S, Krishnakumar V, Sharma Y, Dinda AK, Mohanty S. Mesenchymal Stem Cell Derived Exosomes: A Nano Platform for Therapeutics and Drug Delivery in Combating COVID-19. *Stem Cell Rev Rep* (2021) 17(1):33–43. doi: 10.1007/s12015-020-10002-z
89. Kugeratski FG, Kalluri R. Exosomes as Mediators of Immune Regulation and Immunotherapy in Cancer. *FEBS J* (2021) 288(1):10–35. doi: 10.1111/febs.15558
90. Nanjundappa RH, Wang R, Xie Y, Umeshappa CS, Xiang J. Novel CD8+ T Cell-Based Vaccine Stimulates Gp120-Specific CTL Responses Leading to Therapeutic and Long-Term Immunity in Transgenic HLA-A2 Mice. *Vaccine* (2012) 30(24):3519–25. doi: 10.1016/j.vaccine.2012.03.075
91. Lattanzi L, Federico M. A Strategy of Antigen Incorporation Into Exosomes: Comparing Cross-Presentation Levels of Antigens Delivered by Engineered Exosomes and by Lentiviral Virus-Like Particles. *Vaccine* (2012) 30(50):7229–37. doi: 10.1016/j.vaccine.2012.10.010

92. Barclay RA, Mensah GA, Cowen M, DeMarino C, Kim Y, Pinto DO, et al. Extracellular Vesicle Activation of Latent HIV-1 Is Driven by EV-Associated C-Src and Cellular SRC-1 via the PI3K/AKT/mTOR Pathway. *Viruses* (2020) 12(6):665. doi: 10.3390/v12060665
93. Anyanwu SI, Doherty A, Powell MD, Obialo C, Huang MB, Quarshie A, et al. Detection of HIV-1 and Human Proteins in Urinary Extracellular Vesicles From HIV+ Patients. *Adv Virol* (2018) 2018:7863412. doi: 10.1155/2018/7863412
94. Stroud JC, Oltman A, Han A, Bates DL, Chen L. Structural Basis of HIV-1 Activation by NF-Kappab—a Higher-Order Complex of P50:RelA Bound to the HIV-1 LTR. *J Mol Biol* (2009) 393(1):98–112. doi: 10.1016/j.jmb.2009.08.023
95. Duh EJ, Maury WJ, Folks TM, Fauci AS, Rabson AB. Tumor Necrosis Factor Alpha Activates Human Immunodeficiency Virus Type 1 Through Induction of Nuclear Factor Binding to the NF-Kappa B Sites in the Long Terminal Repeat. *Proc Natl Acad Sci USA*. (1989) 86(15):5974–8. doi: 10.1073/pnas.86.15.5974

Conflict of Interest: The authors declare that the research was conducted in the absence of any commercial or financial relationships that could be construed as a potential conflict of interest.

GLOSSARY

HIV	human immunodeficiency virus
cART	combination antiretroviral therapy
DNA	deoxyribonucleic acid
LRAs	latency reversal agents
EVs	extracellular vesicles
CD63	cluster of differentiation 63
CD9	cluster of differentiation 9
CD81	cluster of differentiation 81
Alix	Programmed cell death 6-interacting protein
Tsg101	tumor susceptibility gene 101 protein
RNA	ribonucleic acid
mRNA	messenger RNA
miRNAs	microRNA (small single-stranded non-coding RNA molecule)
Nef	Negative Regulatory Factor
MHC	major histocompatibility complex
CD4	cluster of differentiation 4
Tat	trans-Activator of Transcription
CCR5	C-C chemokine receptor type 5
CXCR4	C-X-C chemokine receptor type 4
PBMCs	peripheral blood mononuclear cells
Env	Envelope glycoprotein
Gp120	Glycoprotein 120
CD8	cluster of differentiation 8
Tregs	regulatory T cells
IgA	Immunoglobulin A
IgG	Immunoglobulin B
APOBEC3G (A3G)	apolipoprotein B mRNA editing enzyme, catalytic polypeptide-like 3G
TLR	Toll-like receptor
ISG	IFN-stimulated genes
ISG15	IFN-stimulated gene 15
ISG56	IFN-stimulated gene 56
MxB	gene coding for myxovirus resistance protein B
OAS-1	gene coding for 2'-5'-oligoadenylate synthetase 1
GBP5	gene coding for guanylate binding protein 5
RNAsa-L	Ribonuclease L
miRNA-17	micro-RNA 17
miRNA-20	micro-RNA 20
miRNA-28	micro-RNA 28
miRNA-29	micro-RNA 29
miRNA-125b	micro-RNA 125b
IFN	Interferon
LTR	long terminal repeat
NF-kβ	nuclear factor kappa-light-chain-enhancer of activated B cells
DC-SIGN	dendritic Cell-Specific Intercellular adhesion molecule-3-Grabbing Non-integrin
Cdk9	Cyclin-dependent kinase 9
c-Src	proto-oncogene tyrosine-protein kinase Src
PI3K	Phosphatidylinositol 3-kinase
AKT-1	RAC-alpha serine/threonine-protein kinase
mTOR	Mechanistic Target of Rapamycin Kinase
STAT3	Signal transducer and activator of transcription 3
TAR	trans-activation response element
IL-6	interleukin-6
TNF-β	tumor necrosis factor beta
PKR	protein kinase R
vimR88	viral micro-RNA 88
vmiR99	viral micro-RNA 99
TLR8	Toll-like receptor 8
TNFα	tumor necrosis factor α
ADAM17	tumor necrosis factor-α-converting enzyme

frontiers in Immunology

REVIEW
published: 28 January 2022
doi: 10.3389/fimmu.2022.828386

Breast Cancer Vaccines: Disappointing or Promising?

Si-Yuan Zhu[1,2] *and Ke-Da Yu*[1,2*]

[1] Department of Breast Surgery, Fudan University Shanghai Cancer Center, Shanghai, China,
[2] Shanghai Medical College, Fudan University, Shanghai, China

Breast cancer has become the most commonly diagnosed cancer globally. The relapse and metastasis of breast cancer remain a great challenge despite advances in chemotherapy, endocrine therapy, and HER2 targeted therapy in the past decades. Innovative therapeutic strategies are still critically in need. Cancer vaccine is an attractive option as it aims to induce a durable immunologic response to eradicate tumor cells. Different types of breast cancer vaccines have been evaluated in clinical trials, but none has led to significant benefits. Despite the disappointing results at present, new promise from the latest study indicates the possibility of applying vaccines in combination with anti-HER2 monoclonal antibodies or immune checkpoint blockade. This review summarizes the principles and mechanisms underlying breast cancer vaccines, recapitulates the type and administration routes of vaccine, reviews the current results of relevant clinical trials, and addresses the potential reasons for the setbacks and future directions to explore.

Keywords: breast cancer, vaccine, HER2, tumor antigens, E75 peptide vaccine

OPEN ACCESS

Edited by:
Fabio Bagnoli, GlaxoSmithKline, Italy

Reviewed by:
Elizabeth Ann Repasky, University at Buffalo, United States
Ourania Tsitsilonis, National and Kapodistrian University of Athens, Greece

***Correspondence:**
Ke-Da Yu
yukeda@fudan.edu.cn

Specialty section:
This article was submitted to Vaccines and Molecular Therapeutics, a section of the journal Frontiers in Immunology

Received: *03 December 2021*
Accepted: *12 January 2022*
Published: *28 January 2022*

Citation:
Zhu S-Y and Yu K-D (2022) Breast Cancer Vaccines: Disappointing or Promising? Front. Immunol. 13:828386. doi: 10.3389/fimmu.2022.828386

1 INTRODUCTION

Breast cancer has become the most commonly diagnosed cancer globally, with an estimated burden of 2.3 million new cases in 2020 (1). Breast cancer is heterogeneous and clinically classified into three main subtypes according to the status of estrogen receptor (ER), progesterone receptor (PR), and human epidermal growth factor receptor 2 (HER2): luminal subtype that expresses ER and/or PR, HER2-positive subtype that overexpresses HER2, and triple-negative breast cancer (TNBC) (2). Despite advances in endocrine therapy and anti-HER2 therapy in past decades, relapse and metastasis of breast cancer remain a great challenge in clinical practice. Therefore, innovative therapeutic approaches are still critically in need. In recent years, studies have shown that tumor-infiltrating lymphocyte (TIL) is associated with response to treatment and long-term prognosis in patients with breast cancer (3, 4). Coupled with clinical successes of immune checkpoint blockades (ICB) applied in TNBC and other solid tumors (5–7), intensive interest has arisen in immunotherapy for breast cancer (8, 9).

Immune-based treatment strategies can be divided into passive immunotherapy and active immunotherapy. The anti-HER2 targeted intervention *via* monoclonal antibodies such as trastuzumab and pertuzumab falls under the former category (10, 11). Active immunotherapy mainly refers to cancer vaccines. The cancer vaccine is intended to elicit or boost an anti-tumor immune response by activating autologous immune cells in the patient to induce a therapeutic effect (12, 13). This review summarizes the principles and mechanisms underlying breast cancer vaccines, recapitulates the type and administration routes of vaccine, and reviews the current results of

relevant clinical trials. The challenges we face at present and potential directions to explore in the future are discussed in the end.

2 PRINCIPLES OF BREAST CANCER VACCINE

2.1 Immunoediting Throughout Tumor Progression

The immune system plays different roles in breast cancer progression during different stage of tumor development. The paradoxical interaction between the tumor and the immune system is referred to as immunoediting, which generally evolves through three phases: elimination, equilibrium, and escape (**Figure 1**) (14). During the elimination phase, incipient tumor cells can activate innate immunity, including maturation of macrophages, natural killing (NK) cells and dendritic cells (DCs). These cells help prime tumor-specific T cells. Thus the adaptive immune response can cooperate with innate immunity to recognize and eradicate these early transformed tumor cells. The equilibrium phase starts if any tumor subclones survives the selection pressure from the host immunity. Tumor cells can hardly be removed, but meanwhile, their progression is strictly limited or even paused because of the delicate balance between tumor growth and the defense effect of the immune system in this phase. However, tumor subclones with less immunogenicity will eventually arise due to tumor cells' genetic instability and epigenetic modifications (15). These subclones can evade immune recognition and destruction through multiple solutions such as downregulating antigen-presenting molecules and increasing immune checkpoint receptors on the cell surface (16, 17). Therefore, the evolved tumor cells that succeed in escaping constant immunologic pressure will enter the last phase of immunoediting, where the immune system scarcely restrict their progression (18–20).

2.2 Immune Cells Recognizing Tumor Antigens

To produce an anti-tumor immune response, the effector immune cells need to recognize tumor antigens presented by tumor cells directly or by antigen-presenting cells (APCs) *via* major histocompatibility complex (MHC) on the cell surface. $CD8^+$ and $CD4^+$ T cells, which play a core role in the immunoediting process, distinguish these non-self-epitopes of tumor cells displayed by MHC class-I and MHC class-II molecules respectively from normal self-antigens (21–24).

Tumor antigens can be divided into tumor-specific antigens (TSAs) and tumor-associated antigens (TAAs) (25). TSAs are expressed only by tumor cells and not by normal cells. TSAs include oncoviral antigens derived from oncogenic tumor viruses and neoantigens derived from somatic mutations in tumor cells. Therefore there is usually no immune tolerance towards TSAs in humans (26).

TAAs are self-proteins commonly expressed in both tumors and normal tissues, while their expression patterns in tumor cells are abnormal (27). This category includes overexpressed antigens such as HER2 and mucin-1 (MUC-1), tissue differentiation antigens such as carcino-embryonic antigen (CEA), and tumor germline antigens like melanoma-associated antigen (28). The majority of tumor antigens that have been studied in breast cancer vaccines so far are the HER2 protein and other HER2-derived

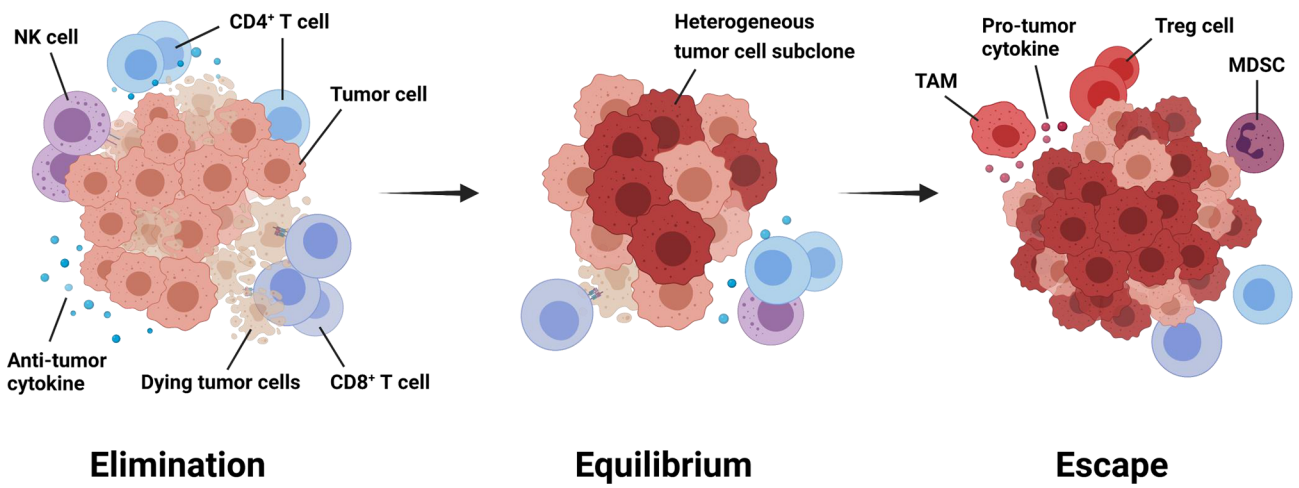

FIGURE 1 | Immunoediting throughout tumorigenesis and progression. Immunoediting generally evolves through three phases: elimination, equilibrium, and escape (14). During the first phase, tumor cells activate anti-tumor immune responses, which mainly performed by $CD8^+$ T cells, $CD4^+$ T cells, and natural killing cells. The equilibrium phase starts if any tumor subclones survive the selection pressure from the host immunity. Tumor cells can hardly be removed, but meanwhile, their progression is strictly limited in this phase. When shifting to the escape phase, tumor cells with less immunogenicity manage to avoid recognition and attack from anti-tumor immune cells through multiple mechanisms. Besides, an immunosuppressive tumor microenvironment will gradually generate to attenuate anti-tumor immunity and favor tumor progression further. MDSC, myeloid-derived suppressor cell; NK, natural killing; TAM, tumor-associated macrophage; Treg cell, regulatory T cell.

peptides (29, 30). In humans, the HER2 protein is generally expressed during fetal development and is weakly detectable in the epithelial cells of many normal tissues in adults (31). Thus immune tolerance to HER2 has usually been established already. In fact, despite the existence of immune tolerance, humoral and cellular immunity against HER2 have been detected in some of breast cancer patients due to the high immunogenicity of the antigen (32, 33). However, the level of the pre-existed anti-HER2 immunity is usually too low to induce an evident therapeutic effect. Therefore, vaccines targeting HER2-related antigens need to overcome the established tolerance to boost an immune response that is strong and durable enough (31). Various strategies, including using novel immunoadjuvants, applying dominant or subdominant epitopes, and altering the natural structure of peptides, have been investigated in breast cancer vaccines to circumvent immune tolerance.

2.3 Tumor Cells Attenuating Anti-Tumor Immunity

To successfully escape immunosurveillance, tumors manage to suppress the host immunity both systemically and locally (34). As mentioned above, when the elimination phase gradually shifts to the escape phase, the immunosuppressive effect will outweigh the antitumoral response in the relatively advanced stage of the disease. During this shift, suppressive immune cells, including regulatory T (Treg) cells, tumor-associated macrophages (TAMs), and myeloid-derived suppressor cells (MDSCs), become increasingly prevalent in the tumor microenvironment (TME) and the draining lymph nodes of the tumor and even appear in peripheral blood (35–39). Increased number of these immunosuppressive cells generally correlates to inferior prognosis (38–42). Moreover, the number and the activity of the cytotoxic lymphocytes (CTLs) and NK cells in the TME are reduced so that the antitumoral response will be further undermined (43–46).

In addition to the transformation of immune cell composition in the TME, cytokines are also involved in generating an immunosuppressive microenvironment in favor of tumor progression (47). For instance, upregulation of the DC-derived cytokine TGFβ promotes the proliferation of Treg cells (48), and Treg cells will correspondingly downregulate the co-stimulatory molecules such as CD80 and CD86 on DCs required for CTL priming (45). The cytokine interleukin-2 (IL-2), which is necessary for CTL activation, can bind to Treg cells at a higher affinity, leaving the CTLs in starvation (46). Moreover, adenosine produced by Treg cells has an immune inhibitory effect on the effector T cells (49, 50). The inhibitory cytokine IL-10 and TGFβ secreted by TAMs are also capable of blocking the function of CTLs (51, 52) and suppress the production of anti-tumor cytokine IL-12 (53).

Furthermore, immune checkpoint receptors such as programmed cell death receptor 1 (PD-1) and cytotoxic T lymphocyte antigen 4 (CTLA-4) are found to be upregulated in tumor progression. PD-1 is the counter-receptor of programmed cell death ligand 1 (PD-L1) (54). In patients with different malignant tumors, high levels of PD-1 expression are detected in TILs, including tumor-specific T cells, and PD-L1 is upregulated in tumor cells and APCs simultaneously. Engagement of PD-L1 and PD-1 results in T cell dysfunction and apoptosis so that the tumor cells can avoid destruction from T cells (55, 56). CTLA-4 is found in the intracellular compartment in resting T cells and it will be transported to the cell surface once the T cell is stimulated (57). It can block the co-stimulatory signals, which is essential for T cell activation, through binding the transmitting molecules CD80 and CD86 on DCs and B cells to prevent the immune response from over-amplification (58). ICB blocks the inhibitory receptors such as PD-1/PD-L1 and CTLA-4, allowing effector T cells to attack the tumor (59). The efficacy of ICB for breast cancer has recently been evaluated. Monoclonal antibody atezolizumab targeting PD-L1 successfully prolonged progression-free survival (PFS) among patients with metastatic TNBC in the IMpassion130 trial (7). However, the same drug failed to show a significant improvement in PFS for advanced HER2-positive breast cancer in combination with trastuzumab emtansine in the KATE2 trial (60).

Collectively, the suppressive immune cells, the cytokines, the metabolites, and immune checkpoint molecules together constitute a complex network of immune suppression that facilitates immune escape and attenuates anti-tumor immunity.

3 APPROACHES OF BREAST CANCER VACCINE

Strategies of vaccination involve optimization of vaccine regimens and administration routes. Breast cancer vaccines can be divided into different types based on platforms and formulations. Nevertheless, they all need to make the targeted antigen recognized by the autologous immune system to induce a therapeutic effect. Adjuvant of the vaccine plays a vital role as they are able to enhance antigen immunogenicity and regulate the immune response. Additionally, administration routes have different influences on the delivery of targeted antigens to DCs. We will briefly review the types of breast cancer vaccines and introduce the adjuvants and administration routes applied currently.

3.1 Types of Breast Cancer Vaccine

Currently, the most common vaccination approach for breast cancer is to utilize peptides derived from tumor antigens. Vaccination of tumor antigen-related protein and carbohydrate has also been explored for long. Tumor cell-based vaccine is one of the traditional methods, while DNA-based and DC-based vaccines represent novel modalities in this field. A different formulation of vaccines and their mechanisms of action are depicted in **Figure 2**.

3.1.1 Peptide Vaccine

Delivering MHC class-I restricted peptide epitopes to activate immune responses against the specific tumor antigen is one of the most common strategies applied for breast cancer. The peptide injected will be processed and presented by APCs to prime immune effector cells, which will then seek out and eradicate cancer cells expressing the shared antigen (61). Compared to other formulations, short amino acid peptides are simple and cheap to manufacture and relatively stable

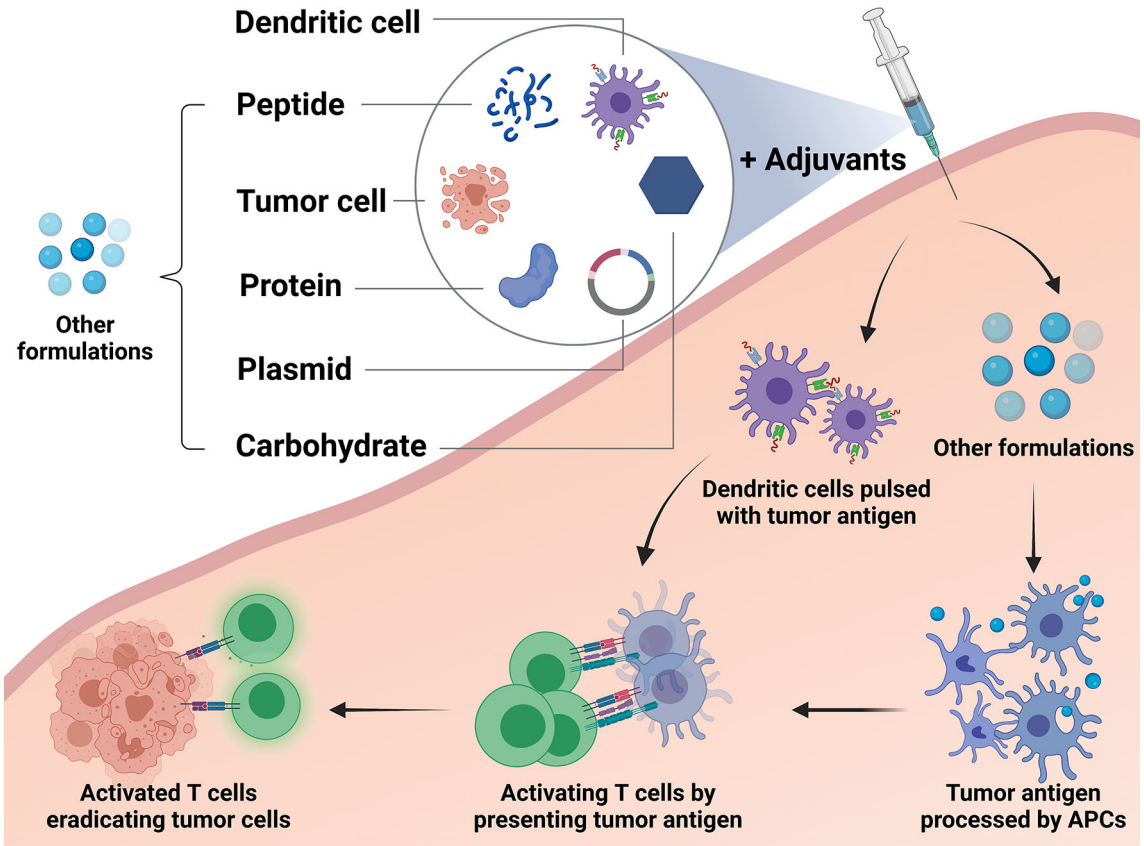

FIGURE 2 | Different types of breast cancer vaccines and their mechanisms. The studied breast cancer vaccines can be divided into the following types according to their formulations and approaches: peptide vaccine, protein-based vaccine, carbohydrate antigen vaccine, DNA-based vaccine, dendritic cell-based (DC-based) vaccine, and tumor cell vaccine. DC-based vaccines utilize *ex vivo* generation of DCs loaded with tumor antigens or transfected to express tumor antigens. These cells process the antigens and present them to T cells directly by themselves in order to activate an immune response. Except the dendritic cells, other formulations applied in the vaccines, including peptide, protein, plasmid, carbohydrate and tumor cell, need to stimulate the autologous antigen presenting cells (APCs). Then the autologous APCs will activate the effector immune cells to boost an anti-tumor reaction.

when transported, which makes large-scale manufacture and transportation possible (62). However, the individual peptide is usually limited to certain human leukocyte antigen (HLA) subtypes and thus patients who do not express the common HLA types cannot be treated with the vaccine (63). In addition, the usual MHC class-I binding peptides do not have a strong ability to activate $CD4^+$ helper T cells, which may cause limited activation of $CD8^+$ cytotoxic T cells and transience of immune responses (64). This issue might be partly overcome by using synthetic peptides that are long enough to include multiple MHC class-I and class-II epitopes. Such peptides containing 23-45 amino acids might lead to superior T cell stimulation through a more efficient processing and presentation pathway (65).

3.2.2 Protein-Based Vaccine

The protein-based vaccine is developed with the whole or shortened fragment of tumor antigen protein whose amino acid sequence is much longer than peptides (64). It enables uptake, processing, and presentation of multiple MHC class-I and class-II peptide epitopes and is not HLA restricted. But the presentation process might be less efficient, and the response to this kind of vaccine is hard to measure due to lack of a specific marker (66).

3.1.3 Carbohydrate Antigen Vaccine

Carbohydrate antigens abnormally expressed by tumor cells can also be distinguished by immune cells. Hence, such carbohydrate antigen becomes an ideal candidate to incorporate in a cancer vaccine. For instance, Sialy-Tn (STn), a disaccharide carbohydrate associated with MUC-1, is expressed uniquely on the cell surface of a variety of cancer cells, including breast cancer (67). Immunization with STn demonstrated tumor regression and prolonged survival in animal studies, and the cancer vaccine towards STn was correspondingly developed (68).

3.1.4 Tumor Cell Vaccine

It is one of the earliest approaches of the cancer vaccine to use whole tumor cells or products of tumor cell lysis to stimulate an

immune response (64). It is based on a pool of unknown antigens derived from autologous or allogeneic tumor cells, and thus a polyvalent immune response will be triggered. The tumor cells are modified to secret cytokines or express co-stimulatory molecules in order to enhance the antigen-presenting ability in some vaccines (69, 70). The disadvantage of the tumor cell vaccine lies in that these vaccines contain endogenous cellular antigens and may cause an autoimmune reaction. There is also a lack of a standardized method for preparing tumor cell vaccines (63).

3.1.5 DNA-Based Vaccine

The DNA-based breast cancer vaccine uses the DNA sequence encoding tumor antigens, which are usually delivered in the forms of plasmids or vectors. The DNA sequence will be incorporated by APCs and translated into the tumor antigen, which will then be processed for presentation for immune cells to stimulate an antigen-specific immunity (71). DNA-based vaccines are easy to construct in large quantities and store at a low cost. However, the immunogenicity is not strong enough due to low efficiency of plasmids uptake and antigen expression (63, 71).

3.1.6 DC-Based Vaccine

DCs are a heterogeneous population of APCs that efficiently take up antigens and then process and present the antigens to $CD4^+$ and $CD8^+$ T cells after migrating to lymph nodes. NK cells and B cells can also be stimulated by DCs (61). The DC-based vaccines usually utilize *ex vivo* generation of DCs loaded with tumor antigens or transfected to express tumor antigens. Monocytes and CD34+ progenitor cells have been tested, and antigens including complex tumor lysates and multiple MHC class-I and class-II peptides have been explored in studies (62). Some vaccines require inoculation in lymph nodes and the DCs delivered can activate the immune cells directly. The production of DC-based vaccines can be technically demanding due to the individualized *ex vivo* process for the maturation of DCs (64). It is therefore difficult to compare trials with a single clinical trial arm and individualized vaccination patterns.

3.1.7 DC-Tumor Cell Fusion Vaccine

One of the efforts to improve the DC-based vaccination strategy is the fusion of DCs with tumor cells. DC-tumor cell hybrids can be created by exposing DCs and tumor cells in polythelene glycol (72). Tumor cells can also be transfected with a viral fusogenic membrane glycoprotein and pelleted with DCs to achieve a DC-tumor hybrid (73). Besides, electrofusion technique has been applied in this strategy (74). Compared with DCs pulsed with single antigens, DC-tumor cell fusion is able to present the entire repertoire of tumor antigens from the parental tumor cell to activate both the MHC class-I and class-II pathways (75). Nevertheless, this kind of vaccine is even harder to produce compared to the DC-based vaccine pulsed with peptides.

3.2 Adjuvants for Breast Cancer Vaccine

Adjuvants are substances that enhance antigen immunogenicity and elicit an immune response when inoculated with antigens (76). Mechanisms of most adjuvants include slowing release of antigens, promoting antigen uptake and presentation of APCs and stimulating proliferation of DCs and macrophages (77–79). In prophylactic vaccines designed for infectious diseases, classical adjuvants, such as alum, mainly induce the type 2 T helper cell-dependent humoral immunity instead of type 1 T helper cell responses that directly destruct tumor cells (80). Different types of adjuvants used in cancer vaccines are listed in **Table 1**.

Granulocyte-macrophage colony-stimulating factor (GM-CSF) is a secreted cytokine that has been widely used as an adjuvant in breast cancer vaccines. It has been shown to be capable of triggering the maturation of myeloid cells such as granulocytes and macrophages and promoting the expansion and activation of DCs (81, 82). Several breast cancer vaccines containing GM-CSF induced detectable immune responses in clinical trials (83–87). And in melanoma patients, locally addition of GM-CSF modestly increased the immune response towards the vaccinated antigen (78, 88). However, in other studies, it was also observed that GM-CSF might be associated with a lower degree of T cell responses and induction of inhibitory MDSCs (89, 90). Therefore, the application of GM-CSF as an adjuvant in cancer vaccines still needs further investigation.

Another popular strategy for adjuvants adopted in DNA-based cancer vaccines is utilizing recombinant viral vectors. Recombinant viral vectors, which usually function as a delivery vehicle for the antigen, can boost immune response as well in that they always contain more or less toll-like receptor (TLR) ligands and pattern recognition receptor ligands to activate DCs (91). The TLR agonists are also able to enhance $CD8^+$ T cell activation and prevent T cell from exhausting (92, 93). The main drawback of such an adjuvant is that the vectors also have other sequences capable of competing with the inserted sequence of targeted antigens (94).

TABLE 1 | Major types of adjuvants for breast cancer vaccine and their functions.

Types of Adjuvants	Examples	Functions
Cytokines	GM-CSF, IL-12	Promoting the maturation and activation of DCs and enhancing antigen uptake and presentation
Microbes and microbial derivatives	BCG, CpG, MPL, poly I:C	Activating DCs through toll-like receptor ligands
Mineral salts	Alum	Enhancing antibody production by plasma cells
Oil emulsions or surfactants	AS02, Montanide, QS21	Decelerating release of antigens and stimulating local DCs at the injection site
Particulates	AS04, polylactide co-glycolide	Functioning as an antigen carrier and enhancing antigen uptake and presentation
Viral vectors	Adenovirus, fowlpox	Delivering antigens and activating DCs through toll-like receptor ligands

AS, adjuvant system; BCG, Bacillus Calmette-Guérin; CpG, cytosine-phosphate diester-guanine; DC, dendritic cell; GM-CSF, Granulocyte-macrophage colony-stimulating factor; IL, interleukin; MPL, monophosphoryl lipid A; QS21, a plant extract derived from Quillaja saponaria.

Nevertheless, difficulty exists when comparing different adjuvant strategies for cancer vaccines since the effects of adjuvants might vary with vaccine formulations, targeted tumor antigens, immunization schedule, and route of administration. Therefore relevant studies on the optimization of adjuvants for breast cancer vaccines are urgently necessary at present.

3.3 Administration Routes of Breast Cancer Vaccine

Administration routes of cancer vaccines help effectively present the antigens to autologous APCs. Different preferred routes were applied for cancer vaccines of different types (**Figure 3**). Several peptide vaccines targeting HER2 have adopted intradermal vaccination strategies as there is a dense network of cutaneous DCs (83–85). Studies demonstrated that intradermal inoculation with low doses of the peptide was safe and stimulated antigen-specific T cell responses in the majority of the healthy population (95). The subcutaneous injection was also practiced in a variety of different breast cancer vaccines and achieved immune responses. However, large volumes of antigen delivered subcutaneously with adjuvants might cause severe injection-site reactions with occasional sterile abscess formation (96), which may lead to discontinuation of vaccination procedure or reduction of vaccine doses. In addition, intramuscular administration was often used to deliver vectors or plasmids for some DNA-based vaccines (97–99). By contrast, some DC-based vaccines required intranodal injection in order to prime the T cells existing in the lymph node directly.

An important factor to consider is how administration routes of vaccines affect the circulating and homing process of T cells towards the cancer-infiltrated tissues. Recent studies showed that intranasal immunization with DCs from the lung parenchyma was able to trigger homing properties on induced $CD8^+$ T cells to the mucosa (100). Much more work is necessary to establish valid rules regarding the delivery routes of cancer vaccines.

4 CLINICAL TRIALS OF BREAST CANCER VACCINE

Some breast cancer vaccines managed to elicit detectable immune responses and demonstrate good tolerance in early trials. Nevertheless, none of them has demonstrated significant clinical benefits in the following phase 3 trials. The Theratope® (STn) vaccine applied in the metastatic setting and the NeuVax™ [Nelipepimut-S (NPS), or E75] vaccine applied in the adjuvant setting both failed to bring clinical benefits in their

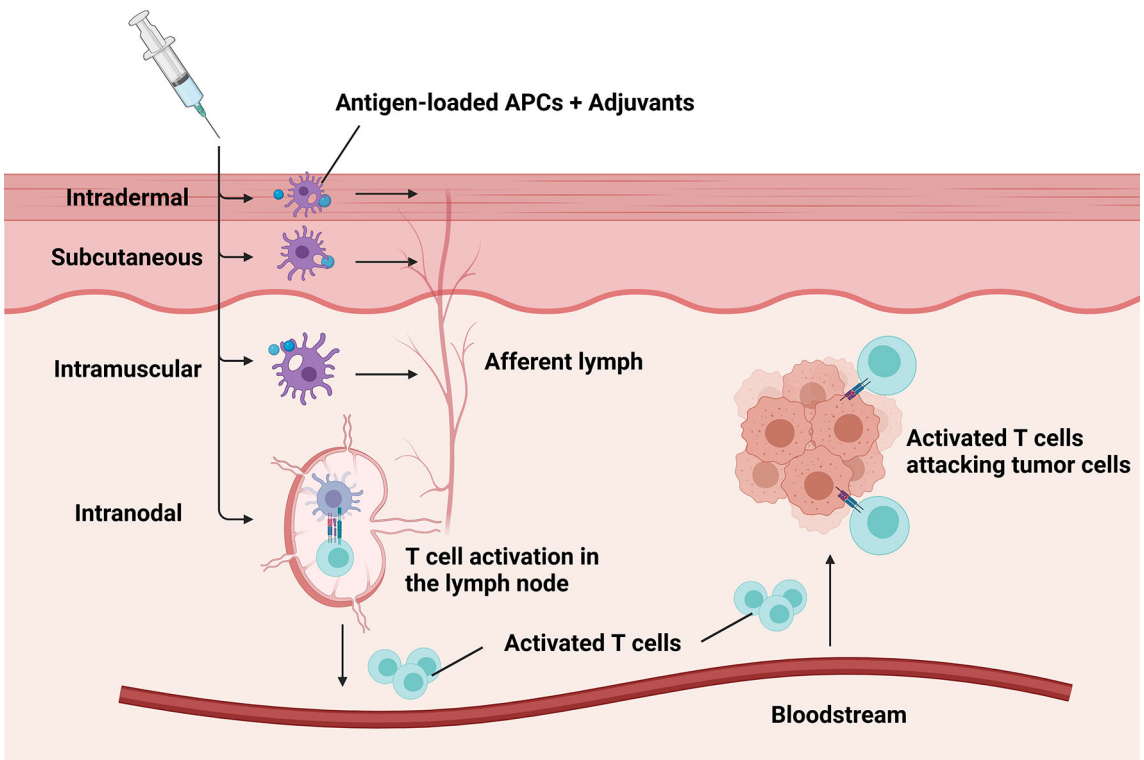

FIGURE 3 | Different administration routes of breast cancer vaccines. Major administration routes of breast cancer vaccines include intradermal, subcutaneous, intramuscular, and intranodal injection. The preferred routes depending on the type of the delivered antigens help effectively present the antigens to autologous antigen-presenting cells (APCs). Then the antigen-loaded APCs transfer to lymph nodes to prime T cells through afferent lymph. Subsequently, activated T cells transport into tumorous tissue with the aid of the bloodstream to eradicate tumor cells.

phase 3 study despite their early success (101, 102). We summarize the current results of clinical trials evaluating breast cancer vaccines according to the antigen they target in the following paragraphs. Major clinical trials targeting HER2-related antigens and non-HER2-related antigens are listed in **Tables 2** and **3**, respectively.

4.1 Vaccines Targeting HER2-Related Antigens

Breast cancer vaccines deliver HER2 or HER2-related antigens through different approaches and formulations. In this field, several peptide vaccines have been studied extensively in phase 2-3 clinical trials. We will introduce the vaccines targeting HER2-related antigens in the order of their types.

4.1.1 Peptide Vaccine—E75

E75 (Nelipepimut-S) vaccine is one of the most extensively studied breast cancer vaccines against HER2. It consists of HLA-A2/A3-restricted, MHC class-I, extracellular HER2-derived peptide E75 and the immunologic adjuvant GM-CSF. In a phase 1 trial initiated in the adjuvant setting, the E75 vaccine was administered to the disease-free patient with any level of HER2 expression [immunohistochemistry (IHC) 1-3+]. An immune response with good tolerance was demonstrated (83). The monthly intradermal dose of 1000mg E75 and 250mg of GM-CSF for 6 months was determined to be optimal (116). In the following phase 2 adjuvant study, 195 patients were randomly assigned to the vaccination arm or the control arm. At the conclusion of 5-year follow up, the disease-free survival (DFS) rate was 89.7% for vaccinated patients and 80.2% for control patients (P=0.08) (103, 116). Interestingly, vaccinated patients with relatively low expression of HER2 (IHC 1-2+) demonstrated a more robust immune response compared to those with higher levels of HER2 expression (IHC 3+), suggesting the possibility of immunologic tolerance to HER2 in some patients with tumors expressing high levels of HER2 (117).

Based on these promising data, the multicenter double-blinded phase 3 PRESENT trial was undertaken in patients with node-positive breast cancer with IHC 1-2+ HER2 expression in the adjuvant setting (102). In total, 758 disease-free patients were randomized to receive NeuVax^{TM} or placebo. The primary endpoint was 3-year DFS. However, this trial was terminated due to futility when an interim analysis, which was triggered after 70 qualifying DFS events occurred, failed to show a significant difference in DFS with vaccination. There were even more DFS events in the vaccinated group than in the control group. Still, the deaths, second cancers, and clinical recurrences were similar at 16.8 months median follow-up.

When combined with anti-HER2 targeted therapy, the efficacy of E75 vaccine in patients with low expression of HER2 (IHC 1-2+) was evaluated in a recently conducted phase 2 adjuvant trial (104). A total of 275 patients were randomized to receive E75 or placebo after receiving 1-year standard trastuzumab-based anti-HER2 treatment. At a median follow up of 25.7 months, estimated DFS did not significantly differ between the vaccination arm and the control arm (P = 0.18). But significant improved DFS was seen in patients with TNBC (IHC 1-2+ and hormone receptor-negative) in a planned exploratory analysis (P = 0.01). This study reflects that the HER2-derived peptide vaccines might be effective when used in parallel to or combined with trastuzumab-based anti-HER2 targeted therapy.

As for HER2 overexpression (IHC 3+) patients, the efficacy of E75 remains ambiguous in that the majority of the HER2 overexpression patients enrolled in the existing trials did not receive trastuzumab as standard anti-HER2 therapy.

4.1.2 Peptide Vaccine—GP2

Although the results of NeuVax^{TM} are not satisfying, new promise comes from other latest studies. GP2 is another HLA-A2/A3-restricted, MHC class-I, an immunogenic peptide derived from the transmembrane domain of HER2. While GP2 has a lower affinity to HLA-A2 than E75, it is as efficacious in inducing a CD8$^+$ T cell response (118). The GP2 vaccine demonstrated a good safety profile and managed to generate GP2-specific T cell responses and GP2-specific delayed-type hypersensitivity (DTH) responses when administered with GM-CSF in a phase 1 adjuvant trial (84). In the following phase 2 adjuvant trial that enrolled 180 patients with tumors expressing HER2 (IHC 1-3+), no significant benefit in DFS in the vaccination group compared with the control group (88% vs. 81%, P=0.43) after a 34-month median follow-up was observed (105). A subgroup analysis showed that HER2-positive (IHC 3+) patients had no recurrences with a trend towards improved DFS in the vaccinated group as compared to the control group (100% vs. 87.2%, P=0.052) (119). Encouraging results came from the final analysis of this trial, which demonstrated that the GP2 vaccine reduced the recurrence rate to 0% in HER 3+ patients, who have received a standard course of trastuzumab after surgery. The estimated 5-year DFS rate in the 46 HER2 3+ vaccinated patients, if the patient completed the primary immunization series, was 100% versus 89.4% in the 50 placebo patients (p=0.034) (106).

4.1.3 Peptide Vaccine—AE37

In addition to E75 and GP2, AE37 is another HER2-related peptide vaccine used in the adjuvant setting of breast cancer. It is an Ii-Key hybrid of AE36, which is derived from the intracellular domain of HER2. The modification was conducted to improve the binding potency of the epitope (120). Unlike E75 and GP2, AE37 is an MHC class-II epitope that mainly induces CD4$^+$ T cell activation. Low toxicity and favorable immune response were demonstrated in a phase 1 trial (85). Levels of Treg cells were measured and found to decrease after vaccination as AE37 stimulates CD4$^+$ helper T cell response (121). In a phase 2 trial of clinically disease-free patients expressing any degree of HER2 (IHC 1-3+), AE37 plus GM-CSF and GM-CSF alone were randomly administered to 153 and 145 patients, respectively (107). The DFS rate was 87.6% in the vaccine group and 86.2% in the control group (P=0.70) after a median follow-up of 30 months. In planned subset analyses of patients with IHC 1-2+ HER2-expressing tumors, DFS was 86.8% in vaccinated patients and 82.0% in control patients(P=0.21). Interestingly, TNBC patients (IHC 1-2+ and hormone receptor-negative) demonstrated a DFS rate of 84.0% in the vaccine group and 64.0% in the control group (P=0.12), suggesting AE37

TABLE 2 | Major clinical trials on breast cancer vaccines targeting HER2-related antigens.

Clinical Trial Reference	Trial Phase	Setting	Targeted Tumor Antigen	Design and Arms	Breast Cancer Subtype	Primary Objectives	Outcomes
PRESENT Trial NCT01479244 (102)	III	Adjuvant	HER2-derived peptide E75	Vaccination Arm: E75 + GM-CSF (N=376) Control Arm: Placebo + GM-CSF (N=382)	HLA-A2/A3+, HER2 low-expressing (IHC 1/2+), node-positive	DFS	RR at 16.8 months interim analysis: 9.8% (vaccinated group) versus 6.3% (control group) (P = 0.07). Based on these data, the study was terminated for futility.
US Military Cancer Institute Clinical Trials Group Study I-01 and I-02 (103)	I/II	Adjuvant	HER2-derived peptide E75	Vaccination Arm: E75 + GM-CSF of different doses (N=108) Control Arm: Observation (N=79)	HLA-A2/A3+, HER2-expressing, node-positive or high-risk node-negative	Safety, optimal dosing of immune response	Five-year DFS: 89.7% (vaccinated group) versus 80.2% (control group) (P = 0.08). Toxicities were minimal.
NCT01570036 (104)	II	Adjuvant	HER2-derived peptide E75	Vaccination Arm: E75 + GM-CSF + trastuzumab (N=136) Control Arm: Placebo + GM-CSF + trastuzumab (N=139)	HLA-A2/A3+, HER2 low-expressing (IHC 1/2+), node-positive	DFS	The estimated 24-month DFS: 89.8% (vaccinated group) versus 83.8% (control group) (P= 0.18).
NCT00524277 (105, 106)	II	Adjuvant	HER2-derived peptide GP2	Vaccination Arm: GP2 + GM-CSF (N=89) Control Arm: GM-CSF alone (N=91)	HLA-A2+, HER2-expressing, node-positive or high-risk node-negative	DFS, RR	The estimated 5-year DFS: 88% (vaccinated group) versus 81% (control group) (P = 0.43); 100% (HER2 3+ vaccinated patients) versus 89% (HER2 3+ placebo patients) (P=0.03).
US Military Cancer Institute Clinical Trials Group Study I-04 (84)	I	Adjuvant	HER2-derived peptide GP2	Single arm: GP2 + GM-CSF of different doses (N=18)	HLA-A2+, HER2-expressing, node-negative	Safety, immune response	Immune response was induced in all the enrolled patients. Toxicities were minimal.
NCT00524277 (107)	II	Adjuvant	HER2-derived peptide AE37	Vaccination Arm: AE37 + GM-CSF (N=153) Control Arm: GM-CSF alone (N=145)	HLA-A2+, HER2-expressing, node-positive or high-risk node-negative	RR	RR at 25-month median follow-up: 12.4% (vaccinated group) versus 13.8% (control group) (P=0.70).
US Military Cancer Institute Clinical Trials Group Study I-03 (85)	I	Adjuvant	HER2-derived peptide AE37	Single arm: AE37 + GM-CSF of different doses (N=15)	HLA-A2+, HER2-expressing, node-negative	Safety, immune response	Immune response was induced in all the enrolled patients. Toxicities were minimal.
NCT00399529 (108)	II	Metastatic	HER2	Single arm: HER2 GM-CSF-secreting tumor cell vaccine + cyclophosphamide + trastuzumab (N=20)	Stage IV, HER2-expressing	Safety, CBR	CBR at 6 months and 1 year was 55% and 40%, respectively. Toxicities were minimal.
NCT00140738 (109)	I/II	Metastatic	HER2	Single arm: recombinant HER2 protein + AS15 (N=40)	Stage IV, HER2-expressing	Safety, CBR	Clinical activity was observed with 2/40 objective responses and prolonged stable disease for 10/40 patients. Immunization was associated with minimal toxicity.
NCT02061332 (110)	II	Neoadjuvant	HER2	Single arm: HER2 dendritic cell vaccine with different routes (N=27)	HER2-expressing DCIS or early invasive breast cancer	Safety, immune and clinical response	Vaccination by all injection routes was well tolerated. There was no significant difference in immune response rates by vaccination route.

CBR, clinical benefit rate; DCIS, ductal carcinoma in situ; DFS, disease-free survival; GM-CSF, granulocyte-macrophage colony-stimulating factor; HER2, human epidermal growth factor receptor 2; HLA, human leukocyte antigen; IHC, immunohistochemistry; RR, recurrence rate.

vaccination may lead to clinical benefits in patients with low HER2-expressing tumors, specifically TNBC.

4.1.4 Protein-Based Vaccine

As for the protein-based vaccine, in a phase 1 study, 29 patients with stage II-IV HER2-overexpressing breast and ovarian cancer were vaccinated with the intracellular domain of HER2 (amino acids 676-1255) plus GM-CSF (86). As a result, 89% of the patients developed HER2-specific T cell immunity, and HER2-specific antibody immunity was observed in 82% of the patients. Cellular immunity was maintained for 9-12 months after completion of immunization in over half of the patients.

In another phase 1 trial, another recombinant HER2 protein with adjuvant AS15 was administered to 61 trastuzumab-naive patients with stage II-III HER2-overexpressing breast cancer after surgical resection and adjuvant therapy (122). Association was found between the vaccination dose, the immunization schedule, and the prevalence of HER2-specific humoral responses. The HER2-specific immunity was maintained for over 5 years in 6/8 patients who received the highest dose of vaccination. In the metastatic setting, the same vaccine regimen was administered to 40 HER2-overexpressing metastatic breast cancer patients as first or second-line therapy following response to trastuzumab-based treatment as maintenance (109).

TABLE 3 | Major clinical trials on breast cancer vaccines targeting non-HER2-related antigens.

Clinical Trial Reference	Trial Phase	Setting	Targeted Tumor Antigen	Breast Cancer Subtype	Primary Objectives	Outcomes
NCT00003638 (101)	III	Metastatic	STn	Stage IV	TTP, OS	TTP: 3.4 months (treatment group) versus 3.0 months (control group) (P=0.35). Median OS: 23.1 months (treatment group) versus 22.3 months (control group) (P=0.91).
Miles DW, et al. (111)	II	Metastatic	STn	Stage IV	Safety, immune and clinical response	Clinical activity was observed with 2/18 minor responses and stable disease for 5/18 patients. Toxicities were minimal.
NCT00179309 (112)	II	Metastatic	Mucin-1, CEA	Stage IV	PFS	Median PFS: 7.9 months (vaccinated arm) versus 3.9 months (control arm) (P=0.09).
Svane IM, et al. (113)	II	Metastatic	p53	Stage IV HLA-A2+	Safety, immune and clinical response	Clinical activity was observed with 8/19 stable disease or minor regression with 11/19 progressive disease. Toxicities were minimal.
Domchek SM, et al. (114)	I	Metastatic	hTERT	Stage IV HLA-A2+	Immune response	High immune response was observed in 9/16 patients and non/low response was seen in 7/16 patients.
NCT00807781 (99)	I	Metastatic	Mammaglobin-A	Stage IV HLA-A2/A3+	Safety, immune response	No serious adverse events and a significant increase in the frequency of MAM-A specific $CD8^+$ T cells after vaccination (0.9% vs. 3.8%, P<0.001) was observed.
Avigan D, et al. (115)	I	Metastatic	Multiple antigens	Stage IV	Safety, clinical response	No significant toxicity or autoimmunity. Clinical activity was observed with 2/10 disease regression and 1/10 disease stabilization.

CEA, carcino-embryonic antigen; HLA, human leukocyte antigen; hTERT, human telomerase reverse transcriptase; OS, overall survival; PFS, progression-free survival; STn, Sialyl-Tn; TTP, time to progression.

The vaccine was well-tolerated and clinical activity was observed with 2 objective responses and prolonged stable disease for 10 patients.

4.1.5 Tumor Cell Vaccine

A HER2-positive tumor cell vaccine that was modified to secret GM-CSF has been evaluated in clinical trials. A total of 28 patients with metastatic breast cancer received the vaccine in combination with cyclophosphamide and doxorubicin to test the hypothesis that the two chemotherapy drugs can enhance vaccine-induced immunity (87). HER2-specific DTH and antibody responses were observed with low toxicity in most patients, and the optimal dose of chemotherapy was cyclophosphamide at $200mg/m^2$ and doxorubicin at $350mg/m^2$. The vaccine was administered to 20 HER2-positive metastatic breast cancer patients with a low dose of cyclophosphamide ($300mg/m^2$) and weekly trastuzumab in another single-arm clinical trial (108). Augmented HER2-specific immunity was also detected by enhanced DTH and $CD8^+$ T cell responses.

4.1.6 DNA-Based Vaccine

In a pilot phase 1 study, the DNA vaccine encoding a full-length signaling-deficient version of HER2 was injected together with GM-CSF and IL-2 to 8 patients with metastatic HER2-positive breast cancer who were also treated by trastuzumab (97). Treatment for 2 patients was discontinued after one vaccine cycle due to rapid tumor progression or disease-related complications. The vaccine was proven to be safe in the trial. Although no T cell responses towards HER2 were observed immediately after vaccination, a significant increase of MHC class-II restricted T cell responses to HER2 was detected at long-term follow-up.

Another multicenter phase 1 study using a DNA vaccine named V930 involved 33 patients with stage II-IV solid tumors expressing HER2 or CEA (98). V930 contained equal amounts of plasmids expressing the extracellular and transmembrane domains of HER2 and a plasmid expressing CEA fused to the B subunit of Escherichia coli heat-labile toxin. Patients were randomly assigned to receive V930 alone or V930 followed by V932, another adenovirus subtype-6 viral vector vaccine coding for the same antigens. In spite of good tolerance in both approaches, no measurable cell-mediated immune response to CEA or HER2 was either detected.

Currently, ongoing clinical trials (NCT00393783, NCT00436254) are evaluating the safety and immunologic activity of DNA-based vaccines encoding different versions of HER2-derived protein in treating HER2-overexpressing breast cancer.

4.1.7 DC-Based Vaccine

The efficacy of a DC-based vaccine towards HER2 was examined in patients with HER2-overexpressing ductal carcinoma *in situ* (DCIS) prior to surgical resection (123). The DC vaccine was loaded with HER2 MHC class-I and class-II peptides and activated *in vitro* with IFN-γ and bacterial lipopolysaccharides to produce cytokine IL-12. The 13 patients enrolled in the study showed high rates of HER2-specific sensitization for both IFN-γ-secreting $CD4^+$ T cells (85%) and $CD8^+$ T cells (80%) and induction of tumor-lytic antibodies. Interestingly, 7 patients demonstrated markedly decreased HER2 expression in surgical tumor specimens, suggesting a possible immunoediting process for HER2-expressing tumor cells. A follow-up trial in the neoadjuvant setting involving 54 HER2-positive patients with DCIS or early invasive breast cancer indicated that clinical and immune responses to the tumor did not vary significantly between different routes (intralesional versus intranodal versus intralesional-plus-intranodal) by which the same DC vaccine is administered (110).

In another clinical study, 7 patients with stage II-IV HER2-overexpressing breast cancer were injected with autologous DCs pulsed with a peptide derived from the intracellular domain of

HER2 after surgery and adjuvant therapy (124). HER2-specific antibodies were detected in six patients, and all of the seven participants were disease-free at a median follow-up of 5 years.

Clinical trials involving DC-based vaccines are moving forward currently. These trials use DCs pulsed with HER2-derived peptide E75 plus trastuzumab and vinorelbine (NCT00266110), and DCs pulsed with HER2 peptides 369-377 and 689-697 (NCT00923143).

4.2 Vaccines Targeting Non-HER2-Related Antigens

Besides HER2 or HER2-related peptides, non-HER2-related antigens are also studied in vaccination for breast cancer, indicating opportunities of using cancer vaccines to treat HER2-negative breast cancers. Mucins, human telomerase reverse transcriptase (hTERT), and p53 are some of the studied targets. Next, breast cancer vaccines targeting non-HER2-related antigens will be introduced in the order of their types.

4.2.1 Carbohydrate Antigen Vaccine—Sialyl-Tn

Theratope®, the STn-keyhole limpet hemocyanin (KLH) vaccine, is a synthetic STn conjugated to the KLH carrier protein. A significantly higher antibody level was observed in patients pretreated with a low dose of cyclophosphamide and vaccinated with STn-KLH in a randomized phase 2 trial (111). In the following double-blinded phase 3 study, a total of 1028 metastatic breast cancer patients across 126 centers in 10 countries were randomized to receive the STn-KLH vaccine or only KLH alone. Patients in both arms also received a low dose of cyclophosphamide (300 mg/m^2) to increase the immunogenicity of the vaccine. The primary endpoint was time to progression (TTP) and overall survival (OS). Despite the fact that significant antibody titers specific for STn were produced in patients treated with the vaccine, no significant improvement in TTP or OS was observed in the trial (101). The TTP was 3.4 months in the treatment group and 3.0 months in the control group (P=0.353). The median survival time was 23.1 months and 22.3 months (P=0.916), respectively, in the treatment and control groups. Lack of more strict eligibility criteria might be part of the reason for the negative results in that only 30%-40% of the breast cancer express STn, and no detection of STn expression was performed on the patients enrolled in the study (125). A subgroup analysis showed that the vaccinated arm had longer TTP and OS compared with the control arm in patients receiving endocrine therapy, indicating using the STn-KLH vaccine in combination with the endocrine therapy might improve clinical outcomes (126).

4.2.2 Peptide Vaccine—hTERT

The hTERT is nearly universally overexpressed in human cancers, including breast cancer, and it can be recognized by CD8$^+$ T cells. Nineteen patients with metastatic breast cancer received hTERT peptide vaccination, and high hTERT-specific CD8$^+$ T cell responses were induced after vaccination in 9 participants (114). An exploratory analysis revealed that the median OS was significantly longer in the patients who achieved an immune response to hTERT compared with those who did not. Trials evaluating hTERT vaccines are underway in the metastatic setting (NCT00573495 and NCT01660529) and the adjuvant setting (NCT02960594 and NCT00753415).

4.2.3 DNA-Based Vaccine—MUC-1, Mammoglobin-A

PANVAC is a recombinant poxviral-vector cancer vaccine consisting of a priming dose with recombinant vector and subsequent doses with recombinant fowlpox vector. Each vector encodes the transgenes for CEA and MUC-1 and transgenes for 3 human co-stimulatory molecules (B7.1, ICAM-1, and LFA3). In a phase 2 clinical trial, 48 patients with metastatic breast cancer of all subtypes were randomized to receive PANVAC plus docetaxel or docetaxel alone (112). A trend towards improvement in progression-free survival (PFS) was detected. The median PFS in the vaccinated arm was 7.9 months compared with 3.9 months in the control arm (P=0.09) at the median potential follow-up of 42.8 months.

Mammoglobin-A (MAM-A) is another breast cancer-associated antigen overexpressed in 40% to 80% of primary breast cancers (127). A phase I clinical trial of a MAM-A DNA vaccine was initiated to evaluate its safety and efficacy. In this study enrolling 14 patients with stable metastatic breast cancer, significant increase in the frequency of MAM-A specific CD8$^+$ T cells and no severe adverse events were observed after vaccination. Exploratory analysis also suggested an improved 6-month PFS rate in the vaccinated patients compared with those who met all eligibility criteria but were not vaccinated because of HLA phenotype (53% vs. 33%, P=0.011) (99).

4.2.4 DC-Based Vaccine—p53

The efficacy of a DC-based vaccine loaded with wild-type p53-derived peptide and stimulated with IL-4 and GM-CSF has been evaluated. This vaccine was administered in combination with low-dose IL-2 to 26 metastatic breast cancer patients in the study (113). Seven patients discontinued vaccination due to rapid disease progression or death. Eight of nineteen evaluable patients attained stable disease or minor regression while the rest of the patients had progressive disease, indicating the effect of p53-specific immune therapy. Surprisingly, the frequency of Treg cells was found to be almost doubled after vaccination in the analysis (128).

4.2.5 DC-Tumor Cell Fusion Vaccine—Multiple Antigens

A phase I clinical trial evaluated the fusion cell vaccination in patients with metastatic breast cancer and renal cancer (115). A total of 32 breast cancer patients were enrolled in the study and vaccine generation was successful in 16 patients. Among them, 6 patients were withdrawn from the study before receiving the vaccine due to significant disease progression. The rest of the patients were vaccinated with autologous fusion cells. As a result, no significant treatment-related toxicity or autoimmunity was observed. Two patients exhibited disease regression and 1 patient had disease stabilization.

5 COMBINATIONAL THERAPY OF BREAST CANCER VACCINE

ICB has reformed the treatment strategy for some solid tumors, including melanoma and non-small cell lung cancer. As for breast

cancer, ICB has already demonstrated its efficacy in treatment for metastatic TNBC (7). However, the addition of ICB to trastuzumab did not show a clinically significant improvement in PFS for HER2-positive metastatic breast cancer and was associated with more adverse events (60). Currently, an area of active investigation is combining the vaccine with ICB to overcome cancer tolerance. As mentioned previously, ICB makes the effector immune cells able to attack the tumor cells by blocking the inhibitory receptors such as PD-1/PD-L1 and CTLA-4 (59). Results of some preclinical studies indicate that tumor vaccines will also upregulate the expression level of inhibitory receptors on the cell surface when activating T cells (129). One underlying mechanism is that increased IFN-γ secreted by tumor-specific T cells can correspondingly upregulate the expression of PD-L1 on tumor cells and APCs, which is set initially to prevent over-amplification of the immune reactions occurring in the body (130). Therefore, the administration of ICB can probably relieve the immunosuppressive effect that attenuates anti-tumor immunity induced by vaccines. The combined use of breast cancer vaccine and ICB represents a promising strategy that may potentially enhance and prolong the duration of the immune response and ultimately lead to significant clinical benefits.

Additionally, applying cancer vaccines in combination with established therapies might also improve efficacy. Growing evidence has shown that some HER2-derived peptide vaccines may work synergistically when combined with anti-HER2 monoclonal antibodies (131). Studies indicates that chemotherapy and radiation therapy are associated with immunogenic cell death (132). Such immune response might help induce durable immune response when the therapies are applid in combination with cancer vaccines. Consistently, the effect of combining cancer vaccination with chemotherapy, targeted therapy, endocrine therapy, and even radiation therapy are also worth exploring (104, 133, 134).

6 CONCLUSION AND FUTURE PERSPECTIVE

Active vaccination therapy for breast cancer has several theoretical advantages compared to conventional chemotherapy and anti-HER2 immunotherapy *via* monoclonal antibodies: better tolerance, lower toxicity, and long-lasting immune response with tumor specificity (64). In addition, some vaccines can elicit immunity to tumors without any HER2 expression if the vaccine target is derived from non-HER2-related antigens.

However, clinical trials evaluating breast cancer vaccines have provided limited evidence of clinical benefits despite the successful induction of immune responses. It was demonstrated that the prognosis of patients who received vaccination is usually associated with the degree of immune responses (114). And in the initial E75 Phase 2 trial, immunity was noted to wane with time, and this corresponded with increased recurrences noted in the vaccine arm (103). Therefore a potential explanation for negative results to date is that the effective anti-tumor immunity stimulated by vaccines is not long-lasting enough to produce significant benefits in survival. The reason why the anti-tumor immune response fades so early may be attributed to the following factors: suboptimal vaccine formulations, the immune tolerance developed to specific tumor antigens, and the immune-suppressive microenvironment. Early trials have acknowledged that a HER2-specific MHC class-I peptide epitope vaccine alone elicits only short-lived $CD8^+$ T cell responses (135). In fact, as previously described, pre-existing immunity against HER2 has been detected in some patients. Nevertheless, the natural immune response is not strong enough to cultivate significant benefits due to immune tolerance. The immune tolerance that gradully builds in a long-term process might be a key factor to both the pre-existing immunity and the decreased immunity stimulated by vaccine. Hence, how to suppress immune tolerance for long and how to effectively exploit the natural immune response in the patients remains vital challenges to improve efficacy of breast cancer vaccines. Additionally, throughout the immunoediting process, the immunosuppressive effect will gradually outweigh the anti-tumor immunity as the tumor progresses. Even though the cancer vaccines manage to enhance the ability of the immune system to recognize specific tumor antigens, the effector immune cells such as CTLs might be incapable of efficiently eradicating the tumor cells in an immunosuppressive TME.

To overcome this issue, the optimal immunization dose and schedule, delivery routes, and choices of immunologic boosters need to be investigated. It was demonstrated that booster inoculations could maintain immunity, and those who received scheduled booster inoculations were less likely to recur (136). Moreover, the results of different peptide vaccines indicate that vaccine formulations should be tailored to the features of the tumor being targeted. Tolerance might be avoided by using subdominant epitopes with lower binding affinity against antigens with higher expression levels. For instance, E75, a dominant epitope of HER2, appears most effective in tumors expressing low degrees of HER2, while GP2, a subdominant epitope of HER2, shows more potential in HER2-overexpressing breast cancer in combination with trastuzumab. AE37, the MHC class-II targeted vaccine, shows the greatest efficacy in TNBC and may be helpful in all HLA subtypes (137).

The immune system maintains the delicate balance in our body to effectively remove non-self antigens and prevent autoimmune diseases at the same time. Despite the various obstacles that we encountered in the development of the breast cancer vaccine, the concept behind cancer vaccines that autologous immune systems can be mobilized to fight cancers has never been abandoned. Although the current results of clinical trials evaluating breast cancer vaccines are not satisfying, we believe novel strategies will eventually lead to improved efficacy as our understanding of cancer immunology deepens.

AUTHOR CONTRIBUTIONS

All authors wrote, read and approved the final manuscript.

FUNDING

Supported by grants from the National Natural Science Foundation of China (82072916), the 2018 Shanghai Youth

Excellent Academic Leader, the Fudan ZHUOSHI Project, Chinese Young Breast Experts Research project (CYBER-2021-A01).

ACKNOWLEDGMENTS

The figures are created with Biorender.com.

REFERENCES

1. Sung H, Ferlay J, Siegel RL, Laversanne M, Soerjomataram I, Jemal A, et al. Global Cancer Statistics 2020: GLOBOCAN Estimates of Incidence and Mortality Worldwide for 36 Cancers in 185 Countries. *CA Cancer J Clin* (2021) 71(3):209–49. doi: 10.3322/caac.21660
2. Loibl S, Poortmans P, Morrow M, Denkert C, Curigliano G. Breast Cancer. *Lancet* (2021) 397(10286):1750–69. doi: 10.1016/S0140-6736(20)32381-3
3. Savas P, Salgado R, Denkert C, Sotiriou C, Darcy PK, Smyth MJ, et al. Clinical Relevance of Host Immunity in Breast Cancer: From TILs to the Clinic. *Nat Rev Clin Oncol* (2016) 13:228–41. doi: 10.1038/nrclinonc.2015.215
4. Criscitiello C, Esposito A, Trapani D, Curigliano G. Prognostic and Predictive Value of Tumor Infiltrating Lymphocytes in Early Breast Cancer. *Cancer Treat Rev* (2016) 50:205–7. doi: 10.1016/j.ctrv.2016.09.019
5. Emens LA, Ascierto PA, Darcy PK, Demaria S, Eggermont AMM, Redmond WL, et al. Cancer Immunotherapy: Opportunities and Challenges in the Rapidly Evolving Clinical Landscape. *Eur J Cancer* (2017) 81:116–29. doi: 10.1016/j.ejca.2017.01.035
6. Lipson EJ, Forde PM, Hammers HJ, Emens LA, Taube JM, Topalian SL. Antagonists of PD-1 and PD-L1 in Cancer Treatment. *Semin Oncol* (2015) 42:587–600. doi: 10.1053/j.seminoncol.2015.05.013
7. Schmid P, Adams S, Rugo HS, Schneeweiss A, Barrios CH, Iwata H, et al. Atezolizumab and Nab-Paclitaxel in Advanced Triple-Negative Breast Cancer. *N Engl J Med* (2018) 379:2108–21. doi: 10.1056/NEJMoa1809615
8. Emens LA. Breast Cancer Immunobiology Driving Immunotherapy: Vaccines and Immune Checkpoint Blockade. *Expert Rev Anticancer Ther* (2012) 12:1597–611. doi: 10.1586/era.12.147
9. Emens LA. Breast Cancer Immunotherapy: Facts and Hopes. *Clin Cancer Res* (2018) 24:511–20. doi: 10.1158/1078-0432.CCR-16-3001
10. Humphries C. Adoptive Cell Therapy: Honing That Killer Instinct. *Nature* (2013) 504:S13–15. doi: 10.1038/504S13a
11. Weiner LM. Building Better Magic Bullets–Improving Unconjugated Monoclonal Antibody Therapy for Cancer. *Nat Rev Cancer* (2007) 7:701–6. doi: 10.1038/nrc2209
12. Coulie PG, Van den Eynde BJ, van der Bruggen P, Boon T. Tumour Antigens Recognized by T Lymphocytes: At the Core of Cancer Immunotherapy. *Nat Rev Cancer* (2014) 14:135–46. doi: 10.1038/nrc3670
13. van der Burg SH. Correlates of Immune and Clinical Activity of Novel Cancer Vaccines. *Semin Immunol* (2018) 39:119–36. doi: 10.1016/j.smim.2018.04.001
14. Schreiber RD, Old LJ, Smyth MJ. Cancer Immunoediting: Integrating Immunity's Roles in Cancer Suppression and Promotion. *Science* (2011) 331:1565–70. doi: 10.1126/science.1203486
15. Riaz N, Havel JJ, Makarov V, Desrichard A, Urba WJ, Sims JS, et al. Et Al: Tumor and Microenvironment Evolution During Immunotherapy With Nivolumab. *Cell* (2017) 171:934–49.e916. doi: 10.1016/j.cell.2017.09.028
16. Chang CC, Pirozzi G, Wen SH, Chung IH, Chiu BL, Errico S, et al. Multiple Structural and Epigenetic Defects in the Human Leukocyte Antigen Class I Antigen Presentation Pathway in a Recurrent Metastatic Melanoma Following Immunotherapy. *J Biol Chem* (2015) 290:26562–75. doi: 10.1074/jbc.M115.676130
17. Ribas A. Adaptive Immune Resistance: How Cancer Protects From Immune Attack. *Cancer Discov* (2015) 5:915–9. doi: 10.1158/2159-8290.CD-15-0563
18. Mittal D, Gubin MM, Schreiber RD, Smyth MJ. New Insights Into Cancer Immunoediting and Its Three Component Phases–Elimination, Equilibrium and Escape. *Curr Opin Immunol* (2014) 27:16–25. doi: 10.1016/j.coi.2014.01.004
19. O'Donnell JS, Teng MWL, Smyth MJ. Cancer Immunoediting and Resistance to T Cell-Based Immunotherapy. *Nat Rev Clin Oncol* (2019) 16:151–67. doi: 10.1038/s41571-018-0142-8
20. Teng MW, Galon J, Fridman WH, Smyth MJ. From Mice to Humans: Developments in Cancer Immunoediting. *J Clin Invest* (2015) 125:3338–46. doi: 10.1172/JCI80004
21. Matsushita H, Vesely MD, Koboldt DC, Rickert CG, Uppaluri R, Magrini VJ, et al. Cancer Exome Analysis Reveals a T-Cell-Dependent Mechanism of Cancer Immunoediting. *Nature* (2012) 482:400–4. doi: 10.1038/nature10755
22. Linnemann C, van Buuren MM, Bies L, Verdegaal EM, Schotte R, Calis JJ, et al. High-Throughput Epitope Discovery Reveals Frequent Recognition of Neo-Antigens by CD4+ T Cells in Human Melanoma. *Nat Med* (2015) 21:81–5. doi: 10.1038/nm.3773
23. Schumacher TN, Schreiber RD. Neoantigens in Cancer Immunotherapy. *Science* (2015) 348:69–74. doi: 10.1126/science.aaa4971
24. Balachandran VP, Luksza M, Zhao JN, Makarov V, Moral JA, Remark R, et al. Identification of Unique Neoantigen Qualities in Long-Term Survivors of Pancreatic Cancer. *Nature* (2017) 551:512–6. doi: 10.1038/nature24462
25. Hollingsworth RE, Jansen K. Turning the Corner on Therapeutic Cancer Vaccines. *NPJ Vaccines* (2019) 4:7. doi: 10.1038/s41541-019-0103-y
26. Lee CH, Yelensky R, Jooss K, Chan TA. Update on Tumor Neoantigens and Their Utility: Why It Is Good to Be Different. *Trends Immunol* (2018) 39:536–48. doi: 10.1016/j.it.2018.04.005
27. Ilyas S, Yang JC. Landscape of Tumor Antigens in T Cell Immunotherapy. *J Immunol* (2015) 195:5117–22. doi: 10.4049/jimmunol.1501657
28. Benvenuto M, Focaccetti C, Izzi V, Masuelli L, Modesti A, Bei R. Tumor Antigens Heterogeneity and Immune Response-Targeting Neoantigens in Breast Cancer. *Semin Cancer Biol* (2019) 72:65–75. doi: 10.1016/j.semcancer.2019.10.023
29. Hammerl D, Smid M, Timmermans AM, Sleijfer S, Martens JWM, Debets R. Breast Cancer Genomics and Immuno-Oncological Markers to Guide Immune Therapies. *Semin Cancer Biol* (2018) 52:178–88. doi: 10.1016/j.semcancer.2017.11.003
30. Solinas C, Aiello M, Migliori E, Willard-Gallo K, Emens LA. Breast Cancer Vaccines: Heeding the Lessons of the Past to Guide a Path Forward. *Cancer Treat Rev* (2020) 84:101947. doi: 10.1016/j.ctrv.2019.101947
31. Disis ML, Gooley TA, Rinn K, Davis D, Piepkorn M, Cheever MA, et al. Generation of T-Cell Immunity to the HER-2/Neu Protein After Active Immunization With HER-2/Neu Peptide-Based Vaccines. *J Clin Oncol* (2002) 20:2624–32. doi: 10.1200/JCO.2002.06.171
32. Disis ML, Knutson KL, Schiffman K, Rinn K, McNeel DG. Pre-Existent Immunity to the HER-2/Neu Oncogenic Protein in Patients With HER-2/Neu Overexpressing Breast and Ovarian Cancer. *Breast Cancer Res Treat* (2000) 62:245–52. doi: 10.1023/A:1006438507898
33. Disis ML CE, McLaughlin G, Murphy AE, Chen W, Groner B, Jeschke M, et al. Existent T-Cell and Antibody Immunity to HER-2/Neu Protein in Patients With Breast Cancer. *Cancer Res* (1994) 54(1):16–20.
34. Rabinovich GA, Gabrilovich D, Sotomayor EM. Immunosuppressive Strategies That are Mediated by Tumor Cells. *Annu Rev Immunol* (2007) 25:267–96. doi: 10.1146/annurev.immunol.25.022106.141609
35. DeNardo DG, Coussens LM. Inflammation and Breast Cancer. Balancing Immune Response: Crosstalk Between Adaptive and Innate Immune Cells During Breast Cancer Progression. *Breast Cancer Res* (2007) 9:212. doi: 10.1186/bcr1746
36. Liyanage UK, Moore TT, Joo HG, Tanaka Y, Herrmann V, Doherty G, et al. Prevalence of Regulatory T Cells is Increased in Peripheral Blood and Tumor Microenvironment of Patients With Pancreas or Breast Adenocarcinoma. *J Immunol* (2002) 169:2756–61. doi: 10.4049/jimmunol.169.5.2756
37. Gabrilovich DI. Myeloid-Derived Suppressor Cells. *Cancer Immunol Res* (2017) 5:3–8. doi: 10.1158/2326-6066.CIR-16-0297
38. Qian BZ, Pollard JW. Macrophage Diversity Enhances Tumor Progression and Metastasis. *Cell* (2010) 141:39–51. doi: 10.1016/j.cell.2010.03.014
39. Zou W. Regulatory T Cells, Tumour Immunity and Immunotherapy. *Nat Rev Immunol* (2006) 6:295–307. doi: 10.1038/nri1806
40. Tanaka A, Sakaguchi S. Regulatory T Cells in Cancer Immunotherapy. *Cell Res* (2017) 27:109–18. doi: 10.1038/cr.2016.151
41. Nakamura R, Sakakibara M, Nagashima T, Sangai T, Arai M, Fujimori T, et al. Accumulation of Regulatory T Cells in Sentinel Lymph Nodes is a

Prognostic Predictor in Patients With Node-Negative Breast Cancer. *Eur J Cancer* (2009) 45:2123–31. doi: 10.1016/j.ejca.2009.03.024
42. Gentles AJ, Newman AM, Liu CL, Bratman SV, Feng W, Kim D, et al. The Prognostic Landscape of Genes and Infiltrating Immune Cells Across Human Cancers. *Nat Med* (2015) 21:938–45. doi: 10.1038/nm.3909
43. Coffelt SB, Wellenstein MD, de Visser KE. Neutrophils in Cancer: Neutral No More. *Nat Rev Cancer* (2016) 16:431–46. doi: 10.1038/nrc.2016.52
44. DeNardo DG, Brennan DJ, Rexhepaj E, Ruffell B, Shiao SL, Madden SF, et al. Leukocyte Complexity Predicts Breast Cancer Survival and Functionally Regulates Response to Chemotherapy. *Cancer Discov* (2011) 1:54–67. doi: 10.1158/2159-8274.CD-10-0028
45. Bauer CA, Kim EY, Marangoni F, Carrizosa E, Claudio NM, Mempel TR. Dynamic Treg Interactions With Intratumoral APCs Promote Local CTL Dysfunction. *J Clin Invest* (2014) 124:2425–40. doi: 10.1172/JCI66375
46. Chinen T, Kannan AK, Levine AG, Fan X, Klein U, Zheng Y, et al. An Essential Role for the IL-2 Receptor in Treg Cell Function. *Nat Immunol* (2016) 17:1322–33. doi: 10.1038/ni.3540
47. Dranoff G. Cytokines in Cancer Pathogenesis and Cancer Therapy. *Nat Rev Cancer* (2004) 4:11–22. doi: 10.1038/nrc1252
48. Ghiringhelli F, Puig PE, Roux S, Parcellier A, Schmitt E, Solary E, et al. Tumor Cells Convert Immature Myeloid Dendritic Cells Into TGF-Beta-Secreting Cells Inducing CD4+CD25+ Regulatory T Cell Proliferation. *J Exp Med* (2005) 202:919–29. doi: 10.1084/jem.20050463
49. Kobie JJ, Shah PR, Yang L, Rebhahn JA, Fowell DJ, Mosmann TR. T Regulatory and Primed Uncommitted CD4 T Cells Express CD73, Which Suppresses Effector CD4 T Cells by Converting 5'-Adenosine Monophosphate to Adenosine. *J Immunol* (2006) 177:6780–6. doi: 10.4049/jimmunol.177.10.6780
50. Allard B, Beavis PA, Darcy PK, Stagg J. Immunosuppressive Activities of Adenosine in Cancer. *Curr Opin Pharmacol* (2016) 29:7–16. doi: 10.1016/j.coph.2016.04.001
51. Schwartz M, Zhang Y, Rosenblatt JD. B Cell Regulation of the Anti-Tumor Response and Role in Carcinogenesis. *J Immunother Cancer* (2016) 4:40. doi: 10.1186/s40425-016-0145-x
52. Sarvaria A, Madrigal JA, Saudemont A. B Cell Regulation in Cancer and Anti-Tumor Immunity. *Cell Mol Immunol* (2017) 14:662–74. doi: 10.1038/cmi.2017.35
53. Ruffell B, Chang-Strachan D, Chan V, Rosenbusch A, Ho CM, Pryer N, et al. Macrophage IL-10 Blocks CD8+ T Cell-Dependent Responses to Chemotherapy by Suppressing IL-12 Expression in Intratumoral Dendritic Cells. *Cancer Cell* (2014) 26:623–37. doi: 10.1016/j.ccell.2014.09.006
54. Freeman GJ, Long AJ, Iwai Y, Bourque K, Chernova T, Nishimura H, et al. Et Al: Engagement of the PD-1 Immunoinhibitory Receptor by a Novel B7 Family Member Leads to Negative Regulation of Lymphocyte Activation. *J Exp Med* (2000) 192:1027–34. doi: 10.1084/jem.192.7.1027
55. Zou W, Chen L. Inhibitory B7-Family Molecules in the Tumour Microenvironment. *Nat Rev Immunol* (2008) 8:467–77. doi: 10.1038/nri2326
56. Zou W, Wolchok JD, Chen L. PD-L1 (B7-H1) and PD-1 Pathway Blockade for Cancer Therapy: Mechanisms, Response Biomarkers, and Combinations. *Sci Transl Med* (2016) 8:328rv324. doi: 10.1126/scitranslmed.aad7118
57. Linsley PS, Bradshaw J, Greene J, Peach R, Bennett KL, Mittler RS. Intracellular Trafficking of CTLA-4 and Focal Localization Towards Sites of TCR Engagement. *Immunity* (1996) 4:535–43. doi: 10.1016/S1074-7613(00)80480-X
58. Buchbinder E, Hodi FS. Cytotoxic T Lymphocyte Antigen-4 and Immune Checkpoint Blockade. *J Clin Invest* (2015) 125:3377–83. doi: 10.1172/JCI80012
59. Pardoll DM. The Blockade of Immune Checkpoints in Cancer Immunotherapy. *Nat Rev Cancer* (2012) 12:252–64. doi: 10.1038/nrc3239
60. Emens LA, Esteva FJ, Beresford M, Saura C, De Laurentiis M, Kim S-B, et al. Trastuzumab Emtansine Plus Atezolizumab Versus Trastuzumab Emtansine Plus Placebo in Previously Treated, HER2-Positive Advanced Breast Cancer (KATE2): A Phase 2, Multicentre, Randomised, Double-Blind Trial. *Lancet Oncol* (2020) 21:1283–95. doi: 10.1016/S1470-2045(20)30465-4
61. Ladjemi MZ, Jacot W, Chardes T, Pelegrin A, Navarro-Teulon I. Anti-HER2 Vaccines: New Prospects for Breast Cancer Therapy. *Cancer Immunol Immunother* (2010) 59:1295–312. doi: 10.1007/s00262-010-0869-2
62. Butterfield LH. Cancer Vaccines. *BMJ* (2015) 350:h988. doi: 10.1136/bmj.h988
63. Shumway NM, Ibrahim N, Ponniah S, Peoples GE, Murray JL. Therapeutic Breast Cancer Vaccines: A New Strategy for Early-Stage Disease. *BioDrugs* (2009) 23:277–87. doi: 10.2165/11313490-000000000-00000
64. Al-Awadhi A, Lee Murray J, Ibrahim NK. Developing Anti-HER2 Vaccines: Breast Cancer Experience. *Int J Cancer* (2018) 143:2126–32. doi: 10.1002/ijc.31551
65. Rosalia RA, Quakkelaar ED, Redeker A, Khan S, Camps M, Drijfhout JW, et al. Dendritic Cells Process Synthetic Long Peptides Better Than Whole Protein, Improving Antigen Presentation and T-Cell Activation. *Eur J Immunol* (2013) 43:2554–65. doi: 10.1002/eji.201343324
66. Milani A, Sangiolo D, Montemurro F, Aglietta M, Valabrega G. Active Immunotherapy in HER2 Overexpressing Breast Cancer: Current Status and Future Perspectives. *Ann Oncol* (2013) 24:1740–8. doi: 10.1093/annonc/mdt133
67. Reddish MA, Jackson L, Koganty RR, Qiu D, Hong W, Longenecker BM. Specificities of Anti-Sialyl-Tn and Anti-Tn Monoclonal Antibodies Generated Using Novel Clustered Synthetic Glycopeptide Epitopes. *Glycoconj J* (1997) 14:549–60. doi: 10.1023/A:1018576224062
68. Holmberg LA, Sandmaier BM. Vaccination With Theratope (STn-KLH) as Treatment for Breast Cancer. *Expert Rev Vaccines* (2004) 3:655–63. doi: 10.1586/14760584.3.6.655
69. Dols A, Smith JW2nd, Meijer SL, Fox BA, Hu HM, Walker E, et al. Vaccination of Women With Metastatic Breast Cancer, Using a Costimulatory Gene (CD80)-Modified, HLA-A2-Matched, Allogeneic, Breast Cancer Cell Line: Clinical and Immunological Results. *Hum Gene Ther* (2003) 14:1117–23. doi: 10.1089/104303403322124828
70. Dranoff G, Jaffee E, Lazenby A, Golumbek P, Levitsky H, Brose K, et al. Vaccination With Irradiated Tumor Cells Engineered to Secrete Murine Granulocyte-Macrophage Colony-Stimulating Factor Stimulates Potent, Specific, and Long-Lasting Anti-Tumor Immunity. *Proc Natl Acad Sci U S A* (1993) 90:3539–43. doi: 10.1073/pnas.90.8.3539
71. Yang B, Jeang J, Yang A, Wu TC, Hung CF. DNA Vaccine for Cancer Immunotherapy. *Hum Vaccin Immunother* (2014) 10:3153–64. doi: 10.4161/21645515.2014.980686
72. Lentz BR. PEG as a Tool to Gain Insight Into Membrane Fusion. *Eur Biophys J* (2007) 36:315–26. doi: 10.1007/s00249-006-0097-z
73. Cheong SC, Blangenois I, Franssen JD, Servais C, Phan V, Trakatelli M, et al. Generation of Cell Hybrids. *Via Fusogenic Cell Line J Gene Med* (2006) 8:919–28. doi: 10.1002/jgm.906
74. Kanduser M, Usaj M. Cell Electrofusion: Past and Future Perspectives for Antibody Production and Cancer Cell Vaccines. *Expert Opin Drug Delivery* (2014) 11:1885–98. doi: 10.1517/17425247.2014.938632
75. Lee WT. Dendritic Cell-Tumor Cell Fusion Vaccines. *Adv Exp Med Biol* (2011) 713:177–86. doi: 10.1007/978-94-007-0763-4_11
76. Melero I, Gaudernack G, Gerritsen W, Huber C, Parmiani G, Scholl S, et al. Therapeutic Vaccines for Cancer: An Overview of Clinical Trials. *Nat Rev Clin Oncol* (2014) 11:509–24. doi: 10.1038/nrclinonc.2014.111
77. Clements CJ, Griffiths E. The Global Impact of Vaccines Containing Aluminium Adjuvants. *Vaccine* (2002) 20:S24–33. doi: 10.1016/S0264-410X(02)00168-8
78. Jger E, Ringhoffer M, Dienes HP, Arand M, Karbach J, Jger D, et al. Granulocyte-Macrophage-Colony-Stimulating Factor Enhances Immune Responses to Melanoma-Associated Peptides *In Vivo*. *Int J Cancer* (1996) 67:54–62. doi: 10.1002/(SICI)1097-0215(19960703)67:1<54::AID-IJC11>3.0.CO;2-C
79. Hailemichael Y, Dai Z, Jaffarzad N, Ye Y, Medina MA, Huang XF, et al. Persistent Antigen at Vaccination Sites Induces Tumor-Specific CD8(+) T Cell Sequestration, Dysfunction and Deletion. *Nat Med* (2013) 19:465–72. doi: 10.1038/nm.3105
80. Grun JL, Maurer PH. Different T Helper Cell Subsets Elicited in Mice Utilizing Two Different Adjuvant Vehicles: The Role of Endogenous Interleukin 1 in Proliferative Responses. *Cell Immunol* (1989) 121:134–45. doi: 10.1016/0008-8749(89)90011-7
81. Hercus TR, Thomas D, Guthridge MA, Ekert PG, King-Scott J, Parker MW, et al. The Granulocyte-Macrophage Colony-Stimulating Factor Receptor: Linking Its Structure to Cell Signaling and its Role in Disease. *Blood* (2009) 114:1289–98. doi: 10.1182/blood-2008-12-164004

82. Yan WL, Shen KY, Tien CY, Chen YA, Liu SJ. Recent Progress in GM-CSF-Based Cancer Immunotherapy. *Immunotherapy* (2017) 9:347–60. doi: 10.2217/imt-2016-0141
83. Peoples GE, Gurney JM, Hueman MT, Woll MM, Ryan GB, Storrer CE, et al. Clinical Trial Results of a HER2/neu (E75) Vaccine to Prevent Recurrence in High-Risk Breast Cancer Patients. *J Clin Oncol* (2005) 23:7536–45. doi: 10.1200/JCO.2005.03.047
84. Carmichael MG, Benavides LC, Holmes JP, Gates JD, Mittendorf EA, Ponniah S, et al. Results of the First Phase 1 Clinical Trial of the HER-2/Neu Peptide (GP2) Vaccine in Disease-Free Breast Cancer Patients: United States Military Cancer Institute Clinical Trials Group Study I-04. *Cancer* (2010) 116:292–301. doi: 10.1002/cncr.24756
85. Holmes JP, Benavides LC, Gates JD, Carmichael MG, Hueman MT, Mittendorf EA, et al. Results of the First Phase I Clinical Trial of the Novel II-Key Hybrid Preventive HER-2/Neu Peptide (AE37) Vaccine. *J Clin Oncol* (2008) 26:3426–33. doi: 10.1200/JCO.2007.15.7842
86. Disis ML, Schiffman K, Guthrie K, Salazar LG, Knutson KL, Goodell V, et al. Effect of Dose on Immune Response in Patients Vaccinated With an Her-2/Neu Intracellular Domain Protein–Based Vaccine. *J Clin Oncol* (2004) 22:1916–25. doi: 10.1200/JCO.2004.09.005
87. Emens LA, Asquith JM, Leatherman JM, Kobrin BJ, Petrik S, Laiko M, et al. Timed Sequential Treatment With Cyclophosphamide, Doxorubicin, and an Allogeneic Granulocyte-Macrophage Colony-Stimulating Factor-Secreting Breast Tumor Vaccine: A Chemotherapy Dose-Ranging Factorial Study of Safety and Immune Activation. *J Clin Oncol* (2009) 27:5911–8. doi: 10.1200/JCO.2009.23.3494
88. Weber J, Sondak VK, Scotland R, Phillip R, Wang F, Rubio V, et al. Granulocyte-Macrophage-Colony-Stimulating Factor Added to a Multipeptide Vaccine for Resected Stage II Melanoma. *Cancer* (2003) 97:186–200. doi: 10.1002/cncr.11045
89. Serafini P, Carbley R, Noonan KA, Tan G, Bronte V, Borrello I. High-Dose Granulocyte-Macrophage Colony-Stimulating Factor-Producing Vaccines Impair the Immune Response Through the Recruitment of Myeloid Suppressor Cells. *Cancer Res* (2004) 64:6337–43. doi: 10.1158/0008-5472.CAN-04-0757
90. Slingluff CL Jr, Petroni GR, Olson WC, Smolkin ME, Ross MI, Haas NB, et al. Effect of Granulocyte/Macrophage Colony-Stimulating Factor on Circulating CD8+ and CD4+ T-Cell Responses to a Multipeptide Melanoma Vaccine: Outcome of a Multicenter Randomized Trial. *Clin Cancer Res* (2009) 15:7036–44. doi: 10.1158/1078-0432.CCR-09-1544
91. van den Boorn JG, Barchet W, Hartmann G. Nucleic Acid Adjuvants: Toward an Educated Vaccine. *Adv Immunol* (2012) 114:1–32. doi: 10.1016/B978-0-12-396548-6.00001-9
92. Liu W, Tang H, Li L, Wang X, Yu Z, Li J. Peptide-Based Therapeutic Cancer Vaccine: Current Trends in Clinical Application. *Cell Prolif* (2021) 54: e13025. doi: 10.1111/cpr.13025
93. Paston SJ, Brentville VA, Symonds P, Durrant LG. Cancer Vaccines, Adjuvants, and Delivery Systems. *Front Immunol* (2021) 12:627932. doi: 10.3389/fimmu.2021.627932
94. Bos R, van Duikeren S, van Hall T, Lauwen MM, Parrington M, Berinstein NL, et al. Characterization of Antigen-Specific Immune Responses Induced by Canarypox Virus Vaccines. *J Immunol* (2007) 179:6115–22. doi: 10.4049/jimmunol.179.9.6115
95. van den Hende M, van Poelgeest MI, van der Hulst JM, de Jong J, Drijfhout JW, Fleuren GJ, et al. Skin Reactions to Human Papillomavirus (HPV) 16 Specific Antigens Intradermally Injected in Healthy Subjects and Patients With Cervical Neoplasia. *Int J Cancer* (2008) 123:146–52. doi: 10.1002/ijc.23502
96. de Vos van Steenwijk PJ, van Poelgeest MI, Ramwadhdoebe TH, Lowik MJ, Berends-van der Meer DM, van der Minne CE, et al. The Long-Term Immune Response After HPV16 Peptide Vaccination in Women With Low-Grade Pre-Malignant Disorders of the Uterine Cervix: A Placebo-Controlled Phase II Study. *Cancer Immunol Immunother* (2014) 63:147–60. doi: 10.1007/s00262-013-1499-2
97. Norell H, Poschke I, Charo J, Wei WZ, Erskine C, Piechocki MP, et al. Vaccination With a Plasmid DNA Encoding HER-2/Neu Together With Low Doses of GM-CSF and IL-2 in Patients With Metastatic Breast Carcinoma: A Pilot Clinical Trial. *J Transl Med* (2010) 8:53. doi: 10.1186/1479-5876-8-53
98. Diaz CM, Chiappori A, Aurisicchio L, Bagchi A, Clark J, Dubey S, et al. Phase 1 Studies of the Safety and Immunogenicity of Electroporated HER2/CEA DNA Vaccine Followed by Adenoviral Boost Immunization in Patients With Solid Tumors. *J Transl Med* (2013) 11:62. doi: 10.1186/1479-5876-11-62
99. Tiriveedhi V, Tucker N, Herndon J, Li L, Sturmoski M, Ellis M, et al. Safety and Preliminary Evidence of Biologic Efficacy of a Mammaglobin-a DNA Vaccine in Patients With Stable Metastatic Breast Cancer. *Clin Cancer Res* (2014) 20:5964–75. doi: 10.1158/1078-0432.CCR-14-0059
100. Sandoval F, Terme M, Nizard M, Badoual C, Bureau MF, Freyburger L, et al. Mucosal Imprinting of Vaccine-Induced CD8(+) T Cells is Crucial to Inhibit the Growth of Mucosal Tumors. *Sci Transl Med* (2013) 5:172ra120. doi: 10.1126/scitranslmed.3004888
101. Miles D, Roche H, Martin M, Perren TJ, Cameron DA, Glaspy J, et al. Phase III Multicenter Clinical Trial of the Sialyl-TN (STn)-Keyhole Limpet Hemocyanin (KLH) Vaccine for Metastatic Breast Cancer. *Oncologist* (2011) 16:1092–100. doi: 10.1634/theoncologist.2010-0307
102. Mittendorf EA, Lu B, Melisko M, Price Hiller J, Bondarenko I, Brunt AM, et al. Efficacy and Safety Analysis of Nelipepimut-S Vaccine to Prevent Breast Cancer Recurrence: A Randomized, Multicenter, Phase III Clinical Trial. *Clin Cancer Res* (2019) 25:4248–54. doi: 10.1158/1078-0432.CCR-18-2867
103. Mittendorf EA, Clifton GT, Holmes JP, Schneble E, van Echo D, Ponniah S, et al. Final Report of the Phase I/II Clinical Trial of the E75 (Nelipepimut-S) Vaccine With Booster Inoculations to Prevent Disease Recurrence in High-Risk Breast Cancer Patients. *Ann Oncol* (2014) 25:1735–42. doi: 10.1093/annonc/mdu211
104. Clifton GT, Hale D, Vreeland TJ, Hickerson AT, Litton JK, Alatrash G, et al. Results of a Randomized Phase IIb Trial of Nelipepimut-S + Trastuzumab Versus Trastuzumab to Prevent Recurrences in Patients With High-Risk HER2 Low-Expressing Breast Cancer. *Clin Cancer Res* (2020) 26:2515–23. doi: 10.1158/1078-0432.CCR-19-2741
105. Mittendorf EA, Ardavanis A, Litton JK, Shumway NM, Hale DF, Murray JL, et al. Primary Analysis of a Prospective, Randomized, Single-Blinded Phase II Trial Evaluating the HER2 Peptide GP2 Vaccine in Breast Cancer Patients to Prevent Recurrence. *Oncotarget* (2016) 7:66192–201. doi: 10.18632/oncotarget.11751
106. Patel SS, McWilliams DB, Patel MS, Fischette CT, Thompson J, Daugherty FJ. "Five Year Median Follow-Up Data From a Prospective, Randomized, Placebo-Controlled, Single-Blinded, Multicenter, Phase IIb Study Evaluating the Reduction of Recurrences Using HER2/neu Peptide GP2 + GM-CSF vs. GM-CSF Alone After Adjuvant Trastuzumab in HER2 Positive Women With Operable Breast Cancersnehal". In: *In San Antonio Breast Cancer Symposium*, vol. PS10-23. San Antonio, TX, United States (2020). Greenwich LifeSciences p. PS10–23.
107. Mittendorf EA, Ardavanis A, Symanowski J, Murray JL, Shumway NM, Litton JK, et al. Primary Analysis of a Prospective, Randomized, Single-Blinded Phase II Trial Evaluating the HER2 Peptide AE37 Vaccine in Breast Cancer Patients to Prevent Recurrence. *Ann Oncol* (2016) 27:1241–8. doi: 10.1093/annonc/mdw150
108. Chen G, Gupta R, Petrik S, Laiko M, Leatherman JM, Asquith JM, et al. A Feasibility Study of Cyclophosphamide, Trastuzumab, and an Allogeneic GM-CSF-Secreting Breast Tumor Vaccine for HER2+ Metastatic Breast Cancer. *Cancer Immunol Res* (2014) 2:949–61. doi: 10.1158/2326-6066.CIR-14-0058
109. Curigliano G, Romieu G, Campone M, Dorval T, Duck L, Canon JL, et al. A Phase I/II Trial of the Safety and Clinical Activity of a HER2-Protein Based Immunotherapeutic for Treating Women With HER2-Positive Metastatic Breast Cancer. *Breast Cancer Res Treat* (2016) 156:301–10. doi: 10.1007/s10549-016-3750-y
110. Lowenfeld L, Mick R, Datta J, Xu S, Fitzpatrick E, Fisher CS, et al. Dendritic Cell Vaccination Enhances Immune Responses and Induces Regression of HER2(pos) DCIS Independent of Route: Results of Randomized Selection Design Trial. *Clin Cancer Res* (2017) 23:2961–71. doi: 10.1158/1078-0432.CCR-16-1924
111. Miles DW, Towlson KE, Graham R, Reddish M, Longenecker BM, Taylor-Papadimitriou J, et al. A Randomised Phase II Study of Sialyl-Tn and DETOX-B Adjuvant With or Without Cyclophosphamide Pretreatment for the Active Specific Immunotherapy of Breast Cancer. *Br J Cancer* (1996) 74:1292–6. doi: 10.1038/bjc.1996.532

112. Heery CR, Ibrahim NK, Arlen PM, Mohebtash M, Murray JL, Koenig K, et al. Docetaxel Alone or in Combination With a Therapeutic Cancer Vaccine (PANVAC) in Patients With Metastatic Breast Cancer: A Randomized Clinical Trial. *JAMA Oncol* (2015) 1:1087–95. doi: 10.1001/jamaoncol.2015.2736
113. Svane IM, Pedersen AE, Johansen JS, Johnsen HE, Nielsen D, Kamby C, et al. Vaccination With P53 Peptide-Pulsed Dendritic Cells is Associated With Disease Stabilization in Patients With P53 Expressing Advanced Breast Cancer; Monitoring of Serum YKL-40 and IL-6 as Response Biomarkers. *Cancer Immunol Immunother* (2007) 56:1485–99. doi: 10.1007/s00262-007-0293-4
114. Domchek SM, Recio A, Mick R, Clark CE, Carpenter EL, Fox KR, et al. Telomerase-Specific T-Cell Immunity in Breast Cancer: Effect of Vaccination on Tumor Immunosurveillance. *Cancer Res* (2007) 67:10546–55. doi: 10.1158/0008-5472.CAN-07-2765
115. Avigan D, Vasir B, Gong J, Borges V, Wu Z, Uhl L, et al. Fusion Cell Vaccination of Patients With Metastatic Breast and Renal Cancer Induces Immunological and Clinical Responses. *Clin Cancer Res* (2004) 10:4699–708. doi: 10.1158/1078-0432.CCR-04-0347
116. Peoples GE, Holmes JP, Hueman MT, Mittendorf EA, Amin A, Khoo S, et al. Combined Clinical Trial Results of a HER2/neu (E75) Vaccine for the Prevention of Recurrence in High-Risk Breast Cancer Patients: U.S. Military Cancer Institute Clinical Trials Group Study I-01 and I-02. *Clin Cancer Res* (2008) 14:797–803. doi: 10.1158/1078-0432.CCR-07-1448
117. Benavides LC, Gates JD, Carmichael MG, Patil R, Holmes JP, Hueman MT, et al. The Impact of HER2/neu Expression Level on Response to the E75 Vaccine: From U.S. Military Cancer Institute Clinical Trials Group Study I-01 and I-02. *Clin Cancer Res* (2009) 15:2895–904. doi: 10.1158/1078-0432.CCR-08-1126
118. Mittendorf EA, Storrer CE, Foley RJ, Harris K, Jama Y, Shriver CD, et al. Evaluation of the HER2/neu-Derived Peptide GP2 for Use in a Peptide-Based Breast Cancer Vaccine Trial. *Cancer* (2006) 106:2309–17. doi: 10.1002/cncr.21849
119. Brown TA2nd, Mittendorf EA, Hale DF, Myers JW3rd, Peace KM, Jackson DO, et al. Prospective, Randomized, Single-Blinded, Multi-Center Phase II Trial of Two HER2 Peptide Vaccines, GP2 and AE37, in Breast Cancer Patients to Prevent Recurrence. *Breast Cancer Res Treat* (2020) 181:391–401. doi: 10.1007/s10549-020-05638-x
120. Humphreys RE, Adams S, Koldzic G, Nedelescu B, von Hofe E, Xu M. Increasing the Potency of MHC Class II-Presented Epitopes by Linkage to Ii-Key Peptide. *Vaccine* (2000) 18:2693–7. doi: 10.1016/S0264-410X(00)00067-0
121. Gates JD, Clifton GT, Benavides LC, Sears AK, Carmichael MG, Hueman MT, et al. Circulating Regulatory T Cells (CD4+CD25+FOXP3+) Decrease in Breast Cancer Patients After Vaccination With a Modified MHC Class II HER2/neu (AE37) Peptide. *Vaccine* (2010) 28:7476–82. doi: 10.1016/j.vaccine.2010.09.029
122. Limentani SA, Campone M, Dorval T, Curigliano G, de Boer R, Vogel C, et al. A Non-Randomized Dose-Escalation Phase I Trial of a Protein-Based Immunotherapeutic for the Treatment of Breast Cancer Patients With HER2-Overexpressing Tumors. *Breast Cancer Res Treat* (2016) 156:319–30. doi: 10.1007/s10549-016-3751-x
123. Czerniecki BJ, Koski GK, Koldovsky U, Xu S, Cohen PA, Mick R, et al. Targeting HER-2/Neu in Early Breast Cancer Development Using Dendritic Cells With Staged Interleukin-12 Burst Secretion. *Cancer Res* (2007) 67:1842–52. doi: 10.1158/0008-5472.CAN-06-4038
124. Morse MA, Hobeika A, Osada T, Niedzwiecki D, Marcom PK, Blackwell KL, et al. Long Term Disease-Free Survival and T Cell and Antibody Responses in Women With High-Risk Her2+ Breast Cancer Following Vaccination Against Her2. *J Transl Med* (2007) 5:42. doi: 10.1186/1479-5876-5-42
125. Soares R, Marinho A, Schmitt F. Expression of Sialyl-Tn in Breast Cancer Correlation With Prognostic Parameters. *Pathol - Res Pract* (1996) 192:1181–6. doi: 10.1016/S0344-0338(96)80148-8
126. Ibrahim NK, Murray JL, Zhou D, Mittendorf EA, Sample D, Tautchin M, et al. Survival Advantage in Patients With Metastatic Breast Cancer Receiving Endocrine Therapy Plus Sialyl Tn-KLH Vaccine. *Post Hoc Anal Large Randomized Trial J Cancer* (2013) 4:577–84. doi: 10.7150/jca.7028
127. Sasaki E, Tsunoda N, Hatanaka Y, Mori N, Iwata H, Yatabe Y. Breast-Specific Expression of MGB1/mammaglobin: An Examination of 480 Tumors From Various Organs and Clinicopathological Analysis of MGB1-Positive Breast Cancers. *Mod Pathol* (2007) 20:208–14. doi: 10.1038/modpathol.3800731
128. Svane IM, Pedersen AE, Nikolajsen K, Zocca MB. Alterations in P53-Specific T Cells and Other Lymphocyte Subsets in Breast Cancer Patients During Vaccination With P53-Peptide Loaded Dendritic Cells and Low-Dose Interleukin-2. *Vaccine* (2008) 26:4716–24. doi: 10.1016/j.vaccine.2008.06.085
129. Fourcade J, Sun Z, Pagliano O, Chauvin JM, Sander C, Janjic B, et al. PD-1 and Tim-3 Regulate the Expansion of Tumor Antigen-Specific CD8(+) T Cells Induced by Melanoma Vaccines. *Cancer Res* (2014) 74:1045–55. doi: 10.1158/0008-5472.CAN-13-2908
130. Blank C, Brown I, Peterson AC, Spiotto M, Iwai Y, Honjo T, et al. PD-L1/B7H-1 Inhibits the Effector Phase of Tumor Rejection by T Cell Receptor (TCR) Transgenic CD8+ T Cells. *Cancer Res* (2004) 64:1140–5. doi: 10.1158/0008-5472.CAN-03-3259
131. Mittendorf EA, Storrer CE, Shriver CD, Ponniah S, Peoples GE. Investigating the Combination of Trastuzumab and HER2/neu Peptide Vaccines for the Treatment of Breast Cancer. *Ann Surg Oncol* (2006) 13:1085–98. doi: 10.1245/ASO.2006.03.069
132. Fucikova J, Kepp O, Kasikova L, Petroni G, Yamazaki T, Liu P, et al. Detection of Immunogenic Cell Death and Its Relevance for Cancer Therapy. *Cell Death Dis* (2020) 11:1013. doi: 10.1038/s41419-020-03221-2
133. Middleton G, Silcocks P, Cox T, Valle J, Wadsley J, Propper D, et al. Gemcitabine and Capecitabine With or Without Telomerase Peptide Vaccine GV1001 in Patients With Locally Advanced or Metastatic Pancreatic Cancer (TeloVac): An Open-Label, Randomised, Phase 3 Trial. *Lancet Oncol* (2014) 15:829–40. doi: 10.1016/S1470-2045(14)70236-0
134. Barker CA, Postow MA. Combinations of Radiation Therapy and Immunotherapy for Melanoma: A Review of Clinical Outcomes. *Int J Radiat Oncol Biol Phys* (2014) 88:986–97. doi: 10.1016/j.ijrobp.2013.08.035
135. Knutson KL, Schiffman K, Disis ML. Immunization With a HER-2/Neu Helper Peptide Vaccine Generates HER-2/Neu CD8 T-Cell Immunity in Cancer Patients. *J Clin Invest* (2001) 107:477–84. doi: 10.1172/JCI11752
136. Holmes JP, Clifton GT, Patil R, Benavides LC, Gates JD, Stojadinovic A, et al. Use of Booster Inoculations to Sustain the Clinical Effect of an Adjuvant Breast Cancer Vaccine: From US Military Cancer Institute Clinical Trials Group Study I-01 and I-02. *Cancer* (2011) 117:463–71. doi: 10.1002/cncr.25586
137. Clifton GT, Mittendorf EA, Peoples GE. Adjuvant HER2/neu Peptide Cancer Vaccines in Breast Cancer. *Immunotherapy* (2015) 7:1159–68. doi: 10.2217/imt.15.81

Conflict of Interest: The authors declare that the research was conducted in the absence of any commercial or financial relationships that could be construed as a potential conflict of interest.

frontiers in Immunology

ORIGINAL RESEARCH
published: 08 March 2022
doi: 10.3389/fimmu.2022.835774

Antibody-Mediated Inhibition of Insulin-Degrading Enzyme Improves Insulin Activity in a Diabetic Mouse Model

Ofir Fursht[1†], Mirit Liran[2†], Yuval Nash[1,3†], Vijay Krishna Medala[1], Dor Ini[2], Tabitha Grace Royal[1,3], Guy Goldsmith[1], Limor Nahary[2], Itai Benhar[2‡] and Dan Frenkel[1,3*‡]*

[1] Department of Neurobiology, School of Neurobiology, Biochemistry and Biophysics, the George S. Wise Faculty of Life Sciences, Tel Aviv University, Tel Aviv, Israel, [2] The Shmunis School of Biomedicine and Cancer Research, the George S. Wise Faculty of Life Sciences, Tel Aviv University, Tel Aviv, Israel, [3] Sagol School of Neuroscience, Tel Aviv University, Tel Aviv, Israel

Diabetes is a metabolic disease that may lead to different life-threatening complications. While insulin constitutes a beneficial treatment, its use may be limited due to increased degradation and an increase in side effects such as weight gain and hypoglycemia. Small molecule inhibitors to insulin-degrading enzyme (IDE) have been previously suggested as a potential treatment for diabetes through their ability to reduce insulin degradation and thus increase insulin activity. Nevertheless, their tendency to bind to the zinc ion in the catalytic site of IDE may affect other important metalloproteases and limit their clinical use. Here, we describe the isolation of an IDE-specific antibody that specifically inhibits insulin degradation by IDE. Using phage display, we generated a human IDE-specific antibody that binds human and mouse IDE with high affinity and specificity and can differentiate between active IDE to a mutated IDE with reduced catalytic activity in the range of 30 nM. We further assessed the ability of that IDE-inhibiting antibody to improve insulin activity *in vivo* in an STZ-induced diabetes mouse model. Since human antibodies may stimulate the mouse immune response to generate anti-human antibodies, we reformatted our inhibitory antibody to a "reverse chimeric" antibody that maintained the ability to inhibit IDE *in vitro*, but consisted of mouse constant regions, for reduced immunogenicity. We discovered that one intraperitoneal (IP) administration of the IDE-specific antibody in STZ-induced diabetic mice improved insulin activity in an insulin tolerance test (ITT) assay and reduced blood glucose levels. Our results suggest that antibody-mediated inhibition of IDE may be beneficial on improving insulin activity in a diabetic environment.

Keywords: antibody, ScFv library, antibody engineering, diabetes, insulin-degrading enzyme (IDE)

OPEN ACCESS

Edited by:
Lee Mark Wetzler, School of Medicine, Boston University, United States

Reviewed by:
Peter M Van Endert, Institut National de la Santé et de la Recherche Médicale (INSERM), France
Alexander G. Gabibov, Institute of Bioorganic Chemistry (RAS), Russia

****Correspondence:***
Dan Frenkel
dfrenkel@tauex.tau.ac.il
Itai Benhar
benhar@tauex.tau.ac.il

[†]These authors have contributed equally to this work

[‡]ORCID:
Dan Frenkel
orcid.org/0000-0002-7494-6857
Itai Benhar
orcid.org/0000-0002-0824-7177

Specialty section:
This article was submitted to Vaccines and Molecular Therapeutics, a section of the journal Frontiers in Immunology

Received: *14 December 2021*
Accepted: *26 January 2022*
Published: *08 March 2022*

Citation:
Fursht O, Liran M, Nash Y, Medala VK, Ini D, Royal TG, Goldsmith G, Nahary L, Benhar I and Frenkel D (2022) Antibody-Mediated Inhibition of Insulin-Degrading Enzyme Improves Insulin Activity in a Diabetic Mouse Model. Front. Immunol. 13:835774. doi: 10.3389/fimmu.2022.835774

INTRODUCTION

Diabetes mellitus (DM) is a metabolic disorder that results in chronic hyperglycemia due to insufficient levels or impaired responses to the hormone insulin that is essential for glucose homeostasis (1, 2). The World Health Organization indicates that one in 10 people has diabetes, reaching more than 422 million people worldwide in 2014 (3). The two most common forms of diabetes are due to either a diminished production of insulin (type I diabetes, T1D) or insufficient response by the body to insulin (type II diabetes, T2D) (4). With the aging population growing in both number and percentage, there is an increase in the importance of developing and studying new methods for alleviating diabetes-related complications such as stroke, cognitive diseases, vascular diseases, and kidney and eye diseases (5–8). Those diseases can affect both the quality of life of the patients and their families and add to the burden on the public healthcare system. About 25% of diabetes patients require administration of insulin (9). The majority of the top diabetes drugs are insulin homologues (10). Nevertheless, the problems with insulin treatment are as follows: maintaining the basal levels, due to degradation (11, 12); reluctance of patients to inject insulin continuously due to side effects (weight gain, hypoglycemia) (13); and continued administration of insulin may lead to enhanced clearance by the immune cells (14).

Insulin-degrading enzyme (IDE, insulysin) is a ~110 kDa zinc metalloprotease and is an enzyme that was reported to be responsible for insulin degradation (15). IDE is highly conserved; human and mouse/rat proteins share 95% amino acid identities and 100% identity of the residues located in the putative catalytic site (15, 16). Structural analysis revealed that human IDE consists of two equally sized (~55 kDa) N- and C-terminal domains. Several proteins were shown to be digested by IDE (17); however, insulin has the highest affinity to IDE ($K_m \approx$ 14 nM) (18). The presence of IDE in multiple cellular compartments has been reported (19), including mitochondria, and secreted to the plasma (20, 21). Studies of IDE inhibition (22–24) have shown that modulating IDE activity could potentially be a new therapeutic strategy for treating diabetes (25). We recently reported that IDE levels are elevated in the serum of prediabetes metabolic syndrome patients in correlation with increase in triglycerides and reduction in HDL levels (26). Nevertheless, the problem with some of the IDE inhibitors is their limited specificity, as in addition to inhibiting IDE, they were shown to inhibit other Zn^{2+} metalloproteases (27).

Antibodies are known for their high affinity and specificity for a binding partner (ligand or antigen) (28). The antibody engineering field has evolved rapidly in the past decades, much due to novel technologies for the *in vitro* isolation of antibodies from combinatorial libraries and their functional expression in various systems (29). Antibody-based therapy aims for the production of antibodies that will eliminate or neutralize its target. Thus, in this work, we aimed to develop IDE-specific antibodies and evaluate their potential as a therapeutic approach for DM in a mouse model.

Abbreviations: DM, diabetes mellitus; IDE, insulin-degrading enzyme; rhIDE, recombinant human IDE; mAb, monoclonal antibody; IP, intraperitoneal; MBP, *E. coli* maltose-binding protein; oGTT, oral glucose tolerance test; ITT, insulin tolerance test; rcIgG, reverse-chimeric IgG (with human variable and mouse constant immunoglobulin domains); RT, room temperature (about 25°C); STZ, streptozotocin; T1D, type 1 diabetes; T2D, type 2 diabetes.

MATERIALS AND METHODS

Expression and Purification of WT and Mutated IDE Proteins

For the studies described herein, we used recombinant human IDE (rhIDE) that we produced in *E. coli* essentially as described in (26). We expressed both the WT form of the protein and, in the same manner, a E111Q mutated form of the enzyme, in which a point mutation at the catalytic site markedly reduces the enzyme's catalytic activity (**Figure 1A**) (30). The genes encoding the two forms of IDE were cloned into a pET28a+ plasmid backbone, with a His tag at their C-terminus.

Affinity Selection (Bio-Panning) of Human Antibody Phage Display Library for Isolating Binders to IDE

The antibody phage display technique was utilized using the "Ronit 1" human synthetic antibody phage display library as previously described (31). Recombinant IDE, WT, and mutated (catalytically inactive E111Q) were obtained as described in *Materials and Methods*. The library was subjected to four affinity-selection cycles on 10 μg WT rhIDE-coated plates for 2 h at RT where WT IDE was used as bait. During two of the cycles, depletion of the library phages on IDE E111Q was carried out prior to positive affinity selection on the WT enzyme, with an intention to isolate antibodies that bind with high affinity to the catalytic site of the WT enzyme. At the end of each affinity-selection cycle, the bound phages were eluted with 100 mM TEA pH = 13 and immediately neutralized with 1M Tris–HCl pH = 7.4. Eluted phages were used to infect XL1-blue *E. coli* and grown to logarithmic phase for clonal amplification. Phage for the next affinity selection cycle were "rescued by" incubation of infected *E. coli* with 10^{10} CFU/ml M13KO7 helper phage overnight at 37°C with shaking at 250 rpm. Virions from bacterial growth supernatant were precipitated in 20% polyethylene glycol (PEG)/NaCl and suspended in phosphate-buffered saline (PBS) before being used in the next affinity-selection (panning) cycle. After the fourth cycle of affinity selection, IDE-specific scFv-displaying phages were identified by monoclonal phage ELISA. Binders were verified for specificity by testing their binding to several control antigens. The three validated binders were reformatted for production as soluble antibodies and tested in three formats: MBP-scFv, human IgG1 produced as "Inclonals," and reverse-chimeric IgGs produced in mammalian cells culture.

Expression and Purification of IDE-Specific "Inclonal" Human IgG

The "Inclonals" expression and refolding protocol were carried out as previously reported (32–34).

Production of Reverses Chimeric Antimouse IDE Antibodies

To convert the antibodies to full-size reverse-chimeric IgGs, they were cloned into pcDNA 3.4 plasmid backbone. These plasmids are based on the CMV promoter-controlled pcDNA3.4 vectors that are provided as the "Antibody Expressing Positive Control Vector" part of the Expi293™ kit for transient transfection-based expression. The kit also provides the Expi293F™ cells (Thermo Fisher, Rockford, IL, USA, #A14635). The cloning antibody variable domains into IgG expression vectors was carried out as previously described (35). Cloning was carried out by PCR amplification of the antibodies heavy and light variable domains followed by cloning into pcDNA 3.4 plasmids already carrying the corresponding constant domains by Gibson assembly (36). Transfection of Expi293F™ cells with the different pcDNA3.4 vectors was performed by ExpiFectamine™ transfection kit (Gibco, #A14524), according to manufacturer recommendations (Life Technologies, Eugene, OR, USA). For each transfection, a total amount of 30 μg plasmid DNA comprised of 3:1 molar ratio of the IgL and IgH, respectively. Transfection, cell growth, and collection of conditioned medium were carried out as recommended by the vendor (Life Technologies Expi293™ kit for transient transfection-based expression). The antibodies-containing conditioned medium was harvested by centrifugation (Sorvall GSA rotor) for 10 min, at 4°C at 8,000 rpm, 6–7 days after transfection. Reverse chimeric mouse IgG1 mAbs were purified on Protein G columns, according to the manufacturer recommendations (GE Healthcare, Chicago, IL, USA). Prior to purification, antibody-containing media were buffered with 20 mM phosphate buffer, pH 7, and filtered. mAbs were eluted in 1 ml fractions, and the pH was neutralized by 0.25 ml of 1.5M Tris–HCl pH 8.8. Buffer exchange to sterile Dulbecco's PBS (DPBS) (Sigma) was performed on 10-kDa Amicon® Ultra Centrifugal Filters (Millipore Sigma, Burlington, MA, USA) or PD-10 desalting columns (GE Healthcare, Chicago, IL, USA).

The antibodies were collected by centrifugation and concentrated to a final concentration of 1–2 mg/ml using a centrifugal filter concentrator. Purified antibodies were stored at −80°C in small aliquots. Protein concentration was determined by measuring the absorbance of the protein at O.D. 280 nm in the Thermo Scientific NanoDrop™ 2000c spectrophotometer and dividing the absorbance value by the extinction coefficient factor of the protein (extinction coefficient was calculated by http://www.expasy.org/tools/protparam.html).

Evaluation of Antibodies Binding to IDE by ELISA

Ninety-six-well ELISA plates (Nunc, Roskilde, Denmark) were coated overnight at 4°C with 2.5–5 μg/ml of rhIDE WT (IDE) or ACE1 or ACE2 or PBS in PBS and non-relevant proteins such as bovine serum albumin (BSA), His trap-purified protein (His), and MBP-LacZ. Following three washes with PBS containing 0.05% Tween-20 (PBST), the wells were blocked for 1 h at room temperature (RT) with 3% w/v skim milk (232100, Difco, Sparks, MD, USA) in PBS. Wells were than incubated for 2 h at RT with IDE-specific antibodies in different formats: as phage displayed scFv clones, with serial dilutions, as MBP-scFv, and as hIgG or as rcIgG in different concentrations. Bound phages were detected with mouse anti-M13 antibody (1 h at RT) followed by incubation with horseradish peroxidase (HRP)-conjugated goat antimouse secondary antibody (115-035-003, Jackson ImmunoResearch Laboratories, West Grove, PA, USA, ME; 1:5,000 in PBS) for 1 h at RT. Human IDE-specific IgG antibodies were incubated with HRP-conjugated goat anti-human (109-035-088, Jackson ImmunoResearch Laboratories, ME; 1:5,000 in PBS) or anti-mouse (115-035-062, Jackson ImmunoResearch Laboratories, ME; 1:5,000 in PBS) for 2 h in RT. Following three washes with PBST, 3,3′,5,5′-tetramethylbenzidine (TMB; eBioscience, San Diego, CA, USA) was added until color appeared. The reaction was stopped by adding 1M H_2SO_4 and analyzed using a microplate ELISA reader at 450 nm.

Fluorescent Labeling of rcH3-IgG

rcH3-IgG was reconstituted in PBS at pH 7.4 at a concentration of 1 mg/ml. For labeling, the pH of 40 μg of protein solution was adjusted to pH 8.3 using 1M $NaHCO_3$ (Merck, Rehovot, Israel) followed by addition of Alexa Fluor 647 NHS ester (Thermo Fisher) at a molar dye-to-protein ratio of 3:1. Samples were incubated at 4°C overnight, and free dye was removed by using a Pierce 1 ml chromatography cartridge desalting (Thermo, USA) with PBS at pH 7.4 as a buffer.

Affinity Measurements of Binary Equilibrium by Microfluidic Diffusional Sizing

All microfluidic experiments were performed on a Fluidity One-W Serum instrument (Fluidic Analytics, Cambridge, UK) (37). Alexa-647-labeled rcH3-IgG (20 nM) was used, and serial dilution of rhIDE starting at 300 nM was performed. To determine the affinity of IDE binding, Alexa-Fluor-647-labeled rcH3-IgG (20 nM) was mixed with unlabeled IDE at decreasing concentrations (300 nM with 6 additional × 3 dilutions) in PBST and incubated at 4°C for 1 h. To measure complex formation by microfluidic diffusional sizing (MDS), 5 μl of sample was pipetted on a microfluidic chip, and analysis was performed at the 1.5–8.0 nm setting on a Fluidity One-W Serum instrument (center wavelength for excitation is 630 nm with a bandwidth of 38 nm and center wavelength for emission is 694 nm with a bandwidth of 44 nm; Fluidic Analytics, Cambridge, UK). Error bars shown in figures are standard deviations from triplicate measurements. The equilibrium dissociation constant (KD) was determined by nonlinear least-squares (NLSQ) fitting (Prism, GraphPad Software).

Comparing Binding of H3 IgG to Native IDE Compared to Binding Heat-Denatured IDE by ELISA

This was carried out to understand whether H3 IgG binds to a linear or to a conformational epitope of IDE. A solution of 5 μg/ml rhIDE in PBS was prepared and either used directly to coat half of an ELISA plate or denatured by heating at 80°C for 20 min

followed by rapid chilling on ice before using it to coat the other half of the ELISA plate. The plate was coated overnight at 4°C with 50 µl/well of either native or denatured rhIDE. On the following day, the plate was washed once with 300 µl/well of PBST and was blocked with 300 µl/well of 3% skim-milk solution in PBS for 1 h at 37°C. Next, the plate was washed three times with 300 µl/well of PBST, and rcH3-IgG at concentrations of 100, 50, 25, 12.5, 6.25, 3.125, and 1.625 nM was applied to the wells of three columns of wells coated with native or with heat-denatured rhIDE. This was followed by washing these wells three times with 300 µl/well of PBST/well followed by adding 50 µl/well of HRP-conjugated goat antihuman IgG diluted × 5,000 in PBST. The plate was left for 1 h at room temperature and then washed three times with 300 µl/well of PBST. Finally, 50 µl/well of the HRP substrate TMB was added until color appeared. The reaction was stopped after 2 min by adding 50 µl/well 1M H_2SO_4 and analyzed using a BioTek microplate ELISA reader. The optical density was measured at 450-nm wavelength. The results are presented as mean ± SEM (n = 3). To quantify total rhIDE coated onto the wells, the other half of the plate was incubated with HRP-conjugated goat anti-His-tag antibody, diluted 2,000×, 4,000×, 8,000×, 16,000×, 16,000×, 32,000×, 64,000×, and 128,000× in PBST. The plate was left for 1 h at room temperature and then washed three times with 300 µl/well of PBST. Finally, 50 µl/well of the HRP substrate TMB were added until color appeared. The reaction was stopped after 2 min by adding 50 µl/well 1M H_2SO_4 and analyzed using a microplate ELISA reader. The optical density was measured at 450-nm wavelength. The results are presented as mean ± SEM (n = 3).

IDE Insulin Digestion Assay

Various concentrations of IDE inhibitors were incubated with 1.5 µg/ml rhIDE for 1/2 h at RT. Next, recombinant human insulin (41-975-100, Biological Industries, Kibbutz Beit Haemek, Israel) diluted in Mercodia ultrasensitive mouse insulin ELISA (10-1249-01) calibrator 0 was added to the tubes and incubated for 1 h at 37°C. From each tube, 25 µl were taken and evaluated for residual insulin concentration using the Mercodia ultrasensitive Mouse Insulin ELISA kit. Absorbance at 450 nm was recorded by a Spectrafluor plus microplate reader (Tecan, Männedorf, Switzerland).

Mice

Male C57BL/6 mice were purchased from the Jackson Laboratory; IDE KO mice were kindly received from Prof. Dennis Selkoe's laboratory (38). All experiments were in accordance with Tel Aviv University guidelines and approved by the Tel Aviv University (TAU) animal care committee for animal research.

Streptozotocin Diabetes Mouse Model

Ten-weeks-old C57BL/6 mice were fasted overnight, after which they were intraperitoneally injected with 150 mg/kg of STZ diluted in 100 nM citrate buffer at pH =4.5. All mice developed hyperglycemia within 2 days from the STZ injection. At day 3 after STZ injection, each mouse was intraperitoneally injected with 10 mg/kg of reverse chimeric mAbs.

Oral Glucose Tolerance Test

Mice were fasted for 2 h after which they received a single i.p. injection of reverse chimeric mAbs (10 mg/kg), followed by additional 4 h of fasting (six in total). At the end of this time period, mice were given glucose orally, using a gavage needle, at a dose of 2 g/kg. Blood glucose was measured prior to glucose administration (time 0) and 15, 30, 60, 90, and 120 min after glucose administration using the Contour blood glucose meter (Bayer, Elkhart, IN, USA).

Testing the Binding Specificity of H3 IgG to Tissue-Expressed IDE by ELISA

C57BL/6 J WT and IDE−/− mice were euthanized under CO_2 and were transcardially perfused with 20 ml ice cold PBS. Mice were then quickly dissected to collect the liver, kidney, and spleen. The isolated organs were cut into small pieces using razor blades on a chilled glass stage and were collected into ice-cold IDE extraction buffer. Tissue was homogenized in extraction buffer using mechanical pestle to obtain a clear lysate. The lysate was left on ice for 30 min and was later centrifuged at 13,000 rpm for 15 min at 4°C. The supernatant was used for subsequent ELISA. The ELISA for quantifying IDE in the cell extracts was carried out as described before for measuring IDE levels in sera (26).

Viability Assay of Stress-Induced HepG2 Cell Line

Human hepatocellular carcinoma cells (HepG2) were seeded, 2.5×10^4 cells/well in 96-well plate, containing Dulbecco's modified Eagle's medium with 1 g/L D-glucose (low glucose), at 37°C, 5% CO_2 for 6 h and later treated with 5 µM Rotenone at 37°C, 5% CO_2 for 4 h. Then, the medium containing Rotenone was replaced by fresh medium, and the plate was kept at 37°C, 5% CO_2 overnight. Next, the cells were treated with or without different antibodies (as indicated) at a final concentration of 1 µM for 22 h. After incubation, 50 µl/well XTT reagent (Biological industries, Israel) was added according to suppliers' recommendations at 37°C, 5% CO_2 for 2 h. Plate was analyzed with an EMax Plus Microplate Reader at 450 and 630 nm. At all stages, volume was 100 µl/well unless mentioned otherwise.

Insulin Tolerance Test

Mice were fasted for 2 h after which they received a single i.p. injection of reverse chimeric mAbs (10 mg/kg), followed by additional 4 h of fasting (6 h in total). At the end of this time period, the mice were given an i.p. injection of insulin (0.5 U/kg, dissolved in PBS). Blood glucose was measured prior to glucose administration (time 0) and 15, 30, 60, and 90 min after glucose administration. The experiment was repeated 11 days later (with no further injection of antibody). In addition to measuring blood glucose levels, we measured blood insulin concentration at 90 min following insulin injection. Blood glucose levels were measured using the Contour blood glucose meter (Bayer, Elkhart, IN, USA); serum insulin levels were measured using the Mercodia ultrasensitive Mouse Insulin ELISA kit as described above.

Serum Collection

Following the ITT and the injection of reverse chimeric mAbs, mice were bled every 3 days from the facial vein using, a 27-G needle. Blood samples (no more than 120 µl each time) were put in 1.5-ml Eppendorf tubes at RT for 1 h. The blood clots were removed from the tubes using a needle, and the tubes were put on ice for 40 min. Next, the tubes were centrifuged for 10 min at 4°C at 2,300 rpm; the clear supernatant was then taken to a new tube for a further cleaning cycle. The supernatant was taken into a new tube and kept at −20°C.

Detection of Reverse-Chimeric Antibodies in Serum Samples

Ninety-six-well ELISA plates were coated over night with 50 µl/well of 5 µg/ml of IDE in PBS at 4°C. Following three washes with 300 µl/well of PBST, wells were blocked with 300 µl/well of 5% (w/v) skim milk in PBS, for 1 h in RT. For the detection of the IDE-specific antibody (rcH3-IgG), serum samples were diluted 1:2,700 in PBS, whereas control antibody-injected samples served as a control. Known concentrations of the rcH3-IgG antibody diluted in a 1:2,700-diluted sample of control mice served as a reference for the measurement of IDE concentrations. Samples were incubated for 2 h at RT. Following three washes, wells were incubated with 50 µl/well of HRP-conjugated goat anti-mouse antibody (1:5,000 in PBS) for 1 h at RT. Following three washes with PBST, 50µl/well of TMB was added until color appeared. The reaction was stopped by adding 50 µl/well of 1 M H_2SO_4 and analyzed using an ELISA reader at 450 nm.

Statistical Analysis

GraphPad software (GraphPad Prism v8) was utilized for all the statistical analyses. Data comparisons were carried out using either an unpaired two-tailed Student's t-test when two groups were compared or one-way ANOVA (with Bonferroni's *post-hoc* test) when three or more groups were analyzed. Each experiment was repeated at least three times. $p < 0.05$ was considered significant.

RESULTS

Expression and Purification of WT and Mutated IDE Proteins

For the studies described herein, we used the recombinant human IDE that we produced in *E. coli* as described in (26). The purified rhIDE was used as the antigen for both the screening and for immunization. We expressed both the WT form of the protein and in the same manner a E111Q-mutated form of the enzyme, in which a point mutation at the catalytic site markedly reduces the enzyme's catalytic activity (30, 39).

Isolation and Characterization of IDE-Specific Antibodies

The purified rhIDE along with the mutated IDE was used as bait in order to isolate specific scFv clones that recognize specific epitopes of WT IDE. Antibody phage display was utilized using the "Ronit 1" human synthetic antibody phage display library (31) as described in *Materials and Methods*. After four cycles of affinity selection on WT IDE, we identified three IDE-specific scFv-displaying phage clones (two of which are not presented herein), one of which, later proven to be an IDE-neutralizing antibody, was named H3 (see **Figure 1B**). As shown in **Figure 2**, serial dilutions of phages displaying the H3 (**Figure 2A**) bind IDE well and show little to no binding to BSA, a His trap-purified recombinant fusion protein (His), and MBP-LacZ proteins that were used as negative controls.

For initial evaluation of full-size IgGs, we first produced the antibodies as "Inclonals"; IgGs expressed in an *E. coli* expression system (32). The isolated "Inclonal" antibody showed a marked binding to IDE and an EC_{50} of about 1 nM (**Figure 2B**). The antibodies showed very little binding to BSA (negative specificity control).

We further examined the ability of human H3 IgG to inhibit IDE activity. We found that it inhibits insulin digestion by IDE in a dose-dependent manner (**Figure 2C**).

We assessed the binding specificity to human H3 IgG to IDE by assessing its ability to recognize IDE from tissue extracts obtained from WT vs. IDE−/− mice, using ELISA as described before (26). As shown in **Figure 3A**, the antibody did not show binding to proteins extracted from IDE−/− mouse tissues but did bind to proteins extracted from WT mouse tissues. Together, these results suggest that the human H3 IgG binds IDE with high affinity and specificity.

While we expected that H3 IgG will affect only the secreted IDE levels, we assessed potential toxicity to liver cells, which were reported (40) (and as shown in **Figure 3A**) to express high IDE levels. We tested the hepatocyte cell line HepG2 (40). Herein, cells were subjected to oxidative stress using rotenone, which is known to increase oxidative stress, which may lead to IDE elevation (41). Cells were treated with 5 µM rotenone for 4 h. Then, media were discarded, and cells were left to recover overnight with human H3 IgG, isotype control, or left untreated, and cell viability was determined and normalized to untreated cells. We could not detect any toxicity associated with human H3 IgG treatment and, as shown in **Figure 3B**, even found a significant increase by ~50% in the survival of cells treated with human H3 IgG compared to the controls. We further tested whether treatment of WT mice with H3 single-chain Fv (scFv) could reduce IDE activity, leading to higher insulin activity and reduced glucose clearance in oGTT. C57/BL6 male mice at the age of 6 months were treated with either H3 scFv (20 mg/kg, n = 5) or PBS (control, n = 5) 30 min prior to glucose administration. Blood glucose was measured prior to oral administration of glucose (0) and 15, 30, 60, 90, and 120 min after. At time intervals 60, 90, and 120, the blood glucose levels of scFv H3-treated mice were significantly lower than the control group and PBS-treated mice (**Figure 3C**).

Conversion of the IDE-Specific Antibodies to Reverse-Chimeric IgGs

Chimeric antibodies were a critical milestone in the history of therapeutic antibody development. Chimeric antibodies are recombinant IgGs where the variable domains are from a

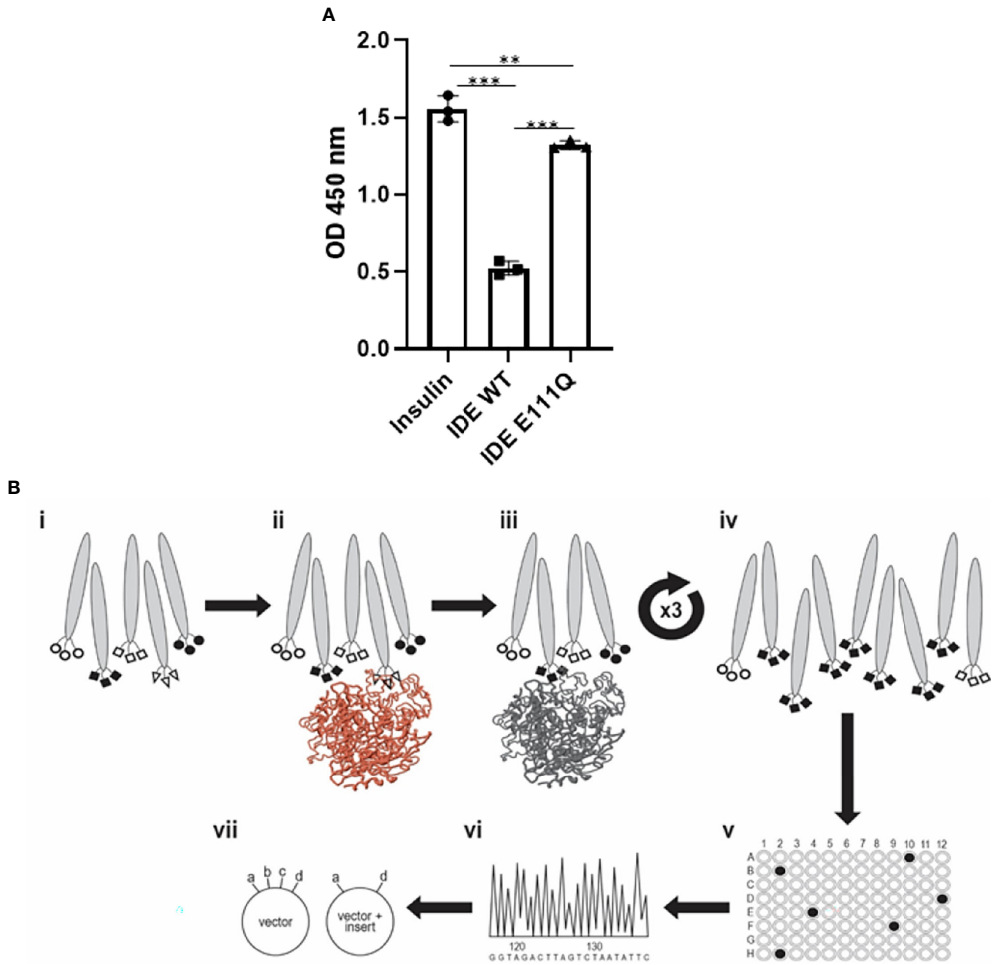

FIGURE 1 | Activity of purified rhIDE wild-type and inactive mutant (E111Q) and their utilization in the antibody discovery process. **(A)** IDE activity assay: incubation of 1.5 µg/L human insulin with PBS (insulin, 1.5 µg/L) or 12 µg/ml rhIDE WT or E111Q for 2 h at 37°C. Residual insulin was later analyzed using Mercodia ultrasensitive mouse insulin ELISA. Results detected on an ELISA plate reader at 450 nm. The results are presented as mean ± SEM (n = 3). **p < 0.01; ***p < 0.001. One-way ANOVA with Bonferroni correction. **(B)** Scheme of the antibody discovery pipeline that was used to obtain rhIDE-binding antibodies: (i) antibody phage display library 2×10^9 antibody clones used as input for the first panning cycle; (ii) depletion: capture on mutant rhIDE (colored brown); (iii) positive selection: capture depleted phages on WT rhIDE; (iv) washed to remove unbound phages, recovered the phages that bound rhIDE, and amplified them by infecting *E. coli* and preparing an enriched population of rhIDE binders to be used as input for the subsequent panning cycles. Repeated three times to obtain a phage population dominated by rhIDE binders; (v) identified phages that bind WT rhIDE by monoclonal phage ELISA; (vi) identified the antibody coding sequences by sequencing of the DNA recovered from monoclonal phages that bind WT rhIDE; (vii) cloned the antibody coding sequences from the phages that bind WT rhIDE to an antibody expression vector to produce soluble purified antibodies.

mouse antibody, while the constant domains are human sequences. Compared to mouse monoclonal antibodies (mAbs), chimeric antibodies are far less immunogenic, limiting the elicitation of human-anti-mouse antibodies upon administration to human patients (42). Conversely, reverse-chimeric antibodies are antibodies with human variable domains and murine constant domains (43). In addition to being useful for antibody discovery in transgenic mice, reverse-chimeric antibodies can be very useful for treating mouse models, to avoid eliciting a mouse-anti-human immune response. In order to evaluate the efficacy of our IDE-specific antibody in mouse models, we converted it to a reverse-chimeric IgG (rcIgG) (mouse IgG1 isotype). The rcH3-IgG was purified as described in *Materials and Methods* to a high level of purity (**Supplementary Figure S1A**). It was tested for binding to IDE, BSA, and the E111Q IDE mutant (**Figure 4A**). Antibody rc2E12 that does not bind IDE served as an isotype control. As shown in **Figure 4A**, rcH3-IgG binds IDE with high affinity (EC_{50} of 1.62 nM), similar to the human H3 Inclonal reported above. In addition to ELISA, we accurately measured the KD of rhIDE to rcH3-IgG by MDS (**Figures 4B**). As the IDE concentration was decreased, less of the fluorescently labeled rcH3-IgG was found in the protein complex, and the effective hydrodynamic radius (Rh) decreased accordingly. Based on a 1:1 equilibrium binding model, the KD was determined to be 30 nM, similar to values that we obtained by ELISA (see **Figure 4A**). It

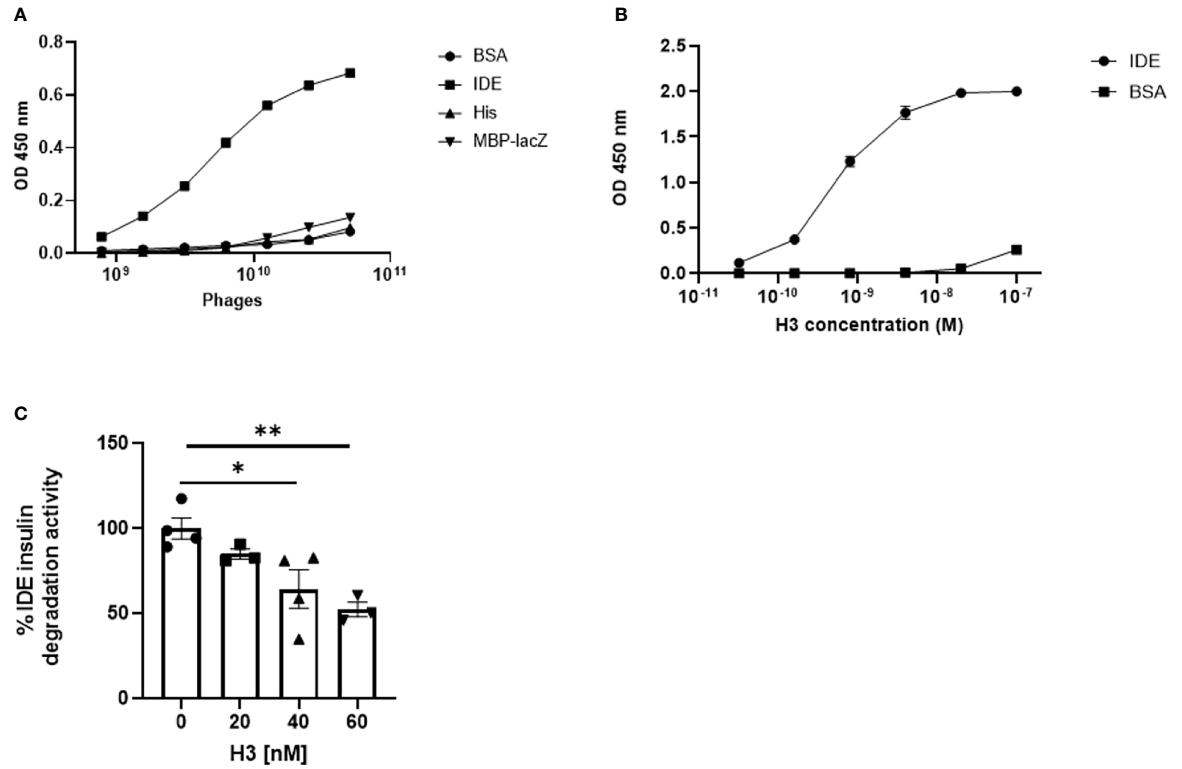

FIGURE 2 | Binding of IDE by IDE-specific phage displayed antibodies and binding and inhibition of IDE by "Inclonal" human IgGs. **(A)** Analysis of IDE binding by H3 scFv displaying phages in ELISA. The analyzed scFv displaying phages were added in serial dilutions to ELISA plate wells previously coated with 2.5 µg/ml of rhIDE WT (IDE) and non-relevant proteins: BSA, a His trap-purified protein (His) and MBP-LacZ. Bound phages were detected with mouse anti-M13 antibody followed by HRP-conjugated goat anti-mouse secondary antibody. The results are presented as mean ± SEM (n = 3). **(B)** Analysis of IDE binding by purified "Inclonal" human IgG in ELISA. The analyzed antibodies were added in serial dilutions to ELISA plate wells coated with 2 µg/ml of IDE WT and BSA. Bound antibodies were detected with a HRP-conjugated goat anti-human secondary antibody. The results are presented as mean ± SEM (n = 4). **(C)** Evaluation of inhibition of IDE-mediated cleavage of insulin by human H3 IgG by ELISA. IDE (1.2 µg/ml) was incubated with 20, 40, or 60 nM of the antibodies 1/2 h at 25°C, followed by incubation of 1.5 µg/L of human insulin 1 h at 37°C. Residual insulin was later analyzed using Mercodia ultrasensitive mouse insulin ELISA kit. The results are presented as mean ± SEM (n = 3–4). *p < 0.02. *p = 0.0227, **p = 0.0075.

was reported that other IDE inhibitors may bind to the zinc in its catalytic site and may interfere with other important similar zinc metalloprotease enzymes, such as angiotensin-converting enzyme (ACE) (44). As presented in **Figure 4C**, the rcH3-IgG showed specificity to IDE and did not bind to other zinc metalloproteinase such as ACE1 or ACE2.

In order to define whether rcH3-IgG recognized the conformation of active rhIDE, we compared the difference in binding to native compared to heat-denatured rhIDE. As shown in **Figure 4D**, thermal denaturation of rhIDE resulted in a very significant reduction in the ELISA signal resulting from detection with rcH3-IgG (down to almost negligible signal). We also evaluated how heat denaturation affected coating of the ELISA plate compared to coating with native IDE in the same plate. As shown in **Supplementary Figure 1B**, we found that thermal denaturation of rhIDE resulted in lowering (but not elimination) of the ELISA signal where rhIDE was detected using serial 2× dilutions of an anti-His-tag antibody (that recognizes a linear epitope), suggesting that denatured rhIDE might also bind less efficiently to the wells of the ELISA plate. Combined, these results suggest that H3 IgG recognizes specifically a conformational epitope of active rhIDE.

IDE-Specific Antibodies Improve Insulin Signaling in a Diabetes Mouse Model

It was previously suggested that inhibition of IDE may improve insulin activity in a diabetes mouse model (22). We further assessed the ability of rcH3-IgG to reduce glucose levels (oGTT) and improve insulin activity (iTT) in STZ-treated mice. We administered i.p. either rcH3-IgG or an isotype control antibody to STZ-treated mice, 1 h prior to testing oGTT and iTT. Following a glucose challenge (oGTT), both control and rcH3-IgG-treated mice exhibited a rise in blood glucose levels. However, rcH3-IgG-treated mice exhibited lower levels of glucose through time, compared to the isotype control-treated mice ($p < 0.05$). *Post-hoc* analysis revealed that rcH3-IgG-treated mice had significantly lower glucose levels 90 min after glucose administration compared to the isotype control-treated mice ($p < 0.05$; **Figure 5A**). These

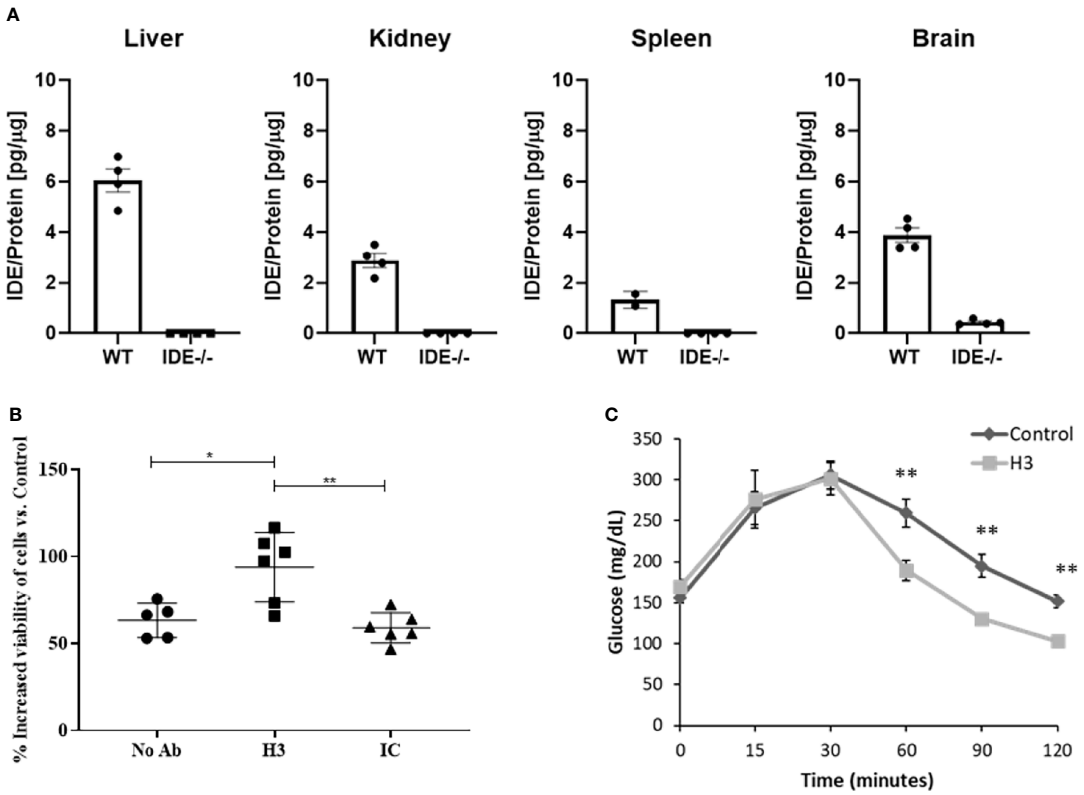

FIGURE 3 | Evaluation of binding specificity of human H3 IgG to tissue-expressed IDE and its activity in cell culture and in mice. **(A)** IDE levels in the liver, kidney, spleen, and brain protein extracts of WT and IDE–/– mice were measured by ELISA. There was no detectable quantity of IDE from any organ in IDE–/– mice. The results are presented as mean ± SEM (n = 4). **(B)** Anti-IDE human H3 IgG protects HepG2 cells from oxidative stress. HepG2 were treated with 5 µM Rotenone for 4 h. Then, media were discarded, and cells were left to recover overnight with 1 µM antibody treatment as indicated. Twenty-four hours later, cell viability was determined by XTT-based cell proliferation kit. The results are presented as mean ± SD (One way ANOVA; *p = 0.0078; **p = 0.002). **(C)** Thirty minutes before oGTT, 6-month-old male mice received a single i.p. injection of scFv at concentration of 2 mg/ml (20 mg/kg) or PBS (control). Blood glucose was measured before glucose administration (0) and 15, 30, 60, 90, and 120 min after. The results are presented as mean ± SEM (n = 5). **p < 0.01. One-way ANOVA with Bonferroni correction was performed.

results suggest that treatment with rcH3-IgG improves glucose levels in a diabetes mouse model. We further assessed the ability of rcH3-IgG to improve insulin activity. We found that while the rcH3-IgG-treated mice exhibited a significant reduction in glucose levels starting from 30 min after the administration of insulin ($p < 0.001$), the isotype control-treated mice exhibited a significant reduction in glucose levels only after 90 min ($p < 0.05$; **Figure 5B**). To assess the long-term effect of rcH3-IgG, we measured glucose 11 days after antibody administration (without additional antibody administration) and found that the blood glucose levels were still significantly lower in the rcH3-IgG-treated mice as compared to the rc2E12-IgG-treated mice (**Figure 5C**). Furthermore, the rcH3-IgG-treated mice showed significantly improved iTT test results (**Figure 5C**). In addition, at this point, we measured serum insulin levels and found that they were higher in the rcH3-IgG-treated mice as compared to the rc2E12-IgG-treated mice (**Figure 5D**). Indeed, we tested the half-life of the rcH3-IgG antibody in the sera of the treated mice and found that it was about 11 days (**Figure 5E**).

DISCUSSION

During our studies focused on IDE, we developed IDE-specific antibody (H3) that inhibits IDE activity. Furthermore, we showed its potential to improve insulin activity in a diabetes mouse model.

IDE is a metalloprotease involved in insulin degradation, and mice and human IDE share 95% amino acid identity with an identical catalytic site. Currently, the use of small molecule inhibitors of IDE is limited in clinical trial due to their non-specificity to other zinc metalloproteinase (45). It has been previously suggested that IDE activity is linked to its conformational stage, and changes within the structure may affect its activity (45). We applied a unique approach for isolating antibodies that may affect the enzyme activity. The isolation process of the IDE-specific scFv-displaying phages was subjected to depletion of rhIDE E111Q binders before positive selection for WT IDE binders. The difference between the two rhIDE isoforms is one amino acid in the catalytic site that renders the enzyme

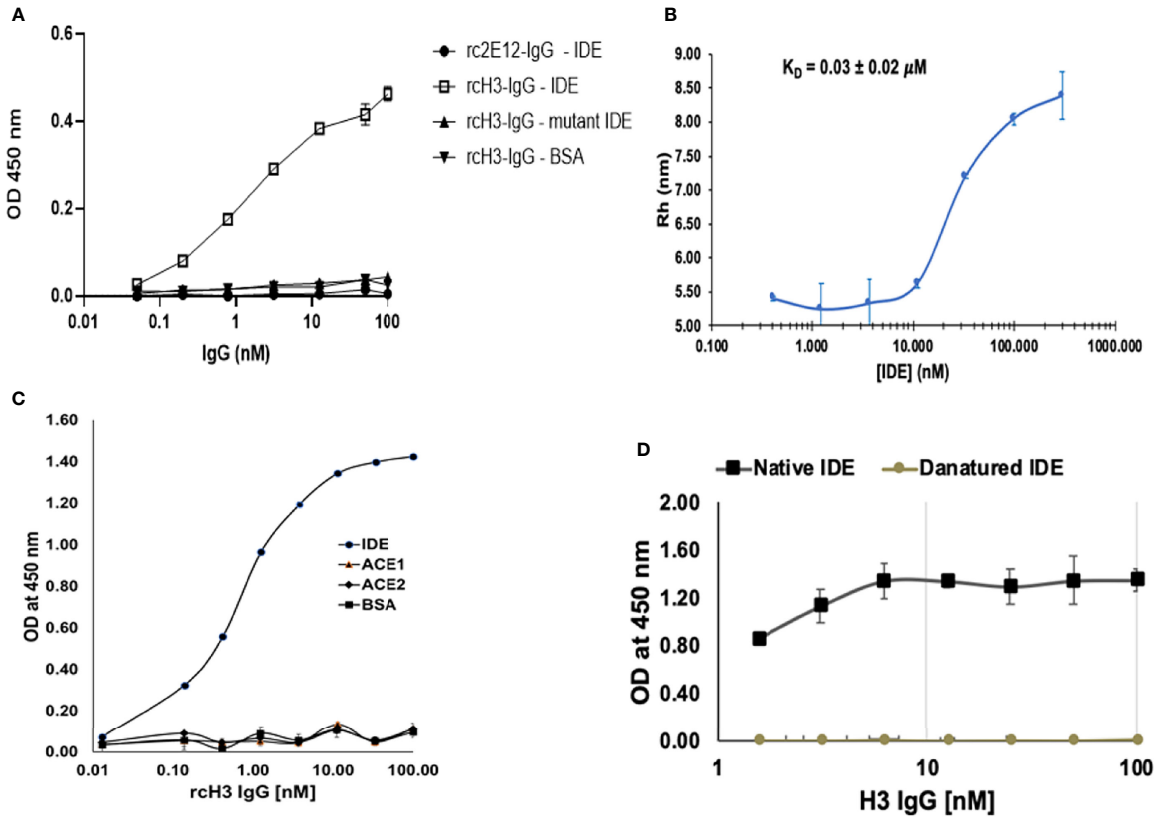

FIGURE 4 | Reverse chimeric H3 IgG binds IDE specifically and in a conformation-dependent manner. **(A)** Evaluation of binding to WT and to mutant IDE by reverse-chimeric H3 and by the isotype control, reverse-chimeric 2E12 IgGs by ELISA. The results are presented as mean ± SEM (n = 3). **(B)** Binding affinity of rcH3 to rhIDE measured by MDS. A binding experiment of rhIDE to Alexa-647-labeled rcH3-IgG using diffusional sizing (MDS) (37). Bars show the average of triplicate measurements with the error bars representing the standard deviation. From the fit, the dissociation constant KD = 30 nM could be calculated. **(C)** Specificity of reverse-chimeric H3 to IDE vs. ACE1 and ACE2 was evaluated by ELISA. **(D)** rcH3-IgG recognizes a conformational epitope on rhIDE. rcH3-IgG at concentrations of 100, 50, 25, 12.5, 6.25, 3.125, and 1.625 nM was applied to the wells of three columns of wells coated with native or with heat-denatured rhIDE. The ELISA was carried out as described in *Materials and Methods*.

catalytically compromised (46). The depletion step probably caused a loss of IDE-specific clones that bind remotely from the catalytic site and improved the chances of recovering antibodies that bind vicinal to the catalytic site. Furthermore, the antibody could detect WT IDE in its native conformation but failed to recognize mutant IDE (**Figure 4A**) or heat-denatured IDE (**Figure 4D**), suggesting that its epitope is conformational.

IDE is an essential enzyme for insulin activity. Indeed, IDE knockout causes hyperinsulinemia and hyperglycemia in mice (38). However, this may be due to its cellular role in monitoring the release of insulin from its receptors (47). Furthermore, partial IDE depletion in IDE-heterozygote mice did not lead to any reported pathology. IDE was shown to regulate the levels of serum insulin (38), and polymorphisms in the *IDE* gene were linked with T2D in rats (48) and humans (49). Recently, we reported an increase in serum IDE concentration in metabolic syndrome patients who are at high risk of developing diabetes (26) Furthermore, inhibition of IDE activity as potential treatment for diabetes was previously suggested (22) and show efficacy without aberrant toxicity (25). H3 antibody shows high specificity to IDE and does not recognize any other tissue proteins isolated from selected tissue such as the liver, kidney, spleen, and brain. Furthermore, while other reports suggest that impairment in IDE activity in liver cells can lead to stress and impaired activity (50), here, we showed that treatment with H3 antibody following oxidative stress in hepatic cell line increase survival. Those results may suggest that targeting the secreted form of IDE by an antibody may prevent interference with essential intercellular IDE activity (50). Of note, H3 antibody did not recognize other essential zinc metalloproteinase such as ACE1 or ACE2, suggesting both its specificity and potential safety.

Due to their large size, unless they bind to a cell-surface internalizing target, antibodies do not penetrate cells. Therefore, under pathological conditions of hypoinsulinemia in diabetes, antibodies inhibiting the secreted form of IDE should increase insulin levels and ameliorate pathological features of the disease. Indeed, we could show that administration of an IDE-specific antibody can improve insulin activity in an environment where

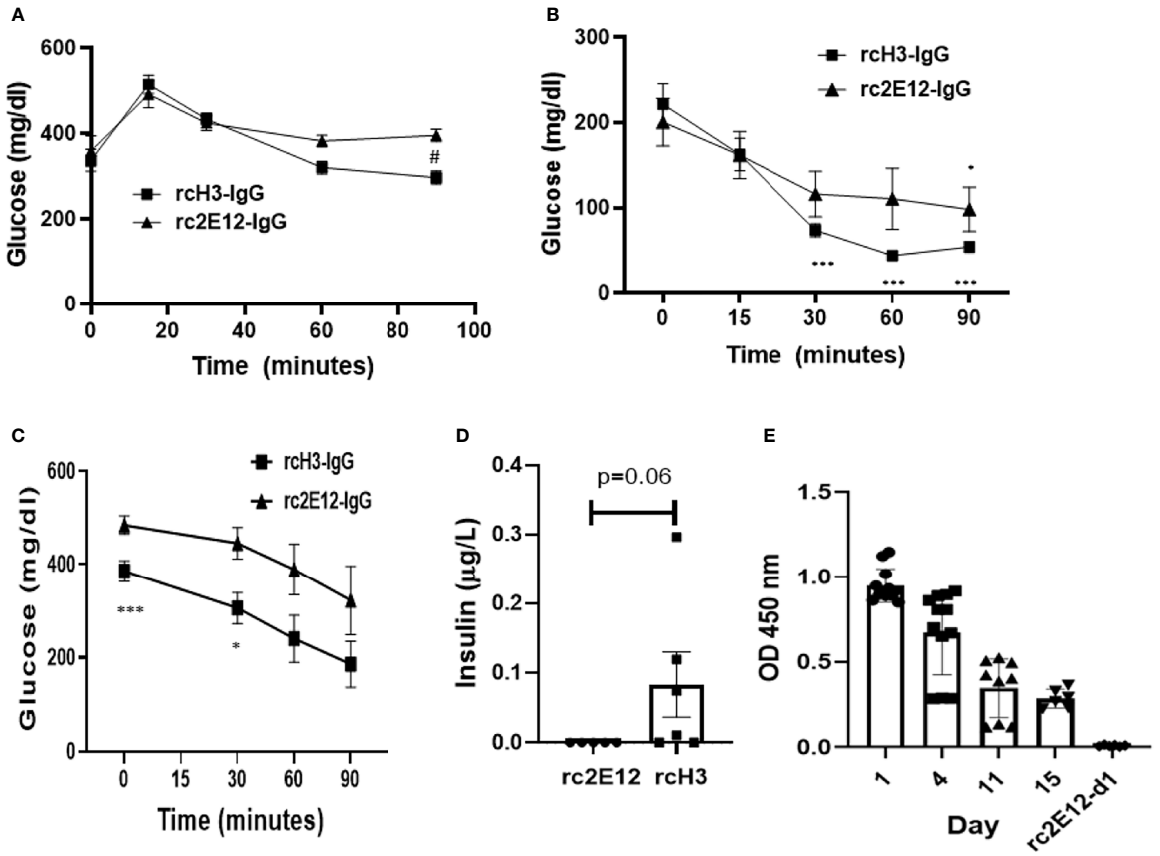

FIGURE 5 | The reverse-chimeric IDE-specific antibody H3 increases blood insulin levels and reduces blood glucose levels in STZ-induced diabetic mice. **(A)** Two days after STZ injection, mice were administrated i.p. with IDE-specific antibody or control antibody and were tested by **(A)** oGTT assay (n = 5–6 mice in each group, $^{\#}p < 0.01$ *between* groups) or **(B)** ITT assay (n = 5 mice in each group, $^{*}p < 0.05$, $^{***}p < 0.001$ *within* group). **(C)** ITT assay following 11 days of antibody administration in STZ-treated mice (n = 5–6 mice in each group, $^{*}p = 0.015$, $^{***}p = 0.008$). **(D)** Insulin serum levels following 11 days of antibody administration in STZ-treated mice assessed by Mercodia ultrasensitive mouse insulin ELISA. The results are presented as mean ± SEM. **(E)** Levels of IDE-specific antibodies at different days following administration (n = 2–4 mice in each group). The results are presented as mean ± SEM.

there are limited insulin levels such as in STZ-treated mice. We also show that H3 MBP-scFv has efficacy in WT mice. In addition, we could detect the rcIgGs up to 11 days following administration, which is in the normal range for murine IgGs in mice (51). Of note, as shown in iTT assay (without additional antibody administration) and by measurement of serum insulin levels at day 11, we found that the glucose levels were lower and insulin levels were higher in rcH3-treated mice compared to rc2E12 (isotype control)-treated mice.

Of note, while small molecules may interfere with intracellular IDE activity, antibodies targeting the cell surface or secreted forms of IDE do not affect the intracellular IDE pool directly, which may be more beneficial for controlling insulin levels. Another advantage may be linked to a reduced clearing of antibodies from the circulation as compared to small molecules. Blocking IDE activity may be beneficial for the maintenance of high circulating insulin levels and other substrates of IDE in pathological conditions such as diabetes. In pathological stages that require exogenous insulin injection, IDE inhibition may serve as a therapeutic intervention, as it will decrease the necessary amounts of administrated insulin and will increase its effective half-life in the serum. Beneficial insulin properties are not limited to glucose regulation but also to the promotion of beta-cell regeneration. Neutralizing antibodies can inhibit IDE-dependent insulin degradation by either directly binding and blocking the active site of IDE or by binding to a site on IDE that affect conformational changes or dimerization. Of note, the H3 antibody preferentially recognizes only the native form of IDE, which suggests that its affect may be linked to the altering active conformational form of the enzyme. Further research needs to be done in order to identify such interactions.

It was suggested that besides IDE, cathepsin may play an important role in the degradation of intracellular insulin (52). Nevertheless, it was reported that fasting serum insulin levels in IDE-KO is higher than those in WT mice (53). While different IDE inhibitors show efficacy in modulating glucose levels, IDE's exact role in glucose metabolism might be complex and needs further investigation (39).

In conclusion, we present here a new approach that may be potentially used to treat diabetes using an antibody targeting IDE. This approach may have limited potential to toxicity due to its high specificity to IDE. Further research using our approach will increase our understanding regarding the role of IDE in diabetes and may provide novel therapeutic approaches in diabetes and related complications.

DATA AVAILABILITY STATEMENT

The original contributions presented in the study are included in the article/**Supplementary Material**. Further inquiries can be directed to the corresponding authors.

ETHICS STATEMENT

The animal study was reviewed and approved by Tel Aviv University guidelines and approved by the TAU animal care committee for animal research.

AUTHOR CONTRIBUTIONS

OF, ML, YN, LN, DI, VM, GG, TGR, IB, and DF designed the research and analyzed data. OF, ML YN, DI, VM, TGR, GG, and LN performed the experiments and collected the data. ML, YN, IB, and DF wrote the manuscript. All authors contributed to the article and approved the submitted version.

FUNDING

The work was supported by Brainboost grant from Sagol School of Neuroscience (DF) grant from Israel Innovation Authority (DF and IB).

SUPPLEMENTARY MATERIAL

The Supplementary Material for this article can be found online at: https://www.frontiersin.org/articles/10.3389/fimmu.2022.835774/full#supplementary-material

REFERENCES

1. Alberti KGMM, Zimmet PZ. Definition, Diagnosis and Classification of Diabetes Mellitus and Its Complications. Part 1: Diagnosis and Classification of Diabetes Mellitus. Provisional Report of a WHO Consultation. *Diabetes Med* (1998) 15:539–53. doi: 10.1002/(SICI)1096-9136(199807)15:7<539::AID-DIA668>3.0.CO;2-S
2. Kahn CR. Insulin Resistance: A Common Feature of Diabetes Mellitus. *N Engl J Med* (1986) 315(4):252–4. doi: 10.1056/nejm198607243150410
3. Roglic G. WHO Global Report on Diabetes: A Summary. *Int J Noncommunicable Dis* (2016) 1:3–8. doi: 10.4103/2468-8827.184853
4. Vinik AI, Fishwick DT, Pittenger G. Advances in Diabetes for the Millennium: Toward a Cure for Diabetes. *Medscape Gen Med* (2004) 6(3 Suppl):12.
5. Mortel KF, Meyer JS, Sims PA, McClintic K. Diabetes Mellitus as a Risk Factor for Stroke. *South Med J* (1990) 83:904–11. doi: 10.1097/00007611-199008000-00014
6. Falanga V. Wound Healing and Its Impairment in the Diabetic Foot. *Lancet* (2005) 366:1736–43. doi: 10.1016/S0140-6736(05)67700-8
7. McCrimmon RJ, Ryan CM, Frier BM. Diabetes and Cognitive Dysfunction. *Lancet* (2012) 379:2291–9. doi: 10.1016/S0140-6736(12)60360-2
8. Kleinridders A, Ferris HA, Cai W, Kahn CR. Insulin Action in Brain Regulates Systemic Metabolism and Brain Function. *Diabetes* (2014) 63 (7):2232–43. doi: 10.2337/db14-0568
9. Cheung BMY, Ong KL, Cherny SS, Sham P-C, Tso AWK, Lam KSL. Diabetes Prevalence and Therapeutic Target Achievement in the United States, 1999 to 2006. *Am J Med* (2009) 122:443–53. doi: 10.1016/J.AMJMED.2008.09.047
10. Rines AK, Sharabi K, Tavares CDJ, Puigserver P. Targeting Hepatic Glucose Metabolism in the Treatment of Type 2 Diabetes. *Nat Rev Drug Discov* (2016) 15:786–804. doi: 10.1038/nrd.2016.151
11. Binder C, Lauritzen T, Faber O, Pramming S. Insulin Pharmacokinetics. *Diabetes Care* (1984) 7:188–99. doi: 10.2337/diacare.7.2.188
12. Williams G, Pickup JC, Keen H. Massive Insulin Resistance Apparently Due to Rapid Clearance of Circulating Insulin. *Am J Med* (1987) 82:1247–52. doi: 10.1016/0002-9343(87)90234-8
13. Brunton SA, Davis SN, Renda SM. Overcoming Psychological Barriers to Insulin Use in Type 2 Diabetes. *Clin Cornerstone* (2006) 8:S19–26. doi: 10.1016/S1098-3597(06)80012-8
14. Porter S. Human Immune Response to Recombinant Human Proteins. *J Pharm Sci* (2001) 90:1–11. doi: 10.1002/1520-6017(200101)90:1<1::AID-JPS1>3.0.CO;2-K
15. Fernandez-Gamba A, Leal M, Morelli L, Castano E. Insulin-Degrading Enzyme: Structure-Function Relationship and Its Possible Roles in Health and Disease. *Curr Pharm Des* (2009) 15:3644–55. doi: 10.2174/138161209789271799
16. Tundo GR, Sbardella D, Ciaccio C, Bianculli A, Orlandi A, Desimio MG, et al. Insulin-Degrading Enzyme (IDE): A Novel Heat Shock-Like Protein. *J Biol Chem* (2013) 288(4):2281–9. doi: 10.1074/jbc.M112.393108
17. Guo Q, Manolopoulou M, Bian Y, Schilling AB, Tang W-J. Molecular Basis for the Recognition and Cleavages of IGF-II, TGF-α, and Amylin by Human Insulin-Degrading Enzyme. *J Mol Biol* (2010) 395:430–43. doi: 10.1016/J.JMB.2009.10.072
18. Duckworth WC, Kitabchi AE. Insulin and Glucagon Degradation by the Same Enzyme. *Diabetes* (1974) 23:536–43. doi: 10.2337/DIAB.23.6.536
19. Duckworth WC, Bennett RG, Hamel FG. Insulin Degradation: Progress and Potential. *Endocr Rev* (1998) 19:608–24. doi: 10.1210/edrv.19.5.0349
20. Hulse RE, Ralat LA, Wei-Jen T. Structure, Function, and Regulation of Insulin-Degrading Enzyme. *Vitam Horm* (2009) 80:635–48. doi: 10.1016/S0083-6729(08)00622-5
21. Glebov K, Schütze S, Walter J. Functional Relevance of a Novel SlyX Motif in Non-Conventional Secretion of Insulin-Degrading Enzyme. *J Biol Chem* (2011) 286:22711–5. doi: 10.1074/jbc.C110.217893
22. Maianti JP, McFedries A, Foda ZH, Kleiner RE, Du XQ, Leissring MA, et al. Anti-Diabetic Activity of Insulin-Degrading Enzyme Inhibitors Mediated by Multiple Hormones. *Nature* (2014) 511:94–8. doi: 10.1038/nature13297
23. Yang D, Qin W, Shi X, Zhu B, Xie M, Zhao H, et al. Stabilized β-Hairpin Peptide Inhibits Insulin Degrading Enzyme. *J Med Chem* (2018) 61:8174–85. doi: 10.1021/acs.jmedchem.8b00418
24. Tang W-J. Targeting Insulin-Degrading Enzyme to Treat Type 2 Diabetes Mellitus. *Trends Endocrinol Metab* (2016) 27:24–34. doi: 10.1016/J.TEM.2015.11.003
25. Nash Y, Ganoth A, Borenstein-Auerbach N, Levy-Barazany H, Goldsmith G, Kopelevich A, et al. From Virus to Diabetes Therapy: Characterization of a Specific Insulin-Degrading Enzyme Inhibitor for Diabetes Treatment. *FASEB J* (2021) 35(5):e21374. doi: 10.1096/FJ.201901945R
26. Sofer Y, Nash Y, Osher E, Fursht O, Goldsmith G, Nahary L, et al. Insulin-Degrading Enzyme Higher in Subjects With Metabolic Syndrome. *Endocrine* (2021) 71(2):357–64. doi: 10.1007/s12020-020-02548-2
27. Deprez-Poulain R, Hennuyer N, Bosc D, Liang WG, Enée E, Marechal X, et al. Catalytic Site Inhibition of Insulin-Degrading Enzyme by a Small Molecule Induces Glucose Intolerance in Mice. *Nat Commun* (2015) 6:8250. doi: 10.1038/ncomms9250

28. Brekke OH, Sandlie I. Therapeutic Antibodies for Human Diseases at the Dawn of the Twenty-First Century. *Nat Rev Drug Discovery* (2003) 2:52–62. doi: 10.1038/nrd984
29. Maynard J, Georgiou G. Antibody Engineering. *Annu Rev BioMed Eng* (2000) 2:339–76. doi: 10.1146/annurev.bioeng.2.1.339
30. Perlman RK, Gehm BD, Kuo W-L, Rich Rosner M. Functional Analysis of Conserved Residues in the Active Site of Insulin-Degrading Enzyme. *J Biol Chem* (1993) 268:21538–44. doi: 10.1016/S0021-9258(20)80575-4
31. Azriel-Rosenfeld R, Valensi M. Benhar I. A Human Synthetic Combinatorial Library of Arrayable Single-Chain Antibodies Based on Shuffling *In Vivo* Formed CDRs Into General Framework Regions. *J Mol Biol* (2004) 335:177–92. doi: 10.1016/J.JMB.2003.10.053
32. Hakim R, Benhar I. "Inclonals": IgGs and IgG-Enzyme Fusion Proteins Produced in an E. Coli Expression-Refolding System. *MAbs* (2009) 1:281–7. doi: 10.4161/mabs.1.3.8492
33. Buchner J, Pastan I, Brinkmann U. A Method for Increasing the Yield of Properly Folded Recombinant Fusion Proteins: Single-Chain Immunotoxins From Renaturation of Bacterial Inclusion Bodies. *Anal Biochem* (1992) 205:263–70. doi: 10.1016/0003-2697(92)90433-8
34. Benhar I, Pastan I. Cloning, Expression and Characterization of the Fv Fragments of the Anti-Carbohydrate Mabs Bl and B5 as Single-Chain Immunotoxins. *"Protein Eng Des Sel* (1994) 7:1509–15. doi: 10.1093/protein/7.12.1509
35. Birnboim-Perach R, Grinberg Y, Vaks L, Nahary L, Benhar I. *Production of Stabilized Antibody Fragments in the E. Coli Bacterial Cytoplasm and in Transiently Transfected Mammalian Cells*. New York, NY: Humana Press (2019) p. 455–80. doi: 10.1007/978-1-4939-8958-4_23
36. Gibson DG, Young L, Chuang R-Y, Venter JC, Hutchison CA, Smith HO. Enzymatic Assembly of DNA Molecules Up to Several Hundred Kilobases. *Nat Methods* (2009) 6:343–5. doi: 10.1038/nmeth.1318
37. Fiedler S, Piziorska MA, Denninger V, Morgunov AS, Ilsley A, Malik AY, et al. Antibody Affinity Governs the Inhibition of SARS-CoV-2 Spike/ACE2 Binding in Patient Serum. *ACS Infect Dis* (2021) 7:2362–9. doi: 10.1021/ACSINFECDIS.1C00047
38. Farris W, Mansourian S, Chang Y, Lindsley L, Eckman EA, Frosch MP, et al. Insulin-Degrading Enzyme Regulates the Levels of Insulin, Amyloid Beta-Protein, and the Beta-Amyloid Precursor Protein Intracellular Domain *In Vivo*. *Proc Natl Acad Sci USA* (2003) 100:4162–7. doi: 10.1073/PNAS.0230450100
39. González-Casimiro CM, Merino B, Casanueva-Álvarez E, Postigo-Casado T, Cámara-Torres P, Fernández-Díaz CM, et al. Modulation of Insulin Sensitivity by Insulin-Degrading Enzyme. *Biomedicines* (2021) 9:1–38. doi: 10.3390/BIOMEDICINES9010086
40. Pivovarova O, Gögebakan Ö, Pfeiffer AFH, Rudovich N. Glucose Inhibits the Insulin-Induced Activation of the Insulin-Degrading Enzyme in HepG2 Cells. *Diabetologia* (2009) 52:1656–64. doi: 10.1007/S00125-009-1350-7/FIGURES/5
41. Tundo GR, Sbardella D, Ciaccio C, Bianculli A, Orlandi A, Desimio MG, et al. Insulin-Degrading Enzyme (IDE): A Novel Heat Shock-Like Protein. *J Biol Chem* (2013) 288:2281–9. doi: 10.1074/jbc.M112.393108
42. Morrison SL, Schlom J. Recombinant Chimeric Monoclonal Antibodies. *Important Adv Oncol* (1990) 3–18.
43. Murphy AJ, Macdonald LE, Stevens S, Karow M, Dore AT, Pobursky K, et al. Mice With Megabase Humanization of Their Immunoglobulin Genes Generate Antibodies as Efficiently as Normal Mice. *PNAS* (2014) 111 (14):5153–8. doi: 10.1073/pnas.1324022111
44. Turner AJ, Hooper NM. The Angiotensin–Converting Enzyme Gene Family: Genomics and Pharmacology. *Trends Pharmacol Sci* (2002) 23:177–83. doi: 10.1016/S0165-6147(00)01994-5
45. Leissring MA, Malito E, Hedouin S, Reinstatler L, Sahara T, Abdul-Hay SO, et al. Designed Inhibitors of Insulin-Degrading Enzyme Regulate the Catabolism and Activity of Insulin. *PloS One* (2010) 5:e10504. doi: 10.1371/journal.pone.0010504
46. Shen Y, Joachimiak A, Rich Rosner M, Tang W-J. Structures of Human Insulin-Degrading Enzyme Reveal a New Substrate Recognition Mechanism. *Nature* (2006) 443:870–4. doi: 10.1038/nature05143
47. Backer JM, Kahn RC, White MF. The Dissociation and Degradation of Internalized Insulin Occur in the Endosomes of Rat Hepatoma Cells. *J Biol Chem* (1990) 265:14828–35. doi: 10.1016/S0021-9258(18)77189-5
48. Fakhrai-Rad H, Nikoshkov A, Kamel A, Fernström M, Zierath JR, Norgren S, et al. Insulin-Degrading Enzyme Identified as a Candidate Diabetes Susceptibility Gene in GK Rats. *Hum Mol Genet* (2000) 9:2149–58. doi: 10.1093/hmg/9.14.2149
49. Karamohamed S, Demissie S, Volcjak J, Liu CY, Heard-Costa N, Liu J, et al. Polymorphisms in the Insulin-Degrading Enzyme Gene Are Associated With Type 2 Diabetes in Men From the NHLBI Framingham Heart Study. *Diabetes* (2003) 52:1562–7. doi: 10.2337/diabetes.52.6.1562
50. Pivovarova O, Von Loeffelholz C, Ilkavets I, Sticht C, Zhuk S, Murahovschi V, et al. Modulation of Insulin Degrading Enzyme Activity and Liver Cell Proliferation. *Cell Cycle* (2015) 14:2293. doi: 10.1080/15384101.2015.1046647
51. Vieira P, Rajewsky K. The Half-Lives of Serum Immunoglobulins in Adult Mice. *Eur J Immunol* (1988) 18:313–6. doi: 10.1002/eji.1830180221
52. Authier F, Tioui MM, Fabrega S, Kouach M, Briand G. Endosomal Proteolysis of Internalized Insulin at the C-Terminal Region of the B Chain by Cathepsin D *. *J Biol Chem* (2002) 277:9437–46. doi: 10.1074/JBC.M110188200
53. Abdul-Hay SO, Kang D, McBride M, Li L, Zhao J, Leissring MA. Deletion of Insulin-Degrading Enzyme Elicits Antipodal, Age-Dependent Effects on Glucose and Insulin Tolerance. *PloS One* (2011) 6(6):e20818. doi: 10.1371/JOURNAL.PONE.0020818

Conflict of Interest: The authors declare that the research was conducted in the absence of any commercial or financial relationships that could be construed as a potential conflict of interest.

frontiers in Immunology

ORIGINAL RESEARCH
published: 30 March 2022
doi: 10.3389/fimmu.2022.867195

CRISPR/Cas9 Approach to Generate an Auxotrophic BCG Strain for Unmarked Expression of LTAK63 Adjuvant: A Tuberculosis Vaccine Candidate

*Luana Moraes [1,2], Monalisa Martins Trentini [1], Dimitrios Fousteris [1,3], Silas Fernandes Eto [4], Ana Marisa Chudzinski-Tavassi [4,5], Luciana Cezar de Cerqueira Leite [1] and Alex Issamu Kanno [1]**

[1] Laboratório de Desenvolvimento de Vacinas, Instituto Butantan, São Paulo, Brazil, [2] Programa de Pós-Graduação Interunidades em Biotecnologia Universidade de São Paulo - Instituto de Pesquisas Tecnológicas - Instituto Butantan (USP-IPT-IB), São Paulo, Brazil, [3] UnivLyon, Université Claude Bernard Lyon 1, Villeurbanne, France, [4] Development and Innovation Laboratory, Instituto Butantan, São Paulo, Brazil, [5] Center of Excellence in New Target Discovery (CENTD) Special Laboratory, Instituto Butantan, São Paulo, Brazil

OPEN ACCESS

Edited by:
Fabio Bagnoli, GlaxoSmithKline, Italy

Reviewed by:
Steven Derrick, Center for Biologics Evaluation and Research (FDA), United States
Angelo Izzo, Royal Prince Alfred Hospital, Australia

***Correspondence:**
Alex Issamu Kanno
alex.kanno@butantan.gov.br

Specialty section:
This article was submitted to Vaccines and Molecular Therapeutics, a section of the journal Frontiers in Immunology

Received: *31 January 2022*
Accepted: *09 March 2022*
Published: *30 March 2022*

Citation:
Moraes L, Trentini MM, Fousteris D, Eto SF, Chudzinski-Tavassi AM, Leite LCC and Kanno AI (2022) CRISPR/Cas9 Approach to Generate an Auxotrophic BCG Strain for Unmarked Expression of LTAK63 Adjuvant: A Tuberculosis Vaccine Candidate. Front. Immunol. 13:867195. doi: 10.3389/fimmu.2022.867195

Tuberculosis is one of the deadliest infectious diseases and a huge healthcare burden in many countries. New vaccines, including recombinant BCG-based candidates, are currently under evaluation in clinical trials. Our group previously showed that a recombinant BCG expressing LTAK63 (rBCG-LTAK63), a genetically detoxified subunit A of heat-labile toxin (LT) from *Escherichia coli*, induces improved protection against *Mycobacterium tuberculosis* (*Mtb*) in mouse models. This construct uses a traditional antibiotic resistance marker to enable heterologous expression. In order to avoid the use of these markers, not appropriate for human vaccines, we used CRISPR/Cas9 to generate unmarked mutations in the *lysA* gene, thus obtaining a lysine auxotrophic BCG strain. A mycobacterial vector carrying *lysA* and *ltak63* gene was used to complement the auxotrophic BCG which co-expressed the LTAK63 antigen (rBCGΔ-LTAK63) at comparable levels to the original construct. The intranasal challenge with *Mtb* confirmed the superior protection induced by rBCGΔ-LTAK63 compared to wild-type BCG. Furthermore, mice immunized with rBCGΔ-LTAK63 showed improved lung function. In this work we showed the practical application of CRISPR/Cas9 in the tuberculosis vaccine development field.

Keywords: recombinant BCG, CRISPR/Cas9, LTAK63 adjuvant, complemented auxotroph, tuberculosis vaccine

INTRODUCTION

The Bacillus Calmette-Guérin (BCG), a live attenuated strain of *Mycobacterium bovis* is the only licensed vaccine against tuberculosis (TB), one of the top 10 causes of mortality (1). BCG is usually administered at birth and is very effective in protecting children against severe forms of the disease. Epidemiological evidence suggests that protection wanes with time and its efficacy in adults against

the pulmonary TB is variable (2) contributing to the 10 million new cases and 1.5 million deaths every year (1). Since the development of BCG, a century ago, no new vaccine has been licensed. Therefore, many vaccine candidates are under evaluation as improved vaccines against TB.

Recombinant BCG (rBCG) is an attractive strategy to generate improved TB vaccines. With the development of mycobacterial expression vectors, many strains of rBCG aiming to improve the immune response and protection against TB were generated (3). One of the most advanced vaccine candidates in clinical trials, VPM1002, is based on the rBCG strategy and expresses a pore-forming toxin – cytolysin (4). The expression of toxin derivatives may modulate the immune response and provide improved protection against *M. tuberculosis* (*Mtb*) challenge. We have previously developed a rBCG strain expressing the genetically detoxified subunit A of the heat-labile toxin from *E. coli*, LTAK63, as adjuvant. In comparison to wild-type BCG, immunization of mice with rBCG-LTAK63 increased the Th1 immune response in the lungs (higher IFN-γ, TNF-α, IL-6 and IL-17 production) and long-term immune responses against *Mtb*. rBCG-LTAK63 also conferred improved protection against *Mtb* challenge, including the hypervirulent Beijing strain (5).

The expression of LTAK63 was dependent on a vector containing an antibiotic resistance marker. In order to move forward to clinical trials, it is important to obtain stable antigen expression without antibiotic resistance. Complemented auxotrophic strains are an interesting approach to obtain unmarked expression of heterologous antigens. In this strategy, an essential gene of the biosynthesis of an amino acid is functionally knocked-out. The respective gene is then provided by a complementation plasmid which maintenance is essential for survival and at the same time, the plasmid can be used to co-express antigens of interest (6). Another advantage over antibiotic resistance markers is that the *in vivo* stability of the vector is usually higher (7). We have previously used auxotrophic complementation to obtain an unmarked rBCG strain expressing the genetically detoxified S1 subunit of the pertussis antigen, S1PT, as vaccine against pertussis (8) and bladder cancer immunotherapy (9, 10) as well as presenting increased features of innate immune memory/trained immunity response (11). In that study, the auxotrophic strain was generated using a mycobacteriophage to knock-out the *lysA* gene, involved in the biosynthesis of lysine. This strategy required the insertion of two selection markers to screen for positive mutants and then an additional counter selection step to remove the markers. Even though this process generates an unmarked deletion it stills leaves a chromosomal "scar" (12).

The CRISPR/Cas technology has emerged as a cutting-edge versatile molecular tool for genome manipulation in several organisms. The technique uses a Cas endonuclease (Cas9), a trans-activating RNA (tracrRNA) and a specific targeting sequence (crRNA). This duplex crRNA:tracrRNA (sgRNA) can bind to Cas9 and drives it to the complementary sequence in the genome. The exchange of the crRNA sequence allows targeting of any sequence of interest, with the only condition of being adjacent to a PAM domain (Protospacer Adjacent Motif) (13). So far, applications of CRISPR/Cas in mycobacteria intended to interfere with gene expression (CRISPRi) in order to analyze gene function (14, 15); or to establish the required conditions to generate gene knock-outs in *M. smegmatis*, *M. marinum* and *Mtb* (16).

In this work, we applied CRISPR/Cas9 to generate an auxotrophic BCG, which was complemented to obtain the stable expression of the LTAK63 adjuvant. The immunization with rBCGΔ-LTAK63 showed superior protection against *Mtb* challenge and conferred improved lung function.

MATERIALS AND METHODS

Strains, Media, and Growth Conditions

Escherichia coli DH5α, *M. smegmatis* mc^2 155, *M. bovis* BCG Danish (American Type Culture Collection, ATCC #35733) and their derivatives were used in the study. *E. coli* was used for the cloning steps and grown in Luria-Bertani (LB) (5 g/L yeast extract, 10 g/L tryptone and 10 g/L NaCl), (Sigma-Aldrich®, Merck KGaA, St. Louis, MO, USA). *M. smegmatis* was grown in Middlebrook 7H9 (MB7H9) (Difco, Detroit, MI, USA), supplemented with 0.5% glycerol (Sigma-Aldrich®) and 0.05% Tween 80 (Sigma-Aldrich®) or plated on Middlebrook 7H10 agar (Difco) supplemented with 0.5% glycerol (MB7H10). BCG was grown in Middlebrook 7H9 supplemented with 10% of OADC (oleic acid-albumin-dextrose-catalase; BBL, Cockeysville, MD, USA), 0.5% glycerol and 0.05% Tween 80 (MB7H9-OADC) or plated on Middlebrook 7H10 agar supplemented with 0.5% glycerol and OADC (MB7H10-OADC). *Mtb* was grown in Middlebrook 7H11 (Difco) supplemented with OADC, glycerol and Tween 80 (MB7H11-OADC). *E. coli* and *M. smegmatis* were grown at 37°C. BCG and *Mtb* were grown at 37°C and 5% CO_2. When indicated, kanamycin sulphate (20 μg/mL) (Sigma-Aldrich®), tetracycline hydrochloride (Tc) (200 ng/mL) (Sigma-Aldrich®) and/or L-lysine (40 μg/mL) (Sigma-Aldrich®) were added.

Preparation and Transformation of Competent Cells

Chemically competent *E. coli* DH5α was prepared according to standard protocols (17). Electrocompetent mycobacteria were prepared as previously described (18). For transformation of mycobacteria, 300-500 ng of plasmid DNA were mixed with competent cells and electroporation performed using a Gene Pulser II device (BioRad, Hercules, CA, UK). Cells were recovered in MB7H9 and plated onto MB7H10 agar until the appearance of visible colonies. Kanamycin, tetracycline, or/and lysine were added to the media, as described above, when required.

Construction of the Mycobacterial CRISPR/Cas9 All-In-One Vectors

Codon-optimized *cas9* expression cassette, the Tet regulator (*tetR*) cassette and the tracrRNA sequences (Genscript, Piscataway, NJ, USA) were sequentially cloned into pJH152 (a kind gift from Dr. Stewart Cole, EPFL, Lausanne, France) using

the restriction enzymes NotI/ClaI, HpaI and NheI (New England Biolabs, Ipswich, MA, USA), respectively, originating pKLM-CRISPR (**Figure 1**). Selection of crRNA was made using the Cas-Designer tool at R-GENOME website (http://www.rgenome.net/cas-designer/). Each crRNAs sequence was inserted using BbsI (New England Biolabs) upstream of tracrRNA in pKLM-CRISPR, generating the sgRNA sequences. The expression of Cas9 and sgRNA are both controlled by tetracycline-inducible promoters (pUV15tetO). The T4g32 transcriptional terminator was added to each cassette end (T). Orientation of the cloned fragments according to **Figure 1** were confirmed by Sanger sequencing. Vectors including crRNA aiming to knock-out *lysA* were named pKLM-CRISPR-*lysA(x)*, where *(x)* represents different crRNA sequences. The list of plasmids and oligonucleotides used are shown in **Supplementary Tables S1, S2**. Alignment of *lysA* from BCG and *M. smegmatis* as well as the relative position of sgRNA targets are represented in **Supplementary Figure 1**.

Construction of Complementation Vectors Expressing LysA and LTAK63

The pAN71-*ltak63* vector containing pAN promoter and driving low expression of the LTAK63 adjuvant was previously constructed by our group (5). A PCR-amplified *lysA* gene (containing a Shine-Dalgarno, SD), or a *lysA* expression cassette digested from pJH152 were used. The pAN71-*ltak63* vector was digested with NotI/PvuII (New England Biolabs) and the *lysA* fragment inserted in tandem with *ltak63* under the same pAN promoter, generating pAN71-*ltak63-lysA*(t) (**Figure 2A**). In this construct, the kanamycin resistance marker was removed by digestion with NsiI (New England Biolabs) and self-ligated. The pAN71-*ltak63* vector was also digested with NotI/ClaI (New England Biolabs) to clone the *lysA* expression cassette, generating pAN71-*ltak63-lysA*(c) (**Figure 2B**). The kanamycin resistance marker was removed by digestion with ClaI (New England Biolabs) and self-ligated. Both vectors were electroporated into *M. smegmatis* mc^2 1493 (lysine auxotroph) (19) and transformants plated onto MB7H10. Transformants were then grown in MB7H9 with and without kanamycin to confirm construction of the unmarked pAN71-*ltak63-lysA* vectors. Plasmid extraction from *M. smegmatis* was performed using Wizard Plus SV Minipreps DNA Purification kit (Promega, Madison, WI, USA) and the extracted plasmids were used to transform the lysine auxotrophic BCG (BCGΔ*lysA*).

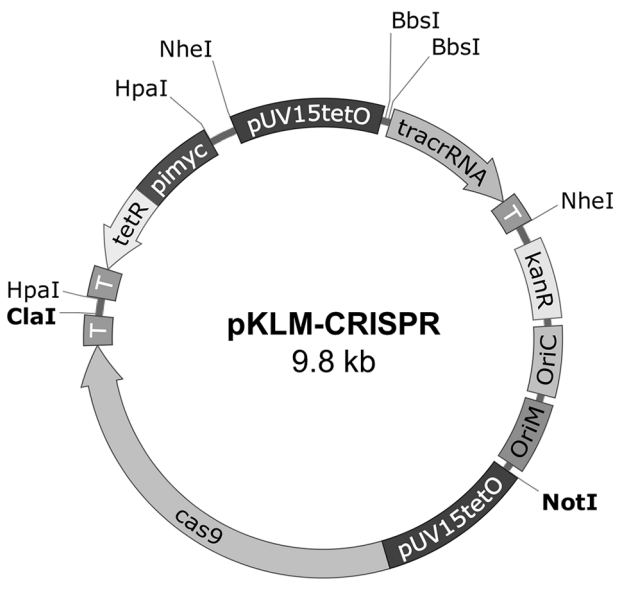

FIGURE 1 | Schematic representation of the pKLM-CRISPR vector. The pKLM-CRISPR vector, contains the expression cassette for codon optimized *cas9* gene and a cassette for expression of sgRNA, both under regulation of pUV15tetO, a tetracycline-inducible promoter. The repressor tetR is expressed constitutively by the pimyc promoter. Transcriptional terminators (T) were introduced after each expression cassette. The restriction sites used for cloning are also indicated. The two BbsI sites were introduced to facilitate the cloning of the crRNA sequences upstream of tracrRNA. The vectors also contain a kanamycin resistance marker (KanR); origin of replication in *E. coli* (oriC) and mycobacteria (oriM).

Induction of Cas9 Expression in Mycobacteria

After transformation of *M. smegmatis* and BCG with pKLM-CRISPR-*lysA(x)*, kanamycin-resistant colonies were recovered and cultured in 5 mL of MB7H9 and MB7H9-OADC, respectively. These cultures were used as pre-inoculum in a fresh culture starting at OD_{600} 0.1. After 2 h (*M. smegmatis*) or 24 h (BCG) of incubation, tetracycline was added to induce expression of Cas9, and the culture was maintained at 37°C for 4-24 h (*M. smegmatis*) or 24-120 h (BCG). After the induction, bacteria were lysed by sonication using an ultrasonic processor GE100 (GE Healthcare, Chicago, IL, USA) and protein extracts separated by SDS-PAGE (BioRad, Hercules, CA, UK), transferred to PVDF membranes (GE Healthcare) and blocked with 5% non-fat dry milk at 4°C for 16 h. The membrane was probed using monoclonal anti-Cas9 antibodies (7A9-3A3, 1:1,000) (Santa Cruz Biotechnology, Dallas, TX, USA) incubated for 90 min and anti-mouse IgG conjugated with peroxidase (A6782, 1:1,000) (Sigma-Aldrich®) for 60 min. *E. coli* DH5α transformed with pCas (20) was used as positive control for Cas9 expression. Chemiluminescent signal was developed using ECL Prime Western Blotting System (GE Healthcare) and images acquired with the LAS4000 digital imaging system (GE Healthcare).

Screening and Characterization of Knock-Out Mutants

After tetracycline induction the cultures were plated onto MB7H10 or MB7H10-OADC, both supplemented with lysine and kanamycin and incubated at 37°C until the appearance of visible colonies. Single colonies were then transferred to mirror plates either containing or not lysine, both in presence of kanamycin. Growth only in the lysine-containing plate revealed positive knock-out clones (Lysine-KO). The Lysine-KO clones were used as template for PCR amplification of the *lysA* region and sequencing. The *lysA* sequences from the Lysine-KO clones were compared with the reference sequences in UNIPROT database (*M. smegmatis*-Q9X5M1 and BCG-P9WIU7).

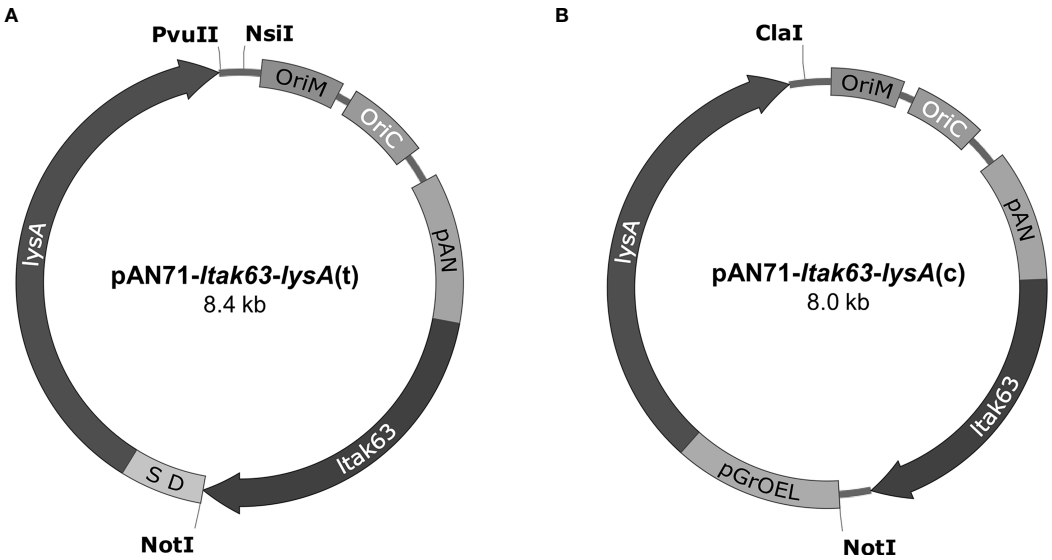

FIGURE 2 | Vectors pAN71-*ltak63-lysA*(t) and pAN71-*ltak63-lysA*(c) used for the complementation of lysine auxotrophic strains. **(A)** In pAN71-*ltak63-lysA*(t) the *lysA* gene is in tandem with *ltak63*, including a Shine-Dalgarno sequence (SD) between the genes. **(B)** In pAN71-*ltak63-lysA*(c) the *lysA* gene is under the control of the pGrOEL promoter. The KanR site was truncated by restriction digestion with NsiI or ClaI, respectively and self- ligated. Both plasmids share the same features such as oriM and oriC, the pAN promoter and the *ltak63* sequence.

In Vitro Stability of BCG Functional KO

To assess reversion to the wild-type phenotype during *in vitro* culturing, rBCGΔ*lysA* strains were serially passaged weekly for up to 8 passages when the cells were plated on MB7H10-OADC containing or not lysine. Additionally, the curing of pKLM-CRISPR-*lysA(x)* was assessed by plating rBCGΔ*lysA* onto mirror plates containing or not kanamycin. Growth only in the plate lacking kanamycin indicated plasmid loss.

Complementation of Auxotrophic Strains

Competent BCGΔ*lysA* were prepared as previously described and transformed with pAN71-*ltak63-lysA*(t) and pAN71-*ltak63-lysA*(c), generating rBCGΔ-LTAK63(t or c), respectively. Selected clones were grown in MB7H9-OADC until an OD_{600} 1.0, when bacteria were recovered, and protein extracts used to detect the expression of LTAK63 by Western blot (20). Detection of LTAK63 was performed using anti-serum of mice previously immunized with rLTK63 (1:1,000) incubated for 60 min and an anti-mouse IgG antibody conjugated with peroxidase (A6782, 1:3,000 Sigma-Aldrich®) incubated for 60 min. Additionally, growth curves of complemented auxotrophs were compared to wild-type BCG to determine whether rBCGΔ-LTAK63(t or c) would show altered *in vitro* growth.

Animals and Immunization

All animal experiments were performed according to Brazilian and international guidelines on animal experimentation and approved by the Ethics Committee of Instituto Butantan, São Paulo-SP (CEUAIB), (Permit number 8591010817). Five to eight-week-old female BALB/c mice were obtained from the Central Animal Facility of the Instituto Butantan, SP, Brazil. BALB/c were immunized through the subcutaneous route (s.c.) with a single dose of BCG or rBCGΔ-LTAK63(t) ($1x10^6$ CFU/100 μL), or saline and challenged after 90 days *via* the intranasal route (i.n.) with *M. tuberculosis* H37Rv (500 CFU/50 μL). Thirty days after challenge, the lungs were collected, homogenized, and 20 μL of serial dilutions (10^{-1}, 10^{-2} and 10^{-3}) were plated on MB7H11-OADC at 37°C and 5% CO_2 for CFU counting.

Histopathology and Quantification of the Lung Inflammation

Thirty days after *Mtb* challenge, lung tissue samples were collected, preserved in 10% neutral buffered formalin, embedded in paraffin, cut into 5-6 μm sections, and stained with hematoxylin and eosin (H&E). The severity of inflammation in the mouse lungs was assessed according to (21). In summary, H&E-stained lung sections were photographed at 40 x magnification using a microscope (Nikon Eclipse Ti-S) coupled to a digital camera (DS-Fi1c, Nikon). Image analysis software (ImageJ, National Institutes of Health, USA) was used to determine the pulmonary area affected. The inflammatory area was measured according to (21) and the functional lung area is represented by the intra-alveolar regions in the lung tissue determined using morphometric analysis according to (22). Briefly, five images at 40 x magnification per lung lobule, totaling 25 images per treatment, were randomly selected, and analyzed for the qualitative evaluation of the cell infiltrate and intra-alveolar regions. To measure the areas of interest the images were transformed into 8-bit and treated with threshold and percentage of the measured area. For leukocyte counting, the Color Deconvolution 2 plugin were used to visualize and separate nuclei from the cytoplasm. For cell counting, the Cell Counter

plugin was used. This analysis is used to facilitate the differential counting of segmented and mononuclear nuclei.

Statistical Analysis

Statistical analysis was performed using the GraphPad Prism (GraphPad Software, Inc.). The significance of differences among groups was calculated by unpaired parametric two-way Student's t-test as described in the figure legends. Differences between mean values were considered significant when $p < 0.05$.

RESULTS

Inducible Expression of Cas9 in Mycobacteria

Transformation of *M. smegmatis* and BCG with pKLM-CRISPR showed that both were able to express Cas9, as determined by the Western blot (~160 kDa). In *M. smegmatis*, the highest expression of Cas9 was observed at 8 h after the induction in a concentration of 200 ng/mL of tetracycline (**Supplementary Figure 2** and **Figure 3A**). In BCG, the highest expression of Cas9 was between 24-48 h after the induction, with decreasing levels being observed from that time until 120 h (**Figure 3B**). Attempts to express the wild-type *S. pyogenes* Cas9 in mycobacteria were unsuccessful (data not shown).

Phenotypic Screening and Characterization of Smeg*ΔlysA* and BCG*ΔlysA*

Mycobacteria were transformed with the gene editing vectors (pKLM-CRISPR containing the specific crRNAs to target *lysA* (n=3 for *M. smegmatis* and n=2 for BCG) (**Supplementary Table 2**), and the expression of Cas9 was induced by tetracycline. After induction, the culture was plated on solid media containing kanamycin to obtain isolated colonies. These were transferred to mirror plates with and without lysine to detect the functional knock-out of LysA. The transformation of *M. smegmatis* with the vector containing crRNA-*lysA820*-Smeg, resulted in 2 out of 8 colonies (25%) that did not grow in the absence of lysine (Smeg*ΔlysA*) (**Figure 4A**). The induction with crRNA-*lysA394*-Smeg did not generate any functional knock-out (0/5), while crRNA-*lysA123*-Smeg did not produce any transformant. In BCG transformed with the vectors containing crRNA-*lysA*88-BCG, 2 out of 50 colonies (4%) did not grow without the supplementation of lysine (BCG*ΔlysA*) (**Figure 4B**). No functional knock-outs were obtained using the vector containing crRNA-*lysA20*-BCG. In the genotypic analysis of *M. smegmatis*, we observed the addition of a single nucleotide (*lysA*_2b) and the deletion of two nucleotides (*lysA*_2c) next to the PAM site (**Figure 4C**). In BCG, we performed an additional round of induction (independent experiment), obtaining a total of five functional knock-outs. Sequencing analysis of BCG*ΔlysA* demonstrated the deletion of two nucleotides (*lysA*_7 and *lysA*_9), deletion of larger fragments (*lysA*_10 and *lysA*_39), 83 and 107 bp (**Figure 4D** and **Supplementary Figure 3**), and a single nucleotide deletion (*lysA*_43). The *in-silico* translation of these sequences revealed that the mutations results in the early interruption of translation or frameshifts impairing the correct translation of LysA (**Supplementary Figure 4**). The possibility of reversion from the auxotrophic phenotype was evaluated by subculturing BCG*ΔlysA* and observation of growth without supplementation of lysine. Even after 8 passages, without the supplementation of lysine, no prototrophic colony was observed (**Supplementary Figure 5**).

LTAK63 Adjuvant Expression in Auxotrophic Mycobacteria

Once reversion to the wild-type phenotype was excluded, the BCG*ΔlysA* lysA_39 (mutant containing the deletion of 107 bp) was selected to be complemented. Before the complementation, the pKLM-CRISPR plasmid was cured. In a single incubation without kanamycin, 35% of the colonies showed plasmid loss (**Supplementary Figure 6**). A single colony was selected and prepared as competent cells. The BCG*ΔlysA* was then transformed with the complementation vectors, pAN71-*ltak63-lysA*(t) and pAN71-*ltak63-lysA*(c) and protein extracts used to detect the expression of LTAK63 (**Figure 5**). More importantly, either when driven by the vectors with *lysA* in tandem or as an expression cassette, the level of LTAK63 expression was comparable to that observed in BCG transformed with the pAN71-*ltak63* vector.

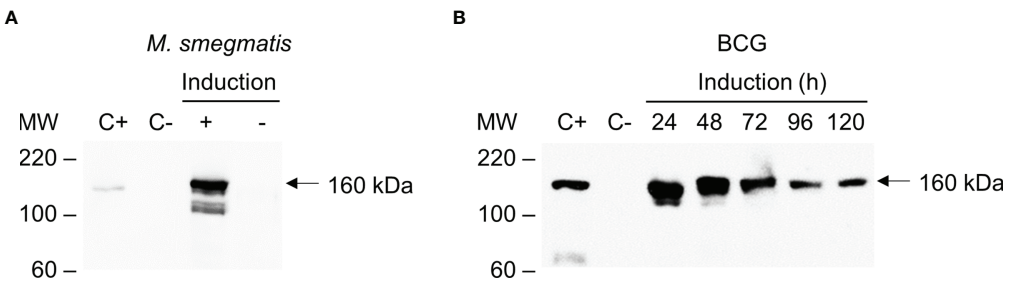

FIGURE 3 | Inducible expression of Cas9 in *M. smegmatis* and BCG. *E. coli* transformed with pCas9 was used as positive control (C+). Total protein extracts of wild-type mycobacterial strains were used as negative controls (C-). **(A)** Western blot of total protein extracts of *M. smegmatis* transformed with pKLM-CRISPR vector with either Cas9 expression induced (+) or not induced (-) with tetracycline. **(B)** Western blot of the expression of Cas9 in BCG induced with tetracycline over time (24, 48, 72, 96 or 120 h). The Western blots were probed with monoclonal anti-Cas9 antibody (1:1,000). Molecular weight markers (MW) are indicated in the left and the expected molecular weight of Cas9 indicated by an arrow (~160 kDa).

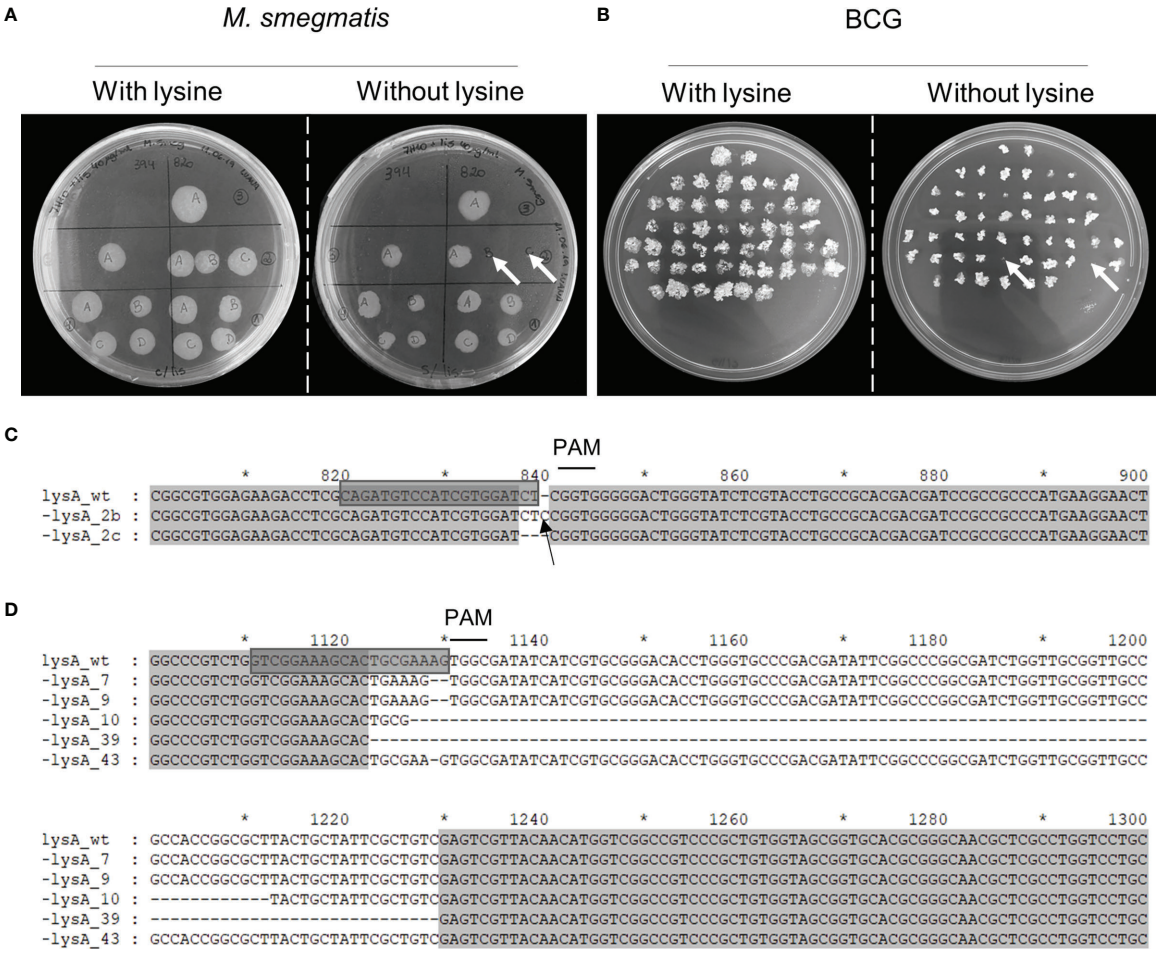

FIGURE 4 | Phenotypic screening and genotypic characterization of Smeg*ΔlysA* and BCG*ΔlysA*. After the induction of Cas9, the cultures were seeded on lysine-supplemented plates to recover all viable bacteria. The colonies of **(A)** *M. smegmatis*, and **(B)** BCG were then seeded on mirror plates with and without lysine. The colonies that did not grow on plates without lysine (white arrows) indicate a positive knock-out. The *lysA* genes from **(C)** Smeg*ΔlysA*, and **(D)** BCG*ΔlysA* were sequenced and compared to the wild-type sequence. The sgRNA used to target *lysA* is highlighted (grey box); the deleted nucleotides are represented by the dashed line; the inserted nucleotide is pointed out with a black arrow and the PAM site (NGG) is indicated with a line above. Numbering and asterisks represent the nucleotide positions regarding the full *lysA* gene sequence.

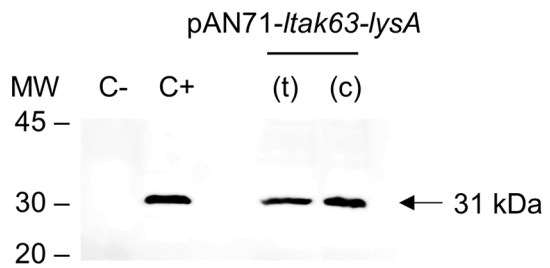

FIGURE 5 | Expression of LTAK63 in complemented auxotrophic BCG. Western blot of total protein extracts of wild-type BCG (C-); rBCG-LTAK63 (C+) and complemented auxotrophic strains obtained by transformation of BCG*ΔlysA* with pAN71-*ltak63-lysA* either in the tandem construct (t) or cassette (c). Western blots were probed with mouse anti-serum raised against rLTAK63 (1:1,000). Molecular weight markers (MW) are indicated and the expected molecular weight of LTAK63 is indicated by an arrow (~31 kDa).

In Vitro Growth of Complemented Auxotrophic BCG

We investigated whether the complemented auxotrophic BCG would show distinct *in vitro* growth in comparison to wild-type mycobacteria. It can be observed that both recombinant BCG strains showed growth comparable to the wild-type (**Supplementary Figure 7**). The rBCGΔ-LTAK63(t) was selected for the *in vivo* experiments, hereafter, named rBCGΔ-LTAK63.

Protection of Immunized Mice Against Intranasal Challenge With *Mtb*

BALB/c mice were immunized with BCG, rBCGΔ-LTAK63 or not immunized and were challenged with *Mtb* 90 days after. The group immunized with rBCGΔ-LTAK63 showed a 1.5 log CFU reduction in the lungs when compared to the control group and 0.5 log reduction when compared to the BCG group (**Figure 6A**). Histopathological findings typical in a *Mtb* infection in the mouse

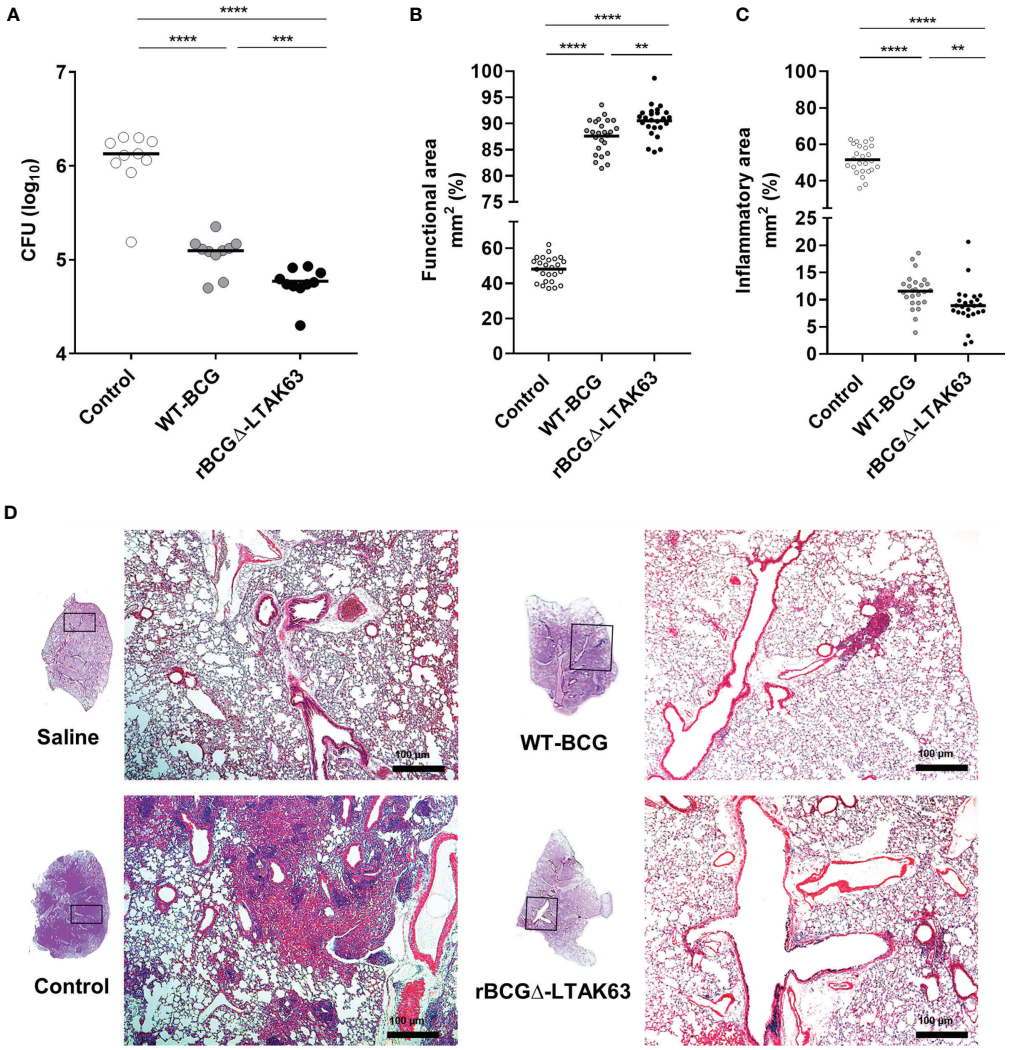

FIGURE 6 | Protection against *Mtb* challenge induced by immunization. Groups of BALB/c mice (n=10/group) immunized s.c. with BCG (WT-BCG), rBCGΔ-LTAK63, or not immunized (Control) were challenged i.n. with 500 CFU of *Mtb*. Thirty days after challenge, the lung was recovered to evaluate CFU **(A)**, functional lung area, represented by the intra-alveolar space **(B)** and inflammatory area **(C)**, represented by the inflammatory infiltrate of lung sections stained with H&E. Functional area and lung inflammation scores are presented as the mean percentage of inflammation for each mouse and the infiltrate is presented as cell counts per mm². **p < 0.01, ***p < 0.001 and ****p < 0.0001. Representative histopathology of lungs from naïve mice (Saline), infected only (Control), or immunized and challenged (BCG and rBCGΔ-LTAK63). Lung sections were stained with H&E (bar, 100 µm) **(D)**. Challenge experiments were performed twice.

model showed a granulomatous inflammatory process spread across the infected lungs. Immunization with rBCGΔ-LTAK63 showed increased protection of the lung tissue compared to BCG as evaluated by the functional lung area (**Figure 6B**). The effect of rBCGΔ-LTAK63 on leukocyte migration differs from that of BCG, displaying a reduction in the inflammatory score (**Figure 6C**). The improvement of the histopathological lesions is shown in the representative lung sections. Mice immunized with rBCGΔ-LTAK63 showed fewer lesions consisting of perivascular and peribronchiolar inflammatory infiltrates when compared with BCG-immunized mice (**Figure 6D**). Characterization of the cellular infiltrate showed the presence of mononuclear cells, neutrophils, and alveolar macrophages in the perivascular and peribronchiolar infiltrates; a general decrease in the total number of these cell types in the lungs of the groups immunized with BCG or rBCGΔ-LTAK63 indicates improved protection against lung pathology upon vaccination (**Figure 7**).

DISCUSSION

BCG is the only licensed vaccine against tuberculosis. It is especially important for children to prevent the development of severe forms of TB. However, its efficacy wanes over time and adults are less protected. In order to develop improved vaccines against tuberculosis, thousands of potential candidates are in

A

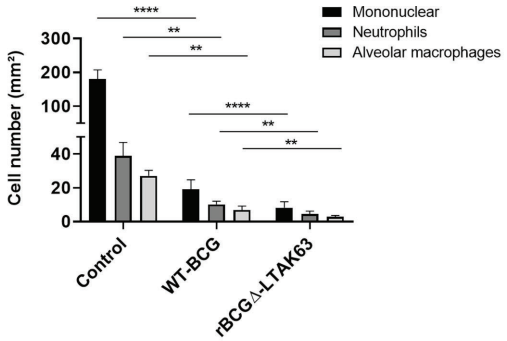

B

	Mononuclear	Neutrophils	Alveolar macrophages	Total cells
Control	180 ± 27.5	38.8 ± 8.0	27 ± 3.3	245.8
	73.2%	15.8%	11%	
WT-BCG	19.2 ± 5.5	10.2 ± 1.9	6.8 ± 2.4	36.2
	53%	28.2%	18.8%	
rBCGΔ-LTAK63	8.2 ± 3.5	4.4 ± 1.8	2.8 ± 0.8	15.4
	53%	28.6%	18.2%	

C

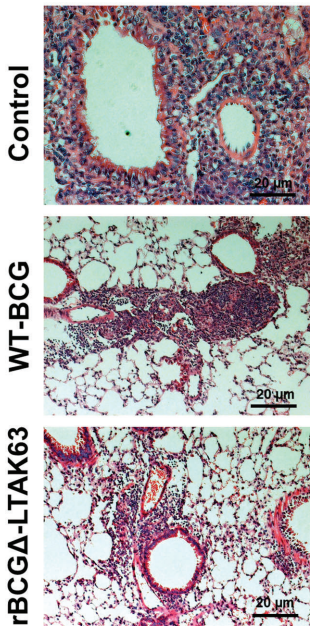

FIGURE 7 | Characterization of the cellular infiltrate in the lungs. Total number of mononuclear cells, neutrophils, and alveolar macrophages in the perivascular and peribronchiolar infiltrates in the lungs of BALB/c mice infected only (Control), or immunized and challenged (BCG and rBCGΔ-LTAK63) represented as cell counts per mm². **p < 0.01 and ****p < 0.0001 **(A)** and the actual cell numbers, percentage and total cell count in each group **(B)**. Five images at 40 x magnification per lung lobule, totaling 25 images per treatment, were randomly selected. For cell counting, ImageJ software and the Color Deconvolution 2 plugin were used to visualize and separate nuclei from the cytoplasm. Representative histopathology of lungs sections stained with H&E (bar, 20 µm) **(C)**. Challenge experiments were performed twice.

the discovery phase, hundreds have undergone preclinical trials in animal models, but only few candidates passed to clinical studies in humans (23). Among the most promising vaccine candidates are the live attenuated VPM1002 and MTBVAC. Interestingly, both vaccines required the generation of genomic mutations. While in VPM1002 it was necessary to disrupt the *ureC* gene – to provide an optimal environment for the cytolysin's activity. The insertion of lysteriolysin gene at the *ureC* locus demanded the use of a hygromycin marker for selection, which removal "was technically extremely challenging" (24). On the other hand, MTBVAC was obtained by deletion of two independent genes, *fadD26* and *phoP* (25). To achieve such mutations, a stepwise insertion/deletion process, comprising 4 different steps, was necessary (26). All these time-consuming and labor-intensive procedures could be avoided with the use of CRISPR/Cas9.

In our approach, we constructed an all-in-one vector containing the CRISPR/Cas9 elements required for the generation of the gene knock-outs in one step. To enable better control over the expression of Cas9 and sgRNA, we chose to use tetracycline-inducible promoters for both. The peak of Cas9 expression was observed at 8 h in *M. smegmatis* and 24-48 h for BCG. Lower levels of Cas9 expression were observed with prolonged incubation. Other studies have also observed that longer incubations are not necessary to induce Cas9 or other nucleases (13). The use and characterization of inducible promoters in CRISPR/Cas systems are important since continuous induction could lead to undesired mutations at unknown genomic *loci*.

To obtain the disruption of *lysA*, three sgRNA for *M. smegmatis* and two for BCG were designed. In *M. smegmatis*, the transformation with one of the selected sgRNA constructs did not produce any transformants. Between the two that did generate transformants, functional knock-outs were observed in only one. In BCG, the two constructs produced transformants, but knock-outs were observed in only one. Interestingly, plasmid constructs that induced the functional knock-out of *lysA* contained sgRNAs targeting the positive strand. It should be noted that we used a phenotypic screening to evaluate knock-outs and therefore silent mutations e.g. those maintaining the original reading frame, were not detected by this approach. All the mutations induced by CRISPR/Cas9 were characterized by the removal of nucleotides which indicates the action of non-homologous end-joining (NHEJ) DNA repair mechanisms in these cases. In *M. smegmatis*, one of the knock-outs had an extra nucleotide near the PAM site which is also a possibility in this particular strain (16). While most bacteria employ homologous recombination (HR) to repair double-strand breaks (DBS) in their DNA, mycobacteria have developed additional repair mechanisms. Besides HR, NHEJ and SSA (single-strand

annealing) are functional and described as not redundant but rather defined as distinct DSB repair pathways (27). As CRISPR/Cas9 exploits the DNA repair mechanisms to generate the mutations in the host genomes, further studies to understand the interplay between these repair systems are necessary. For instance, it may be possible to favor the HR repair and the consequently knock-in of sequences by disrupting key gene proteins (such as *ku* and *ligD*) to abolish NHEJ-mediated repair, or by inducing the overexpression of HR-related proteins (27).

We applied CRISPR/Cas9 to obtain an unmarked and scarless gene editing, thus resulting in a lysine auxotrophic BCG strain which was later complemented to stably express the LTAK63 adjuvant. The use of auxotrophic complementation is an interesting approach to obtain unmarked heterologous expression and increase the stability of the construct. On the other hand, it can also result in impaired growth since the level of LysA expressed can be different from that of the original wild-type strain. Here, we evaluated two different constructs using *lysA* complementation either in tandem with *ltak63* [pAN71-*ltak63-lysA*(t)] or each gene with its own expression cassette [pAN71-*ltak63-lysA*(c)]. The construct in tandem is driven by the pAN promoter, which is considered a weak mycobacterial promoter (28). If the expression of LysA is too low, then it could also affect BCG's fitness and the protection induced against *Mtb*. Alternatively, the pAN71-*ltak63-lysA*(c) construct includes another promoter for the expression of *lysA*, the pGrOEL. The addition of another expression cassette may decrease plasmid stability and compromise the expression of LTAK63. Our data show that whichever strategy used for the expression of LTAK63 and LysA, the growth of recombinant BCG strains is comparable to the wild-type strain. More importantly, the complemented strains generated here were able to express the LTAK63 antigen at levels comparable to the original rBCG-LTAK63 construct, which is imperative in order to obtain improved protection against *Mtb* (5).

Immunization of mice with the complemented auxotrophic BCG expressing LTAK63 (rBCGΔ-LTAK63) confirmed its superior protection against *Mtb* challenge. Previews reports demonstrated that mice immunized with rBCG-LTAK63 and challenged intratracheally with *Mtb* displayed a 1-2 log reduction of CFU in the lungs in comparison to wild-type BCG. Here, we observed that mice immunized with rBCGΔ-LTAK63 and challenged with *Mtb* exhibit a 0.5 log reduction in comparison to wild-type BCG. This difference may be explained by the distinct routes and bacterial loads involved in the challenge (intratracheal, $1x10^5$ CFU, and intranasal, 500 CFU) (5). The intranasal route has the advantage of being less invasive and better mimics the natural *Mtb* infection (29). Accordingly, the protective effects on lung tissue during the clinical course of the infection was clear in the groups of mice immunized with BCG or rBCGΔ-LTAK63. However, it is notorious that immunization with rBCGΔ-LTAK63 intensified the protective effects evaluated as functional lung area and modulated the leukocyte response in comparison to BCG. The reduction in the cellular infiltrate after the *Mtb* challenge may, in fact, be associated with a faster and improved resolution of the infection induced by the immunization of rBCGΔ-LTAK63.

In this work we produced lysine-deficient mutants using a one-step induction of CRISPR/Cas9; furthermore, we demonstrated the efficient complementation with *lysA*-containing vectors also expressing LTAK63 adjuvant. Immunization with rBCGΔ-LTAK63 induced better protection against *Mtb* challenge. The data presented here shows the practical application of CRISPR/Cas9 towards the generation of new and improved TB vaccines.

DATA AVAILABILITY STATEMENT

The original contributions presented in the study are included in the article/**Supplementary Material**. Further inquiries can be directed to the corresponding author.

ETHICS STATEMENT

The animal study was reviewed and approved by Ethics Committee of Instituto Butantan (CEUAIB) (Permit number 8591010817).

AUTHOR CONTRIBUTIONS

LL and AK conceived and designed the experiments. LM, MT, DF, and SE performed the experiments and collected data. LM, MT, DF, SE, AC-T, LL, and AK processed and analyzed the data. LM, MT, SE, LL, and AK wrote the manuscript. All authors contributed to the article and approved the submitted version.

FUNDING

We acknowledge the support from FAPESP (Projects 2017/24832-6, 2017/17218-0 and 2019/06454-0) and Fundação Butantan.

ACKNOWLEDGMENTS

We would like to thank Drs. Stewart Cole and Brigitte Gicquel, from Institut Pasteur, Paris, for kindly providing the pJH152 and pLA71 vectors, respectively.

SUPPLEMENTARY MATERIAL

The Supplementary Material for this article can be found online at: https://www.frontiersin.org/articles/10.3389/fimmu.2022.867195/full#supplementary-material

REFERENCES

1. World Health O. *Global Tuberculosis Report 2020*. Geneva: World Health Organization (2020).
2. Andersen P, Doherty TM. The Success and Failure of BCG — Implications for a Novel Tuberculosis Vaccine. *Nat Rev Microbiol* (2005) 3(8):656–62. doi: 10.1038/nrmicro1211
3. Marques-Neto LM, Piwowarska Z, Kanno AI, Moraes L, Trentini MM, Rodriguez D, et al. Thirty Years of Recombinant BCG: New Trends for a Centenary Vaccine. *Expert Rev Vaccines* (2021) 0(0):1–11. doi: 10.1080/14760584.2021.1951243
4. Nieuwenhuizen NE, Kulkarni PS, Shaligram U, Cotton MF, Rentsch CA, Eisele B, et al. The Recombinant Bacille Calmette–Guérin Vaccine VPM1002: Ready for Clinical Efficacy Testing. *Front Immunol* (2017) 8:1147. doi: 10.3389/fimmu.2017.01147
5. Nascimento IP, Rodriguez D, Santos CC, Amaral EP, Rofatto HK, Junqueira-Kipnis AP, et al. Recombinant BCG Expressing LTAK63 Adjuvant Induces Superior Protection Against Mycobacterium Tuberculosis. *Sci Rep* (2017) 7(1):2109. doi: 10.1038/s41598-017-02003-9
6. Borsuk S, Mendum TA, Fagundes MQ, Michelon M, Cunha CW, McFadden J, et al. Auxotrophic Complementation as a Selectable Marker for Stable Expression of Foreign Antigens in Mycobacterium Bovis BCG. *Tuberculosis (Edinburgh Scotland)* (2007) 87(6):474–80. doi: 10.1016/j.tube.2007.07.006
7. Seixas FK, Borsuk S, Fagundes MQ, Hartwig DD, Silva ÉFD, Cerqueira GM, et al. Stable Expression of Leptospira Interrogans Antigens in Auxotrophic Mycobacterium Bovis BCG. *Biol Res* (2010) 43(1):13–8. doi: 10.4067/S0716-97602010000100003
8. Nascimento IP, Dias WO, Quintilio W, Hsu T, Jacobs WR, Leite LCC. Construction of an Unmarked Recombinant BCG Expressing a Pertussis Antigen by Auxotrophic Complementation: Protection Against Bordetella Pertussis Challenge in Neonates. *Vaccine* (2009) 27(52):7346–51. doi: 10.1016/j.vaccine.2009.09.043
9. Andrade PM, Chade DC, Borra RC, Nascimento IP, Villanova FE, Leite LCC, et al. The Therapeutic Potential of Recombinant BCG Expressing the Antigen S1PT in the Intravesical Treatment of Bladder Cancer. *Urol Oncol: Semin Orig Investigations* (2010) 28(5):520–5. doi: 10.1016/j.urolonc.2008.12.017
10. Rodriguez D, Goulart C, Pagliarone AC, Silva EP, Cunegundes PS, Nascimento IP, et al. *In Vitro* Evidence of Human Immune Responsiveness Shows the Improved Potential of a Recombinant BCG Strain for Bladder Cancer Treatment. *Front Immunol* (2019) 10:1460. doi: 10.3389/fimmu.2019.01460
11. Kanno AI, Boraschi D, Leite LCC, Rodriguez D. Recombinant BCG Expressing the Subunit 1 of Pertussis Toxin Induces Innate Immune Memory and Confers Protection Against Non-Related Pathogens. *Vaccines* (2022) 10(2). doi: 10.3390/vaccines10020234
12. Malaga W, Perez E, Guilhot C. Production of Unmarked Mutations in Mycobacteria Using Site-Specific Recombination. *FEMS Microbiol Lett* (2003) 219(2):261–8. doi: 10.1016/S0378-1097(03)00003-X
13. Doudna JA, Charpentier E. Genome Editing. The New Frontier of Genome Engineering With CRISPR-Cas9. *Sci (New York NY)* (2014) 346(6213):1258096. doi: 10.1126/science.1258096
14. Choudhary E, Thakur P, Pareek M, Agarwal N. Gene Silencing by CRISPR Interference in Mycobacteria. *Nat Commun* (2015) 6:6267. doi: 10.1038/ncomms7267
15. Singh AK, Carette X, Potluri L-P, Sharp JD, Xu R, Prisic S, et al. Investigating Essential Gene Function in Mycobacterium Tuberculosis Using an Efficient CRISPR Interference System. *Nucleic Acids Res* (2016) 44(18):e143. doi: 10.1093/nar/gkw625
16. Yan M-Y, Li S-S, Ding X-Y, Guo X-P, Jin Q, Sun Y-C. A CRISPR-Assisted Nonhomologous End-Joining Strategy for Efficient Genome Editing in Mycobacterium Tuberculosis. *mBio* (2020) 11(1). doi: 10.1128/mBio.02364-19
17. Bergmans HE, van Die IM, Hoekstra WP. Transformation in Escherichia Coli: Stages in the Process. *J Bacteriol* (1981) 146(2):564–70. doi: 10.1128/jb.146.2.564-570.1981
18. Parish T, Stoker NG. Electroporation of Mycobacteria. *Methods Mol Biol (Clifton NJ)* (1998) 101:129–44. doi: 10.1385/0-89603-471-2:129
19. Pavelka MS, Jacobs WR. Comparison of the Construction of Unmarked Deletion Mutations in Mycobacterium Smegmatis, Mycobacterium Bovis Bacillus Calmette-Guérin, and Mycobacterium Tuberculosis H37Rv by Allelic Exchange. *J Bacteriol* (1999) 181(16):4780–9. doi: 10.1128/JB.181.16.4780-4789.1999
20. Jiang Y, Chen B, Duan C, Sun B, Yang J, Yang S. Multigene Editing in the Escherichia Coli Genome *via* the CRISPR-Cas9 System. *Appl Environ Microbiol* (2015) 81(7):2506–14. doi: 10.1128/AEM.04023-14
21. Mukundan R. Analysis of Image Feature Characteristics for Automated Scoring of HER2 in Histology Slides. *J Imaging* (2019) 5(3):35. doi: 10.3390/jimaging5030035
22. Salaets T, Tack B, Gie A, Pavie B, Sindhwani N, Jimenez J, et al. A Semi-Automated Method for Unbiased Alveolar Morphometry: Validation in a Bronchopulmonary Dysplasia Model. *PloS One* (2020) 15(9):e0239562. doi: 10.1371/journal.pone.0239562
23. Martin C, Aguilo N, Marinova D, Gonzalo-Asensio J. Update on TB Vaccine Pipeline. *Appl Sci* (2020) 10(7):2632. doi: 10.3390/app10072632
24. Kaufmann SH, Cotton MF, Eisele B, Gengenbacher M, Grode L, Hesseling AC, et al. The BCG Replacement Vaccine VPM1002: From Drawing Board to Clinical Trial. *Expert Rev Vaccines* (2014) 13(5):619–30. doi: 10.1586/14760584.2014.905746
25. Arbues A, Aguilo JI, Gonzalo-Asensio J, Marinova D, Uranga S, Puentes E, et al. Construction, Characterization and Preclinical Evaluation of MTBVAC, the First Live-Attenuated M. Tuberculosis-Based Vaccine to Enter Clinical Trials. *Vaccine* (2013) 31(42):4867–73. doi: 10.1016/j.vaccine.2013.07.051
26. Martin C, Williams A, Hernandez-Pando R, Cardona PJ, Gormley E, Bordat Y, et al. The Live Mycobacterium Tuberculosis phoP Mutant Strain Is More Attenuated Than BCG and Confers Protective Immunity Against Tuberculosis in Mice and Guinea Pigs. *Vaccine* (2006) 24(17):3408–19. doi: 10.1016/j.vaccine.2006.03.017
27. Gupta R, Barkan D, Redelman-Sidi G, Shuman S, Glickman MS. Mycobacteria Exploit Three Genetically Distinct DNA Double-Strand Break Repair Pathways. *Mol Microbiol* (2011) 79(2):316–30. doi: 10.1111/j.1365-2958.2010.07463.x
28. Nascimento LV, Santos CC, Leite LCC, Nascimento IP. Characterisation of Alternative Expression Vectors for Recombinant Bacillus Calmette-Guérin as Live Bacterial Delivery Systems. *Memórias Do Instituto Oswaldo Cruz* (2020) 115:e190347. doi: 10.1590/0074-02760190347
29. Logan KE, Gavier-Widen D, Hewinson RG, Hogarth PJ. Development of a Mycobacterium Bovis Intranasal Challenge Model in Mice. *Tuberculosis (Edinburgh Scotland)* (2008) 88(5):437–43. doi: 10.1016/j.tube.2008.05.005

Conflict of Interest: LL has a patent application on the use of rBCG-LTAK63 as vaccine against *Mtb*. The funders had no role in the design of the study, in the collection, analyses, or interpretation of data, in the writing of the manuscript, or in the decision to publish the results.

The remaining authors declare that the research was conducted in the absence of any commercial or financial relationships that could be construed as a potential conflict of interest.

frontiers in Immunology

ORIGINAL RESEARCH
published: 31 March 2022
doi: 10.3389/fimmu.2022.848835

Early-Life Antibiotic Exposure Associated With Varicella Occurrence and Breakthrough Infections: Evidence From Nationwide Pre-Vaccination and Post-Vaccination Cohorts

Teng-Li Lin[1,2], Yi-Hsuan Fan[3], Yi-Ling Chang[2], Hsiu J. Ho[4], Li-Lin Liang[5], Yi-Ju Chen[2,6,7] and Chun-Ying Wu[4,7,8,9,10]**

[1] Department of Dermatology, Dalin Tzu Chi Hospital, Buddhist Tzu Chi Medical Foundation, Chiayi, Taiwan, [2] Department of Dermatology, Taichung Veterans General Hospital, Taichung, Taiwan, [3] Department of Pediatrics, Chung Shan Medical University Hospital, Taichung, Taiwan, [4] Institute of Biomedical Informatics and Research Center for Epidemic Prevention, National Yang Ming Chiao Tung University, Taipei, Taiwan, [5] Institute of Public Health, School of Medicine, National Yang Ming Chiao Tung University, Taipei, Taiwan, [6] School of Life Sciences, National Chung-Hsing University, Taichung, Taiwan, [7] Faculty of Medicine and Institute of Clinical Medicine, National Yang Ming Chiao Tung University, Taipei, Taiwan, [8] Division of Translational Research, Taipei Veterans General Hospital, Taipei, Taiwan, [9] Department of Public Health, China Medical University, Taichung, Taiwan, [10] National Institute of Cancer Research and Institute of Population Health Science, National Health Research Institutes, Miaoli, Taiwan

Background: Antibiotic-driven dysbiosis may impair immune function and reduce vaccine-induced antibody titers.

Objectives: This study aims to investigate the impacts of early-life antibiotic exposure on subsequent varicella and breakthrough infections.

Methods: This is a nationwide matched cohort study. From Taiwan's National Health Insurance Research Database, we initially enrolled 187,921 children born from 1997 to 2010. Since 2003, the Taiwan government has implemented a one-dose universal varicella vaccination program for children aged 1 year. We identified 82,716 children born during the period 1997 to 2003 (pre-vaccination era) and 48,254 children born from July 1, 2004, to 2009 (vaccination era). In the pre-vaccination era, 4,246 children exposed to antibiotics for at least 7 days within the first 2 years of life (Unvaccinated A-cohort) were compared with reference children not exposed to antibiotics (Unvaccinated R-cohort), with 1:1 matching for gender, propensity score, and non-antibiotic microbiota-altering medications. Using the same process, 9,531 children in the Vaccinated A-cohort and Vaccinated R-cohort were enrolled from the vaccination era and compared. The primary outcome was varicella. In each era, demographic characteristics were compared, and cumulative incidences of varicella were calculated. Cox proportional hazards model was used to examine associations.

OPEN ACCESS

Edited by:
Lee Mark Wetzler, Boston University, United States

Reviewed by:
Anastasia N. Vlasova, The Ohio State University, United States
Talia Sainz, University Hospital La Paz, Spain

***Correspondence:**
Yi-Ju Chen
yjchenmd@vghtc.gov.tw
Chun-Ying Wu
dr.wu.taiwan@gmail.com

Specialty section:
This article was submitted to Vaccines and Molecular Therapeutics, a section of the journal Frontiers in Immunology

Received: *05 January 2022*
Accepted: *10 March 2022*
Published: *31 March 2022*

Citation:
Lin T-L, Fan Y-H, Chang Y-L, Ho HJ, Liang L-L, Chen Y-J and Wu C-Y (2022) Early-Life Antibiotic Exposure Associated With Varicella Occurrence and Breakthrough Infections: Evidence From Nationwide Pre-Vaccination and Post-Vaccination Cohorts. Front. Immunol. 13:848835. doi: 10.3389/fimmu.2022.848835

Results: In the pre-vaccination era, the 5-year cumulative incidence of varicella in the Unvaccinated A-cohort (23.45%, 95% CI 22.20% to 24.70%) was significantly higher than in the Unvaccinated R-cohort (16.72%, 95% CI 15.62% to 17.82%) (p<.001). In the vaccination era, a significantly higher 5-year cumulative incidence of varicella was observed in the Vaccinated A-cohort (1.63%, 95% 1.32% to 1.93%) than in the Vaccinated R-cohort (1.19%, 95% CI 0.90% to 0.45%) (p=0.006). On multivariate analyses, early-life antibiotic exposure was an independent risk factor for varicella occurrence in the pre-vaccination (adjusted hazard ratio [aHR] 1.92, 95% CI 1.74 to 2.12) and vaccination eras (aHR 1.66, 95% CI 1.24 to 2.23). The use of penicillins, cephalosporins, macrolides, or sulfonamides in infancy was all positively associated with childhood varicella regardless of vaccine administration.

Conclusions: Antibiotic exposure in early life is associated with varicella occurrence and breakthrough infections.

Keywords: varicella, breakthrough infection, vaccine, antibiotic, microbiota, dysbiosis, pediatric population

INTRODUCTION

The early-life microbiome has a fundamental role in human immunity. Indigenous microbiota provides crucial signals for maturation and modulation of the immune system (1, 2). In contrast, dysbiosis in infancy might cause stunting and dysregulation of immunity (3, 4). The composition of gut microbiota also correlates with vaccine immunogenicity (5). Evidence has suggested the association between early-life microbial colonization and sustainable vaccine-specific memory T-cells and antibody responses (6).

Exposure to medications, particularly antibiotics, is a common cause of dysbiosis (7, 8). Even short-term or low-dose antibiotics can disturb the delicate ecosystem of the infant microbiome (9, 10). Early-life antibiotic exposure has been linked to a higher risk of various conditions, including inflammatory bowel disease, type 2 diabetes, and atopic disorders (11–13). However, little is known about the effect of infantile antibiotic exposure on susceptibility to later-life infections. In addition, although antibiotic-driven dysbiosis has been found to impair vaccine responses (10, 14, 15), limitations are that most studies were conducted with a small sample size and in animal models or adults. Whether early-life antibiotic exposures decrease vaccine efficacy or increase the risk of breakthrough infections in the pediatric population remains to be elucidated.

Varicella was once associated with a significant impact on public health in Taiwan (16). Since the implementation of universal varicella vaccination (UVV) in 2003, disease transmission has been successfully controlled (17). However, varicella outbreaks among schoolchildren still occurred occasionally (18), and breakthrough infections continue to be reported despite high rates of national vaccination coverage (19). The present study was aimed to investigate the effect of early-life antibiotic exposure on childhood varicella risk and breakthrough infections.

MATERIALS AND METHODS

Data Source

We conducted a nationwide cohort study using Taiwan's National Health Insurance Research Database (NHIRD) from 1997 to 2013. The NHIRD contains detailed healthcare information from more than 99% of Taiwan's population of 25 million people. Diagnoses are documented in the NHIRD using codes based on the International Classification of Diseases, Revision 9, Clinical Modification (ICD-9-CM). The accuracy of diagnosis in the NHIRD has been validated (20, 21), and the data have been used extensively in clinical epidemiology and health service research (22, 23). Personal information, including body weight, height, lifestyle, occupation, and cluster history, is unavailable from the database. This study has been approved by the ethical review board of Taichung Veterans General Hospital (No. CE20224B).

Vaccination

The live attenuated varicella vaccine was approved for use in Taiwan in 1997. Two brands of OKA-strain varicella vaccines, Varivax (Merck) and Varilrix (GlaxoSmithKline) are available in Taiwan. The vaccines have been first provided free to children aged 1 year in Taipei City and Taichung City since 1998 and 1999, respectively. In 2003, the Taiwan government implemented the UVV program, targeting 1-year-old children. The self-paid second-dose booster has been recommended for children aged 4 to 6 years. Despite unavailable 2-dose vaccination rates, the cumulative coverage rate of at least one dose of varicella vaccine among children born after July 1, 2004, has reached more than 94% to date (24).

Study Design and Population

From the NHIRD, children born from 1997 to 2010 were eligible for enrollment. Children born from 1997 to 2003 and living in regions other than Taipei City and Taichung City were

considered unvaccinated (pre-vaccination era). Children born during July 1, 2004, and 2009 were deemed vaccinated (vaccination era). We excluded children with a follow-up period of less than one year, death registration, malignancy, immunodeficiency disorders, white blood cell disorders, transplantation, chemotherapy, or immunotherapy before varicella development. The diagnostic codes for these comorbidities are presented in **Supplemental Table 1**.

Early life, especially from conception to 2 years of age, is a critical window for microbiota development and immune maturation (25, 26). In the vaccination era, children who received antibiotics for at least 7 days within the first 2 years of life were included in the antibiotic cohort (Vaccinated A-cohort). The reference cohort (Vaccinated R-cohort) comprised children who had not received antibiotics. We identified the Unvaccinated A-cohort and the Unvaccinated R-cohort in the pre-vaccination era using the same process.

The index date was defined as the first day of the third year of life. All sampled children were followed up from age 2 years to the development of outcome of interest or death. Each child was followed up for a maximum of 5 years.

In each era, 1:1 matching of children in both cohorts was carried out for gender, propensity score, and non-antibiotic microbiota-altering medications. The propensity score was calculated *via* logistic regression model (27) that included infectious diseases, non-bacterial gastroenteritis, and constipation (**Supplemental Table 1**). These have been common pediatric comorbidities that promote intestinal dysbiosis. Histamine type-2 receptor antagonists (H2RAs), proton pump inhibitors (PPIs), and laxatives have been found to cause perturbation of gut microbiota (28). Non-antibiotic microbiota-altering medication exposure was defined as using any of these drugs for at least 7 days within the first 2 years of life.

Outcome Measurement

The primary outcome was varicella with diagnostic code (ICD-9-CM code 052) in the NHIRD. Children with varicella before the index date were still censored during the follow-up. However, to evaluate the association between early-life antibiotic exposure and subsequent varicella, only varicella that occurred in children after 2 years of age was identified.

Breakthrough varicella has been defined as varicella occurring over 6 weeks after at least one dose of vaccination (17, 19). Since the age at varicella vaccination in Taiwan was previously reported to be 1 to 1.97 years (17), the identified varicella cases in the vaccination era were considered breakthrough events.

Covariate Assessment

Demographic factors such as gender, comorbidities, and medication were considered potential confounders. Comorbidities were defined as diseases based on diagnostic codes (**Supplemental Table 1**) after the index date. Exposure to drugs related to dysbiosis, including H2RAs, PPIs, or laxatives, was defined as the use of such medications for at least 7 days within the first 2 years of life. Exposure to immunomodulatory drugs, such as systemic corticosteroids and disease-modifying antirheumatic drugs, was defined as using these drugs for more than 30 days per year on average. The aforementioned medication is listed in **Supplemental Table 2**.

Statistical Analysis

We first analyzed the demographic data, comorbidities, and medications. The categorical variables and prevalence rates of varicella in the study cohorts of each era were compared using the chi-square test. The cumulative incidences of varicella were calculated using the Kaplan-Meier method. The differences in the full time-to-event distributions between the two cohorts of each era were tested *via* the 2-tailed log-rank test.

We next performed multivariate analyses with modified Cox proportional hazard models to determine whether antibiotic exposure is an independent risk factor for subsequent varicella. The adjusted variables were gender, hospital visit number during the follow-up period, and well-known factors for dysbiosis, including antibiotic exposure, use of non-antibiotic microbiota-altering medications, infectious diseases, non-bacterial gastroenteritis, and constipation. We also conducted sub-analyses to examine the risk of exposure to different antibiotics in early life on varicella development.

All data were managed *via* SAS 9.4 software (SAS Institute Inc., Cary, NC, USA) and the "cmprsk" package of R. The results are expressed as an estimated number with 95% confidence interval (CI).

RESULTS

Demographic Characteristics of the Study Cohorts

We initially enrolled 187,921 children born from 1997 to 2010 from Taiwan's NHIRD. Among them, 82,716 children not living in Taipei City or Taichung City were born from 1997 to 2003, and 48,254 children were born from July 1, 2004, to 2009. A total of 8,293 children with a follow-up period of less than 1 year or with comorbidities or therapy that may increase the risk of infections before the occurrence of varicella were excluded. Finally, 81,596 children were included in the pre-vaccination era group and 47,533 were included in the vaccination era group (**Figure 1**). The baseline characteristics of the children in both groups are presented in **Supplemental Table 3**.

In the pre-vaccination era, 69,430 children exposed to antibiotics for at least 7 days within the first 2 years were included in the Unvaccinated A-cohort, and 4,975 children in the reference group not exposed to antibiotics within the first 2 years of life were included in the Unvaccinated R-cohort. The baseline characteristics of children in both cohorts are shown in **Supplemental Table 4**. After matching for gender, propensity score, and non-antibiotic microbiota-altering medications at a ratio of 1:1, there were 4,246 children in each cohort (**Figure 1**). Using the same process, we selected subjects from the vaccination era, with 9,531 children each in the Vaccinated A-cohort and the Vaccinated R-cohort (**Figure 1**).

Demographic characteristics and comorbidities were comparable between the cohorts in each era, except higher

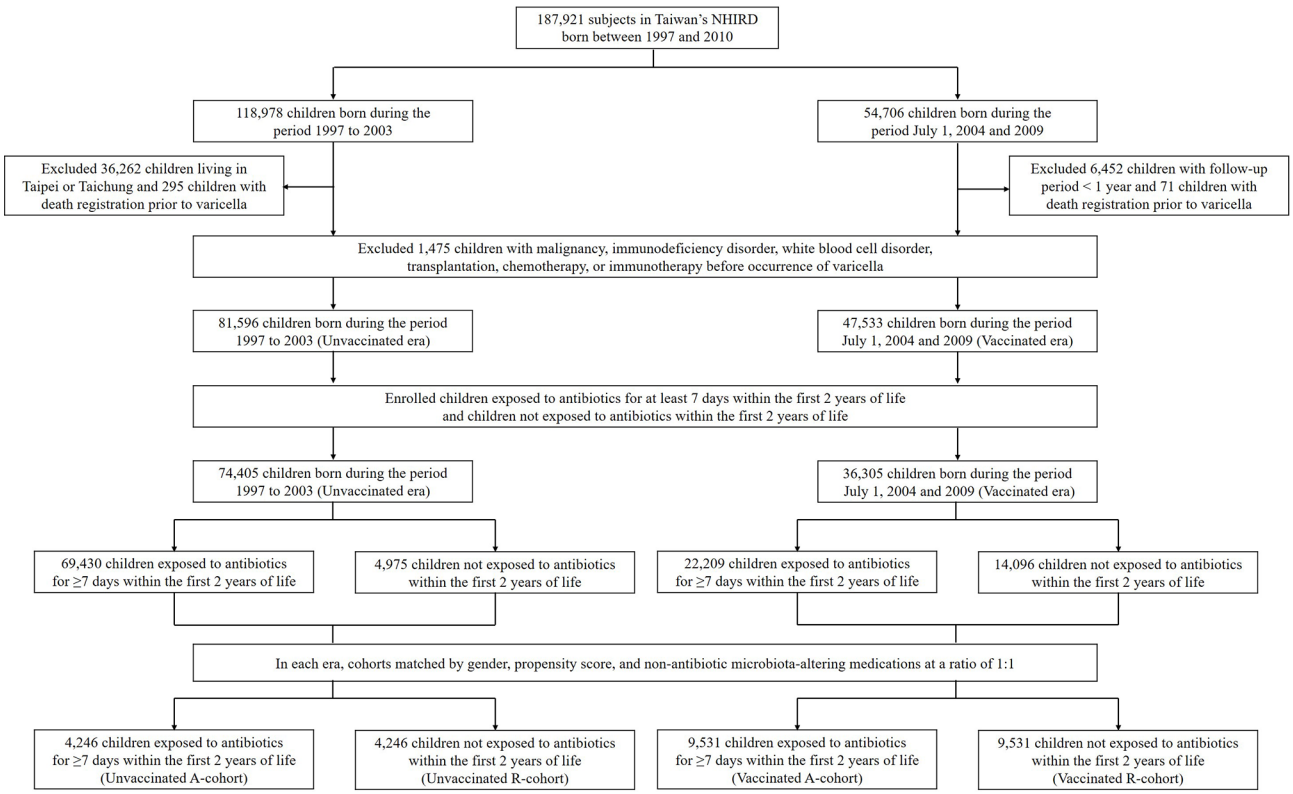

FIGURE 1 | Flow chart of the patient selection process. NHIRD, National Health Insurance Research Database; A-cohort, antibiotic cohort; R-cohort, reference cohort.

numbers of hospital visits in both A-cohorts compared to the respective R-cohorts (median 72 vs. 59 in pre-vaccination era, and 77 vs.71 in vaccination era) (**Table 1**). In the Unvaccinated A-cohort, penicillins (59.6%) were most common, followed by cephalosporins (33.4%), macrolides (32.0%), and sulfonamides (22.7%). In the Vaccinated A-cohort, penicillins (61.1%) and cephalosporins (15.4%) were most common (**Supplemental Table 5**). Ages at varicella occurrence and hospitalization for varicella were comparable between the cohorts in each era.

Cumulative Incidences of Varicella

A significantly higher 5-year cumulative incidence of varicella was observed in the pre-vaccination era group (22.22%, 95% confidence interval [CI] 21.94-22.51%) than in the vaccination era group (1.40%, 95% CI 1.27-1.53%) (p<.001) (**Supplemental Figure 1**).

In the pre-vaccination era, the 5-year cumulative incidence of varicella in the Unvaccinated A-cohort (23.45%, 95% CI 22.20-24.70%) was significantly higher than in the Unvaccinated R-cohort (16.72%, 95% CI 15.62-17.82%) (p<.001) (**Figure 2A**). In the vaccination era, a significantly higher 5-year cumulative incidence of varicella was observed in the Vaccinated A-cohort (1.63%, 95% 1.32-1.93%) than in the Vaccinated R-cohort (1.19%, 95% CI 0.90-1.45%) (p=0.006) (**Figure 2B**).

Multivariate Analyses

In the pre-vaccination era, antibiotic exposure for at least 7 days within the first 2 years of life was independently associated with varicella occurrence (adjusted hazard ratio [aHR] 1.92, 95% CI 1.74-2.12). This risk was weaker but still significant among children born in the vaccination era (aHR 1.66, 95% CI 1.24-2.23) (**Table 2**).

Further analyses demonstrated that exposure to a specific type of the commonly-used antibiotics, including penicillins (aHR 1.47, 95% CI 1.31-1.66), cephalosporins (aHR 1.19, 95% CI 1.04-1.36), macrolides (aHR 1.46, 95% CI 1.28-1.67), and sulfonamides (aHR 1.27, 95% CI 1.09-1.48), were also independent risk factors for varicella occurrence in the pre-vaccination era. However, exposure to these antibiotics in the vaccination era was positively associated with subsequent varicella but without statistical significance (**Table 2**).

DISCUSSION

This nationwide cohort study suggests that antibiotic exposure early in life is an independent risk factor for childhood varicella. Even though herd immunity has been reached in the vaccination era, a significantly higher incidence of breakthrough varicella is

TABLE 1 | Demographic characteristics and outcomes of matched study subjects in antibiotic and reference cohorts in the pre-vaccination and vaccination eras.

	Pre-vaccination era			Vaccination era		
	Antibiotic cohort[a] (N=4,426)	Reference cohort[a] (N=4,426)	P-value	Antibiotic cohort[a] (N=9,531)	Reference cohort[a] (N=9,531)	P-value
Age, years						
Mean ± SD	3.0 ± 0.0	3.0 ± 0.0	NA	3.0 ± 0.0	3.0 ± 0.0	NA
Median (IQR)	3.0 (3.0-3.0)	3.0 (3.0-3.0)	NA	3.0 (3.0-3.0)	3.0 (3.0-3.0)	NA
Gender, N (%)			>.999			>.999
Female	2,371 (53.6%)	2,371 (53.6%)		4,693 (49.2%)	4,693 (49.2%)	
Male	2,055 (46.4%)	2,055 (46.4%)		4,838 (50.8%)	4,838 (50.8%)	
Follow-up, years						
Mean ± SD	4.4 ± 1.3	4.5 ± 1.2	<.001	3.6 ± 1.3	3.5 ± 1.3	<.001
Median (IQR)	5.0 (5.0-5.0)	5.0 (5.0-5.0)	<.001	4.0 (2.5-5.0)	3.7 (2.3-5.0)	<.001
Hospital visits, N						
Mean ± SD	82.7 ± 59.2	70.5 ± 56.0	<.001	88.9 ± 58.3	81.0 ± 54.3	<.001
Median (IQR)	72.0 (41.0-113.0)	59.0 (29.0-99.8)	<.001	77.0 (47.0-118.0)	71.0 (42.0-109.0)	<.001
Antibiotic exposure, days						
Mean ± SD	39.2 ± 32.1	NA	NA	21.5 ± 24.5	NA	0.187
Median (IQR)	29.0 (16.0-52.0)	NA	NA	15.0 (10.0-24.0)	NA	0.220
Non-antibiotic microbiota-altering medication exposure,[b] N (%)	270 (6.1%)	270 (6.1%)	>.999	1,000 (10.5%)	1,000 (10.5%)	>.999
Immunomodulatory drugs,[c] N (%)						
Corticosteroids	13 (0.3%)	13 (0.3%)	>.999	29 (0.3%)	26 (0.3%)	0.787
DMARDs	1 (0.0%)	NA	>.999	1 (0.0%)	NA	>.999
Early-life infectious diseases,[d] N (%)						
All infections[e]	2,162 (48.8%)	2,148 (48.5%)	0.782	7,777 (81.6%)	7,748 (81.3%)	0.602
Chronic sinusitis	51 (1.2%)	49 (1.1%)	0.920	72 (0.8%)	89 (0.9%)	0.205
Acute otitis media	82 (1.9%)	88 (2.0%)	0.699	559 (5.9%)	549 (5.8%)	0.781
Acute upper respiratory infections	3,846 (86.9%)	3,847 (86.9%)	>.999	9,520 (99.9%)	9,523 (99.9%)	0.646
Acute bronchitis/bronchiolitis	2,460 (55.6%)	2,447 (55.3%)	0.797	8,502 (89.2%)	8,474 (88.9%)	0.531
Pneumonia	411 (9.3%)	415 (9.4%)	0.913	2,563 (26.9%)	2,569 (27.0%)	0.935
Urinary tract infections	29 (0.7%)	32 (0.7%)	0.797	142 (1.5%)	140 (1.5%)	0.952
Meningitis	6 (0.1%)	7 (0.2%)	>.999	4 (0.0%)	8 (0.1%)	0.386
Sepsis	49 (1.1%)	48 (1.1%)	>.999	60 (0.6%)	67 (0.7%)	0.593
Cellulitis/abscess	162 (3.7%)	163 (3.7%)	>.999	927 (9.7%)	955 (10.0%)	0.512
Impetigo	88 (2.0%)	95 (2.1%)	0.654	221 (2.3%)	220 (2.3%)	>.999
Comorbidities,[f] N (%)						
Congenital anomalies of heart	76 (1.7%)	53 (1.2%)	0.051	187 (2.0%)	117 (1.2%)	<.001
Kawasaki disease	9 (0.2%)	12 (0.3%)	0.662	42 (0.4%)	15 (0.2%)	<.001
Non-bacterial gastroenteritis	2,414 (54.5%)	2,419 (54.7%)	0.932	6,303 (66.1%)	6,250 (65.6%)	0.427
Constipation	851 (19.2%)	855 (19.3%)	0.936	2,189 (23.0%)	2,176 (22.8%)	0.836
Intussusception	190 (4.3%)	173 (3.9%)	0.391	317 (3.3%)	297 (3.1%)	0.436
Appendicitis	20 (0.5%)	22 (0.5%)	0.877	33 (0.3%)	25 (0.3%)	0.357
Febrile convulsion	10 (0.2%)	19 (0.4%)	0.137	86 (0.9%)	98 (1.0%)	0.415
Epilepsy	37 (0.8%)	34 (0.8%)	0.812	75 (0.8%)	51 (0.5%)	0.040
Outcomes						
Varicella, N (%)	1,038 (23.5%)	740 (16.7%)	<.001	117 (1.2%)	75 (0.8%)	0.003
Age at varicella onset, years						
Mean ± SD	5.3 ± 1.2	5.2 ± 1.2	0.664	5.1 ± 1.3	5.3 ± 1.3	0.187
Median (IQR)	5.2 (4.4~6.0)	5.2 (4.3~6.1)	0.688	5.0 (3.8~6.0)	5.3 (4.4~6.2)	0.220
Hospitalization for varicella	7 (0.2%)	3 (0.1%)	0.343	1 (0.0%)	2 (0.0%)	>.999

N, number; SD, standard deviation; IQR, interquartile range; NA, not available; DMARDs, disease-modifying antirheumatic drugs.

[a]*In each era, the antibiotic cohort and the reference cohort were matched by gender, propensity score, and non-antibiotics microbiota-altering medications at a ratio of 1:1.*

[b]*Non-antibiotic microbiota-altering medication exposure refer to the use of histamine type-2 receptor antagonists, proton pump inhibitors, or laxatives for at least 7 days within the first 2 years of life.*

[c]*Immunomodulatory drug exposure refers to the use of corticosteroids or DMARDs for at least 30 days after the index date.*

[d]*Early-life infectious diseases refer to infections with diagnostic code recorded in the database at least once before the index date.*

[e]*All infections include infectious diseases with codes 001-039 but 042 in the International Classification of Diseases, Ninth Revision [ICD-9].*

[f]*Comorbidities refer to comorbidities with diagnostic code recorded in the database at least once after the index date.*

observed in children exposed to antibiotics in early life. The present study adds to the mounting evidence that antibiotic-driven dysbiosis during infancy may cause sequelae linked with immune dysfunction, including increased susceptibility to infections.

Commensal-pathogen interactions involve the direct microbiota-related colonization resistance and the indirect microbiome-mediated immune modulation (29). Commensal microbiota can limit colonization of the invading pathogen through upregulating epithelial barrier function, competition

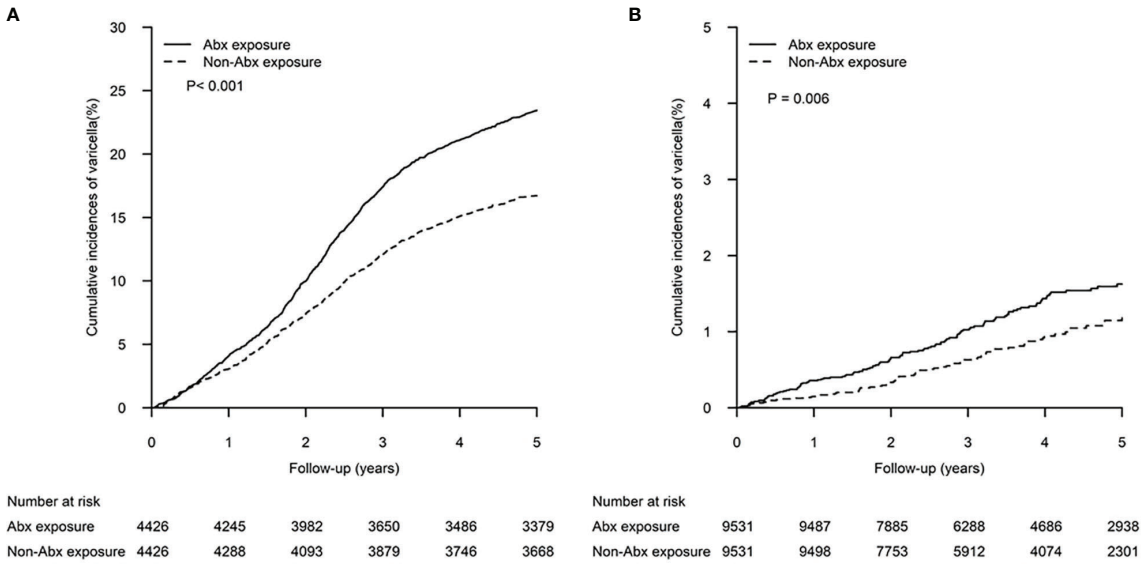

FIGURE 2 | Cumulative incidences of varicella in patients exposed to antibiotics within the first 2 years of life and matched controls. The differences between the two study cohorts in the **(A)** pre-vaccination era and **(B)** vaccination era were determined by log-rank test.

TABLE 2 | Multivariate analyses of antibiotic effects for varicella in the pre-vaccination and vaccination eras.

	aHR (95% CI)[a]	
	Pre-vaccination era	**Vaccination era**
Antibiotic exposures	1.92 (1.74-2.12)	1.66 (1.24-2.23)
Penicillins[b]	1.47 (1.31-1.66)	1.28 (0.94-1.74)
Cephalosporins[b]	1.19 (1.04-1.36)	1.41 (0.88-2.26)
Macrolides[b]	1.46 (1.28-1.67)	1.25 (0.67-2.34)
Sulfonamides[b]	1.27 (1.09-1.48)	1.27 (0.59-2.73)

aHR, adjusted hazard ratio; CI, confidence interval.

[a]*Adjusted for gender, hospital visit number, antibiotic exposure, non-antibiotic microbiota-altering medication, infections within the first 2 years of life, non-bacterial gastroenteritis, and constipation.*

[b]*Substitution of specific type of antibiotic for any type of antibiotic in the same model on multivariate analyses.*

for specific resources, and bactericidal or bacteriostatic effects (29, 30). Eubiotic microbiota also supports healthy immune development, shaping optimal innate and acquired immune responses against infective challenges (1, 2).

Evidence has demonstrated that a decrease in bacterial taxa, vacant nutrient niches, and metabolic environment changes after antibiotic administration predispose individuals to certain infections (31, 32), whereas the commensals may progressively return to baseline following antibiotic cessation (33). On the other hand, antibiotic-driven dysbiosis, especially in early life, might result in enduring immune alterations and long-lasting health impacts (3, 4). Animal studies have demonstrated that infant mice exposed to antibiotics had reduced and dysfunctional interferon-γ-producing CD8 T cells, resulting in subsequent increased mortality from vaccinia virus infection (34). In humans, children exposed to early-life antibiotics have been found to exhibit lower infection-induced cytokines, including interleukin 1β, interferon α, interferon γ, tumor necrosis factor α, and IP10 protein (35). Our results align with these immunological findings and support the microbiome-immune-infection axis theory. Early-life antibiotic exposure is associated with dysbiosis and impaired anti-infectious immunity and increases susceptibility to future varicella infections.

The role of the microbiome in the modulation of vaccine immunogenicity has recently been addressed (5). Several observational studies have documented the correlation between microbiota composition, such as the abundance of Bifidobacterium and Bacteroides species, and vaccine responses (6, 36, 37). Immunomodulatory molecules derived from microbiota, such as flagellin, peptidoglycan, and lipopolysaccharides, regulate T cell priming and immunoglobulin production in response to antigenic stimulation (36, 38, 39). Increasing data also suggests that epitopes encoded by the microbiota can cross-reactive with pathogen-encoded epitopes, presumably with vaccine-encoded epitopes (40, 41).

Despite the association between microbiome and vaccine responses, controversy exists over the influence of microbial perturbation on immunization. Antibiotic-driven dysbiosis impairs vaccine immunogenicity in infant mice but not in adult mice (14). From human research, adults with low pre-existing immunity have been found to present markedly reduced post-vaccination antibody titers after experiencing antibiotic treatment (10). Nevertheless, antibiotic exposure in early life has not significantly affected immunogenicity induced by routine infant vaccines, while sample sizes of these studies were modest (42, 43). Additionally, effects of prebiotics or probiotics on vaccine response are variable, depending on the antigens, probiotic strains, and population (44–46). To date, none of these microbiota-targeted interventions have been transferred from research into clinical practice. Our study assessed incidence

of breakthrough varicella among children exposed to early-life antibiotics. Although the UVV program has provided robust protection, infantile antibiotic exposure was still an independent risk factor for childhood breakthrough varicella. Such risk might result from increased varicella pathogenicity following antibiotic exposure overwhelming the vaccine protective efficacy or alteration of vaccine responses induced by antibiotic-driven dysbiosis. Further studies are needed to clarify the effects of early-life antibiotic exposure on immunization and vaccine efficacy.

The microbiota changes related to antibiotics depend on the type of antibiotic used. Previous studies have suggested that almost all types of antibiotics affect gut microbiota. The penicillin family of antibiotics, such as amoxicillin, piperacillin, and ticarcillin, may increase the abundance of Enterococcus spp. and decrease the abundance of anaerobes (47). Cephalosporins, quinolones, and sulfonamides have been associated with abundant Enterobacteriaceae except for Escherichia coli (47). Macrolide treatment has been linked to long-term gut microbiota perturbations among pre-school children, including depletion of Actinobacteria and increases in Bacteroidetes and Proteobacteria (48). The antimicrobial spectrum also influences the impact of antibiotics on the immune response to vaccination. An adult study has demonstrated that the proportion of vaccinees with a more than 2-fold anti-rotavirus antibody titer by 7 days post-vaccination was significantly higher among subjects treated with vancomycin only than those treated with broad-spectrum antibiotics (15). In the present study, early-life exposure to penicillins, cephalosporins, macrolides, or sulfonamides were all independent risk factors for childhood varicella in the pre-vaccination era. The risk of breakthrough varicella due to exposure to these antibiotics in the vaccination era was also observed, although without statistical significance owing to the small number of cases. Relationship between the risk and antimicrobial spectrum of the administered antibiotic remains to be elucidated, since we only examined the effects of using different types of antibiotics rather than the specific antibiotic on varicella occurrence. Overall, caution is warranted in prescribing any type of antibiotic to infants despite their benefits. It should also be taken into account the effects on the human microbiome when administering antibiotic therapy.

Our study has several strengths. The population-based cohort study design enabled us to assess the association between antibiotic exposure and varicella infections. By utilizing the nationwide NHIRD, we enrolled a large sample size, which prevented selection bias, allowing us to identify relatively rare conditions such as post-vaccination infection, and provide reliability in terms of statistics with a smaller margin of error.

Despite these strengths, there are several limitations. First, as this was an observational study, we could only report an association between antibiotic exposure and subsequent varicella but could not infer causality. Second, patient-specific information such as lifestyle, contact history, seeking healthcare in private practice, and over-the-counter medication use was unavailable from the NHIRD. To minimize biases, cohorts possessed comparable characteristics after matching gender, propensity score, and non-antibiotic microbiota-altering medications. We also performed multivariable analyses to adjust for potential confounders. Third, the specific date of vaccination, the total number of varicella vaccines administered, whether concomitant vaccinations were used or not, and the interval from antibiotic exposure to vaccination were not recorded in the dataset. Therefore, it is difficult to assess the effects of antibiotic exposure on immunization. Instead, we reported the association between antibiotic therapy in infancy and varicella during childhood regardless of herd immunity. Finally, as our study focused on varicella, the generalizability of our results may be limited. Nevertheless, it provided valuable information on the microbiome-immune-infection axis theory.

CONCLUSIONS

In conclusion, children exposed to antibiotics in infancy are associated with varicella later in life. Antibiotic exposure is an independent risk factor for varicella occurrence, even though herd immunity has been reached. These findings suggest caution when administering antibiotics in early life to prevent increased infection susceptibility and poor vaccine efficacy.

DATA AVAILABILITY STATEMENT

The data analyzed in this study is subject to the following licenses/restrictions: All researchers who wish to use the NHIRD and its data subsets are required to sign a written agreement declaring that they have no intention of attempting to obtain information that could potentially violate the privacy of patients or care providers. Requests to access these datasets should be directed to Center for Biomedical Resources of NHRI, https://nhird.nhri.org.tw/en/Data_Protection.html.

ETHICS STATEMENT

The studies involving human participants were reviewed and approved by the ethical review board of Taichung Veterans General Hospital (No. CE20224B). Written informed consent from the participants' legal guardian/next of kin was not required to participate in this study in accordance with the national legislation and the institutional requirements.

AUTHOR CONTRIBUTIONS

Study concept and design: T-LL, Y-HF, Y-JC, C-YW. Statistical analysis: Y-LC, HH. Analysis and interpretation of data: T-LL, L-LL, Y-JC. Drafting of the manuscript: T-LL, Y-JC. Critical revision of the manuscript for important intellectual content: T-LL, C-YW, Y-JC. All authors read and approved the final manuscript.

FUNDING

This work is supported in part by the Ministry of Science and Technology, Taiwan (MOST 109-2327-B-010-005; 109-2410-H-110-016-MY2).

SUPPLEMENTARY MATERIAL

The Supplementary Material for this article can be found online at: https://www.frontiersin.org/articles/10.3389/fimmu.2022.848835/full#supplementary-material

REFERENCES

1. Gensollen T, Iyer SS, Kasper DL, Blumberg RS. How Colonization by Microbiota in Early Life Shapes the Immune System. *Science* (2016) 352:539–44. doi: 10.1126/science.aad9378
2. Rooks MG, Garrett WS. Gut Microbiota, Metabolites and Host Immunity. *Nat Rev Immunol* (2016) 16:341–52. doi: 10.1038/nri.2016.42
3. Tamburini S, Shen N, Wu HC, Clemente JC. The Microbiome in Early Life: Implications for Health Outcomes. *Nat Med* (2016) 22:713–22. doi: 10.1038/nm.4142
4. Ruff WE, Greiling TM, Kriegel MA. Host-Microbiota Interactions in Immune-Mediated Diseases. *Nat Rev Microbiol* (2020) 18:521–38. doi: 10.1038/s41579-020-0367-2
5. Lynn DJ, Benson SC, Lynn MA, Pulendran B. Modulation of Immune Responses to Vaccination by the Microbiota: Implications and Potential Mechanisms. *Nat Rev Immunol* (2022) 22:33–46. doi: 10.1038/s41577-021-00554-7
6. Huda MN, Ahmad SM, Alam MJ, Khanam A, Kalanetra KM, Taft DH, et al. Bifidobacterium Abundance in Early Infancy and Vaccine Response at 2 Years of Age. *Pediatrics.* (2019) 143:e20181489. doi: 10.1542/peds.2018-1489
7. Vangay P, Ward T, Gerber JS, Knights D. Antibiotics, Pediatric Dysbiosis, and Disease. *Cell Host Microbe* (2015) 175:553–64. doi: 10.1016/j.chom.2015.04.006
8. Ianiro G, Tilg H, Gasbarrini A. Antibiotics as Deep Modulators of Gut Microbiota: Between Good and Evil. *Gut.* (2016) 65:1906–15. doi: 10.1136/gutjnl-2016-312297
9. Rodriguez JG, Rogers AB, Robine N, Loke P, Blaser MJ. Altering the Intestinal Microbiota During a Critical Developmental Window has Lasting Metabolic Consequences. *Cell.* (2014) 158:705–21. doi: 10.1016/j.cell.2014.05.052
10. Hagan T, Cortese M, Rouphael N, Boudreau C, Linde C, Maddur MS, et al. Antibiotics-Driven Gut Microbiome Perturbation Alters Immunity to Vaccines in Humans. *Cell.* (2019) 178:1313–28.e1313. doi: 10.1016/j.cell.2019.08.010
11. Kronman MP, Zaoutis TE, Haynes K, Feng R, Coffin SE. Antibiotic Exposure and IBD Development Among Children: A Population-Based Cohort Study. *Pediatrics.* (2012) 130:e794–803. doi: 10.1542/peds.2011-3886
12. Mikkelsen KH, Knop FK, Frost M, Hallas J, Pottegård A. Use of Antibiotics and Risk of Type 2 Diabetes: A Population-Based Case-Control Study. *J Clin Endocrinol Metab* (2015) 100:3633–40. doi: 10.1210/jc.2015-2696
13. Mitre E, Susi A, Kropp LE, Schwartz DJ, Gorman GH, Nylund CM. Association Between Use of Acid-Suppressive Medications and Antibiotics During Infancy and Allergic Diseases in Early Childhood. *JAMA Pediatr* (2018) 172:e180315. doi: 10.1001/jamapediatrics.2018.0315
14. Lynn MA, Tumes DJ, Choo JM, Sribnaia A, Blake SJ, Leong LEX, et al. Early-Life Antibiotic-Driven Dysbiosis Leads to Dysregulated Vaccine Immune Responses in Mice. *Cell Host Microbe* (2018) 23:653–60.e655. doi: 10.1016/j.chom.2018.04.009
15. Harris VC, Haak BW, Handley SA, Jiang B, Velasquez DE, Hykes BL Jr, et al. Effect of Antibiotic-Mediated Microbiome Modulation on Rotavirus Vaccine Immunogenicity: A Human, Randomized-Control Proof-Of-Concept Trial. *Cell Host Microbe* (2018) 24:197–207.e194. doi: 10.1016/j.chom.2018.07.005
16. Lin YH, Huang LM, Chang IS, Tsai FY, Chang LY. Disease Burden and Epidemiological Characteristics of Varicella in Taiwan From 2000 to 2005. *J Microbiol Immunol Infect* (2009) 42:5–12.
17. Cheng HY, Chang LY, Lu CY, Huang LM. Epidemiology of Breakthrough Varicella After the Implementation of a Universal Varicella Vaccination Program in Taiwan, 2004-2014. *Sci Rep* (2018) 8:17192. doi: 10.1038/s41598-018-35451-y
18. Lai CC, Chen SC, Jiang DD. An Outbreak of Varicella Among Schoolchildren in Taipei. *BMC Public Health* (2011) 11:226. doi: 10.1186/1471-2458-11-226
19. Huang WC, Huang LM, Chang IS, Tsai FY, Chang LY. Varicella Breakthrough Infection and Vaccine Effectiveness in Taiwan. *Vaccine.* (2011) 29:2756–60. doi: 10.1016/j.vaccine.2011.01.092
20. Lin CC, Lai MS, Syu CY, Chang SC, Tseng FY. Accuracy of Diabetes Diagnosis in Health Insurance Claims Data in Taiwan. *J Formos Med Assoc* (2005) 104:157–63.
21. Cheng CL, Kao YH, Lin SJ, Lee CH, Lai ML. Validation of the National Health Insurance Research Database With Ischemic Stroke Cases in Taiwan. *Pharmacoepidemiol Drug Saf* (2011) 20:236–42. doi: 10.1002/pds.2087
22. Lin TL, Fan YH, Chang YL, Ho HJ, Wu CY, Chen YJ. Early-Life Infections in Association With the Development of Atopic Dermatitis in Infancy and Early Childhood: A Nationwide Nested Case-Control Study. *J Eur Acad Dermatol Venereol* (2022) 36:615–22. doi: 10.1111/jdv.17908
23. Lin TL, Wu CY, Fan YH, Chang YL, Ho HJ, Chen YJ. Association Between Early Life Laxative Exposure and Risk of Allergic Diseases. *Ann Allergy Asthma Immunol* (2022) 128:291–98. doi: 10.1016/j.anai.2021.12.016
24. Taiwan Centers for Disease Control. *Statistics of Communicable Diseases and Surveillance Report*. Available at: https://www.cdc.gov.tw/InfectionReport/List/DRiONFTwYxu8T162Hm6yFw (Accessed 30 December 2021).
25. Wopereis H, Oozeer R, Knipping K, Belzer C, Knol J. The First Thousand Days - Intestinal Microbiology of Early Life: Establishing a Symbiosis. *Pediatr Allergy Immunol* (2014) 25:428–38. doi: 10.1111/pai.12232
26. Robertson RC, Manges AR, Finlay BB, Prendergast AJ. The Human Microbiome and Child Growth - First 1000 Days and Beyond. *Trends Microbiol* (2019) 27:131–47. doi: 10.1016/j.tim.2018.09.008
27. Rosenbaum PR, Rubin DB. Reducing Bias in Observational Studies Using Subclassification on the Propensity Score. *Am Stat Assoc* (1984) 79:516–24. doi: 10.1080/01621459.1984.10478078
28. Weersma RK, Zhernakova A, Fu J. Interaction Between Drugs and the Gut Microbiome. *Gut.* (2020) 69:1510–9. doi: 10.1136/gutjnl-2019-320204
29. Libertucci J, Young VB. The Role of the Microbiota in Infectious Diseases. *Nat Microbiol* (2019) 4:35–45. doi: 10.1038/s41564-018-0278-4
30. George S, Aguilera X, Gallardo P, Farfán M, Lucero Y, Torres JP, et al. Bacterial Gut Microbiota and Infections During Early Childhood. *Front Microbiol* (2022) 12:793050. doi: 10.3389/fmicb.2021.793050
31. Ng KM, Ferreyra JA, Higginbottom SK, Lynch JB, Kashyap PC, Gopinath S, et al. Microbiota-Liberated Host Sugars Facilitate Post-Antibiotic Expansion of Enteric Pathogens. *Nature.* (2013) 502:96–9. doi: 10.1038/nature12503
32. Theriot CM, Koenigsknecht MJ, Carlson PE Jr, Hatton GE, Nelson AM, Li B, et al. Antibiotic-Induced Shifts in the Mouse Gut Microbiome and Metabolome Increase Susceptibility to Clostridium Difficile Infection. *Nat Commun* (2014) 5:3114. doi: 10.1038/ncomms4114
33. Ng KM, Aranda-Díaz A, Tropini C, Frankel MR, Van Treuren W, O'Loughlin CT, et al. Recovery of the Gut Microbiota After Antibiotics Depends on Host Diet, Community Context, and Environmental Reservoirs. *Cell Host Microbe* (2019) 26:650–65.e654. doi: 10.1016/j.chom.2019.10.011
34. Gonzalez-Perez G, Hicks AL, Tekieli TM, Radens CM, Williams BL, Lamousé-Smith ES. Maternal Antibiotic Treatment Impacts Development of the Neonatal Intestinal Microbiome and Antiviral Immunity. *J Immunol* (2016) 196:3768–79. doi: 10.4049/jimmunol.1502322
35. Semic-Jusufagic A, Belgrave D, Pickles A, Telcian AG, Bakhsoliani E, Sykes A, et al. Assessing the Association of Early Life Antibiotic Prescription With Asthma Exacerbations, Impaired Antiviral Immunity, and Genetic Variants in 17q21: A Population-Based Birth Cohort Study. *Lancet Respir Med* (2014) 2:621–30. doi: 10.1016/S2213-2600(14)70096-7
36. Harris VC, Armah G, Fuentes S, Korpela KE, Parashar U, Victor JC, et al. Significant Correlation Between the Infant Gut Microbiome and Rotavirus Vaccine Response in Rural Ghana. *J Infect Dis* (2017) 215:34–41. doi: 10.1093/infdis/jiw518
37. Harris V, Ali A, Fuentes S, Korpela K, Kazi M, Tate J, et al. Rotavirus Vaccine Response Correlates With the Infant Gut Microbiota

Composition in Pakistan. *Gut Microbes* (2018) 9:93–101. doi: 10.1080/19490976.2017.1376162
38. Oh JZ, Ravindran R, Chassaing B, Carvalho FA, Maddur MS, Bower M, et al. TLR5-Mediated Sensing of Gut Microbiota Is Necessary for Antibody Responses to Seasonal Influenza Vaccination. *Immunity*. (2014) 41:478–92. doi: 10.1016/j.immuni.2014.08.009
39. Kim D, Kim YG, Seo SU, Kim DJ, Kamada N, Prescott D, et al. Nod2-Mediated Recognition of the Microbiota Is Critical for Mucosal Adjuvant Activity of Cholera Toxin. *Nat Med* (2016) 22:524–30. doi: 10.1038/nm.4075
40. Bremel RD, Homan EJ. Extensive T-Cell Epitope Repertoire Sharing Among Human Proteome, Gastrointestinal Microbiome, and Pathogenic Bacteria: Implications for the Definition of Self. *Front Immunol* (2015) 6:538. doi: 10.3389/fimmu.2015.00538
41. Carrasco Pro S, Lindestam Arlehamn CS, Dhanda SK, Carpenter C, Lindvall M, Faruqi AA, et al. Microbiota Epitope Similarity Either Dampens or Enhances the Immunogenicity of Disease-Associated Antigenic Epitopes. *PloS One* (2018) 13:e0196551. doi: 10.1371/journal.pone.0196551
42. Grassly NC, Praharaj I, Babji S, Kaliappan SP, Giri S, Venugopal S, et al. The Effect of Azithromycin on the Immunogenicity of Oral Poliovirus Vaccine: A Double-Blind Randomised Placebo-Controlled Trial in Seronegative Indian Infants. *Lancet Infect Dis* (2016) 16:905–14. doi: 10.1016/S1473-3099(16)30023-8
43. Zimmermann P, Perrett KP, Ritz N, Flanagan KL, Robins-Browne R, van der Klis FRM, et al. Biological Sex Influences Antibody Responses to Routine Vaccinations in the First Year of Life. *Acta Paediatr* (2020) 109:147–57. doi: 10.1111/apa.14932
44. Soh SE, Ong DQ, Gerez I, Zhang X, Chollate P, Shek LP, et al. Effect of Probiotic Supplementation in the First 6 Months of Life on Specific Antibody Responses to Infant Hepatitis B Vaccination. *Vaccine*. (2010) 28:2577–9. doi: 10.1016/j.vaccine.2010.01.020
45. Matsuda F, Chowdhury MI, Saha A, Asahara T, Nomoto K, Tarique AA, et al. Evaluation of a Probiotics, Bifidobacterium Breve BBG-01, for Enhancement of Immunogenicity of an Oral Inactivated Cholera Vaccine and Safety: A Randomized, Double-Blind, Placebo-Controlled Trial in Bangladeshi Children Under 5 Years of Age. *Vaccine*. (2011) 29:1855–8. doi: 10.1016/j.vaccine.2010.12.133
46. Maruyama M, Abe R, Shimono T, Iwabuchi N, Abe F, Xiao JZ. The Effects of Non-Viable Lactobacillus on Immune Function in the Elderly: A Randomised, Double-Blind, Placebo-Controlled Study. *Int J Food Sci Nutr* (2016) 67:67–73. doi: 10.3109/09637486.2015.1126564
47. Zimmermann P, Curtis N. The Effect of Antibiotics on the Composition of the Intestinal Microbiota - a Systematic Review. *J Infect* (2019) 796:471–89. doi: 10.1016/j.jinf.2019.10.008
48. Korpela K, Salonen A, Virta LJ, Kekkonen RA, Forslund K, Bork P, et al. Intestinal Microbiome Is Related to Lifetime Antibiotic Use in Finnish Pre-School Children. *Nat Commun* (2016) 7:10410. doi: 10.1038/ncomms10410

Conflict of Interest: The authors declare that the research was conducted in the absence of any commercial or financial relationships that could be construed as a potential conflict of interest.

Publisher's Note: All claims expressed in this article are solely those of the authors and do not necessarily represent those of their affiliated organizations, or those of the publisher, the editors and the reviewers. Any product that may be evaluated in this article, or claim that may be made by its manufacturer, is not guaranteed or endorsed by the publisher.

frontiers | Frontiers in Immunology

REVIEW
published: 05 April 2022
doi: 10.3389/fimmu.2022.834942

Advances in Pathogenesis, Progression, Potential Targets and Targeted Therapeutic Strategies in SARS-CoV-2-Induced COVID-19

Hong Zhou[1†], Wei-Jian Ni[2,3†], Wei Huang[4†], Zhen Wang[5], Ming Cai[6,7*] and Yan-Cai Sun[1*]*

[1] Department of Pharmacy, Anhui Provincial Cancer Hospital, The First Affiliated Hospital of USTC, Division of Life Sciences and Medicine, University of Science and Technology of China, Hefei, China, [2] Inflammation and Immune Mediated Diseases Laboratory of Anhui Province, The Key Laboratory of Anti-inflammatory of Immune Medicines, Ministry of Education, Anhui Institute of Innovative Drugs, School of Pharmacy, Anhui Medical University, Hefei, China, [3] Anhui Provincial Hospital, The First Affiliated Hospital of USTC, Division of Life Sciences and Medicine, University of Science and Technology of China, Hefei, China, [4] The Third People's Hospital of Hefei, The Third Clinical College of Anhui Medical University, Hefei, China, [5] Anhui Provincial Children's Hospital, Children's Hospital of Fudan University-Anhui Campus, Hefei, China, [6] Department of Pharmacy, The Second Affiliated Hospital of Anhui University of Chinese Medicine, Hefei, China, [7] School of Pharmacy, Anhui University of Chinese Medicine, Hefei, China

OPEN ACCESS

Edited by:
Fabio Bagnoli, GlaxoSmithKline, Italy

Reviewed by:
Shetty Ravi Dyavar, Adicet Bio, Inc, United States
Wen Zhang, Zhejiang University of Technology, China
Tomohiro Tanaka, Tokyo University of Science, Japan

***Correspondence:**
Wei-Jian Ni
niweijian@ustc.edu.cn
Ming Cai
caiming@ahtcm.edu.cn
Yan-Cai Sun
13349293359@163.com

[†]These authors have contributed equally to this work and share first authorship

Specialty section:
This article was submitted to Vaccines and Molecular Therapeutics, a section of the journal Frontiers in Immunology

Received: *14 December 2021*
Accepted: *07 March 2022*
Published: *05 April 2022*

Citation:
Zhou H, Ni W-J, Huang W, Wang Z, Cai M and Sun Y-C (2022) Advances in Pathogenesis, Progression, Potential Targets and Targeted Therapeutic Strategies in SARS-CoV-2-Induced COVID-19. Front. Immunol. 13:834942. doi: 10.3389/fimmu.2022.834942

As the new year of 2020 approaches, an acute respiratory disease quietly caused by severe acute respiratory syndrome coronavirus 2 (SARS-CoV-2), also known as coronavirus disease 2019 (COVID-19) was reported in Wuhan, China. Subsequently, COVID-19 broke out on a global scale and formed a global public health emergency. To date, the destruction that has lasted for more than two years has not stopped and has caused the virus to continuously evolve new mutant strains. SARS-CoV-2 infection has been shown to cause multiple complications and lead to severe disability and death, which has dealt a heavy blow to global development, not only in the medical field but also in social security, economic development, global cooperation and communication. To date, studies on the epidemiology, pathogenic mechanism and pathological characteristics of SARS-CoV-2-induced COVID-19, as well as target confirmation, drug screening, and clinical intervention have achieved remarkable effects. With the continuous efforts of the WHO, governments of various countries, and scientific research and medical personnel, the public's awareness of COVID-19 is gradually deepening, a variety of prevention methods and detection methods have been implemented, and multiple vaccines and drugs have been developed and urgently marketed. However, these do not appear to have completely stopped the pandemic and ravages of this virus. Meanwhile, research on SARS-CoV-2-induced COVID-19 has also seen some twists and controversies, such as potential drugs and the role of vaccines. In view of the fact that

research on SARS-CoV-2 and COVID-19 has been extensive and in depth, this review will systematically update the current understanding of the epidemiology, transmission mechanism, pathological features, potential targets, promising drugs and ongoing clinical trials, which will provide important references and new directions for SARS-CoV-2 and COVID-19 research.

Keywords: severe acute respiratory syndrome coronavirus 2 (SARS-CoV-2), coronavirus disease 2019 (COVID-19), small molecular inhibitor, vaccine, traditional Chinese medicine, potential target, targeted therapeutic strategy

INTRODUCTION

To date, the 2019 coronavirus disease (COVID-19) pandemic caused by severe acute respiratory syndrome coronavirus 2 (SARS-CoV-2) has infected 440 million people and caused approximately 5.97 million deaths, and these data are still growing rapidly (https://coronavirus.jhu.edu/map.html). This terrible disease not only causes a large number of casualties, but also seriously affects the world economy and peaceful development (1). Therefore, elucidating the possible mechanisms and potential targets of the disease and exploring effective therapeutic drugs and strategies are the most urgent efforts worldwide.

Studies have confirmed that SARS-CoV-2 is a single-stranded RNA-positive Sarbecovirus subgenus β-coronavirus (2). Homology analysis found that the genome sequence of SARS-CoV-2 is approximately 79% homologous with that of the previous SARS-CoV, and more than 50% homologous with that of MERS-CoV, which provides a certain basis and direction for its research (3). However, due to the extremely unstable genetic material of SARS-CoV-2, it is prone to mutations, producing mutant strains or promoting rapid virus evolution (**Table 1**), promoting the continued progress of COVID-19 and a wave of turbulence. This once again threatens the prevention and research of COVID-19 (39). Therefore, the need for targeted drugs and promising treatment strategies is urgent.

In view of this, this article will comprehensively analyze the epidemiological and pathological characteristics of SARS-CoV-2 to promote further research on COVID-19. In-depth discussion of promising therapeutic targets and possible pathogenesis during SARS-CoV-2 infection will accelerate the development of promising drugs, including small molecule drugs, vaccines and biological products, traditional Chinese medicines (TCMs) and symptomatic drugs, and the exploration of effective treatment strategies will eventually promote their clinical applications to overcome SARS-CoV-2-induced COVID-19.

STRUCTURAL INFORMATION, EPIDEMIOLOGY AND PATHOLOGY FEATURES OF SARS-COV-2

According to statistics, there are currently two types (highly pathogenic and minimally pathogenic) of six coronaviruses (CoVs) that can cause human diseases. Among them, highly pathogenic CoVs, including SARS-CoV (Guangdong, China, 2002), Middle East respiratory syndrome coronavirus (MERS-CoV, Saudi Arabia, 2012) and the existing SARS-CoV-2 can cause severe human lung infections and multiple organ dysfunctions (40). The specific development trend of these CoVs is included in **Figure 1**. With the help of the latest omics, structural biology and other technologies, researchers have initially mastered the genome and structural information of SARS-CoV-2 (41). Specifically, the structure of SARS-CoV-2 is composed of the nucleocapsid (N) protein wrapped with RNA as genetic material located in the core region, accompanied by spike (S) protein, envelope (E) protein and membrane (M) protein scattered in the peripheral area, and the genome structure is mainly composed of multiple open reading frames (ORFs) (42). According to the current gene bank annotation (NC_045512.2), 2 functional ORFs (ORF1a and ORF1b) are translated into replicase complexes, and 4 functional ORFs encode S, E, M and N proteins in the 5'-3' direction, while the remaining ORFs are distributed in the abovementioned functional genes, encoding multiple accessory proteins, including 3a/3b, 6, 7a/7b, 8a/8b and 9b (43). Further research found that the ORF1a- and ORF1b-translated viral replicase/transcriptase protein complex is cleaved to form up to 16 kinds of nonstructural proteins (nsps) by the virus/host proteolytic enzymes, including 3C-like main protease ($3CL^{pro}$ or M^{pro}) and papain-like protease (PL^{pro}) (44). During this process, PL^{pro} cuts the N-terminus of the polyprotein to form nsp1, nsp2 and nsp3, which are required for SARS-CoV-2 replication, while $3CL^{pro}$ cleaves and separates the polyprotein pp1ab to generate nsp4-16 to form multiple active proteins, including RdRp and helicases, which are essential requirements for the life cycle of SARS-CoV-2 in host cells (45). The useful information shown in **Figure 2** will help scientists better discover potential targets that interfere with the replication, spread, and pathogenicity of SARS-CoV-2 and develop promising vaccines, small molecule drugs and TCMs that can be used in the clinic.

Meanwhile, the initial epidemiological research results indicate that SARS-CoV-2 spreads from person to person mainly through the respiratory tract, droplets or aerosols (46). However, based on multiple studies, it can be seen that SARS-CoV-2 can be spread not only through the abovementioned channels but also through other means, which is mainly manifested as follows: 1. There have been cases showing that SARS-CoV-2 can spread by the placenta, but vertical transmission rarely occurs. 2. According to existing research,

TABLE 1 | Characteristics of the current concerned SARS-CoV-2 variant strains.

Variant Name	Discovery Time	Original Location	Epidemiological Characteristics	Reference
B.1.1.7 (Alpha)	September 2020	United Kingdom	The infectivity of this type of variant strain has changed, and the transmission speed has increased by approximately 50%; the sensitivity to monoclonal antibody therapy remains unchanged; it can be effectively neutralized by vaccines or antibodies produced by natural infections	Sabino et al. (4) Thye et al. (5)
B.1.351 (Beta) B.1.351.2 B.1.351.3	May 2020	South Africa	The infectivity of this variant strain increases by approximately 50%; the sensitivity to monoclonal antibody treatment is reduced; the neutralizing effect of antibodies produced by vaccines or natural infections is also significantly reduced	Martin et al. (6) Benton et al. (7)
B.1.1.28.1 (P.1/Gamma)	November 2020	Japan/Brazil	This type of variant strain is less sensitive to monoclonal antibody therapy; the neutralizing effect of antibodies produced by vaccines or natural infections is also significantly reduced	Faria et al. (8) Hemmer et al. (9)
B.1.617.1 (Kappa) B.1.617.2 (Delta)	October 2020	India	The infectivity of this type of variant strain is enhanced; the sensitivity to monoclonal antibody therapy may be reduced; the neutralizing effect of antibodies produced by vaccines or natural infections may be reduced	Mishra et al. (10) Kannan et al. (11)
B.1.1.28.2 (P.2/Zeta)	April 2020	Brazil	Potential depletion in neutralization by convalescent and postvaccination sera or monoclonal antibody treatments	Sapkal et al. (12) Zhang et al. (13)
B.1.427/ B.1.429 (Epsilon)	June 2020	United States	The mutant strain has enhanced toxicity and immune escape ability, resulting in low efficacy or even ineffectiveness of various serum vaccines and neutralizing antibodies, ~20% increased transmissibility	McCallum et al. (14) Deng et al. (15)
C.37 (Lambda)	December 2020	Peru	This mutant strain will affect the effectiveness of vaccines and neutralizing antibodies, and is believed to promote the virus to invade host cells and help the virus escape the host immune system	Romero et al. (16) Darvishi et al. (17)
B.1.621 (Mu) B.1.621.1	January 2021	Colombia	The mutant strain is highly resistant to COVID-19 convalescent serum and vaccines vaccinated thus far, with enhanced transmission and pathogenicity, and is likely to have immune escape and natural derivation capabilities	Laiton-Donato et al. (18) Uriu et al. (19)
B.1.1.28.3 (P.3/Theta)	March 2021	Philippine	The mutant strain may show stronger transmission, while reducing the neutralization of vaccine and convalescent serum	Shuai et al. (20) Moubarak et al. (21)
B.1.1.523	May 2020	Russia	The enhanced immune escape ability of the mutant strain leads to weakened vaccine effectiveness	van der Veer et al. (22)
C.1.2	March 2021	South Africa	The mutation degree of this mutant strain far exceeds that of other strains, the gene mutation rate is higher but the incidence rate is low, and the infectivity and immune escape ability are enhanced	Albayat et al. (23) Yang et al. (24)
R.1	January 2021	Japan	This variant strain is easier to spread and may have the ability to actively evade vaccine antibodies	Nagano et al. (25) Sekizuka et al. (26)
C.36.3	January 2021	Thailand-Egypt	This strain has been listed by the WHO as a "mutant strain under surveillance", which means that the strain is potentially dangerous	https://www.who.int/en/activities/tracking-SARS-CoV-2-variants/
B.1.1.519	November 2020	Mexico	This variant strain reduces the activity of some monoclonal antibodies, but does not show changes in immune escape ability and pathogenicity	Rodríguez-Maldonado et al. (27)
B.1.1.318	February 2021	United Kingdom	This variant strain is highly transmissible and may impair the efficacy of the vaccine	Laine et al. (28) Manouana et al. (29)
B.1.466.2	November 2020	Indonesia	This mutant strain has a high infection rate in Indonesia (approximately 48%), but the overseas infection rate is low (<0.5%)	Fibriani et al. (30) Sam et al. (31)
B.1.620	February 2021	Europe	This mutant strain carries mutations and missing information of a variety of strains of interest, and is likely to have antibody-mediated immune escape. It may be ineffective against mRNA vaccines and is widely spread in central Africa.	Dudas et al. (32) Zahradník et al. (33)
B.1.526 (Iota)	November 2020	United States	The mutant strain has a faster transmission speed and a higher lethality rate, is partially or completely resistant to monoclonal antibodies, and is not sensitive to the neutralization effect of plasma and serum during the recovery period.	Annavajhala et al. (34) Thompson et al. (35)
B.1.525 (Eta)	December 2020	Nigeria/ United Kingdom	The mutant strain has strong transmission and immune escape ability, which can weaken the neutralization efficiency of vaccines and antibodies	Bugembe et al. (36)
B.1.630	March 2021	Dominican Republic	This mutant strain has a large number of spike protein mutation points, but weaker transmissibility than the Delta variant. It still needs attention	https://www.who.int/en/activities/tracking-SARS-CoV-2-variants/
B.1.1.529 (Omicron)	November 2021	South Africa Botswana	The mutant strain has more mutation sites and significantly enhanced infectivity, which is 10× and 2× higher than the original virus or Delta mutant strain, respectively; the immune escape ability is enhanced and twice that of the Delta mutant strain, resulting in a decreased efficiency of monoclonal antibodies and resistant to vaccines; the speed of virus infection has increased, and there is an increased risk of reinfection	Abdool and de Oliveira (37), Chen et al. (38)

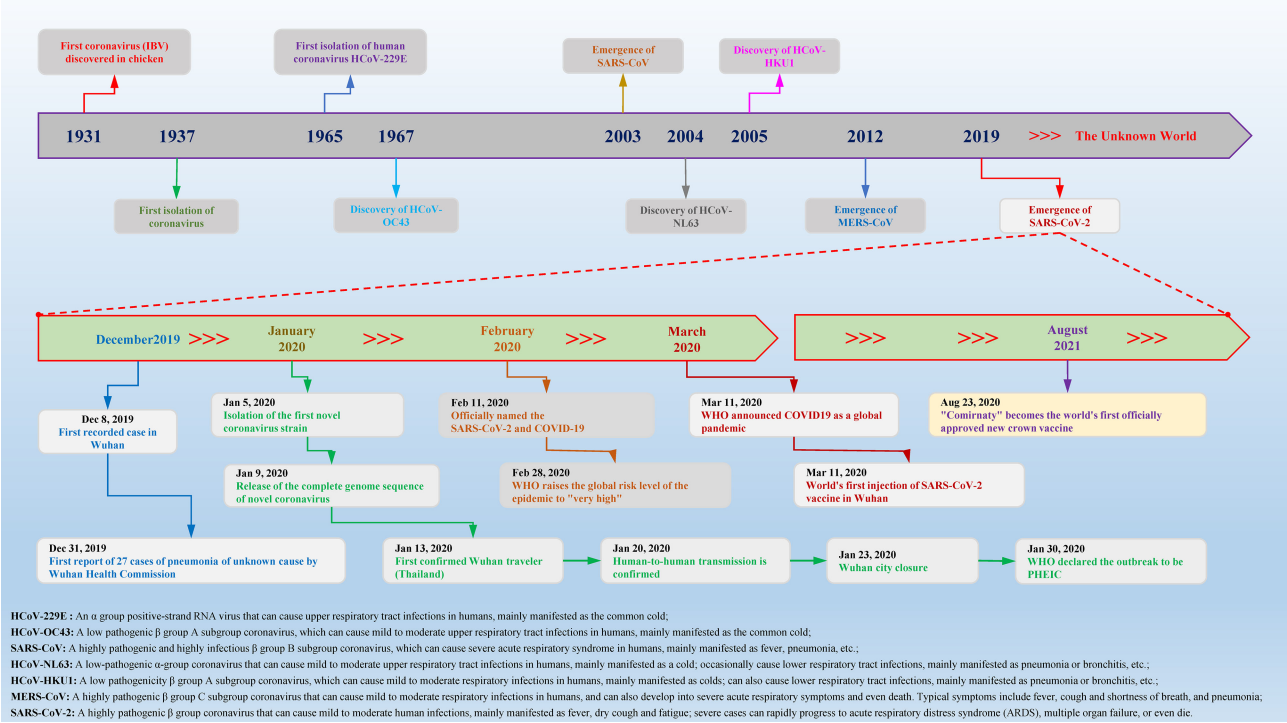

FIGURE 1 | Timeline of key events for coronavirus discovery and research. Coronavirus was first isolated from chickens in 1937. With the passage of time and changes in the environment, in the past 84 years, a variety of different species and subgroups of coronaviruses have been discovered, identified, named, and researched. In December 2019, Wuhan, China, reported a novel coronavirus case for the first time. In a short period of time, the COVID-19 epidemic caused by SARS-CoV-2 spread to the world and caused major disasters and epidemics. In the past two years, there have been more than 440 million confirmed cases worldwide, causing approximately 5.97 million deaths, which has caused great social upheavals and dangers.

the virus can spread among minks and can infect humans. Meanwhile, cats and ferrets have been confirmed to be able to transmit to each other, but there are no reported cases of transmission to humans. 3. There have been studies speculating that this virus can also be spread by direct contact and pollutants, but this may be just an unusual route of transmission. 4. Although live virus has been isolated from saliva and feces, viral RNA has also been detected in semen and blood transfusions (47). There are currently no reports of sexual or blood transmission and only one report of possible fecal-respiratory transmission (48), which will provide us with important guidance for all-round protection.

Researchers conducted a systematic analysis of SARS-CoV-2-infected patients and found that almost all patients had frosted glass shadows on both sides of their lungs (49). The initial symptoms of the patient mainly included fever, cough and sputum, hemoptysis, headache and myalgia or fatigue, diarrhea, dyspnea, etc. As the disease progresses, symptoms such as inflammation, fibrosis and edema appear in the lungs, which gradually develop into acute respiratory distress syndrome (ARDS) and cause lung failure (50). Meanwhile, SARS-CoV-2 infection also causes damage to multiple organ functions, including digestive system injury, such as liver degeneration and spot necrosis, and the epithelium of the esophagus, stomach and intestine mucosa show varying degrees of degeneration, necrosis and exfoliation; brain and nervous system damage, such as cerebral congestion and edema, some neuronal degeneration and ischemic changes; cardiovascular system damage, such as increased blood pressure and arrhythmia, increases the probability of myocardial infarction, causes myocardial ischemia, necrosis, thrombosis and cardiac insufficiency; genitourinary system damage, including glomerular congestion, segmental hyperplasia or necrosis, protein exudation in the glomerular capsule, and acute kidney injury (**Figure 3**); and some patients still die after treatment (51). Based on this, being familiar with the pathological changes caused by SARS-CoV-2 will lay the foundation for clinical diagnosis and targeted therapy.

At present, new cases of COVID-19 are caused by multiple SARS-CoV-2 variants in many countries (52). Currently, a number of major variants are rapidly growing and causing concern, including alpha (B.1.1.7), beta (B.1.351), gamma (B.1.1.28.1), delta (B.1.617.2) and omicron (B.1.1.529), and the characteristics of these variants are shown in **Table 1**. Meanwhile, different mutant strains have different characteristics. For example, the gamma variants increase toxicity and increase the risk of hospitalization and death, while Delta strains are highly infectious and spread quickly, especially the shortened incubation period or passage interval, which increases the risk of global epidemics (10, 53).

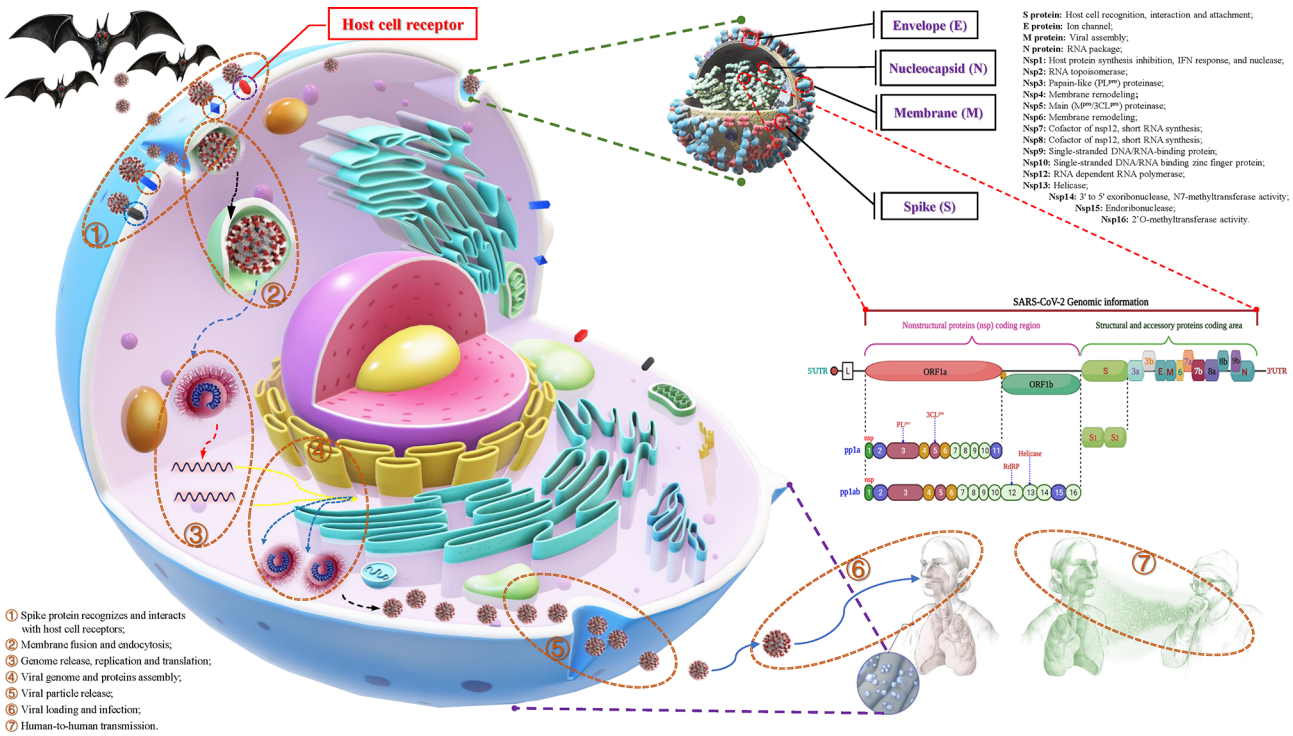

FIGURE 2 | The structural features, potential functions and transmission process of SARS-CoV-2. Structurally, the outer side of SARS-CoV-2 is surrounded by a capsid, which is mainly composed of spike (S), membrane (M), and envelope (E) proteins, while the nucleocapsid (N) protein is accompanied by the genome. The genomic structure of SARS-CoV-2 is based on a single-stranded positive-stranded RNA, which contains a 5'-methylated cap and a 3'-polyadenylic acid tail, arranged in the following order: 5'-end; nonstructural protein (nsp) coding region [open reading frame (ORF1a/b)]; structure and accessory protein coding regions such as S, E, M, N and 3a, 3b, 6, 7a, 7b, 8a, 8b, 9b. Among them, the open reading frame (ORF) 1a/b is responsible for encoding a variety of nonstructural proteins, mainly RNA-dependent RNA polymerase (RdRP), papain-like protease (PL^{pro}) and 3C-like protease ($3CL^{pro}$). The putative functions of these proteins are mentioned in the figure. During the infection process, SARS-CoV-2 recognizes and interacts with host cell surface receptors and enters the host cell through membrane fusion and endocytosis. After entering the host cell, SARS-CoV-2 releases its genome and translates a large number of nsps, including RdRP, PL^{pro} and $3CL^{pro}$. Under the action of these enzymes, it synthesizes the new RNA genome and assembles to form virus particles, which are then released into the extracellular space through exocytosis. Uncontrolled replication promotes SARS-CoV-2 infection, leading to immune disorders and inflammatory cytokine storms and ultimately leading to damage to multiple organs, especially the lungs.

Authoritative research shows that SARS-CoV-2 has evolved more than 800 different subtypes or branches, and its variants may have exceeded 1,000 (54). In general, the direction of the mutation and evolution of the new coronavirus is mainly to break through immunity, avoid vaccines, increase exponential replication, and be highly infectious (37). Although the mutant strains are terrible, their diversity, transmission, epidemic, and pathogenic characteristics will provide important clues for the in-depth study of virus mutation mechanisms, exploration of novel potential targets, and development of effective vaccines, drugs, and therapeutic strategies.

POTENTIAL THERAPEUTIC TARGETS OF SARS-COV-2

Combining the research experience of SARS- and MERS-CoV to explore the potential therapeutic targets of SARS-CoV-2, the following aspects should be considered: enzymes and functional proteins that affect RNA synthesis and viral replication; structural proteins that affect virus entry and the self-assembly process; virulence factors that affect the host immune regulation; and host cell surface proteins and receptors (**Figure 4**). Correspondingly, therapeutic strategies are also divided into targeting SARS-CoV-2 and targeting host cells and the body's immune system (55). Authoritative research shows that SARS-CoV-2 can encode a variety of proteins, including nsps, structural proteins, and several virulence factors (56). Moreover, multiple specific host cell surface receptors, coreceptors, and auxiliary proteases, including angiotensin converting enzyme 2 (ACE2), transmembrane protease serine 2 (TMPRSS2), cluster of differentiation 147 (CD147) tyrosine-protein kinase receptor UFO (AXL) and nonmuscle myosin heavy chain IIA (MYH9) (38, 57, 58), have been identified. Obviously, these targets will be the most promising targets for fighting the COVID-19 outbreak caused by SARS-CoV-2.

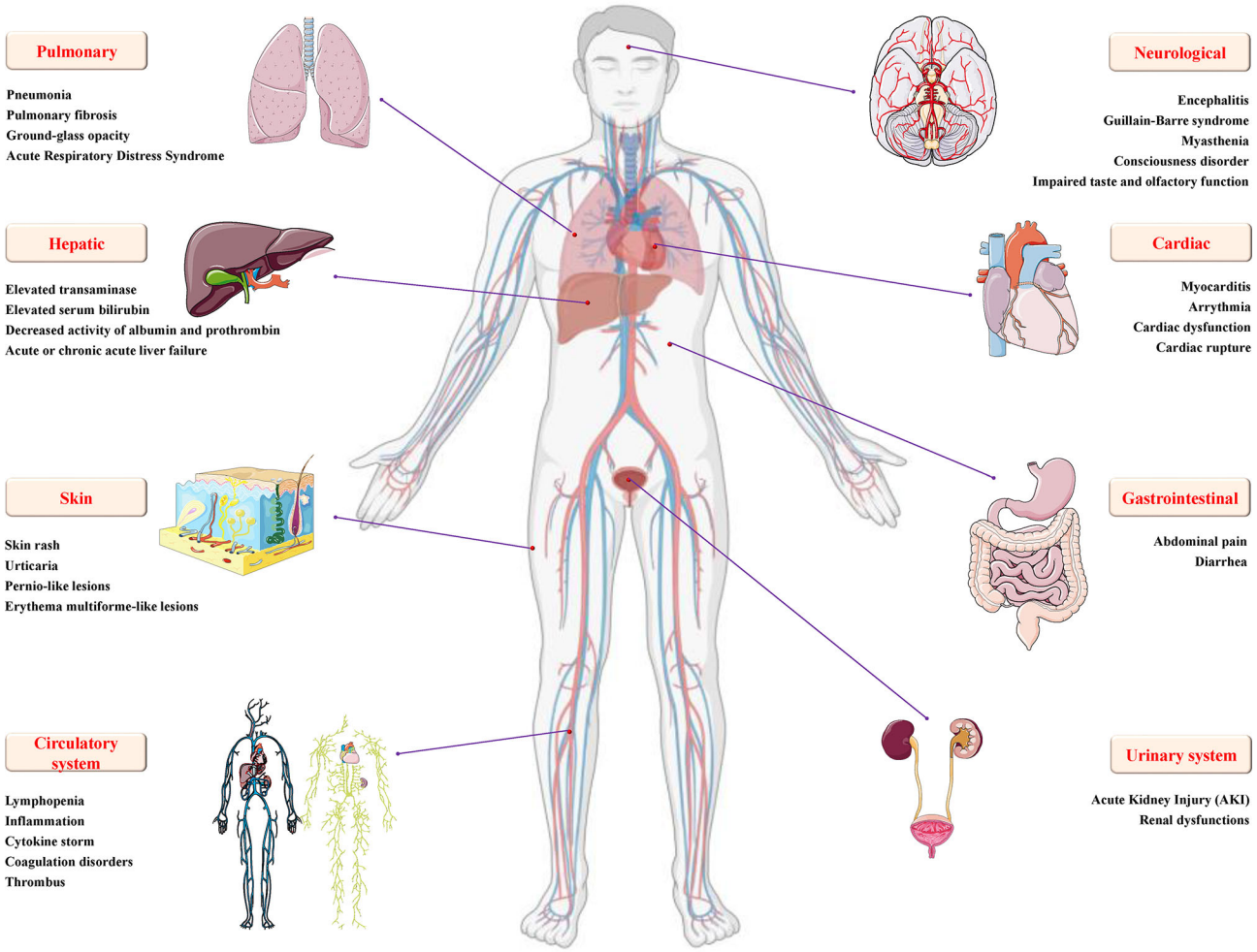

FIGURE 3 | Details of multiple organ injury caused by SARS-CoV-2. In addition to varying degrees of pulmonary inflammation, embolism, and acute respiratory distress syndrome, COVID-19 caused by SARS-CoV-2 infection can also cause various organ dysfunctions and damages, including but not limited to encephalitis, Gillan-Barre syndrome, muscle weakness and other nervous system dysfunction; increased blood pressure, arrhythmia, myocardial ischemia, cardiac insufficiency, rupture and other cardio/cerebrovascular system damage; urogenital system damage, such as glomerular congestion and acute kidney injury; digestive system damage, such as diarrhea, increased transaminase/serum bilirubin, decreased albumin/prothrombin activity, acute or chronic acute liver failure, and skin and circulatory diseases, such as skin rash, urticaria, pernio-like lesions, inflammation, cytokine storm, coagulopathy and thrombosis.

RNA Synthesis and Replication Protease Targets

Nsps have proven to be widely involved in SARS-CoV-2 recognition, entry, inheritance, replication, and infection. Together with their key biological functions and relatively clear structure and active site, the main nsps, including PL^{pro}, $3CL^{pro}$, RNA-dependent RNA polymerase (RdRP) and helicase, have become the first batch of targets to be considered for the development of small molecular inhibitors (**Figure 4**) (59).

$3CL^{pro}$, the aforementioned nsp5, was found to cut 11 sites on the polyprotein body encoded by ORF1ab and then release mature nsp4-nsp16, which is crucial to the life cycle of SARS-CoV-2 (60). Structural analysis showed that the protease monomer mainly contains a domain I (residues 8-101) and a long loop connected domain II (residues 102-184) and a domain III (residues 185-200), and the active site is located in the gap between domains I and II (61). Mature research on the function, structure and active site of $3CL^{pro}$ makes it a powerful target for anti-SARS-CoV-2 drugs such as small molecules and peptide inhibitors.

Unlike $3CL^{pro}$, PL^{pro} mainly cuts from the N-terminus of the polyprotein to release nsp1, 2 and 3, which will affect the accuracy of SARS-CoV-2 replication. Research on MERS-/SARS-CoV suggests that it has a powerful role in antihost innate immunity (62). Moreover, homology analysis found that SARS-CoV-2 and SARS-CoV PL^{pro} share approximately 83% of the sequence at the protein level. Combined with its indispensable role in virus replication and infection, PL^{pro}

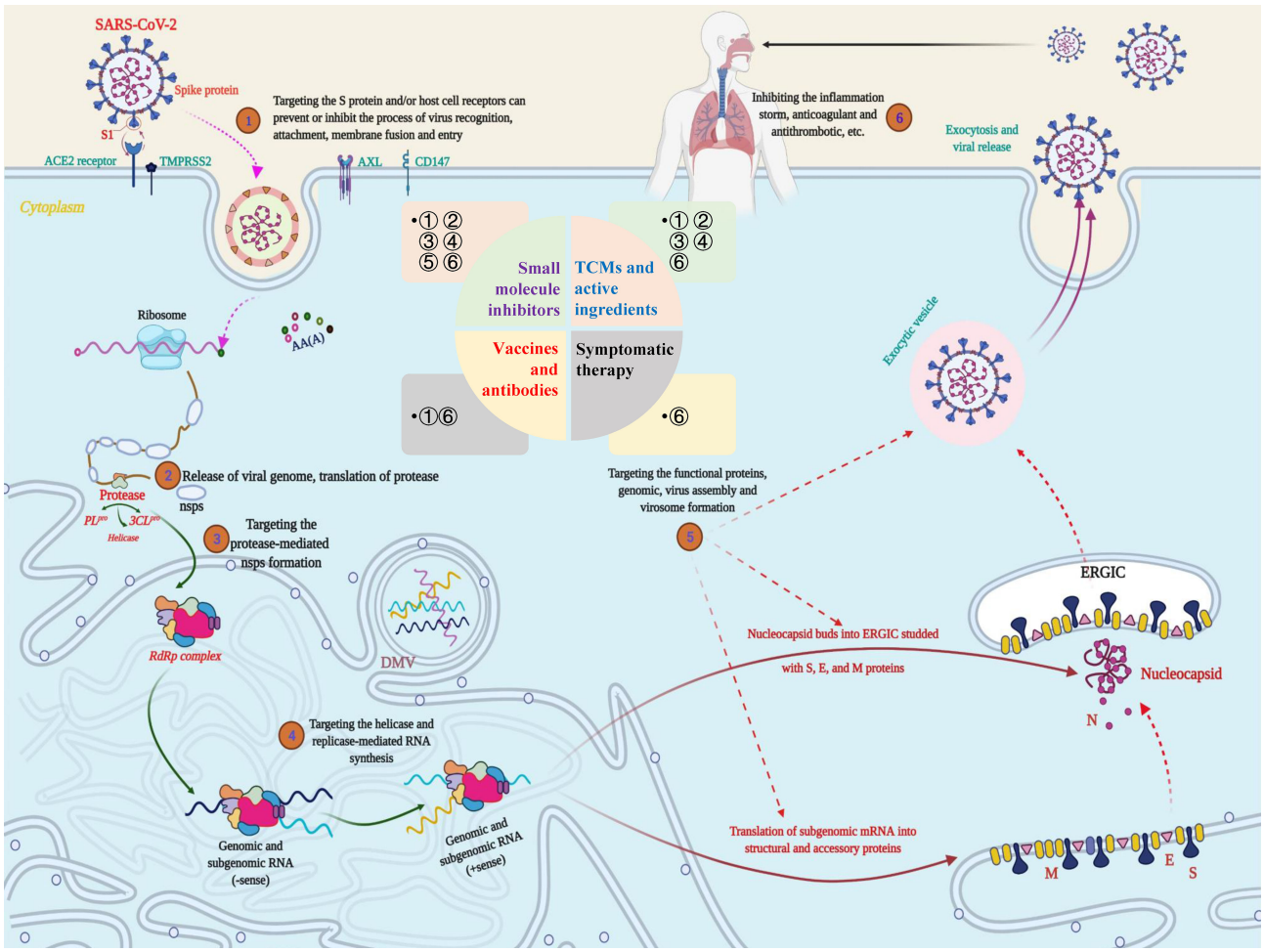

FIGURE 4 | Potential targets and targeted therapeutic strategies for combating SARS-CoV-2-induced COVID-19. Scheme of the potential targets, intervention strategies and types of therapeutic drugs in the cycle of SARS-CoV-2 infection, replication, and transmission. During the infection stage, SARS-CoV-2 recognizes and interacts with host cell surface receptors through the spike (S) protein or transmembrane glycoprotein CD147 and enters the host cell through membrane fusion and endocytosis. After the virus enters the host cell, SARS-CoV-2 releases its nucleocapsid and genome into the cytoplasm and translates a large number of nonstructural proteins (nsps) including coding RNA-dependent RNA polymerase (RdRP), papain-like protease (PL^{pro}) and 3C-like protease ($3CL^{pro}$). Under the action of these enzymes, a full-length negative antisense genome template is synthesized to produce the new RNA genome and assembled to form virus particles, which are then released into the extracellular space through exocytosis. Uncontrolled replication promotes SARS-CoV-2 infection, leading to immune disorders and inflammatory cytokine storms and ultimately leading to damage to multiple organs, especially the lungs. The whole process exposed multiple potential targets, providing important guidance for research on anti-SARS-CoV-2 targets, drugs and treatment strategies.

should be a valuable target for SARS-CoV-2 inhibitor research. Meanwhile, the use of X-ray crystallography and other techniques to analyze the structure of PL^{pro} will further facilitate the study of PL^{pro} inhibitors against SARS-CoV-2 (63, 64).

In the RNA replication of CoVs, RdRP promotes their evolution by affecting the fidelity of replication and mutation rates to help them adapt to the environment or host cells (65). Homology analysis found that SARS-CoV and SARS-CoV-2 share approximately 82% of the homologous sequence at the genome level, while RdRP shares a sequence of more than an astonishing 96% at the protein level (66). These findings remind us that RdRP will become one of the most promising targets for the study and treatment of SARS-CoV-2. High-resolution structural analysis revealed that the functional domain of SARS-CoV-2 RdRP is located at the C-terminus of the protein, where there is a conserved Ser-Asp-Asp motif. At the RNA level, nsp8 can control the *de novo* synthesis of up to 6 nucleotides, which will provide primers for nsp12/RdRP RNA synthesis. Meanwhile, the nsp7-nsp8 complex can increase the activity of RdRP, which in turn affects its binding to RNA (67). All these studies provide valuable references and directions for research on anti-SARS-CoV-2 targeting RdRP.

SARS-CoV-2 helicase (nsp13) is a multifunctional nucleoside triphosphate (NTP)-dependent protein. Structural analysis revealed that helicase contains a metal binding domain (MBD)

composed of 26 cysteine residues at the N-terminus and a helicase domain (Hel) consisting of a conserved motif at the C-terminus (68). Functional studies found that, helicase can unwind double-stranded (ds) DNA and RNA in an NTP-dependent manner along the 5'-3' direction during (69). It was found that the sequence of the helicase of SARS-CoV-2 is conserved and indispensable and is an essential component of virus replication. Based on these studies, helicase is expected to become a viable target against SARS-CoV-2 infection.

Structural Protein Targets

Based on the current research results, the spike protein is one of the most critical structural proteins of SARS-CoV-2, which forms a special flower crown structure on the outer surface of the virus in the form of a trimer. Meanwhile, studies have found that the spike protein can directly affect the recognition, receptor binding, interaction, and virus entry between SARS-CoV-2 and host cells to determine the tissue or host preference in the initial stage of infection (70). In the spike (S)-mediated infection process, certain proteases in the host cell, such as TMPRSS2, can cleave the spike protein into two subtypes, the S1 subunit and the S2 subunit. The responsibility of the S1 subunit is to recognize and bind to host cell surface receptors, while the main task of the S2 subunit is to mediate the virus-cell and cell membrane fusion process (71). From the perspective of the mechanism, the structural integrity, cleavage and activation of the S protein perform crucial roles during host cell invasion and virulence. Therefore, it will have far-reaching significance to develop drugs and vaccines that affect the viral spike protein or specific receptors on the host cell surface to prevent SARS-CoV-2 from entering and infecting. Except for the outermost spike protein, the N protein is a highly immunogenic phosphoprotein and also a core and highly conserved component of SARS-CoV-2 (72). In the process of virion assembly, N protein combines with viral genomic RNA to produce a spiral nucleocapsid and is related to viral genome replication and regulation of cell signaling pathways. During this process, the N-terminal domain (NTD) and C-terminal domain (CTD) are necessary structures for effective binding to viral RNA (73). Meanwhile, studies have pointed out that the E protein mainly affects the structural integrity and virulence of SARS-CoV-2 (74). In addition, these proteins also exhibit the interferon (IFN) antagonistic properties. In particular, the M protein can prevent the formation of the MAVS-traf3-tbk1 complex and antagonize the production of IFN-I by interacting with MAVS (74, 75). Based on the above research, S (S1 and S2 subunit), N (NTD and CTD domain), E and M proteins are all have great potential to become targets for the development of anti-SARS-CoV-2 drugs and vaccines (**Figure 4**).

Virulence Factor Targets

Virulence factors (VFs) are molecules with virulence properties such as invasiveness and toxins produced by the metabolism of viruses and bacteria, which mainly inhibit or evade the host's immune response when infecting the host and obtain nutrients from the host for self-proliferation (76). At present, little is known about the virulence factors of SARS-CoV-2, and there are three virulence factors, namely nsp1, nsp3c and ORF7a, which are considered to be most likely involved in interfering with the innate immunity of the host to assist in immune escape of the virus (77–79). Specifically, nsp1 induces the degradation of mRNA and inhibits the production of IFN-I by interacting with host cell 40S ribosomal subunits, while nsp3c combines with host cell ADP-ribose to resist innate immunity (77, 80). In addition, ORF7a of SARS-CoV-2 directly binds to bone marrow stromal antigen 2 (BST-2), which reduces its activity by blocking the glycosylation of BST-2 and ultimately inhibits the release of the assembled virus (79). In view of the high feasibility of virulence factors as potential targets for SARS-CoV-2 research, the development of drugs that affect the production and effects of virulence factors will be another important clue to explore the fight against SARS-CoV-2-induced COVID-19.

Hose Specific Receptor or Enzyme Targets

Authoritative studies have confirmed that host cell ACE2 is the specific receptor to which the SARS-CoV S protein receptor binding domain (RBD) binds. The latest research has found that the host receptors of SARS-CoV-2 and SARS-CoV have a high degree of consistency, which indicates that there is also an important interaction between the spike RBD of SARS-CoV-2 and ACE2 (81). During the infection stage, the RBD of the S protein S1 subunit recognizes and binds to the cell surface ACE2 receptor, which promotes the weakening or disappearance of the interaction between S1 and the S2 subunit, thereby exposing the S2 subunit (82). Subsequently, the S2 subunit changes conformation by inserting the fusion peptide (FP) into the host cell membrane, resulting in the formation of a six-helix bundle (6HB) between HR1 and HR2, which ultimately promotes fusion of the viral membrane with the host cell membrane (83). According to the receptor binding motif (RBM) analysis, a large number of amino acid residues necessary for binding to ACE2 are completely retained in the S protein of SARS-CoV-2, which is consistent with the previous discovery that the virus uses ACE2 to enter the host cell (84). Based on a number of authoritative studies, ACE2 will be the most valuable host cell target in preventing the entry and infection of SARS-CoV-2.

In addition, TMPRSS2 can cut off the spike to trigger SARS- and MERS-CoV infection. In a study of SARS-CoV-2, it was found that the virus uses TMPRSS2 instead of cathepsin B and L (CatB/L) to activate the S protein, and the spreading process may also be closely related to the activity of TMPRSS2 (85). Another study found that TMPRSS2 inhibitors can significantly inhibit the SARS-CoV-2 spike protein from entering a cell line expressing TMPRSS2, while promoting the expression of TMPRSS2 can cancel this inhibitory effect, which indicates that the initiation of the SARS-CoV-2 spike protein is dependent on TMPRSS2 (86). Furthermore, an *in vitro* study showed that camostat mesylate, a serine protease inhibitor, can potently stop the virus from entering Caco-2 ($TMPRSS2^+$) cells rather than 293T ($TMPRSS2^-$) cells by inhibiting the activity of TMPRSS2 (87). The above results suggest that inhibiting TMPRSS2 to treat patients with SARS-CoV-2 infection will be a promising and valuable therapeutic strategy.

CD147 is a highly glycosylated single-pass transmembrane glycoprotein that has been found to play an indelible role in tumor development, plasmodium invasion, virus infection and other processes (88). During SARS-CoV invasion of host cells, CD147 molecules can interact with cyclophilin A (CyPA) to mediate a similar mechanism of action in HIV-1 invasion, while the CD147 antagonist peptide (AP)-9 can strongly bind to HEK293 cells and exert its anti-SARS-CoV effect (89). In view of the high similarity between SARS-CoV and SARS-CoV-2, some studies have attempted to explore the possible role of CD147 in host cell invasion by SARS-CoV-2 (90). The results show that blocking host cell CD147 can significantly inhibit SARS-CoV-2 infection, suggesting that CD147 is likely to be another potential surface receptor independent of ACE2 (91). A study used the humanized anti-CD147 monoclonal antibody called meplazeumab (60 μg/ml), which can prevent virus invasion and the subsequent inflammation caused by SARS-CoV-2 and its variants, including variants α, β, γ and δ, with inhibition rates of 68.7, 75.7, 52.1, 52.1 and 62.3%, respectively (92). Furthermore, CD147 genetically modified mice are more sensitive to SARS-CoV-2 and variants such as α and β, causing the same pathological changes as COVID-19 (93). In addition, surface plasmon resonance analysis confirmed that there is an interaction between CD147 and the S protein (90). This evidence indicates that SARS-CoV-2 can also enter host cells by binding to the CD147 receptor. However, the question of whether CD147 is a coreceptor, a secondary receptor or a completely independent new receptor still needs more research to be verified. However, CD147 is a novel potential therapeutic target with further exploration value in research on fighting SARS-CoV-2 infection. While researchers have multiplied their hopes for discovering this new infection mechanism, several studies have suggested that there is no direct interaction between RBD and CD147, raising doubts about its role as a coreceptor and potential as a therapeutic target (94, 95). Science has always been developed through constant questioning. The conflicting results do not discourage us but instead provide us with new research clues. In any case, more research needs to be done to strengthen the reliability of this finding.

SARS-CoV-2 infection mainly relies on the interaction of the viral surface S protein and the well-known host cell surface receptor ACE2. However, the low expression of ACE2 in the respiratory system makes it difficult to fully explain why SARS-CoV-2 mainly infects the human respiratory system. Along with the continuous deepening of exploration, researchers proved that the AXL protein on lung cells can bind to the spike protein and show a relatively obvious colocalization phenomenon on the cell membrane through large-scale screening and a series of biochemical cellular experiments (96). Interestingly, AXL does not bind to the RBD of the S protein but instead binds to the NTD region at the N-terminus. Meanwhile, a study also found that AXL has significant retention in almost all types of airway cells, including type I/II lung epithelial cells, fibroblasts, basal cells, endothelial cells, smooth muscle cells and myeloid cells. In addition, overexpression of AXL can effectively promote the invasion of SARS-CoV-2, while knocking out AXL in human lung epithelial cells significantly reduces SARS-CoV-2 infection (97). At the same time, clinical data from patients with SARS-CoV-2 also show that the expression level of AXL is highly correlated with severe infections (98). The use of soluble AXL protein can effectively antagonize SARS-CoV-2 infection of lung cells, suggesting that AXL is another potential target during SARS-CoV-2 infection, and targeted or AXL-based drugs may be used for future clinical interventions against SARS-CoV-2 infection.

POTENTIAL THERAPEUTIC STRATEGIES AND PROMISING ANTI-SARS-COV-2 DRUGS

Small Molecule Inhibitors

Drawing lessons from the research and development experience of SARS-CoV and MERS therapeutic drugs and the current authoritative research about SARS-CoV-2, we need to explore small molecule inhibitors that can prevent the novel coronavirus and its epidemic from two directions (99): 1. This type of inhibitor targets viral proteins, such as the S protein, viral enzymes (PL^{pro}, $3CL^{pro}$, RdRP and helicase) and some important structural proteins; 2. This type of inhibitor interacts with host cell surface proteins, such as receptor (ACE2 or AXL) or coreceptor (heparin sulfate), serine protease TMPRSS2, etc., to block virus invasion and some signal regulators of the human immune system, as shown in **Figure 4**. At the same time, the corresponding development strategies are mainly divided into three categories: 1. Virtual screening: High-throughput screening is carried out to identify possible lead compounds from existing compound databases, such as ZINC, DrugBank, or ChemDiv, on the basis of structural biology and homology modeling analysis of protein structure. 2. Experimental high-throughput screening (HTS): Identify small molecules in the active compound library, including approved drugs, clinical trial candidates, and even internal compound databases. 3. Reposition the application of clinical and preclinical drugs (100, 101). That is the so-called "new use of old medicine". In addition, the computer-aided design and fragment-based drug exploration are also important strategies.

Under the guidance of these strategies, a variety of small molecule inhibitors targeting different stages of the SARS-CoV-2 life cycle have been discovered. When trying to block SARS-CoV-2 entry by targeting the S protein, the researchers found that Arbidol, Bictegravir, Dolutegravir, and Tizoxanide all have such a conformation that they can bind to the key sites of the S protein with a very high binding energy (102). Arbidol mainly binds to the S1 and S2 subunits of SARS-CoV-2 to promote tight subunit binding, which not only prevents the S1 subunit from falling off, but also impedes the membrane fusion function of the S2 subunit, eventually preventing virus entry. *In vitro* experiments showed that Arbidol has satisfactory activity against SARS-CoV-2 with IC_{50} and 50% cytotoxic concentration (CC_{50}) values of 4.11 and 31.79 μmol/L,

respectively, and the selectivity index (SI) was 7.73 (103). Bictegravir and Dolutegravir combine between the RBD and NTD of two adjacent S1 monomers, which can prevent SARS-CoV-2 entry by restricting the interaction between the spike RBD and ACE2 receptor (104). In addition, Tizoxanide not only affects the stability of the S1 subunit through hydrogen bonds and van der Waals forces to prevent the RBD in the metastable conformation of the S1 subunit from binding to ACE2 but also affects the membrane fusion of the S2 subunit and host cell (105). Importantly, structural optimization of these molecules produces 9 new small molecules with better anti-SARS-CoV-2 activity, which provides important references for the discovery, development and optimization of small molecule inhibitors targeting the S protein (102). According to the research experience of SARS/MERS-CoV, the design of viral fusion interference peptides based on the properties of heptad repeat 1 (HR1) and heptad repeat 2 (HR2) of the S2 subunit is also an important strategy for the research of small molecule inhibitors of SARS-CoV-2. A pancoronavirus fusion inhibitor peptide, EK1, was designed to inhibit a variety of CoVs and inhibit SARS-CoV-2 S protein-mediated membrane fusion and pseudovirus infection in a dose-dependent manner. Subsequently, its improved version, lipopeptide EK1C4 was designed to have the same inhibitory effect at $IC_{50\ values}$ of 1.3 and 15.8 nmol/L, and these two results were 241- and 149-fold those of the former, respectively (106). In addition, another lipopeptide, IPB02, designed based on the HR2 sequence also showed a similar effect (107). Furthermore, SARS-CoV-2-HR2P, a peptide directly based on the amino acid sequence of SARS-CoV-2 HR2, showed a potent membrane fusion inhibition with an IC_{50} of 0.18 mmol/L (106). Unlike SARS-CoV-2-HRP2, which is designed on a single amino acid, [SARSHRC-PEG4]2-chol, as a dimeric lipopeptide has better membrane fusion inhibition and lower cytotoxicity against SARS-CoV-2 entry (108). After that, one study designed a peptide SBP1 composed of 23-mer peptides to prevent the virus from entering the host cell by disrupting the combination of SARS-CoV-2-RBD and ACE2 (109). To inhibit the combination of viral S protein and ACE2, a study designed two types of peptide inhibitors, AHB1/2 and LCB1/3, by two *de novo* synthesis approaches around the ACE2 helix structure and RBD motif, which have a strong SARS-CoV-2 neutralization effect with $IC_{50\ values}$ of 35/15.5 nmol/L and 23.54/48.1 pmol/L, respectively (110). A study identified a fibronectin-derived anticancer peptide ATN-161 from existing peptides that can prevent the binding of the S protein to ACE2, thereby reducing SARS-CoV-2 infection with an IC_{50} of 3.16 mmol/L (111). In light of this, the design of small molecule inhibitors for the S protein should focus on the protein structure, amino acid sequence and motif characteristics of the RBD, S1 and S2 subunits. When targeting the host cell ACE2 receptor, it has recently been suggested that ACE2 inhibitors, such as captopril and enalapril, may be effective for those who have experienced SARS-CoV-2-induced pneumonia (112). Nicotinamide analogs, such as nicotinamide riboside (NR) and nicotinamide mononucleotide (NMN), are an important class of natural vitamin derivatives. A relevant study found that it can effectively inhibit ACE2, so it is considered a potential inhibitor for the treatment of COVID-19 (113). However, these are only theoretical speculations and almost no basic or clinical research verification. It is possible that such suggestions will gradually fade out of people's field of vision. At present, the development of anti-SARS-CoV-2 drugs targeting ACE2 is mainly focused on peptides, antibodies and other biochemical products, including ACE2 antibody, ACE2-scFv, ACE2 nanobody, and ACE2-Fc (114, 115). Although TMPRSS2 is the gateway for SARS-CoV-2 host cells to enter, there have not been many breakthroughs in the research of small molecule inhibitors against this target. The known TMPRSS2 inhibitor camostat in a clinical trial against COVID-19 shows excellent abilities to reduce the death risk and hospital stay (87). Recently, a study demonstrated that the camostat-like drug nafamostat mesylate can prevent the SARS-CoV-2 membrane fusion caused by TMPRSS2 at a concentration of its less than one tenth, suggesting that nafamostat mesylate may be a promising inhibitor against SARS-CoV-2 infection by targeting TMPRSS2 (116). Other studies identified a variety of serine protease experimental inhibitors (DB03782, DB03213, and DB04107) and potential molecules (Z126202570, Z46489368, and Z422255982) through homology modeling and molecular docking/dynamic simulation and embraced binding free energy calculations that may effectively inhibit the TMPRSS2, which all contain a positively charged warhead similar to nafamostat and camostat (117). However, these molecules need to be determined by in-depth mechanistic research. A recent study discovered a covalent small molecule ketobenzothiazole (kbt) serine protease inhibitor, MM3122, whose structure is completely different from camostat and nafamostat and is said to be effective (86). All these results indicate that the study of small molecule inhibitors targeting TMPRSS2 for SARS-CoV-2 will be a good choice. In addition to the ACE2-mediated virus entry pathway, CD147-mediated viral entry is likely to become the second pathway of SARS-CoV-2 invasion. Although still controversial, this does not affect the research of drugs targeting CD147 in the prevention of SARS-CoV-2 infection (90). At present, the drugs targeting CD147 are mainly monoclonal antibodies, and research on small molecule compounds is rarely involved, which will be a breakthrough in future research. The latest research suggests that AXL is a candidate receptor for SARS-CoV-2, which can promote the infection of lung and bronchial epithelial cells (97). As a receptor tyrosine kinase (RTK), there is currently no report on the use of small molecule compounds targeting AXL for the treatment of SARS-CoV-2 infection, but we can refer to the research of RTK small molecule inhibitors in tumors to discover potential small molecule inhibitors of AXL for preventing the entry of SARS-CoV-2.

When considering inhibiting SARS-CoV-2 replication, the study found a variety of promising small molecule inhibitors. $3CL^{pro}$ (nsp5) is one of the most ideal targets for discovering inhibitors of SARS-CoV-2. The study found that the amino Cys145 residue in the catalytic pocket of $3CL^{pro}$ is an effective target for exploring small molecular covalent inhibitors of SARS-CoV-2 and other coronaviruses (118). A fluorescence resonance

energy transfer study found that the 8-aminoquinoline antimalarial drug tafenoquine can induce the transformation of $3CL^{pro}$ to expose the hydrophobic pocket and promote the protein aggregation, ultimately reducing the activity of $3CL^{pro}$ and repressing SARS-CoV-2 RNA replication with an IC_{50} near 2.5 μmol/L, which is appropriately 1/4 that of hydroxychloroquine (119). Although Lopinavir-Ritonavir (*Kaletra*) was initially used in the treatment of SARS-CoV-2 because of its ability to block the replication of SARS-CoV and MERS by inhibiting $3CL^{pro}$, the latest research results do not support its use in the treatment of COVID-19 (120). A study screened FDA-approved drug libraries and found that the anticoagulant dipyridamole (DIP) may bind to $3CL^{pro}$ to inhibit more than 50% of SARS-CoV-2 replication in Vero E6 cells at 100 nmol/L. After 2 weeks of DIP treatment, 8 critically ill patients improved significantly (121). With the continuous understanding of the structure of the $3CL^{pro}$ protein, more small molecule inhibitors have been discovered, and some of them have been in clinical trials. Compounds 11a and 11b have been screened and confirmed to have a strong inhibitory effect on SARS-CoV-2 $3CL^{pro}$, with $IC_{50\ values}$ of 0.053 μmol/L and 0.040 μmol/L, respectively; $EC_{50\ values}$ of 0.53 μmol/L and 0.72 μmol/L, respectively; and have good pharmacokinetic properties (122). At present, 11a (DC402234) has submitted a clinical application registration declaration and has obtained FDA conditional clinical trial approval (Phase I: NCT04766931). After screening, the *in vivo* antiviral test results of the small molecule compounds MI-09 and MI-30 showed that oral or intraperitoneal injection of these compounds can significantly reduce the lung viral load and lung pathological damage in a SARS-CoV-2-infected transgenic mouse model (123). Although various research results and different inhibitors of $3CL^{pro}$ have been shown in front of people one after another, the clinical entry is extremely limited; only the four inhibitors (PF-07304814 [phase III: NCT04501978] and PF-07321332 [phase III: NCT05047601] developed by Pfizer, USA; the aforementioned 11a (DC402234 made by Frontiers, China [phase I: NCT04766931]; and the code-named S-217622 produced by Shionogi Inc., Japan [phase II/III: jRCT2031210350) are in clinical trial (124). PL^{pro} (nsp3) has also received much attention due to its important role in the replication and invasion of SARS-CoV-2. Some noncovalent small molecule inhibitors (rac3j, rac3k and rac5c) that have been effective against SARS-CoV can target SARS-CoV-2 PL^{pro} to prevent the self-processing of nsp3 in cells, thus reducing viral-induced CPE at high concentrations (33 μmol/L) (125). Based on the crystal structure of SARS-CoV-2 PL^{pro}, researchers obtained useful data from the FDA-approved drug database and identified 147 potential inhibitors of SARS-CoV-2 PL^{pro}. In Vero E6 cells, dronedarone, an ion channel modifier, has good antiviral activity against SARS-CoV-2-induced CPE with an IC_{50} of 4.5 μmol/L (CC_{50} of 12.1 μmol/L) (126). The naphthalene-based inhibitor, GRL-0617, can effectively inhibit the activity of SARS-CoV-2 PL^{pro} with an IC_{50} of 2.2 μmol/L, and its mechanism is not limited to occupying the substrate pocket but expands to seal the substrate binding entrance cleft, thereby preventing the binding of the substrate (62). At present, the crystal structure of PL^{pro} has been completely resolved (PDB code: 6W9C), and more small molecule compounds will be discovered as the crystal structure is fully analyzed. To date, no small molecule inhibitors against PL^{pro} have entered clinical studies, which suggests that there is still a long way to go in the development of PL^{pro}-targeted small molecule inhibitors against SARS-CoV-2. RdRP (nsp 12) has become an important target for the development of anti-SARS-CoV-2 drugs because it participates in the virus replication process as a key enzyme that catalyzes the synthesis of the SARS-CoV-2 genome. A research group from Shanghai, China, successfully analyzed the three-dimensional structure of the RdRP-nsp7-nsp8 complex at near-atomic resolution (with an overall resolution of 2.9 Å) using cryo-electron microscopy, which lays a solid foundation for the design of antiviral inhibitors based on the RdRP structure (127). As research on SARS-CoV-2 RdRP continues, multiple potential drugs have been discovered and confirmed. Remdesivir [GS-5734], a nucleotide analog originally used to fight Ebola virus, was first proposed for the treatment of COVID-19 patients because it can be used as a substrate for the RdRP. In Vero E6 cells at a SARS-CoV-2 MOI of 0.05, remdesivir shows an ideal potential to fight SARS-CoV-2 with IC_{50} = 0.77 μmol/L, CC_{50} > 100 μmol/L and SI > 129.87, which also quickly promotes the quick access of RdRP small molecule inhibitors to global phase III clinical trials and their direct use in some regions (128). However, things are always dramatic. The latest clinical trial results published by the WHO do not seem to be optimistic about this small molecule inhibitor (129). As far as COVID-19 hospitalized patients are concerned, it has little or no impact on indicators such as overall mortality and duration of hospital stay. Regardless of the outcome, the emergence of remdesivir has provided an important reference and motivation for the research of small molecule inhibitors targeting RdRP. A subsequent study screened a century-old classic drug, suramin, and a variety of derivatives, which exhibited a more than 20-fold ability to fight SARS-CoV-2 infection with remdesivir by targeting RdRP (66). Another small-molecule inhibitor called favipiravir (T-705) targets RdRP to mildly resist SARS-CoV-2 infection with an IC_{50} of 61.88 μmol/L, CC_{50} > 400 μmol/L and SI > 6.46 (130). Several clinical trials (ChiCTR2000029600/200030254, etc.) have shown that favipiravir may accelerate virus clearance and alleviate the progression of COVID-19, which lays a solid foundation for its clinical application and provides a structural basis and strong evidence for the development of broad-spectrum antiviral drugs based on the strategy of "old drugs and new use". A study reported that the oral broad-spectrum ribonucleoside analog β-D-N4-hydroxycytidine [EIDD-1931] showed good anti-SARS-CoV-2 activity in Vero cells with an IC_{50} of 0.3 μmol/L (131). In addition, the oral EIDD-1931 prodrug molnupiravir (MK-4482, EIDD-2801, Merck Sharp & Dohme Corp, USA), due to its ideal anti-coronavirus effect, has ended phase III clinical trials (NCT04575584, NCT04575597 and NCT04939428) ahead of schedule and is expected to be launched in the United States soon (131). The oral purine nucleotide prodrug AT-527 developed by Roche is expected to have a good phase III clinical trial (NCT04889040) result (132). These studies provide hopes and directions for the development of small molecule inhibitors targeting RdRP during SARS-CoV-2 infection. At present, there

are already several small molecule inhibitors that target helicases, such as bananins, 5-hydroxychromone derivatives, and SSYA10-001, which are expected to be used in SARS-CoV-2-related experiments (133). In addition, authoritative studies suggest that the classic old drug clofazimine has the ability to inhibit the helicase activity of SARS-CoV-2, suggesting that it may play a role in controlling the current COVID-19 pandemic and the emergence of CoVs in the future (134). Although there has been hope, the greatest challenge is the relatively low selectivity of small molecule inhibitors targeting helicase, and there is no drug targeting helicase that exceeds preclinical development. However, the development of small molecule helicase inhibitors may provide another effective treatment option for the COVID-19 pandemic.

Studies are also concerned that several small molecule inhibitors can fight SARS-CoV-2 *via* immunoregulatory and inflammatory functions, and the specific details are introduced in the "Significant Symptomatic Therapeutic Agents" section.

At present, the continuous rapid screening of small molecule databases based on SARS-CoV-2 potential targets has found some effective lead compounds or candidate drugs, which will promote the continuation of basic research and clinical trials of small molecule inhibitors for COVID-19 (**Table 2**). In addition, computer-based drug design is icing on the cake for accelerating the screening and development of small molecule inhibitors, but it is conservatively estimated that new targeted interventions will still take some time. Considering the current spread of the novel coronavirus disease and the continuing case fatality rate, rapid screening of FDA-approved and clinical trial drugs is a more practical method because "old drugs and new use" may reduce development costs and shorten development time (232). To date, a large number of small molecule inhibitors against SARS-CoV-2 infection have been screened; however, many of these studies have not been fully implemented (233). Meanwhile, the safety of some confirmed promising anti-SARS-CoV-2 small molecule inhibitors or drugs is also unknown, especially reproductive toxicity, which imposes more difficulties on the clinical translation of small molecule inhibitors. Therefore, adequate research needs to be carried out to maximize safety and avoid false positive effects. The mutation of the virus and the SARS-CoV-2 epidemic have made the discovery of vaccines and drugs more uncertain. In the long run, there is still much work to be done in the screening, validation, clinical research and clinical application of specific or broad-spectrum small molecule inhibitors for SARS-CoV-2 virus entry, replication, or prevention.

Vaccines

The main therapeutic strategies for infectious diseases include controlling the source of infection, blocking the route of transmission and protecting the susceptible. Among them, vaccines, as an effective means to protect susceptible persons and block transmission, have always been the main weapon for humans to fight infectious diseases (234). Given that the current effective treatments against the new coronavirus are not fully recognized, the development of vaccines against SARS-CoV-2 is particularly important. At present, a variety of vaccine platforms against SARS-CoV-2 are rapidly being established and developed, including inactivated vaccines and live attenuated vaccines and viral vector vaccines and nucleic acid vaccines (DNA and mRNA) (**Figure 5**) (235). With the joint efforts of scientists from all over the world, more than 322 candidate vaccines have been developed, which are in the preclinical, Phase I, Phase II through to Phase III efficacy studies and include Phase IV registered as interventional studies (https://www.who.int/publications/m/item/draft-landscape-of-covid-19-candidate-vaccines) **(Table 2)**. The rapid development of vaccine research has brought dawn to the control of the epidemic, but there are many shortcomings that need to be considered and improved.

Regarding inactivated vaccines, there are preliminary statistics of 15 such vaccines that have entered different clinical trials, including BBIBP-CorV, CoronaVac, WIBP vaccines, and Covaxin, which have entered Phase III (236). CoronaVac (Sinovac Biotech, China) can produce a wide range of neutralizing antibodies against 10 different virus strains in a variety of animals with a titer of over 90, and it has complete protection against SARS-CoV-2 infection after three immunizations (6 μg/dose) in macaques (151). Currently, CoronaVac is undergoing Phase III clinical trials in Brazil, of which 90,000 healthy participants are or will be registered. Another inactivated vaccine, covaxin, developed by an Indian Pharmaceutical company, has shown good safety and effectiveness in phase 1/2 clinical trials. At present, Covaxin is also undergoing phase III clinical trials, of which 26,000 volunteers participated (237). Other candidate inactivated vaccines are being rapidly developed in China and have been confirmed to have higher antibody titers and better safety in phase 1/2 clinical trials. Just now, a Phase III clinical trial with 15,000 participants has been launched in the United Arab Emirates (238). The development of inactivated vaccines gives us confidence in the development of vaccines against SARS-CoV-2. However, we must also recognize some of the shortcomings of inactivated vaccines and improve them. For example, the inoculation dose is large, the protection time is short, the need for multiple vaccinations, and the formation of antibody-dependent enhancement effects may aggravate viral infections.

The development of live attenuated vaccines against SARS-CoV-2 has been slow, mainly due to the limitations of the longer transformation or screening time of attenuated strains, heavy workload, and high biosafety protection standards. At present, only one attenuated influenza virus vector vaccine developed by China has entered a phase I clinical trial (ChiCTR2000037782), and three live attenuated vaccines developed by India and Turkey are undergoing preclinical evaluation (239). However, we should also realize that live attenuated vaccines can retain the complete structure of the virus and have good immunogenicity; they can simulate the natural infection process to induce humoral and cellular immunity and can produce long-lasting protection; no adjuvant is required (240). If the transformation time of attenuated strains can be optimized and biosafety is ensured, live attenuated vaccines can be an alternative direction.

At present, approximately 20 SARS-CoV-2 vaccines are being developed around the world that use the viral vector method.

TABLE 2 | List of drugs that may be effective in the preclinical and clinical phases for COVID-19.

Drug Name	Drug Type	Target	Study Phase	Test Effect	Reference Doi
Arbidol	Small molecule compound	S1/S2 subunit of Spike protein	Phase IV (NCT04252885; NCT04260594)	Prevents S1 subunit from falling off and membrane fusion of S2 subunit, and SARS-CoV-2 entry	Wang et al. (103)
Bictegravir	Small molecule compound	S2 subunit of Spike protein	Preclinical	Prevents the SARS-CoV-2 entry by restricting the interaction between Spike RBD and ACE2	Sun et al. (102)
Dolutegravir	Small molecule compound	S2 subunit of Spike protein	Preclinical	Prevents the SARS-CoV-2 entry by restricting the interaction between Spike RBD and ACE2	Sun et al. (102)
Tizoxanide	Small molecule compound	S1/S2 subunit of Spike protein	Preclinical	Prevents the S1 subunit from binding to ACE2, and S2 subunit membrane fusion	Sun et al. (102)
EK1	Peptide	Spike protein HR2	Preclinical	Against Spike protein-mediated membrane fusion and pseudovirus infection	Xia et al. (135)
EK1C4	Lipopeptide	Spike protein HR2	Preclinical	Against Spike protein-mediated membrane fusion and pseudovirus infection	Xia et al. (106)
IPB02	Lipopeptide	Spike protein HR2	Preclinical	Against Spike protein-mediated celle-cell fusion and pseudovirus infection	Zhu et al. (107)
SARS-CoV-2-HR2P	Peptide	Spike protein HR2	Preclinical	Against Spike protein-mediated membrane fusion and pseudovirus infection	Xia et al. (106)
$[SARS_{HRC}\text{-}PEG_4]_2$-chol	Dimeric lipopeptide	Spike protein HR2	Preclinical	Against Spike protein-mediated membrane fusion and SARS-CoV-2 entry	de Vries et al. (108)
SBP1	23-mer peptide fragment	SARS-CoV-2-RBD	Preclinical	Block the interaction between Spike protein and ACE2, and SARS-CoV-2 entry	Ucar et al. (109)
AHB1/3	Peptide	SARS-CoV-2-RBD	Preclinical	Inhibit the SARS-CoV-2 attachment between Spike protein and ACE2, and viral neutralization	Cao et al. (110)
LCB1/3	Peptide	SARS-CoV-2-RBD	Preclinical	Inhibit the SARS-CoV-2 attachment between Spike protein and ACE2, and viral neutralization	Cao et al. (110)
ATN-161	Integrin binding peptide	Spike protein, ACE2	Preclinical	Inhibit SARS-CoV-2 attachment through $\alpha5\beta1$ integrin-based mechanism	Beddingfield et al. (111)
Captopril	ACE inhibitor	ACE2	Phase II (NCT04355429)	Inhibit the interaction between Spike protein and ACE2, and viral neutralization	Milne et al. (136)
Enalapril	ACE inhibitor	ACE2	Phase III (NCT04591210)	Inhibit the interaction between Spike protein and ACE2, and viral neutralization	Bauer, et al. (112)
Camostat mesylate	Serine protease inhibitor	TMPRSS2	Phase II (NCT04455815)	Blocks the TMPRSS2 activity induced Spike protein priming and SARS-CoV-2 entry	Hoffmann et al. (137)
Nafamostat mesylate	Serine protease inhibitor	TMPRSS2	Phase II/III (NCT04455815)	Blocks the TMPRSS2 activity induced Spike protein priming and SARS-CoV-2 entry	Hempel et al. (138)
Z126202570; Z46489368; Z422255982	Serine protease inhibitor	TMPRSS2	Preclinical	Blocks the TMPRSS2 activity induced Spike protein priming and SARS-CoV-2 entry	Alzain and Elbadwi, et al. (117)
MM3122	Serine protease inhibitor	TMPRSS2	Preclinical	Blocks the TMPRSS2 activity induced Spike protein priming and SARS-CoV-2 entry	Mahoney et al. (86)
Tafenoquine	8-aminoquinoline antimalarial drug	$3CL^{pro}$	Preclinical	Induces the transformation of $3CL^{pro}$ conception, inhibits the activity of $3CL^{pro}$ and represses the SARS-CoV-2 RNA replication	Achutha et al. (119)
Dipyridamole (DIP)	Anticoagulant	$3CL^{pro}$	Preclinical	Inhibits the activity of $3CL^{pro}$ and represses the SARS-CoV-2 RNA replication	Liu et al. (121)
Compound 11a	Pseudopeptide lead compound	$3CL^{pro}$	Phase I (NCT04766931)	Inhibits the activity of $3CL^{pro}$ and represses the SARS-CoV-2 RNA replication	Dai et al. (122)
Compound 11b	Pseudopeptide lead compound	$3CL^{pro}$	Preclinical	Inhibits the activity of $3CL^{pro}$ and represses the SARS-CoV-2 RNA replication	Dai et al. (122)
MI-09	Boceprevir or telaprevir derivatives	$3CL^{pro}$	Preclinical	Inhibits the activity of $3CL^{pro}$ and represses the SARS-CoV-2 RNA replication	Qiao et al. (123)
MI-30	Boceprevir or telaprevir derivatives	$3CL^{pro}$	Preclinical	Inhibits the activity of $3CL^{pro}$ and represses the SARS-CoV-2 RNA replication	Qiao et al. (123)
PF-07304814	Phosphate prodrug of PF-00835231	$3CL^{pro}$	Phase I (NCT04535167)	Inhibits the activity of $3CL^{pro}$ and represses the SARS-CoV-2 RNA replication	Yap et al. (139)
PF-07321332	Orally active pseudopeptide $3CL^{pro}$ inhibitor	$3CL^{pro}$	Phase III (NCT04960202)	Inhibits the activity of $3CL^{pro}$ and represses the SARS-CoV-2 RNA replication	Zhao et al. (140)
S-217622	Orally active reversible covalent $3CL^{pro}$ inhibitor	$3CL^{pro}$	Phase II/III (jRCT2031210350)	Inhibits the activity of $3CL^{pro}$ and represses the SARS-CoV-2 RNA replication	https://www.shionogi.com/jp/ja/news/2021/10/211021_2.html

(Continued)

TABLE 2 | Continued

Drug Name	Drug Type	Target	Study Phase	Test Effect	Reference Doi
GRL-0617	Naphthalene-based selective noncovalent PL^{pro} inhibitor	PL^{pro}	Preclinical	Inhibits of PL^{pro} to impair the SARS-CoV-2-induced cytopathogenic effect, maintain the antiviral interferon pathway and reduce viral replication	Pitsillou et al. (141) Shin et al. (62)
Remdesivir	Monophosphoramidate prodrug of adenosine analogue	RdRP	Phase II/III (NCT04431453)	Blocks the RdRP activity to block the SARS-CoV-2 replication and infection, thus reducing the time to recovery in COVID-19 patients	Kokic et al. (142)
Suramin	Non-nucleoside RdRP inhibitor	RdRP	Phase II (ChiCTR2000030029)	Inhibits the RdRP activity to block the SARS-CoV-2 replication and infection	Yin et al. (143)
Favipiravir	Nucleotide analogue	RdRP	Phase III (NCT04558463)	Inhibits the RdRP activity to block the SARS-CoV-2 replication and infection	Naydenova et al. (144) Ninove et al. (145)
EIDD-1931	Ribonucleoside analogue	RdRP	Phase I/II (NCT04746183)	Prevents the synthesis of RdRP and promotes the mutation of SARS-CoV-2 RNA bases to kill the virus, reduce the viral load and finally clear the infection	Miller et al. (146) Jena et al. (147)
EIDD-2801 (molnupiravir)	Oral EIDD-1931 prodrug (ribonucleoside analogue)	RdRP	Phase II (NCT04405570)	Anti-SARS-CoV-2 after being metabolized into EIDD-1931 in the body	Wölfel et al. (148) Sheahan et al. (131)
AT-527	Double Prodrug of a Guanosine Nucleotide Analog	RdRP	Phase III (NCT04889040)	It selectively inhibits the RdRP activity to block the SARS-CoV-2 replication and infection	Good et al. (132)
Bananins	Drug-like compound	Helicase	Preclinical	Blocks the virus replication and load by inhibiting the helicase activity	Spratt et al. (133)
SSYA10-001	Drug-like compound	Helicase (nsp13)	Preclinical	Blocks the virus replication and load by inhibiting the helicase activity	Spratt et al. (133)
Clofazimine	Anti-tuberculosis drug	Helicase Spike protein	Phase II (NCT04465695)	Inhibits the spike-dependent entry, reduces viral load by disrupting the helicase induced virus replication, and also prevents cytokine storm associated with viral infection	Yuan et al. (134)
BBIBP-CorV	Inactivated (Vero cells) vaccine	Spike protein	Phase III (NCT04993560); Approved for emergency utilization worldwide	Elicits high levels of neutralizing antibodies (anti-receptor-binding domain (RBD) IgG, as well as anti-spike protein (S) IgG and IgA antibodies) and T cell-mediated immune responses	Wang (149) Xia et al. (150)
CoronaVac	Inactivated (Vero cells) vaccine	S1 domain and RBD of Spike protein	Phase III (NCT05077176); Approved for emergency utilization worldwide	Elicits the development of humoral immunity against SARS-CoV-2, particularly Ig anti-RBD	Zhang et al. (151) Vacharathit et al. (152)
WIBP vaccine	Inactivated (Vero cells) vaccine	Spike protein	Phase III (NCT04510207)	Elicits high levels of neutralizing antibodies and T cell-mediated immune responses	Al et al. (153)
BBV152 (Covaxin)	Whole-virion inactivated (Vero cells) vaccine	Spike protein	Phase III (NCT04641481)	Induces high titres of specific IgG and neutralizing antibodies and enhances cytokine and chemokine responses	Ella et al. (154) Ella et al. (155)
ChAdOx1 nCoV-19/ AZD1222	Non-replicating adenovirus vectored vaccine	Spike protein	Phase III (NCT05059106)	Induces high anti-spike neutralizing antibody titers, as well as Fc-mediated functional antibody responses	Voysey et al. (156) Ramasamy et al. (157)
Ad26.COV2.S	Non-replicating adenovirus 26 vectored vaccine	Spike protein	Phase III (NCT04505722)	Induces high titres and stable neutralizing antibodies and enhances T-cell responses	Sadoff et al. (158)
Ad5-nCoV	Non-replicating adenovirus type 5 vectored vaccine	Spike protein	Phase III (NCT04540419); Approved for emergency utilization in China	It generates S1 IgG antibodies to induce strong humoral and cellular immune responses	Guzmán-Martínez et al. (159) Wu et al. (160)
Gam-COVID-Vac	Non-replicating adenovirus 5 and 26 vectored vaccine	Spike protein	Phase III (NCT04642339) Approved for emergency utilization in Russia	Induces high titres of specific IgG and neutralizing antibodies and enhances T-cell responses	González et al. (161) Logunov et al. (162)
GRAd-COV2	Non-replicating defective Simian adenovirus vectored vaccine	Spike protein	Phase II/III (NCT04791423)	Elicits both functional antibodies that neutralize SARS-CoV-2 infection and block Spike protein binding to the ACE2 receptor, and a robust, T helper (Th)1 dominated cellular response	Lanini et al. (163)

(Continued)

TABLE 2 | Continued

Drug Name	Drug Type	Target	Study Phase	Test Effect	Reference Doi
VXA-CoV2-1	Non-replicating adenovirus Ad5 vectored vaccine	Spike protein	Phase I (NCT04563702)	Induces anti-spike IgG and neutralizing antibodies with the sera demonstrating neutralizing activity	Johnson et al. (164)
hAd5-S-Fusion+N-ETSD	Non-replicating adenovirus Ad5 vectored vaccine	Spike protein N protein	Phase I/II (NCT04845191)	Induces neutralizing antibodies and Th1-prone N- and S-specific T-cell responses, providing complete protection of the nasal cavity and lungs against SARS-CoV-2 infection	Gabitzsch et al. (165)
LV-SMENP-DC	Minigenes engineered based on multiple viral genes, lentiviral vectored (NHP/TYF) modified dendritic cell vaccine	Spike protein	Phase I/II (NCT04276896)	Induces neutralizing antibodies and T-cell responses	Mahrosh et al. (166)
Pathogen-specific aAPC	Minigenes engineered based on multiple viral genes, lentiviral vectored (NHP/TYF) vaccine	Antigen presenting cells	Phase I (NCT04299724)	Induces neutralizing antibodies and T-cell responses	Mahrosh et al. (166)
DelNS1-2019-nCoV-RBD-OPT1	Replicating intranasal based-RBD flu vectored vaccine	Spike protein	Phase II/III (ChiCTR2100048316/ ChiCTR2100051391)	Simulates the natural infection pathway of respiratory viruses to activate local and systemic T-cell immune response to prevent the SARS-CoV-2 infection	Wang et al. (167)
VSV-ΔG-SARS-CoV-2-S/IIBR-100	Replicating viral VSV vectored vaccine	Spike protein	Phase II/III (NCT04990466)	It develops spike-specific antibodies in antisera to prevent the SARS-CoV-2 infection	Yahalom-Ronen et al. (168)
TMV-083/V-591	Attenuated measles-vector based vaccine	Spike protein	Phase I/II (NCT04497298/ NCT04498247); Stop R&D	Increases the geometric mean titers (GMTs) of anti-SARS-CoV-2 Spike protein serum neutralizing antibody to prevent the SARS-CoV-2 infection	Scarabel, Lucia, et al. (169)
V590	Recombinant VSV-vector based vaccine	Spike protein	Phase I (NCT04569786); Stop R&D	Increases the geometric mean titers (GMTs) of anti-SARS-CoV-2 Spike protein serum neutralizing antibody	Scarabel et al. (169)
MVA-SARS-2-S	Nonreplicating modified vaccinia virus Ankara vectored vaccine	Spike protein	Phase I (NCT04569383)	The robust expression of Spike protein as antigen to produce S-specific CD8+ T cells and serum antibodies binding to Spike protein that neutralized SARS-CoV-2.	Tscherne et al. (170)
ZyCoV-D	DNA vaccine	Spike protein	Phase I/II (CTRI/2020/07/ 02635); Approved for clinical use in India	It encodes and translate the SARS-CoV-2 Spike protein, which stimulates the host to produce high titres of virus-neutralizing antibodies and robust T cell immune response, thereby completely blocking the virus entry and subsequent infection	Momin et al. (171) Dey et al. (172)
INO-4800	DNA vaccine	Spike protein	Phase III (NCT04642638)	It induces antibodies to block SARS-CoV-2 Spike protein binding to the host receptor ACE2 and produces high titres of virus-neutralizing antibodies and robust cell immune response, thereby completely blocking the virus entry and subsequent infection	Tebas et al. (173) Smith et al. (174)
BNT162b2	Nucleoside-modified mRNA vaccine	Spike protein	Phase III (NCT04955626); Approved for clinical use	It mimics and encodes the SARS-CoV-2 spike protein, which stimulates the host to produce high titres of virus-neutralizing antibodies and robust T cell immune response, thereby completely blocking the virus entry and subsequent infection	Polack et al. (175) Liu et al. (176)
mRNA-1273	Lipid nanoparticle-encapsulated mRNA vaccine	Spike protein	Phase III (NCT04860297)	It mimics and encodes the SARS-CoV-2 spike protein, which stimulates the host to produce high titres of virus-neutralizing antibodies and robust immune response, thereby completely blocking the virus entry and subsequent infection	Baden et al. (177) Jackson et al. (178)
CVnCoV	Lipid nanoparticle-encapsulated naturally occurring nucleotides mRNA vaccine	Spike protein	Phase III (NCT04860258)	It mimics and encodes the SARS-CoV-2 surface spike protein, which stimulates the host to produce high titres of virus-neutralizing antibodies and robust T-cell responses, thereby completely blocking the virus entry and subsequent infection	Alexandersen et al. (179) Rauch et al. (180)
ARCT-021	Self-replicating mRNA and nanoparticle delivery system vaccine	Spike protein	Phase II (NCT04728347)	It mimics and encodes the virus surface spike protein, which stimulates the host to produce antibodies to activate cell-mediated immunity, thereby completely blocking the entry of SARS-CoV-2 and subsequent infection	Rappaport et al. (181)

(Continued)

TABLE 2 | Continued

Drug Name	Drug Type	Target	Study Phase	Test Effect	Reference Doi
LNP-nCoVsaRNA	Self-amplifying mRNA vaccine	Spike protein	Phase I (ISRCTN17072692)	It mimics the virus surface spike protein gene, triggers the virus to produce spike protein, stimulates the host to produce antibodies and completely blocks the entry of SARS-CoV-2 and subsequent infection	Karpiński et al. (182)
ARCoV	Lipid nanoparticle thermostable mRNA-based Vaccine	Spike protein RBD	Phase III (NCT04847102)	It encodes the viral Spike protein RBD to elicit robust neutralizing antibodies against SARS-CoV-2 as well as a Th1-biased cellular response against the viral challenge	Zhang et al. (183)
hrsACE2	Human recombinant soluble ACE2	ACE2	Preclinical	It prevents the interaction between Spike protein and ACE2, reduce early SARS-CoV-2 infections, and effectively inhibit the viral proliferation in human vascular organs and kidney organs	Monteil et al. (115) Abd et al. (184)
LY-CoV555 LY3819253	S protein neutralizing antibody	Spike protein	Phase II/III (NCT04427501)	It high-affinity binds to the Spike protein RBD to inhibit the ACE2 binding and reduce the viral replication in the upper and lower respiratory tract	Chen et al. (185) Yang et al. (186)
BRII-196 BRII-198	S protein neutralizing antibody	Spike protein	Phase III (NCT04501978)	It binds to different highly conserved epitope on the Spike protein to block viral entry and neutralize live SARS-CoV-2 infection	Yang et al. (186)
SCTA01 HB27	S protein neutralizing antibody	Spike protein RBD	Phase II/III (NCT04644185)	It engages the Spike protein RBD to efficiently neutralize SARS-CoV-2 pseudoviruses as well as authentic SARS-CoV-2	Yang et al. (186) Li et al. (187)
NVX-CoV2373	Recombinant nanoparticle spike protein subunit vaccine	Spike protein	Phase II (NCT05112848)	It elicits high titer anti-S IgG that blocks hACE2 receptor binding, neutralize virus infection and antigen-specific-cells, and protects against SARS-CoV-2 challenge	Tian et al. (188) Keech et al. (189)
RBD219-N1C1	Recombinant protein heterologous vaccine	Spike protein RBD	Preclinical	Stimulate SARS-CoV-2 to produce IgG neutralizing antibodies and induce T-cell immunity	Chen et al. (190) Lee et al. (191)
HR2P polypeptide	Peptide-based membrane fusion inhibitor	Spike protein HR2 domain	Preclinical	It can effectively inhibit SARS-CoV-2 replication and the Spike protein-mediated cell-cell fusion for treating the viral infection	Xia et al. (192) Lu et al. (193)
Lianhua Qingwen Capsule	TCM	multiple targets such as Akt1, MAPK1, IL6, HSP90AA1, TNF, and CCL2, et al	Real World Study	The main ingredients can inhibit multiple protein targets such as Akt1, MAPK1, IL6, HSP90AA1, TNF, and CCL2, et al, to reduce the inflammatory storm, tissue damage and help eliminate virus infection	Xia et al. (194) Yan et al. (195)
Qingfei Paidu Decoction	TCM	$3CL^{pro}$, and multiple targets such as CXCR4, ICAM1, CXCL8, CXCL10, IL6, IL2, CCL2, IL1B, IL4, et al	Real World Study	Multiple main ingredients can inhibit the $3CL^{pro}$ mediated SARS-CoV-2 replication, and invasion, and anti-inflammatory and immune regulation, and repairing body damage	Yang et al. (196) Li et al. (197)
Huoxiang Zhengqi formula	TCM	$3CL^{pro}$, PI3K/Akt	Real World Study	Multiple main ingredients can inhibit the $3CL^{pro}$ mediated SARS-CoV-2 replication and improve the PI3K/Akt mediated inflammatory cytokine release and inflammatory storm	Du et al. (198)
Xuebijing injection	TCM	$3CL^{pro}$, ACE2	Real World Study	Multiple components combine with 3CLpro and ACE2 to act on targets such as IL6, CCL2, TNF and PTGS2 to reduce SARS-CoV-2 entry inflammation responses and regulate the immune functions	Qin et al. (199) Feng et al. (200)
Jinhua Qinggan Granules	TCM	$3CL^{pro}$, ACE2	Real World Study	Multiple components combine with $3CL^{pro}$ and ACE2 to act on targets such as PTGS2, HSP90AB1, HSP90AA1, PTGS1, and NCOA2 to shorten the fever time, increase the recovery rate of lymphocytes and white blood cells, and improve related immunological indicators	Zhang et al. (201) Liu et al. (202)
Tanreqing Injection	TCM	$3CL^{pro}$, $CD3^+$ T cell	Real World Study	Multiple main ingredients can inhibit the $3CL^{pro}$ mediated SARS-CoV-2 replication and improve the $CD3^+$ T-cell level to enhance immune function	Zhang et al. (203)
Huashi Baidu Decoction	TCM	$3CL^{pro}$, ACE2	Real World Study	Blocks the ACE2 receptor mediated SARS-CoV-2 host cell entry and inhibits the $3CL^{pro}$-mediated viral replication and infection	Tao et al. (204) Cai et al. (205)
Shufeng Jiedu Capsule	TCM	$3CL^{pro}$, NF-κB	Real World Study	Inhibits the NF-κB signaling pathway and $3CL^{pro}$ to reduce the SARS-CoV-2 load, cytokine storm, inflammation and regulate immune response	Chen et al. (206) Xia et al. (207)
Xuanfei Baidu Decoction	TCM	NF-κB signaling pathway	Real World Study	Inhibits the NF-κB mediated cytokine storm and blunts the THP-1-derived macrophages pinocytosis	Li et al. (208)

(Continued)

TABLE 2 | Continued

Drug Name	Drug Type	Target	Study Phase	Test Effect	Reference Doi
Reduning injection	TCM	Carbonic anhydrases (CAs), matrix metallopeptidases (MMPs) and multiple pathways like PI3K/Akt, MAPK	Real World Study	Inhibits the overexpression of MAPKs, PKC and p65 NF-κB to reduce cytokine storm, inflammation and lung damage	Cao et al. (209) Xu et al. (210) Jia et al. (211)
Shenmai injection	TCM	Bcl2, MAPK3 and IL-6	Real World Study	Immune regulation for COVID-19	Yang et al. (212)
Quercetin	Plant flavonoid active ingredients of TCM	Multiple enzymes including $3CL^{pro}$, PL^{pro}, RDRP, Spike protein and ACE2	Preclinical	Inhibits multiple SARS-CoV-2 enzymes mediated viral replication, attachment and entry and infection	Derosa et al. (213) Pan et al. (214) Saakre et al. (215)
Kaempferol	The main flavonoid polyphenols of kaempferol galanga L	ACE2 and $3CL^{pro}$	Preclinical	Blocks the ACE2 receptor mediated SARS-CoV-2 cell entry and inhibits the $3CL^{pro}$-mediated viral replication and infection	Khan et al. (216) Pan et al. (214)
Luteolin	Main flavonoid in honeysuckle	$3CL^{pro}$ and cytokine storm	Preclinical	Blocks 3CLpro-mediated SARS-CoV-2 replication and infection, inhibits the cytokine storm caused by mast cells secreting proinflammatory cytokines	Theoharides (217) Shawan et al. (218)
Isorhamnetin	Flavonoid ingredient in hippophae rhamnoides	Spike protein and $3CL^{pro}$	Preclinical	Inhibits the $3CL^{pro}$ mediated SARS-CoV-2 replication and Spike protein mediated viral attachment	Zhan et al. (219) Tejera et al. (220)
Naringenin	Active ingredients of TCM	$3CL^{pro}$, cytokine storm and ACE2	Preclinical	Inhibits the $3CL^{pro}$ mediated SARS-CoV-2 replication, cytokine production induced cytokine storm and ACE2 mediated viral entry	Clementi et al. (221) Maurya et al. (222) D'Amore et al. (223)
Wogonin	Active ingredients of TCM	$3CL^{pro}$ and Akt1	Preclinical	Inhibits the $3CL^{pro}$ mediated SARS-CoV-2 replication and Akt1 induced infection, lung injury and lung fibrogenesis	Xia, Lu, et al. (207) Xia et al. (194)
Salvianolic acid C	Active hydrophilic compound of Danshen	Spike protein	Preclinical	Inhibits SARS-CoV-2 infection by blocking the formation of six-helix bundle core of spike protein and the binding of its RBD and ACE2	Yang et al. (224) Wang et al. (225) Hu et al. (226)
Baicalin	Active components of Scutellaria B.	$3CL^{pro}$, RdRP and PL^{pro}	Preclinical	Inhibits SARS-CoV-2 replication by interfering the $3CL^{pro}$, RdRP and PL^{pro}	Jo et al. (227) Zandi et al. (228) Rehman et al. (229)
Baicalein	Active components of Scutellaria B.	$3CL^{pro}$, RdRP, and Mitochondrial	Preclinical	Inhibits SARS-CoV-2 replication by interfering mitochondrial oxidative phosphorylation, ^{3CLpro} and RdRP	Huang et al. (230) Liu et al. (231) Zandi et al. (228)

These vector vaccines are mainly divided into two categories: nonreplicating vector vaccines based on adenovirus and lentivirus and replicating vector vaccines based on measles, influenza, etc. The most concerning adenovirus vectors include ChAdOx1 nCoV-19/AZD1222 (Oxford University & AstraZeneca, etc., UK; D8110C00001) (241) and Ad26.COV2.S (Johnson & Johnson, USA; NCT04505722) (242), Ad5-nCoV (Academy of Military Medical Sciences & CanSino Biologics Inc, China; NCT04526990) (160) and Gam-COVID-Vac (Gamaleya, Russia; NCT04656613) (162). In addition, the 2019-nCOV candidate (Academy of Military Medical Sciences, China; ChiCTR2000031781) and defective simian adenovirus vector GRAd-COV2 (ReiThera, Italy; NCT04791423) are in phase II, with two vaccines: VXA-CoV2-1 (Vaxart, USA; NCT04563702) and hAd5-S-Fusion+N-ETSD (ImmunityBio, Inc., USA; NCT04710303) are in phase I. Lentiviral vector-based vaccines under development include LV-SMENP-DC currently in phase I/II and pathogen-specific aAPC vaccine in phase I (Shenzhen Geno-Immune Medical Institute, China; NCT04299724/NCT04276896). Phase II of the clinical trial was the intranasal influenza virus vector DelNS1-2019-nCoV-RBD-OPT1 (Beijing Wantai Biological Pharmacy, China; ChiCTR2000039715), and phase I/II of the clinical trial was the replication VSV vector rVSV-SARS-CoV-2-S/IIBR-100 vaccine (Israel Institute of Biology, Israel; NCT04608305) and three replication virus vector vaccines in Phase I: the intranasal influenza virus vector the measles vector TMV-083/V-591 (Institut Pasteur & Themis Bioscience, Austria; NCT04497298) and the VSV vector V590-001 (MSD Corp., USA; NCT04569786) and modified Ankara vector MVA-SARS-2-S (Universitätsklinikum Hamburg-Eppendorf, Germany; NCT04569383). Relying on the characteristics of few adverse reactions, good safety, and a mature production system, this type of vaccine has been developed rapidly. However, neutralizing antibodies of the vector may exist in the body, which will cause the vector to be attacked, thereby reducing the vaccine effect. Therefore, improving the effectiveness will be an important direction for the improvement of these vector vaccines.

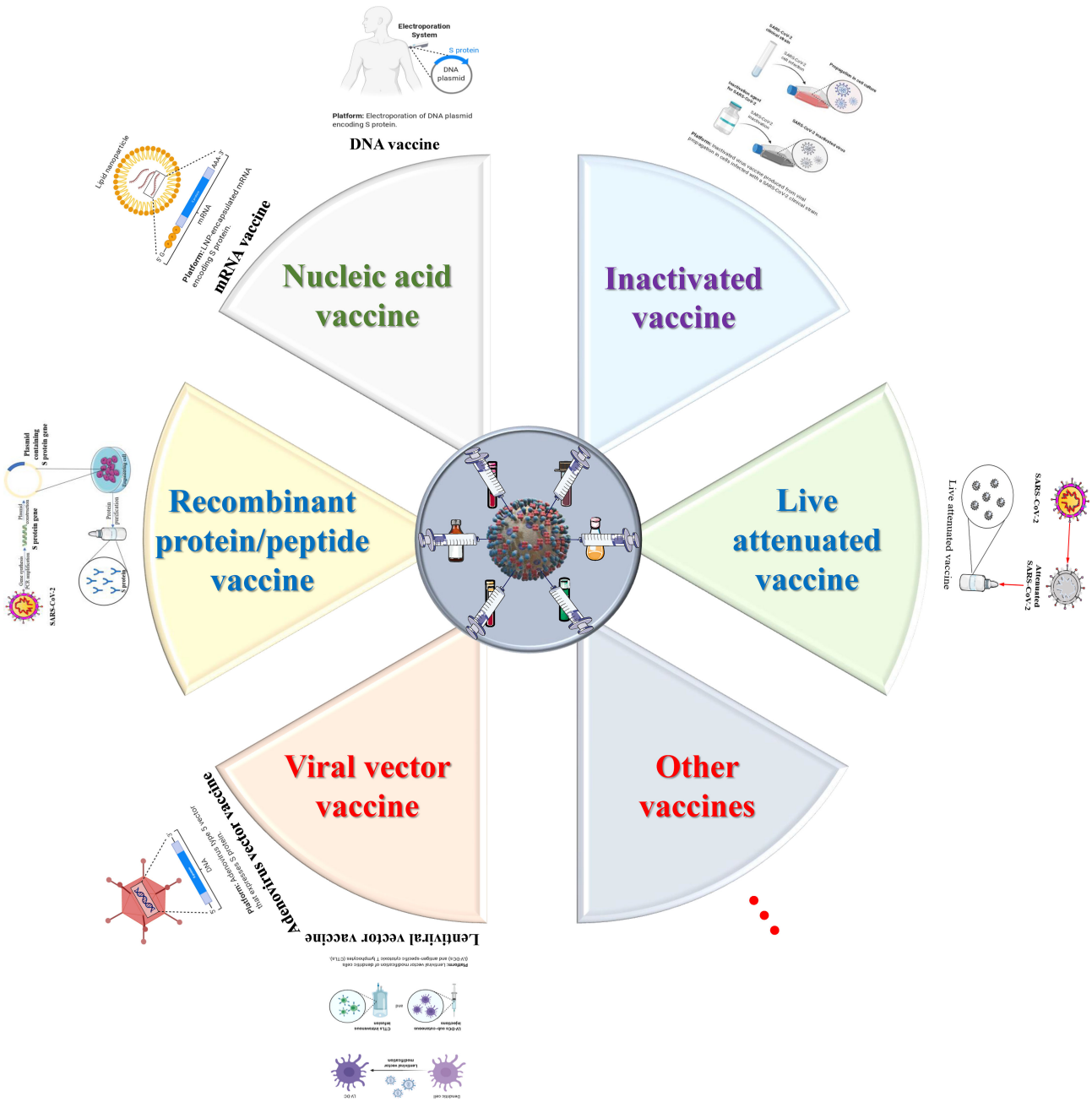

FIGURE 5 | The design and development model of SARS-CoV-2/COVID-19 vaccines. One of the most important intervention strategies for COVID-19 is vaccine control. To date, six major types of vaccine candidates (live attenuated vaccines, recombinant protein/peptide vaccines, inactivated vaccines, viral vector vaccines, nucleic acid vaccines and other types of vaccines) are under development, clinical trials, authorized emergency use, and routine preventive use. These six types of candidate vaccines represent the direction of SARS-CoV-2 and even the entire coronavirus vaccine research.

The SARS-CoV-2 nucleic acid vaccine has quickly become the focus of vaccine research and development due to its simple development and operation, low production cost, short development and production cycle, and rapid response (243). At present, the research of such vaccines is divided into two major directions, namely, DNA vaccines and mRNA vaccines. Currently, there are 27 DNA vaccines under research in the world, 11 of which have entered the clinical trial stage, and this number will slowly increase as the technology continues to mature. ZyCoV-D is a new type of DNA vaccine candidate mainly composed of plasmid DNA loaded with the viral spike gene and signal peptide coding gene (171). The results of clinical trials (CTRI/2020/07/026352) have verified a good safety profile and induced cellular and humoral responses, which will support its further development

to prevent COVID-19-related infection and death in the global population. Meanwhile, the emergency use of the ZyCoV-D vaccine in India has brought more possibilities and hopes for the development of DNA vaccines. INO-4800 is a DNA vaccine expressing S protein particles developed by Inovio Pharmaceuticals (174). Clinical trial (NCT04336410) data prove that the INO-4800 vaccine maintains one or both cells and humoral arms of the immune response for the emerging SARS-CoV-2 variant, which may be the key factor affecting the ongoing COVID-19 pandemic. Taking into account the advantages of DNA vaccines, the results of phase I clinical trials of INO-4800 (NCT04447781) and the status of entering phase II/III clinical trials (NCT04642638) once again brought great encouragement to the development of DNA vaccines. Although we have seen great hopes for DNA vaccines against the new coronavirus, we should also clearly recognize that the challenge for DNA vaccines is that they need to reach the nucleus all the way, which forces us to do more research to improve and develop a delivery system to meet the delivery efficiency of DNA vaccines (244). In addition to DNA vaccines, the development of mRNA vaccines is also in full swing. mRNA vaccines can express intracellular antigens similar to DNA vaccines, but they solve the problem of low immunogenicity of DNA vaccines and generate nonspecific immunity against the vector and delivery efficiency, so they have received more attention from researchers. Currently, two mRNA vaccines have been approved for marketing, namely BNT162b2 developed by BioNTech & Pfizer and mRNA-1273 produced by Moderna (175, 177). The results of clinical trials (NCT04368728/NCT04470427) show that the effectiveness, safety and immunogenicity of the two mRNA vaccines meet the ideal requirements. With further in-depth research on SARS-CoV-2, more mRNA vaccines have entered clinical trials, such as CVnCoV (CureVac AG; Phase II: NCT04515047), ARCT-021 (Arcturus Therapeutics, Inc.; Phase I/II: NCT04480957), LNP-nCoVsaRNA (Imperial College London; Phase I: ISRCTN17072692) and ARCoV (Academy of Military Medical Sciences; Phase I: ChiCTR2000034112), etc., and preclinical research (more than 19 candidate mRNA vaccines). Evidence from clinical trials thus far shows that mRNA vaccines are very likely to become a new platform that is fast, safe and efficient. However, to become a viable clinical alternative to traditional vaccines, mRNA vaccines must overcome two major problems related to the immunogenicity and stability of mRNA vaccines (245).

In addition to the above vaccine development strategies, recombinant protein and peptide vaccines such as human recombinant soluble ACE2 (hrsACE2), recombinant S protein nanoparticle vaccine (NVX-CoV2373), recombinant RBD protein vaccine (RBD219-N1), HR2P polypeptide and EK1C4 vaccine, etc. It can effectively induce humoral and cellular immunity to produce a wider cross-reaction, which is also an important choice for the development of SARS-CoV-2 vaccines. Each vaccine development strategy has many advantages, while at the same time, there are more or fewer shortcomings (246). The current main goal is to develop a safe and effective vaccine to curb the pandemic of SARS-CoV-2. However, we should be clearly aware that while avoiding the risks of existing vaccines, the ultimate goal of vaccine development is to develop single or mixed general vaccines for different CoVs or to establish a research and development and production platform. Only in this way can we withstand the current and future virus damage.

Traditional Chinese Medicine

Traditional Chinese medicine (TCM) has played an important role in the prevention and treatment of infectious diseases, and its theories and methods have been traced in many classic Chinese medical works (247). Meanwhile, these TCMs achieved good results in fighting against SARS-CoV infection in 2003. Moreover, in the 74187 confirmed cases of SARS-CoV-2 infection reported in China, the effective rate of receiving TCM treatment was more than 90%, and its main effect was to significantly improve and shorten the course of disease, delay disease progression, and reduce mortality (248). At the same time, traditional Chinese medicine has also been confirmed to have a low incidence of adverse reactions and often self-healing in the treatment of COVID-19 patients (249). Given that, TCM is a valuable resource for combating the epidemic of SARS-CoV-2.

Among the abundant resources of TCM, some representative drugs have shown good anti-SARS-CoV-2 activity in terms of direct anti-virus, regulation of inflammatory immunity, and organ protection, as shown in **Figure 4**. Analysis of cytopathic effects and plaque reduction showed that the active ingredients of Lianhua Qingwen capsule significantly inhibited the replication of SARS-CoV-2 in a dose-dependent manner through Akt signaling (194). In Vero E6 cells infected with 100 TCID50 SARS-CoV-2, the IC_{50} value was 411.2 μg/mL (250). In addition, Qingfei Paidu Decoction has the effect of directly inhibiting the invasion and replication of SARS-CoV-2 by acting on the host cell ACE2 and $3CL^{pro}$, respectively (251). In addition, the ingredients of Huoxiang Zhengqi capsule and Xuebijing injection are reported as potential $3CL^{pro}$ inhibitors, which could inhibit SARS-CoV-2 replication by targeting PIK3CG and E2F1 through the PI3K/Akt pathway. Moreover, network pharmacology and molecular docking studies found that the active ingredients of multiple TCMs, including Jinhua Qinggan granules, Tanreqing injection and Huashi Baidu Decoction, can all act on replicating enzymes or host cell receptor proteins to inhibit the replication and invasion of SARS-CoV-2 (252). In addition to directly blocking the replication and invasion of SARS-CoV-2, several active ingredients in Qingfei Baidu Decoction, Xuanfei Baidu Decoction, Huashi Baidu Decoction, Jinhua Qinggan Granules, Huoxiang Zhengqi Capsules, Lianhua Qingwen Capsules, Shufeng Jiedu Capsules, Xuebi Jing injection, Reduning injection, Tanreqing injection and Shenmai injection have been proven to not only reduce inflammation and inflammatory storms but also regulate cytokines and immune dysfunction by regulating multiple signal pathway abnormalities in patients, thus alleviating SARS-CoV-2-induced COVID-19 (253). In the process of studying the damage of SARS-CoV-2 to organ function, clinical analysis found that Qingfei Paidu Decoction, Jinhua Qinggan Granules, Lianhua Qingwen Capsules, and Shufeng Jiedu Capsules may play a protective role in organ damage through the effects of expectorant, anti-inflammatory, antioxidant, and antifibrosis (248, 252).

The mechanisms of TCMs for anti-SARS-CoV-2 and organs protection are quite complicated. On this basis, it will be a great

deal for the TCM treatment of SARS-CoV-2 if the specific active ingredients can be clarified. In this context, based on the TCM system pharmacology database and analysis platform (TCMSP) and literature, researchers have discovered that quercetin, kaempferol, luteolin, isorhamnetin, baicalein, naringenin, and wogonin (the latter three are in the same ranking) are the most promising important ingredients for anti-SARS-CoV-2 by comprehensive analysis using network pharmacology, bioinformation analysis, molecular docking, animal experiments, and clinical trials (252). In addition, as many as 401 compounds were found to have antiviral activity, and many ingredients have shown good therapeutic effects in experiments. A recent study found that salvianolic acid C, an active hydrophilic compound of Danshen, can effectively inhibit SARS-CoV-2 infection and block the formation of the S protein 6-HB core, with an IC_{50} value of 3.41 μmol/L (224). In a cell-based system, baicalin and baicalein, as the key active components of Scutellaria B., show strong antiviral ability by significantly inhibiting $3CL^{pro}$ activity, with $IC_{50\ values}$ of 10.27 and 1.69 μmol/L, respectively (254). The above findings suggest that TCM resources are very abundant, and many ingredients or compounds can be considered as lead compounds for the development of anti-SARS-CoV-2 drugs (**Table 2**). Perhaps the active ingredients of TCM can form a more promising small molecule inhibitor library in the future. Therefore, we should pay attention to and devote certain resources to screening, discovering and developing promising TCM compounds and extracts for the treatment of SARS-CoV-2.

We know that TCM prescriptions are produced in long-term exploration and practice, and their compatibility, toxicity, safety and other issues can be guaranteed. However, the abovementioned problems exist when the active ingredients and monomers of TCM are used (249, 255). We hope that TCM can be more widely used in the treatment of COVID-19, but at the same time, safety issues such as compatibility, toxicity, and adverse reactions of active ingredients and monomers of TCM should also be more studied and explored (256).

Significant Symptomatic Therapeutic Strategy

During COVID-19, aggressive inflammation and dysfunctional immune responses are the most basic, common and important pathological features that trigger cytokine storms and mediate multiple organ system damage (257). If not well controlled, the situation will worsen and even lead to death. In severe cases, most patients experience severe lung inflammation and thrombosis (258). Therefore, anti-inflammatory and anticoagulant drugs have been proposed and implemented, including the application of low molecular weight heparin to hospitalized patients as one of the standard symptomatic therapeutic strategies (**Figure 4**). In the serum of most COVID-19 patients, the levels of proinflammatory cytokines, including IL-1β, IL-2, IL-6, IL-8, IL-17, G/GM-CSF, MCP1, CCL3 and TNF, are significantly elevated, which is considered a cytokine storm (259). Among these cytokines, IL-6 has become a stable indicator of poor prognosis and has been used in the neutralization treatment of several inflammatory diseases. Therefore, targeting serum IL-6 levels to reduce inflammation may become an important symptomatic treatment strategy (260). One clinical study (ChiCTR2000029765) showed that tocilizumab, an IL-6 receptor-targeted monoclonal antibody, could reduce the risk of severe SARS-CoV-2 infection in patients with invasive mechanical ventilation or death (261). A randomized double-blind phase III clinical trial (NCT04320615) showed that tocilizumab (8 mg/kg, intravenous injection) can significantly shorten the intensive care unit by 5.8 days (9.8 days of standard care) and shorten the discharge time by 8 days (20 days of standard care) (262). Currently, tocilizumab has registered more than 70 SARS-CoV-2-related clinical trials. CVL218 was originally discovered through a data-driven drug reuse framework that can effectively inhibit the replication of SARS-CoV-2 with an EC_{50} of 5.12 μM. In-depth studies have shown that CVL218 (1 and 3 μM) treatment for 12 h can significantly reduce the production of IL-6 by 50% and 73% in peripheral blood mononuclear cells induced by CpG (microbial DNA sequence containing unmethylated CpG dinucleotides), respectively. *In vivo* studies have shown that CVL218 is mainly distributed in lung tissues and has no obvious toxicity (263). The above results suggest that CVL218 has a significant anti-inflammatory cytokine effect on SARS-CoV-2-induced immunopathological symptoms. Based on this, we think that targeted intervention of inflammatory cytokines is an important SARS-CoV-2 treatment strategy that can be studied in depth.

Multiple studies suggest that excessive inflammatory production of proinflammatory cytokines such as IL-6 and TNF-α may trigger ARDS, which will accelerate disease progression and increase the risk of death in COVID-19 patients (264, 265). Therefore, controlling the development of ARDS may also be a feasible treatment strategy for COVID-19. At present, a number of clinical studies (NCT04244591/NCT04327401/NCT04476992/NCT04306393…) are using strategies such as glucocorticoids, small molecule drugs, recombinant interferon and NO inhalation to explore the effectiveness of intervening in ARDS to affect COVID-19 (266, 267). Perhaps this strategy will provide more evidence for the safety and efficacy of treating COVID-19.

Immunomodulators are an important class of substances that affect the function of the immune system. Among them, pegylated interferon-α, which is approved for the treatment of hepatitis B/C viruses (HBV/HCV), can be used to stimulate the innate antiviral response of patients infected with SARS-CoV-2 (ChiCTR2000029387) (268). A retrospective study showed that pegylated interferon-α aerosol (5 million IU, bid) and arbidol (600 mg/day) treatment can significantly reduce the upper respiratory tract viral load and shorten the time for the inflammatory response indicators (IL-6 and CRP) in blood to return to normal with no obvious adverse reaction (269). Meanwhile, some clinical trials evaluated the therapeutic effect of glucocorticoids and found that they can significantly reduce the cytokine storm and relieve the corresponding tissue damage, which is beneficial to the treatment of severe COVID-19 (reduced 1/3 of mortality rate in patients using ventilators) and may affect the clearance of the virus in mild patients (270). The above results indicate that the use of immunomodulators to affect immune function will be a symptomatic treatment strategy for COVID-19 that can be considered. Although it is not given

priority, the indications, dosage and course of treatment can be strictly controlled in consideration of the patient's situation to ensure the maximum benefit of the patient.

The use of antibodies contained in the plasma of convalescent patients to suppress viremia for passive immunotherapy is considered to be a promising option for anti-SARS-CoV-2 infection. Currently, there have been clinical trials to test the effectiveness of plasma in recovering patients, and a study showed that the mortality rate of patients receiving convalescent plasma therapy is significantly lower than that of patients not receiving plasma therapy (271). *In vitro* experiments showed that antibodies in the serum of SARS-CoV-2-infected patients can effectively neutralize SARS-CoV-2. Moreover, clinical trials of administering convalescent plasma to 5,000 COVID-19 hospitalized patients in the early stages have also proven to be safe because the incidence of serious adverse events is very low (272). Therefore, convalescent plasma seems to be a good symptomatic treatment strategy in the case of solving the problems of ionomer safety and whether it needs a different storage method from ordinary plasma.

In addition, blood purification, NK-cell therapy, MSC transplantation therapy and Treg cell therapy have also been mentioned and are being studied. These therapies mainly alleviate and eliminate the pathological symptoms of patients, including inflammation, immune dysfunction, organ failure, etc., by adjusting immune function, removing inflammatory cytokines from the body, and directly killing SARS-CoV-2 infections (186). Changes such as lymphopenia and increased inflammatory cytokines in COVID-19 patients can induce symptoms of inflammation, immune function, and organ system dysfunction, which can be considered potential biomarkers and intervention targets for disease progression (273). Therefore, symptomatic treatments such as improving lymphopenia, reducing inflammation, and regulating immunity will become promising treatment strategies.

PERSPECTIVES AND CONCLUSIONS

The continuous outbreak of SARS-CoV-2 and the endless emergence of new mutant strains once again emphasize the urgency of continuing to explore, screen, and prevent COVID-19 globally. All this urgently requires precise target determination and mechanism elucidation in order to develop specific or broad-spectrum drugs for SARS-CoV-2 virus entry, replication, pathological changes or prevention.

While exploring and determining the effective targets for fighting against SARS-CoV-2, we should highly combine the experience of the three CoV pandemics, clarify the SARS-CoV-2 genome and structural information, and lay the foundation for screening targets; comprehensively consider the pathophysiological characteristics and mechanisms of viral entry, replication, assembly, infection and pathogenic processes to accurately analyze the crystal structure of related enzymes and proteins, and provide direct evidence for the target; and combine omics, bioinformatics, computer virtual screening and artificial intelligence and other technologies to explore, screen and confirm targets with maximum efficiency.

Furthermore, the development of vaccines and drugs needs to be carried out at multiple levels. Specifically, considering the lethality and disability of COVID-19, short-term research focuses on "old drugs and new use", rapid screening of FDA-approved drugs and clinical trials, and cooperation with other medication considerations to speed up the treatment of patients. After multichannel experience accumulation, developing innovative drugs targeted at different populations with good activity and selectivity against viruses through virtual screening and computer drug design, candidate drug preclinical research, and corresponding protective measures are key to future prevention and treatment. Moreover, it is necessary to minimize the occurrence and impact of drug resistance to maintain the efficacy of these innovative drugs; from a long-term perspective, broad-spectrum anti-CoV drugs should be developed to provide sufficient R&D experience and test platforms for possible future outbreaks.

Currently, there are only a few clinically approved drugs, vaccines and corresponding therapeutic strategies for COVID-19, and we cannot control the long-term consequences. Therefore, through the existing vaccination prevention, contact tracing, isolation of infected persons, and effective supportive treatment of SARS-CoV-2-infected persons, the diagnosis of symptomatic and asymptomatic persons and their close contacts as soon as possible is still the key means to prevent the further spread and control the disease. Furthermore, we should also realize that focusing on international cooperation and sharing anti-epidemic experiences will provide new impetus for the dissemination and confirmation of treatment strategies.

AUTHOR CONTRIBUTIONS

HZ and W-JN contributed to the conception or design of the review. HZ and W-JN wrote the manuscript. WH, MC, ZW, and Y-CS collected and analyzed the latest literature and intelligence on the pandemic. W-JN, MC, and ZW revised the original draft. W-JN, MC, and Y-CS critically reviewed and edited the latest version for important intellectual content. All authors contributed to the article and approved the submitted version.

FUNDING

This work was supported by the Science Foundation of Anhui Provincial Cancer Hospital (No. 2020YJQN008), the National Natural Science Foundation of China (No. 81803602), the Natural Science Foundation of Anhui Province (No. 1708085QH207), and the Fundamental Research Funds for the Central Universities (No. WK9110000018).

ACKNOWLEDGMENTS

We thank the American Journal Experts (AJE) for their guidance on the grammar and language of this article. We thank Microsoft Office and Bio Render for providing materials to help us better beautify the figures.

REFERENCES

1. Zhu N, Zhang D, Wang W, Li X, Yang B, Song J, et al. A Novel Coronavirus From Patients With Pneumonia in China, 2019. *N Engl J Med* (2020) 382:727–33. doi: 10.1056/NEJMoa2001017
2. Gussow AB, Auslander N, Faure G, Wolf YI, Zhang F, Koonin EV. Genomic Determinants of Pathogenicity in SARS-CoV-2 and Other Human Coronaviruses. *Proc Natl Acad Sci USA* (2020) 117:15193–9. doi: 10.1073/pnas.2008176117
3. Tang X, Ying R, Yao X, Li G, Wu C, Tang Y, et al. Evolutionary Analysis and Lineage Designation of SARS-CoV-2 Genomes. *Sci Bull (Beijing)* (2021) 66:2297–311. doi: 10.1016/j.scib.2021.02.012
4. Sabino EC, Buss LF, Carvalho M, Prete CJ, Crispim M, Fraiji NA, et al. Resurgence of COVID-19 in Manaus, Brazil, Despite High Seroprevalence. *Lancet* (2021) 397:452–5. doi: 10.1016/S0140-6736(21)00183-5
5. Thye AY, Law JW, Pusparajah P, Letchumanan V, Chan KG, Lee LH. Emerging SARS-CoV-2 Variants of Concern (VOCs): An Impending Global Crisis. *Biomedicines* (2021) 9:1303. doi: 10.3390/biomedicines9101303
6. Martin DP, Weaver S, Tegally H, San JE, Shank SD, Wilkinson E, et al. The Emergence and Ongoing Convergent Evolution of the SARS-CoV-2 N501Y Lineages. *Cell* (2021) 184:5189–200. doi: 10.1016/j.cell.2021.09.003
7. Benton DJ, Wrobel AG, Roustan C, Borg A, Xu P, Martin SR, et al. The Effect of the D614G Substitution on the Structure of the Spike Glycoprotein of SARS-CoV-2. *Proc Natl Acad Sci USA* (2021) 118:e2022586118. doi: 10.1073/pnas.2022586118
8. Faria NR, Mellan TA, Whittaker C, Claro IM, Candido D, Mishra S, et al. Genomics and Epidemiology of the P.1 SARS-CoV-2 Lineage in Manaus, Brazil. *Science* (2021) 372:815–21. doi: 10.1126/science.abh2644
9. Hemmer CJ, Lobermann M, Reisinger EC. [COVID-19: Epidemiology and Mutations: An Update]. *Radiologe* (2021) 61:880–7. doi: 10.1007/s00117-021-00909-0
10. Mishra A, Kumar N, Bhatia S, Aasdev A, Kanniappan S, Sekhar AT, et al. SARS-CoV-2 Delta Variant Among Asiatic Lions, India. *Emerg Infect Dis* (2021) 27:2723–5. doi: 10.3201/eid2710.211500
11. Kannan SR, Spratt AN, Cohen AR, Naqvi SH, Chand HS, Quinn TP, et al. Evolutionary Analysis of the Delta and Delta Plus Variants of the SARS-CoV-2 Viruses. *J Autoimmun* (2021) 124:102715. doi: 10.1016/j.jaut.2021.102715
12. Sapkal G, Yadav PD, Ella R, Abraham P, Patil DY, Gupta N, et al. Neutralization of VUI B.1.1.28 P2 Variant With Sera of COVID-19 Recovered Cases and Recipients of Covaxin an Inactivated COVID-19 Vaccine. *J Travel Med* (2021) 28:taab077. doi: 10.1093/jtm/taab077
13. Zhang L, Cui Z, Li Q, Wang B, Yu Y, Wu J, et al. Ten Emerging SARS-CoV-2 Spike Variants Exhibit Variable Infectivity, Animal Tropism, and Antibody Neutralization. *Commun Biol* (2021) 4:1196. doi: 10.1038/s42003-021-02728-4
14. McCallum M, Bassi J, De Marco A, Chen A, Walls AC, Di Iulio J, et al. SARS-CoV-2 Immune Evasion by the B.1.427/B.1.429 Variant of Concern. *Science* (2021) 373:648–54. doi: 10.1126/science.abi7994
15. Deng X, Garcia-Knight MA, Khalid MM, Servellita V, Wang C, Morris MK, et al. Transmission, Infectivity, and Neutralization of a Spike L452R SARS-CoV-2 Variant. *Cell* (2021) 184:3426–37. doi: 10.1016/j.cell.2021.04.025
16. Romero PE, Davila-Barclay A, Salvatierra G, Gonzalez L, Cuicapuza D, Solis L, et al. The Emergence of Sars-CoV-2 Variant Lambda (C.37) in South America. *Microbiol Spectr.* (2021) 9:e78921. doi: 10.1128/Spectrum.00789-21
17. Darvishi M, Rahimi F, Talebi BAA. SARS-CoV-2 Lambda (C.37): An Emerging Variant of Concern? *Gene Rep* (2021) 25:101378. doi: 10.1016/j.genrep.2021.101378
18. Laiton-Donato K, Franco-Munoz C, Alvarez-Diaz DA, Ruiz-Moreno HA, Usme-Ciro JA, Prada DA, et al. Characterization of the Emerging B.1.621 Variant of Interest of SARS-CoV-2. *Infect Genet Evol* (2021) 95:105038. doi: 10.1016/j.meegid.2021.105038
19. Uriu K, Kimura I, Shirakawa K, Takaori-Kondo A, Nakada TA, Kaneda A, et al. Neutralization of the SARS-CoV-2 Mu Variant by Convalescent and Vaccine Serum. *N Engl J Med* (2021) 385:2397–9. doi: 10.1056/NEJMc2114706
20. Shuai H, Chan JF, Yuen TT, Yoon C, Hu JC, Wen L, et al. Emerging SARS-CoV-2 Variants Expand Species Tropism to Murines. *Ebiomedicine* (2021) 73:103643. doi: 10.1016/j.ebiom.2021.103643
21. Moubarak M, Kasozi KI, Hetta HF, Shaheen HM, Rauf A, Al-Kuraishy HM, et al. The Rise of SARS-CoV-2 Variants and the Role of Convalescent Plasma Therapy for Management of Infections. *Life (Basel).* (2021) 11:734. doi: 10.3390/life11080734
22. van der Veer BMJW, Dingemans J, van Alphen LB, Hoebe CJPA, Savelkoul PHM. A Novel B.1.1.523 SARS-CoV-2 Variant That Combines Many Spike Mutations Linked to Immune Evasion With Current Variants of Concern. *bioRxiv* (2021), 2021–9. doi: 10.1101/2021.09.16.460616
23. Albayat SS, Arshad S, Arshad MA, Jabbar A, Ullah I. Precautionary Measures for More Transmissible C.1.2 COVID-19 Variant: A Caution for Qatar and the Rest of the World. *J Med Virol* (2022) 94:842–3. doi: 10.1002/jmv.27438
24. Yang X. SARS-COV-2 C.1.2 Variant is Highly Mutated But may Possess Reduced Affinity for ACE2 Receptor. *bioRxiv* (2021), 2010–21. doi: 10.1101/2021.10.16.464644
25. Nagano K, Tani-Sassa C, Iwasaki Y, Takatsuki Y, Yuasa S, Takahashi Y, et al. SARS-CoV-2 R.1 Lineage Variants That Prevailed in Tokyo in March 2021. *J Med Virol* (2021) 93:6833–6. doi: 10.1002/jmv.27240
26. Sekizuka T, Itokawa K, Hashino M, Okubo K, Ohnishi A, Goto K, et al. A Discernable Increase in the Severe Acute Respiratory Syndrome Coronavirus 2 R.1 Lineage Carrying an E484K Spike Protein Mutation in Japan. *Infect Genet Evol* (2021) 94:105013. doi: 10.1016/j.meegid.2021.105013
27. Rodriguez-Maldonado AP, Vazquez-Perez JA, Cedro-Tanda A, Taboada B, Boukadida C, Wong-Arambula C, et al. Emergence and Spread of the Potential Variant of Interest (VOI) B.1.1.519 of SARS-CoV-2 Predominantly Present in Mexico. *Arch Virol* (2021) 166:3173–7. doi: 10.1007/s00705-021-05208-6
28. Laine P, Nihtila H, Mustanoja E, Lyyski A, Ylinen A, Hurme J, et al. SARS-CoV-2 Variant With Mutations in N Gene Affecting Detection by Widely Used PCR Primers. *J Med Virol* (2021) 94:1227–31. doi: 10.1002/jmv.27418
29. Manouana GP, Nzamba MM, Bikangui R, Oye BS, Ondo NG, Honkpehedji JY, et al. Emergence of B.1.1.318 SARS-CoV-2 Viral Lineage and High Incidence of Alpha B.1.1.7 Variant of Concern in the Republic of Gabon. *Int J Infect Dis* (2022) 114:151–4. doi: 10.1016/j.ijid.2021.10.057
30. Fibriani A, Stephanie R, Alfiantie AA, Siregar A, Pradani G, Yamahoki N, et al. Analysis of SARS-CoV-2 Genomes From West Java, Indonesia. *Viruses* (2021) 13:2097. doi: 10.3390/v13102097
31. Sam IC, Chong YM, Abdullah A, Fu J, Hasan MS, Jamaluddin FH, et al. Changing Predominant SARS-CoV-2 Lineages Drives Successive COVID-19 Waves in Malaysia, February 2020 to March 2021. *J Med Virol* (2021) 94:1146–53. doi: 10.1002/jmv.27441
32. Dudas G, Hong SL, Potter BI, Calvignac-Spencer S, Niatou-Singa FS, Tombolomako TB, et al. Emergence and Spread of SARS-CoV-2 Lineage B.1.620 With Variant of Concern-Like Mutations and Deletions. *Nat Commun* (2021) 12:5769. doi: 10.1038/s41467-021-26055-8
33. Zahradnik J, Marciano S, Shemesh M, Zoler E, Harari D, Chiaravalli J, et al. SARS-CoV-2 Variant Prediction and Antiviral Drug Design are Enabled by RBD. *Vitro Evol Nat Microbiol* (2021) 6:1188–98. doi: 10.1038/s41564-021-00954-4
34. Annavajhala MK, Mohri H, Wang P, Nair M, Zucker JE, Sheng Z, et al. Emergence and Expansion of the SARS-CoV-2 Variant B.1.526 Identified in New York. *medRxiv* (2021). doi: 10.1101/2021.02.23.21252259
35. Thompson CN, Hughes S, Ngai S, Baumgartner J, Wang JC, McGibbon E, et al. Rapid Emergence and Epidemiologic Characteristics of the SARS-CoV-2 B.1.526 Variant - New York City, New York, January 1-April 5, 2021. *MMWR Morb Mortal Wkly Rep* (2021) 70:712–6. doi: 10.15585/mmwr.mm7019e1
36. Bugembe DL, Phan M, Abias AG, Ayei J, Deng LL, Lako R, et al. SARS-CoV-2 Variants, South Sudan, January-March 2021. *Emerg Infect Dis* (2021) 27:3133–6. doi: 10.3201/eid2712.211488
37. Abdool KS, de Oliveira T. New SARS-CoV-2 Variants - Clinical, Public Health, and Vaccine Implications. *N Engl J Med* (2021) 384:1866–8. doi: 10.1056/NEJMc2100362
38. Chen J, Fan J, Chen Z, Zhang M, Peng H, Liu J, et al. Nonmuscle Myosin Heavy Chain IIA Facilitates SARS-CoV-2 Infection in Human Pulmonary Cells. *Proc Natl Acad Sci U S A* (2021) 118:e2111011118. doi: 10.1073/pnas.2111011118
39. Fontanet A, Autran B, Lina B, Kieny MP, Karim S, Sridhar D. SARS-CoV-2 Variants and Ending the COVID-19 Pandemic. *Lancet* (2021) 397:952–4. doi: 10.1016/S0140-6736(21)00370-6

40. Cui J, Li F, Shi ZL. Origin and Evolution of Pathogenic Coronaviruses. *Nat Rev Microbiol* (2019) 17:181–92. doi: 10.1038/s41579-018-0118-9
41. Finkel Y, Mizrahi O, Nachshon A, Weingarten-Gabbay S, Morgenstern D, Yahalom-Ronen Y, et al. The Coding Capacity of SARS-CoV-2. *Nature* (2021) 589:125–30. doi: 10.1038/s41586-020-2739-1
42. Lu R, Zhao X, Li J, Niu P, Yang B, Wu H, et al. Genomic Characterisation and Epidemiology of 2019 Novel Coronavirus: Implications for Virus Origins and Receptor Binding. *Lancet* (2020) 395:565–74. doi: 10.1016/S0140-6736(20)30251-8
43. Jungreis I, Sealfon R, Kellis M. SARS-CoV-2 Gene Content and COVID-19 Mutation Impact by Comparing 44 Sarbecovirus Genomes. *Nat Commun* (2021) 12:2642. doi: 10.1038/s41467-021-22905-7
44. Jackson B, Boni MF, Bull MJ, Colleran A, Colquhoun RM, Darby AC, et al. Generation and Transmission of Interlineage Recombinants in the SARS-CoV-2 Pandemic. *Cell* (2021) 184:5179–88. doi: 10.1016/j.cell.2021.08.014
45. Artese A, Svicher V, Costa G, Salpini R, Di Maio VC, Alkhatib M, et al. Current Status of Antivirals and Druggable Targets of SARS CoV-2 and Other Human Pathogenic Coronaviruses. *Drug Resist Updat* (2020) 53:100721. doi: 10.1016/j.drup.2020.100721
46. Rolf JD. Clinical Characteristics of Covid-19 in China. *N Engl J Med* (2020) 382:1860. doi: 10.1056/NEJMc2005203
47. Hu B, Guo H, Zhou P, Shi ZL. Characteristics of SARS-CoV-2 and COVID-19. *Nat Rev Microbiol* (2021) 19:141–54. doi: 10.1038/s41579-020-00459-7
48. Guo M, Tao W, Flavell RA, Zhu S. Potential Intestinal Infection and Faecal-Oral Transmission of SARS-CoV-2. *Nat Rev Gastroenterol Hepatol* (2021) 18:269–83. doi: 10.1038/s41575-021-00416-6
49. Oude MB, Worp N, Nieuwenhuijse DF, Sikkema RS, Haagmans B, Fouchier R, et al. The Next Phase of SARS-CoV-2 Surveillance: Real-Time Molecular Epidemiology. *Nat Med* (2021) 27:1518–24. doi: 10.1038/s41591-021-01472-w
50. Yang B, Fan J, Huang J, Guo E, Fu Y, Liu S, et al. Clinical and Molecular Characteristics of COVID-19 Patients With Persistent SARS-CoV-2 Infection. *Nat Commun* (2021) 12:3501. doi: 10.1038/s41467-021-23621-y
51. Guan WJ, Ni ZY, Hu Y, Liang WH, Ou CQ, He JX, et al. Clinical Characteristics of Coronavirus Disease 2019 in China. *N Engl J Med* (2020) 382:1708–20. doi: 10.1056/NEJMoa2002032
52. Deng H, Yan X, Yuan L. Human Genetic Basis of Coronavirus Disease 2019. *Signal Transduct Target Ther* (2021) 6:344. doi: 10.1038/s41392-021-00736-8
53. Abdelnabi R, Boudewijns R, Foo CS, Seldeslachts L, Sanchez-Felipe L, Zhang X, et al. Comparing Infectivity and Virulence of Emerging SARS-CoV-2 Variants in Syrian Hamsters. *Ebiomedicine* (2021) 68:103403. doi: 10.1016/j.ebiom.2021.103403
54. McCormick KD, Jacobs JL, Mellors JW. The Emerging Plasticity of SARS-CoV-2. *Science* (2021) 371:1306–8. doi: 10.1126/science.abg4493
55. Zumla A, Chan JF, Azhar EI, Hui DS, Yuen KY. Coronaviruses - Drug Discovery and Therapeutic Options. *Nat Rev Drug Discov* (2016) 15:327–47. doi: 10.1038/nrd.2015.37
56. V'Kovski P, Kratzel A, Steiner S, Stalder H, Thiel V. Coronavirus Biology and Replication: Implications for SARS-CoV-2. *Nat Rev Microbiol* (2021) 19:155–70. doi: 10.1038/s41579-020-00468-6
57. Xiang R, Yu Z, Wang Y, Wang L, Huo S, Li Y, et al. Recent Advances in Developing Small-Molecule Inhibitors Against SARS-CoV-2. *Acta Pharm Sin B* (2021) 12:995–1026. doi: 10.1016/j.apsb.2021.06.016
58. Zhou H, Fang Y, Xu T, Ni WJ, Shen AZ, Meng XM. Potential Therapeutic Targets and Promising Drugs for Combating SARS-CoV-2. *Br J Pharmacol* (2020) 177:3147–61. doi: 10.1111/bph.15092
59. Wu C, Liu Y, Yang Y, Zhang P, Zhong W, Wang Y, et al. Analysis of Therapeutic Targets for SARS-CoV-2 and Discovery of Potential Drugs by Computational Methods. *Acta Pharm Sin B* (2020) 10:766–88. doi: 10.1016/j.apsb.2020.02.008
60. Kneller DW, Phillips G, O'Neill HM, Jedrzejczak R, Stols L, Langan P, et al. Structural Plasticity of SARS-CoV-2 3cl M(pro) Active Site Cavity Revealed by Room Temperature X-Ray Crystallography. *Nat Commun* (2020) 11:3202. doi: 10.1038/s41467-020-16954-7
61. Zhang L, Lin D, Sun X, Curth U, Drosten C, Sauerhering L, et al. Crystal Structure of SARS-CoV-2 Main Protease Provides a Basis for Design of Improved Alpha-Ketoamide Inhibitors. *Science* (2020) 368:409–12. doi: 10.1126/science.abb3405
62. Shin D, Mukherjee R, Grewe D, Bojkova D, Baek K, Bhattacharya A, et al. Papain-Like Protease Regulates SARS-CoV-2 Viral Spread and Innate Immunity. *Nature* (2020) 587:657–62. doi: 10.1038/s41586-020-2601-5
63. Gao X, Qin B, Chen P, Zhu K, Hou P, Wojdyla JA, et al. Crystal Structure of SARS-CoV-2 Papain-Like Protease. *Acta Pharm Sin B* (2021) 11:237–45. doi: 10.1016/j.apsb.2020.08.014
64. Osipiuk J, Azizi SA, Dvorkin S, Endres M, Jedrzejczak R, Jones KA, et al. Structure of Papain-Like Protease From SARS-CoV-2 and its Complexes With non-Covalent Inhibitors. *Nat Commun* (2021) 12:743. doi: 10.1038/s41467-021-21060-3
65. Gao Y, Yan L, Huang Y, Liu F, Zhao Y, Cao L, et al. Structure of the RNA-Dependent RNA Polymerase From COVID-19 Virus. *Science* (2020) 368:779–82. doi: 10.1126/science.abb7498
66. Yin W, Mao C, Luan X, Shen DD, Shen Q, Su H, et al. Structural Basis for Inhibition of the RNA-Dependent RNA Polymerase From SARS-CoV-2 by Remdesivir. *Science* (2020) 368:1499–504. doi: 10.1126/science.abc1560
67. Hillen HS, Kokic G, Farnung L, Dienemann C, Tegunov D, Cramer P. Structure of Replicating SARS-CoV-2 Polymerase. *Nature* (2020) 584:154–6. doi: 10.1038/s41586-020-2368-8
68. White MA, Lin W, Cheng X. Discovery of COVID-19 Inhibitors Targeting the SARS-CoV-2 Nsp13 Helicase. *J Phys Chem Lett* (2020) 11:9144–51. doi: 10.1021/acs.jpclett.0c02421
69. Chen J, Malone B, Llewellyn E, Grasso M, Shelton P, Olinares P, et al. Structural Basis for Helicase-Polymerase Coupling in the SARS-CoV-2 Replication-Transcription Complex. *Cell* (2020) 182:1560–73. doi: 10.1016/j.cell.2020.07.033
70. Walls AC, Park YJ, Tortorici MA, Wall A, McGuire AT, Veesler D. Structure, Function, and Antigenicity of the SARS-CoV-2 Spike Glycoprotein. *Cell* (2020) 181:281–92. doi: 10.1016/j.cell.2020.02.058
71. Watanabe Y, Allen JD, Wrapp D, McLellan JS, Crispin M. Site-Specific Glycan Analysis of the SARS-CoV-2 Spike. *Science* (2020) 369:330–3. doi: 10.1126/science.abb9983
72. Carlson CR, Asfaha JB, Ghent CM, Howard CJ, Hartooni N, Safari M, et al. Phosphoregulation of Phase Separation by the SARS-CoV-2 N Protein Suggests a Biophysical Basis for Its Dual Functions. *Mol Cell* (2020) 80:1092–103. doi: 10.1016/j.molcel.2020.11.025
73. Peng Y, Du N, Lei Y, Dorje S, Qi J, Luo T, et al. Structures of the SARS-CoV-2 Nucleocapsid and Their Perspectives for Drug Design. *EMBO J* (2020) 39:e105938. doi: 10.15252/embj.2020105938
74. Mandala VS, McKay MJ, Shcherbakov AA, Dregni AJ, Kolocouris A, Hong M. Structure and Drug Binding of the SARS-CoV-2 Envelope Protein Transmembrane Domain in Lipid Bilayers. *Nat Struct Mol Biol* (2020) 27:1202–8. doi: 10.1038/s41594-020-00536-8
75. Lu S, Ye Q, Singh D, Cao Y, Diedrich JK, Yates JR, et al. The SARS-CoV-2 Nucleocapsid Phosphoprotein Forms Mutually Exclusive Condensates With RNA and the Membrane-Associated M Protein. *Nat Commun* (2021) 12:502. doi: 10.1038/s41467-020-20768-y
76. Liu B, Zheng D, Jin Q, Chen L, Yang J. VFDB 2019: A Comparative Pathogenomic Platform With an Interactive Web Interface. *Nucleic Acids Res* (2019) 47:D687–92. doi: 10.1093/nar/gky1080
77. Schuller M, Correy GJ, Gahbauer S, Fearon D, Wu T, Diaz RE, et al. Fragment Binding to the Nsp3 Macrodomain of SARS-CoV-2 Identified Through Crystallographic Screening and Computational Docking. *Sci Adv* (2021) 7:eabf8711. doi: 10.1126/sciadv.abf8711
78. Yuan S, Peng L, Park JJ, Hu Y, Devarkar SC, Dong MB, et al. Nonstructural Protein 1 of SARS-CoV-2 Is a Potent Pathogenicity Factor Redirecting Host Protein Synthesis Machinery Toward Viral RNA. *Mol Cell* (2020) 80:1055–66. doi: 10.1016/j.molcel.2020.10.034
79. Nemudryi A, Nemudraia A, Wiegand T, Nichols J, Snyder DT, Hedges JF, et al. SARS-CoV-2 Genomic Surveillance Identifies Naturally Occurring Truncation of ORF7a That Limits Immune Suppression. *Cell Rep* (2021) 35:109197. doi: 10.1016/j.celrep.2021.109197
80. Thoms M, Buschauer R, Ameismeier M, Koepke L, Denk T, Hirschenberger M, et al. Structural Basis for Translational Shutdown and Immune Evasion by the Nsp1 Protein of SARS-CoV-2. *Science* (2020) 369:1249–55. doi: 10.1126/science.abc8665
81. Xiao T, Lu J, Zhang J, Johnson RI, McKay L, Storm N, et al. A Trimeric Human Angiotensin-Converting Enzyme 2 as an Anti-SARS-CoV-2

Agent. *Nat Struct Mol Biol* (2021) 28:202–9. doi: 10.1038/s41594-020-00549-3
82. Benton DJ, Wrobel AG, Xu P, Roustan C, Martin SR, Rosenthal PB, et al. Receptor Binding and Priming of the Spike Protein of SARS-CoV-2 for Membrane Fusion. *Nature* (2020) 588:327–30. doi: 10.1038/s41586-020-2772-0
83. Starr TN, Greaney AJ, Hilton SK, Ellis D, Crawford K, Dingens AS, et al. Deep Mutational Scanning of SARS-CoV-2 Receptor Binding Domain Reveals Constraints on Folding and ACE2 Binding. *Cell* (2020) 182:1295–310. doi: 10.1016/j.cell.2020.08.012
84. Shang J, Ye G, Shi K, Wan Y, Luo C, Aihara H, et al. Structural Basis of Receptor Recognition by SARS-CoV-2. *Nature* (2020) 581:221–4. doi: 10.1038/s41586-020-2179-y
85. Koch J, Uckeley ZM, Doldan P, Stanifer M, Boulant S, Lozach PY. TMPRSS2 Expression Dictates the Entry Route Used by SARS-CoV-2 to Infect Host Cells. *EMBO J* (2021) 40:e107821. doi: 10.15252/embj.2021107821
86. Mahoney M, Damalanka VC, Tartell MA, Chung DH, Lourenco AL, Pwee D, et al. A Novel Class of TMPRSS2 Inhibitors Potently Block SARS-CoV-2 and MERS-CoV Viral Entry and Protect Human Epithelial Lung Cells. *Proc Natl Acad Sci USA* (2021) 118:e2108728118. doi: 10.1073/pnas.2108728118
87. Hoffmann M, Kleine-Weber H, Schroeder S, Kruger N, Herrler T, Erichsen S, et al. SARS-CoV-2 Cell Entry Depends on ACE2 and TMPRSS2 and Is Blocked by a Clinically Proven Protease Inhibitor. *Cell* (2020) 181:271–80. doi: 10.1016/j.cell.2020.02.052
88. Zhang MY, Zhang Y, Wu XD, Zhang K, Lin P, Bian HJ, et al. Disrupting CD147-RAP2 Interaction Abrogates Erythrocyte Invasion by Plasmodium Falciparum. *Blood* (2018) 131:1111–21. doi: 10.1182/blood-2017-08-802918
89. Chen Z, Mi L, Xu J, Yu J, Wang X, Jiang J, et al. Function of HAb18G/CD147 in Invasion of Host Cells by Severe Acute Respiratory Syndrome Coronavirus. *J Infect Dis* (2005) 191:755–60. doi: 10.1086/427811
90. Wang K, Chen W, Zhang Z, Deng Y, Lian JQ, Du P, et al. CD147-Spike Protein is a Novel Route for SARS-CoV-2 Infection to Host Cells. *Signal Transduct Target Ther* (2020) 5:283. doi: 10.1038/s41392-020-00426-x
91. Chen H, Zou TH, Xuan B, Yan Y, Yan T, Shen C, et al. Single Cell Transcriptome Revealed SARS-CoV-2 Entry Genes Enriched in Colon Tissues and Associated With Coronavirus Infection and Cytokine Production. *Signal Transduct Target Ther* (2020) 5:121. doi: 10.1038/s41392-020-00237-0
92. Bian H, Zheng ZH, Wei D, Wen A, Zhang Z, Lian JQ, et al. Safety and Efficacy of Meplazumab in Healthy Volunteers and COVID-19 Patients: A Randomized Phase 1 and an Exploratory Phase 2 Trial. *Signal Transduct Target Ther* (2021) 6:194. doi: 10.1038/s41392-021-00603-6
93. Geng J, Chen L, Yuan Y, Wang K, Wang Y, Qin C, et al. CD147 Antibody Specifically and Effectively Inhibits Infection and Cytokine Storm of SARS-CoV-2 and Its Variants Delta, Alpha, Beta, and Gamma. *Signal Transduct Target Ther* (2021) 6:347. doi: 10.1038/s41392-021-00760-8
94. Ragotte RJ, Pulido D, Donnellan FR, Hill ML, Gorini G, Davies H, et al. Human Basigin (CD147) Does Not Directly Interact With SARS-CoV-2 Spike Glycoprotein. *mSphere* (2021) 6:e64721. doi: 10.1128/mSphere.00647-21
95. Shilts J, Crozier T, Greenwood E, Lehner PJ, Wright GJ. No Evidence for Basigin/CD147 as a Direct SARS-CoV-2 Spike Binding Receptor. *Sci Rep* (2021) 11:413. doi: 10.1038/s41598-020-80464-1
96. Morales A, Rojo RS, Cristobal H, Fiz-Lopez A, Arribas E, Mari M, et al. Growth Arrest-Specific Factor 6 (GAS6) Is Increased in COVID-19 Patients and Predicts Clinical Outcome. *Biomedicines* (2021) 9:335. doi: 10.3390/biomedicines9040335
97. Wang S, Qiu Z, Hou Y, Deng X, Xu W, Zheng T, et al. AXL is a Candidate Receptor for SARS-CoV-2 That Promotes Infection of Pulmonary and Bronchial Epithelial Cells. *Cell Res* (2021) 31:126–40. doi: 10.1038/s41422-020-00460-y
98. Bouhaddou M, Memon D, Meyer B, White KM, Rezelj VV, Correa MM, et al. The Global Phosphorylation Landscape of SARS-CoV-2 Infection. *Cell* (2020) 182:685–712. doi: 10.1016/j.cell.2020.06.034
99. Beeraka NM, Sadhu SP, Madhunapantula SV, Rao PR, Svistunov AA, Nikolenko VN, et al. Strategies for Targeting SARS CoV-2: Small Molecule Inhibitors-The Current Status. *Front Immunol* (2020) 11:552925. doi: 10.3389/fimmu.2020.552925
100. Jan JT, Cheng TR, Juang YP, Ma HH, Wu YT, Yang WB, et al. Identification of Existing Pharmaceuticals and Herbal Medicines as Inhibitors of SARS-CoV-2 Infection. *Proc Natl Acad Sci USA* (2021) 118:e2021579118. doi: 10.1073/pnas.2021579118
101. Riva L, Yuan S, Yin X, Martin-Sancho L, Matsunaga N, Pache L, et al. Discovery of SARS-CoV-2 Antiviral Drugs Through Large-Scale Compound Repurposing. *Nature* (2020) 586:113–9. doi: 10.1038/s41586-020-2577-1
102. Sun C, Zhang J, Wei J, Zheng X, Zhao X, Fang Z, et al. Screening, Simulation, and Optimization Design of Small Molecule Inhibitors of the SARS-CoV-2 Spike Glycoprotein. *PloS One* (2021) 16:e245975. doi: 10.1371/journal.pone.0245975
103. Wang X, Cao R, Zhang H, Liu J, Xu M, Hu H, et al. The Anti-Influenza Virus Drug, Arbidol is an Efficient Inhibitor of SARS-CoV-2 *In Vitro*. *Cell Discov* (2020) 6:28. doi: 10.1038/s41421-020-0169-8
104. Khan RJ, Jha RK, Amera GM, Jain M, Singh E, Pathak A, et al. Targeting SARS-CoV-2: A Systematic Drug Repurposing Approach to Identify Promising Inhibitors Against 3C-Like Proteinase and 2'-O-Ribose Methyltransferase. *J Biomol Struct Dyn* (2021) 39:2679–92. doi: 10.1080/07391102.2020.1753577
105. Yamamoto KA, Blackburn K, Migowski E, Goshe MB, Brown DT, Ferreira DF, et al. Quantitative Proteomic Analysis of the Tizoxanide Effect in Vero Cells. *Sci Rep* (2020) 10:14733. doi: 10.1038/s41598-020-71634-2
106. Xia S, Zhu Y, Liu M, Lan Q, Xu W, Wu Y, et al. Fusion Mechanism of 2019-Ncov and Fusion Inhibitors Targeting HR1 Domain in Spike Protein. *Cell Mol Immunol* (2020) 17:765–7. doi: 10.1038/s41423-020-0374-2
107. Zhu Y, Yu D, Yan H, Chong H, He Y. Design of Potent Membrane Fusion Inhibitors Against SARS-CoV-2, an Emerging Coronavirus With High Fusogenic Activity. *J Virol* (2020) 94:e00635–20. doi: 10.1128/JVI.00635-20
108. de Vries RD, Schmitz KS, Bovier FT, Predella C, Khao J, Noack D, et al. Intranasal Fusion Inhibitory Lipopeptide Prevents Direct-Contact SARS-CoV-2 Transmission in Ferrets. *Science* (2021) 371:1379–82. doi: 10.1126/science.abf4896
109. Ucar B, Acar T, Arayici PP, Derman S. A Nanotechnological Approach in the Current Therapy of COVID-19: Model Drug Oseltamivir-Phosphate Loaded PLGA Nanoparticles Targeted With Spike Protein Binder Peptide of SARS-CoV-2. *Nanotechnology* (2021) 32:485601. doi: 10.1088/1361-6528/ac1c22
110. Cao L, Goreshnik I, Coventry B, Case JB, Miller L, Kozodoy L, et al. *De Novo* Design of Picomolar SARS-CoV-2 Miniprotein Inhibitors. *Science* (2020) 370:426–31. doi: 10.1126/science.abd9909
111. Beddingfield BJ, Iwanaga N, Chapagain PP, Zheng W, Roy CJ, Hu TY, et al. The Integrin Binding Peptide, ATN-161, as a Novel Therapy for SARS-CoV-2 Infection. *JACC Basic Transl Sci* (2021) 6:1–8. doi: 10.1016/j.jacbts.2020.10.003
112. Bauer A, Schreinlechner M, Sappler N, Dolejsi T, Tilg H, Aulinger BA, et al. Discontinuation Versus Continuation of Renin-Angiotensin-System Inhibitors in COVID-19 (ACEI-COVID): A Prospective, Parallel Group, Randomised, Controlled, Open-Label Trial. *Lancet Respir Med* (2021) 9:863–72. doi: 10.1016/S2213-2600(21)00214-9
113. Esam Z, Akhavan M, Lotfi M, Bekhradnia A. Molecular Docking and Dynamics Studies of Nicotinamide Riboside as a Potential Multi-Target Nutraceutical Against SARS-CoV-2 Entry, Replication, and Transcription: A New Insight. *J Mol Struct* (2022) 1247:131394. doi: 10.1016/j.molstruc.2021.131394
114. Huo J, Le Bas A, Ruza RR, Duyvesteyn H, Mikolajek H, Malinauskas T, et al. Neutralizing Nanobodies Bind SARS-CoV-2 Spike RBD and Block Interaction With ACE2. *Nat Struct Mol Biol* (2020) 27:846–54. doi: 10.1038/s41594-020-0469-6
115. Monteil V, Kwon H, Prado P, Hagelkruys A, Wimmer RA, Stahl M, et al. Inhibition of SARS-CoV-2 Infections in Engineered Human Tissues Using Clinical-Grade Soluble Human Ace2. *Cell* (2020) 181:905–13. doi: 10.1016/j.cell.2020.04.004
116. Zhuravel SV, Khmelnitskiy OK, Burlaka OO, Gritsan AI, Goloshchekin BM, Kim S, et al. Nafamostat in Hospitalized Patients With Moderate to Severe COVID-19 Pneumonia: A Randomised Phase II Clinical Trial. *EClinicalMedicine* (2021) 41:101169. doi: 10.1016/j.eclinm.2021.101169
117. Alzain AA, Elbadwi FA. Identification of Novel TMPRSS2 Inhibitors for COVID-19 Using E-Pharmacophore Modelling, Molecular Docking, Molecular Dynamics and Quantum Mechanics Studies. *Inform Med Unlocked* (2021) 26:100758. doi: 10.1016/j.imu.2021.100758
118. Vuong W, Khan MB, Fischer C, Arutyunova E, Lamer T, Shields J, et al. Feline Coronavirus Drug Inhibits the Main Protease of SARS-CoV-2 and

Blocks Virus Replication. *Nat Commun* (2020) 11:4282. doi: 10.1038/s41467-020-18096-2
119. Achutha AS, Pushpa VL, Suchitra S. Theoretical Insights Into the Anti-SARS-CoV-2 Activity of Chloroquine and Its Analogs and In Silico Screening of Main Protease Inhibitors. *J Proteome Res* (2020) 19:4706–17. doi: 10.1021/acs.jproteome.0c00683
120. Cao B, Wang Y, Wen D, Liu W, Wang J, Fan G, et al. A Trial of Lopinavir-Ritonavir in Adults Hospitalized With Severe Covid-19. *N Engl J Med* (2020) 382:1787–99. doi: 10.1056/NEJMc2008043
121. Liu X, Li Z, Liu S, Sun J, Chen Z, Jiang M, et al. Potential Therapeutic Effects of Dipyridamole in the Severely Ill Patients With COVID-19. *Acta Pharm Sin B* (2020) 10:1205–15. doi: 10.1016/j.apsb.2020.04.008
122. Dai W, Zhang B, Jiang XM, Su H, Li J, Zhao Y, et al. Structure-Based Design of Antiviral Drug Candidates Targeting the SARS-CoV-2 Main Protease. *Science* (2020) 368:1331–5. doi: 10.1126/science.abb4489
123. Qiao J, Li YS, Zeng R, Liu FL, Luo RH, Huang C, et al. SARS-CoV-2 M(pro) Inhibitors With Antiviral Activity in a Transgenic Mouse Model. *Science* (2021) 371:1374–8. doi: 10.1126/science.abf1611
124. Wu Y, Li Z, Zhao YS, Huang YY, Jiang MY, Luo HB. Therapeutic Targets and Potential Agents for the Treatment of COVID-19. *Med Res Rev* (2021) 41:1775–97. doi: 10.1002/med.21776
125. Huynh T, Cornell W, Luan B. In Silico Exploration of Inhibitors for SARS-CoV-2's Papain-Like Protease. *Front Chem* (2020) 8:624163. doi: 10.3389/fchem.2020.624163
126. Xiao X, Wang C, Chang, Wang Y, Dong X, Jiao T, et al. Identification of Potent and Safe Antiviral Therapeutic Candidates Against SARS-CoV-2. *Front Immunol* (2020) 11:586572. doi: 10.3389/fimmu.2020.586572
127. Wang Q, Wu J, Wang H, Gao Y, Liu Q, Mu A, et al. Structural Basis for RNA Replication by the SARS-CoV-2 Polymerase. *Cell* (2020) 182:417–28. doi: 10.1016/j.cell.2020.05.034
128. Grein J, Ohmagari N, Shin D, Diaz G, Asperges E, Castagna A, et al. Compassionate Use of Remdesivir for Patients With Severe Covid-19. *N Engl J Med* (2020) 382:2327–36. doi: 10.1056/NEJMc2015312
129. Wang Y, Zhang D, Du G, Du R, Zhao J, Jin Y, et al. Remdesivir in Adults With Severe COVID-19: A Randomised, Double-Blind, Placebo-Controlled, Multicentre Trial. *Lancet* (2020) 395:1569–78. doi: 10.1016/S0140-6736(20)31022-9
130. Kaptein S, Jacobs S, Langendries L, Seldeslachts L, Ter Horst S, Liesenborghs L, et al. Favipiravir at High Doses has Potent Antiviral Activity in SARS-CoV-2-Infected Hamsters, Whereas Hydroxychloroquine Lacks Activity. *Proc Natl Acad Sci USA* (2020) 117:26955–65. doi: 10.1073/pnas.2014441117
131. Sheahan TP, Sims AC, Zhou S, Graham RL, Pruijssers AJ, Agostini ML, et al. An Orally Bioavailable Broad-Spectrum Antiviral Inhibits SARS-CoV-2 in Human Airway Epithelial Cell Cultures and Multiple Coronaviruses in Mice. *Sci Transl Med* (2020) 12:eabb5883. doi: 10.1126/scitranslmed.abb5883
132. Good SS, Westover J, Jung KH, Zhou XJ, Moussa A, La Colla P, et al. AT-527, a Double Prodrug of a Guanosine Nucleotide Analog, Is a Potent Inhibitor of SARS-CoV-2 *In Vitro* and a Promising Oral Antiviral for Treatment of COVID-19. *Antimicrob Agents Chemother* (2021) 65:e02479–20. doi: 10.1128/AAC.02479-20
133. Spratt AN, Gallazzi F, Quinn TP, Lorson CL, Sonnerborg A, Singh K. Coronavirus Helicases: Attractive and Unique Targets of Antiviral Drug-Development and Therapeutic Patents. *Expert Opin Ther Pat* (2021) 31:339–50. doi: 10.1080/13543776.2021.1884224
134. Yuan S, Yin X, Meng X, Chan JF, Ye ZW, Riva L, et al. Clofazimine Broadly Inhibits Coronaviruses Including SARS-CoV-2. *Nature* (2021) 593:418–23. doi: 10.1038/s41586-021-03431-4
135. Xia S, Yan L, Xu W, Agrawal AS, Algaissi A, Tseng CK, et al. A Pan-Coronavirus Fusion Inhibitor Targeting the HR1 Domain of Human Coronavirus Spike. *Sci Adv* (2019) 5:v4580. doi: 10.1126/sciadv.aav4580
136. Milne S, Yang CX, Timens W, Bosse Y, Sin DD. SARS-CoV-2 Receptor ACE2 Gene Expression and RAAS Inhibitors. *Lancet Respir Med* (2020) 8:e50–1. doi: 10.1016/S2213-2600(20)30224-1
137. Hoffmann M, Arora P, Gross R, Seidel A, Hornich BF, Hahn AS, et al. SARS-CoV-2 Variants B.1.351 and P.1 escape From Neutralizing Antibodies. *Cell* (2021) 184:2384–93. doi: 10.1016/j.cell.2021.03.036
138. Hempel T, Elez K, Kruger N, Raich L, Shrimp JH, Danov O, et al. Synergistic Inhibition of SARS-CoV-2 Cell Entry by Otamixaban and Covalent Protease Inhibitors: Pre-Clinical Assessment of Pharmacological and Molecular Properties. *Chem Sci* (2021) 12:12600–9. doi: 10.1039/d1sc01494c
139. Vandyck K, Deval J. Considerations for the Discovery and Development of 3-Chymotrypsin-Like Cysteine Protease Inhibitors Targeting SARS-CoV-2 Infection. *Curr Opin Virol* (2021) 49:36–40. doi: 10.1016/j.coviro.2021.04.006
140. Zhao Y, Fang C, Zhang Q, Zhang R, Zhao X, Duan Y, et al. Crystal Structure of SARS-CoV-2 Main Protease in Complex With Protease Inhibitor PF-07321332. *Protein Cell* (2021) 13:1–5. doi: 10.1007/s13238-021-00883-2
141. Pitsillou E, Liang J, Ververis K, Lim KW, Hung A, Karagiannis TC. Identification of Small Molecule Inhibitors of the Deubiquitinating Activity of the SARS-CoV-2 Papain-Like Protease: In Silico Molecular Docking Studies and *In Vitro* Enzymatic Activity Assay. *Front Chem* (2020) 8:623971. doi: 10.3389/fchem.2020.623971
142. Kokic G, Hillen HS, Tegunov D, Dienemann C, Seitz F, Schmitzova J, et al. Mechanism of SARS-CoV-2 Polymerase Stalling by Remdesivir. *Nat Commun* (2021) 12:279. doi: 10.1038/s41467-020-20542-0
143. Yin W, Luan X, Li Z, Zhou Z, Wang Q, Gao M, et al. Structural Basis for Inhibition of the SARS-CoV-2 RNA Polymerase by Suramin. *Nat Struct Mol Biol* (2021) 28:319–25. doi: 10.1038/s41594-021-00570-0
144. Naydenova K, Muir KW, Wu LF, Zhang Z, Coscia F, Peet MJ, et al. Structure of the SARS-CoV-2 RNA-Dependent RNA Polymerase in the Presence of Favipiravir-RTP. *Proc Natl Acad Sci USA* (2021) 118:e2021946118. doi: 10.1073/pnas.2021946118
145. Ninove L, Nougairede A, Gazin C, Thirion L, Delogu I, Zandotti C, et al. RNA and DNA Bacteriophages as Molecular Diagnosis Controls in Clinical Virology: A Comprehensive Study of More Than 45,000Routine PCR Tests. *PloS One* (2011) 6:e16142. doi: 10.1371/journal.pone.0016142
146. Miller SR, McGrath ME, Zorn KM, Ekins S, Wright SH, Cherrington NJ. Remdesivir and EIDD-1931 Interact With Human Equilibrative Nucleoside Transporters 1 and 2: Implications for Reaching SARS-CoV-2 Viral Sanctuary Sites. *Mol Pharmacol* (2021) 100:548–57. doi: 10.1124/molpharm.121.000333
147. Jena NR. Role of Different Tautomers in the Base-Pairing Abilities of Some of the Vital Antiviral Drugs Used Against COVID-19. *Phys Chem Chem Phys* (2020) 22:28115–22. doi: 10.1039/d0cp05297c
148. Wolfel R, Corman VM, Guggemos W, Seilmaier M, Zange S, Muller MA, et al. Virological Assessment of Hospitalized Patients With COVID-2019. *Nature* (2020) 581:465–9. doi: 10.1038/s41586-020-2196-x
149. Wang H, Zhang Y, Huang B, Deng W, Quan Y, Wang W, et al. Development of an Inactivated Vaccine Candidate, BBIBP-CorV, With Potent Protection Against SARS-CoV-2. *Cell* (2020) 182:713–21. doi: 10.1016/j.cell.2020.06.008
150. Xia S, Zhang Y, Wang Y, Wang H, Yang Y, Gao GF, et al. Safety and Immunogenicity of an Inactivated SARS-CoV-2 Vaccine, BBIBP-CorV: A Randomised, Double-Blind, Placebo-Controlled, Phase 1/2 Trial. *Lancet Infect Dis* (2021) 21:39–51. doi: 10.1016/S1473-3099(20)30831-8
151. Zhang Y, Zeng G, Pan H, Li C, Hu Y, Chu K, et al. Safety, Tolerability, and Immunogenicity of an Inactivated SARS-CoV-2 Vaccine in Healthy Adults Aged 18-59 Years: A Randomised, Double-Blind, Placebo-Controlled, Phase 1/2 Clinical Trial. *Lancet Infect Dis* (2021) 21:181–92. doi: 10.1016/S1473-3099(20)30843-4
152. Vacharathit V, Aiewsakun P, Manopwisedjaroen S, Srisaowakarn C, Laopanupong T, Ludowyke N, et al. CoronaVac Induces Lower Neutralising Activity Against Variants of Concern Than Natural Infection. *Lancet Infect Dis* (2021) 21:1352–4. doi: 10.1016/S1473-3099(21)00568-5
153. Al KN, Zhang Y, Xia S, Yang Y, Al QM, Abdulrazzaq N, et al. Effect of 2 Inactivated SARS-CoV-2 Vaccines on Symptomatic COVID-19 Infection in Adults: A Randomized Clinical Trial. *JAMA* (2021) 326:35–45. doi: 10.1001/jama.2021.8565
154. Ella R, Reddy S, Jogdand H, Sarangi V, Ganneru B, Prasad S, et al. Safety and Immunogenicity of an Inactivated SARS-CoV-2 Vaccine, BBV152: Interim Results From a Double-Blind, Randomised, Multicentre, Phase 2 Trial, and 3-Month Follow-Up of a Double-Blind, Randomised Phase 1 Trial. *Lancet Infect Dis* (2021) 21:950–61. doi: 10.1016/S1473-3099(21)00070-0
155. Ella R, Reddy S, Blackwelder W, Potdar V, Yadav P, Sarangi V, et al. Efficacy, Safety, and lot-to-lot Immunogenicity of an Inactivated SARS-CoV-2 Vaccine (BBV152): Interim Results of a Randomised, Double-Blind,

Controlled, Phase 3 Trial. *Lancet* (2021) 398:2173–84. doi: 10.1016/S0140-6736(21)02000-6
156. Voysey M, Clemens S, Madhi SA, Weckx LY, Folegatti PM, Aley PK, et al. Safety and Efficacy of the ChAdOx1 nCoV-19 Vaccine (AZD1222) Against SARS-CoV-2: An interim Analysis of Four Randomised Controlled Trials in Brazil, South Africa, and the UK. *Lancet* (2021) 397:99–111. doi: 10.1016/S0140-6736(20)32661-1
157. Ramasamy MN, Minassian AM, Ewer KJ, Flaxman AL, Folegatti PM, Owens DR, et al. Safety and Immunogenicity of ChAdOx1 nCoV-19 Vaccine Administered in a Prime-Boost Regimen in Young and Old Adults (COV002): A Single-Blind, Randomised, Controlled, Phase 2/3 Trial. *Lancet* (2021) 396:1979–93. doi: 10.1016/S0140-6736(20)32466-1
158. Sadoff J, Gray G, Vandebosch A, Cardenas V, Shukarev G, Grinsztejn B, et al. Safety and Efficacy of Single-Dose ad26.COV2.s Vaccine Against Covid-19. *N Engl J Med* (2021) 384:2187–201. doi: 10.1056/NEJMoa2101544
159. Guzman-Martinez O, Guardado K, de Guevara EL, Navarro S, Hernandez C, Zenteno-Cuevas R, et al. IgG Antibodies Generation and Side Effects Caused by Ad5-nCoV Vaccine (CanSino biologics) and BNT162b2 Vaccine (Pfizer/BioNTech) Among Mexican Population. *Vaccines (Basel)* (2021) 9:999. doi: 10.3390/vaccines9090999
160. Wu S, Huang J, Zhang Z, Wu J, Zhang J, Hu H, et al. Safety, Tolerability, and Immunogenicity of an Aerosolised Adenovirus Type-5 Vector-Based COVID-19 Vaccine (Ad5-Ncov) in Adults: Preliminary Report of an Open-Label and Randomised Phase 1 Clinical Trial. *Lancet Infect Dis* (2021) 21:1654–64. doi: 10.1016/S1473-3099(21)00396-0
161. Gonzalez S, Olszevicki S, Salazar M, Calabria A, Regairaz L, Marin L, et al. Effectiveness of the First component of Gam-COVID-Vac (Sputnik V) on Reduction of SARS-CoV-2 Confirmed Infections, Hospitalisations and Mortality in Patients Aged 60-79: A Retrospective Cohort Study in Argentina. *EClinicalMedicine* (2021) 40:101126. doi: 10.1016/j.eclinm.2021.101126
162. Logunov DY, Dolzhikova IV, Shcheblyakov DV, Tukhvatulin AI, Zubkova OV, Dzharullaeva AS, et al. Safety and Efficacy of an Rad26 and Rad5 Vector-Based Heterologous Prime-Boost COVID-19 Vaccine: An Interim Analysis of a Randomised Controlled Phase 3 Trial in Russia. *Lancet* (2021) 397:671–81. doi: 10.1016/S0140-6736(21)00234-8
163. Lanini S, Capone S, Antinori A, Milleri S, Nicastri E, Camerini R, et al. GRAd-COV2, a Gorilla Adenovirus-based Candidate Vaccine Against COVID-19, Is Safe and Immunogenic in Younger and Older Adults. *Sci Transl Med* (2022) 14:j1996. doi: 10.1126/scitranslmed.abj1996
164. Johnson S, Martinez CI, Tedjakusuma SN, Peinovich N, Dora EG, Birch SM, et al. Oral Vaccination Protects Against Severe Acute Respiratory Syndrome Coronavirus 2 in a Syrian Hamster Challenge Model. *J Infect Dis* (2022) 225:34–41. doi: 10.1093/infdis/jiab561
165. Gabitzsch E, Safrit JT, Verma M, Rice A, Sieling P, Zakin L, et al. Complete Protection of Nasal and Lung Airways Against SARS-CoV-2 Challenge by Antibody Plus th1 Dominant n- and S-Specific T-Cell Responses to Subcutaneous Prime and Thermally-Stable Oral Boost Bivalent hAd5 Vaccination in an NHP Study. *bioRxiv* (2021) 2012–20. doi: 10.1101/2020.12.08.416297
166. Mahrosh HS, Mustafa G. The COVID-19 Puzzle: A Global Nightmare. *Environ Dev Sustain* (2021) 23:12710–37. doi: 10.1007/s10668-021-01224-3
167. Wang P, Zheng M, Lau SY, Chen P, Mok BW, Liu S, et al. Generation of DelNS1 Influenza Viruses: A Strategy for Optimizing Live Attenuated Influenza Vaccines. *Mbio* (2019) 10:e02180–19. doi: 10.1128/mBio.02180-19
168. Yahalom-Ronen Y, Tamir H, Melamed S, Politi B, Shifman O, Achdout H, et al. A Single Dose of Recombinant VSV-G-Spike Vaccine Provides Protection Against SARS-CoV-2 Challenge. *Nat Commun* (2020) 11:6402. doi: 10.1038/s41467-020-20228-7
169. Scarabel L, Guardascione M, Dal Bo M, Toffoli G. Pharmacological Strategies to Prevent SARS-CoV-2 Infection and Treat the Early Phases of COVID-19. *Int J Infect Dis* (2021) 104:441–51. doi: 10.1016/j.ijid.2021.01.035
170. Tscherne A, Schwarz JH, Rohde C, Kupke A, Kalodimou G, Limpinsel L, et al. Immunogenicity and Efficacy of the COVID-19 Candidate Vector Vaccine MVA-SARS-2-S in Preclinical Vaccination. *Proc Natl Acad Sci USA* (2021) 118:e2026207118. doi: 10.1073/pnas.2026207118
171. Momin T, Kansagra K, Patel H, Sharma S, Sharma B, Patel J, et al. Safety and Immunogenicity of a DNA SARS-CoV-2 Vaccine (ZyCoV-D): Results of an Open-Label, non-Randomized Phase I Part of Phase I/II Clinical Study by Intradermal Route in Healthy Subjects in India. *EClinicalMedicine* (2021) 38:101020. doi: 10.1016/j.eclinm.2021.101020
172. Dey A, Chozhavel RT, Chandra H, Pericherla H, Kumar S, Choonia HS, et al. Immunogenic Potential of DNA Vaccine Candidate, ZyCoV-D Against SARS-CoV-2 in Animal Models. *Vaccine* (2021) 39:4108–16. doi: 10.1016/j.vaccine.2021.05.098
173. Tebas P, Yang S, Boyer JD, Reuschel EL, Patel A, Christensen-Quick A, et al. Safety and Imunogenicity of INO-4800 DNA Vaccine Against SARS-CoV-2: A Preliminary Report of an Open-Label, Phase 1 Clinical Trial. *EClinicalMedicine* (2021) 31:100689. doi: 10.1016/j.eclinm.2020.100689
174. Smith T, Patel A, Ramos S, Elwood D, Zhu X, Yan J, et al. Immunogenicity of a DNA Vaccine Candidate for COVID-19. *Nat Commun* (2020) 11:2601. doi: 10.1038/s41467-020-16505-0
175. Polack FP, Thomas SJ, Kitchin N, Absalon J, Gurtman A, Lockhart S, et al. Safety and Efficacy of the BNT162b2 mRNA Covid-19 Vaccine. *N Engl J Med* (2020) 383:2603–15. doi: 10.1056/NEJMoa2034577
176. Liu Y, Liu J, Xia H, Zhang X, Zou J, Fontes-Garfias CR, et al. BNT162b2-Elicited Neutralization Against New SARS-CoV-2 Spike Variants. *N Engl J Med* (2021) 385:472–4. doi: 10.1056/NEJMc2106083
177. Baden LR, El SH, Essink B, Kotloff K, Frey S, Novak R, et al. Efficacy and Safety of the mRNA-1273 SARS-CoV-2 Vaccine. *N Engl J Med* (2021) 384:403–16. doi: 10.1056/NEJMoa2035389
178. Jackson LA, Anderson EJ, Rouphael NG, Roberts PC, Makhene M, Coler RN, et al. An mRNA Vaccine against SARS-CoV-2 - Preliminary Report. *N Engl J Med* (2020) 383:1920–31. doi: 10.1056/NEJMoa2022483
179. Alexandersen S, Chamings A, Bhatta TR. SARS-CoV-2 Genomic and Subgenomic RNAs in Diagnostic Samples Are not an Indicator of Active Replication. *Nat Commun* (2020) 11:6059. doi: 10.1038/s41467-020-19883-7
180. Rauch S, Roth N, Schwendt K, Fotin-Mleczek M, Mueller SO, Petsch B. MRNA-Based SARS-CoV-2 Vaccine Candidate CVnCoV Induces High Levels of Virus-Neutralising Antibodies and Mediates Protection in Rodents. *NPJ Vaccine* (2021) 6:57. doi: 10.1038/s41541-021-00311-w
181. Rappaport AR, Hong S, Scallan CD, Gitlin L, Akoopie A, Boucher GR, et al. A Self-Amplifying mRNA COVID-19 Vaccine Drives Potent and Broad Immune Responses at Low Doses That Protects Non-Human Primates Against SARS-CoV-2. *bioRxiv* (2021) 2011–21. doi: 10.1101/2021.11.08.467773
182. Karpinski TM, Ozarowski M, Seremak-Mrozikiewicz A, Wolski H, Wlodkowic D. The 2020 Race Towards SARS-CoV-2 Specific Vaccines. *Theranostics* (2021) 11:1690–702. doi: 10.7150/thno.53691
183. Zhang NN, Li XF, Deng YQ, Zhao H, Huang YJ, Yang G, et al. A Thermostable mRNA Vaccine Against COVID-19. *Cell* (2020) 182:1271–83. doi: 10.1016/j.cell.2020.07.024
184. Abd ET, Stockand JD. Recent Progress and Challenges in Drug Development Against COVID-19 Coronavirus (SARS-CoV-2) - An Update on the Status. *Infect Genet Evol* (2020) 83:104327. doi: 10.1016/j.meegid.2020.104327
185. Chen P, Nirula A, Heller B, Gottlieb RL, Boscia J, Morris J, et al. SARS-CoV-2 Neutralizing Antibody LY-CoV555 in Outpatients With Covid-19. *N Engl J Med* (2021) 384:229–37. doi: 10.1056/NEJMoa2029849
186. Yang L, Liu S, Liu J, Zhang Z, Wan X, Huang B, et al. COVID-19: Immunopathogenesis and Immunotherapeutics. *Signal Transduct Target Ther* (2020) 5:128. doi: 10.1038/s41392-020-00243-2
187. Li Y, Qi L, Bai H, Sun C, Xu S, Wang Y, et al. Safety, Tolerability, Pharmacokinetics, and Immunogenicity of a Monoclonal Antibody (SCTA01) Targeting SARS-CoV-2 in Healthy Adults: A Randomized, Double-Blind, Placebo-Controlled, Phase I Study. *Antimicrob Agents Chemother* (2021) 65:e106321. doi: 10.1128/AAC.01063-21
188. Tian JH, Patel N, Haupt R, Zhou H, Weston S, Hammond H, et al. SARS-CoV-2 Spike Glycoprotein Vaccine Candidate NVX-CoV2373 Immunogenicity in Baboons and Protection in Mice. *Nat Commun* (2021) 12:372. doi: 10.1038/s41467-020-20653-8
189. Keech C, Albert G, Cho I, Robertson A, Reed P, Neal S, et al. Phase 1-2 Trial of a SARS-CoV-2 Recombinant Spike Protein Nanoparticle Vaccine. *N Engl J Med* (2020) 383:2320–32. doi: 10.1056/NEJMoa2026920
190. Chen WH, Hotez PJ, Bottazzi ME. Potential for Developing a SARS-CoV Receptor-Binding Domain (RBD) Recombinant Protein as a Heterologous

Human Vaccine Against Coronavirus Infectious Disease (COVID)-19. *Hum Vaccin Immunother* (2020) 16:1239–42. doi: 10.1080/21645515.2020.1740560
191. Lee J, Liu Z, Chen WH, Wei J, Kundu R, Adhikari R, et al. Process Development and Scale-Up Optimization of the SARS-CoV-2 Receptor Binding Domain-Based Vaccine Candidate, RBD219-N1C1. *Appl Microbiol Biotechnol* (2021) 105:4153–65. doi: 10.1007/s00253-021-11281-3
192. Xia S, Yan L, Xu W, Agrawal AS, Algaissi A, Tseng CK, et al. A Pan-Coronavirus Fusion Inhibitor Targeting the HR1 Domain of Human Coronavirus Spike. *Sci Adv* (2019) 5:v4580. doi: 10.1126/sciadv.aav4580
193. Lu L, Liu Q, Zhu Y, Chan KH, Qin L, Li Y, et al. Structure-Based Discovery of Middle East Respiratory Syndrome Coronavirus Fusion Inhibitor. *Nat Commun* (2014) 5:3067. doi: 10.1038/ncomms4067
194. Xia QD, Xun Y, Lu JL, Lu YC, Yang YY, Zhou P, et al. Network Pharmacology and Molecular Docking Analyses on Lianhua Qingwen Capsule Indicate Akt1 is a Potential Target to Treat and Prevent COVID-19. *Cell Prolif* (2020) 53:e12949. doi: 10.1111/cpr.12949
195. Yan H, Zou C. Mechanism and Material basis of Lianhua Qingwen Capsule for Improving Clinical Cure Rate of COVID-19: A Study Based on Network Pharmacology and Molecular Docking Technology. *Nan Fang Yi Ke Da Xue Xue Bao* (2021) 41:20–30. doi: 10.12122/j.issn.1673-4254.2021.01.03
196. Yang R, Liu H, Bai C, Wang Y, Zhang X, Guo R, et al. Chemical Composition and Pharmacological Mechanism of Qingfei Paidu Decoction and Ma Xing Shi Gan Decoction Against Coronavirus Disease 2019 (COVID-19): In Silico and Experimental Study. *Pharmacol Res* (2020) 157:104820. doi: 10.1016/j.phrs.2020.104820
197. Li X, Tang H, Tang Q, Chen W. Decoding the Mechanism of Huanglian Jiedu Decoction in Treating Pneumonia Based on Network Pharmacology and Molecular Docking. *Front Cell Dev Biol* (2021) 9:638366. doi: 10.3389/fcell.2021.638366
198. Du H, Wang P, Ma Q, Li N, Ding J, Sun T, et al. Preliminary Study on the Effective Components and Mechanism of Huoxiang Zhengqi Decoction in Inhibiting the Replication of Novel Coronavirus. *World Sci Technol-Modern Tradit Chin Med Mater Med* (2020) 22:645–51. doi: 10.11842/wst.20200221002
199. Qin F, Li S, Sun Y, Liu Y, Peng S. Molecular Mechanism of Xuebijing Treating ARDS Caused by SARS-CoV-2 Based on Network Pharmacology and Molecular Docking. *Pharmacol Clinics Chin Mater Med* (2020) 36:21–8. doi: 10.13412/j.cnki.zyyl.20200528.001
200. Feng Y, Xie Y, Wang Y, Lian Q, Wang Y, Luo G, et al. Molecular Mechanism of Xuebijing Injection in treatment of Sepsis According to "Drug-Target-Pathway" Network. *Acta Pharm Sin* (2017) 52:556–62. doi: 10.16438/j.0513-4870.2016-1048
201. Zhang Q, Cao F, Wang Y, Xu X, Sun Y, Li J, et al. The Efficacy and Safety of Jinhua Qinggan granule (JHQG) in the Treatment of Coronavirus Disease 2019 (COVID-19): A Protocol for Systematic Review and Meta Analysis. *Med (Baltimore)* (2020) 99:e20531. doi: 10.1097/MD.0000000000020531
202. Liu Z, Li X, Gou C, Li L, Luo X, Zhang C, et al. Effect of Jinhua Qinggan Granules on Novel Coronavirus Pneumonia in Patients. *J Tradit Chin Med* (2020) 40:467–72. doi: 10.19852/j.cnki.jtcm.2020.03.016
203. Zhang X, Xue Y, Chen X, Wu JM, Su ZJ, Sun M, et al. Effects of Tanreqing Capsule on the Negative Conversion Time of Nucleic Acid in Patients With COVID-19: A Retrospective Cohort Study. *J Integr Med* (2021) 19:36–41. doi: 10.1016/j.joim.2020.10.002
204. Tao Q, Du J, Li X, Zeng J, Tan B, Xu J, et al. Network Pharmacology and Molecular Docking Analysis on Molecular Targets and Mechanisms of Huashi Baidu Formula in the Treatment of COVID-19. *Drug Dev Ind Pharm* (2020) 46:1345–53. doi: 10.1080/03639045.2020.1788070
205. Cai Y, Zeng M, Chen YZ. The Pharmacological Mechanism of Huashi Baidu Formula for the Treatment of COVID-19 by Combined Network Pharmacology and Molecular Docking. *Ann Palliat Med* (2021) 10:3864–95. doi: 10.21037/apm-20-1759
206. Chen X, Yin YH, Zhang MY, Liu JY, Li R, Qu YQ. Investigating the Mechanism of ShuFeng JieDu Capsule for the Treatment of Novel Coronavirus Pneumonia (COVID-19) Based on Network Pharmacology. *Int J Med Sci* (2020) 17:2511–30. doi: 10.7150/ijms.46378
207. Xia L, Shi Y, Su J, Friedemann T, Tao Z, Lu Y, et al. Shufeng Jiedu, a Promising Herbal Therapy for Moderate COVID-19: Antiviral and Anti-Inflammatory Properties, Pathways of Bioactive Compounds, and a Clinical Real-World Pragmatic Study. *Phytomedicine* (2021) 85:153390. doi: 10.1016/j.phymed.2020.153390
208. Li Y, Li B, Wang P, Wang Q. Traditional Chinese Medicine, Qingfei Paidu Decoction and Xuanfei Baidu Decoction, Inhibited Cytokine Production *via* NF-kappaB Signaling Pathway in Macrophages: Implications for Coronavirus Disease 2019 (COVID-19) Therapy. *Front Pharmacol* (2021) 12:722126. doi: 10.3389/fphar.2021.722126
209. Cao C, Zhen Z, Kuang S, Xu T. Reduning Injection Combined With Western Medicine for Pneumonia: A pProtocol for Systematic Review and Meta-Analysis. *Med (Baltimore)* (2020) 99:e22757. doi: 10.1097/MD.0000000000022757
210. Xu X, Zhang J, Zheng W, Yang Z, Zhao X, Wang C, et al. Efficacy and Safety of Reduning Injection in the Treatment of COVID-19: A Randomized, Multicenter Clinical Study. *Ann Palliat Med* (2021) 10:5146–55. doi: 10.21037/apm-20-2121
211. Jia S, Luo H, Liu X, Fan X, Huang Z, Lu S, et al. Dissecting the Novel Mechanism of Reduning Injection in Treating Coronavirus Disease 2019 (COVID-19) Based on Network Pharmacology and Experimental Verification. *J Ethnopharmacol* (2021) 273:113871. doi: 10.1016/j.jep.2021.113871
212. Wang Y, Lu C, Li H, Qi W, Ruan L, Bian Y, et al. Efficacy and Safety Assessment of Severe COVID-19 Patients With Chinese Medicine: A Retrospective Case Series Study at Early Stage of the COVID-19 Epidemic in Wuhan, China. *J Ethnopharmacol* (2021) 277:113888. doi: 10.1016/j.jep.2021.113888
213. Derosa G, Maffioli P, D'Angelo A, Di Pierro F. A Role for Quercetin in Coronavirus Disease 2019 (COVID-19). *Phytother Res* (2021) 35:1230–6. doi: 10.1002/ptr.6887
214. Pan B, Fang S, Zhang J, Pan Y, Liu H, Wang Y, et al. Chinese Herbal Compounds Against SARS-CoV-2: Puerarin and Quercetin Impair the Binding of Viral S-Protein to ACE2 Receptor. *Comput Struct Biotechnol J* (2020) 18:3518–27. doi: 10.1016/j.csbj.2020.11.010
215. Saakre M, Mathew D, Ravisankar V. Perspectives on Plant Flavonoid Quercetin-Based Drugs for Novel SARS-CoV-2. *Beni Suef Univ J Basic Appl Sci* (2021) 10:21. doi: 10.1186/s43088-021-00107-w
216. Khan A, Heng W, Wang Y, Qiu J, Wei X, Peng S, et al. In Silico and *In Vitro* Evaluation of Kaempferol as a Potential Inhibitor of the SARS-CoV-2 Main Protease (3CLpro). *Phytother Res* (2021) 35:2841–5. doi: 10.1002/ptr.6998
217. Theoharides TC. COVID-19, Pulmonary Mast Cells, Cytokine Storms, and Beneficial Actions of Luteolin. *Biofactors* (2020) 46:306–8. doi: 10.1002/biof.1633
218. Shawan M, Halder SK, Hasan MA. Luteolin and Abyssinone II as Potential Inhibitors of SARS-CoV-2: An In Silico Molecular Modeling Approach in Battling the COVID-19 Outbreak. *Bull Natl Res Cent* (2021) 45:27. doi: 10.1186/s42269-020-00479-6
219. Zhan Y, Ta W, Tang W, Hua R, Wang J, Wang C, et al. Potential Antiviral Activity of Isorhamnetin Against SARS-CoV-2 Spike Pseudotyped Virus *In Vitro*. *Drug Dev Res* (2021) 82:1124–30. doi: 10.1002/ddr.21815
220. Tejera E, Perez-Castillo Y, Toscano G, Noboa AL, Ochoa-Herrera V, Giampieri F, et al. Computational Modeling Predicts Potential Effects of the Herbal Infusion "Horchata" Against COVID-19. *Food Chem* (2022) 366:130589. doi: 10.1016/j.foodchem.2021.130589
221. Clementi N, Scagnolari C, D'Amore A, Palombi F, Criscuolo E, Frasca F, et al. Naringenin Is a Powerful Inhibitor of SARS-CoV-2 Infection *In Vitro*. *Pharmacol Res* (2021) 163:105255. doi: 10.1016/j.phrs.2020.105255
222. Maurya VK, Kumar S, Prasad AK, Bhatt M, Saxena SK. Structure-Based Drug Designing for Potential Antiviral Activity of Selected Natural Products From Ayurveda Against SARS-CoV-2 Spike Glycoprotein and Its Cellular Receptor. *Virusdisease* (2020) 31:179–93. doi: 10.1007/s13337-020-00598-8
223. D'Amore A, Gradogna A, Palombi F, Minicozzi V, Ceccarelli M, Carpaneto A, et al. The Discovery of Naringenin as Endolysosomal Two-Pore Channel Inhibitor and Its Emerging Role in SARS-CoV-2 Infection. *Cells-Basel* (2021) 10:1130. doi: 10.3390/cells10051130
224. Yang C, Pan X, Xu X, Cheng C, Huang Y, Li L, et al. Salvianolic Acid C Potently Inhibits SARS-CoV-2 Infection by Blocking the Formation of Six-Helix Bundle Core of Spike Protein. *Signal Transduct Target Ther* (2020) 5:220. doi: 10.1038/s41392-020-00325-1

225. Wang W, Li SS, Xu XF, Yang C, Niu XG, Yin SX, et al. Danshensu Alleviates Pseudo-typed SARS-CoV-2 Induced Mouse Acute Lung Inflammation. *Acta Pharmacol Sin* (2021) 0:1–10. doi: 10.1038/s41401-021-00714-4
226. Hu S, Wang J, Zhang Y, Bai H, Wang C, Wang N, et al. Three Salvianolic Acids Inhibit 2019-nCoV Spike Pseudovirus viropexis by Binding to Both Its RBD and Receptor ACE2. *J Med Virol* (2021) 93:3143–51. doi: 10.1002/jmv.26874
227. Jo S, Kim S, Shin DH, Kim MS. Inhibition of SARS-CoV 3CL Protease by Flavonoids. *J Enzyme Inhib Med Chem* (2020) 35:145–51. doi: 10.1080/14756366.2019.1690480
228. Zandi K, Musall K, Oo A, Cao D, Liang B, Hassandarvish P, et al. Baicalein and Baicalin Inhibit SARS-CoV-2 RNA-Dependent-RNA Polymerase. *Microorganisms* (2021) 9:893. doi: 10.3390/microorganisms9050893
229. Rehman M, Akhter S, Batool AI, Selamoglu Z, Sevindik M, Eman R, et al. Effectiveness of Natural Antioxidants Against SARS-CoV-2? Insights From the In-Silico World. *Antibiotics (Basel)* (2021) 10:1011. doi: 10.3390/antibiotics10081011
230. Huang S, Liu Y, Zhang Y, Zhang R, Zhu C, Fan L, et al. Baicalein Inhibits SARS-CoV-2/VSV Replication With Interfering Mitochondrial Oxidative Phosphorylation in a mPTP Dependent Manner. *Signal Transduct Target Ther* (2020) 5:266. doi: 10.1038/s41392-020-00353-x
231. Liu H, Ye F, Sun Q, Liang H, Li C, Li S, et al. Scutellaria Baicalensis Extract and Baicalein Inhibit Replication of SARS-CoV-2 and Its 3C-Like Protease *In Vitro*. *J Enzyme Inhib Med Chem* (2021) 36:497–503. doi: 10.1080/14756366.2021.1873977
232. Sadegh S, Matschinske J, Blumenthal DB, Galindez G, Kacprowski T, List M, et al. Exploring the SARS-CoV-2 Virus-Host-Drug Interactome for Drug Repurposing. *Nat Commun* (2020) 11:3518. doi: 10.1038/s41467-020-17189-2
233. Su H, Zhou F, Huang Z, Ma X, Natarajan K, Zhang M, et al. Molecular Insights Into Small-Molecule Drug Discovery for SARS-CoV-2. *Angew Chem Int Ed Engl* (2021) 60:9789–802. doi: 10.1002/anie.202008835
234. DeFrancesco L. Whither COVID-19 Vaccines? *Nat Biotechnol* (2020) 38:1132–45. doi: 10.1038/s41587-020-0697-7
235. Sempowski GD, Saunders KO, Acharya P, Wiehe KJ, Haynes BF. Pandemic Preparedness: Developing Vaccines and Therapeutic Antibodies For COVID-19. *Cell* (2020) 181:1458–63. doi: 10.1016/j.cell.2020.05.041
236. Dong Y, Dai T, Wei Y, Zhang L, Zheng M, Zhou F. A Systematic Review of SARS-CoV-2 Vaccine Candidates. *Signal Transduct Target Ther* (2020) 5:237. doi: 10.1038/s41392-020-00352-y
237. Dash GC, Subhadra S, Turuk J, Parai D, Rath S, Sabat J, et al. Breakthrough SARS-CoV-2 Infections Among BBV-152 (COVAXIN(R)) and AZD1222 (COVISHIELD(TM)) Recipients: Report From the Eastern State of India. *J Med Virol* (2021) 94:1201–5. doi: 10.1002/jmv.27382
238. Awadasseid A, Wu Y, Tanaka Y, Zhang W. Current Advances in the Development of SARS-CoV-2 Vaccines. *Int J Biol Sci* (2021) 17:8–19. doi: 10.7150/ijbs.52569
239. Cevik M, Grubaugh ND, Iwasaki A, Openshaw P. COVID-19 Vaccines: Keeping Pace With SARS-CoV-2 Variants. *Cell* (2021) 184:5077–81. doi: 10.1016/j.cell.2021.09.010
240. Jeyanathan M, Afkhami S, Smaill F, Miller MS, Lichty BD, Xing Z. Immunological Considerations for COVID-19 Vaccine Strategies. *Nat Rev Immunol* (2020) 20:615–32. doi: 10.1038/s41577-020-00434-6
241. van Doremalen N, Lambe T, Spencer A, Belij-Rammerstorfer S, Purushotham JN, Port JR, et al. ChAdOx1 Ncov-19 Vaccine Prevents SARS-CoV-2 Pneumonia in Rhesus Macaques. *Nature* (2020) 586:578–82. doi: 10.1038/s41586-020-2608-y
242. Yu J, Tostanoski LH, Mercado NB, McMahan K, Liu J, Jacob-Dolan C, et al. Protective Efficacy of Ad26.COV2.S Against SARS-CoV-2 B.1.351 in Macaques. *Nature* (2021) 596:423–7. doi: 10.1038/s41586-021-03732-8
243. Pushparajah D, Jimenez S, Wong S, Alattas H, Nafissi N, Slavcev RA. Advances in Gene-Based Vaccine Platforms to Address the COVID-19 Pandemic. *Adv Drug Deliv Rev* (2021) 170:113–41. doi: 10.1016/j.addr.2021.01.003
244. Yu J, Tostanoski LH, Peter L, Mercado NB, McMahan K, Mahrokhian SH, et al. DNA Vaccine Protection Against SARS-CoV-2 in Rhesus Macaques. *Science* (2020) 369:806–11. doi: 10.1126/science.abc6284
245. Wang Z, Schmidt F, Weisblum Y, Muecksch F, Barnes CO, Finkin S, et al. mRNA Vaccine-Elicited Antibodies to SARS-CoV-2 and Circulating Variants. *Nature* (2021) 592:616–22. doi: 10.1038/s41586-021-03324-6
246. Callaway E. Coronavirus Vaccines Leap Through Safety Trials - But Which Will Work is Anybody's Guess. *Nature* (2020) 583:669–70. doi: 10.1038/d41586-020-02174-y
247. Atanasov AG, Zotchev SB, Dirsch VM, Supuran CT. Natural Products in Drug Discovery: Advances and Opportunities. *Nat Rev Drug Discov* (2021) 20:200–16. doi: 10.1038/s41573-020-00114-z
248. Lyu M, Fan G, Xiao G, Wang T, Xu D, Gao J, et al. Traditional Chinese Medicine in COVID-19. *Acta Pharm Sin B* (2021) 11:3337–63. doi: 10.1016/j.apsb.2021.09.008
249. Xing D, Liu Z. Effectiveness and Safety of Traditional Chinese Medicine in Treating COVID-19: Clinical Evidence From China. *Aging Dis* (2021) 12:1850–6. doi: 10.14336/AD.2021.0906
250. Runfeng L, Yunlong H, Jicheng H, Weiqi P, Qinhai M, Yongxia S, et al. Lianhuaqingwen Exerts Anti-Viral and Anti-Inflammatory Activity Against Novel Coronavirus (SARS-CoV-2). *Pharmacol Res* (2020) 156:104761. doi: 10.1016/j.phrs.2020.104761
251. Yan H, Zou Y, Zou C. [Mechanism of Qingfei Paidu Decoction for Treatment of COVID-19: Analysis Based on Network Pharmacology and Molecular Docking Technology]. *Nan Fang Yi Ke Da Xue Xue Bao* (2020) 40:616–23. doi: 10.12122/j.issn.1673-4254.2020.05.02
252. Huang YF, Bai C, He F, Xie Y, Zhou H. Review on the Potential Action Mechanisms of Chinese Medicines in Treating Coronavirus Disease 2019 (COVID-19). *Pharmacol Res* (2020) 158:104939. doi: 10.1016/j.phrs.2020.104939
253. Tong T, Wu YQ, Ni WJ, Shen AZ, Liu S. The Potential Insights of Traditional Chinese Medicine on Treatment of COVID-19. *Chin Med* (2020) 15:51. doi: 10.1186/s13020-020-00326-w
254. Su H, Yao S, Zhao W, Li M, Liu J, Shang W, et al. Discovery of Baicalin and Baicalein as Novel, Natural Product Inhibitors of SARS-CoV-2 3CL Protease *In Vitro*. *bioRxiv* (2020), 2020–4. doi: 10.1101/2020.04.13.038687
255. Wang H, Xu B, Zhang Y, Duan Y, Gao R, He H, et al. Efficacy and Safety of Traditional Chinese Medicine in Coronavirus Disease 2019 (COVID-19): A Systematic Review and Meta-Analysis. *Front Pharmacol* (2021) 12:609213. doi: 10.3389/fphar.2021.609213
256. Liu M, Gao Y, Yuan Y, Yang K, Shi S, Zhang J, et al. Efficacy and Safety of Integrated Traditional Chinese and Western Medicine for Corona Virus Disease 2019 (COVID-19): A Systematic Review and Meta-Analysis. *Pharmacol Res* (2020) 158:104896. doi: 10.1016/j.phrs.2020.104896
257. Naldi L, Cazzaniga S. More on Covid-19 in Immune-Mediated Inflammatory Diseases. *N Engl J Med* (2020) 383:795–6. doi: 10.1056/NEJMc2018011
258. Ramlall V, Thangaraj PM, Meydan C, Foox J, Butler D, Kim J, et al. Immune Complement and Coagulation Dysfunction in Adverse Outcomes of SARS-CoV-2 Infection. *Nat Med* (2020) 26:1609–15. doi: 10.1038/s41591-020-1021-2
259. Xu Z, Shi L, Wang Y, Zhang J, Huang L, Zhang C, et al. Pathological Findings of COVID-19 Associated With Acute Respiratory Distress Syndrome. *Lancet Respir Med* (2020) 8:420–2. doi: 10.1016/S2213-2600(20)30076-X
260. Kim JS, Lee JY, Yang JW, Lee KH, Effenberger M, Szpirt W, et al. Immunopathogenesis and Treatment of Cytokine Storm in COVID-19. *Theranostics* (2021) 11:316–29. doi: 10.7150/thno.49713
261. Wang P, Nair MS, Liu L, Iketani S, Luo Y, Guo Y, et al. Antibody Resistance of SARS-CoV-2 Variants B.1.351 and B.1.1.7. *Nature* (2021) 593:130–5. doi: 10.1038/s41586-021-03398-2
262. Soin AS, Kumar K, Choudhary NS, Sharma P, Mehta Y, Kataria S, et al. Tocilizumab Plus Standard Care Versus Standard Care in Patients in India With Moderate to Severe COVID-19-Associated Cytokine Release Syndrome (COVINTOC): An Open-Label, Multicentre, Randomised, Controlled, Phase 3 Trial. *Lancet Respir Med* (2021) 9:511–21. doi: 10.1016/S2213-2600(21)00081-3
263. Ge Y, Tian T, Huang S, Wan F, Li J, Li S, et al. An Integrative Drug Repositioning Framework Discovered a Potential Therapeutic Agent Targeting COVID-19. *Signal Transduct Target Ther* (2021) 6:165. doi: 10.1038/s41392-021-00568-6
264. Perez-Fernandez XL, Sabater-Riera J, Fuset-Cabanes M. COVID-19 ARDS: Getting Ventilation Right. *Lancet* (2022) 399:22. doi: 10.1016/S0140-6736(21)02439-9
265. O'Donnell JS, Peyvandi F, Martin-Loeches I. Pulmonary Immuno-Thrombosis in COVID-19 ARDS Pathogenesis. *Intensive Care Med* (2021) 47:899–902. doi: 10.1007/s00134-021-06419-w
266. Aslan A, Aslan C, Zolbanin NM, Jafari R. Acute Respiratory Distress Syndrome in COVID-19: Possible Mechanisms and Therapeutic Management. *Pneumonia (Nathan)* (2021) 13:14. doi: 10.1186/s41479-021-00092-9

267. Dyavar SR, Singh R, Emani R, Pawar GP, Chaudhari VD, Podany AT, et al. Role of Toll-Like Receptor 7/8 Pathways in Regulation of Interferon Response and Inflammatory Mediators During SARS-CoV2 Infection and Potential Therapeutic Options. *BioMed Pharmacother* (2021) 141:111794. doi: 10.1016/j.biopha.2021.111794
268. Li G, De Clercq E. Therapeutic Options for the 2019 Novel Coronavirus (2019-Ncov). *Nat Rev Drug Discov* (2020) 19:149–50. doi: 10.1038/d41573-020-00016-0
269. Yin P, Meng J, Chen J, Gao J, Wang D, Liu S, et al. Antiviral Drugs Arbidol and Interferon Alpha-1b Contribute to Reducing the Severity of COVID-19 Patients: A Retrospective Cohort Study. *Virol J* (2021) 18:142. doi: 10.1186/s12985-021-01617-w
270. Matthay MA, Thompson BT. Dexamethasone in Hospitalised Patients With COVID-19: Addressing Uncertainties. *Lancet Respir Med* (2020) 8:1170–2. doi: 10.1016/S2213-2600(20)30503-8
271. Casadevall A, Joyner MJ, Pirofski LA. SARS-CoV-2 Viral Load and Antibody Responses: The Case for Convalescent Plasma Therapy. *J Clin Invest* (2020) 130:5112–4. doi: 10.1172/JCI139760
272. Duan K, Liu B, Li C, Zhang H, Yu T, Qu J, et al. Effectiveness of Convalescent Plasma Therapy in Severe COVID-19 Patients. *Proc Natl Acad Sci U S A* (2020) 117:9490–6. doi: 10.1073/pnas.2004168117
273. Song JW, Zhang C, Fan X, Meng FP, Xu Z, Xia P, et al. Immunological and Inflammatory Profiles in Mild and Severe Cases of COVID-19. *Nat Commun* (2020) 11:3410. doi: 10.1038/s41467-020-17240-2

Conflict of Interest: The authors declare that the research was conducted in the absence of any commercial or financial relationships that could be construed as a potential conflict of interest.

Publisher's Note: All claims expressed in this article are solely those of the authors and do not necessarily represent those of their affiliated organizations, or those of the publisher, the editors and the reviewers. Any product that may be evaluated in this article, or claim that may be made by its manufacturer, is not guaranteed or endorsed by the publisher.

frontiers | Frontiers in Immunology

ORIGINAL RESEARCH
published: 19 May 2022
doi: 10.3389/fimmu.2022.851642

Bomidin: An Optimized Antimicrobial Peptide With Broad Antiviral Activity Against Enveloped Viruses

Rongrong Liu[1†], Ziyu Liu[1†], Haoran Peng[2†], Yunhua Lv[1], Yunan Feng[1], Junjun Kang[3], Naining Lu[3], Ruixue Ma[1], Shiyuan Hou[1], Wenjie Sun[1], Qikang Ying[1], Fang Wang[1], Qikang Gao[4], Ping Zhao[2], Cheng Zhu[5], Yixing Wang[6*] and Xingan Wu[1*]*

[1] Department of Microbiology, School of Basic Medicine, Fourth Military Medical University, Xi'an, China, [2] Department of Microbiology, Second Military Medical University, Shanghai, China, [3] Department of Neurobiology, School of Basic Medicine, Fourth Military Medical University, Xi'an, China, [4] Analysis Center of Agrobiology and Environmental Sciences, Zhejiang University, Hangzhou, China, [5] Tianjin Key Laboratory of Function and Application of Biological Macromolecular Structures, School of Life Sciences, Tianjin University, Tianjin, China, [6] Jiangsu Genloci Biotech Inc., Nanjing, China

OPEN ACCESS

Edited by:
Denise L. Doolan,
James Cook University, Australia

Reviewed by:
Gill Diamond,
University of Louisville, United States
Joshua A. Jackman,
Sungkyunkwan University,
South Korea

***Correspondence:**
Cheng Zhu
cheng_zhu@tju.edu.cn
Yixing Wang
wangyx@genloci.com
Xingan Wu
wuxingan@fmmu.edu.cn

[†]These authors contributed equally to this work

Specialty section:
This article was submitted to Vaccines and Molecular Therapeutics, a section of the journal Frontiers in Immunology

Received: 10 January 2022
Accepted: 19 April 2022
Published: 19 May 2022

Citation:
Liu R, Liu Z, Peng H, Lv Y, Feng Y, Kang J, Lu N, Ma R, Hou S, Sun W, Ying Q, Wang F, Gao Q, Zhao P, Zhu C, Wang Y and Wu X (2022) Bomidin: An Optimized Antimicrobial Peptide With Broad Antiviral Activity Against Enveloped Viruses. Front. Immunol. 13:851642. doi: 10.3389/fimmu.2022.851642

The rapid evolution of highly infectious pathogens is a major threat to global public health. In the front line of defense against bacteria, fungi, and viruses, antimicrobial peptides (AMPs) are naturally produced by all living organisms and offer new possibilities for next-generation antibiotic development. However, the low yields and difficulties in the extraction and purification of AMPs have hindered their industry and scientific research applications. To overcome these barriers, we enabled high expression of bomidin, a commercial recombinant AMP based upon bovine myeloid antimicrobial peptide-27. This novel AMP, which can be expressed in Escherichia coli by adding methionine to the bomidin sequence, can be produced in bulk and is more biologically active than chemically synthesized AMPs. We verified the function of bomidin against a variety of bacteria and enveloped viruses, including severe acute respiratory syndrome coronavirus-2 (SARS-CoV-2), herpes simplex virus (HSV), dengue virus (DENV), and chikungunya virus (CHIKV). Furthermore, based on the molecular modeling of bomidin and membrane lipids, we elucidated the possible mechanism by which bomidin disrupts bacterial and viral membranes. Thus, we obtained a novel AMP with an optimized, efficient heterologous expression system for potential therapeutic application against a wide range of life-threatening pathogens.

Keywords: antimicrobial peptide, AVP, SARS-CoV-2, HSV-2, DENV-2, CHIKV

INTRODUCTION

The Coronavirus disease 2019 (COVID-19) pandemic has led to high mortality and new infections in many countries (1). Recently, the emergence or re-emergence of multiple viruses (severe acute respiratory syndrome coronavirus-2 [SARS-CoV-2], herpes simplex virus [HSV], Dengue virus [DENV], chikungunya virus [CHIKV], etc.), as well as drug-resistant pathogenic strains, has constantly threatened the lives of humans and animals (2). To overcome the immediate threat posed by constantly evolving pathogens and prevent future epidemics (3), broad-spectrum

antimicrobial agents and novel drugs against drug-resistant strains are urgently needed (4). Antimicrobial peptides (AMPs) are amphiphilic peptides that selectively target and eliminate various microbial pathogens at low micromolar concentrations (5, 6), with little or no induction of drug resistance (7) (8). AMPs are classified into synthetic peptides and natural antibiotics. In mammals, cathelicidins and defensins constitute two prominent AMP families (9). Notably, AMPs potentially possess antiviral abilities through physical interactions with membrane or fusion proteins (10), alternation of virion morphology (11), and inducing virion aggregations (11). For example, LL-37, protegrin-1, and indolizidine have been reported to inhibit HIV infections (12). Furthermore, AMPs have attracted considerable attention as therapeutics against infectious viral pathogens such as HSV (13), DENV, Zika virus (ZIKV), Ebola virus (EBOV) (14), CHIKV (15), and, recently, SARS-CoV-2 (16–18).

Primary HSV infection usually causes a self-limited oral labia infection (HSV-1) or genital infection and subsequent persistence of latent HSV in nerve root ganglia (HSV-2) (19). Moreover, the outbreak of HSV infection may be spontaneous or induced by external stimuli such as emotional stress, ultraviolet radiation, or immunosuppression. HSV-2 infections affect more than one-half of the world's population and can persist in sacral ganglia or trigeminal nerves with intermittent reappearance (20). Dengue hemorrhagic fever (DHF) and dengue shock syndrome (DSS) are caused by DENV-1, DENV-2, DENV-3, and DENV-4 (21). DENV-2 is the predominant cause of outbreaks (22). CHIKV is a re-emerging human arthropod-transmitted virus that may also lead to global outbreaks. It has become a serious health problem due to the lack of an antiviral treatment/vaccine. In addition, CHIKV can cause self-healing febrile diseases with joint pain. Extensive studies have been conducted to target different proteins in CHIKV to curb the spread of the virus (15).

More than 60 approved peptide drugs are currently available for sale in the United States, Europe, Japan, and Asian countries. In addition, peptide-based antiviral therapies have been approved for HIV, influenza virus, and Hepatitis virus (B and C) (23). In this new generation of compounds, AMP has antiviral activity, and its mechanism and biological properties have attracted people's attention. The current antimicrobial peptides (APD) database is dedicated to natural antimicrobial peptides, with 190 peptides annotated as antiviral. Among these AVPs, there are 138 animals, 30 plants, 2 fungi, 1 protozoa, 14 bacteria, and 5 synthetic peptides. In addition, four famous AVP families are isolated from different natural sources-antimicrobial peptides, cecropin, cyclopeptides, and defensins (24). Applying AH-D antiviral peptides in early pregnancy can prevent Zika virus replication and offspring death (25). In addition, the peptide crossed the blood-brain barrier to reduce viral loads and damage caused by ZIKV (26). In studying the membrane binding of HCV non-structural 5A (NS5A) protein, the development of 27-polymer AH peptide preferentially ruptures lipid vesicles less than ~ 100nm in diameter. In addition to the AH peptide, the 18-mer amphiphilic α-helix C5A peptide was initially identified when screening a peptide library from HCV polyproteins and effectively inhibited various envelope viruses *in vitro*, including HCV, HIV, DENV, West Nile virus, HSV, RSV, and MV. These characteristics led to the design of C5A variants with improved antiviral selectivity and applicability for nanoparticles (27).

Because of its broad-spectrum mechanism and huge potential sequence diversity, peptides that inhibit viral entry may potentially meet the demand for new antiviral therapy; however, to optimize or evolve sequence design to combat a wide range of viral diseases, their mechanisms need to be better understood (28). Notably, the low yields and difficulties in the extraction and purification of AMPs have hindered their industry and scientific research applications. To our knowledge, only polylysine and nisin (29) can be produced industrially (29). Therefore, we developed an optimized heterologous expression system to increase AMP yields significantly, achieve efficient purification and structural AMP optimization, and improve AMP therapeutic activity (30).

The amphiphilic nature of most AMPs determines their structural flexibility. Based on their secondary structures, AMPs are usually classified into four categories: linear α-helical peptides, β-sheet peptides, β-hairpin, or loop peptides (29). Notably, the helical peptide shows an unstructured conformation in an aqueous solution, but when the peptide contacts a biological membrane, it becomes an amphiphilic spiral structure (29). BMAP-27 is a well-known peptide derived from bovine sources with a cationic NH_2 terminus that forms an amphipathic α-helix (31). BMAP-18 is a truncated form of BMAP-27. Its toxicity in mammalian and insect cells is reduced, but it is still directly toxic to parasites *in vitro* (32). Bomidin is BMAP-18 with a methionine added to the N-terminus of the primary sequence, which enables its expression in *E. coli*.

Bomidin (CAS#: 2374916-29-5) is a biologically extracted polypeptide containing 19 L-amino acids and with a molecular weight of 2474 Da. In the current study, we optimized the codon of the bomidin gene, induced the expression of bomidin in *Escherichia coli* BL21(DE3), and ultimately extracted and purified bomidin with purity ≥95% by ion-exchange chromatography and reversed-phase chromatography. Bomidin has shown a significant antibacterial effect against *Vibrio parahaemolyticus* and, therefore, has recognized therapeutic potential against *Macrobrachium rosenbergii* in aquaculture applications (33). To investigate the possibility of bomidin as a novel antibacterial and antiviral agent, we characterized the ability of bomidin to inhibit multiple bacterial strains and enveloped viruses (SARS-CoV-2, HSV-2, DENV-2, and CHIKV). In addition, we demonstrated the mechanism by which bomidin destroys bacterial and viral membrane structures. Our results suggest that bomidin can be further developed as a safe and efficient peptide-based therapy for treating and preventing a wide range of infections.

METHODS

Cells, Viruses, and AMPs

Vero-E6 (African green monkey kidney cell line) and Huh7 (hepatocellular carcinoma cell line) were cultured in DMEM (Thermo Fisher Scientific, Waltham, USA) containing 10% fetal

bovine serum in a 5% CO2 incubator at 37°C. DENV-2, HSV-2, and HTNV were kept in our lab and propagated in Huh7 and Vero-E6 cells. The SARS-CoV-2 virus (PubMed No: MT627325) was isolated, processed, and maintained in the ABSL-3 laboratory. In addition, CHIKV and SARS-CoV-2 were gifts from the Second Military Medical University and propagated in Vero-E6 cells. Detection of virus titers was performed using plaque-formation assays (SARS-CoV-2, HSV-2, and CHIKV), fluorescent focus assays (DENV2), and ELISAs (HTNV). Bomidin: MGRFKRFRKKFKKLFKKLS (CAS#: 2374916-29-5) was provided by Genloci Biotech with purity > 95%. (Nanjing, China). In addition, BMAP-18 (GRFKRFRKKFKKLFKKIS) (34) and RI-10 (RIVQRIKDFL) (14) control peptides were synthesized by GenScript (Genscript Biotech Corporation China). All peptide AMPs were dissolved in ddH_2O at a dose of 1 mM and diluted in the medium as required before the assay.

Character Determination of Bomidin

The molecular weight of Bomidin was obtained using an ultra-extreme mass spectrometer (Bruker Daltonik GmbH, Leipzig, Germany). The data are collected for a mass range from m/z 500–3000 Da in positive reflection mode. At a laser frequency of 1000 Hz, 1000 excitations are obtained at each point.

Cytotoxicity Measurement

The cell suspension (2×10^4 cells/well) was inoculated in a 96-well culture plate and grown overnight to 90% confluence at 37°C. The cells were treated with different concentrations of AMPs for 1 hour, and the same concentration of PBS was used as a control. After 48 hours of cell culture, 10% CCK8 solution was added to each well and incubated at 37°C for 1 hour. The absorbance was measured at 450 nm using a microplate reader. The CC50 represents the drug concentration required for the uninfected cells' 50% cell killing (cytotoxicity).

In Vitro Antibacterial Assays

The test strain's minimal inhibitory concentration (MIC) was determined by the microbroth dilution method recommended by the Clinical and Laboratory Standards Institute (CLSI) M07-A11. The MIC of compounds to fungi was determined by the micro liquid-based dilution method recommended by [Reference Method for Broth Dilution Antifungal Susceptibility Testing of Yeast; Approved Standard-third Edition (Vol, 28, No. l4); M27-A3]. The MIC assay was performed according to the method described in the **Supplementary Materials**.

Fluorescent Focus Assay

Huh, 7 cells were seeded in 12-well plates and incubated under 5% CO2 at 37°C overnight. Viruses were mixed with different concentrations of Bomidin (0 μM, 10 μM, 20 μM, 40 μM, and 80 μM) for 30 min and infected the cells for 2 hours. After adsorption, an overlay of DMEM, 5% FBS, and 0.8% carboxymethylcellulose (CMC, ICN Biomedicals, Aurora, OH) was added. The infected monolayer cells were cultured in a 5% CO2 incubator at 37°C. The covering solution of the culture medium infected for 2 days was removed, and cold phosphate-buffered saline (PBS) was added. After incubating for 5 minutes, the PBS was discarded, and the cells were fixed with cold absolute methanol (Sigma–Aldrich Co., St. Louis, MO) for 10 minutes and then washed with PBS. Next, the cells were incubated with an antibody diluted with PBS for 1 hour at 37°C, washed three times, and then stained with a secondary antibody. The fluorescent foci of infection were observed and counted by fluorescence microscopy.

Immunofluorescence Assay

Different viruses were mixed with antimicrobial peptides for 10 min, infected cells for 1 h, and cultured with DMEM containing 10% serum for 48 h. After discarding the supernatant and washing it three times with PBS, it was permeated with PBS containing 0.2% Triton X-100 (containing 0.1% BSA) at room temperature for 30 minutes. Then, the cells were mixed with an antiviral antibody at 4°C overnight. After washing with PBS three times, the cells were incubated with fluorescence-conjugated secondary antibodies at room temperature for 1 hour. Cell nuclei were stained using 4',6'-diamidino-2-phenylindole (DAPI) in the dark for 5 min, and images were obtained by Fluorescence microscope.

Plaque Forming Assay

The cells were cultured overnight in a 6-well plate (1×106 cells/well). Two hours after adding viruses to the wells, the cells were further incubated with a maintenance medium containing 2% methylcellulose (Sigma, Saint Louis, USA) for 48 hours at 37°C. After incubation, the maintenance medium was removed, and the cells were washed with phosphate-buffered saline (PBS) and stained with methylene blue.

Quantitative Real-Time PCR Assay

Cellular RNA was isolated using a standard protocol, and qRT–PCR analysis was performed using SYBR Green (BIO-RAD, California, USA) according to the manufacturer's protocol. Viral RNA expression was calculated using the 2-delta delta C.T. (cycle threshold) method normalized to GAPDH expression. qPCR primers sequences are as follows: SARS-CoV-2: Fwd-5'GGGGA ACTTCTCCTGCTAGAAT 3', Rev 5'CAGACATTTTGCT CTCAAGCTG 3' | HSV-2: Fwd-5' AATGTGGTTTAGCT CCCGCA-3', Rev-5' CCAGTTGGCGTGTCTGTTTC-3' | DENV-2: Fwd-5' GGTTTTGGGAGCTGGTTGAC, Rev-5' ACTCTAAGAAGCGTGCTCCA |CHIKV:Fwd-5'TCTATAACATGGACTACCCGCCC, Rev-5' AGCCAGATGGTGCCTGAGAGT

Western Blotting

The cells were washed twice with DPBS, lysed with 1×SDS protein loading buffer at 4°C for 30 minutes, and harvested. The supernatant was collected by centrifugation (13,000 rpm) at 4°C for 30 minutes. Next, the same amount of protein was boiled at 95°C for 10 minutes, separated by SDS–PAGE with different concentrations, and then transferred to a polyvinylidene fluoride membrane by electrophoresis. After blocking with 5% skim milk in 1×TBS, the membrane was incubated with primary antibody (Abs), and then the secondary Abs were labeled with infrared dye. The Odyssey infrared imaging system (LI-COR Biosciences)

was used to visualize the signal on the polyvinylidene fluoride film and then the whole W.B. program.

Transmission Electron Microscopy

After predehydration with graded ethanol, the bacteria were transferred to anhydrous acetone for 20 minutes. At room temperature, the sample was placed in a 1:1 mixture of absolute acetone and final Spoor resin mixture for 1 hour and then transferred to a 1:3 mixture of absolute acetone and final resin mixture for 3 hours. The final Spoor resin mixture was incubated overnight. Next, the sample was placed in an Eppendorf tube containing Spoor resin and heated at 70°C for more than 9 hours. Samples were sliced in a Leica EMUC7 ultramome, and the slices were stained with uranyl acetate and essential lead citrate for 5 to 10 minutes and observed with a Hitachi H-7650TEM.

Virus-infected cells were collected by centrifugation to prepare cell particles, fixed in cacodylate sodium buffer containing 1% glutaraldehyde (0.2 M, pH 7.2), and fixed in 1% osmium tetroxide. Then, the fixed sample was dehydrated by acetone solution and embedded in epoxy resin. Finally, the sample was polymerized at 60°C for 3 days. The resin block was used to prepare ultrathin slices (50-70 nm thick). These sections were supported by copper mesh, negatively stained with uranyl acetate and lead citrate (electron microscopy) and observed with a JEM100SX transmission electron microscope (JEOL, Tokyo, Japan).

Molecular Dynamics Simulations

The all-atom M.D. simulations were performed on Gromacs 2019.6 with CHARMM36 force field (35, 36). The initial model of the bomidin peptide and various lipids, along with 150 mM NaCl and explicit water molecules, were constructed by CHARMM-GUI and equilibrated as an NPT ensemble at 303.15 K (37, 38). The simulations were carried out with LINCS constraints on H-bonds and a time step of 2 fs. The nonbonded interaction cutoff for electrostatic calculations was set as 10 Å, and the particle mesh Ewald (PME) method was used to calculate long-range electrostatic interactions.

Statistical Analysis

Statistical analysis was performed by GraphPad Prism software (version 9.0, GraphPad Software Inc.). Data are expressed as the means ± S.D. Unpaired Student's t tests determined statistical significance between the two groups. One-way ANOVA determined the significance of the variability between different groups. $p < 0.05$ was considered statistically significant, and $p > 0.05$ was considered statistically nonsignificant (*$p < 0.05$; **$p < 0.01$; ***$p < 0.001$; NS, no significance).

RESULTS

Peptide Prediction and Characterization

We simulated the structure, hydrophilicity, and hydrophobicity of bomidin, which is an αα-helical peptide (**Figure 1A**), with positively charged lysine and arginine residues scattered among the hydrophobic parts on both sides (**Figure 1B**). In a dissolved state, bomidin has a charge number related to the pH of the solution. The mass spectrum in **Figure 1C** shows the multiple charge states (from +7 to +3) of the bomidin ion detected. Considering that as many as 10 in the bomidin sequence as a primary amino acid, we speculate that Bomidin may also have ions of various valence states in a neutral solution (**Figure 1C**). The mass of bomidin was 2474 Da.

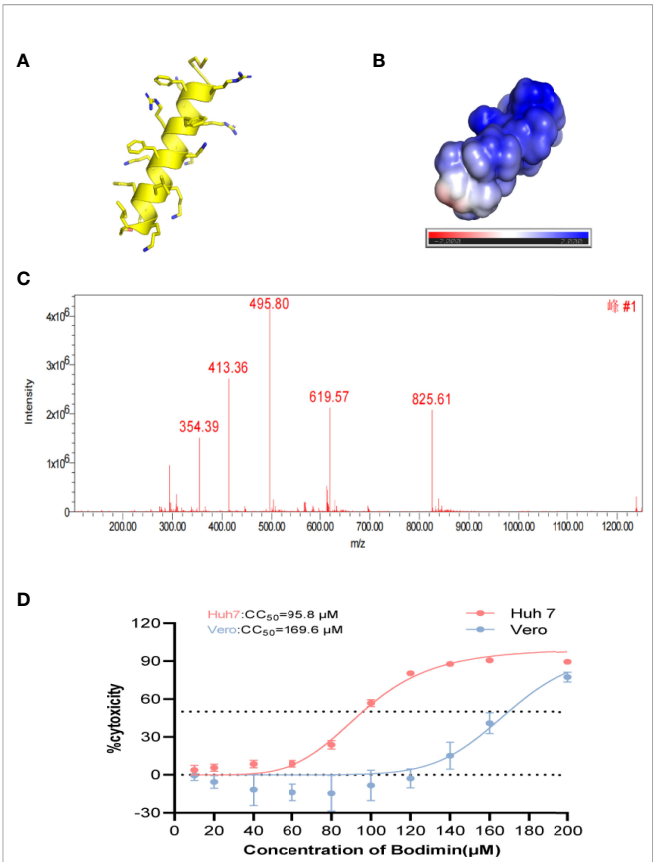

FIGURE 1 | The structural characteristics of bomidin. **(A)** The α-helix of bomidin. **(B)** Total solvent accessibility of bomidin; blue, hydrophobic; red, hydrophilic regions. **(C)** Mass analysis of bomidin. **(D)** Cytotoxic effects of bomidin in cells. The cytotoxicity induced by bomidin in Vero E6 and Huh7 cells was determined by CCK-8 assay 48 h after treatment. CC50 is the bomidin concentration required to reduce cell viability by 50%.

Bomidin Inhibits 12 Bacterial Species and 2 Fungal Strains

AMPs featured high specificity against bacteria and relatively low cytotoxicity toward mammalian cells. Therefore, we first examined the impact of bomidin on cell viability. The 50% cytotoxicity (CC50) value in virus-susceptible cells was 169.6 ± 1.1 μM in Vero cell lines and 95.8 ± 1.1 μM in Hu7 cell lines (**Figure 1D**). We then established that bomidin inhibited 12 bacterial species, including 41 strains. To assess the effects of bomidin on common bacteria, we measured the minimum inhibitory concentration (MIC) using

the microbroth dilution method (39). We determined the effects of bomidin on other bacterial strains, including 8 gram-positive and 4 gram-negative bacteria species (**Table 1**). The MICs were in the range of 1-4 μM in common. For the more tolerant gram-positive bacterium *Enterococcus faecalis* and the fungus *Candida albicans*, the MIC value ranged from 8 to 32 μM. (**Table 1**).

Specifically, we characterized the antimicrobial effects of bomidin on 5 common pathogenic drug-resistant strains from hospitals. These drug-resistant strains (extended-spectrum β-lactamase (ESBL)-producing *E. coli*, vancomycin-resistant *Staphylococcus aureus*, multidrug-resistant *Acinetobacter baumannii, Klebsiella* and *Pseudomonas aeruginosa*) were cultured on blood agar plates with complete hemolytic rings (*β*-hemolytic phenotype). Treatment with bomidin significantly reduced the populations of these pathogens. At a 100 μM dose, bomidin abolished the growth of *Klebsiella* and *P. aeruginosa* within 30 minutes, while its effects on the cultures of *S. aureus, A. baumannii*, and ESBL-producing *E. coli* were evident within 24 h (**Figure 2A** and **Supplementary Figure 1**).

We then used a scanning electron microscope to directly observe the bomidin-treated bacterial samples. The morphology of the untreated cells was intact (**Figure 2B**, left column). In contrast, the membrane surface of the bomidin-treated cells was swollen, the cell surface was rough, and the morphology showed changes (**Figure 2B**). After 10 min or 30 min of bomidin treatment, the number of bacteria (*B. subtilis, E. coli*, and *S. aureus*) decreased, and their size also reduced. In addition, perforations, vesicular structures, and flocculent material aggregates were observed on the membranes, and some bacteria had ruptured, presenting fragmented, unclear structures (**Figure 2B**). Hence, bomidin disrupted the integrity of the bacterial membranes.

TABLE 1 | MICs of Bomidin against various bacteria and fungi.

Organism		MIC range (μM)
Gram Positive Bacteria	*Staphylococcus aureus* (4 strains)	2∼4
	Bacillus megaterium Bm 11	2
	Bacillus subtilis KCTC 3068	4
	Staphylococcus epidermidis KCTC 1917	4
	Enterococcus faecalis (10 strains)	8∼> 32
	Enterococcus faecium (5 strains)	8∼> 32
	Streptococcus agalactiae (3 strains)	1∼4
	Acinetobacter baumanni (10 strains)	0.5∼16
Gram Negative Bacteria	*Escherichia coli* (3 strains)	2∼4
	Salmonella typhimurium ATCC 14028	4
	Pseudomonas aeruginosa ATCC 27853	1
	Serratia marcescens ATCC 8100	2
Fungi	*Candida albicans*	16
	Cryptococcus neoformans	4
Drug-resistant Bacteria	Vancomycin-resistant *Staphylococcus aureus*	> 50
	Extended-spectrum β-lactamases (ESBLs)-producing *Escherichia coli*	> 50
	Multiple drug-resistant *Pseudomonas aeruginosa*	> 50
	Multiple drug-resistant *Acinetobacter baumanni*	> 50
	Multiple drug-resistant *Klebsiella*	50

The effects of Bomidin on other bacterial strains, including 8 Gram-positive bacteria and 4 Gram-negative bacteria, and the MICs were in the range of 1-4 μM. For the more tolerant Gram-positive bacteria Enterococcus faecalis and the fungi Candida albicans, the MIC value ranges from 8-32μM. For the drug-resistant bacteria, the MIC value is greater than or equal to 50μM.

Bomidin Inhibits a Broad Range of Enveloped Viruses at the mRNA and Protein Levels

As enveloped viruses (SARS-CoV-2, HSV-2, CHIKV, DENV-2, etc.) contain viral membranes, we were interested in testing the antiviral effects of bomidin on these representative viruses. After incubating bomidin and the viruses for 10 minutes, we infected these susceptible cells with SARS-CoV-2, HSV-2, CHIKV, or DENV-2. We quantified the replication ability of the remaining viruses at the protein level using immunofluorescence (live SARS-CoV-2 and DENV-2) or GFP reporter genes (for pseudotyped CHIKV) (**Figures 3A, B**). Bomidin inhibited the infectability of each virus in a dose-responsive manner. Specifically, 10 μM bomidin was enough to reduce the population of DENV-2 or HSV by 50%, while 80 μM bomidin significantly inhibited SARS-CoV-2 growth. We also corroborated the inhibitory effects at the mRNA level. Consistent with the measurements of GFP signals, the DENV-2 and HSV mRNA levels were susceptible to increased bomidin concentrations (**Figure 3C**).

Electron Microscopy Revealed That the Number of Viral Particles Decreased Significantly After Bomidin Treatment

We directly compared viral particles in cells with or without bomidin treatment using electron microscopy. In cells without bomidin, dark-colored viral particles of SARS-CoV-2, HSV-2, CHIKV, or DENV-2 were apparent. With 20μM, 40 μM or 80 μM bomidin pretreatment, no viral particles were observed, suggesting an antiviral inhibition percentage greater than 90% (**Figures 4A–D, a-c**). Bomidin did not affect the integrity of the mammalian cell membrane (**Figures 4A–D, d**).

Compared With Other Reported Antibacterial Peptides, Including BMAP-18, Bomidin Shows a More Significant Inhibitory Effect on Virus Infection

We compared the antiviral activities of the mammalian cathelicidins BMAP-18 and bomidin and the control peptide RI-10 (RIVQRIKDFL) (14). As shown in spot tests, immunofluorescence assays, and plaque tests, the ability of bomidin to inhibit infection (DENV-2, CHIKV, and HSV-2) was significantly higher than that of the other two peptides (**Figures 5A–C**).

Bomidin Can Pass Through Bacterial and Viral Membranes in Simulated Systems But Does Not Damage Eukaryotic Cell Membranes

To evaluate the impacts of the bomidin peptide on different components of cellular or viral membranes, we computationally modeled systems containing bomidin and common membrane lipids (**Figure 6** and **Supplementary Table 1**) (phosphatidylserine, P.S.; phosphatidylinositol, P.I.; phosphatidylcholine, P.C.; phosphatidylethanolamine, P.E.; cholesterol, Chol; and sphingomyelin, S.M.). In current study, the components of viral membrane were adapted from shared lipidome of DENV (40),

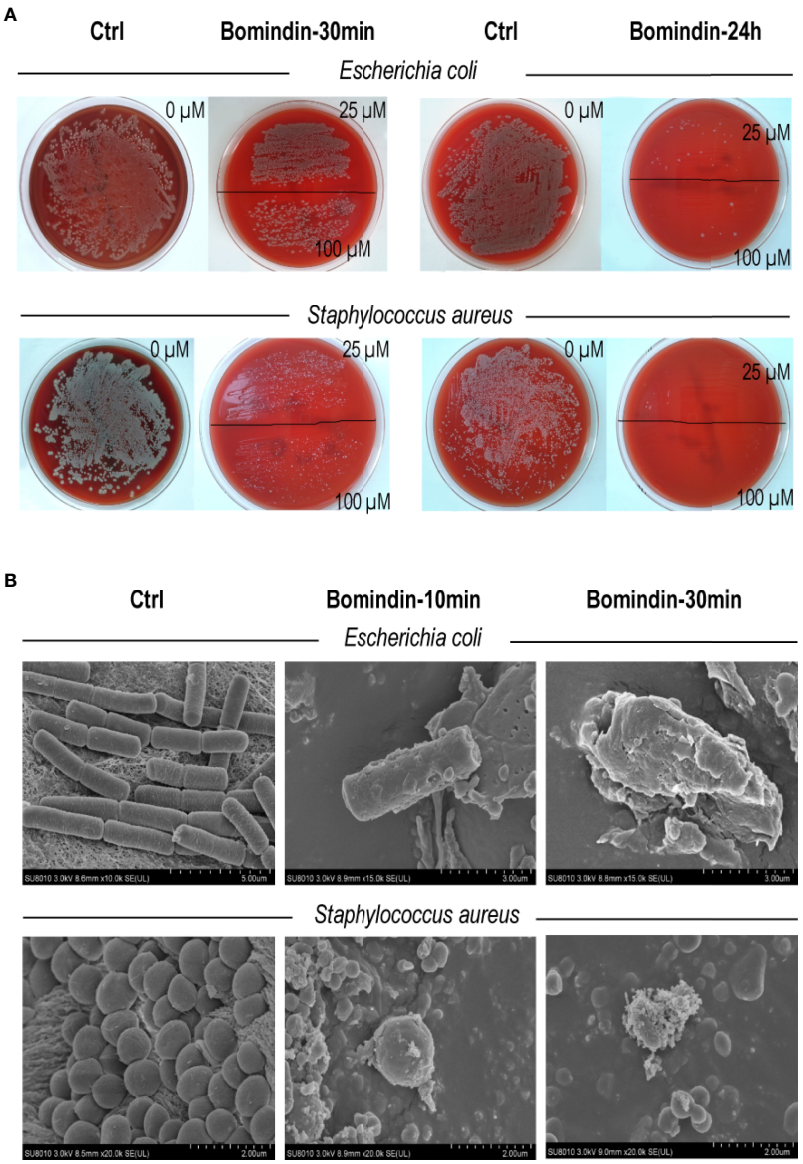

FIGURE 2 | Assessment of bomidin as an inhibitor of bacterial growth. **(A)** The 25 μM and 100 μM doses of bomidin treatment significantly reduced bacterial populations within 30 min while abolishing the growth of ESBL-producing *Escherichia coli* and *Staphylococcus aureus* within 24 h. **(B)** After 30 min or 1 h of bomidin treatment, the number and size of bacteria (*B. subtilis, E coli*, and *S. aureus*) decreased. Perforations, vesicular structures, and some flocculent material aggregates were observed on the membranes, and some bacteria ruptured into fragmented, unclear structures.

SARS-CoV-2 (41), HSV-2 (42), E. Coli and mammalian cell membranes (43) were used as the model system. Notably, the mammalian cell plasma membrane contains significant amounts (~20%) of cholesterol, while a majority of viral membranes are composed of P.C. (~60%), P.E. (~20%), and P.I. (~10%) lipids. When embedded inside the bilayers of a viral or bacterial membrane model, bomidin disrupted the surrounding lipid molecules and emerged from one side of the membrane bilayer (**Figure 6A** and **Supplementary Video 1**), possibly leading to the perforations or vesicular structures observed in the electron microscopy images. In contrast, bomidin resides in the plasma membrane without disturbing its overall integrity, likely because the enriched components of cholesterol reduced the fluidity of human plasma membranes. We postulated that the efficacy of bomidin was sensitive to the chemical nature of lipids it interacted. As control simulations, we also evaluated the effects of several known AMPs with varying lengths/conformations (**Supplementary Video 2**, two antibacterial peptides and one anti-HCV peptide). The results of our control simulations indicated that the bilayer system we constructed for molecular dynamics simulations reflected the antimicrobial activities; all three peptides caused membrane permeation and disruption.

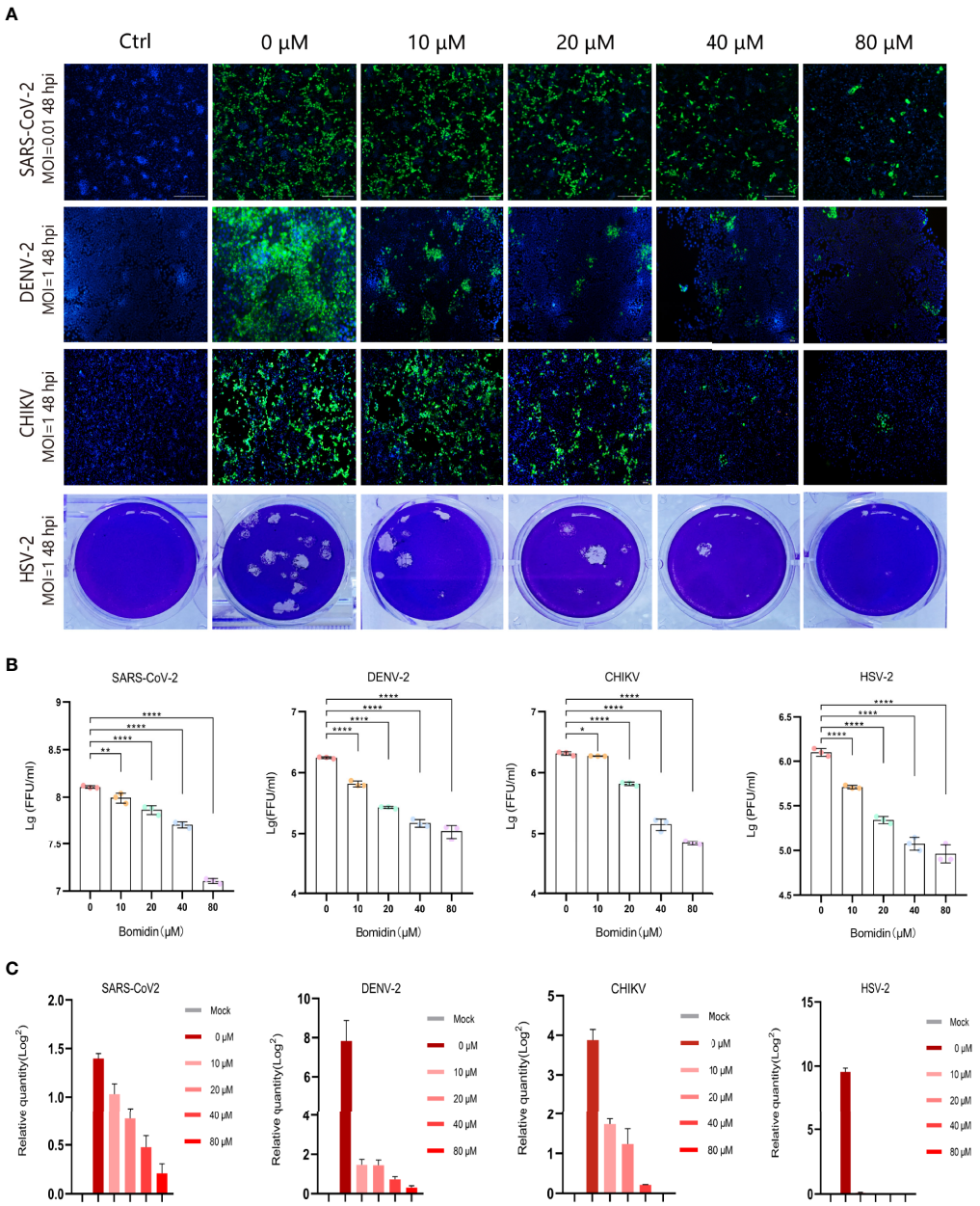

FIGURE 3 | Broad spectrum antiviral activity of bomidin against viral infection in cells. **(A)** The dose-dependent inhibitory effect of bomidin at different concentrations (0 μM, 10 μM, 20 μM, 40 μM and 80 μM) was determined by an immunofluorescence assay (SARS-CoV-2, DENV-2 and CHIKV) and a plaque forming assay (HSV-2) 48 h postinfection. Cell nuclei were stained with DAPI (blue). The viral proteins are indicated in green. **(B)** Fluorescence quantification. **(C)** Bomidin inhibition of virus RNA formation at different concentrations (0 μM, 10 μM, 20 μM, 40 μM and 80 μM) was determined by quantitative real-time PCR 48 h postinfection, and GAPDH was used as the housekeeping gene for normalization. The data are shown as the means ± S.D.; n = 3 cell cultures per experiment. *p < 0.05; **p < 0.01; ****p < 0.0001.

DISCUSSION

Collectively, our results demonstrated the potential of bomidin as a broad-spectrum inhibitor of bacteria and multiple enveloped viral infections. As a family of cationic peptides, the antimicrobial or antiviral activity is usually associated with its ability to adsorb on bacterial/viral surfaces or with interactions with innate immune system components to enhance nucleic acid-sensing (44). Specifically, AMP membrane-targeting mechanisms can be described through pore models or carpet models (45). AMPs vertically embedded in the cell membrane accumulate and then bend to form a circular hole with a 1–2 nm diameter (also known as the toroidal pore or wormhole model, **Figure 6B**) (45). Interestingly, our data indicated that Bomidin

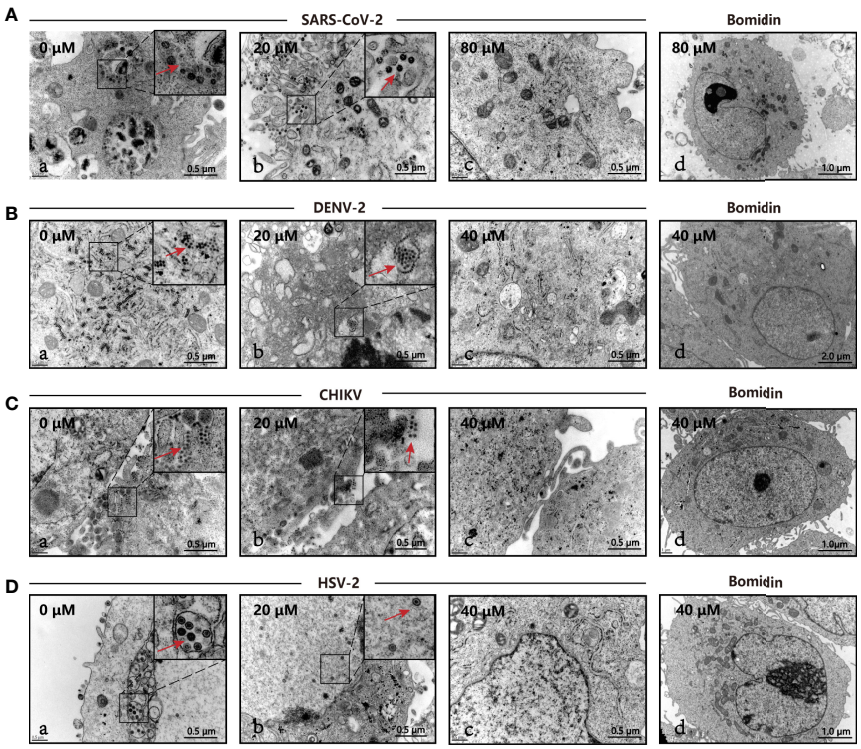

FIGURE 4 | The antiviral activity of bomidin against viral infection was determined by transmission electron microscopy (TEM). The different viruses were mixed with the respective concentrations of bomidin-treated cells for 2 hours and detected by TEM 48 h postinfection. **(A)** SARS-CoV-2, **(B)** DENV-2, **(C)** CHIKV, **(D)** HSV-2. **(a)** Virus-infected cells; **(b, c)** Bomidin-treated viral cultures for 10-30 min at 37°C with infected cells; red arrows: viral particles. **(d)** Bomidin control.

disrupted flavivirus membranes but did not affect the integrity of Hantaan virus (HTNV) membranes (**Supplementary Figure 3**) or eukaryotic cell membranes. Previous studies have suggested that flavivirus membranes are derived from internal endoplasmic reticulum membranes of infected cells (46). Hence, we postulated that the function of bomidin as an antiviral peptide depended on the lipid composition and chemical properties of the membranes with which it interacts. Indeed, molecular modeling showed that bomidin readily disrupted viral membranes (with components similar to those in the endoplasmic reticulum) and bacterial membranes but did not alter the overall structures of the cell membranes, corroborating our experimental observations.

The recent trend of virus epidemics shows that enveloped viruses are the main threat to global health. Therefore, it will be beneficial to formulate a widely applicable anti-virus strategy for a wide range of enveloped viruses. The phospholipid membrane, including the viral envelope, is a suitable target, especially if the strategy based on nanotechnology can be further optimized to target the viral membrane selectively (47). Previous studies suggested the lipid composition of the virion envelope reflects that of the membrane where budding took place (48). The Lipid Envelope Antiviral Disruption (LEAD) molecules (such as CLR01) were shown to broadly inhibit mosquito-borne viruses (such as DENV and ZIKV) and other lipid membrane-enveloped viruses (49). It disrupts the lipid envelope surrounding virions, abrogates viral infectivity, and reduces viral load (49).

We observed broad-spectrum inhibitory activities against over forty different bacteria and four enveloped viruses, suggesting that the bomidin peptide could target lipid components shared among the bacteria and viruses. Furthermore, based on recently published lipidome experiments of viruses, specifically DENV (40), SARS-CoV-2 (41), HSV (42), and studies of E. Coli and mammalian cell membranes (43). We constructed model systems of commonly shared lipid components from a consensus of lipidomic measurements to investigate the role of bomidin on the model membrane (48). Hence, we further divided our membrane models into those resembling the endoplasmic reticulum/Golgi or those resembling the plasma membrane. A notable difference between these two is the enrichment of cholesterol esters and sphingomyelin (50). Using these models, we could explain why bomidin readily inhibited viruses budding from the E.R./Golgi (such as Dengue and SARS-CoV-2) but was not as effective against HSV-1 (high amount of sphingomyelin) or HTNV (budding from the plasma membrane) (**Supplementary Figure 3**). The lipid components of E. Coli inner membrane and human cell plasma membrane were used as positive controls and negative controls, respectively, in our simulations (43). An emerging paradigm for broad-spectrum antimicrobial molecules focused on the lipids of

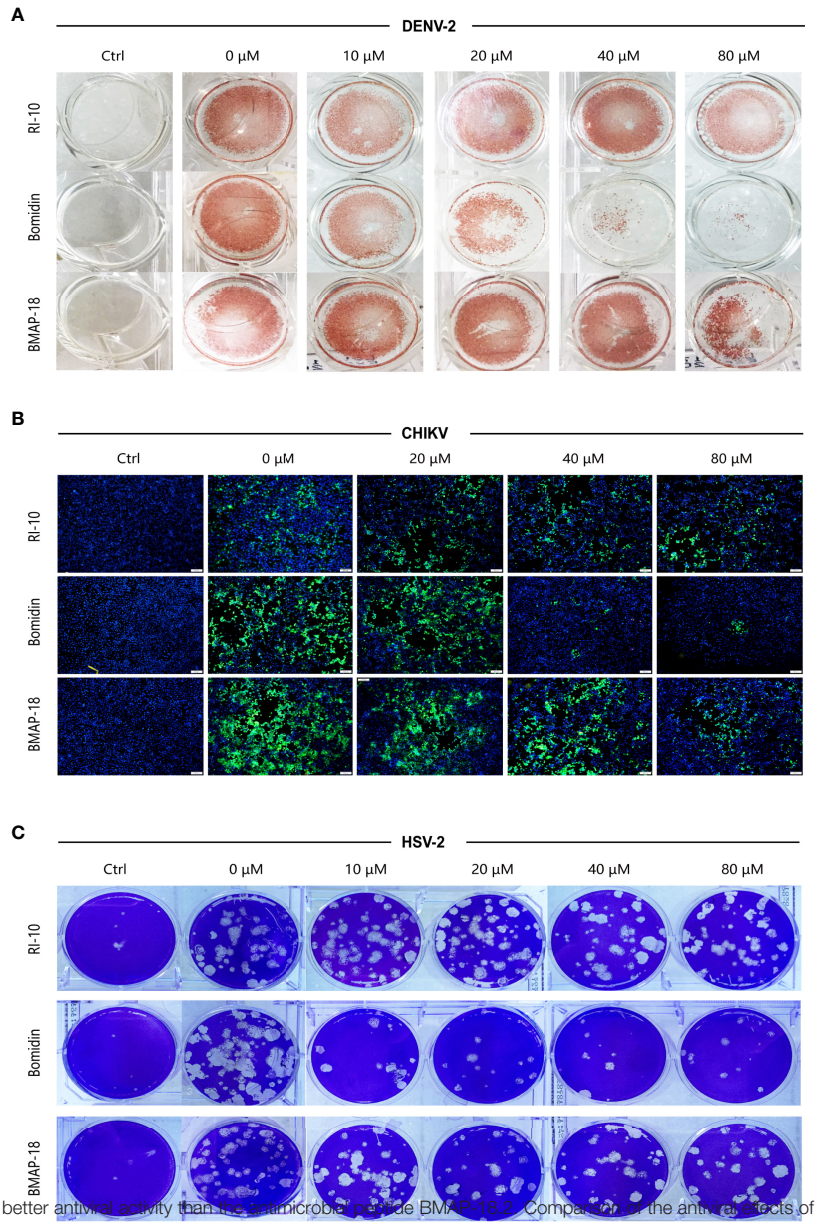

FIGURE 5 | Bomidin shows better antiviral activity than the antimicrobial peptide BMAP-18.2. Comparison of the antiviral effects of the antimicrobial peptides bomidin and BMAP-18 on different viruses. The viruses were mixed with varying concentrations of the antimicrobial peptide to infect cells for 2 h. The effects were detected by various methods **(A)** fluorescence focus assay; **(B)** immunofluorescence assay; **(C)** plaque-forming assay) 48 h postinfection. RI-10: nonantimicrobial control peptide; BMAP-18: antimicrobial control peptide; bomidin: BMAP18-derived antimicrobial peptide.

the virus and bacteria (51), and our results reinforced that interfacial activity of AMPs correlated with their broad-spectrum antimicrobial activities (11).

More than 400 peptide drugs are currently in clinical trials, and the FDA has approved approximately 60 kinds of peptide drugs (23). In sharp contrast, few peptides have been approved for use in antiviral treatment. Therefore, strategies are being developed to improve drug properties, such as permeability, oral bioavailability, and blood and cell stability (29). Despite a few potential limitations (such as limited mass production), peptides exhibit advantages over small-molecule drugs (organics), including superior binding affinity and fewer side effects (14, 23, 52). Furthermore, the backbone and side chains of natural AMPs can be conveniently adapted to carry a circular structure consisting of D-amino acids (53), which significantly increases the stability of the peptides and improves their drug properties in the presence of peptidases (29).

In summary, the protective effects of bomidin reported here suggest further expansion of the antiviral arsenal. Furthermore,

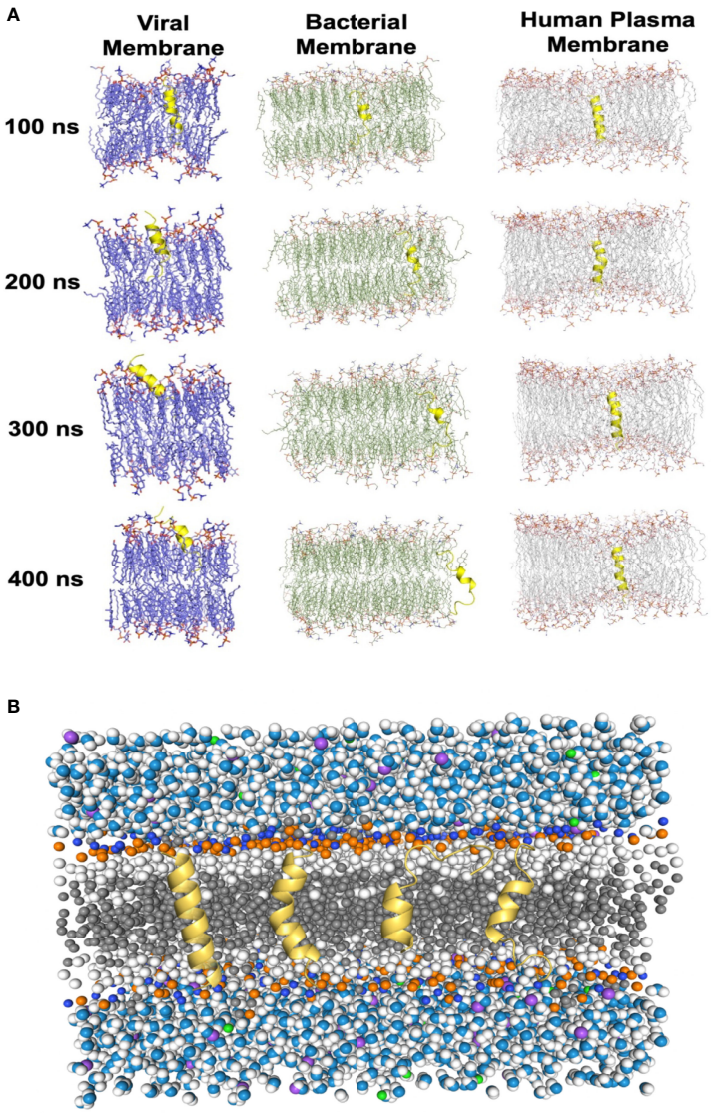

FIGURE 6 | Molecular dynamics simulations of the Bomidin–membrane interactions. **(A)** Snapshots of the Bomidin and bilayer membrane dynamic systems throughout the 400 ns trajectories. Bomidin interacted strongly with anionic phospholipid bilayers with a preference for fluid layers. Membrane penetrations or disruptions were observed for viral/bacterial membrane models (left/middle panel). The elevated cholesterol-to-phospholipid molar ratio (commonly seen in mammalian plasma membranes) and decrease in membrane fluidity can shield the membrane from the action of the peptide (right panel). **(B)** Lateral view of the overall simulated system with a bilayer of lipids (dark gray) immersed in water (blue/white spheres) and ions (purple/green spheres). Conformations sampled by Bomidin (yellow) are shown.

our rational engineering of bomidin has enabled its mass production. It generates new opportunities for future manufacturing and applications, such as loaded bomidin acting as nanocarriers to achieve sustained drug release, external medicines, nasally administered mist sprays, or wound dressings. Overall, we expect that the systemic administration and development of bomidin into antibiotics and broad-spectrum antiviral drugs will contribute to our constant fight against drug-resistant bacterial infections and viruses and stall the spread of worldwide pandemic-causing pathogens.

DATA AVAILABILITY STATEMENT

The raw data supporting the conclusions of this article will be made available by the authors, without undue reservation.

AUTHOR CONTRIBUTIONS

RL: Conceptualization, data curation, formal analysis, investigation, methodology, software, validation, visualization.

ZL: Data curation, formal analysis, methodology, software, validation, visualization, writing—original draft, writing—review and editing. HP: Data curation, formal analysis, methodology. YL: Methodology. YF: Investigation, writing—original draft. JK: Data curation, methodology, software. NL: Data curation. RM, Methodology. SH: Methodology. WS: Methodology. QY: Methodology. FW: Methodology, supervision. QG: Conceptualization, methodology, resources. PZ: Data curation, formal analysis, resources, supervision. CZ: Data curation, formal analysis, funding acquisition, methodology, validation, visualization, writing—review and editing. YW: Conceptualization, data curation, funding acquisition, methodology, resources. XW: Funding acquisition, methodology, project administration, resources, supervision, writing—review and editing. All authors contributed to the article and approved the submitted version.

FUNDING

This work was supported by the National Natural Science Foundation of China (Nos. 81772167, 81971563 to XW), the Key Research and Development Project of Shaanxi Province (No. 2019ZDLSF02-03 to XW), the National Key Research and Development Program of China (2020YFA0908501 to CZ), the National Natural Science Foundation of China (22007071 and 22077094 to CZ), and the project of Shaanxi Social Development of Science and Technology (NO.2016SF-112 to ZL).

SUPPLEMENTARY MATERIAL

The Supplementary Material for this article can be found online at: https://www.frontiersin.org/articles/10.3389/fimmu.2022.851642/full#supplementary-material

REFERENCES

1. Keni R, Alexander A, Nayak PG, Mudgal J, Nandakumar K. COVID-19: Emergence, Spread, Possible Treatments, and Global Burden. *Front Public Health* (2020) 8:216. doi: 10.3389/fpubh.2020.00216
2. Coelho AC, García Díez J. Biological Risks and Laboratory-Acquired Infections: A Reality That Cannot be Ignored in Health Biotechnology. *Front Bioeng Biotechnol* (2015) 3:56. doi: 10.3389/fbioe.2015.00056
3. Brice DC, Diamond G. Antiviral Activities of Human Host Defense Peptides. *Curr Med Chem* (2020) 27:1420–43. doi: 10.2174/0929867326666190805151654
4. Yang PL. Call for Papers: Antiviral Therapeutics. *ACS Infect Dis* (2020) 6:1527–8. doi: 10.1021/acsinfecdis.0c00399
5. Lehrer RI, Barton A, Daher KA, Harwig SS, Ganz T, Selsted ME. Interaction of Human Defensins With Escherichia Coli. Mechanism of Bactericidal Activity. *J Clin Invest* (1989) 84:553–61. doi: 10.1172/JCI114198
6. Zasloff M. Magainins, a Class of Antimicrobial Peptides From Xenopus Skin: Isolation, Characterization of Two Active Forms, and Partial cDNA Sequence of a Precursor. *Proc Natl Acad Sci USA* (1987) 84:5449–53. doi: 10.1073/pnas.84.15.5449
7. Lalani S, Gew LT, Poh CL. Antiviral Peptides Against Enterovirus A71 Causing Hand, Foot and Mouth Disease. *Peptides* (2021) 136:170443. doi: 10.1016/j.peptides.2020.170443
8. Lei J, Sun L, Huang S, Zhu C, Li P, He J, et al. The Antimicrobial Peptides and Their Potential Clinical Applications. *Am J Transl Res* (2019) 11(7):3919–31.
9. Zasloff M. Antimicrobial Peptides of Multicellular Organisms. *Nature* (2002) 415:389–95. doi: 10.1038/415389a
10. Badani H, Garry RF, Wimley WC. Peptide Entry Inhibitors of Enveloped Viruses: The Importance of Interfacial Hydrophobicity. *Biochim Biophys Acta BBA - Biomembr* (2014) 1838:2180–97. doi: 10.1016/j.bbamem.2014.04.015
11. Hoffmann AR, Guha S, Wu E, Ghimire J, Wang Y, He J, et al. Broad-Spectrum Antiviral Entry Inhibition by Interfacially Active Peptides. *J Virol* (2020) 94:e01682–20. doi: 10.1128/JVI.01682-20
12. Wang G, Watson KM, Buckheit RW. Anti-Human Immunodeficiency Virus Type 1 Activities of Antimicrobial Peptides Derived From Human and Bovine Cathelicidins. *Antimicrob Agents Chemother* (2008) 52:3438–40. doi: 10.1128/AAC.00452-08
13. Cully M. Antiviral Therapy Targets Latent HSV Infections. *Nat Rev Drug Discov* (2021) 20:586–6. doi: 10.1038/d41573-021-00113-8
14. Yu Y, Cooper CL, Wang G, Morwitzer MJ, Kota K, Tran JP, et al. Engineered Human Cathelicidin Antimicrobial Peptides Inhibit Ebola Virus Infection. *iScience* (2020) 23:100999. doi: 10.1016/j.isci.2020.100999
15. Ghildiyal R, Gabrani R. Antiviral Therapeutics for Chikungunya Virus. *Expert Opin Ther Pat* (2020) 30:467–80. doi: 10.1080/13543776.2020.1751817
16. Chowdhury SM, Talukder SA, Khan AM, Afrin N, Ali MA, Islam R, et al. Antiviral Peptides as Promising Therapeutics Against SARS-CoV-2. *J Phys Chem B* (2020) 124:9785–92. doi: 10.1021/acs.jpcb.0c05621
17. Elnagdy S, AlKhazindar M. The Potential of Antimicrobial Peptides as an Antiviral Therapy Against COVID-19. *ACS Pharmacol Amp Transl Sci* (2020) 3:780–2. doi: 10.1021/acsptsci.0c00059
18. Maiti BK. Potential Role of Peptide-Based Antiviral Therapy Against SARS-CoV-2 Infection. *ACS Pharmacol Amp Transl Sci* (2020) 3:783–5. doi: 10.1021/acsptsci.0c00081
19. Culver EL, Travis SPL. How to Manage the Infectious Risk Under Anti-TNF in Inflammatory Bowel Disease. *Curr Drug Targets* (2010) 11:198–218. doi: 10.2174/138945010790310009
20. Sharma A, Bhomia M, Yeh T-J, Singh J, Maheshwari RK. Miltefosine Inhibits Chikungunya Virus Replication in Human Primary Dermal Fibroblasts. *F1000Research* (2018) 7:9. doi: 10.12688/f1000research.13242.1
21. Rey FA, Stiasny K, Heinz FX. Flavivirus Structural Heterogeneity: Implications for Cell Entry. *Curr Opin Virol* (2017) 24:132–9. doi: 10.1016/j.coviro.2017.06.009
22. Afreen N, Deeba F, Naqvi I, Shareef M, Ahmed A, Broor S, et al. Molecular Investigation of 2013 Dengue Fever Outbreak From Delhi, India. *PloS Curr* (2014) 6. doi: 10.1371/currents.outbreaks.0411252a8b82aa933f6540abb54a855f
23. Agarwal G, Gabrani R. Antiviral Peptides: Identification and Validation. *Int J Pept Res Ther* (2021) 27:149–68. doi: 10.1007/s10989-020-10072-0
24. Zakaryan H, Chilingaryan G, Arabyan E, Serobian A, Wang G. Natural Antimicrobial Peptides as a Source of New Antiviral Agents. *J Gen Virol* (2021) 102. doi: 10.1099/jgv.0.001661
25. Camargos VN, Foureaux G, Medeiros DC, da Silveira VT, Queiroz-Junior CM, Matosinhos ALB, et al. In-Depth Characterization of Congenital Zika Syndrome in Immunocompetent Mice: Antibody-Dependent Enhancement and an Antiviral Peptide Therapy. *EBioMedicine* (2019) 44:516–29. doi: 10.1016/j.ebiom.2019.05.014
26. Jackman JA, Costa VV, Park S, Real ALCV, Park JH, Cardozo PL, et al. Therapeutic Treatment of Zika Virus Infection Using a Brain-Penetrating Antiviral Peptide. *Nat Mater* (2018) 17:971–7. doi: 10.1038/s41563-018-0194-2
27. Jackman JA. Antiviral Peptide Engineering for Targeting Membrane-Enveloped Viruses: Recent Progress and Future Directions. *Biochim Biophys Acta BBA - Biomembr* (2022) 1864:183821. doi: 10.1016/j.bbamem.2021.183821
28. Kuroki A, Tay J, Lee GH, Yang YY. Broad-Spectrum Antiviral Peptides and Polymers. *Adv Healthc Mater* (2021) 10:2101113. doi: 10.1002/adhm.202101113
29. Moretta A, Scieuzo C, Petrone AM, Salvia R, Manniello MD, Franco A, et al. Antimicrobial Peptides: A New Hope in Biomedical and Pharmaceutical Fields. *Front Cell Infect Microbiol* (2021) 11:668632. doi: 10.3389/fcimb.2021.668632
30. Sampaio de Oliveira KB, Leite ML, Rodrigues GR, Duque HM, da Costa RA, Cunha VA, et al. Strategies for Recombinant Production of Antimicrobial Peptides With Pharmacological Potential. *Expert Rev Clin Pharmacol* (2020) 13:367–90. doi: 10.1080/17512433.2020.1764347
31. Schaduangrat N, Nantasenamat C, Prachayasittikul V, Shoombuatong W. ACPred: A Computational Tool for the Prediction and Analysis of Anticancer Peptides. *Molecules* (2019) 24:1973. doi: 10.3390/molecules24101973

32. Haines LR, Thomas JM, Jackson AM, Eyford BA, Razavi M, Watson CN, et al. Killing of Trypanosomatid Parasites by a Modified Bovine Host Defense Peptide, BMAP-18. *PloS Negl Trop Dis* (2009) 3:e373. doi: 10.1371/journal.pntd.0000373
33. Zhang M, Yu Y, Lian L, Li W, Ren J, Liang Y, et al. Functional Mechanism of Antimicrobial Peptide Bomidin and Its Safety for Macrobrachium Rosenbergii. *Probiotics Antimicrob Proteins* (2022) 14:169–79. doi: 10.1007/s12602-021-09857-6
34. He M, Zhang H, Li Y, Wang G, Tang B, Zhao J, et al. Cathelicidin-Derived Antimicrobial Peptides Inhibit Zika Virus Through Direct Inactivation and Interferon Pathway. *Front Immunol* (2018) 9:722. doi: 10.3389/fimmu.2018.00722
35. Brooks BR, Brooks CL, Mackerell AD, Nilsson L, Petrella RJ, Roux B, et al. CHARMM: The Biomolecular Simulation Program. *J Comput Chem* (2009) 30:1545–614. doi: 10.1002/jcc.21287
36. Hess B, Kutzner C, van der Spoel D, Lindahl E. GROMACS 4: Algorithms for Highly Efficient, Load-Balanced, and Scalable Molecular Simulation. *J Chem Theory Comput* (2008) 4:435–47. doi: 10.1021/ct700301q
37. Jo S, Lim JB, Klauda JB, Im W. CHARMM-GUI Membrane Builder for Mixed Bilayers and Its Application to Yeast Membranes. *Biophys J* (2009) 97:50–8. doi: 10.1016/j.bpj.2009.04.013
38. Wu EL, Cheng X, Jo S, Rui H, Song KC, Dávila-Contreras EM, et al. CHARMM-GUI Membrane Builder Toward Realistic Biological Membrane Simulations. *J Comput Chem* (2014) 35:1997–2004. doi: 10.1002/jcc.23702
39. Wiegand I, Hilpert K, Hancock REW. Agar and Broth Dilution Methods to Determine the Minimal Inhibitory Concentration (MIC) of Antimicrobial Substances. *Nat Protoc* (2008) 3:163–75. doi: 10.1038/nprot.2007.521
40. Reddy T, Sansom MSP. The Role of the Membrane in the Structure and Biophysical Robustness of the Dengue Virion Envelope. *Structure* (2016) 24:375–82. doi: 10.1016/j.str.2015.12.011
41. Theken KN, Tang SY, Sengupta S, FitzGerald GA. The Roles of Lipids in SARS-CoV-2 Viral Replication and the Host Immune Response. *J Lipid Res* (2021) 62:100129. doi: 10.1016/j.jlr.2021.100129
42. van Genderen IL, Brandimarti R, Torrisi MR, Campadelli G, van Meer G. The Phospholipid Composition of Extracellular Herpes Simplex Virions Differs From That of Host Cell Nuclei. *Virology* (1994) 200:831–6. doi: 10.1006/viro.1994.1252
43. Teixeira V, Feio MJ, Bastos M. Role of Lipids in the Interaction of Antimicrobial Peptides With Membranes. *Prog Lipid Res* (2012) 51:149–77. doi: 10.1016/j.plipres.2011.12.005
44. Baumann A, Kiener MS, Haigh B, Perreten V, Summerfield A. Differential Ability of Bovine Antimicrobial Cathelicidins to Mediate Nucleic Acid Sensing by Epithelial Cells. *Front Immunol* (2017) 8:59. doi: 10.3389/fimmu.2017.00059
45. Huan Y, Kong Q, Mou H, Yi H. Antimicrobial Peptides: Classification, Design, Application and Research Progress in Multiple Fields. *Front Microbiol* (2020) 11:582779. doi: 10.3389/fmicb.2020.582779
46. Romero-Brey I, Bartenschlager R. Endoplasmic Reticulum: The Favorite Intracellular Niche for Viral Replication and Assembly. *Viruses* (2016) 8:160. doi: 10.3390/v8060160
47. Yoon BK, Jeon W-Y, Sut TN, Cho N-J, Jackman JA. Stopping Membrane-Enveloped Viruses With Nanotechnology Strategies: Toward Antiviral Drug Development and Pandemic Preparedness. *ACS Nano* (2021) 15:125–48. doi: 10.1021/acsnano.0c07489
48. Ivanova PT, Myers DS, Milne SB, McClaren JL, Thomas PG, Brown HA. Lipid Composition of the Viral Envelope of Three Strains of Influenza Virus—Not All Viruses Are Created Equal. *ACS Infect Dis* (2015) 1:435–42. doi: 10.1021/acsinfecdis.5b00040
49. Jackman JA, Shi P-Y, Cho N-J. Targeting the Achilles Heel of Mosquito-Borne Viruses for Antiviral Therapy. *ACS Infect Dis* (2019) 5:4–8. doi: 10.1021/acsinfecdis.8b00286
50. van Meer G, de Kroon AIPM. Lipid Map of the Mammalian Cell. *J Cell Sci* (2011) 124:5–8. doi: 10.1242/jcs.071233
51. Vigant F, Santos NC, Lee B. Broad-Spectrum Antivirals Against Viral Fusion. *Nat Rev Microbiol* (2015) 13:426–37. doi: 10.1038/nrmicro3475
52. Na M, Kmp R, Nt S. Peptide-Based Antiviral Drugs. *Antivir Drug Discov Dev* (2021) 1322:261–84. doi: 10.1007/978-981-16-0267-2_10
53. Bhardwaj G, Mulligan VK, Bahl CD, Gilmore JM, Harvey PJ, Cheneval O, et al. Accurate *De Novo* Design of Hyperstable Constrained Peptides. *Nature* (2016) 538:329–35. doi: 10.1038/nature19791

Conflict of Interest: Author YW was employed by the company Jiangsu Genloci Biotech Inc.

The remaining authors declare that the research was conducted in the absence of any commercial or financial relationships that could be construed as a potential conflict of interest.

Publisher's Note: All claims expressed in this article are solely those of the authors and do not necessarily represent those of their affiliated organizations, or those of the publisher, the editors and the reviewers. Any product that may be evaluated in this article, or claim that may be made by its manufacturer, is not guaranteed or endorsed by the publisher.

frontiers | Frontiers in Immunology

ORIGINAL RESEARCH
published: 09 June 2022
doi: 10.3389/fimmu.2022.887219

Meta-Analysis of Human Antibodies Against *Plasmodium falciparum* Variable Surface and Merozoite Stage Antigens

Eizo Takashima[1†], Bernard N. Kanoi[2†], Hikaru Nagaoka[1], Masayuki Morita[1], Ifra Hassan[1], Nirianne M. Q. Palacpac[3], Thomas G. Egwang[4], Toshihiro Horii[3], Jesse Gitaka[2] and Takafumi Tsuboi[5*]*

[1] Division of Malaria Research, Proteo-Science Center, Ehime University, Matsuyama, Japan, [2] Centre for Research in Infectious Diseases, Directorate of Research and Innovation, Mount Kenya University, Thika, Kenya, [3] Department of Malaria Vaccine Development, Research Institute for Microbial Diseases, Osaka University, Suita, Japan, [4] Med Biotech Laboratories, Kampala, Uganda, [5] Division of Cell-Free Sciences, Proteo-Science Center, Ehime University, Matsuyama, Japan

OPEN ACCESS

Edited by:
Denise L. Doolan,
James Cook University, Australia

Reviewed by:
Virander Singh Chauhan,
International Centre for Genetic Engineering and Biotechnology, India
Yaw Aniweh,
University of Ghana, Ghana

***Correspondence:**
Eizo Takashima
takashima.eizo.mz@ehime-u.ac.jp
Takafumi Tsuboi
tsuboi.takafumi.mb@ehime-u.ac.jp

[†]These authors have contributed equally to this work

Specialty section:
This article was submitted to Vaccines and Molecular Therapeutics, a section of the journal Frontiers in Immunology

Received: 01 March 2022
Accepted: 11 May 2022
Published: 09 June 2022

Citation:
Takashima E, Kanoi BN, Nagaoka H, Morita M, Hassan I, Palacpac NMQ, Egwang TG, Horii T, Gitaka J and Tsuboi T (2022) Meta-Analysis of Human Antibodies Against Plasmodium falciparum Variable Surface and Merozoite Stage Antigens. Front. Immunol. 13:887219. doi: 10.3389/fimmu.2022.887219

Concerted efforts to fight malaria have caused significant reductions in global malaria cases and mortality. Sustaining this will be critical to avoid rebound and outbreaks of seasonal malaria. Identifying predictive attributes that define clinical malaria will be key to guide development of second-generation tools to fight malaria. Broadly reactive antibodies against variable surface antigens that are expressed on the surface of infected erythrocytes and merozoites stage antigens are targets of naturally acquired immunity and prime candidates for anti-malaria therapeutics and vaccines. However, predicting the relationship between the antigen-specific antibodies and protection from clinical malaria remains unresolved. Here, we used new datasets and multiple approaches combined with re-analysis of our previous data to assess the multi-dimensional and complex relationship between antibody responses and clinical malaria outcomes. We observed 22 antigens (17 PfEMP1 domains, 3 RIFIN family members, merozoite surface protein 3 (PF3D7_1035400), and merozoites-associated armadillo repeats protein (PF3D7_1035900) that were selected across three different clinical malaria definitions (1,000/2,500/5,000 parasites/μl plus fever). In addition, Principal Components Analysis (PCA) indicated that the first three components (Dim1, Dim2 and Dim3 with eigenvalues of 306, 48, and 29, respectively) accounted for 66.1% of the total variations seen. Specifically, the Dim1, Dim2 and Dim3 explained 52.8%, 8.2% and 5% of variability, respectively. We further observed a significant relationship between the first component scores and age with antibodies to PfEMP1 domains being the key contributing variables. This is consistent with a recent proposal suggesting that there is an ordered acquisition of antibodies targeting PfEMP1 proteins. Thus, although limited, and further work on the significance of the selected antigens will be required, these approaches may provide insights for identification of drivers of naturally acquired protective immunity as well as guide development of additional tools for malaria elimination and eradication.

Keywords: ***Plasmodium falciparum*, variable surface antigens, PfEMP1, RIFIN, malaria immunity, PCA**

INTRODUCTION

There is a common agreement that sustainable elimination of malaria will require multiple approaches (1). The need to develop efficacious vaccines remains an integral component of this fight, supported by strong evidence showing that naturally acquired protective immunity against *Plasmodium falciparum* is acquired among individuals living in malaria-endemic regions (2, 3). Specifically, antibody-mediated immunity against *P. falciparum* malaria is acquired with age and repeated exposure (2). This immunity mainly targets antigens of the parasite asexual blood-stages; however, the complete repertoire of the specific targets has not been unequivocally defined. Based on this understanding, several approaches are being applied to select the most appropriate vaccine candidates.

Focused and unbiased immuno-epidemiology studies have reported, identified, or characterized most of the leading candidate vaccines in the developmental pipeline. Most recently, high-throughput immunoscreening to simultaneously investigate proteins as potential vaccine candidates or as immune correlates of protection has been a major strategy (4–7) with antigens such as PfRh5, CelTOS, MSP3, and GLURP (7–9) being identified. These antigens are in the vaccine development pipeline. However, most data, to date has limited our ability to prioritize antigens, enrich the pool of vaccine candidates, and link immunological data with clinical outcomes.

Over the years, we have developed and optimized a robust and high-throughput eukaryotic wheat germ cell-free protein synthesis system (WGCFS) coupled with a homogeneous high-throughput AlphaScreen platform for antibody profiling and mechanistic characterization of proteins that have a role in merozoites invasion of erythrocytes, or induction of protective immunity in malaria naturally exposed individuals (9–11). Leveraging this approach, we have prioritized, from hundreds of parasite proteins expressed in multiple parasite stages, several *P. falciparum* antigens for inclusion in the vaccine development pipeline. Recently, a total of 1,827 recombinant proteins drawn from different *P. falciparum* stages (sporozoites, merozoites, trophozoites, schizonts, and gametocytes) were used to probe individual serum samples obtained from residents of a malaria endemic region in Uganda. Protein immunoreactivity was observed at 54% with 128 antigens inducing antibody responses that significantly associated with reduced risk to clinical malaria episodes (defined as fever ≥37.5 ˚C and asexual parasitemia of ≥2,500/μl of blood) during a 12-months follow-up period. Of these antigens, 53 were down-selected as the most viable vaccine candidates by virtue of having a signal peptide (SP) and/or transmembrane domain (TM) (4, 5, 7) suggesting their putative expression on the surface of merozoites and/or sporozoites, or on the infected erythrocytes. Similarly, by focusing on parasite protein families that are exported to the surface of infected red blood cells such as erythrocyte membrane protein 1 (PfEMP1), repetitive interspersed family (RIFIN) proteins, subtelomeric variable open reading frame (STEVOR), and surface-associated interspersed gene family (SURFIN) (12), we observed that more than 95% of the antigens were reactive with serum samples obtained from Uganda (11, 13). These studies demonstrated that the repertoire of potentially protective antigens that correlated with protective immunity against clinical malaria is wider than thought and offers multiple options for the identification of malaria vaccine candidates, aside from those that are currently under clinical or pre-clinical evaluation (9).

Previous studies with our follow-up cohort in Uganda (14) and similar immunoepidemiology studies (4, 7, 15) have largely focused on a single definition of clinical malaria based on the incidence within a specified geographic area. However, ongoing field trials/studies further strengthen the argument that clinical definitions of malaria are also influenced by factors that are related to host immunity (age, transmission, co-infections, etc), and parasitaemia accompanied by symptoms do not necessarily imply clinical malaria especially in endemic areas (16–19). Moreover, malaria transmission heterogeneity (ranging from high, stable, and declining), as well as absence of robust correlates of protection highlights the complexity involved in evaluating new and future interventions. In this study, to obtain a wider picture, and considering the declining malaria transmission in endemic areas, we sought to re-evaluate the previously published data together with new data sets generated against merozoites stage antigens that are considered potential targets of protective immunity, to assess the relationship between antibody responses and clinical malaria outcomes categorized by different clinical malaria definitions. Further, using the Principal Component Analysis (PCA) for the antibody responses we highlight antigens that are robustly identified by different protein based global immunological screens.

MATERIALS AND METHODS

Study Setting and Ethical Statement

Serum samples used in this study were obtained from residents of Lira Municipality, Northern Uganda, that were taking part in a prospective study of 66 non-vaccinated participants aged 6–20 years. The region was characterized by high malaria transmission (14, 20–23). Study protocols and permission to use the samples were approved by the Institutional Research and Ethics Committee of Lacor Hospital (LHIREC 023/09/13), Uganda National Council for Science and Technology (HS1403) in Uganda; and Ethics Committees of the Research Institute for Microbial Diseases, Osaka University, and Ehime University, Japan. Written informed consents were obtained from all participants and/or their parents or guardians before the study. Aside from parental consent, assent was obtained from children aged 8-17 years. The study was conducted in compliance with the International Conference on Harmonisation Good Clinical Practices guidelines and the Declaration of Helsinki.

Production of a *P. falciparum* Parasite Protein Library

The comprehensive protein library consisted of 579 proteins representing the asexual erythrocytic stages of *P. falciparum* (**Table S1**). Newly synthesized asexual blood-stage proteins

(BSP: n = 46) selected from our previous study based on their significant immunoreactivities (9) were asssessd together with data from previously published libraries of proteins derived from cysteine-rich interdomain regions of *P. falciparum* erythrocyte membrane protein 1 (PfEMP1) (CIDR: n = 108), Duffy binding–like domains of PfEMP1 (DBL: n = 163) (11), repetitive interspersed family proteins (RIFIN: n = 176), subtelomeric variable open reading frame proteins (STEVOR: n = 53), and surface-associated interspersed gene family proteins (SURFIN: n = 33) (13). All proteins were synthesized using the optimized WGCFS protocol and assayed alongside biotinylated rabbit IgG standard for plate-to-plate and day-to-day normalization (11).

All the proteins were expressed from sequences derived from the *P. falciparum* 3D7 reference strain. Briefly, the DNA sequences representing the ectodomains while excluding the SP and/or TM domains were amplified by using high fidelity PrimeSTAR Max DNA polymerase (Takara Bio, Kusatsu, Japan) and cloned into the WGCFS dedicated pEU plasmid vector (CellFree Sciences, Matsuyama, Japan) using the In-Fusion HD Cloning Kit (Takara Bio). A semi-automated GenDecoder1000 robotic protein synthesizer (CellFree Sciences) was used for *in vitro* transcription and mono-biotinylated recombinant protein synthesis with WGCFS.

Human Antibodies Quantification by AlphaScreen

We used the AlphaScreen platform to assess serum antibodies in malaria exposed individuals as described (9, 24). The system exploits the existence of mono-biotinylation on each recombinant *P. falciparum* protein. Specifically, the proteins were dispensed into a 384-well OptiPlate using a JANUS Automated Workstation dispenser (PerkinElmer, Waltham, MA) and mixed with 10 µl of 4000-fold diluted sera in reaction buffer (100 mM Tris-HCl [pH 8.0], 0.01% [v/v] Tween-20, and 0.1% [w/v] bovine serum albumin). After 30 min incubation at 26°C, 10 µl of detection mixture containing streptavidin-coated donor beads (PerkinElmer) and protein G (Thermo Scientific, Waltham, MA) conjugated acceptor beads (PerkinElmer) were added, to make a final concentration of 12 µg/ml for both beads. The plate was then incubated in the dark for 1 hr at 26°C to allow optimal binding of the donor and acceptor beads to the biotinylated protein and human antibody, respectively. Luminescence emitted by acceptor beads upon excitation of the donor beads was detected using an EnVision plate reader (PerkinElmer) and captured as AlphaScreen Counts (ASC). To account for day-to-day and plate-to-plate assay variability, serially diluted biotinylated rabbit IgG (PerkinElmer) was included in each plate, and subsequently used to generate a 5-parameter logistic standardization curve. The assays were randomized to minimize experimental bias.

Statistical Analysis

All data analyses were performed using R software (Version 4.0.1, R Foundation for Statistical Computing). As previously described, protein seropositivity cut off point to human sera was set at half the lowest non-negative ASC value from that of the assayed samples (25), and a protein was considered immunoreactive if more than 10% of the volunteers had ASC levels above the seropositivity cut-off.

For survival analysis, the time-to-first clinical malaria episode from baseline (defined as the time from first sampling when all enrolled individuals were blood-smear negative) was used as the endpoint (14). For detailed analyses, three different definitions for clinical malaria were used: fever ≥37.5°C and asexual parasitemia of (i) ≥1,000/µl, (ii) ≥2,500/µl, and (iii) ≥5,000/µl blood, with no sign(s) of complicated disease. Although some children may have multiple parasitic or febrile malaria episodes as defined above, only the first febrile episode was considered in the analysis. To assess whether the presence of antigen-specific antibodies was associated with overall survival, Cox proportional hazards model was used to calculate hazard ratios (HR) and 95% confidence intervals (CIs) between 'High Responders' (individuals with an ASC value above the population median for that antigen) or 'Low Responders' (7, 9, 26, 27). Potential protective efficacy (PPE) relative to different definitions of malaria was computed as 1- hazard ratio (PPE% = (1- HR) × 100%). For multivariate survival analysis, data was adjusted for bednet use and age as a categorical variable (6-10 years, 11-15 years, and 16-20 years).

To simultaneously evaluate antibodies developed in response to different proteins among patients with and without clinical malaria, we used Principal Component Analysis (PCA). PCA essentially reduces the dimensionality of antibody responses by generating fewer composite variables to capture as much variance in that dataset. The model then assesses and compares the relationship between the scores obtained for each of these components per subject. To generate the global antigen derived principal components, all immunoreactive antigens were used without prespecified groupings (BSP, PfEMP1-CIDR, PfEMP1-DBL, RIFIN, STEVOR, and SURFIN) to determine group-based variance. To identify PCA derived clusters of antibody responses that were involved in protection against clinical malaria, we selected principal components where at least three variables were loaded, and the eigenvalue was greater than 2 or the proportion of variance explained was >5% (28). Individuals displaying outlier PCA coordinates were excluded. Individual contributions to the PCA were assessed in association with age, gender, and clinical malaria outcome.

RESULTS

Seroprevalence of Antibodies to Different *P. falciparum* Proteins

We assessed the human antibody reactivities to the protein library (**Table S1**) obtained from the samples (n = 66) taken at the beginning of the study, prior to the rainy season. All the blood-stage proteins (BSP) were newly measured in this study and they were all immunoreactive with seroprevalence above the threshold cut-off point of 10%. Seroprevalence of the other protein groups was reported previously (11, 13). Briefly, 99%

immunoreactivity was observed for PfEMP1 (CIDR and DBL), RIFIN, STEVORs, and SURFINs (11, 13) (**Figure 1**). The seroprevalence varied widely among the protein groups/families: BSP (16-100%), CIDR domains (22-92%), DBL domains (12-100%), RIFIN (10-93%), STEVORs (12-83%) and SURFINs (21-100%) (Kruskal-Wallis Test, $p = 0.001$) with STEVORs having significantly lower median levels, and SURFINs the highest compared to other groups. Although this may represent cross-reactivity within the assessed families (12), a strong Spearman's rank correlation between antibody levels measured in the samples and across different groups, as shown by the correlation matrix (**Figure S1**) suggests that antibodies to different antigens are co-acquired in this population.

Relationship Between Antibodies and Incidence of Febrile Malaria

To gain further insight into the relationship between individual protein reactivity and clinical malaria outcomes, we determined the hazard ratios based on time-to-event using three parasite thresholds for clinical malaria in univariate analysis. Based on the lower threshold of 1,000 parasites/μl blood, antigen-specific antibodies to 43 proteins associated with protection. This changed to 26 and 32 proteins when assessed at 2,500 parasites/μl blood and a higher threshold of 5,000 parasites/μl blood, respectively (**Figure 2A**). In the multivariable-adjusted survival analysis, the correlation between antibodies and the risk of febrile malaria was generally reduced. Twenty-two antigens were selected across the three definitions (**Table 1**) by the unadjusted analysis. The 22 antigens included 17 PfEMP1 domains, 3 RIFIN family members, merozoite surface protein 3 (PF3D7_1035400), and merozoite-associated armadillo repeats protein (PF3D7_1035900). The number of antigens that remained significantly associated with reduced risk of clinical malaria after adjusting for age (24) and bed-net use was 2 for 1,000 parasites/μl blood, 1 for 2,500 parasites/μl blood, and 2 antigens for 5,000 parasites/μl blood (summarized in **Figure 2B**).

Principal Component Analysis of the Antibody Responses

Since the antibody responses and the corresponding semi-protective immunity involve numerous antibodies acting simultaneously but targeting different proteins (26, 29), we performed PCA with all the proteins assayed and with different protein families to capture the effects of all antibodies in a single analysis and extract important associations. The analysis indicated that the first three components (with eigenvalues of 306, 48, and 29, respectively) accounted for 66.1% of the total variation in these data (**Figure 3A**). The analysis showed that the participants who did not experience clinical malaria were more dispersed while those with malaria episodes clustered together (**Figures 3B–D**). The first component (Dim1) explained 52.8% of variability and gave the greatest weights to antibodies against PfEMP1 domains [PF3D7_1240300_DBLβ8 (contributing 0.3), PF3D7_0632500_DBLe2 (0.3), PF3D7_0200100_CIDRα2.2 (0.29), PF3D7_1000300 (0.29) and PF3D7_1373500_CIDRβ6 (0.28)] (**Table 2**; **Figure S2**), while principal component 2 (Dim2) was mainly reflective of anti-PF3D7_1372800 (0.78), PF3D7_0401400 (0.77), PF3D7_0632100 (0.74), PF3D7_0500400 (0.72), and PF3D7_0425900 (0.67) and accounted for 8.2% of the variation. The third component (Dim3), which explained slightly above 5.0% of data variability, gave the strongest weight to antibodies against PF3D7_1200100_DBLα0.9 (2.44), PF3D7_1150400_CIDRγ2 (2.33), PF3D7_0712300_CIDRα0.1 (2.21), PF3D7_0400400_DBLδ1 (2.07), and PF3D7_1200400_DBLγ14 (1.86) (**Table 2**; **Figure S2**). These findings suggest that PfEMP1 domains are major

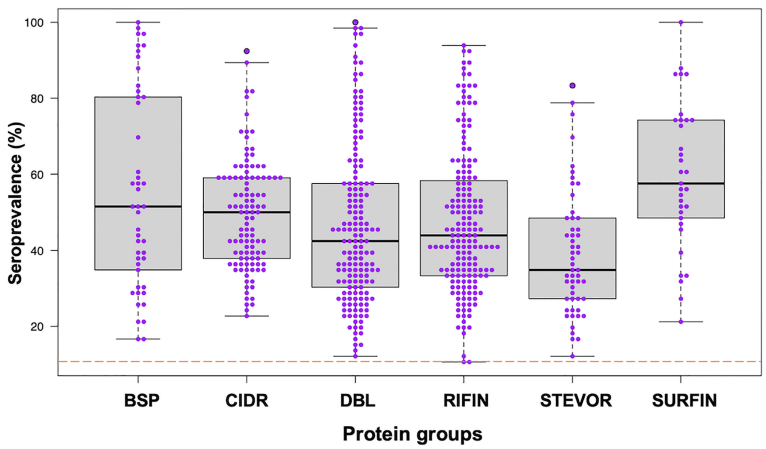

FIGURE 1 | Seroprevalence of antibodies to different *P. falciparum* proteins. Antibodies immunoreactive to BSP (blood-stage proteins), CIDR (cysteine-rich interdomain regions of PfEMP1), DBL (Duffy binding–like domains of PfEMP1), RIFIN (repetitive interspersed family proteins), STEVOR (subtelomeric variable open reading frame proteins), and SURFIN (surface-associated interspersed gene family proteins) are shown. Box plots illustrate medians with 25th and 75th and whiskers for 10th and 90th percentiles with the horizontal line in each group denoting the overall median per group. The dashed red horizontal line indicates 10% seroprevalence that was set as protein immunoreactivity cut-off point. The data in BSP were newly measured in this study. The data in other protein groups, CIDR and DBL from PfEMP1, RIFIN, STEVOR and SURFIN were reported previously (11, 13).

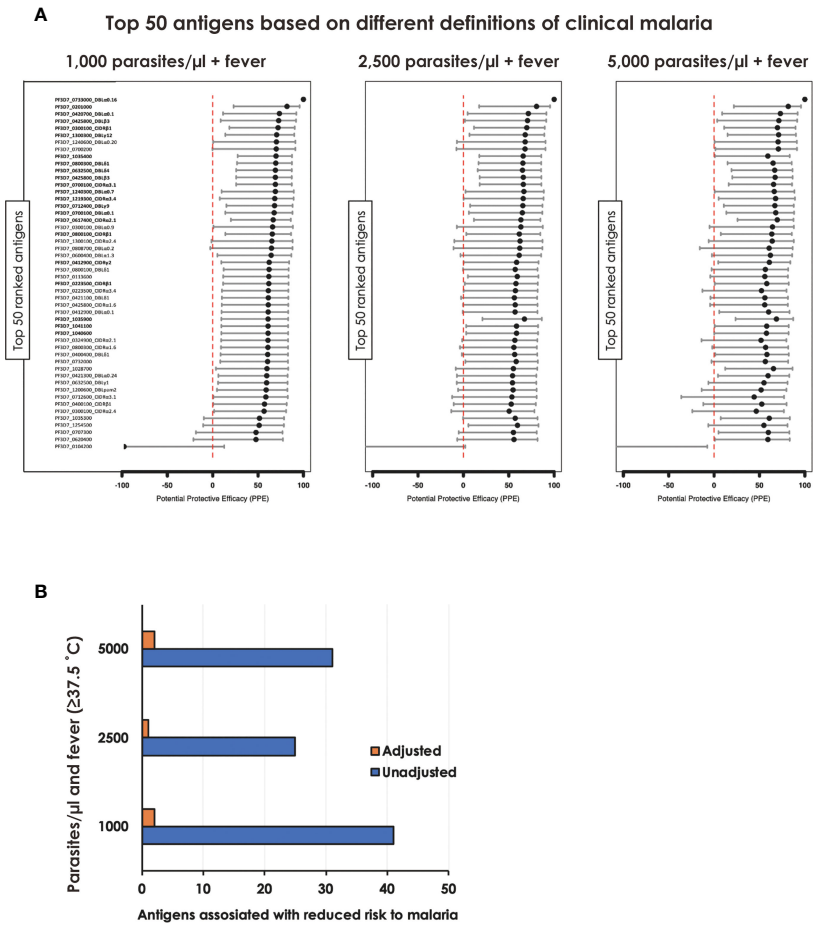

FIGURE 2 | Associations between antibody levels and risk of *P. falciparum* febrile malaria. Complete list of the data for potential protective efficacy (PPE), and 95% confidence interval, is provided in **Table 1**. **(A)** Unadjusted association between antibody levels and risk of *P. falciparum* febrile malaria for each of the antigens tested in the cohort. The top-50 antigens are ranked - top to bottom - by the strength of their PPE. PPE for each antigen was derived from the hazard ratio (HR) calculated by the unadjusted Cox-regression hazard model analysis (comparing children with high vs. low antibody responses). Black dots indicate the percentage protection, and error bars indicate the 95% confidence interval. The red vertical line represents a PPE of 0% (i.e. HR = 1). The 22 cross-selected antigens are labeled in bold. **(B)** The bars represent the number of antigens that associated with protection to clinical malaria in univariate and multivariate analysis. Red bar: Adjusted, Blue bar: Unadjusted.

determinants of the variability observed in individuals experiencing clinical malaria and are consistent with the findings of the Cox analysis model (**Figure 2A**). Specifically, the PF3D7_0425800_DBLβ3 was the only domain selected by the multi-approach analysis and appeared as well in the top 50 antigens by PCA.

When assessing the representation of antibody responses to different protein groups based on Dim1 and Dim2, we observed that most clinical malaria cases clustered together irrespective of the protein group or family (**Figure S3**); and both components are the major drivers of the observed variability. This was again in agreement with the observation in Cox analysis which suggested that multiple, and probably specific antigens may be associated with protective immunity (**Figure 2A**).

We then assessed the relationship between the scores obtained from PCA on one hand and age and malaria clinical outcome to identify patterns of specific antibody responses that could be important in malaria. Age was significantly positively correlated with the scores of the first principal component (Dim1, R = 0.5; P <0.001) but not with Dim2 (R = 0.04, P = 0.8) or Dim3 (R = -0.05, P = 0.7) (**Figure 4**). This, further strengthens the observation on previous studies that age is an important factor on naturally acquired immunity (2).

DISCUSSION

Here, using antibody response data from our previous publications on multi-gene families (9, 11, 13) plus newly generated data from merozoite surface antigens, and expanding the analysis to include wider definition of clinical malaria (categorized according to different parasitemia thresholds), we re-assessed antibody responses in a malaria exposed

TABLE 1 | Associations between antibody levels and risk of *P. falciparum* clinical malaria.

		Unadjusted PPE (1,000 parasites/μl)				Unadjusted PPE (2,500 parasites/μl)				Unadjusted PPE (5,000 parasites/μl)			
Product ID	GeneID*	PPE %	Lower 95%CI	Upper 95%CI	P value**	PPE %	Lower 95%CI	Upper 95%CI	P value**	PPE %	Lower 95%CI	Upper 95%CI	P value**
DC150	**PF3D7_0733000_DBLα0.16**	1.000	0.990	1.000	0.001	1.000	0.990	1.000	0.001	1.000	0.990	1.000	0.001
RS23	**PF3D7_0201000**	0.819	0.230	0.957	0.021	0.806	0.174	0.954	0.027	0.817	0.218	0.957	0.022
DC54	**PF3D7_0420700_DBLα0.1**	0.735	0.114	0.921	0.031	0.716	0.046	0.915	0.042	0.730	0.089	0.920	0.035
DC72	**PF3D7_0425800_DBLβ3**	0.727	0.087	0.918	0.035	0.707	0.017	0.913	0.047	0.714	0.035	0.915	0.044
DC21	**PF3D7_0300100_CIDRβ1**	0.720	0.184	0.904	0.020	0.698	0.117	0.897	0.029	0.698	0.111	0.898	0.030
DC266	**PF3D7_1300300_DBLγ12**	0.705	0.139	0.899	0.026	0.681	0.066	0.891	0.037	0.711	0.148	0.902	0.024
DC251	PF3D7_1240600_DBLα0.20	0.702	0.004	0.911	0.049	0.680	(0.072)	0.905	0.065	0.705	0.005	0.913	0.049
RS89	PF3D7_0700200	0.700	(0.002)	0.910	0.050	0.679	(0.076)	0.904	0.066	0.708	0.015	0.914	0.047
5400	**PF3D7_1035400**	0.698	0.275	0.874	0.007	0.658	0.175	0.859	0.017	0.592	0.009	0.832	0.048
DC169	**PF3D7_0800300_DBLδ1**	0.695	0.268	0.873	0.008	0.655	0.167	0.857	0.018	0.650	0.148	0.856	0.021
DC110	**PF3D7_0632500_DBLδ4**	0.691	0.259	0.871	0.008	0.651	0.157	0.855	0.019	0.668	0.191	0.864	0.015
DC73	**PF3D7_0425800_DBLβ3**	0.691	0.259	0.871	0.009	0.660	0.179	0.859	0.016	0.672	0.201	0.866	0.014
DC119	**PF3D7_0700100_CIDRα3.1**	0.691	0.259	0.871	0.009	0.660	0.179	0.859	0.016	0.655	0.160	0.858	0.019
DC242	**PF3D7_1240300_DBLα0.7**	0.691	0.098	0.894	0.032	0.667	0.024	0.886	0.045	0.663	0.007	0.885	0.049
DC239	**PF3D7_1219300_CIDRα3.4**	0.684	0.078	0.891	0.035	0.659	0.001	0.883	0.050	0.678	0.051	0.890	0.040
DC137	**PF3D7_0712400_DBLγ9**	0.681	0.151	0.881	0.022	0.655	0.074	0.871	0.035	0.669	0.108	0.878	0.029
DC118	**PF3D7_0700100_DBLα0.1**	0.677	0.139	0.879	0.024	0.650	0.061	0.869	0.037	0.679	0.135	0.881	0.025
DC102	**PF3D7_0617400_CIDRα2.1**	0.666	0.200	0.861	0.014	0.634	0.115	0.848	0.026	0.696	0.259	0.875	0.009
DC18	PF3D7_0300100_DBLα0.9	0.660	0.008	0.883	0.048	0.633	(0.073)	0.875	0.067	0.643	(0.050)	0.879	0.061
DC158	**PF3D7_0800100_CIDRβ1**	0.657	0.140	0.863	0.023	0.616	0.032	0.848	0.043	0.636	0.073	0.857	0.034
DC260	PF3D7_1300100_CIDRα2.4	0.652	(0.014)	0.881	0.053	0.624	(0.100)	0.872	0.074	0.641	(0.059)	0.878	0.063
DC175	PF3D7_0808700_DBLα0.2	0.648	(0.027)	0.879	0.056	0.621	(0.110)	0.870	0.077	0.607	(0.158)	0.866	0.090
DC99	PF3D7_0600400_DBLα1.3	0.644	0.051	0.867	0.039	0.615	(0.032)	0.856	0.058	0.621	(0.024)	0.860	0.056
DC49	**PF3D7_0412900_CIDRγ2**	0.622	0.094	0.842	0.029	0.586	0.001	0.829	0.050	0.609	0.045	0.840	0.039
DC157	PF3D7_0800100_DBLδ1	0.621	0.121	0.837	0.024	0.571	(0.004)	0.816	0.051	0.565	(0.028)	0.816	0.058
RS264	PF3D7_0113600	0.619	0.115	0.836	0.025	0.594	0.049	0.826	0.038	0.559	(0.041)	0.813	0.062
DC17	**PF3D7_0223500_CIDRβ1**	0.618	0.114	0.835	0.025	0.579	0.015	0.820	0.046	0.580	0.008	0.822	0.048
DC15	PF3D7_0223500_CIDRα3.4	0.613	0.102	0.833	0.027	0.573	0.002	0.817	0.050	0.522	(0.129)	0.798	0.092
DC64	PF3D7_0421100_DBLδ1	0.613	0.102	0.833	0.027	0.561	(0.026)	0.812	0.057	0.559	(0.040)	0.813	0.061
DC71	PF3D7_0425800_CIDRα1.6	0.612	0.101	0.833	0.027	0.571	(0.004)	0.816	0.051	0.558	(0.044)	0.813	0.063
DC46	PF3D7_0412900_DBLα0.1	0.611	0.097	0.832	0.028	0.569	(0.007)	0.816	0.052	0.601	0.057	0.831	0.036
WE35	**PF3D7_1035900**	0.610	0.095	0.832	0.028	0.673	0.209	0.864	0.013	0.687	0.236	0.872	0.011
RS163	**PF3D7_1041100**	0.610	0.095	0.832	0.028	0.585	0.031	0.823	0.042	0.579	0.007	0.822	0.048
RS158	**PF3D7_1040600**	0.610	0.095	0.832	0.028	0.585	0.031	0.823	0.042	0.577	0.001	0.821	0.050
DC23	PF3D7_0324900_CIDRα2.1	0.609	0.093	0.831	0.029	0.567	(0.013)	0.815	0.053	0.517	(0.139)	0.795	0.097
DC166	PF3D7_0800300_CIDRα1.6	0.608	0.092	0.831	0.029	0.556	(0.038)	0.810	0.061	0.568	(0.021)	0.817	0.056
DC36	PF3D7_0400400_DBLδ1	0.606	0.086	0.830	0.030	0.565	(0.018)	0.814	0.055	0.582	0.013	0.823	0.047
RS99	PF3D7_0732000	0.605	0.084	0.830	0.030	0.581	0.021	0.821	0.045	0.564	(0.029)	0.816	0.058
WE29	PF3D7_1028700	0.598	0.036	0.832	0.041	0.551	(0.085)	0.814	0.075	0.654	0.122	0.864	0.026
DC66	PF3D7_0421300_DBLα0.24	0.595	0.062	0.826	0.035	0.542	(0.072)	0.804	0.072	0.595	0.043	0.828	0.039
DC109	PF3D7_0632500_DBLγ1	0.594	0.059	0.825	0.036	0.541	(0.074)	0.804	0.073	0.550	(0.064)	0.809	0.069
DC232	PF3D7_1200600_DBLpam2	0.589	0.047	0.823	0.038	0.547	(0.058)	0.806	0.067	0.518	(0.137)	0.796	0.096
DC139	PF3D7_0712600_CIDRα3.1	0.586	0.007	0.827	0.048	0.534	(0.124)	0.807	0.089	0.441	(0.362)	0.771	0.200
DC30	PF3D7_0400100_CIDRβ1	0.571	0.005	0.815	0.049	0.527	(0.106)	0.798	0.084	0.525	(0.120)	0.799	0.089
DC19	PF3D7_0300100_CIDRα2.4	0.566	0.016	0.808	0.046	0.504	(0.134)	0.783	0.096	0.465	(0.240)	0.769	0.145
WE50.1	PF3D7_1035300	0.515	(0.097)	0.786	0.082	0.571	(0.004)	0.817	0.051	0.608	0.073	0.834	0.033
RS189	PF3D7_1254500	0.512	(0.105)	0.784	0.085	0.596	0.055	0.827	0.037	0.549	(0.065)	0.809	0.069
WE48	PF3D7_0707300	0.477	(0.185)	0.769	0.120	0.551	(0.051)	0.808	0.065	0.598	0.048	0.830	0.038
MSP10_1-1	PF3D7_0620400	0.477	(0.214)	0.774	0.131	0.558	(0.068)	0.817	0.070	0.593	0.009	0.833	0.048
WE27	PF3D7_0104200	(0.977)	(3.478)	0.127	0.102	(1.293)	(4.364)	0.019	0.056	(1.618)	(5.368)	(0.076)	0.034

**In bold are the proteins cross-selected by the three malaria definations.*

***Yellow highlighted P values: statistically significant by the unadjusted analysis.*

population in Northern Uganda to capture as much immunological information as possible within the context of protective immunity from one population. This comprehensive approach would help identify further key antigenic targets or signature(s) of protective immunity. We observed 22 antigens, that included 17 PfEMP1 domains, 3 RIFIN family members, merozoite surface protein 3 (MSP3; PF3D7_1035400), and merozoite-associated armadillo repeats protein (PfMAAP; PF3D7_1035900), selected by the three clinical malaria definitions (1,000/2,500/5,000 parasites/μl blood plus fever). This suggest that these proteins have a key role in protection against clinical malaria.

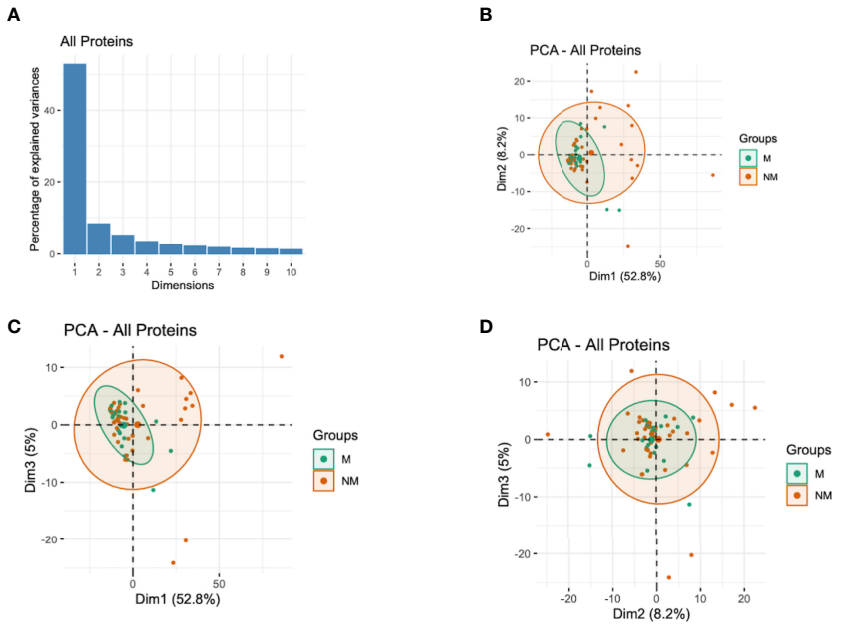

FIGURE 3 | Principal Components Analysis (PCA) of the antibody responses. **(A)** Distribution of principal components (first 10 dimensions) that explained the highest variance of the antibody responses derived from all the immunoreactive proteins. **(B–D)** The plots of the distribution of individuals by type of antibody responses to different proteins. The principal components (Dim)1 vs 2 **(B)**, Dim1 vs 3 **(C)**, and Dim2 vs 3 **(D)** that explained the highest percentage of the variance (percentage in parenthesis) of the antibody responses are presented. Green and red represent malaria (M) and no malaria (NM) cases, respectively. Light green and light red eclipses represent distribution of individuals with and without clinical malaria episodes, respectively.

We observed strong immune responses with high seroprevalence in the different protein families. This could be due to high level of exposure to these abundantly expressed proteins or cross-reactivity among the conserved regions of the domains (12). Although it could be argued that, likely, only highly expressed proteins can be flagged down in terms of antigen discovery and could be restrictive, the potential cross-reactivity could also be a strong point in terms of cross-protection. For instance, recent data suggests that despite their huge sequence diversity, CIDRα1 are structurally and functionally conserved for binding to EPCR (30, 31). Importantly, CIDRα1-EPCR interaction can be blocked by antibodies obtained from individuals naturally infected with malaria in Tanzania (30). The function of other multi-gene families in malaria infection and pathogenicity, to date, remains unclear but it is expected that the parasite could be using these proteins as alternative ligands to evade human immune system for host colonization.

Among them, PF3D7_0425800_DBLβ3, a PfEMP1 domain was selected by the multi-definition analyses, and appeared as well in the top 50 antigens by PCA. The molecule is a domain cassette 4 (DC4) family member consisting of a combination of short tandems that is associated with severe malaria (32–34). Antibodies against DBLβ3 can broadly inhibit PfEMP1 binding to intercellular adhesion molecule 1 (ICAM1) and are cross-reactive to DC4 derived from genetically distant parasite isolates (35). DBLβ3 was also identified in the previous analyses (32, 34) and the approach used here affirmed the importance of this domain in protection against symptomatic malaria. In addition, 3 members of the RIFIN family were selected. This is consistent with recent data which pointed to an important role of these molecules as ligands for opsonization of infected RBCs (36). Studies have suggested that anti-RIFIN antibodies correlate with parasite clearance, abrogation of symptoms of clinical malaria in children (37), and have a role in protection against severe malaria in Tanzanian patients (38). However, we do note that targeting RIFIN alone, as with PfEMP1 domains, for vaccine/as possible intervention tools may not be sufficient or highly effective due to the clonal expression of these proteins (39). We hypothesize that cross-conserved domains, either linear or structural, within the RIFINs may offer better and wider protective base than targeting only a single protein or domain. A recent study has pointed that this is indeed possible as broadly reactive antibodies were generated through insertion of a large DNA fragment between V and DJ segments of antigen binding domains able to recognize RIFINs of different *P. falciparum* isolates (36). Identification and characterization of the cross-protective mechanisms need to be critically pursued.

MSP3 was first identified in 1994 (40), has been a well-known target of naturally acquired immunity, and has been considered to be a promising asexual blood-stage malaria vaccine candidate (41). After the decades of research and development efforts, MSP3 is now under the clinical development as GMZ2, an asexual blood-stage malaria vaccine in combination with another surface antigen, *P. falciparum* glutamate-rich protein (GLURP) (42–44). PfMAAP was recently identified by Aniweh

TABLE 2 | Top 50 antigens based on respective contributions to variability in principal components 1, 2 and 3 (Dim1, Dim2, Dim3).

Product ID	GeneID	Dim1*	Dim2*	Dim3*
DC244	PF3D7_1240300_DBLβ8	**0.299**	0.033	0.014
DC113	PF3D7_0632500_DBLe2	**0.298**	0.022	0.014
DC12	PF3D7_0200100_CIDRα2.2	**0.293**	0.091	0.056
RS146	PF3D7_1000300	**0.287**	0.030	0.044
DC273	PF3D7_1373500_CIDRβ6	**0.286**	0.100	0.102
RS68	PF3D7_0425900	0.159	**0.673**	0.006
RS69	PF3D7_0500400	0.145	**0.722**	0.063
RS83	PF3D7_0632100	0.044	**0.739**	0.135
RS206	PF3D7_1372800	0.014	**0.778**	0.132
RS60	PF3D7_0401400	0.013	**0.769**	0.040
DC228	PF3D7_1200400_DBLγ14	0.097	0.039	**1.864**
DC36	PF3D7_0400400_DBLδ1	0.044	0.154	**2.074**
DC131	PF3D7_0712300_CIDRα0.1	0.043	0.028	**2.209**
DC220	PF3D7_1150400_CIDRγ2	0.037	0.049	**2.331**
DC221	PF3D7_1200100_DBLα0.9	0.028	0.112	**2.443**
DC231	PF3D7_1200600_DBLpam1	0.286	0.160	0.011
DC5	PF3D7_0100300_DBLα1.3	0.285	0.031	0.001
DC237	PF3D7_1200600_DBLe10	0.282	0.071	0.009
DC75	PF3D7_0425800_DBLδ1	0.281	0.076	0.058
DC25	PF3D7_0324900_CIDRβ7	0.281	0.183	0.036
DC180	PF3D7_0809100_CIDRα2.2	0.280	0.136	0.064
DC13	PF3D7_0200100_DBLγ11	0.278	0.185	0.000
RS184	PF3D7_1254100	0.278	0.049	0.050
RS204	PF3D7_1372600	0.278	0.107	0.029
RS63	PF3D7_0413200	0.278	0.053	0.021
DC78	PF3D7_0426000_CIDRα4	0.277	0.234	0.041
DC4	PF3D7_0100100_CIDRβ1	0.275	0.151	0.018
DC171	PF3D7_0808600_DBLα0.15	0.275	0.240	0.062
DC73	PF3D7_0425800_DBLβ3	0.275	0.034	0.017
RS185	PF3D7_1254200	0.274	0.030	0.042
DC224	PF3D7_1200100_CIDRβ1	0.221	0.016	0.676
DC132	PF3D7_0712300_DBLδ1	0.199	0.001	0.626
DC127	PF3D7_0712000_CIDRα3.1	0.195	0.622	0.078
DC143	PF3D7_0712800_CIDRα2.4	0.193	0.555	0.205
DC31	PF3D7_0400400_DBLα1.2	0.185	0.048	0.613
DC130	PF3D7_0712300_DBLα0.1	0.183	0.012	1.129
RS67	PF3D7_0425700	0.171	0.580	0.098
DC147	PF3D7_0712900_CIDRα3.1	0.164	0.638	0.154
DC149	PF3D7_0712900_CIDRβ1	0.163	0.619	0.115
DC213	PF3D7_1100200_CIDRβ4	0.152	0.535	0.005
DC35	PF3D7_0400400_DBLγ11	0.152	0.000	1.322
DC236	PF3D7_1200600_DBLepam5	0.142	0.127	0.980
DC152	PF3D7_0733000_DBLδ1	0.140	0.648	0.226
DC126	PF3D7_0712000_DBLα0.17	0.133	0.011	1.412
DC46	PF3D7_0412900_DBLα0.1	0.129	0.009	1.524
RS110	PF3D7_0800500	0.128	0.642	0.001
DC234	PF3D7_1200600_DBLpam3	0.125	0.031	1.079
RS101	PF3D7_0732200	0.119	0.001	0.758
DC232	PF3D7_1200600_DBLpam2	0.099	0.000	1.112

In bold are the proteins with the highest contribution to principle component.

et al. (45). Recently studied for its viability as vaccine candidate, PfMAAP was found localized to the apical region of merozoites, anti-PfMAAP antibodies inhibited merozoite invasion of erythrocytes *in vitro*, and naturally acquired human antibodies to the conserved N- and C- terminal regions of PfMAAP were associated with reduced risk to malaria. Independent analyses and association with protection in this study supports the vaccine candidacy of both MSP3 and PfMAAP, similar to the highly immunogenic erythrocyte surface antigens.

The need for continued development of robust malaria intervention tools including vaccines across different malaria endemicities (46) calls for "flexible" definitions of clinical malaria (47). Moreover, given that malaria can be defined in very diverse ways since clinical presentations vary widely, it is not obvious what aspects are key to supporting accurate monitoring in the face of changing epidemiology (48). We show that three different parasitemia cut-off points yielded almost similar results (**Figure 2A**) suggesting that, for immunological studies, combination of antigens provide an important signature that can be true in different geographical settings. We do acknowledge that there are challenges to attribute fever (or other symptoms) with observed parasitemia (49) and additional studies will be needed to validate or optimize our findings in different settings and in a larger dataset.

We investigated whether a specific combination of antibody responses to the recombinant proteins evaluated could be associated with key malaria severity factors such as age. PCA is useful for exploring multi-dimensional data, mixed infections and complex host-parasite interactions. To this end, and to capture the joint effects of all antibodies in a single analysis in biological conditions, we investigated the relationship between the overall antibody responses by PCA, a factor analysis approach accommodating the fact that protective antibody responses are likely to involve a number of antibodies working together. With the current dataset, the first three principal components accounted for the majority of the outcomes observed (**Figure 3A**). The analyses only showed a significant relationship between first (Dim1) component scores and age; with PfEMP1 domains being the top contributing variables (**Figure 4**; **Table 2**). This is consistent with a recent proposal suggesting that there are ordered acquisition of antibodies targeting PfEMP1 (50). Taken together, these findings suggest that antibodies to multiple proteins may be acquired with age, and continuous exposure is a key factor in protection against clinical disease and protective immunity (2).

Multiple *P. falciparum* protein microarrays have been designed over the past decade to identify malaria vaccine candidate antigens. One of the most important characteristic in this study is the use of WGCFS for recombinant protein production. In contrast to *E. coli*- (5, 51) and mammalian cell-based protein microarray (52) systems which may cause an artefactual change in protein folding (53), WGCFS can express large and complex non-glycosylated proteins in their near-native forms without codon optimization (54). The AlphaScreen immunoscreening platform does not require protein purification and conjugation. Based on these characteristics, therefore, WGCFS/AlphaScreen platform provides a rapid, straightforward tool for screening and identification of parasite antigenic targets as well as protein-protein interactions important for immunity and pathogenesis (55–57), overcoming most challenges attributed to the *E. coli*-based systems (58, 59) resulting to robust evaluations of immunoreactivities across different proteins families and groups.

In conclusion, the large platform of malaria antigens and the analysis approach applied in this study improved our ability to

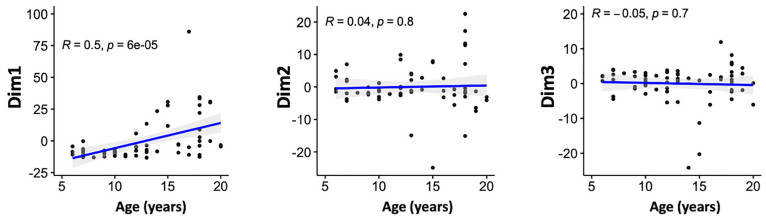

FIGURE 4 | Associations between the antibody responses and age. Correlation between the scores of the principal components 1–3 and age (in years) of the participants. Blue line represent linear regression lines and shading represents 95% confidence intervals. Only the first principal component (Dim1) correlated with age.

interrelate immunological data with clinical outcomes and highlighted antigens for future work aimed towards developing additional tools for malaria elimination and eradication.

DATA AVAILABILITY STATEMENT

The original contributions presented in the study are included in the article/**Supplementary Material**. Further inquiries can be directed to the corresponding authors.

ETHICS STATEMENT

The studies involving human participants were reviewed and approved by Institutional Review Committees of Ehime University and Institutional Review Committees of Research Institute for Microbial Diseases, Osaka University, Japan. In Uganda, the studies were reviewed and approved by Lacor Hospital (LHIREC 023/09/13), and Uganda National Council for Science and Technology (HS866, HS1403). Written informed consent to participate in this study was provided by the participants' legal guardian/next of kin.

AUTHOR CONTRIBUTIONS

ET and BK conceived and designed experiments. HN, MM, and IH conducted experiments. ET, BK, and TT analyzed the data. ET, BK, NP, TE, TH, JG, and TT wrote the manuscript. All authors discussed and edited the manuscript.

FUNDING

This work was funded in part by JSPS KAKENHI (grant numbers JP20H03481, JP21H02724, JP21KK0138) and in part by Strategic Promotion of International Cooperation to Accelerate Innovation in Africa by MEXT, Japan. BK is an EDCTP Fellow under EDCTP2 programme supported by the European Union grant number TMA2020CDF-3203. The funders had no role in study design, data collection and analysis, decision to publish, or preparation of the manuscript.

ACKNOWLEDGMENTS

We appreciate the study volunteers from Lira, Northern Uganda; and thank the research teams from Med Biotech Laboratories, Lira Medical Center, Uganda, and Research Institute for Microbial Diseases, Osaka University for their technical assistance in obtaining the field samples.

SUPPLEMENTARY MATERIAL

The Supplementary Material for this article can be found online at: https://www.frontiersin.org/articles/10.3389/fimmu.2022.887219/full#supplementary-material

REFERENCES

1. WHO. *Global Technical Strategy for Malaria 2016-2030, 2021 Update* Vol. Vol. 2021. Geneva, Switzerland: World Health Organization (2021).
2. Doolan DL, Dobano C, Baird JK. Acquired Immunity to Malaria. *Clin Microbiol Rev* (2009) 22:13–36. doi: 10.1128/CMR.00025-08
3. Barry A, Hansen D. Naturally Acquired Immunity to Malaria. *Parasitology* (2016) 143:125–8. doi: 10.1017/S0031182015001778
4. Osier FH, Mackinnon MJ, Crosnier C, Fegan G, Kamuyu G, Wanaguru M, et al. New Antigens for a Multicomponent Blood-Stage Malaria Vaccine. *Sci Transl Med* (2014) 6:247ra102. doi: 10.1126/scitranslmed.3008705
5. Crompton PD, Kayala MA, Traore B, Kayentao K, Ongoiba A, Weiss GE, et al. A Prospective Analysis of the Ab Response to *Plasmodium falciparum* Before and After a Malaria Season by Protein Microarray. *Proc Natl Acad Sci USA* (2010) 107:6958–63. doi: 10.1073/pnas.1001323107
6. Doolan DL, Mu Y, Unal B, Sundaresh S, Hirst S, Valdez C, et al. Profiling Humoral Immune Responses to *P. falciparum* Infection With Protein Microarrays. *Proteomics* (2008) 8:4680–94. doi: 10.1002/pmic.200800194
7. Richards JS, Arumugam TU, Reiling L, Healer J, Hodder AN, Fowkes FJ, et al. Identification and Prioritization of Merozoite Antigens as Targets of Protective Human Immunity to *Plasmodium falciparum* Malaria for Vaccine and Biomarker Development. *J Immunol* (2013) 191:795–809. doi: 10.4049/jimmunol.1300778
8. Dodoo D, Aikins A, Kusi KA, Lamptey H, Remarque E, Milligan P, et al. Cohort Study of the Association of Antibody Levels to AMA1, MSP119,

MSP3 and GLURP With Protection From Clinical Malaria in Ghanaian Children. *Malaria J* (2008) 7:142. doi: 10.1186/1475-2875-7-142
9. Kanoi BN, Takashima E, Morita M, White MT, Palacpac NM, Ntege EH, et al. Antibody Profiles to Wheat Germ Cell-Free System Synthesized *Plasmodium falciparum* Proteins Correlate With Protection From Symptomatic Malaria in Uganda. *Vaccine* (2017) 35:873–81. doi: 10.1016/j.vaccine.2017.01.001
10. Ntege EH, Takashima E, Morita M, Nagaoka H, Ishino T, Tsuboi T. Blood-Stage Malaria Vaccines: Post-Genome Strategies for the Identification of Novel Vaccine Candidates. *Expert Rev Vaccines* (2017) 16:769–79. doi: 10.1080/14760584.2017.1341317
11. Kanoi BN, Nagaoka H, Morita M, White MT, Palacpac NMQ, Ntege EH, et al. Comprehensive Analysis of Antibody Responses to *Plasmodium falciparum* Erythrocyte Membrane Protein 1 Domains. *Vaccine* (2018) 36:6826–33. doi: 10.1016/j.vaccine.2018.08.058
12. Chan JA, Fowkes FJ, Beeson JG. Surface Antigens of *Plasmodium falciparum*-Infected Erythrocytes as Immune Targets and Malaria Vaccine Candidates. *Cell Mol Life Sci* (2014) 71:3633–57. doi: 10.1007/s00018-014-1614-3
13. Kanoi BN, Nagaoka H, White MT, Morita M, Palacpac NMQ, Ntege EH, et al. Global Repertoire of Human Antibodies Against *Plasmodium falciparum* RIFINs, SURFINs, and STEVORs in a Malaria Exposed Population. *Front Immunol* (2020) 11:893. doi: 10.3389/fimmu.2020.00893
14. Palacpac NM, Ntege E, Yeka A, Balikagala B, Suzuki N, Shirai H, et al. Phase 1b Randomized Trial and Follow-Up Study in Uganda of the Blood-Stage Malaria Vaccine Candidate BK-Se36. *PLoS One* (2013) 8:e64073. doi: 10.1371/journal.pone.0064073
15. Stanisic DI, Fowkes FJ, Koinari M, Javati S, Lin E, Kiniboro B, et al. Acquisition of Antibodies Against *Plasmodium falciparum* Merozoites and Malaria Immunity in Young Children and the Influence of Age, Force of Infection, and Magnitude of Response. *Infect Immun* (2015) 83:646–60. doi: 10.1128/IAI.02398-14
16. Bejon P, Williams TN, Liljander A, Noor AM, Wambua J, Ogada E, et al. Stable and Unstable Malaria Hotspots in Longitudinal Cohort Studies in Kenya. *PLoS Med* (2010) 7:e1000304. doi: 10.1371/journal.pmed.1000304
17. Greenwood BM, Armstrong JR. Comparison of Two Simple Methods for Determining Malaria Parasite Density. *Trans R Soc Trop Med Hyg* (1991) 85:186–8. doi: 10.1016/0035-9203(91)90015-Q
18. Schellenberg JR, Smith T, Alonso PL, Hayes RJ. What Is Clinical Malaria? Finding Case Definitions for Field Research in Highly Endemic Areas. *Parasitol Today* (1994) 10:439–42. doi: 10.1016/0169-4758(94)90179-1
19. Mwangi TW, Ross A, Snow RW, Marsh K. Case Definitions of Clinical Malaria Under Different Transmission Conditions in Kilifi District, Kenya. *J Infect Dis* (2005) 191:1932–9. doi: 10.1086/430006
20. Egwang TG, Apio B, Riley E, Okello D. *Plasmodium falciparum* Malariometric Indices in Apac District, Northern Uganda. *East Afr Med J* (2000) 77:413–6.
21. Proietti C, Pettinato DD, Kanoi BN, Ntege E, Crisanti A, Riley EM, et al. Continuing Intense Malaria Transmission in Northern Uganda. *Am J Trop Med Hyg* (2011) 84:830–7. doi: 10.4269/ajtmh.2011.10-0498
22. Yeka A, Gasasira A, Mpimbaza A, Achan J, Nankabirwa J, Nsobya S, et al. Malaria in Uganda: Challenges to Control on the Long Road to Elimination: I. Epidemiology and Current Control Efforts. *Acta Trop* (2012) 121:184–95. doi: 10.1016/j.actatropica.2011.03.004
23. Okello PE, Van Bortel W, Byaruhanga AM, Correwyn A, Roelants P, Talisuna A, et al. Variation in Malaria Transmission Intensity in Seven Sites Throughout Uganda. *Am J Trop Med Hyg* (2006) 75:219–25. doi: 10.4269/ajtmh.2006.75.219
24. Matsuoka K, Komori H, Nose M, Endo Y, Sawasaki T. Simple Screening Method for Autoantigen Proteins Using the N-Terminal Biotinylated Protein Library Produced by Wheat Cell-Free Synthesis. *J Proteome Res* (2010) 9:4264–73. doi: 10.1021/pr9010553
25. Longley RJ, White MT, Takashima E, Morita M, Kanoi BN, Li Wai Suen CSN, et al. Naturally Acquired Antibody Responses to More Than 300 *Plasmodium Vivax* Proteins in Three Geographic Regions. *PloS Negl Trop Dis* (2017) 11:e0005888. doi: 10.1371/journal.pntd.0005888
26. Osier FH, Fegan G, Polley SD, Murungi L, Verra F, Tetteh KK, et al. Breadth and Magnitude of Antibody Responses to Multiple *Plasmodium falciparum* Merozoite Antigens are Associated With Protection From Clinical Malaria. *Infect Immun* (2008) 76:2240–8. doi: 10.1128/IAI.01585-07
27. Rono J, Osier FH, Olsson D, Montgomery S, Mhoja L, Rooth I, et al. Breadth of Anti-Merozoite Antibody Responses is Associated With the Genetic Diversity of Asymptomatic *Plasmodium falciparum* Infections and Protection Against Clinical Malaria. *Clin Infect Dis* (2013) 57:1409–16. doi: 10.1093/cid/cit556
28. Jolliffe I. Principal Component Analysis. In: *Encyclopedia of Statistics in Behavioral Science* (New York, NY: Springer) (2005).
29. Fowkes FJ, Richards JS, Simpson JA, Beeson JG. The Relationship Between Anti-Merozoite Antibodies and Incidence of *Plasmodium falciparu*m Malaria: A Systematic Review and Meta-Analysis. *PLoS Med* (2010) 7:e1000218. doi: 10.1371/journal.pmed.1000218
30. Lau CK, Turner L, Jespersen JS, Lowe ED, Petersen B, Wang CW, et al. Structural Conservation Despite Huge Sequence Diversity Allows EPCR Binding by the PfEMP1 Family Implicated in Severe Childhood Malaria. *Cell Host Microbe* (2015) 17:118–29. doi: 10.1016/j.chom.2014.11.007
31. Turner L, Lavstsen T, Berger SS, Wang CW, Petersen JE, Avril M, et al. Severe Malaria is Associated With Parasite Binding to Endothelial Protein C Receptor. *Nature* (2013) 498:502–5. doi: 10.1038/nature12216
32. Jensen AT, Magistrado P, Sharp S, Joergensen L, Lavstsen T, Chiucchiuini A, et al. *Plasmodium falciparum* Associated With Severe Childhood Malaria Preferentially Expresses PfEMP1 Encoded by Group A Var Genes. *J Exp Med* (2004) 199:1179–90. doi: 10.1084/jem.20040274
33. Tonkin-Hill GQ, Trianty L, Noviyanti R, Nguyen HHT, Sebayang BF, Lampah DA, et al. The *Plasmodium falciparum* Transcriptome in Severe Malaria Reveals Altered Expression of Genes Involved in Important Processes Including Surface Antigen-Encoding Var Genes. *PLoS Biol* (2018) 16:e2004328. doi: 10.1371/journal.pbio.2004328
34. Bengtsson A, Joergensen L, Rask TS, Olsen RW, Andersen MA, Turner L, et al. A Novel Domain Cassette Identifies *Plasmodium falciparum* PfEMP1 Proteins Binding ICAM-1 and Is a Target of Cross-Reactive, Adhesion-Inhibitory Antibodies. *J Immunol* (2013) 190:240–9. doi: 10.4049/jimmunol.1202578
35. Lennartz F, Bengtsson A, Olsen RW, Joergensen L, Brown A, Remy L, et al. Mapping the Binding Site of a Cross-Reactive *Plasmodium falciparum* PfEMP1 Monoclonal Antibody Inhibitory of ICAM-1 Binding. *J Immunol* (2015) 195:3273–83. doi: 10.4049/jimmunol.1501404
36. Tan J, Pieper K, Piccoli L, Abdi A, Perez MF, Geiger R, et al. A LAIR1 Insertion Generates Broadly Reactive Antibodies Against Malaria Variant Antigens. *Nature* (2016) 529:105–9. doi: 10.1038/nature16450
37. Abdel-Latif MS, Dietz K, Issifou S, Kremsner PG, Klinkert MQ. Antibodies to *Plasmodium falciparum* Rifin Proteins are Associated With Rapid Parasite Clearance and Asymptomatic Infections. *Infect Immun* (2003) 71:6229–33. doi: 10.1128/IAI.71.11.6229-6233.2003
38. Saito F, Hirayasu K, Satoh T, Wang CW, Lusingu J, Arimori T, et al. Immune Evasion of *Plasmodium falciparum* by RIFIN *via* Inhibitory Receptors. *Nature* (2017) 552:101–5. doi: 10.1038/nature24994
39. Fernandez V, Hommel M, Chen Q, Hagblom P, Wahlgren M. Small, Clonally Variant Antigens Expressed on the Surface of the *Plasmodium falciparum*-Infected Erythrocyte are Encoded by the Rif Gene Family and are the Target of Human Immune Responses. *J Exp Med* (1999) 190:1393–404. doi: 10.1084/jem.190.10.1393
40. Oeuvray C, Bouharoun-Tayoun H, Grass-Masse H, Lepers JP, Ralamboranto L, Tartar A, et al. A Novel Merozoite Surface Antigen of *Plasmodium falciparum* (MSP-3) Identified by Cellular-Antibody Cooperative Mechanism Antigenicity and Biological Activity of Antibodies. *Mem Inst Oswaldo Cruz* (1994) 89 Suppl 2:77–80. doi: 10.1590/S0074-02761994000600018
41. Singh S, Soe S, Mejia JP, Roussilhon C, Theisen M, Corradin G, et al. Identification of a Conserved Region of *Plasmodium falciparum* MSP3 Targeted by Biologically Active Antibodies to Improve Vaccine Design. *J Infect Dis* (2004) 190:1010–8. doi: 10.1086/423208
42. Sirima SB, Mordmuller B, Milligan P, Ngoa UA, Kironde F, Atuguba F, et al. A Phase 2b Randomized, Controlled Trial of the Efficacy of the GMZ2 Malaria Vaccine in African Children. *Vaccine* (2016) 34:4536–42. doi: 10.1016/j.vaccine.2016.07.041
43. Dassah S, Adu B, Sirima SB, Mordmuller B, Ngoa UA, Atuguba F, et al. Extended Follow-Up of Children in a Phase2b Trial of the GMZ2 Malaria Vaccine. *Vaccine* (2021) 39:4314–9. doi: 10.1016/j.vaccine.2021.06.024

44. Dejon-Agobe JC, Ateba-Ngoa U, Lalremruata A, Homoet A, Engelhorn J, Nouatin OP, et al. Controlled Human Malaria Infection of Healthy Adults With Lifelong Malaria Exposure to Assess Safety, Immunogenicity, and Efficacy of the Asexual Blood Stage Malaria Vaccine Candidate Gmz2. *Clin Infect Dis* (2019) 69:1377–84. doi: 10.1093/cid/ciy1087
45. Aniweh Y, Nyarko PB, Charles-Chess E, Ansah F, Osier FHA, Quansah E, et al. *Plasmodium falciparum* Merozoite Associated Armadillo Protein (PfMAAP) Is Apically Localized in Free Merozoites and Antibodies Are Associated With Reduced Risk of Malaria. *Front Immunol* (2020) 11:505. doi: 10.3389/fimmu.2020.00505
46. Nasir SMI, Amarasekara S, Wickremasinghe R, Fernando D, Udagama P. Prevention of Re-Establishment of Malaria: Historical Perspective and Future Prospects. *Malaria J* (2020) 19:452. doi: 10.1186/s12936-020-03527-8
47. Hay SI, Okiro EA, Gething PW, Patil AP, Tatem AJ, Guerra CA, et al. Estimating the Global Clinical Burden of *Plasmodium falciparum* Malaria in 2007. *PLoS Med* (2010) 7:e1000290. doi: 10.1371/journal.pmed.1000290
48. Nkumama IN, O'Meara WP, Osier FH. Changes in Malaria Epidemiology in Africa and New Challenges for Elimination. *Trends Parasitol* (2016) 33 (2):128–40. doi: 10.1016/j.pt.2016.11.006
49. Koram KA, Molyneux ME. When Is "Malaria" Malaria? The Different Burdens of Malaria Infection, Malaria Disease, and Malaria-Like Illnesses. *Am J Trop Med Hyg* (2007) 77:1–5. doi: 10.4269/ajtmh.77.6.suppl.1
50. Thomson-Luque R, Votborg-Novel L, Ndovie W, Andrade CM, Niangaly M, Attipa C, et al. *Plasmodium falciparum* Transcription in Different Clinical Presentations of Malaria Associates With Circulation Time of Infected Erythrocytes. *Nat Commun* (2021) 12:4711. doi: 10.1038/s41467-021-25062-z
51. Finney OC, Danziger SA, Molina DM, Vignali M, Takagi A, Ji M, et al. Predicting Antidisease Immunity Using Proteome Arrays and Sera From Children Naturally Exposed to Malaria. *Mol Cell Proteomics* (2014) 13:2646–60. doi: 10.1074/mcp.M113.036632
52. Kamuyu G, Tuju J, Kimathi R, Mwai K, Mburu J, Kibinge N, et al. KILchip V1.0: A Novel *Plasmodium falciparum* Merozoite Protein Microarray to Facilitate Malaria Vaccine Candidate Prioritization. *Front Immunol* (2018) 9:2866. doi: 10.3389/fimmu.2018.02866
53. Romanov V, Davidoff SN, Miles AR, Grainger DW, Gale BK, Brooks BD. A Critical Comparison of Protein Microarray Fabrication Technologies. *Analyst* (2014) 139:1303–26. doi: 10.1039/C3AN01577G
54. Kanoi BN, Nagaoka H, Morita M, Tsuboi T, Takashima E. Leveraging the Wheat Germ Cell-Free Protein Synthesis System to Accelerate Malaria Vaccine Development. *Parasitol Int* (2021) 80:102224. doi: 10.1016/j.parint.2020.102224
55. Nagaoka H, Kanoi BN, Ntege EH, Aoki M, Fukushima A, Tsuboi T, et al. Antibodies Against a Short Region of PfRipr Inhibit *Plasmodium falciparum* Merozoite Invasion and PfRipr Interaction With Rh5 and SEMA7A. *Sci Rep* (2020) 10:6573. doi: 10.1038/s41598-020-63611-6
56. Nagaoka H, Sasaoka C, Yuguchi T, Kanoi BN, Ito D, Morita M, et al. PfMSA180 Is a Novel *Plasmodium falciparum* Vaccine Antigen That Interacts With Human Erythrocyte Integrin Associated Protein (CD47). *Sci Rep* (2019) 9:5923. doi: 10.1038/s41598-019-42366-9
57. Yuguchi T, Kanoi BN, Nagaoka H, Miura T, Ito D, Takeda H, et al. *Plasmodium Yoelii* Erythrocyte Binding Like Protein Interacts With Basigin, an Erythrocyte Surface Protein. *Front Cell Infect Microbiol* (2021) 11:656620. doi: 10.3389/fcimb.2021.656620
58. Arumugam TU, Ito D, Takashima E, Tachibana M, Ishino T, Torii M, et al. Application of Wheat Germ Cell-Free Protein Expression System for Novel Malaria Vaccine Candidate Discovery. *Expert Rev Vaccines* (2014) 13:75–85. doi: 10.1586/14760584.2014.861747
59. Rui E, Fernandez-Becerra C, Takeo S, Sanz S, Lacerda MV, Tsuboi T, et al. *Plasmodium Vivax*: Comparison of Immunogenicity Among Proteins Expressed in the Cell-Free Systems of Escherichia Coli and Wheat Germ by Suspension Array Assays. *Malaria J* (2011) 10:192. doi: 10.1186/1475-2875-10-192

Conflict of Interest: The authors declare that the research was conducted in the absence of any commercial or financial relationships that could be construed as a potential conflict of interest.

frontiers | Frontiers in Immunology

BRIEF RESEARCH REPORT
published: 10 June 2022
doi: 10.3389/fimmu.2022.898520

The Cross-Protective Immunity Landscape Among Different SARS-CoV-2 Variant RBDs

Wenqiang Sun[1,2,3], *Lihong He*[1,4], *Huicong Lou*[1,3], *Wenhui Fan*[1], *Limin Yang*[1], *Gong Cheng*[2,5], *Wenjun Liu*[1,2,3,4*] *and Lei Sun*[1,4*]

[1] CAS Key Laboratory of Pathogenic Microbiology and Immunology, Institute of Microbiology, Chinese Academy of Sciences, Beijing, China, [2] Shenzhen Bay Laboratory, Institute of Infectious Diseases, Shenzhen, China, [3] State Key Laboratory for Conservation and Utilization of Subtropical Agro-Bioresources & Laboratory of Animal Infectious Diseases, College of Animal Sciences and Veterinary Medicine, Guangxi University, Nanning, China, [4] Savaid Medical School, University of Chinese Academy of Sciences, Beijing, China, [5] Tsinghua-Peking Center for Life Sciences, School of Medicine, Tsinghua University, Beijing, China

OPEN ACCESS

Edited by:
Lee Mark Wetzler,
Boston University, United States

Reviewed by:
Stephanie Longet,
University of Oxford, United Kingdom
Shilpi Jain,
Centers for Disease Control and Prevention (CDC), United States

***Correspondence:**
Wenjun Liu
liuwj@im.ac.cn
Lei Sun
sunlei362@im.ac.cn

Specialty section:
This article was submitted to Vaccines and Molecular Therapeutics, a section of the journal Frontiers in Immunology

Received: *17 March 2022*
Accepted: *17 May 2022*
Published: *10 June 2022*

Citation:
Sun W, He L, Lou H, Fan W, Yang L, Cheng G, Liu W and Sun L (2022) The Cross-Protective Immunity Landscape Among Different SARS-CoV-2 Variant RBDs. Front. Immunol. 13:898520. doi: 10.3389/fimmu.2022.898520

Despite the fact that SARS-CoV-2 vaccines have been available in most parts of the world, the epidemic status remains grim with new variants emerging and escaping the immune protection of existing vaccines. Therefore, the development of more effective antigens and evaluation of their cross-protective immunity against different SARS-CoV-2 variants are particularly urgent. In this study, we expressed the wild type (WT), Alpha, Beta, Delta, and Lambda RBD proteins to immunize mice and evaluated their cross-neutralizing activity against different pseudoviruses (WT, Alpha, Beta, Delta, Lambda, and Omicron). All monovalent and pentavalent RBD antigens induced high titers of IgG antibodies against different variant RBD antigens. In contrast, WT RBD antigen-induced antibodies showed a lower neutralizing activity against Beta, Delta, Lambda, and Omicron pseudoviruses compared to neutralization against itself. Interestingly, Beta RBD antigen and multivalent antigen induced broader cross-neutralization antibodies than other variant RBD antigens. These data provide a reference for vaccine strain selection and universal COVID-19 vaccine design to fight the constant emergence of new SARS-CoV-2 variants.

Keywords: SARS-CoV-2, variant, vaccine, RBD, cross-protective immunity

INTRODUCTION

Since the COVID-19 outbreak, the virus has spread around the world and posed a huge threat to human health (1–4). SARS-COV-2 is an enveloped, unsegmented, single-stranded RNA virus with four structural proteins, namely, E envelope protein, M membrane protein, N nucleoprotein, and S spike protein (5). Among them, S protein contains two subunits, S1 and S2, in which receptor-binding domain (RBD) exists in S1 subunit and is responsible for binding to hACE2 (6–8). Therefore, S and RBD were often selected as targets for SARS-CoV-2 vaccine development (9–12).

Currently, the clinically used SARS-CoV-2 vaccines, including inactivated vaccines, mRNA vaccines, subunit vaccines, adenovirus vector vaccines, and so on, are all based on the wild type (WT) strain (13–20). However, SARS-CoV-2 has been undergoing mutations. Variant Alpha

(B.1.1.7), Beta (B.1.351), Gamma (P.1), Iota (B.1.526), Delta (B.1.617.2), Lambda (C.37), and Omicron (B.1.1.529) have been reported successively (21–25). The N501Y mutation was found in RBD of Alpha variant in the UK and has been shown to increase transmissivity and slightly decrease neutralizing activity in recovered patients and immune sera (15, 26, 27). Beta variant was first identified in South Africa, which had three mutations (K417N, E484K, and N501Y) in RBD. These mutations have been reported to affect its binding to human ACE2 and seriously evade neutralizing antibodies (28–31). The Delta variant was first reported in India in 2020 and subsequently became the dominant pandemic strain in the world, where it is still circulating. Two mutation sites (T478K and L452R) exist in Delta RBD. Studies have shown that these two mutations do not participate in its binding to hACE2 (32). Several studies have reported a decrease (mild to moderate) in the neutralization activity of serum of vaccine and recovered patients to Delta variant (33–35). It is possible that the involvement of mutations in other positions cannot be excluded. Lambda variant was first reported in Peru and circulating in parts of Latin America. Two mutation sites (L452Q and F490S) exist in RBD of Lambda. Substantial evidence shows that the Lambda variant exhibits strong immune evasion against vaccines and convalescent sera (33, 36, 37). Omicron was first reported from South Africa in late 2021 and is currently the most dominant strain worldwide. There were 15 mutations in RBD, which affected the receptor-binding motif of RBD interacting with hACE2 (32). The Omicron variant exhibits the most severe immune evasion than other variants (19, 34, 38–40). Therefore, there is an urgent need to develop more effective antigens and evaluate their cross-protective immunity against different SARS-CoV-2 variants.

In this study, we analyzed the genetic evolution and protein structure of different variant RBDs and examined their binding affinity to hACE2. Furthermore, mice were immunized with these variant RBD antigens and the cross-neutralization activity against different variant pseudoviruses were evaluated.

MATERIALS AND METHODS

Cells and Animals

Human embryonic kidney 293T (HEK293T) cells stably expressing hACE2 (293T/hACE2) were kindly provided by Dr. Zhendong Zhao (Institute of Pathogen Biology, Chinese Academy of Medical Sciences & Peking Union Medical College). HEK293T cells (ATCC CRL-3216) were maintained in Dulbecco's modified Eagle's medium (DMEM, Gibco) supplemented with 10% fetal bovine serum (FBS, Gibco) and penicillin (100 U/ml)-streptomycin (100 mg/mL) (Thermo Fisher Scientific, Waltham, MA, USA). All cell lines are tested negative for mycoplasma contamination (Mycoplasma Detection Kit, Solarbio, Beijing, China). Female C57BL/6 mice were purchased from Beijing Vital River Animal Technology Co., Ltd. (licensed by Charles River) and housed and bred under 18 ~ 22°C and 50 ~ 60% humidity conditions.

Construction and Expression of RBD Protein

The different variant RBD proteins were fused with human IgG Fc (hFc) and IL-10 signal peptide, and the amino acid sequences were optimized by human preference codons and constructed into pcDNA3.4 vector. The recombinant plasmid was confirmed by sequencing by Nanjing Genscript Company. Different variant RBD plasmids were transfected into HEK293T cells and the supernatant was harvested 72 h later. Then, the supernatant was purified using Protein A column and proteins were eluted with citric acid buffer (pH 3.4). The eluted proteins were dialyzed in PBS buffer. The purity and molecular weight of proteins were determined by SDS-PAGE. The protein concentration was measured by NanoDrop microspectrophotometer (Thermo Fisher Scientific). Finally, the RBD proteins were frozen to -80°C.

Affinity Between RBD Proteins and hACE2

Ninety-six well ELISA plates (Corning, USA) were coated with the hACE2 protein (2 μg/mL, SinoBiological) overnight at 4°C and blocked with 4% bull serum albumin. The different variant RBD proteins were diluted to a uniform concentration (1 mg/mL), and then two-fold diluted. The plates were incubated with Goat Anti-Human IgG-HRP (Abcam) and developed by the addition of 100 μL of 3,3',5',5-tetramethylbenzidine (TMB) to each well. Finally, 100 μL of 2 mmol/L H_2SO_4 was added to terminate the reaction, and the light absorption of the plate was measured at 450 nm using a microplate reader (Thermo Scientific). The fitted curves and EC_{50} were created using Graphpad software (version 8.0). Each experiment was performed three times.

Mouse Experiments

To evaluate the immune efficacy of different variant RBDs, aged 6-8 weeks naive C57BL/6 mice (four independent mice in each group) were immunized intramuscularly with monovalent and multivalent RBD antigens pre-bound to Alum-adjuvant (antigen and aluminum adjuvant (Imject® Alum, Thermo Scientific) were mixed in a 1:1 volume ratio and gently stirred for 30 min to allow the aluminum adjuvant to effectively adsorb antigen). The immune dose was 10 μg each variant RBD protein per mouse of monovalent RBD antigen and pentavalent RBD antigens were a 10 μg RBD protein mixture including each 2 μg variant RBD protein. Mice immunized with PBS were identified as placebo control. Priming and booster vaccinations were spaced at 3 weeks. Serum samples were collected, inactivated at 56°C for 30 min, and stored at −20°C for subsequent use.

In immunization animal experiments, the clinical status and food intake of the mice were monitored and recorded daily.

Enzyme Linked Immunosorbent Assay (ELISA)

Ninety-six well ELISA plates (Corning, USA) were coated respectively with six different RBD-hFc protein (1 μg/mL) overnight at 4°C and blocked with 4% bull serum albumin.

The serum was threefold diluted and added to each well, and the plates were incubated with Rabbit Anti-Mouse IgG-HRP (Light Chain Specific, CST) and developed by the addition of 100 μL of 3,3',5',5-tetramethylbenzidine (TMB) to each well. Finally, 100 μL of 2 mmol/L H_2SO_4 was added to terminate the reaction, and the light absorption of the plate was measured at 450 nm using a microplate reader (Thermo Scientific). The endpoint of serum antibody titers was determined as the reciprocal of the highest dilution that was 2.1-fold higher than the optical absorbance value of the negative control. Each experiment was performed three times.

Pseudovirus Neutralization Assay

For pseudovirus production, the codon-optimized full-length S protein of wild-type (WT) SARS-CoV-2 S protein was cloned in pCAGGS plasmids and the full-length S protein plasmids of Alpha, Beta, Delta, Lambda, and Omicron variants were modified from pCAGGS-WT. The plasmid pCAGGS-S-WT, pCAGGS-S-Alpha, pCAGGS-S-Beta, pCAGGS-S-Delta, pCAGGS-S-Lambda, and pCAGGS-S-Omicron were cotransfected with psPAX2 and pLenti-GFP into HEK293T cells at a mass ratio of 1:1:1. After 72 h, the supernatant containing pseudovirus was harvested and stored at −80°C for subsequent use. The $TCID_{50}$ was determined in 293T/hACE2 cells according to the previous described method (41).

HEK293T/hACE2 cells were inoculated before the experiment. Starting with a 1:10 dilution, each serum sample was continuously diluted twice in a 96-well plate. Equal volumes of WT or variant pseudoviruses were mixed with each diluted serum sample and incubated for 1.5 h at 37°C. The mixture of virus-serum was added to the cells. After 72 h, the cells-supernatant mixture was collected. The firefly luciferase activity in the cells was detected by chemiluminescence, and the luciferase activity was quantified to measure the transduction efficiency. To calculate the neutralization efficiency, a pseudovirus without serum sample was used as a positive control. Each sample was assessed in three repeat wells. Positive values were determined to be relative luminescence unit (RLU) values that were tenfold higher than that of only the cell background. The half-maximum neutralization titer (NT_{50}) value was the reciprocal of the dilution of half of the mean RLU value of the positive control.

Statistical Analysis

All of the data are presented as the mean ± SEM. P-values were determined by one-way ANOVA. All graphs were generated with GraphPad Prism version 8.0 software.

RESULTS

Bioinformatics Analysis of SARS-CoV-2 Variant RBD

The binding of SARS-CoV-2 RBD to hACE2 is crucial to the virus infection. Several key amino acid mutations are found in the RBD of variants (32). We further analyzed the relationship between RBD sequences of different variants and their antigenicity. More striking, there are 15 amino acid mutations in Omicron RBD. Moreover, there were common mutation sites among different RBDs. For example, Beta RBD (K417N, E484K, N501Y) has the same mutation sites as Alpha (N501Y) and Omicron (K417N, N501Y) (**Figure 1A**). Genetic evolution analysis of RBD amino acid sequences of different variants revealed that Delta and Lambda variants formed a cluster, and Beta and Omicron variants formed another cluster (**Figure 1B**), suggesting that the RBDs in the same cluster of phylogenetic trees might have similar antigenicity. Crystal structure analysis of WT RBD and ACE2 complex indicated that the amino acid residues K417, G446, Y449, N487, Q493, G496, Q498, T500, N501, G502, and Y505 were involved in the interaction of virus and host cell receptor (**Figure 1C**). A recent study showed that the amino acid mutations of RBD binding sites to hACE2 have emerged. For instance, Omicron RBD possesses eight substitutions on the hACE2 recognizing interface, namely K417N, G446S, E484A, Q493R, G496S, Q498R, N501Y, and Y505H, compared with what was seen on the WT RBD (32). In addition, the same amino acid substitutions of RBD were found among different variants. N501Y mutation existed in Alpha, Beta, and Omicron variants, K417N was found in Beta and Omicron variants, and T478K was found in Delta and Omicron variants (**Figure 1D**). Importantly, these mutations have been reported to play important roles in host adaptation and immune evasion (42). Together, the above results indicate that the mutation sites among different RBDs might affect their antigenicity, which provides a reference for the selection of vaccines against different variants.

Increased Affinity Between Variant RBD and hACE2

To determine the affinity between different variant RBD and hACE2, five RBD proteins (WT, Alpha, Beta, Delta, and Lambda) were fused with human IgG Fc and expressed in HEK293T cells (**Figure 2A**). SDS-PAGE gel electrophoresis showed that all RBD proteins were expressed in dimer form and the purity was more than 95% (**Figure 2B**). The affinity between different variant RBD and hACE2 receptors was measured by enzyme linked immunosorbent assays (ELISA). The results showed that the binding affinity of different variant RBDs to hACE2 receptors (Alpha: EC50 = 18.65 ng/ml; Beta: EC50 = 7.53 ng/ml; Delta: EC50 = 16.02 ng/ml; Lambda: EC50 = 27.19 ng/ml) were increased to varying degrees compared with that of WT RBD (WT: EC50 = 27.35 ng/ml) (**Figure 2C**). Particularly, Beta RBD has the highest affinity to hACE2 (3.6-fold compared to WT) among these variants.

Beta and Multivalent RBD Antigens Induce Broad Spectrum Neutralization Antibodies

We prepared five RBD proteins (WT, Alpha, Beta, Delta, Lambda) and immunized mice to obtain antiserums for evaluation of the cross-immune reaction against different

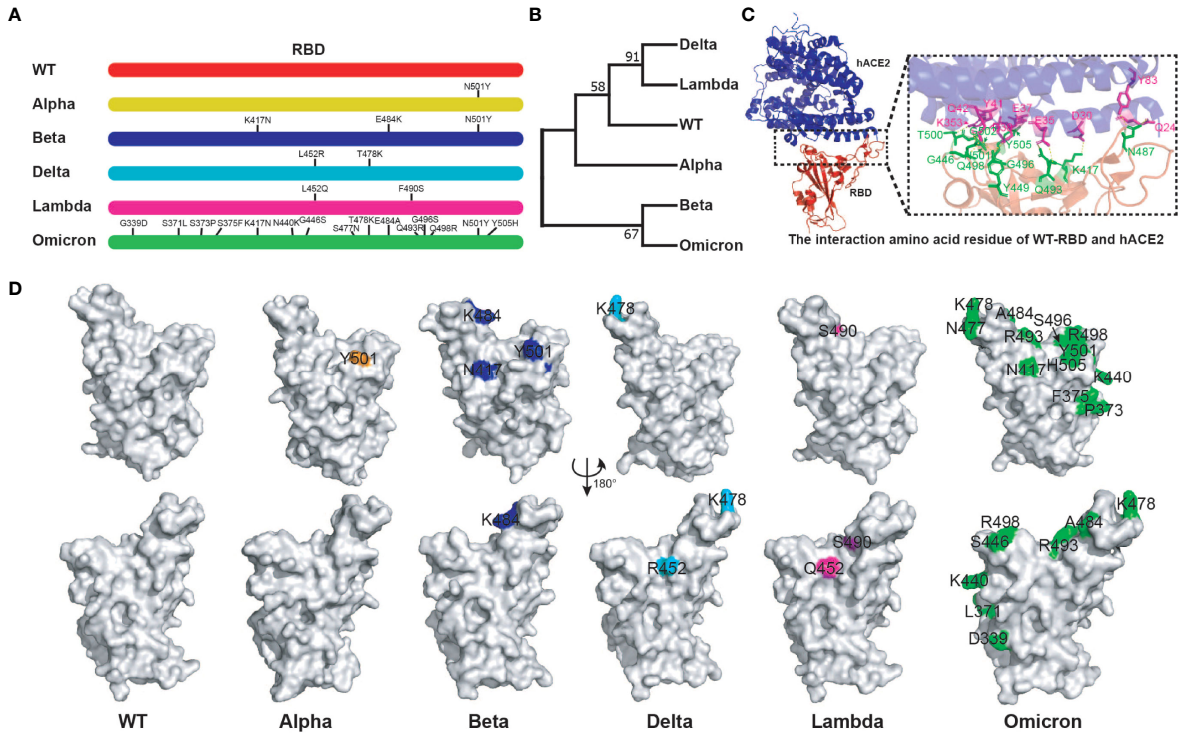

FIGURE 1 | Bioinformatics analysis of SARS-CoV-2 variant RBD. **(A)** The mutation sites of different variant RBDs. **(B)** The evolutionary trees of different variant RBDs. The phylogenetic tree was constructed using the maximum likelihood method within MEGA software (version 11.0). **(C)** The interaction amino acid residues of WT RBD with hACE2 (PDB:6MOJ). Green: RBD amino acid residue; Purple: hACE2 amino acid residue. The image was rendered in PyMOL (version 4.60). **(D)** The distribution of mutant amino acids on RBD structures of different variants. Source of protein crystal structure data from PDB database: WT (6MOJ), Alpha (7EDF), Beta (7PS4), Delta (7WBQ), and Omicron (7WBP). The crystal structure of Lambda RBD was constructed using Swiss-Model online tools. The image was rendered in PyMOL (version 4.60).

SARS-CoV-2 variants. Naive C57BL/6 mice (n=4) were immunized intramuscularly with monovalent or multivalent RBD antigens pre-bound to Alum-adjuvant. The priming and booster vaccinations were spaced at 3 weeks (**Figure 3A**). The immune dose was 10 μg each variant RBD protein per mouse for monovalent RBD antigen. Pentavalent RBD antigens were a 10 μg RBD protein mixture including each 2 μg variant RBD proteins. Blood samples were collected, and antiserum was separated at 3 weeks after the boost immunization. To detect the anti-RBD IgG antibody titers, the ELISA plates were coated with six different RBD protein respectively (WT, Alpha, Beta, Delta, Lambda, or Omicron). The OD value of each dilution is present in **Figures 3B–F**. In addition, there was no significant difference in the endpoint dilution of serum (IgG titers, ~ 10^5) among different monovalent and pentavalent RBD antigen-induced antibodies against different variant RBD proteins (**Figures 3G–K**), which might be attributable to the whole structures of RBDs from all the variants were not significantly changed compared to that of WT. Furthermore, the neutralization titers (NT_{50}) of the sera were measured using HIV-based pseudovirus neutralization assays. We observed that WT RBD antigen-induced antibodies showed a lower neutralizing activity against Beta, Delta, Lambda, and even Omicron pseudoviruses compared to neutralization against itself (**Figure 3L**). Immunization with WT RBD induced 26.8-fold lower neutralization titers against the Omicron pseudovirus compared to WT pseudovirus, indicating that the WT strain vaccine has lower cross-protective immunity against the Omicron variant. Similarly, Alpha (**Figure 3M**), Delta (**Figure 3O**), and Lambda (**Figure 3P**) RBD-induced antibodies exhibited high neutralizing titers against itself, but not against the Omicron variant. In contrast, Beta RBD antigen induced high neutralization antibodies against the Omicron variant (**Figure 3N**). Moreover, Beta RBD antigen (**Figure 3N**) and multivalent RBD antigen (**Figure 3Q**) induced broader cross-neutralization antibodies than other variant RBD antigens.

DISCUSSION

The SARS-CoV-2 variants have brought new challenges to the prevention and control of COVID-19 (42, 43). There is an urgent need for a universal vaccine that could protect people

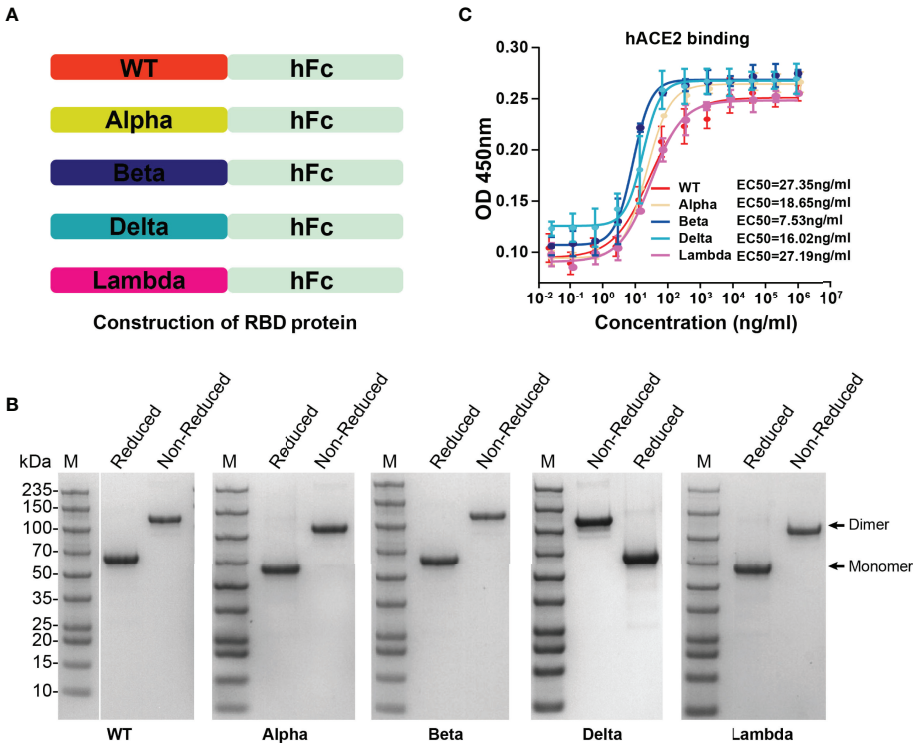

FIGURE 2 | The expression of SARS-CoV-2 variant RBD proteins and determination of affinity between variant RBD and hACE2. **(A)** The construction strategy of WT and variant RBD proteins. The RBD proteins were expressed in HEK293T cells by fusion of human IgG Fc tag in the form of secretion. **(B)** SDS-PAGE gel images of purified RBD proteins. **(C)** The ability of different variant RBDs to bind to hACE2 was test by ELISA. ELISA plate was coated with hACE2 protein (2 μg/ml). The fitted curves and half maximal effective concentration (EC50) were created using Graphpad software (version 8.0).

from multiple COVID-19 variants. He *et al.* developed a SARS-CoV-2 bivalent recombinant vaccine (WT and Beta) targeting the S1 protein, which induces neutralizing antibodies against both SARS-CoV-2 variants and wild-type of the virus (44). Another study showed that the SARS-CoV-2 mRNA bivalent vaccine (WT and Beta) produced a broad-spectrum neutralization response against WT, Beta, CAL.20C, and P1 variants (45). Here, we expressed the five different RBD proteins (WT, Alpha, Beta, Delta, Lambda) and evaluated their cross-neutralizing activity against different pseudoviruses. The results demonstrate that Beta RBD antigen induces broader cross-neutralization antibodies against WT, Alpha, Beta, Delta, Lambda, and Omicron variant pseudoviruses compared with other monovalent RBD antigens, which is supported by the observation that rVSV-S Beta elicits cross-reactive neutralizing antibodies against WT strain, Alpha, and Beta variants (46).

We noticed that the multivalent RBD antigen induces broader cross-neutralization antibodies and higher neutralization titers against Omicron compared to the monovalent antigens. This indicates that there might be conserved neutralizing epitopes between different RBD variants, and more antibodies against conserved neutralizing epitopes were generated after repeated immunization with RBD multivalent antigens. There were similar cases of flu vaccines; the chimeric influenza HA vaccine contains different HA heads and the same HA stem, and more antibodies against the stem region can be produced after multiple immunizations (47–50).

Current studies suggest that the Omicron variant vaccine is not the best choice against the Omicron variant. It does not produce high neutralization titer and broad-spectrum neutralization ability against itself and other variants (51, 52). Interestingly, among these monovalent RBD antigens, only Beta RBD antigen induces high neuralization titers against Omicron, which might be attributable to the similar mutation sites (**Figure 1A**) and antigen sequences (**Figure 1B**) of Beta and Omicron RBDs.

In summary, our results showed that the cross-protective immunity of WT strain SARS-CoV-2 RBD antigen against the currently circulating variants was significantly reduced. In contrast, Beta RBD and multivalent RBD antigens both induced broad spectrum neutralization antibodies compared with other monovalent RBD antigens. Therefore, it is necessary to update or develop new COVID-19 vaccines. This study provides a reference for vaccine strain selection and universal

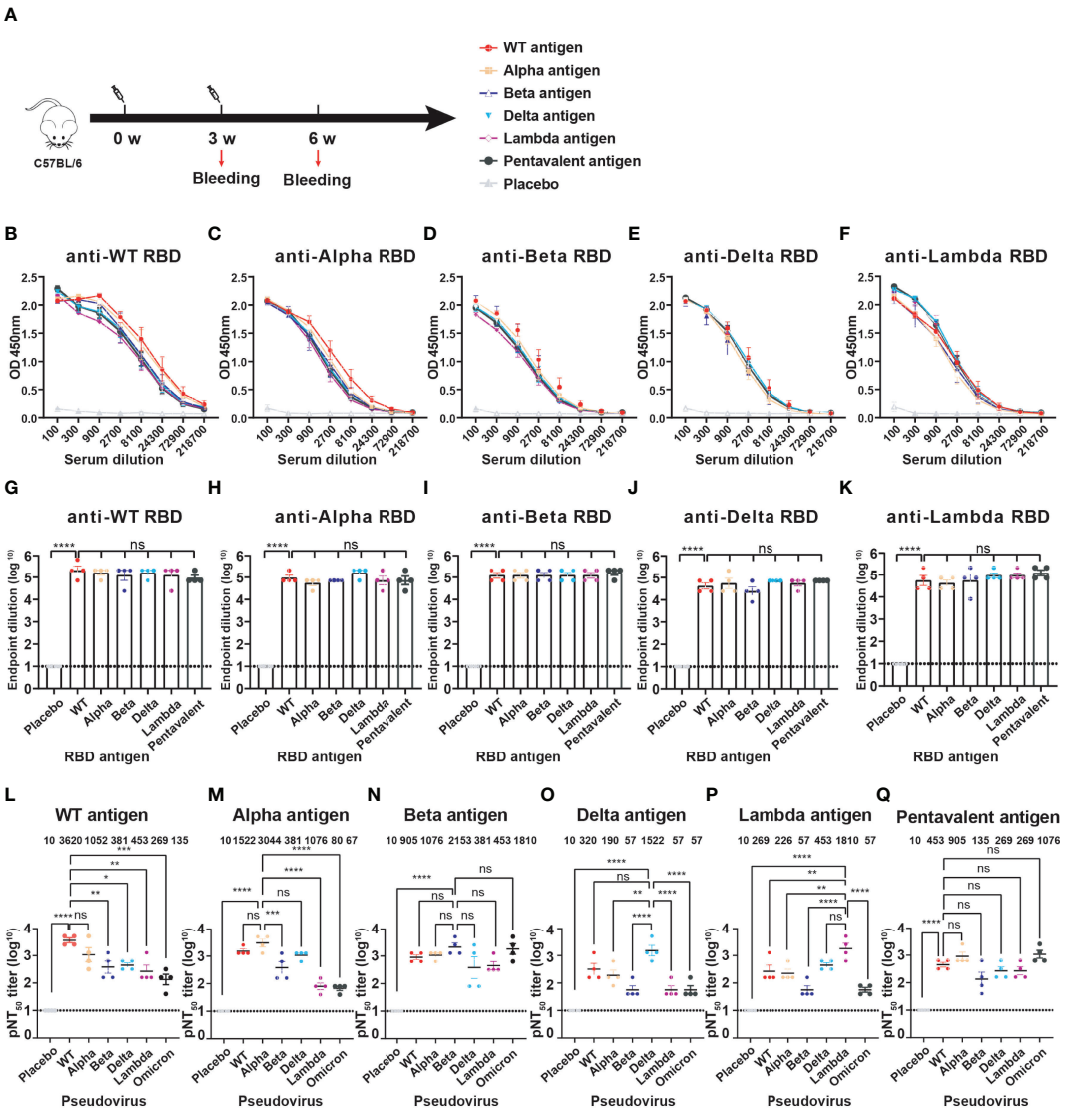

FIGURE 3 | The cross-immunity evaluation of different variant RBD antigens. **(A)** The diagram of the immune program of monovalent and multivalent RBD antigens. Naive C57BL/6 mice (n = 4) were muscularly immunized and bled at the indicated time points. The immune dose is 10 μg per mouse of each variant RBD protein; Pentavalent RBD antigens was a mixture of 2 μg each variant RBD protein. Mice immunized with PBS defined as placebo control. **(B–F)** Detection of the specific IgG against different SARS-CoV-2 variant RBDs by ELISA. Serum samples were collected after 3-week boost immunization. A placebo formulation was given as the control. **(G–K)** The endpoint dilution titers of anti-different variant RBD antibodies induced by different monovalent and pentavalent RBD antigens. **(L–Q)** Neutralizing titers of different variant RBD antigens against different variant pseudoviruses. The data are shown as the mean ± SEM. The dotted horizontal lines indicate the limits of quantification for endpoint dilution and NT_{50} titers. P values were determined by one-way ANOVA (ns, $p > 0.05$; *$p < 0.05$; **$p < 0.01$; ***$p < 0.001$; ****$p < 0.0001$).

COVID-19 vaccine design to fight the constant emergence of new SARS-CoV-2 variants.

DATA AVAILABILITY STATEMENT

The original contributions presented in the study are included in the article/supplementary material. Further inquiries can be directed to the corresponding authors.

ETHICS STATEMENT

The animal study was reviewed and approved by The Experimental Animal Ethics and Welfare Committee of IMCAS.

AUTHOR CONTRIBUTIONS

WL and LS initiated the project and supervised the project. LS, WL, and WS designed the experiments, analyzed the

data, and wrote the paper. WS performed the experiments; LH, HL, and WF helped with some experiments. GC and LY helped analyze the data and revised the manuscript. All authors contributed to the article and approved the submitted version.

FUNDING

This work was supported by grants from the Strategic Priority Research Program of Chinese Academy of Sciences (XDB29010000).

REFERENCES

1. Wu J, Liang B, Chen C, Wang H, Fang Y, Shen S, et al. Sars-Cov-2 Infection Induces Sustained Humoral Immune Responses in Convalescent Patients Following Symptomatic Covid-19. *Nat Commun* (2021) 12(1):1813. doi: 10.1038/s41467-021-22034-1
2. Lu X, Zhang L, Du H, Zhang J, Li YY, Qu J, et al. Sars-Cov-2 Infection in Children. *N Engl J Med* (2020) 382(17):1663–5. doi: 10.1056/NEJMc2005073
3. Helms J, Kremer S, Merdji H, Clere-Jehl R, Schenck M, Kummerlen C, et al. Neurologic Features in Severe Sars-Cov-2 Infection. *N Engl J Med* (2020) 382 (23):2268–70. doi: 10.1056/NEJMc2008597
4. Costiniuk CT, Jenabian M-A. Acute Inflammation and Pathogenesis of Sars-Cov-2 Infection: Cannabidiol as a Potential Anti-Inflammatory Treatment? *Cytokine Growth Factor Rev* (2020) 53:63–5. doi: 10.1016/j.cytogfr.2020.05.008
5. Cevik M, Kuppalli K, Kindrachuk J, Peiris M. Virology, Transmission, and Pathogenesis of Sars-Cov-2. *BMJ* (2020) 371:m3862. doi: 10.1136/bmj.m3862
6. Walls AC, Park YJ, Tortorici MA, Wall A, McGuire AT, Veesler D. Structure, Function, and Antigenicity of the Sars-Cov-2 Spike Glycoprotein. *Cell* (2020) 181(2):281–92.e6. doi: 10.1016/j.cell.2020.02.058
7. Lan J, Ge J, Yu J, Shan S, Zhou H, Fan S, et al. Structure of the SARS-CoV-2 Spike Receptor-Binding Domain Bound to the ACE2 Receptor. *Nature* (2020) 581(7807):215–20. doi: 10.1038/s41586-020-2180-5
8. Wrapp D, Wang N, Corbett KS, Goldsmith JA, Hsieh CL, Abiona O, et al. Cryo-Em Structure of the 2019-Ncov Spike in the Prefusion Conformation. *Science* (2020) 367(6483):1260–3. doi: 10.1126/science.abb2507
9. Huang Q, Ji K, Tian S, Wang F, Huang B, Tong Z, et al. A Single-Dose Mrna Vaccine Provides a Long-Term Protection for Hace2 Transgenic Mice From Sars-Cov-2. *Nat Commun* (2021) 12:776. doi: 10.1038/s41467-021-21037-2
10. Liu Z, Xu W, Xia S, Gu C, Wang X, Wang Q, et al. Rbd-Fc-Based Covid-19 Vaccine Candidate Induces Highly Potent Sars-Cov-2 Neutralizing Antibody Response. *Signal transduction targeted Ther* (2020) 5(1):282. doi: 10.1038/s41392-020-00402-5
11. Yang J, Wang W, Chen Z, Lu S, Yang F, Bi Z, et al. A Vaccine Targeting the Rbd of the S Protein of Sars-Cov-2 Induces Protective Immunity. *Nature* (2020) 586(7830):572–7. doi: 10.1038/s41586-020-2599-8
12. Chen WH, Strych U, Hotez PJ, Bottazzi ME. The Sars-Cov-2 Vaccine Pipeline: An Overview. *Curr Trop Med Rep* (2020) 7:61–4. doi: 10.1007/s40475-020-00201-6
13. Zhao X, Li D, Ruan W, Chen Z, Zhang R, Zheng A, et al. Effects of a Prolonged Booster Interval on Neutralization of Omicron Variant. *N Engl J Med* (2022) 386(9):894–6. doi: 10.1056/NEJMc2119426
14. Collier DA, De Marco A, Ferreira I, Meng B, Datir RP, Walls AC, et al. Sensitivity of Sars-Cov-2 B.1.1.7 to Mrna Vaccine-Elicited Antibodies. *Nature* (2021) 593(7857):136–41. doi: 10.1038/s41586-021-03412-7
15. Graham MS, Sudre CH, May A, Antonelli M, Murray B, Varsavsky T, et al. Changes in Symptomatology, Reinfection, and Transmissibility Associated With the Sars-Cov-2 Variant B.1.1.7: An Ecological Study. *Lancet Public Health* (2021) 6(5):e335–e45. doi: 10.1016/s2468-2667(21)00055-4
16. Edara VV, Norwood C, Floyd K, Lai L, Davis-Gardner ME, Hudson WH, et al. Infection- and Vaccine-Induced Antibody Binding and Neutralization of the B.1.351 Sars-Cov-2 Variant. *Cell Host Microbe* (2021) 29(4):516–21.e3. doi: 10.1016/j.chom.2021.03.009
17. Planas D, Bruel T, Grzelak L, Guivel-Benhassine F, Staropoli I, Porrot F, et al. Sensitivity of Infectious Sars-Cov-2 B.1.1.7 and B.1.351 Variants to Neutralizing Antibodies. *Nat Med* (2021) 27(5):917–24. doi: 10.1038/s41591-021-01318-5
18. Wang P, Nair MS, Liu L, Iketani S, Luo Y, Guo Y, et al. Antibody Resistance of Sars-Cov-2 Variants B.1.351 and B.1.1.7. *Nature* (2021) 593(7857):130–5. doi: 10.1038/s41586-021-03398-2
19. Zhang L, Li Q, Liang Z, Li T, Liu S, Cui Q, et al. The Significant Immune Escape of Pseudotyped Sars-Cov-2 Variant Omicron. *Emerging Microbes infect* (2022) 11(1):1–5. doi: 10.1080/22221751.2021.2017757
20. Sun W, He L, Zhang H, Tian X, Bai Z, Sun L, et al. The Self-Assembled Nanoparticle-Based Trimeric Rbd Mrna Vaccine Elicits Robust and Durable Protective Immunity Against Sars-Cov-2 in Mice. *Signal transduction targeted Ther* (2021) 6(1):1–11. doi: 10.1038/s41392-021-00750-w
21. Lippi G, Mattiuzzi C, Henry BM. Updated Picture of Sars-Cov-2 Variants and Mutations. *Diagnosis* (2022) 9(1):11–7. doi: 10.1515/dx-2021-0149
22. Tegally H, Wilkinson E, Giovanetti M, Iranzadeh A, Fonseca V, Giandhari J, et al. Detection of a Sars-Cov-2 Variant of Concern in South Africa. *Nature* (2021) 592(7854):438–43. doi: 10.1038/s41586-021-03402-9
23. Tang JW, Tambyah PA, Hui DS. Emergence of a New Sars-Cov-2 Variant in the Uk. *J infect* (2021) 82(4):e27–e8. doi: 10.1016/j.jinf.2020.12.024
24. Tao K, Tzou PL, Nouhin J, Gupta RK, de Oliveira T, Kosakovsky Pond SL, et al. The Biological and Clinical Significance of Emerging Sars-Cov-2 Variants. *Nat Rev Genet* (2021) 22(12):757–73. doi: 10.1038/s41576-021-00408-x
25. Baric RS. Emergence of a Highly Fit Sars-Cov-2 Variant. *N Engl J Med* (2020) 383(27):2684–6. doi: 10.1056/NEJMcibr2032888
26. Volz E, Mishra S, Chand M, Barrett JC, Johnson R, Geidelberg L, et al. Assessing Transmissibility of Sars-Cov-2 Lineage B.1.1.7 in England. *Nature* (2021) 593(7858):266–9. doi: 10.1038/s41586-021-03470-x
27. Supasa P, Zhou D, Dejnirattisai W, Liu C, Mentzer AJ, Ginn HM, et al. Reduced Neutralization of Sars-Cov-2 B. 1.1. 7 Variant by Convalescent and Vaccine Sera. *Cell* (2021) 184(8):2201–11. e17. doi: 10.1016/j.cell.2021.02.033
28. Laffeber C, de Koning K, Kanaar R, Lebbink JH. Experimental Evidence for Enhanced Receptor Binding by Rapidly Spreading Sars-Cov-2 Variants. *J Mol Biol* (2021) 433(15):167058. doi: 10.1016/j.jmb.2021.167058
29. Li Q, Nie J, Wu J, Zhang L, Ding R, Wang H, et al. Sars-Cov-2 501y. V2 Variants Lack Higher Infectivity But Do Have Immune Escape. *Cell* (2021) 184(9):2362–71. e9. doi: 10.1016/j.cell.2021.02.042
30. Nelson G, Buzko O, Spilman P, Niazi K, Rabizadeh S, Soon-Shiong P. Molecular Dynamic Simulation Reveals E484k Mutation Enhances Spike Rbd-Ace2 Affinity and the Combination of E484k, K417n and N501y Mutations (501y. V2 Variant) Induces Conformational Change Greater Than N501y Mutant Alone, Potentially Resulting in an Escape Mutant. *BioRxiv* (2021) 10.1101/2021.01.13.426558. doi: 10.1101/2021.01.13.426558
31. Zhou D, Dejnirattisai W, Supasa P, Liu C, Mentzer AJ, Ginn HM, et al. Evidence of Escape of Sars-Cov-2 Variant B. 1.351 From Natural and Vaccine-Induced Sera. *Cell* (2021) 184(9):2348–61. e6. doi: 10.1016/j.cell.2021.02.037
32. Han P, Li L, Liu S, Wang Q, Zhang D, Xu Z, et al. Receptor Binding and Complex Structures of Human Ace2 to Spike Rbd From Omicron and Delta Sars-Cov-2. *Cell* (2022) 185(4):630–40. doi: 10.1016/j.cell.2022.01.001
33. Carreño JM, Alshammary H, Singh G, Raskin A, Amanat F, Amoako A, et al. Evidence for Retained Spike-Binding and Neutralizing Activity Against Emerging Sars-Cov-2 Variants in Serum of Covid-19 Mrna Vaccine Recipients. *EBioMedicine* (2021) 73:103626. doi: 10.1016/j.ebiom.2021.103626
34. Planas D, Saunders N, Maes P, Guivel-Benhassine F, Planchais C, Buchrieser J, et al. Considerable Escape of Sars-Cov-2 Omicron to Antibody Neutralization. *Nature* (2022) 602(7898):671–5. doi: 10.1038/s41586-021-04389-z
35. Mlcochova P, Kemp SA, Dhar MS, Papa G, Meng B, Ferreira IATM, et al. Sars-Cov-2 B.1.617.2 Delta Variant Replication and Immune Evasion. *Nature* (2021) 599(7883):114–9. doi: 10.1038/s41586-021-03944-y
36. Tada T, Zhou H, Dcosta BM, Samanovic MI, Mulligan MJ, Landau NR. Sars-Cov-2 Lambda Variant Remains Susceptible to Neutralization by Mrna

Vaccine-Elicited Antibodies and Convalescent Serum. *BioRxiv* (2021) 10.1101/2021.07.02.450959. doi: 10.1101/2021.07.02.450959
37. Wang M, Zhang L, Li Q, Wang B, Liang Z, Sun Y, et al. Reduced Sensitivity of the Sars-Cov-2 Lambda Variant to Monoclonal Antibodies and Neutralizing Antibodies Induced by Infection and Vaccination. *Emerging Microbes infect* (2022) 11(1):18–29. doi: 10.1080/22221751.2021.2008775
38. Cameroni E, Bowen JE, Rosen LE, Saliba C, Zepeda SK, Culap K, et al. Broadly Neutralizing Antibodies Overcome Sars-Cov-2 Omicron Antigenic Shift. *Nature* (2021) 602(7898):664–70. doi: 10.1038/s41586-021-04386-2
39. Pulliam JR, van Schalkwyk C, Govender N, von Gottberg A, Cohen C, Groome MJ, et al. Increased Risk of Sars-Cov-2 Reinfection Associated With Emergence of the Omicron Variant in South Africa. *Science* (2022) 376(6593):eabn4947. doi: 10.1126/science.abn4947
40. Schmidt F, Muecksch F, Weisblum Y, Da Silva J, Bednarski E, Cho A, et al. Plasma Neutralization of the Sars-Cov-2 Omicron Variant. *N Engl J Med* (2021) 386(6):599–601. doi: 10.1056/NEJMc2119641
41. Nie J, Li Q, Wu J, Zhao C, Hao H, Liu H, et al. Establishment and Validation of a Pseudovirus Neutralization Assay for Sars-Cov-2. *Emerging Microbes infect* (2020) 9(1):680–6. doi: 10.1080/22221751.2020.1743767
42. Krause PR, Fleming TR, Longini IM, Peto R, Briand S, Heymann DL, et al. Sars-Cov-2 Variants and Vaccines. *N Engl J Med* (2021) 385(2):179–86. doi: 10.1056/NEJMsr2105280
43. Tian D, Sun Y, Zhou J, Ye Q. The Global Epidemic of Sars-Cov-2 Variants and Their Mutational Immune Escape. *J Med Virol* (2022) 94(3):847–57. doi: 10.1002/jmv.27376
44. He C, Yang J, He X, Hong W, Lei H, Chen Z, et al. A Bivalent Recombinant Vaccine Targeting the S1 Protein Induces Neutralizing Antibodies Against Both Sars-Cov-2 Variants and Wild-Type of the Virus. *MedComm* (2021) 2 (3):430–41. doi: 10.1002/mco2.72
45. Wu K, Choi A, Koch M, Elbashir S, Ma L, Lee D, et al. Variant Sars-Cov-2 Mrna Vaccines Confer Broad Neutralization as Primary or Booster Series in Mice. *Vaccine* (2021) 39(51):7394–400. doi: 10.1016/j.vaccine.2021.11.001
46. Ding LS, Zhang Y, Wen D, Ma J, Yuan H, Li H, et al. Growth, Antigenicity, and Immunogenicity of Sars-Cov-2 Spike Variants Revealed by a Live Rvsv-Sars-Cov-2 Virus. *Front Med* (2022) 8:2764–. doi: 10.3389/fmed.2021.793437
47. Ermler ME, Kirkpatrick E, Sun W, Hai R, Amanat F, Chromikova V, et al. Chimeric Hemagglutinin Constructs Induce Broad Protection Against Influenza B Virus Challenge in the Mouse Model. *J Virol* (2017) 91(12): e00286–17. doi: 10.1128/JVI.00286-17
48. Hai R, Krammer F, Tan GS, Pica N, Eggink D, Maamary J, et al. Influenza Viruses Expressing Chimeric Hemagglutinins: Globular Head and Stalk Domains Derived From Different Subtypes. *J Virol* (2012) 86(10):5774–81. doi: 10.1128/JVI.00137-12
49. Krammer F, Margine I, Hai R, Flood A, Hirsh A, Tsvetnitsky V, et al. H3 Stalk-Based Chimeric Hemagglutinin Influenza Virus Constructs Protect Mice From H7n9 Challenge. *J Virol* (2014) 88(4):2340–3. doi: 10.1128/JVI.03183-13
50. Krammer F, Pica N, Hai R, Margine I, Palese P. Chimeric Hemagglutinin Influenza Virus Vaccine Constructs Elicit Broadly Protective Stalk-Specific Antibodies. *J Virol* (2013) 87(12):6542–50. doi: 10.1128/JVI.00641-13
51. He C, He X, Yang J, Lei H, Hong W, Song X, et al. Spike Protein of Sars-Cov-2 Omicron (B.1.1.529) Variant Has a Reduced Ability to Induce the Immune Response. *Signal transduction targeted Ther* (2022) 7(1):119. doi: 10.1038/s41392-022-00980-6
52. Gagne M, Moliva JI, Foulds KE, Andrew SF, Flynn BJ, Werner AP, et al. Mrna-1273 or Mrna-Omicron Boost in Vaccinated Macaques Elicits Similar B Cell Expansion, Neutralizing Responses, and Protection From Omicron. *Cell* (2022) 185(9):15567–71.e18. doi: 10.1016/j.cell.2022.03.038

Conflict of Interest: The authors declare that the research was conducted in the absence of any commercial or financial relationships that could be construed as a potential conflict of interest.

Publisher's Note: All claims expressed in this article are solely those of the authors and do not necessarily represent those of their affiliated organizations, or those of the publisher, the editors and the reviewers. Any product that may be evaluated in this article, or claim that may be made by its manufacturer, is not guaranteed or endorsed by the publisher.

frontiers | Frontiers in Immunology

REVIEW
published: 15 June 2022
doi: 10.3389/fimmu.2022.855078

MIR4435-2HG Is a Potential Pan-Cancer Biomarker for Diagnosis and Prognosis

Chenming Zhong[1,2], *Zijun Xie*[2], *Ling-hui Zeng*[1], *Chunhui Yuan*[1*] *and Shiwei Duan*[1,2,3*]

[1] Department of Clinical Medicine, School of Medicine, Zhejiang University City College, Hangzhou, China, [2] Medical Genetics Center, School of Medicine, Ningbo University, Ningbo, China, [3] Institute of Translational Medicine, Zhejiang University City College, Hangzhou, China

The lncRNA MIR4435-2 host gene (MIR4435-2HG) is located on human chromosome 2q13, and its expression is up-regulated in 18 tumors. MIR4435-2HG participates in 6 signaling pathways to promote tumorigenesis, including the TGF-β signaling pathway, Wnt/β-catenin signaling pathway, MDM2/p53 signaling pathway, PI3K/AKT signaling pathway, Hippo signaling pathway, and MAPK/ERK signaling pathway. MIR4435-2HG competitively binds with 20 miRNAs to form a complex ceRNA network, thereby regulating the expression of downstream target genes. The high expression of MIR4435-2HG is also closely related to the clinicopathological characteristics and poor prognosis of a variety of tumors. Also, the high expression of MIR4435-2HG in peripheral blood or serum has the value of predicting the risk of 9 tumors. In addition, MIR4435-2HG participates in the mechanism of action of three cancer drugs, including resveratrol for the treatment of lung cancer, cisplatin for non-small cell lung cancer and colon cancer, and carboplatin for triple-negative breast cancer. This article systematically summarizes the diagnostic and prognostic value of MIR4435-2HG in a variety of tumors and outlines the ceRNA network and signaling pathways related to MIR4435-2HG, which will provide potential directions for future MIR4435-2HG research.

Keywords: MIR4435-2HG, cancer, competing endogenous RNA, diagnosis, prognosis

OPEN ACCESS

Edited by:
Lee Mark Wetzler,
Boston University, United States

Reviewed by:
Jun Ma,
University of Minnesota Twin Cities, United States
Hua Yang,
University of South Florida, United States

***Correspondence:**
Shiwei Duan
duansw@zucc.edu.cn
Chunhui Yuan
ch_yuan@zju.edu.cn

Specialty section:
This article was submitted to Vaccines and Molecular Therapeutics, a section of the journal Frontiers in Immunology

Received: *14 January 2022*
Accepted: *23 May 2022*
Published: *15 June 2022*

Citation:
Zhong C, Xie Z, Zeng L-h, Yuan C and Duan S (2022) MIR4435-2HG Is a Potential Pan-Cancer Biomarker for Diagnosis and Prognosis. Front. Immunol. 13:855078. doi: 10.3389/fimmu.2022.855078

INTRODUCTION

Long non-coding RNAs (lncRNAs) are transcripts longer than 200 nucleotides that can not be translated into proteins. With the rapid development of high-throughput sequencing technology, more and more lncRNAs have been reported to participate in tumor differentiation, stemness, migration, invasion, apoptosis, and proliferation (1).

The lncRNA MIR4435-2 host gene (MIR4435-2HG) is located on human chromosome 2q13, also known as lncRNA-AWPPH, LINC00978, and AK001796. In 2015, MIR4435-2HG was first discovered to be involved in the cell growth inhibition of resveratrol in lung cancer (2). At present, MIR4435-2HG has been proven to be an oncogenic lncRNA, and its abnormal up-regulation can promote the occurrence and development of 18 tumors. In addition, MIR4435-2HG is abnormally up-regulated in the blood of patients with at least 9 tumors, suggesting that MIR4435-2HG can be used as a non-invasive diagnostic marker for these 9 tumors.

Competitive endogenous RNA (ceRNA) can sponge miRNA to regulate downstream mRNA of miRNA (3). MIR4435-2HG is the ceRNA of 20 miRNAs, which can regulate many downstream genes. MIR4435-2HG participates in at least 6 signaling pathways, including TGF-β signaling pathway, Wnt/β-catenin signaling pathway, MDM2/p53 signaling pathway, PI3K/AKT signaling pathway, Hippo signaling pathway, and MAPK/ERK signaling pathway.

The abnormal up-regulation of MIR4435-2HG is closely related to the clinicopathological characteristics of 11 tumors, including tumor size, TNM stage, lymph node metastasis, etc. The high expression of MIR4435-2HG12 is associated with the poor prognosis of 12 tumors. In addition, MIR4435-2HG is related to the mechanism of action of cancer drugs, including resveratrol for the treatment of lung cancer (2), cisplatin for non-small cell lung cancer and colon cancer (4, 5), and carboplatin for triple-negative breast cancer (6).

There is no comprehensive overview related to MIR4435-2HG. Here, this article summarizes the diagnostic and prognostic value of MIR4435-2HG in tumors, clarifies its gene regulatory network, and discusses the future directions and challenges of MIR4435-2HG research.

ABNORMAL REGULATION AND BIOLOGICAL EFFECTS OF MIR4435-2HG IN CANCERS

Pan-Cancer Analysis of MIR4435-2HG Using TCGA Database

We downloaded the expression data of MIR4435-2HG in TCGA, TARGET, and GTEx of 32 cancer types from the UCSC Xena (https://xenabrowser.net/) database, and further performed log2 (x+1) transform for the expression data.

We compared the expression differences of MIR4435-2HG between normal and tumor samples in each cancer type using the unpaired Wilcoxon Test method of R software (version 4.1.1). As shown in **Figure 1A**, we observed significant upregulation of

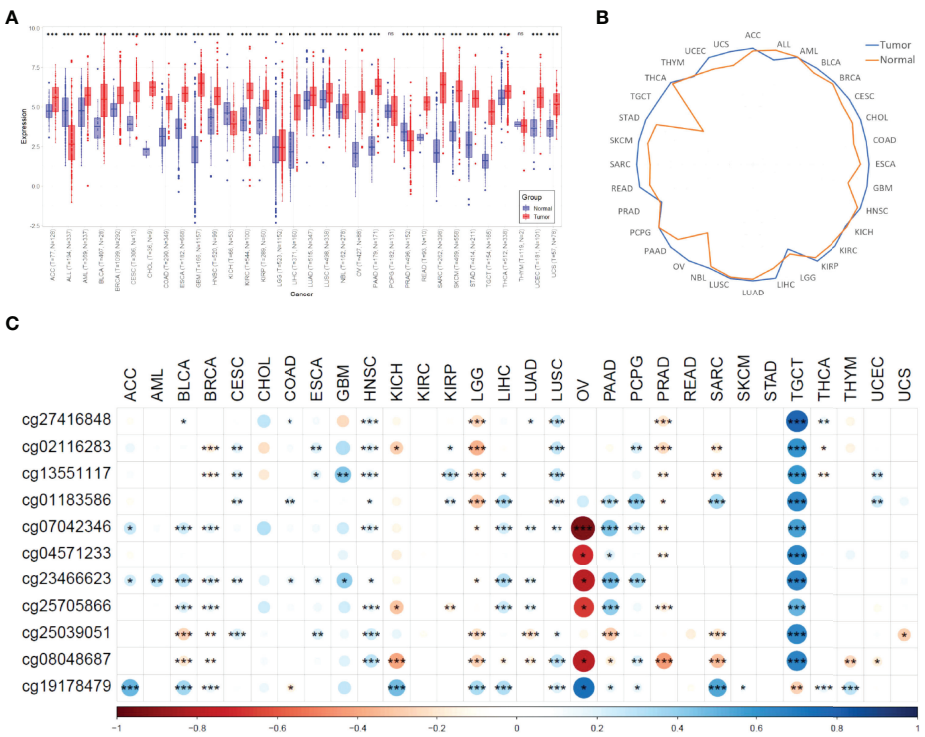

FIGURE 1 | A pan-cancer analysis of MIR4435-2HG. **(A)** MIR4435-2HG is dysregulated in 32 cancer types. (*** means $p < 0.001$, ** means $p<0.01$, * means $p<0.05$, ns means no significant difference); **(B)** quantile expression of MIR4435-2HG in 32 cancer types; **(C)** The correlation tests between MIR4435-2HG expression and methylation of MIR4435-2HG CpG sites (*** means $p<0.001$, ** means $p<0.01$, * means $p<0.05$). ACC, Adrenocortical carcinoma; ALL, Acute lymphoblastic leukemia; AML, Acute myeloid leukemia; BLCA, Bladder urothelial carcinoma; BRCA, Breast invasive carcinoma; CESC, Cervical squamous cell carcinoma and endocervical adenocarcinoma; CHOL, Cholangiocarcinoma; COAD, Colon adenocarcinoma; ESCA, Esophageal carcinoma; GBM, Glioblastoma multiforme; HNSC, Head and Neck squamous cell carcinoma; KICH, Kidney chromophobe; KIRC, Kidney renal clear cell carcinoma; KIRP, Kidney renal papillary cell carcinoma; LGG, Brain lower grade glioma; LIHC, Liver hepatocellular carcinoma; LUAD, Lung adenocarcinoma; LUSC, Lung squamous cell carcinoma; NBL, Neuroblastoma; OV, Ovarian serous cystadenocarcinoma; PAAD, Pancreatic adenocarcinoma; PCPG, Pheochromocytoma and Paraganglioma; PRAD, Prostate adenocarcinoma; READ, Rectum adenocarcinoma; SARC, Sarcoma; STAD, Stomach adenocarcinoma; SKCM, Skin cutaneous melanoma; TGCT, Testicular germ cell tumors; THCA, Thyroid carcinoma; THYM, Thymoma; UCEC, Uterine corpus endometrial carcinoma; UCS, Uterine carcinosarcoma.

MIR4435-2HG in 27 tumors, significant downregulation of MIR4435-2HG in 3 tumors (ALL, PRAD, and KICH), and no significant difference in 2 tumors (PCPG and THYM). In addition, we evaluated the median expression of MIR4435-2HG among all ncRNAs in 32 tumors and corresponding non-tumor tissues. As shown in **Figure 1B**, expression of MIR4435-2HG exceeded at least 75% of lncRNAs in all tumors, suggesting the value of MIR4435-2HG in pan-cancer.

Research Progress of MIR4435-2HG Related Studies

At present, MIR4435-2HG has been confirmed to be an oncogenic lncRNA of 18 cancers. These cancers involve the digestive, respiratory, reproductive, urinary, and nervous systems in humans (**Table 1**). Among them, the experimental results in most tumors were consistent with the bioinformatic analysis results, except for ALL and prostate cancer.

As shown in **Figure 2**, the expression of MIR4435-2HG is up-regulated in the five digestive system cancers. MIR4435-2HG is highly expressed in blood and tumor cell lines of oral squamous cell carcinoma (OSCC) (7), in tumor tissues and tumor cell lines of esophageal squamous cell carcinoma and hepatocellular carcinoma (8, 9, 18–23), and in serum, tumor tissues, and tumor cell lines of gastric cancer and colorectal cancer (1, 10–12, 14–17).

MIR4435-2HG is highly expressed in lung cancer tissues and tumor cell lines (2, 24–27, 29). Abnormal up-regulation of MIR4435-2HG was also detected in whole blood and serum of non-small cell lung cancer patients (27–30).

Among reproductive system cancers, MIR4435-2HG is highly expressed in tumor tissues and tumor cell lines of ovarian cancer (31–33), cervical cancer (34), and breast cancer (6, 35–37). In addition, MIR4435-2HG is highly expressed in prostate cancer cell lines and whole blood (38, 39), in serum and plasma of ovarian cancer patients (31, 32), and in plasma of triple negative breast cancer (TNBC) patients (6, 37).

In tumors of the urinary system, MIR4435-2HG is abnormally upregulated in cancer tissues and cancer cell lines of clear cell renal cell carcinoma and bladder cancer (3, 40, 41). In nervous system tumors, MIR4435-2HG is highly expressed in plasma, cancer tissues and cancer cell lines of glioma (42, 43), and in cancer tissues and cancer cell lines of glioblastoma (**Figure 3**) (44).

In addition, MIR4435-2HG was abnormally up-regulated in tissues and cell lines of osteosarcoma and head and neck squamous cell carcinoma (HNSC) and melanoma (45–48). MIR44435-2HG is highly expressed in childhood T-cell acute lymphoblastic leukemia (T-ALL) bone marrow and cell lines and nasopharyngeal carcinoma cell lines (**Figure 4**) (49, 50).

In the bioinformatics analysis of TCGA data, we analyzed tissue samples from prostate cancer and ALL. In experimental studies of prostate cancer, MIR4435-2HG expression was implicated in plasma and cell line samples (38, 39). In an experimental study of T-ALL, the expression of MIR4435-2HG was involved in the bone marrow and cell lines (49). Therefore, discrepancies in MIR4435-2HG results in prostate cancer and ALL may be due to sample differences. Further validation of the role of MIR4435-2HG in prostate cancer and ALL is required in the future.

The abnormal expression of MIR4435-2HG is closely related to cancer cell proliferation, apoptosis, invasion and migration. Cell cycle arrest can promote cell apoptosis and effectively inhibit cell proliferation (10). Inhibition of cell cycle progression is related to increased expression of genes that block the cell cycle and decreased expression of genes required for progression in G1, S, and M phases (2). p21 is a cyclin-dependent kinase (CDK) inhibitor, which is down-regulated in a variety of cancers. p21 can directly bind to kinases related to G1/S conversion and play a key role in cell cycle progression (21). In esophageal squamous cell carcinom (9), gastric cancer and hepatocellular carcinoma (12, 21), MIR4435-2HG knockdown can promote p21 expression. In addition, MIR4435-2HG knockdown can also reduce the expression of CCND1 and promote the cleavage of PARP and caspase-3 (12, 21). In gastric cancer and hepatocellular carcinoma (10–12, 20, 21), MIR4435-2HG knockdown can increase the proportion of G1 cells. In esophageal squamous cell carcinom (9), MIR4435-2HG knockdown can increase the ratio of G2/M-phase cells, decrease the ratio of S-phase cells, and promote cell apoptosis (**Figure 4**).

Epithelial-mesenchymal transition (EMT) usually induces the invasion and metastasis of cancer cells (24). EMT is essential in the early events of tumor cell metastasis. EMT can make cells more motile and aggressive, and it can confer cancer stem cell (CSC)-like traits on tumor cells (24). Transcription factors such as Snail1, SLUG, ZEB1, and TWIST1 can up-regulate the mesenchymal markers Vimentin and N-cadherin, and ultimately inhibit the expression of E-cadherin, a marker of epithelial status (24). In gastric cancer (10, 12), colorectal cancer (12), hepatocellular carcinoma (21), lung cancer (24), ovarian cancer (33), clear cell renal cell carcinoma (40), and HNSC (47), abnormal upregulation of MIR435-2HG can up-regulate the above-mentioned transcription factors, and ultimately promote the EMT process.

The Relationship Between the Methylation of MIR4435-2HG CpG Sites and the Expression of MIR4435-2HG

A study has shown that lncRNA expression can be activated by DNA hypomethylation in tumors (51). In glioma, Li et al. found that the up-regulation of MIR4435-2HG may be related to its abnormal methylation through HM450K methylation microarray data (52). Here, we systematically analyzed the correlation between the expression of MIR4435-2HG and the CpG methylation of MIR4435-2HG using the Pearson method. As shown in **Figure 1C**, the methylation of cg07042346 in OV was significantly reversely correlated with the expression of MIR4435-2HG ($r<-0.5$, $p<0.01$). However, in SARC and TGCT, the CpG sites of MIR4435-2HG were significantly positively correlated with the expression of MIR4435-2HG ($r>0.5$, $p<0.01$).

TABLE 1 | Expression level and biological functions of MIR4435-2HG in human cancers.

System	Tumor type	Sample size	Assessed cell lines	Animals	Expression	Related genes	Effect *in vitro*	Effect *in vivo*	Ref.
Digestive system	OSCC	Blood specimens of 44 OSCC patients and 38 healthy controls	OSCC (SCC25 (HPV negative) and SCC090 (HPV positive))		Upregulation	TGF-β1↑ E-cadherin↓	proliferation↑ migration↑ invasion↑		(7)
	ESCC	175 pairs of tissues			Upregulation				(8)
		50 pairs of tissues	ESCC (Eca-109 and TE-1)	6 BALB/c nude mice (5-week-old)	Upregulation	MDM2↑ p53↓ p21↓	proliferation↑ cell cycle↑ apoptosis↓		(9)
	GC	57 pairs of tissues	GC (SNU5, HGC-27, and SGC-7901); Normal (GES-1)	10 athymic BALB/c mice (3 to 4-week-old, male)	Upregulation	N-cadherin↑ Vimentin↑ MMP9↑ VEGF↑ α-SMA↑ MYC↑ β-catenin↑ CCND1↑ DSP↓ E-cadherin↓	proliferation↑ migration↑ invasion↑ cell cycle↑ EMT↑ apoptosis↓	tumor growth↑	(10)
		150 pairs of tissues	GC (BGC-823, AGS, SGC-7901, and MGC-803); Normal (GES-1)		Upregulation	miR-497-5p↓/NTRK3↑; CDK6↑ CDK4↑ CCND1↑ MYC↑ N-cadherin↑ Vimentin↑ MMP-9↑ MMP-3↑ MMP-2↑ Bcl-2↑ Mcl-1↑ E-cadherin↓ Bim↓ Bax↓	proliferation↑ migration↑ invasion↑ apoptosis↓		(11)
		72 pairs of tissues; Serum specimens of 50 GC patients and 50 healthy controls	GC (MGC-803, SGC-7901, BGC-823, and HGC-27); Normal (GES-1)	10 BALB/c nude mice (4-week-old, male)	Upregulation	TGF-β1↑ SMAD2↑ MMP9↑ Bcl-2↑ p21↓	proliferation↑ migration↑ invasion↑ cell cycle↑ EMT↑ apoptosis↓	tumor growth↑	(12)
		343 GC tissues and 30 normal tissues (from TCGA database); 60 pairs of tissues (from 18 patients)	GC (HGC-27, AGS, SGC-7901, and MGC-803); Normal (GES-1)	10 nude athymic mice (5 to 6-week-old, male)	Upregulation	miR-138-5p↓/Sox4↑; Vimentin fibronectin↑ Sox4↑ E-cadherin↓	proliferation↑ migration↑ invasion↑ EMT↑	tumor growth↑	(53)
		40 pairs of tissues	GC (HGC-27, BGC-823, SGC-7901, and MKN-45); Normal (GES-1)		Downregulation	miR-203a-3p↑/DKK2↓	proliferation↓ invasion↓		(13)
	CRC	90 pairs of tissues	CRC (HT29, SW620, LoVo, LS123, and HCT116); Normal (NCM460)	10 nude athymic BALB/c (nu/nu) mice (5-week-old, male)	Upregulation	miR-206-3p↓/YAP1↑; CTGF↑ AREG↑ Vimentin↑ Snail↑ Slug↑ Twist1↑ E-cadherin↓	proliferation↑ migration↑ invasion↑ EMT↑	tumor growth↑	(1)
		102 pairs of tissues	CRC (LoVo, SW620, SW480, LS174T, HCT116, and HT29); Normal (HUVEC)		Upregulation		proliferation↑ apoptosis↓		(14)
		70 pairs of tissues			Upregulation	β-catenin↑			(15)
	Colon cancer	Serum specimens of 46 colon cancer patients and 42 healthy controls			Upregulation	GLUT-1↑	proliferation↑		(16)
	COAD	86 pairs of tissues; Whole blood specimens of 86 patients and 56 healthy controls	Colorectal adenocarcinoma (HT-29, Hs 698.T, and SNU-C1)		Upregulation	TGF-β1↑	proliferation↑		(17)
	HCC	22 pairs of tissues	HCC (Huh7, SMMC7721, BEL-7402, and HepG2); Normal (LO2)	6 nude mice	Upregulation	miR-22-3p↓/YWHAZ↑	proliferation↑ migration↑ invasion↑	tumor growth↑	(18)
		64 pairs of tissues	HCC (SNU-398 and SNU-182)		Upregulation	miR-487a↑	proliferation↑		(19)

(Continued)

TABLE 1 | Continued

System	Tumor type	Sample size	Assessed cell lines	Animals	Expression	Related genes	Effect *in vitro*	Effect *in vivo*	Ref.
		49 pairs of tissues	HCC (SK-Hep1, Bel-7404, Huh7, Hep3B, and HepG2); Normal (LO2)	24 BALB/c nude mice (male)	Upregulation	ERK↑ p38↑ JNK↑	proliferation↑ cell cycle↑ apoptosis↓	tumor growth↑	(20)
		120 pairs of tissues (from GEO database); 33 pairs of tissues (from 33 patients); Serum specimens of 58 HCC patients, 49 liver benign disease patients and 45 healthy controls	HCC (7721, 7402, HepG2, and LM3); Normal (7702)	10 BALB/c nude mice (4-week-old, male)	Upregulation	EZH2↑ Bcl-2↑ CCND1↑ N-cadherin↑ Vimentin↑ Slug↑ Snail↑ Twist1↑ p21↓ E-cadherin↓	proliferation↑ migration↑ invasion↑ cell cycle↑ EMT↑ apoptosis↓	tumor growth↑ metastasis↑	(21)
		88 pairs of HCC tissues and 20 PVTT tissues	HCC (SMMC-7721, HCCLM3, Huh7, and HepG2); Normal (QSG-7701)	12 athymic BALB/c nude mice (male)	Upregulation	Snail1↑ PI3K↑	proliferation↑ migration↑	tumor growth↑ metastasis↑	(22)
		73 pairs of tissues	HCC (SMMC-7721, Huh-7, MHCC-97H, and MHCC-97L); Normal (LO2)		Upregulation		proliferation↑ invasion↑		(23)
Respiratory system	LC	52 pairs of tissues	Lung cancer (A549, H1770, H596, H1975, H1650, and H1299); Normal (16HBE)	2 athymic BALB/c nude mice (4 to 6-week-old, female)	Upregulation	N-cadherin↑ Vimentin↑ N-Twist1↑ E-cadherin↓	proliferation↑ migration↑ invasion↑ EMT↑ cancer stem cell traits↑	tumor growth↑ metastasis↑	(24)
		42 pairs of tissues	Lung cancer (A549 and H446); Normal (BEAS2B and 16HBE)	16 BALB/c nude mice (5-week-old)	Upregulation		proliferation↑ cell cycle↑	tumor growth↑	(2)
	NSCLC	39 pairs of tissues	NSCLC (H1299, H1650, A549, and PC9); Normal (16HBE)		Upregulation	miR-6754-5p↓	proliferation↑ migration↑ invasion↑ apoptosis↓		(25)
		Number not shown	Lung cancer (A549, NCI-H1650, and HCC827); Normal (HBE)		Upregulation	miR-204-5p↓/CDK6↑	proliferation↑ migration↑ invasion↑		(26)
		Lung tissues and serum specimens of 138 NSCLC patients and 32 healthy controls	NSCLC (H1581 and H1993); Normal (NuLi-1)		Upregulation	TGF-β1↑	migration↑ invasion↑		(27)
		Blood specimens of 128 NSCLC patients and 30 healthy controls	NSCLC (H1993 and H2170); Normal (IMR-90)		Upregulation	TGF-β1↑	migration↑ invasion↑		(28)
		88 pairs of tissues; Serum specimens of 88 NSCLC patients and 88 healthy controls	NSCLC (NCI-H23 and NCI-H522); Normal (WI-38)		Upregulation	β-catenin↑	proliferation↑ apoptosis↓		(29)
		Blood specimens of 26 SCLC patients, 29 patients NSCLC patients, and 32 healthy controls	Lung cancer (H1770, A549, H1975, H596, H1299, and H1650); Normal (BEAS2B)		Upregulation	TGF-β1↑	proliferation↑ migration↑		(30)
Reproductive system	OC	58 pairs of tissues; Serum specimens of 58 OC patients and 46 healthy controls	OC (UWB1.289 and UWB1.289 +BRCA1)		Upregulation	β-catenin↑	proliferation↑ migration↑ invasion↑		(31)
			OC (UWB1.289 and UWB1.289 +BRCA1)		Upregulation	TGF-β1↑	migration↑ invasion↑		(32)

(Continued)

TABLE 1 | Continued

System	Tumor type	Sample size	Assessed cell lines	Animals	Expression	Related genes	Effect *in vitro*	Effect *in vivo*	Ref.
		23 pairs of tissues; Plasma specimens of 66 OC patients and 54 healthy controls							
		42 pairs of tissues	OC (SKOV3, Caov-3, A2780, and OVCAR3); Normal (ISOE80)	6 BALB/c nude mice (4-week-old, female)	Upregulation	miR-128-3p↓/CKD14↑; Bcl-2↑ Vimentin↑ E-cadherin↓	proliferation↑ migration↑ invasion↑ EMT↑ apoptosis↓	tumor growth↑	(33)
	CC	306 CESC and 13 normal tissues (from TCGA database); 59 pairs of tissues (from 59 patients)	CC (siha/hela); Normal (HCerEpiC)		Upregulation	miR-128-3p↓/MSI2↑	proliferation↑ migration↑ invasion↑		(34)
	BC	1085 breast cancer tissues and 112 normal tissues (from GEPIA database)	Breast cancer (MDA-MB-231 MCF-7); Normal (MCF-10A)		Upregulation	β-catenin↑ N-cadherin↑ Vimentin↑ ZEB1↑ Bcl2↑ PCNA↑ E-cadherin↓ Bax↓	proliferation↑ migration↑ invasion↑ apoptosis↓		(35)
		195 breast cancer patients; 36 pairs of tissues	Breast cancer (T47D, ZR751, MCF-7, MDA-MB-453, BCAP37, ZR7530, MDA-MB-436, SKBR3, MDA-MB-468, MDA-MB-231, MDA-MB-231HM, and BT549); Normal (MCF10A)		Upregulation				(36)
	TNBC	68 pairs of tissues; Plasma specimens of 68 TNBC patients and 62 healthy controls	TNBC (MDA-MB-231 and BT-20)		Upregulation	FZD7↑	proliferation↑		(37)
		Plasma specimens of 72 TNBC patients 44 healthy controls	TNBC (MDA-MB-231 and BT-20)		Upregulation		proliferation↑		(6)
	PCa	Blood specimens of 68 PCa patients and 62 healthy controls	PCa (22Rv1)		Upregulation	TGF-β1↑	migration↑ invasion↑		(38)
			PCa (VCaP, LNCaP, DU145, and PC-3); Normal (WPMY-1)	20 nude mice were (6 to 8-week-old, male)	Upregulation	ST8SIA1↑ β-catenin↑ MYC↑ CCND1↑	proliferation↑ migration↑ invasion↑	tumor growth↑	(39)
Urinary system	ccRCC	40 pairs of tissues	ccRCC (786-O, 769-P, Caki-1, Caki-2, ACHN, and A498); Normal (HK-2)	3 BALB/c (nu/nu) nude mice (4 to 6-week-old, female)	Upregulation	miR-513a-5p↓/KLF6↑	proliferation↑ invasion↑	tumor growth↑	(3)
		118 pairs of tissues	ccRCC (786-O and OSRC-2); Normal (HK-2)	16 athymic nude mice (6-week-old, male)	Upregulation	PC↑	proliferation↑ migration↑ invasion↑ cell cycle↑ EMT↑ apoptosis↓		(40)
	BCa	60 pairs of tissues	BCa (T24, J82, UMUC3, and 5637); Normal (SV-HUC-1)		Upregulation	miR-4288-3p↓	proliferation↑ migration↑ invasion↑		(41)
Nervous system	Glioma	Plasma specimens of 34 metastatic glioma patients, 32 non-metastatic	Glioma (Hs 683 and CCD-25Lu)		Upregulation	HIF1α↑	migration↑ invasion↑		(42)

(Continued)

TABLE 1 | Continued

System	Tumor type	Sample size	Assessed cell lines	Animals	Expression	Related genes	Effect *in vitro*	Effect *in vivo*	Ref.
		glioma patients, and 42 healthy controls							
		48 glioma tissues; Plasma specimens of 22 metastatic glioma patients, 26 non-metastatic glioma patients, and 38 healthy controls	Glioma (Hs 683 and CCD-25Lu)		Upregulation	TGF-β1↑	migration↑ invasion↑		(43)
	GBM	163 GBM tissues and 207 normal tissues (from GEPIA database); 40 pairs of tissues (from 40 patients)	GBM (LN229, U87MG, U87, and U251); Normal human astrocytes (NHAs)	10 athymic BALB/c mice (4 to 5-week-old, male)	Upregulation	miR-1224-5p↓/TGFBR2↑	proliferation↑ invasion↑	tumor growth↑	(44)
Others	Osteosarcoma	36 pairs of tissues	Osteosarcoma (U2OS, SAOS2, HOS, and 143B); Normal (hFOB 1.19)		Upregulation	miR-93-3p↓/FZD7↑, MYC↑ SOX4↑ CCND1↑	proliferation↑ migration↑ invasion↑		(45)
		30 pairs of tissues	Osteosarcoma (MG-63 and U2OS); Normal (hFOB1.19)		Upregulation	Bcl-2↑ Bax↓	proliferation↑ migration↑ invasion↑ apoptosis↓		(46)
	HNSC	519 HNSCC tissues and 44 normal tissues (from GEPIA database); 18 pairs of tissues (from 18 patients)	HNSCC (CAL27 and SCC25)	10 BALB/c nude mice (4-week-old)	Upregulation	miR-383-5p↓/RBM3↑, Vimentin ↑ E-cadherin↓	proliferation↑ migration↑ invasion↑ EMT↑	tumor growth↑	(47)
	Melanoma	28 pairs of tissues	Melanoma (A375 and A2058); Normal (HEMa-LP)		Upregulation	miR-802-5p↓/FLOT2↑	proliferation↑ migration↑ invasion↑		(48)
	T-ALL	Bone marrow with malignant cells of 32 pediatric T-ALL patients and 32 healthy controls	T-ALL (Loucy)		Upregulation	ROCK2↑	proliferation↑ apoptosis↓		(49)
	NPC		NPC (5-8F, CNE1, CNE2, and HONE1); Normal (HNEpC)		Upregulation	LSD1 (in cytoplasm)↑ PTEN (in nucleus)↓	proliferation↑ migration↑ apoptosis↓		(50)

OSCC, oral squamous cell carcinoma; ESCC, esophageal squamous-cell carcinoma; GC, gastric cancer; CRC, colorectal cancer; COAD, Colon adenocarcinoma; HCC, hepatocellular carcinoma; PVTT, portal vein tumor thrombus; LC, lung cancer; SCLC small cell lung cancer; NSCLC, nonsmall cell lung cancer; OC, ovarian cancer; CC, cervical cancer; BC, breast cancer; TNBC, triple-negative breast cancer; PCa, prostate carcinoma; ccRCC, clear cell renal cell carcinoma; BCa, bladder cancer; GBM, glioblastoma; HNSC, head and neck squamous cell carcinoma; T–ALL, T–cell acute lymphoblastic leukemia; NPC, nasopharyngeal carcinoma.
↑, Promotion; ↓, Inhibition.

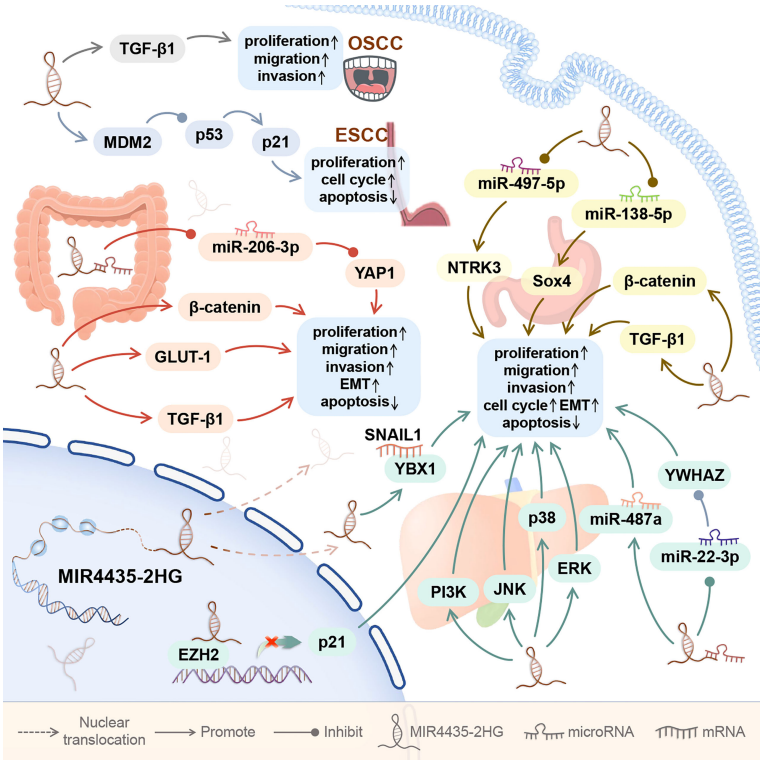

FIGURE 2 | The role of MIR4435-2HG in digestive system cancer. In the digestive system, MIR4435-2HG can promote the growth of 5 types of tumors, including oral squamous cell carcinoma (OSCC), esophageal squamous cell carcinoma (ESCC), hepatocellular carcinoma (HCC), gastric cancer (GC), and colorectal cancer (CRC). By regulating downstream genes, MIR4435-2HG can affect tumor cell proliferation, migration, invasion, apoptosis, EMT, and cell cycle.

THE SIX SIGNALING PATHWAYS RELATED TO MIR4435-2HG IN CANCERS

The oncogenic effect of MIR4435-2HG is related to the regulation of six signaling pathways, including the TGF-β signaling pathway, Wnt/β-catenin signaling pathway, MDM2/p53signalling pathway, PI3K/AKT signaling pathway, Hippo signaling pathway, and MAPK/ERK signaling pathway (**Figure 5**).

The TGF-β Signaling Pathway

Transforming growth factor β (TGF-β) can bind to cell surface receptors and trigger the activation of multiple signal transduction pathways (54). In the early stage of the tumor, TGF-β can inhibit the proliferation of cancer cells, and TGF-β can promote tumor metastasis in the late stage of the tumor (55). In ovarian cancer, TGF-β targeted therapy needs to be carried out cautiously according to the cancer stage (32). The activation of the TGF-β signaling pathway is widely present in the development of tumors (17).

Overexpression of MIR4435-2HG can up-regulate TGF-β1 and promote the metastasis of 7 kinds of tumors, including oral squamous cell carcinoma (OSCC) (7), gastric cancer (12), colorectal adenocarcinoma (17), and non-small cell lung cancer (27, 28, 30), ovarian cancer (32), prostate cancer and glioma (38, 43). In addition, in OSCC and colorectal adenocarcinoma (7, 17), the up-regulation of MIR4435-2HG and TGF-β1 expression can promote tumor growth and metastasis. TGF-β is the main regulator of EMT and a key marker for the metastasis and progression of different malignant tumors (56). In gastric cancer and non-small cell lung cancer (12, 27), the upregulation of MIR4435-2HG and TGF-β1 can promote the EMT of tumor cells. In non-small cell lung cancer, the up-regulation of MIR4435-2HG and TGF-β1 is also closely related to postoperative tumor recurrence (28).

In OSCC (7), non-small cell lung cancer (27, 28, 30), ovarian cancer (32), prostate cancer (38), and glioma (43), the expression levels of MIR4435-2HG and TGF-β1was positively correlated with each other, while no correlation between MIR4435-2HG and TGF-β1 was found in plasma of healthy persons. Overexpression of MIR4435-2HG can up-regulate the expression of TGF-β1, while exogenous TGF-β1 treatment has no effect on the expression of MIR4435-2HG. In gastric cancer (10), colorectal cancer (15), lung cancer (24, 29), ovarian cancer (31), breast cancer (35), and osteosarcoma (45), the overexpression of MIR4435-2HG can increase β-catenin and promote tumorigenesis. β-catenin has been shown to interact with TGF-β (57). Therefore, β-catenin may mediate the interaction between MIR4435-2HG and TGF-β1 (32, 38, 43), but this still needs further research and verification.

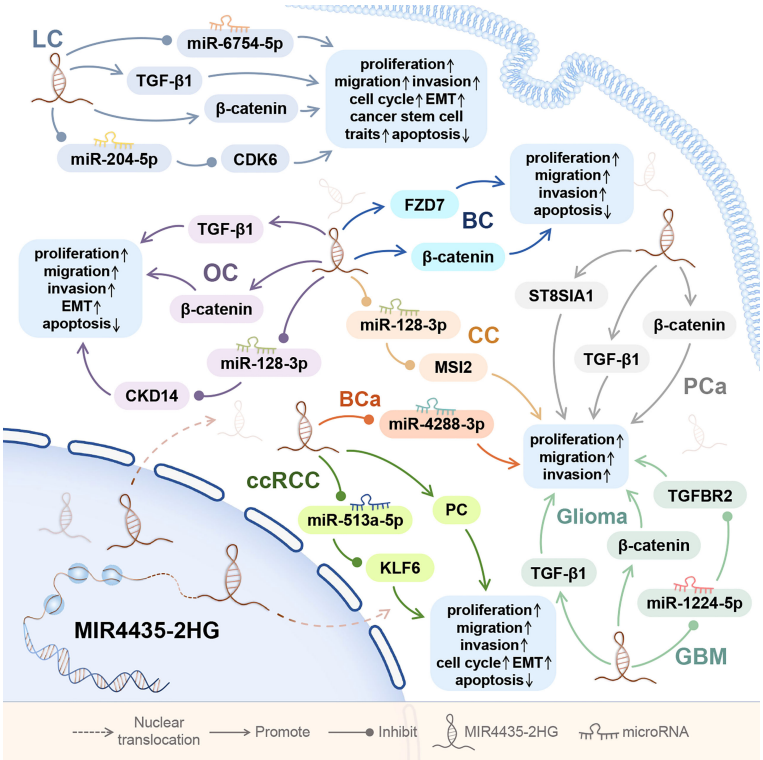

FIGURE 3 | The role of MIR4435-2HG in tumors of the respiratory system, reproductive system, urinary system, and nervous system. MIR4435-2HG can also affect the proliferation, migration, invasion, apoptosis, EMT, and cell cycle of tumor cells by regulating downstream genes. Tumor of the respiratory system consists of lung cancer (LC); Tumors of the reproductive system consist of ovarian cancer (OC), cervical cancer (CC), breast (BC), and prostate cancer (PCa); Tumors of the urinary system include clear cell renal cell carcinoma (ccRCC) and bladder cancer (BCa); and tumor of the nervous system includes gliomas.

The Wnt/β-Catenin Signaling Pathway

β-catenin is located in the cell nucleus, and by controlling gene transcription, it can promote canceration and cancer cell metastasis, and induce cancer cell stemness and drug resistance (15, 24). β-catenin is a well-known oncogene and plays a key role in regulating the Wnt signaling pathway. The Wnt/β-catenin signaling pathway plays a key role in the growth of a variety of tumors (58). The increased cytoplasmic β-catenin content is a sign of the abnormal activation of Wnt/β-catenin pathway. β-catenin plays a key role in regulating the Wnt signaling pathway, and it controls the transcription of target genes in the nucleus (15).

In stomach cancer (10), colorectal cancer (15), lung cancer (24, 29), ovarian cancer (31), breast cancer and osteosarcoma (35, 37, 45), MIR4435-2HG can up-regulate the expression of β-catenin proportionally. In gastric cancer, desmoplakin (DSP) is the most abundant desmosomal protein. MIR4435-2HG can bind to DSP and inhibit DSP and its cascade reaction, thereby activating Wnt/β-catenin signal transduction, promoting tumor growth, metastasis, and EMT (10).

In lung cancer, MIR4435-2HG up-regulates β-catenin, promotes tumor growth, metastasis and EMT both *in vivo* and *in vitro*, and maintains the stemness of cancer cells (24). In non-small cell lung cancer, MIR4435-2HG can up-regulate β-catenin to promote cell proliferation and inhibit cell apoptosis (29). In ovarian cancer, overexpression of MIR4435-2HG significantly promotes the expression of β-catenin and promotes the growth, invasion, and migration of tumor cells (31). In addition, in breast cancer, MIR4435-2HG promotes tumor growth, invasion, metastasis, and EMT by activating Wnt/β-catenin signal transduction, and inhibits cell apoptosis (35); meanwhile, MIR44352HG knockdown can decreases the expression of total and nuclear β-catenin, reduces the expression of anti-apoptotic marker (Bcl2), proliferation marker (PCNA), and mesenchymal markers (N-cadherin, vimentin, and ZEB1), upregulates the cleaved PARP and the epithelial marker (E-cadherin), and activate caspase 3 and Bax of the apoptotic pathway (35).

Frizzled family receptor 7 (FZD7) is a Wnt signaling receptor, which is involved in the maintenance of cancer cell stemness and cancer progression. In triple-negative breast cancer (TNBC), overexpression of MIR4435-2HG promotes frizzled homolog 7 (FZD7) expression in cells, thereby activating the Wnt/β-catenin signaling pathway (37). In osteosarcoma, through the miR-93-3p/FZD7 axis, MIR4435-2HG can also up-regulate FZD7 and activate the Wnt/β-catenin signaling pathway, thereby promoting the proliferation, invasion, and migration of osteosarcoma cells (45). In addition, in prostate cancer tissues and cells, MIR4435-2GH increases the expression levels of β-catenin, p-FAK, p-AKT, c-MYC, and CCND1 by up-regulating ST8SIA1 (39).

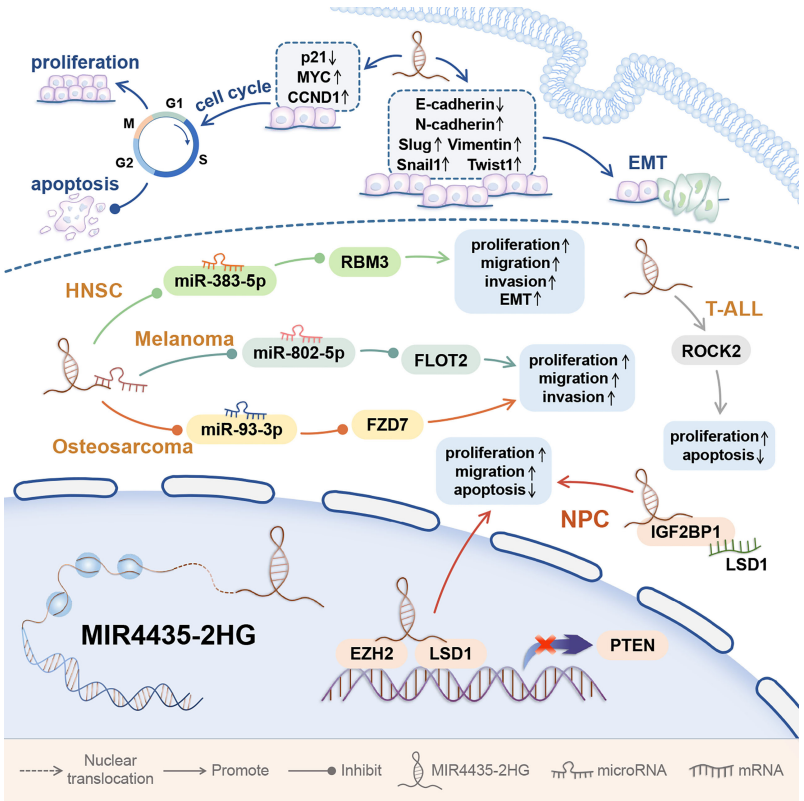

FIGURE 4 | The mechanism of MIR4435-2HG affecting the behavior of tumor cells in other Systems. MIR4435-2HG can promote the progression of tumors in other systems, and affect the proliferation, invasion, migration, apoptosis, and EMT of tumor cells. Affecting EMT and cell cycle is an important mechanism for MIR4435-2HG to promote tumorigenesis. Head and neck squamous cell carcinoma (HNSC); T-cell acute lymphoblastic leukemia (T-ALL); nasopharyngeal carcinoma (NPC).

In the above tumors, MIR4435-2HG can promote the expression of β-catenin, but the activation of Wnt/β-catenin signal transduction has no effect on the expression of MIR4435-2HG. Therefore, MIR4435-2HG is an upstream activator of the Wnt/β-catenin signaling pathway, which plays a role in the occurrence and development of cancer.

The MDM2/p53 Signaling Pathway

MDM2/p53 is one of the important signaling pathways, which can regulate cell growth and cell cycle (59). Mouse double minute 2 (MDM2) is an E3 ubiquitin ligase, which not only inhibits the transcriptional activity of p53, but also promotes the ubiquitination and degradation of p53 (9). p53 is an important tumor suppressor, which is activated in response to various stresses, thereby promoting cell apoptosis (9).

In esophageal squamous cell carcinoma tissues, both MIR4435-2HG and MDM2 were significantly up-regulated. Knockdown of MIR4435-2HG resulted in G2/M phase arrest in esophageal squamous cell carcinom cell lines (Eca-109 and TE-1), as well as decreased expression of MDM2, and increased expression of downstream p53 and p21 (9). The above shows that MIR4435-2HG promotes cell proliferation and cell cycle and inhibits cell apoptosis by regulating the MDM2/p53 signaling pathway.

The PI3K/AKT Signaling Pathway

When PI3K binds to growth factor receptors such as EGFR, RAS and PTEN, it can change the protein structure of AKT and activate AKT and its downstream effectors, thereby regulating cell proliferation, differentiation, apoptosis, and migration (60). The PI3K/AKT pathway is involved in the occurrence and development of a variety of cancers (60).

In the nucleus of hepatocellular carcinoma (HCC) cells, the interaction between MIR4435-2HG and the DNA binding protein Y-box binding protein 1 (YBX1) can enhance the binding of YBX1 to the PI3K promoter, thereby promoting the transcription of PI3K. MIR4435-2HG can activate the PI3K/AKT pathway, promote the proliferation and migration of HCC cells, and promote tumor growth and metastasis in mice. In the cytoplasm of HCC, MIR4435-2HG can interact with YBX1, up-regulate Snail1, and promote tumor progression (22). In prostate cancer tissues and cell lines, MIR4435-2HG promotes ST8SIA1 and up-regulates p-AKT levels (39).

In osteosarcoma cell lines (MG-63 and U2OS), MIR4435-2HG can up-regulate the protein levels of p-PI3K and p-AKT, suggesting that MIR4435-2HG may activate the PI3K/AKT pathway to promote the growth of osteosarcoma cells, Invasion, migration and apoptosis (46).

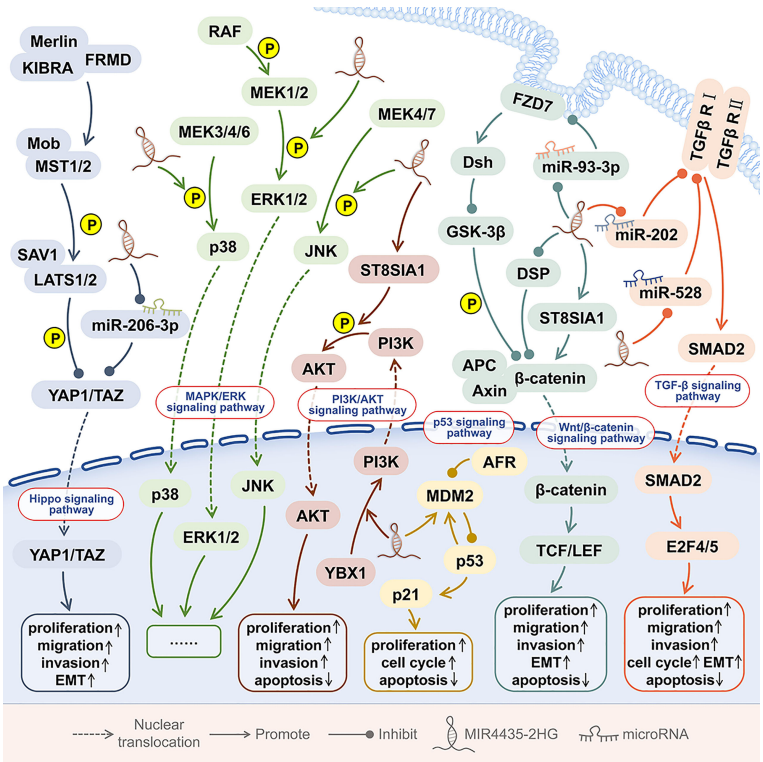

FIGURE 5 | The signaling pathways involved in MIR4435-2HG. In human tumors, MIR4435 participates in at least 6 signaling pathways, including the TGF-β signaling pathway, Wnt/β-catenin signaling pathway, MDM2/p53 signaling pathway, PI3K/AKT signaling pathway, Hippo signaling pathway, and MAPK/ERK signaling pathway.

The Hippo Signaling Pathway

YAP1 is a Hippo signaling pathway gene, which is amplified in a variety of human cancers (61). YAP1 is a transcriptional regulator that is widely activated in human malignancies and can induce the proliferation, metastasis, stemness and chemotherapy resistance of cancer cells (61). In colorectal cancer, MIR4435-2HG binds miR-206-3p to up-regulate downstream YAP1 expression. MIR4435-2HG promotes the proliferation, invasion, migration and EMT of colorectal cancer cells by activating the Hippo signaling pathway, and promotes tumor growth *in vivo* (1).

The MAPK/ERK Signaling Pathway

The MAPK/extracellular signal-regulated kinase (ERK) signaling pathway is highly conserved. The MAPK/ERK signaling pathway involves a variety of biological events, including metabolic reprogramming, cell proliferation, survival, and differentiation (62). In the MAPK/ERK signaling pathway, mutations and dysfunctions of key genes are very common events in various human malignancies (62). In HCC cells, MIR4435-2HG can promote the phosphorylation of ERK, p38, and c-Jun N-terminal kinase (JNK), and activate the MAPK/ERK signaling pathway, thereby promoting HCC cell proliferation, cell cycle progression, and survival (20).

THE CERNA NETWORK OF MIR44350-2HG

The competing endogenous RNA (ceRNA) hypothesis describes that lncRNA and mRNA may bind to the same miRNA through their miRNA response element (MRE) (52). lncRNAs and miRNAs are the two main subgroups of ncRNAs, and both have been shown to be key players in cancer biology (19).

Here, this article outlines the ceRNA network centered on MIR4435-2HG and its biological significance (**Figure 6**). MIR4435-2HG can be used as the ceRNA of 20 miRNAs, 19 of which are found in 14 cancers, including miR-22-3p (18), miR-206-3 (1), miR-296-5p (1), miR-497-5p (11), miR-138-5p (53), miR-203a-3p (13), miR-6754-5p (25), miR-204-5p (26), miR-528 (30), miR-202 (30), miR-125a-5p (52), miR125b-5p (52), miR-1224-5p (44), miR-4288-3p (41), miR-513a-5p (3), miR-128- 3p (33), miR-93-3p (45), miR-802-5p (48), and miR-383-5p (47). In addition, in osteoarthritis, MIR4435-2HG was found to sponge miR-510-3p (63).

In the digestive system, MIR4435-2HG can up-regulate YWHAZ and YAP1 by competitively binding miR-22-3p and miR-206-3p to promote the progression of hepatocellular carcinoma and colorectal cancer, respectively (1, 18). In oral squamous cell carcinoma, the MIR4435-2HG/miR-296-5p axis

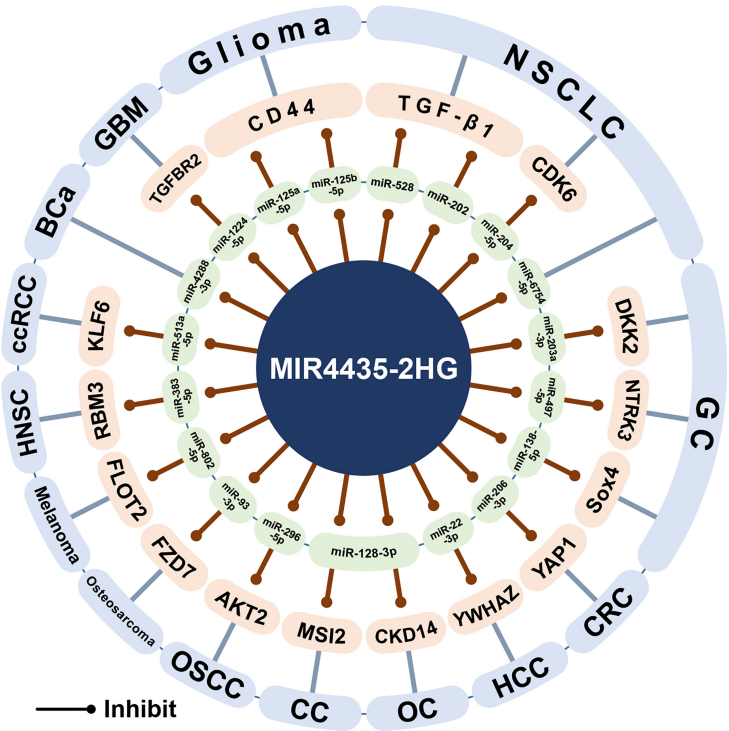

FIGURE 6 | The ceRNA network of MIR4435-2HG. MIR4435-2HG can interact with 19 miRNAs in at least 14 cancers and osteoarthritis, and regulate the expression of its downstream target genes. HCC, Hepatocellular carcinoma; CRC, Colorectal cancer; OSCC, Oral squamous cell carcinoma; GC, Gastric cancer; NSCLC, Non-small cell lung cancer; GBM, Glioblastoma; BCa, Bladder cancer; ccRCC, clear cell renal cell carcinoma; OC, Ovarian cancer; CC, Cervical cancer; HNSC, Head and neck squamous cell carcinoma.

inhibits AKT2, thereby promoting the expression of Snail1, an important transcription factor regulating EMT (64). In gastric cancer, MIR4435-2HG has been shown to promote gastric cancer progression through the miR-497-5p/NTRK3 axis (11) and the miR-138-5p/Sox4 axis (53). However, another study showed that the expression of MIR4435-2HG decreased in gastric cancer, and DKK2 was down-regulated through the MIR4435-2HG/miR-203a-3p axis to inhibit tumor progression (13). It is worth noting that the results of three gastric cancer studies have shown that the expression of MIR4435-2HG in gastric cancer cell lines (HGC-27, BGC-823, SGC-7901, SNU5, AGS, and MGC-803) is higher than that in gastric mucosal cell lines (GES-1) (10–12). However, one study showed that the expression of MIR4435-2HG in four gastric cancer cell lines (HGC-27, BGC-823, SGC-7901, and MKN-45) was lower than that of gastric mucosal cell line (GES-1) (13).

In non-small cell lung cancer, MIR4435-2HG can sponge miR-528 and miR-202, and subsequently up-regulate TGF-β1 to promote tumor growth (30). In addition, MIR4435-2HG/miR-204-5p/CDK6 axis and MIR4435-2HG/miR-6754-5p axis can promote the growth and invasion of non-small cell lung cancer (25, 26). In gliomas, MIR4435-2HG/miR-125a-5p axis and MIR4435-2HG/miR125b-5p axis can up-regulate CD44 and promote tumor progression (52). In glioblastoma, MIR4435-2HG competitively binds miR-1224-5p, thereby up-regulating TGFBR2 and promoting tumor growth (44). In bladder cancer, MIR4435-2HG can sponge miR-4288-3p and promote tumor growth and invasion (41). In clear cell renal cell carcinoma, MIR4435-2HG/miR-513a-5p promotes tumorigenesis and development by promoting the expression of KLF6 (3). In ovarian cancer and cervical cancer (33, 34), MIR4435-2HG can competitively bind miR-128-3p and up-regulate CKD14 and MSI2, thereby promoting tumor progression. In osteosarcoma, the MIR4435-2HG/miR-93-3p axis can up-regulate FZD7 and promote tumor progression (45). In melanoma, the MIR4435-2HG/miR-802-5p axis can promote FLOT2 expression and promote tumor growth and invasion (48). In HNSC, the MIR4435-2HG/miR-383-5p axis can up-regulate RBM3, thereby promoting tumor progression (47). In addition, in osteoarthritis, low expression of MIR4435-2HG can attenuate the MIR4435-2HG/miR-510-3p/IL-17A axis signal and activate the NF-κB signaling pathway, thereby mediating the process of osteoarthritis (63).

In summary, the carcinogenic effect of MIR4435-2HG is through sponging miRNAs to regulate the expression of the downstream target genes. In addition, in osteoarthritis, the low expression of MIR4435-2HG promotes the process of osteoarthritis through the ceRNA network.

THE RELATIONSHIP BETWEEN MIR4435-2HG AND CLINICOPATHOLOGICAL CHARACTERISTICS

As shown in **Table 2**, the abnormal up-regulation of MIR4435-2HG is closely related to the clinicopathological characteristics of 11 tumors. In tumors of the digestive system, high expression of MIR4435-2HG is associated with larger tumors, advanced TNM staging and lymph node metastasis in esophageal squamous cell carcinom (9), gastric cancer (10–12), colorectal cancer (1, 14, 16), and hepatocellular carcinoma (18–20, 23). In esophageal squamous cell carcinom, the upregulation of MIR4435-2HG is also related to tumor differentiation and advanced UICC (Union for International Cancer Control) staging (8, 9). In colorectal cancer, the up-regulated MIR4435-2HG is positively correlated with tumor grade and patient age (15). In hepatocellular carcinoma, high expression of MIR4435-2HG is significantly correlated with distant metastasis, advanced Edmondson grade, incomplete encapsulation, microvascular invasion, and advanced BCLC stage (18, 20, 22).

In breast cancer, MIR4435-2HG is negatively correlated with hormone receptor levels (36). In TNBC, the up-regulated MIR4435-2HG also points to larger tumors and higher TNM stages (37). In ovarian cancer and cervical cancer (33, 34), the high expression level of MIR4435-2HG is also related to advanced FIGO (Federation of Gynecology and Obstetrics) stage and lymph node metastasis. In ovarian cancer, MIR4435-2HG is also closely related to larger tumors and distant metastasis of tumors (31, 33). In lung cancer, high expression of MIR4435-2HG is significantly associated with larger tumors, higher TNM stages, stronger lymph node metastasis, and distant metastasis of the tumor (24, 25, 27, 29). The expression level of MIR4435-2HG in lung cancer tissues and serum of lung cancer patients is significantly positively correlated with tumor size and smoking habits (29). In addition, in clear cell renal cell carcinoma (40), HNSC (47), and osteosarcoma (45), MIR4435-2HG was found to be closely related to advanced TNM stages. In addition, MIR4435-2HG also points to large tumor size and advanced Fuhrman grade in clear cell renal cell carcinoma and distant metastasis of tumors in osteosarcoma (40, 45).

THE PROGNOSTIC AND DIAGNOSTIC VALUE OF MIR4435-2HG

Abnormal up-regulation of MIR4435-2HG has potential value for cancer diagnosis and prognosis. The high expression of MIR4435-2HG is associated with a significant reduction in the overall survival (OS) of patients with 12 types of tumors (**Table 2**), including esophageal squamous cell carcinoma (8, 9), gastric cancer (11), colorectal cancer (1, 14, 17), hepatocellular carcinoma (18, 20, 22, 23), triple-negative breast cancer (TNBC) (37), ovarian cancer (31, 33), prostate cancer (38), lung cancer (24, 26, 29), glioblastoma (44), clear cell renal cell carcinoma (40), HNSC (47), and osteosarcoma (45). Among them, high MIR4435-2HG expression is significantly associated with shorter disease-free survival (DFS) in patients with esophageal squamous cell carcinoma (8), colorectal cancer (1, 14), breast cancer (36), or HNSC (47). In addition, high expression of MIR4435-2HG is also associated with shorter recurrence-free survival (RFS) in patients with hepatocellular carcinoma (22), clear cell renal cell carcinoma (40), or osteosarcoma (45). MIR4435-2HG is also positively correlated with postoperative distant recurrence in patients with non-small cell lung cancer (28).

As shown in **Table 2**, the high expression level of MIR4435-2HG in the tumor tissues and/or blood (whole blood, serum, and plasma) of cancer patients has proved to be of great diagnostic value in 9 cancers. In the tissues and serum of gastric cancer (12), colorectal cancer (15, 17), and non-small cell lung cancer (29), high expression of MIR4435-2HG can distinguish tumor patients from normal controls. In hepatocellular carcinoma serum (21), clear cell renal cell carcinoma tissue (40), and childhood T-ALL bone marrow (49), higher expression levels of MIR4435-2HG can distinguish tumor patients from normal controls. It is worth noting that the high expression of MIR4435-2HG in the serum of colon cancer and the plasma of TNBC and ovarian cancer can effectively distinguish patients with early-stage tumors (stage I-II) and healthy controls Group (6, 16, 32), suggesting that MIR4435-2HG may be used as an early diagnostic marker for these three tumors. In addition, in gliomas, the highly expressed MIR4435-2HG can distinguish metastatic tumors from healthy controls, but cannot effectively distinguish non-metastatic gliomas from normal healthy controls. This indicates that MIR4435-2HG may be involved in the process of glioma metastasis and can be used to diagnose glioma metastasis (42).

MIR4435-2HG AND TUMOR DRUG TREATMENT

MIR4435-2HG has also been shown to be involved in the mechanism of action of a variety of tumor treatment drugs, including resveratrol for the treatment of lung cancer (2), cisplatin for non-small cell lung cancer and colon cancer (4, 5), and carboplatin for three-negative breast cancer (**Figure 7**) (6).

Resveratrol is a natural polyphenol, found in various plants and Chinese herbal medicines. Due to its relatively low toxicity, it can promote cancer by targeting a variety of signaling molecules for cell survival and tumor growth. It is considered an ideal chemopreventive agent (2). As an oncogenic lncRNA, MIR4435-2HG is highly expressed in lung cancer cell lines, and its expression is down-regulated after resveratrol treatment, thereby inhibiting the proliferation and growth of lung cancer cells (2).

Cisplatin is widely used in the treatment of various cancers, but the emergence of cisplatin resistance is a serious clinical problem (5). In non-small cell lung cancer, MIR4435-2HG knockdown can reduce the cisplatin resistance and cell viability of the cisplatin-resistant cell line A549/DDP, and cause cell cycle arrest, which significantly increases the ratio in the G0/G1 phase. Meanwhile,

TABLE 2 | Clinicopathologic significance of MIR4435-2HG in human cancers.

System	Tumor type	Sample size	Expression	Clinicopathological features	Prognostic value	Diagnostic value	Ref.
Digestive system	ESCC	50 patients	Upregulation	Positively associated with tumor diferentiation, large tumor size, advanced TNM stage, and lymph node metastasis	Negatively associated with OS		(9)
		175 patients	Upregulation	Positively associated with advanced UICC stage and lymph node metastasis	Negatively associated with DFS and OS		(8)
	GC	57 patients	Upregulation	Positively associated with advanced TNM stage			(10)
		150 patients	Upregulation	Positively associated with advanced TNM stage	Negatively associated with OS		(11)
		72 patients	Upregulation	Positively associated with large tumor size, advanced TNM stage, and lymph node metastasis		AUC = 0.746, sensitivity = 0.53, specificity = 0.92 (in tissue); AUC = 0.831, sensitivity = 0.80, specificity = 0.70 (in serum)	(12)
		60 patients	Upregulation	Positively associated with advanced TNM stage and lymph node metastasis	Negatively associated with OS		(53)
	CRC	90 patients	Upregulation	Positively associated with large tumor size and advanced TNM stage	Negatively associated with DFS and OS		(1)
		102 patients	Upregulation	Positively associated with large tumor size, advanced TNM stage, and lymph node metastasis	Negatively associated with DFS and OS		(14)
		70 patients	Upregulation	Positively associated with tumor grade and age		AUC = 0.81, specificity = 0.8095, sensitivity = 0.7273	(15)
	COAD	86 patients	Upregulation		Negatively associated with OS	AUC: = 0.9065 (in serum)	(17)
	Colon cancer	46 patients	Upregulation	Positively associated with large tumor size		AUC = 0.8481 (in serum, I-II stage)	(16)
	HCC	64 patients	Upregulation	Positively associated with large tumor size			(19)
		22 patients	Upregulation	Positively associated with advanced TNM stage and distant metastasis	Negatively associated with OS		(18)
		49 patients	Upregulation	Positively associated with large tumor size, advanced Edmondson grade, advanced TNM stage, and lymph node metastasis	Negatively associated with OS		(20)
		88 patients	Upregulation	Positively associated with encapsulation incomplete, microvascular invasion, advanced BCLC stage, and advanced TNM stage	Negatively associated with RFS and OS		(22)
		73 patients	Upregulation	Positively associated with large tumor size and advanced TNM stage	Negatively associated with OS		(23)
		58 patients	Upregulation			AUC = 0.910, sensitivity = 0.76, specificity = 0.96 (in serum)	(21)
Reproductive system	BC	195 patients	Upregulation	Negatively associated with HR status	Negatively associated with DFS		(36)
	TNBC	68 patients	Upregulation	Positively associated with large tumor size and advance TNM stage	Negatively associated with OS	AUC = 0.8927 (in plasma)	(37)
		72 patients	Upregulation			AUC = 0.7980 (in plasma, I-II stage)	(6)
	OC	42 patients	Upregulation				(33)

(Continued)

TABLE 2 | Continued

System	Tumor type	Sample size	Expression	Clinicopathological features	Prognostic value	Diagnostic value	Ref.
				Positively associated with large tumor size, advanced FIGO stage and lymph node metastasis	Negatively associated with OS		
		58 patients	Upregulation	Positively associated with large tumor size and distant metastasis	Negatively associated with OS	AUC = 0.9082 (in serum)	(31)
		28 patients	Upregulation	Positively associated with distant metastasis		AUC = 0.8824 (in plasma, I-II stage)	(32)
	CC	59 patients	Upregulation	Positively associated with advanced FIGO stage and lymph node metastasis			(34)
	PCa	68 patients	Upregulation		Negatively associated with OS		(38)
Respiratory system	LC	52 patients	Upregulation	Positively associated with advanced TNM stage and lymph node metastasis	Negatively associated with OS		(24)
	NSCLC	39 patients	Upregulation	Positively associated with advanced TNM stage and lymph node metastasis			(25)
		138 patients	Upregulation	Positively associated with distant metastasis			(27)
		128 patients	Upregulation		Positively associated with distant recurrence		(28)
		Number not shown	Upregulation		Negatively associated with OS		(26)
		88 patients	Upregulation	Positively associated with large tumor size and smoking habit	Negatively associated with OS	AUC = 0.8686 (in tissue); AUC = 0.8569 (in serum)	(29)
Nervous system	Glioma	34 metastatic glioma patients and 32 non-metastatic glioma patients	Upregulation			AUC = 0.8640 (metastatic glioma) (in plasma)	(42)
	GBM	40 patients	Upregulation		Negatively associated with OS		(44)
Urinary system	ccRCC	118 patients	Upregulation	Positively associated with large tumor size, advanced Fuhrman grade, and advanced TNM stage	Negatively associated with RFS and OS	AUC = 0.946 (in tissue)	(40)
Others	T-ALL	32 patients	Upregulation			AUC = 0.8954 (in bone marrow)	(49)
	HNSC	18 patients	Upregulation	Positively associated with advanced TNM stage	Negatively associated with DFS and OS		(47)
	Osteosarcoma	36 patients	Upregulation	Positively associated with large tumor size, advance TNM stage and distant metastasis	Negatively associated with RFS and OS		(45)

ESCC, esophageal squamous-cell carcinoma; GC, gastric cancer; CRC, colorectal cancer; HCC, hepatocellular carcinoma; BC, breast cancer; TNBC, triple-negative breast cancer; OC, ovarian cancer; CC, cervical cancer; PCa, prostate carcinoma; LC, lung cancer; NSCLC, nonsmall cell lung cancer; GBM, glioblastoma; ccRCC, clear cell renal cell carcinoma; T-ALL, T-cell acute lymphoblastic leukemia; HNSC, head and neck squamous cell carcinoma; TNM, tumor-node-metastasis; UICC, Union for International Cancer Control; BCLC, Barcelona Clinic Liver Cancer; FIGO, Federation of Gynecology and Obstetrics; HR, hormone receptor; DFS, isease-free survival; OS, overall survival; RFS, recurrence-free survival; AUC, area under the curve.

MIR4435-2HG knockdown positively induced the expression of apoptosis-related factors (CCNC and BIRC5), and inhibited the expression of cell cycle-related factors (CDK1 and GTSE5), thereby promoting cell apoptosis (4). In colon cancer, MIR4435-2HG is highly expressed in the cisplatin-resistant cell line HCT116R, and MIR4435-2HG knockdown can significantly restore the sensitivity of cells to cisplatin, inhibit cell proliferation, and promote cell apoptosis (5). In addition, in colon cancer, MIR4435-2HG

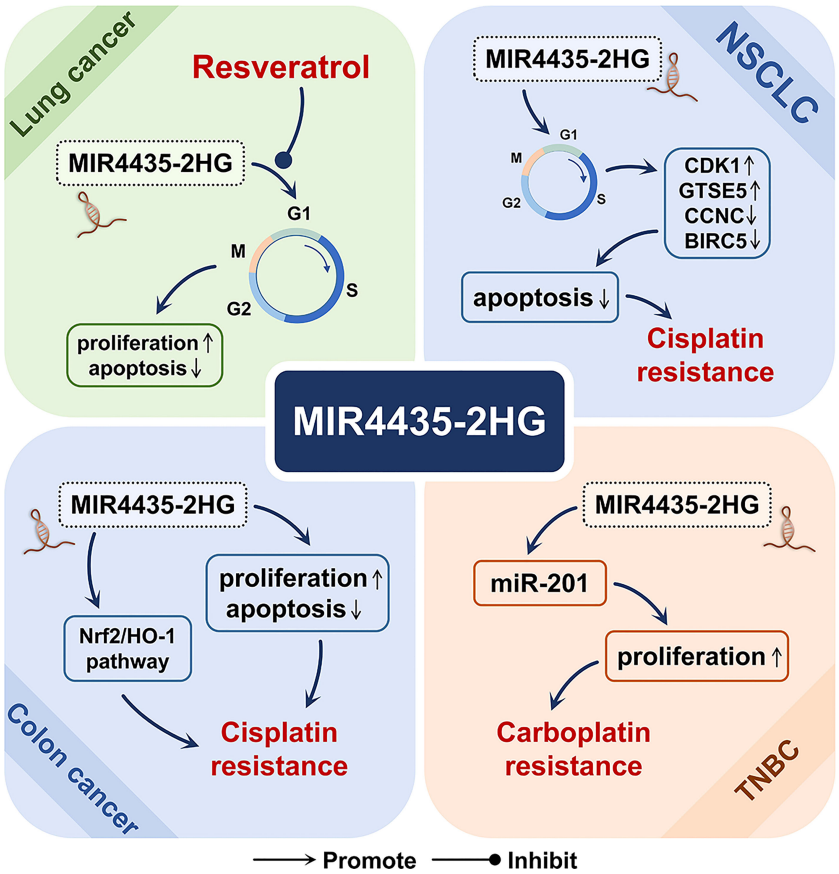

FIGURE 7 | The role of MIR4435-2HG in cancer drugs. In lung cancer, MIR4435-2HG may be involved in the inhibitory effect of resveratrol on the growth of lung cancer cells. In non-small cell lung cancer (NSCLC) and colon cancer, MIR4435-2HG may be a driving factor for cisplatin resistance. In triple-negative breast cancer (TNBC), MIR4435-2HG may be involved in the development of carboplatin resistance.

knockdown can reduce the transcription levels of key molecules (Nrf2 and HO-1) in the oxidative stress pathway (5).

Carboplatin is a cisplatin derivative with broad-spectrum anti-tumor activity. It can be used as a single drug or combined to treat multiple tumors (65). In triple-negative breast cancer (TNBC), overexpression of MIR4435-2HG and miR-21 can promote the proliferation of cancer cells treated with carboplatin, improve the viability of cancer cells, and induce chemotherapy resistance (6).

In summary, MIR4435-2HG may be involved in the inhibitory effect of resveratrol on the growth of lung cancer cells and may be an important driving factor for cisplatin and carboplatin resistance.

CONCLUSIONS AND PERSPECTIVES

MIR4435-2HG is a lncRNA with great potential, which can be used as a diagnostic and prognostic biomarker for a variety of tumors, and a therapeutic target for a variety of tumors. MIR4435-2HG was abnormally up-regulated in tumor tissues and cell lines as an oncogene in 18 tumors, and its overexpression was also detected in the blood, plasma, or serum of 9 tumors. At the same time, MIR4435-2HG is closely related to the clinical characteristics and poor prognosis of 12 tumors. This may mean that MIR4435-2HG can be highly expressed and detected in human blood besides tumor tissues. In the future, the relationship between MIR4435-2HG and tumor development can be studied in more tumors. In addition, there is only one study on the methylation of MIR4435-2HG in gliomas (52), and the mechanism of MIR4435-2HG overexpression in these tumors has not been elucidated. Epigenetic research can provide hints for elucidating the molecular mechanism of MIR4435-2HG.

MIR4435-2HG can participate in at least 6 signal pathways and form a ceRNA network with miRNAs to promote the occurrence and development of tumors. In tumors, MIR4435-2HG can participate in the regulation of signaling pathways and affect different biological processes of tumors. For example, non-small cell lung cancer is involved in TGF-β signaling (27, 28, 30) and Wnt/β-catenin signaling (29). Colorectal cancer is involved in the Wnt/β-catenin signaling pathway (15) and the Hippo signaling pathway (1). This may provide ideas for exploring new tumor

treatment strategies. However, the specific mechanism of MIR4435-2HG in the pathway has not been well explained. Meanwhile, the existing research on MIR4435-2HG mostly focuses on the "lncRNA-miRNA-mRNA" axis, however, the research on the relationship between other non-coding RNAs of MIR4435-2HG is still lacking. For example, MIR4435-2HG and BCL2L11 genes co-localize to chr2 q13, and the lncRNA Morrbid (a myeloid RNA regulator of BCL2L11-induced cell death) is involved in the regulation of N-ras splicing in mouse hepatocytes and is associated with tumorigenesis (66). In the future, it is necessary to further study the regulatory mechanism of MIR4435-2HG and improve its ceRNA network. In addition, the expression of MIR4435-2HG may also be closely associated with nearby genetic variants. For example, the rs17041869 site located in the enhancer of BCL2L11 can regulate the expression of the BCL2L11 gene near MIR4435-2HG (67), suggesting the need to explore genetic variants associated with MIR4435-2HG in the future.

In addition, it needs to be further explored for the application of MIR4435-2HG in the blood of tumor patients in the diagnosis and prognosis of tumors. The connection between MIR4435-2HG and tumor treatment drugs lays the foundation for the clinical treatment of tumors. In the future, it is necessary to test the role of MIR4435-2HG in the treatment of more cancer drugs.

AUTHOR CONTRIBUTIONS

SD, CY, and CZ contributed to the conception, design and final approval of the submitted version. CZ and ZX collected and analyzed literature. CZ, ZX, L-hZ, CY, and SD contributed to manuscript writing. All the authors conceived and gave the approval of the final manuscript.

FUNDING

The research was supported by National Natural Science Foundation of China (32100521) and Qiantang Scholar Fund in Zhejiang University City College.

REFERENCES

1. Dong X, Yang Z, Yang H, Li D, Qiu X. Long Non-Coding RNA MIR4435-2hg Promotes Colorectal Cancer Proliferation and Metastasis Through miR-206/YAP1 Axis. *Front Oncol* (2020) 10:160. doi: 10.3389/fonc.2020.00160
2. Yang Q, Xu E, Dai J, Liu B, Han Z, Wu J, et al. A Novel Long Noncoding RNA AK001796 Acts as an Oncogene and is Involved in Cell Growth Inhibition by Resveratrol in Lung Cancer. *Toxicol Appl Pharmacol* (2015) 285(2):79–88. doi: 10.1016/j.taap.2015.04.003
3. Zhu K, Miao C, Tian Y, Qin Z, Xue J, Xia J, et al. lncRNA MIR4435-2HG Promoted Clear Cell Renal Cell Carcinoma Malignant Progression *via* miR-513a-5p/KLF6 Axis. *J Cell Mol Med* (2020) 24(17):10013–26. doi: 10.1111/jcmm.15609
4. Liu B, Pan CF, Ma T, Wang J, Yao GL, Wei K, et al. Long Noncoding RNA AK001796 Contributes to Cisplatin Resistance of Nonsmall Cell Lung Cancer. *Mol Med Rep* (2017) 16(4):4107–12. doi: 10.3892/mmr.2017.7081
5. Luo P, Wu SG, Ji KB, Yuan X, Li HM, Chen JP, et al. LncRNA MIR4435-2HG Mediates Cisplatin Resistance in HCT116 Cells by Regulating Nrf2 and HO-1. *PLoS One* (2020) 15(11):e0223035. doi: 10.1371/journal.pone.0223035
6. Liu AN, Qu HJ, Gong WJ, Xiang JY, Yang MM, Zhang W. LncRNA AWPPH and miRNA-21 Regulates Cancer Cell Proliferation and Chemosensitivity in Triple-Negative Breast Cancer by Interacting With Each Other. *J Cell Biochem* (2019) 120(9):14860–6. doi: 10.1002/jcb.28747
7. Shen H, Sun B, Yang Y, Cai X, Bi L, Deng L, et al. MIR4435-2HG Regulates Cancer Cell Behaviors in Oral Squamous Cell Carcinoma Cell Growth by Upregulating TGF-Beta1. *Odontology* (2020) 108(4):553–9. doi: 10.1007/s10266-020-00488-x
8. Zong MZ, Shao Q, An XS. Expression and Prognostic Significance of Long Noncoding RNA AK001796 in Esophageal Squamous Cell Carcinoma. *Eur Rev Med Pharmacol Sci* (2019) 23(1):181–6.
9. Liu B, Pan CF, Yao GL, Wei K, Xia Y, Chen YJ. The Long non-Coding RNA AK001796 Contributes to Tumor Growth *via* Regulating Expression of P53 in Esophageal Squamous Cell Carcinoma. *Cancer Cell Int* (2018) 18:38. doi: 10.1186/s12935-018-0537-8
10. Wang HY, Wu MJ, Lu YM, He KF, Cai XL, Yu XF, et al. LncRNA MIR4435-2HG Targets Desmoplakin and Promotes Growth and Metastasis of Gastric Cancer by Activating Wnt/β-Catenin Signaling. *Aging* (2019) 11(17):6657–73. doi: 10.18632/aging.102164
11. Bu JY, Lv WZ, Liao YF, Xiao XY, Lv BJ. Long non-Coding RNA LINC00978 Promotes Cell Proliferation and Tumorigenesis *via* Regulating microRNA-497/NTRK3 Axis in Gastric Cancer. *Int J Biol Macromol* (2019) 123:1106–14. doi: 10.1016/j.ijbiomac.2018.11.162
12. Fu M, Huang Z, Zang X, Pan L, Liang W, Chen J, et al. Long Noncoding RNA LINC00978 Promotes Cancer Growth and Acts as a Diagnostic Biomarker in Gastric Cancer. *Cell Prolif* (2018) 51(1). doi: 10.1111/cpr.12425
13. Li L, Kou J, Zhong B. Up-Regulation of Long non-Coding RNA AWPPH Inhibits Proliferation and Invasion of Gastric Cancer Cells *via* miR-203a/DKK2 Axis. *Hum Cell* (2019) 32(4):495–503. doi: 10.1007/s13577-019-00277-x
14. Shen MY, Zhou GR, Zhang ZY. LncRNA MIR4435-2HG Contributes Into Colorectal Cancer Development and Predicts Poor Prognosis. *Eur Rev Med Pharmacol Sci* (2020) 24(4):1771–7.
15. Ghasemian M, Rajabibazl M, Mirfakhraie R, Razavi AE, Sadeghi H. Long Noncoding RNA LINC00978 Acts as a Potential Diagnostic Biomarker in Patients With Colorectal Cancer. *Exp Mol Pathol* (2021) 122:104666. doi: 10.1016/j.yexmp.2021.104666
16. Bai J, Xu J, Zhao J, Zhang R. Downregulation of lncRNA AWPPH Inhibits Colon Cancer Cell Proliferation by Downregulating GLUT-1. *Oncol Lett* (2019) 18(2):2007–12. doi: 10.3892/ol.2019.10515
17. Liu C, Han B, Xin J, Yang C. LncRNA-AWPPH Activates TGF-Beta1 in Colorectal Adenocarcinoma. *Oncol Lett* (2019) 18(5):4719–25. doi: 10.3892/ol.2019.10794
18. Shen XL, Ding YT, Lu F, Yuan HT, Luan WK. Long Noncoding RNA MIR4435-2HG Promotes Hepatocellular Carcinoma Proliferation and Metastasis Through the miR-22-3p/YWHAZ Axis. *Am J Transl Res* (2020) 12(10):6381–94. doi: 10.3389/fonc.2020.00160
19. Kong Q, Liang C, Jin Y, Pan Y, Tong D, Kong Q, et al. The lncRNA MIR4435-2HG is Upregulated in Hepatocellular Carcinoma and Promotes Cancer Cell Proliferation by Upregulating miRNA-487a. *Cell Mol Biol Lett* (2019) 24:26. doi: 10.1186/s11658-019-0148-y
20. Zhang Q, Cheng S, Cao L, Yang J, Wang Y, Chen Y. LINC00978 Promotes Hepatocellular Carcinoma Carcinogenesis Partly *via* Activating the MAPK/ERK Pathway. *Biosci Rep* (2020) 40(3). doi: 10.1042/BSR20192790
21. Xu X, Gu J, Ding X, Ge G, Zang X, Ji R, et al. LINC00978 Promotes the Progression of Hepatocellular Carcinoma by Regulating EZH2-Mediated Silencing of P21 and E-Cadherin Expression. *Cell Death Dis* (2019) 10(10):752. doi: 10.1038/s41419-019-1990-6
22. Zhao X, Liu Y, Yu S. Long Noncoding RNA AWPPH Promotes Hepatocellular Carcinoma Progression Through YBX1 and Serves as a Prognostic Biomarker. *Biochim Biophys Acta Mol Basis Dis* (2017) 1863(7):1805–16. doi: 10.1016/j.bbadis.2017.04.014

23. Han QL, Chen BT, Zhang KJ, Xia ST, Zhong WW, Zhao ZM. The Long non-Coding RNA AK001796 Contributes to Poor Prognosis and Tumor Progression in Hepatocellular Carcinoma. *Eur Rev Med Pharmacol Sci* (2019) 23(5):2013–9.
24. Qian H, Chen L, Huang J, Wang X, Ma S, Cui F, et al. The lncRNA MIR4435-2HG Promotes Lung Cancer Progression by Activating Beta-Catenin Signalling. *J Mol Med (Berl)* (2018) 96(8):753–64. doi: 10.1007/s00109-018-1654-5
25. Li X, Ren Y, Zuo T. Long Noncoding RNA LINC00978 Promotes Cell Proliferation and Invasion in Nonsmall Cell Lung Cancer by Inhibiting Mir67545p. *Mol Med Rep* (2018) 18(5):4725–32. doi: 10.3892/mmr.2018.9463
26. Wu D, Qin BY, Qi XG, Hong LL, Zhong HB, Huang JY. LncRNA AWPPH Accelerates the Progression of non-Small Cell Lung Cancer by Sponging miRNA-204 to Upregulate CDK6. *Eur Rev Med Pharmacol Sci* (2020) 24 (8):4281–7.
27. Huo Y, Li A, Wang Z. LncRNA AWPPH Participates in the Metastasis of non-Small Cell Lung Cancer by Upregulating TGF-Beta1 Expression. *Oncol Lett* (2019) 18(4):4246–52. doi: 10.3892/ol.2019.10754
28. Tang L, Wang T, Zhang Y, Zhang J, Zhao H, Wang H, et al. Long Non-Coding RNA AWPPH Promotes Postoperative Distant Recurrence in Resected Non-Small Cell Lung Cancer by Upregulating Transforming Growth Factor Beta 1 (TGF-Beta1). *Med Sci Monit* (2019) 25:2535–41. doi: 10.12659/MSM.912876
29. Song Z, Du J, Zhou L, Sun B. lncRNA AWPPH Promotes Proliferation and Inhibits Apoptosis of Nonsmall Cell Lung Cancer Cells by Activating the Wnt/betacatenin Signaling Pathway. *Mol Med Rep* (2019) 19(5):4425–32. doi: 10.3892/mmr.2019.10089
30. Yang M, He X, Huang X, Wang J, He Y, Wei L. LncRNA MIR4435-2HG-Mediated Upregulation of TGF-Beta1 Promotes Migration and Proliferation of Nonsmall Cell Lung Cancer Cells. *Environ Toxicol* (2020) 35(5):582–90. doi: 10.1002/tox.22893
31. Yu G, Wang W, Deng J, Dong S. LncRNA AWPPH Promotes the Proliferation, Migration and Invasion of Ovarian Carcinoma Cells *via* Activation of the Wnt/betacatenin Signaling Pathway. *Mol Med Rep* (2019) 19(5):3615–21. doi: 10.3892/mmr.2019.10029
32. Gong J, Xu X, Zhang X, Zhou Y. LncRNA MIR4435-2HG is a Potential Early Diagnostic Marker for Ovarian Carcinoma. *Acta Biochim Biophys Sin (Shanghai)* (2019) 51(9):953–9. doi: 10.1093/abbs/gmz085
33. Zhu L, Wang A, Gao M, Duan X, Li Z. LncRNA MIR4435-2HG Triggers Ovarian Cancer Progression by Regulating miR-128-3p/CKD14 Axis. *Cancer Cell Int* (2020) 20:145. doi: 10.1186/s12935-020-01227-6
34. Wang R, Liu L, Jiao J, Gao D. Knockdown of MIR4435-2hg Suppresses the Proliferation, Migration and Invasion of Cervical Cancer Cells *via* Regulating the miR-128-3p/MSI2 Axis *In Vitro*. *Cancer Manag Res* (2020) 12:8745–56. doi: 10.2147/CMAR.S265545
35. Chen D, Tang P, Wang Y, Wan F, Long J, Zhou J, et al. Downregulation of Long non-Coding RNA MR4435-2HG Suppresses Breast Cancer Progression *via* the Wnt/beta-Catenin Signaling Pathway. *Oncol Lett* (2021) 21(5):373. doi: 10.3892/ol.2021.12634
36. Deng LL, Chi YY, Liu L, Huang NS, Wang L, Wu J. LINC00978 Predicts Poor Prognosis in Breast Cancer Patients. *Sci Rep* (2016) 6:37936. doi: 10.1038/srep37936
37. Wang K, Li X, Song C, Li M. LncRNA AWPPH Promotes the Growth of Triple-Negative Breast Cancer by Up-Regulating Frizzled Homolog 7 (FZD7). *Biosci Rep* (2018) 38(6). doi: 10.1042/BSR20181223
38. Zhang H, Meng H, Huang X, Tong W, Liang X, Li J, et al. lncRNA MIR4435-2HG Promotes Cancer Cell Migration and Invasion in Prostate Carcinoma by Upregulating TGF-Beta1. *Oncol Lett* (2019) 18(4):4016–21. doi: 10.3892/ol.2019.10757
39. Xing P, Wang Y, Zhang L, Ma C, Lu J. Knockdown of lncRNA MIR44352HG and ST8SIA1 Expression Inhibits the Proliferation, Invasion and Migration of Prostate Cancer Cells *In Vitro* and *In Vivo* by Blocking the Activation of the FAK/AKT/betacatenin Signaling Pathway. *Int J Mol Med* (2021) 47(6). doi: 10.3892/ijmm.2021.4926
40. Wu K, Hu L, Lv X, Chen J, Yan Z, Jiang J, et al. Long non-Coding RNA MIR4435-1HG Promotes Cancer Growth in Clear Cell Renal Cell Carcinoma. *Cancer biomark* (2020) 29(1):39–50. doi: 10.3233/CBM-201451
41. Wang W, Xu Z, Wang J, Chen R. LINC00978 Promotes Bladder Cancer Cell Proliferation, Migration and Invasion by Sponging Mir4288. *Mol Med Rep* (2019) 20(2):1866–72. doi: 10.3892/mmr.2019.10395
42. Zhang T, Wang F, Liao Y, Yuan L, Zhang B. LncRNA AWPPH Promotes the Invasion and Migration of Glioma Cells Through the Upregulation of HIF1alpha. *Oncol Lett* (2019) 18(6):6781–6. doi: 10.3892/ol.2019.11018
43. Dai B, Xiao Z, Mao B, Zhu G, Huang H, Guan F, et al. lncRNA AWPPH Promotes the Migration and Invasion of Glioma Cells by Activating the TGF-Beta Pathway. *Oncol Lett* (2019) 18(6):5923–9. doi: 10.3892/ol.2019.10918
44. Xu H, Zhang B, Yang Y, Li Z, Zhao P, Wu W, et al. LncRNA MIR4435-2HG Potentiates the Proliferation and Invasion of Glioblastoma Cells *via* Modulating miR-1224-5p/TGFBR2 Axis. *J Cell Mol Med* (2020) 24 (11):6362–72. doi: 10.1111/jcmm.15280
45. Li C, Wang F, Wei B, Wang L, Kong D. LncRNA AWPPH Promotes Osteosarcoma Progression *via* Activation of Wnt/beta-Catenin Pathway Through Modulating miR-93-3p/FZD7 Axis. *Biochem Biophys Res Commun* (2019) 514(3):1017–22. doi: 10.1016/j.bbrc.2019.04.203
46. Ding W, Wu D, Ji F, Zhang H. Inhibition of Long non-Coding RNA-AWPPH Decreases Osteosarcoma Cell Proliferation, Migration and Invasion. *Oncol Lett* (2019) 18(5):5055–62. doi: 10.3892/ol.2019.10898
47. Wang S, Chen X, Qiao T. Long Noncoding RNA MIR44352HG Promotes the Progression of Head and Neck Squamous Cell Carcinoma by Regulating the Mir3835p/RBM3 Axis. *Oncol Rep* (2021) 45(6). doi: 10.3892/or.2021.8050
48. Ma DM, Sun D, Wang J, Jin DH, Li Y, Han YE. Long non-Coding RNA MIR4435-2HG Recruits miR-802 From FLOT2 to Promote Melanoma Progression. *Eur Rev Med Pharmacol Sci* (2020) 24(5):2616–24. doi: 10.26355/eurrev_202003_20530
49. Li X, Song F, Sun H. Long non-Coding RNA AWPPH Interacts With ROCK2 and Regulates the Proliferation and Apoptosis of Cancer Cells in Pediatric T-Cell Acute Lymphoblastic Leukemia. *Oncol Lett* (2020) 20(5):239. doi: 10.3892/ol.2020.12102
50. Guo DQ, Liu F, Zhang L, Bian NN, Liu LY, Kong LX, et al. Long non-Coding RNA AWPPH Enhances Malignant Phenotypes in Nasopharyngeal Carcinoma *via* Silencing PTEN Through Interacting With LSD1 and EZH2. *Biochem Cell Biol* (2021) 99(2):195–202. doi: 10.1139/bcb-2019-0497
51. Wang ZH, Yang B, Zhang M, Guo WW, Wu ZY, Wang Y, et al. lncRNA Epigenetic Landscape Analysis Identifies EPIC1 as an Oncogenic lncRNA That Interacts With MYC and Promotes Cell-Cycle Progression in Cancer. *Cancer Cell* (2018) 33(4):706–20. doi: 10.1016/j.ccell.2018.03.006
52. Li ZJ, Tan H, Zhao WL, Xu YG, Zhang ZG, Wang MD, et al. Integrative Analysis of DNA Methylation and Gene Expression Profiles Identifies MIR4435-2HG as an Oncogenic lncRNA for Glioma Progression. *Gene* (2019) 5:705. doi: 10.1016/j.gene.2019.144012
53. Gao LF, Li W, Liu YG, Zhang C, Gao WN, Wang L. Inhibition of MIR4435-2HG on Invasion, Migration, and EMT of Gastric Carcinoma Cells by Mediating MiR-138-5p/Sox4 Axis. *Front Oncol* (2021) 11:661288. doi: 10.3389/fonc.2021.661288
54. Wakefield LM, Roberts AB. TGF-β Signaling: Positive and Negative Effects on Tumorigenesis. *Curr Opin Genet Dev* (2002) 12(2):22–9. doi: 10.1016/S0959-437X(01)00259-3
55. Mirzaei H, Faghihloo E. Viruses as Key Modulators of the TGF-Beta Pathway; a Double-Edged Sword Involved in Cancer. *Rev Med Virol* (2018) 28(2). doi: 10.1002/rmv.1967
56. Katsuno Y, Lamouille S, Derynck R. TGF-β Signaling and Epithelial-Mesenchymal Transition in Cancer Progression. *Curr Opin Oncol* (2013) 25 (1):76–84. doi: 10.1097/CCO.0b013e32835b6371
57. Nishita M, Hashimoto MK, Ogata S, Laurent MN, Ueno N, Shibuya H, et al. Interaction Between Wnt and TGF-Beta Signalling Pathways During Formation of Spemann's Organizer. *Nature* (2000) 403(6771):781–5. doi: 10.1038/35001602
58. Li ZW, Zhao L, Wang QG. Overexpression of Long non-Coding RNA HOTTIP Increases Chemoresistance of Osteosarcoma Cell by Activating the Wnt/β-Catenin Pathway. *Am J Transl Res* (2016) 8(5):2385–93.
59. Giannikaki E, Kouvidou C, Tzardi M, Stefanaki K, Koutsoubi K, Gregoriou M, et al. P53 Protein Expression in Breast Carcinomas. Comparative Study With the Wild Type P53 Induced Proteins Mdm2 and P21/Waf1. *Anticancer Res* (1997) 17(3C):2123–7.
60. Porta C, Paglino C, Mosca A. Targeting PI3K/Akt/mTOR Signaling in Cancer. *Front Oncol* (2014) 4:64. doi: 10.3389/fonc.2014.00064
61. Zanconato F, Cordenonsi M, Piccolo S. YAP/TAZ at the Roots of Cancer. *Cancer Cell* (2016) 29(6):783–803. doi: 10.1016/j.ccell.2016.05.005

62. Asl ER, Amini M, Najafi S, Mansoori B, Mokhtarzadeh A, Mohammadi A, et al. Interplay Between MAPK/ERK Signaling Pathway and MicroRNAs: A Crucial Mechanism Regulating Cancer Cell Metabolism and Tumor Progression. *Life Sci* (2021) 278:119499. doi: 10.1016/j.lfs.2021.119499
63. Liu Y, Yang Y, Ding L, Jia Y, Ji Y. LncRNA MIR4435-2HG Inhibits the Progression of Osteoarthritis Through miR-510-3p Sponging. *Exp Ther Med* (2020) 20(2):1693–701. doi: 10.3892/etm.2020.8841
64. Zhang S, Li C, Liu J, Geng F, Shi X, Li Q, et al. Fusobacterium Nucleatum Promotes Epithelial-Mesenchymal Transiton Through Regulation of the lncRNA MIR4435-2hg/miR-296-5p/Akt2/SNAI1 Signaling Pathway. *FEBS J* (2020) 287(18):4032–47. doi: 10.1111/febs.15233
65. Lynce F, Nunes R. Role of Platinums in Triple-Negative Breast Cancer. *Curr Oncol Rep* (2021) 23(5):50. doi: 10.1007/s11912-021-01041-x
66. Fefilova A, Melnikov P, Prikazchikova T, Abakumova T, Kurochkin I, Mazin PV, et al. Murine Long Noncoding RNA Morrbid Contributes in the Regulation of NRAS Splicing in Hepatocytes *In Vitro*. *Int J Mol Sci* (2020) 21(16):5605. doi: 10.3390/ijms21165605
67. Kar SP, Beesley J, Olama AAA, Michailidou K, Tyrer J, Kote-Jarai Z, et al. Genome-Wide Meta-Analyses of Breast, Ovarian, and Prostate Cancer Association Studies Identify Multiple New Susceptibility Loci Shared by at Least Two Cancer Types. *Cancer Discov* (2016) 6(8):1052–67. doi: 10.1158/2159-8290.CD-15-1227

Conflict of Interest: The authors declare that the research was conducted in the absence of any commercial or financial relationships that could be construed as a potential conflict of interest.

Publisher's Note: All claims expressed in this article are solely those of the authors and do not necessarily represent those of their affiliated organizations, or those of the publisher, the editors and the reviewers. Any product that may be evaluated in this article, or claim that may be made by its manufacturer, is not guaranteed or endorsed by the publisher.

frontiers | Frontiers in Immunology

TYPE Systematic Review
PUBLISHED 09 August 2022
DOI 10.3389/fimmu.2022.863162

OPEN ACCESS

EDITED BY
Lee Mark Wetzler,
Boston University, United States

REVIEWED BY
Xionglin Fan,
Huazhong University of Science and Technology, China
Kamran Zaman,
Indian Council of Medical Research - Regional Medical Research Centre (ICMR - RMRC) Gorakhpur, India

*CORRESPONDENCE
Sheikh Mansoor
mansoorshafi21@gmail.com

SPECIALTY SECTION
This article was submitted to Vaccines and Molecular Therapeutics, a section of the journal Frontiers in Immunology

RECEIVED 26 January 2022
ACCEPTED 27 June 2022
PUBLISHED 09 August 2022

CITATION
Ahmed TI, Rishi S, Irshad S, Aggarwal J, Happa K and Mansoor S (2022) Inactivated vaccine Covaxin/ BBV152: A systematic review. *Front. Immunol.* 13:863162. doi: 10.3389/fimmu.2022.863162

Inactivated vaccine Covaxin/ BBV152: A systematic review

Tousief Irshad Ahmed[1], Saqib Rishi[2], Summaiya Irshad[3], Jyoti Aggarwal[4], Karan Happa[5] and Sheikh Mansoor[6]*

[1]Department of Clinical Biochemistry, Sher-I-Kashmir Institute of Medical Sciences, Srinagar, JK, India, [2]Department of Microbiology, Government Medical College, Srinagar, JK, India, [3]Department of Ophthalmology, Government Medical College, Jammu, JK, India, [4]Department of Biochemistry, Maharishi Markandeshwar Institute of Medical Sciences and Research (MMIMSR), Ambala, HR, India, [5]Department of General Medicine, Sher-I-Kashmir Institute of Medical Sciences, Srinagar, JK, India, [6]Advanced Centre for Human Genetics, Sher-I-Kashmir Institute of Medical Sciences, Srinagar, JK, India

We systematically reviewed and summarized studies focusing on Bharat Biotech's Whole Virion Inactivated Corona Virus Antigen BBV152 (Covaxin), which is India's indigenous response to fighting the SARS-CoV-2 pandemic. Studies were searched for data on the efficacy, immunogenicity, and safety profile of BBV152. All relevant studies published up to March 22, 2022, were screened from major databases, and 25 studies were eventually inducted into the systematic review. The studies focused on the virus antigen (6 µg) adjuvanted with aluminium hydroxide gel and/or Imidazo quinolin gallamide (IMDG), aTLR7/8 agonist. Pre-clinical, phase I, and II clinical trials showed appreciable immunogenicity. Both neutralizing and binding antibody titers were significant and T cell responses were Th1-biased. Phase III trials on the 6 µg +Algel-IMDG formulation showed a 93.4% efficacy against severe COVID-19. Data from the trials revealed an acceptable safety profile with mostly mild-moderate local and systemic adverse events. No serious adverse events or fatalities were seen, and most studies reported milder and lesser adverse events with Covaxin when compared with other vaccines, especially Oxford-Astra Zeneca's AZD1222 (Covishield). The immunogenicity performance of Covaxin, which provided significant protection only after the second dose, was mediocre and it was consistently surpassed by Covishield. One study reported adjusted effectiveness against symptomatic infection to be just 50% at 2 weeks after the second dose. Nonetheless, appreciable results were seen in previously infected individuals administered both doses. There was some evidence of coverage against the Alpha, Beta, and Delta variants. However, neither Covaxin nor Covishield showed sufficient protection against the Omicron variant. Two studies reported super-additive results on mixing Covaxin with Covishield. Further exploration of heterologous prime-boost vaccination with a combination of an inactivated vaccine and an adenoviral vector-based vaccine for tackling future variants may be beneficial.

KEYWORDS

BBV152, Covaxin, inactivated vaccine, Covishield, efficacy, immunogenicity, safety

Introduction

With SARS-CoV-2 infections affecting more than half a billion and resulting in around 6.3 million deaths at the time of writing, more than 220 countries faced a monumental task in combating the devastation inflicted by this virus (1). Extensive vaccination efforts were initiated and successfully concluded all over the world in record times. Unfortunately, the huge number of cases of SARS-CoV-2 worldwide provided fertile ground for genomic changes precipitating the emergence of newer variants, such as the Alpha variant (B.1.1.7), which emerged in the UK, Beta variant (B.1.351) in South Africa, Gamma (P.1) in Brazil, Epsilon (B.1.429) emerging from California, and Iota (B.1.526) in New York. The phenomenal increase in SARS-CoV-2 infections in the Indian subcontinent during the second wave and the flouting of social distancing norms at religious and political gatherings provided the opportunity for the emergence of new variants, the Delta and Kappa (1.617.1 and 1.617.2, respectively) emerging in the country around December 2020 (2).

Bharat Biotech's Covaxin (BBV152) was the second-most administered vaccine in India at 327 million doses received at the time of writing (3). It is a β-propiolactone inactivated vaccine (4). The inactivated whole-virion structure is combined with an adjuvant, Imidazo -quinoline gallamide, which is a toll-like receptor 7/8 agonist molecule adsorbed to alum (Algel-IMDG). The formulation improves homing of vaccine antigen onto draining lymph nodes without systemic spillage. A genetically stable strain NIV-2020-770 containing the Asp614Gly mutation used for making Covaxin was isolated from an asymptomatic SARS-CoV-2 positive patient at the National Institute of Virology (NIV), Pune (5). Biosafety level 3 (BSL3) manufacturing facilities with a vero cell manufacturing platform were utilized in the manufacturing process (6). The strain used is 99.7% identical to Wuhan Hu-1 (7). Five to 10% newborn calf serum in Dulbecco's Modified Eagle medium (DMEM) was used to grow Vero CCL-81 cells in tissue culture flasks and cell stacks. Further virus propagation was achieved in bioreactors which maintained a temperature of 36 ± 1°C. Harvesting was done at 36-72 h post-infection and supernatants were processed. Additional purification and concentration were done by column chromatography and a tangential flow filtration system, respectively (8). The purified final bulk obtained from the inactivation procedure has been found to contain spike and nucleocapsid protein. Transmission electron microscopy (TEM) shows intact, oval structures with the characteristic crown shape (7). Covaxin got early approval from Indian Drug regulatory agencies (9). Studies on vaccine safety have always presented challenges. Antibody-dependent enhancement (ADE) has been a worrying concern with inactivated vaccines and the changes in conformations of spike proteins on inactivation with β-propiolactone may be a cause for concern (10). Autoimmune glomerular disorders have been reported 2 weeks after vaccination with Covaxin (11). A case of Cutaneous small-vessel vasculitis was reported 5 days after inoculation (12). There was also a report of varicella zoster reactivation in a 72-year-old woman a week after receiving the vaccine (13). Coronary thromboembolic phenomena have also been seen, though on a much lesser scale compared to other vaccines (14). Nonetheless, the WHO accorded Emergency use listing (EUL) approval to Covaxin on 3 November 2021 after several delays, its Strategic Advisory Group of Experts on Immunization (SAGE) having previously recommended two doses spaced 4 weeks apart in all adults (15). Several South American and African nations have also been using it in their programs, though not without reservations (16, 17).

We aim to systematically review the overall efficacy, immunogenicity, and safety of BBV152 Covaxin vaccine, which could potentially guide public health policy in relation to combating the threat posed by SARS-CoV-2, especially in those countries that are actively considering adding it to their regimens.

Methods

Search strategy

The Preferred Reporting Items for Systematic Reviews and Meta-Analyses Statement (PRISMA) recommendations were followed in this analysis. (Figure 1) A systematic literature search with no language restriction was performed in electronic databases, including PubMed, Google Scholar, Directory of Open Access Journals (DOAJ), as well as Lancet, to identify eligible studies published up to March 22, 2022. The search strategy was based on the following keywords and MeSH terms: "BBV152", "Covaxin", "vaccine", "vaccination", "safety" and "efficacy". Reference lists of selected studies were also screened. In addition, internet engines were utilized to search for web pages that might have references of interest.

Study selection

Two investigators (TIA and SR) independently performed the literature screening to identify eligible studies. Studies eligible for inclusion were studies of any design (case–control, case–cohort, prospective cohort, randomized control trials, cross-sectional, human, as well as non-human studies), which reported the effectiveness of the BBV152 vaccine to prevent reverse transcription–polymerase chain reaction (RT-PCR) confirmed COVID-19 (through comparison between vaccinated and unvaccinated individuals) and adjusted for covariates. For multiple studies based on the same data, or where preprints were succeeded by publication in indexed journals, the most recent ones were mentioned. Studies involving heterologous administration of BBV152 with other

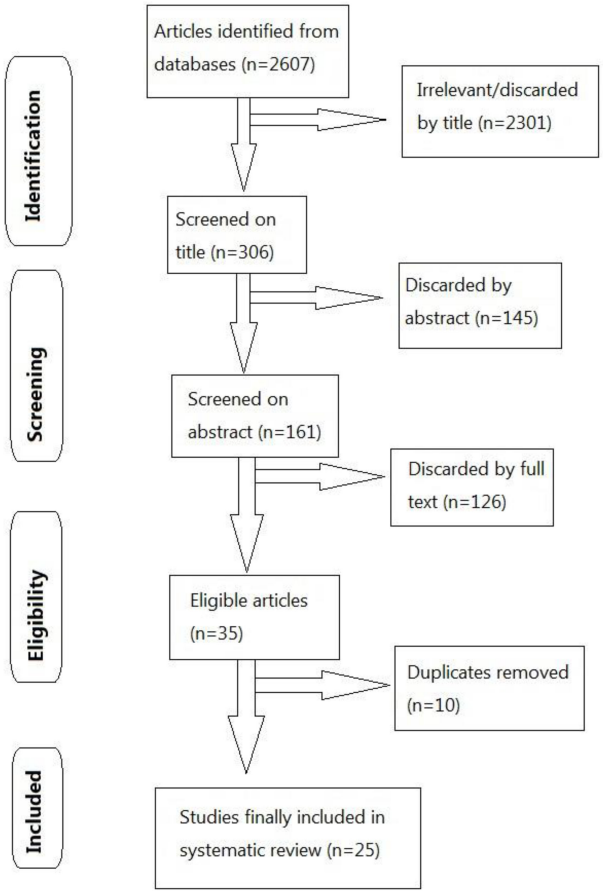

FIGURE 1
Flow diagram utilizing PRISMA (Preferred Reporting Items for Systematic Reviews and Meta-analyses) for study selection.

vaccines had interesting results and were included. One study focusing on chemokine and cytokine subsets elicited was not excluded. Studies comparing BBV152 with other vaccines or involving individuals previously infected with SARS-CoV-2 were included.

Exclusion criteria

We excluded studies that reported unadjusted effectiveness estimates, or which did not use RT-PCR to confirm the diagnosis of COVID-19. Uncorrected manuscripts and pre-prints were not included. One study focusing on breakthrough infections had to be excluded as data for both Covaxin and another vaccine codenamed AZD1222 (brand name Covishield) were grouped together and individual data for Covaxin could not be retrieved (18). Two other studies also had to be excluded due to a lack of Covaxin-specific subgroup analysis (19, 20).

Studies were presented chronologically wherever possible.

We had three outcomes of interest, BBV-152

(a) vaccine efficacy, which is defined as 'a proportionate reduction in disease attack rate (AR) between the unvaccinated (ARU) and vaccinated (ARV) study cohorts' (21),

(b) immunogenicity of the vaccine, measured by estimating either binding antibodies by Enzyme-linked immunosorbent assays (ELISA) or Neutralizing Antibodies (NAb), by plaque reduction neutralization assays ($PRNT_{90}$ or $PRNT_{50}$), focus reduction neutralization titer ($FRNT_{50}$), or microneutralization assay (MNT_{50}), as well as cytokine and chemokine profiles, and

(c) vaccine safety.

Studies examining either efficacy, immunogenicity, or safety, or any combination of the three, were included. Each included study was studied independently by two investigators (TIA and SR), who also obtained details of the same under the headings of first author's surname, study design, sample population and subgroups, number of participants, the incidence of COVID-19 (either asymptomatic, symptomatic with more than one grade of severity) in both vaccinated and unvaccinated individuals, and adjusted vaccine effectiveness estimates and covariates. Two investigators (SM and SI) utilized the Newcastle-Ottawa Scale to

gauge the quality of included observational studies, and a score >7 was considered high quality and suitable for inclusion (22).

Results

A total of 25 articles met inclusion and quality criteria. Of these, three focused on efficacy, 19 examined immunogenicity, 10 included safety assessments. Three were animal-based studies. Full papers were assessed. Except for two articles based in Iran, all the studies were conducted in India. The articles were published in English between December 2020 and March 22, 2022. Several of the studies had the involvement of employees of Bharat Biotech, the company producing Covaxin.

Discussion

Inactivated vaccines have been traditionally used successfully for protection against historically notorious diseases like smallpox, polio, rabies, among others. Theoretically, the intact yet inactivated pathogen elicits a broader immune response compared to other platforms. Epitope coverage of inactivated vaccines is extensive and less prone to circumvention by newer variants (8). The pre-clinical animal studies on the Syrian Hamsters and Rhesus macaques suggested satisfactory efficacy and dose-sparing effect of the 3 µg BBV152 vaccine + Algel-IMDG (in comparison to the 6 µg + Algel-IMDG and other combinations). These animal studies showed high Nab titers, displayed prompt viral clearance from the lower respiratory tract, and displayed no evidence of radiographic abnormalities by the 7th day post-inoculation (8, 23). In the third animal study on three species, 100% seroconversion was observed in 21 days and peak titers were seen on day 28. This study showed sufficient levels of binding Ab and Nab lasting up to 98 days after the first dose. The reliability of the Algel-IMDG adjuvant was also established, as it was found to be non-mutagenic and induced Th1-biased antibody response (7).

The phase I trials presented a Th1-skewed response. Post second dose Seroconversion rates of both the Algel-IMDG adjuvanted combinations of 3 µg and 6 µg were found to be comparable (6). Both cell-mediated and humoral immunity appeared to be sufficiently stimulated. An impressive safety profile with local and systemic adverse events in the range of 17%-21% (none severe) paved the way for phase II trials. In both the phase II trials as well as the follow-up to the phase I trials, the 6 µg + Algel-IMDG combination was found to have the highest immunogenicity and was eventually selected for phase III trials (Table 1) (24). These trials revealed a 93.4% efficacy against severe COVID-19, although efficacy against the Delta variant was lower at 65.2%. There were minimal lot-to-lot variations and the safety profile was similar to placebo (25). Notwithstanding the impressive safety profile (just 12.4% adverse events) established in the trials, an Iranian study reported 92.9% incidence of adverse events, with most of the complaints being of injection site pain. However, the Iranian study included only 42 Covaxin recipients compared to the much larger number in phase III trials. Also, similarly high adverse events were reported for the other vaccines, Oxford-Astra Zeneca's AZD1222(Covishield) and Sputnik V, included in the study (10). The COVAT study showed an increased incidence of mild-moderate adverse events after the first dose in Covaxin (31.2%) compared to second dose (11.1%) and a 2.2% breakthrough infection rate. These rates were found to be better than that seen with AZD1222 recipients, who experienced 46.7% adverse events after the first dose, 18.1% after the second dose, and 5.5% breakthrough events (26). Basavaraja et al. also reported lower incidence rates for Covaxin compared to Covishield, mostly related to vaccination anxiety (27). On the other hand, on comparing two equally sized groups, Choudhary et al. reported higher breakthrough events with Covaxin compared to Covishield (28). Sharma et al. also reported a slightly higher breakthrough infection rate with Covaxin compared to Covishield (29). However, in the COVAT follow-up studies, breakthrough infection rates were similar for the two vaccines (30). Incidence rates varied from the high values reported by the Iranian study to the much lower values of 0.57% reported by Basavaraja et al. (27) The latter utilized spontaneous reporting of adverse events and supervised assessment was conducted for only 30 minutes, which might have resulted in under-reporting of any events occurring after that period. In another Iranian study, adenovirus-vector-based recipients, especially those getting Covishield, reported more numerous and intense side effects compared to vaccinees receiving inactivated formulations. This was attributed to the increased elicitation of cytokine/chemokine responses in the viral vector vaccines (31). Suffice to mention that no serious adverse events or deaths were reported with BBV152 in any study we included, and injection site pain was the decisively predominant adverse event.

Immunogenicity assessments of Covaxin did not usually outperform that observed with other vaccines. In the COVAT study, Covishield surpassed BBV152 in the observed NAb titers and seropositivity rates after the first dose itself, which was barely equaled even after two doses of Covaxin had been administered (Table 2). Among fully vaccinated recipients, Covaxin could elicit an anti-spike Ab geometric mean titer (GMT) of only 48.3 AU/ml, which was less than half that observed with Covishield. The former also elicited a seropositivity of anti-Spike Ab of just 80% compared to 98.1% observed in the latter (26). This superiority in seroprevalence and peak GMT of Covishield was maintained at all time points from 1 to 6 months after the second dose, as seen in the follow-up to the COVAT study. Nonetheless, the declines in peak values were just as rapid, so that by the end of 6 months post the second dose, there was a narrowing of the Ab titer gap between the two vaccines. While Covishield showed a peak of almost 100% seropositivity 3 weeks after the second dose, Covaxin showed

TABLE 1 Phase I, II & III trials on the BBV152/Covaxin.

Study	Type of study	Number of participants	Study groups involved	Findings on immunogenicity/efficacy	Findings on safety	Additional comments
Ella et al. (6)	Double-blind, randomised, phase 1 trial	100	Covaxin 6 µg with Alum	Post 2nd dose Seroconversion rates (MNT_{50}) 82.8% Post 2nd dose Seroconversion rates ($PRNT_{50}$) 86.6%	Local and systemic adverse events in 14 (14%; 8·1–22·7) One report of a serious adverse event	2 dose study (Day 0,14) demonstrated induction of cell-mediated as well as humoral responses. CD4+ and CD8+ T-cell responses detected in 16 from both alum-IMDG groups. Covaxin formulations, especially Alum-IMDG, were Th1 skewed with IgG1/IgG4 ratios>1.
		100	Covaxin 3 µg with Alum-IMDG (Imidazoquinoline class)	Post 2nd dose Seroconversion rates (MNT_{50}) 87·9% Post 2nd dose Seroconversion rates ($PRNT_{50}$) 93.4% similar anti-spike, anti-receptor binding, and anti-nucleoprotein IgG titers (GMTs)	Local and systemic adverse events in 17 (17%; 95% CI 10·5–26·1)	
		100	Covaxin 6 µg with Alum-IMDG	Post 2nd dose Seroconversion rates (MNT_{50}) 91.9% Post 2nd dose Seroconversion rates ($PRNT_{50}$) 86.4%	Local and systemic adverse events in 21 (21%; 13·8–30·5)	
		75	Algel only (controls)	Post 2nd dose Seroconversion rates (MNT_{50}) 8%	Local and systemic adverse events in 10 (10%; 6·9–23·6)	
Ella et al. (24)	double-blind, randomised, multicentre, phase 2 clinical trial	190	3 µg + Algel-IMDG group	Day 56- Geometric mean titers (GMTs; $PRNT_{50}$)- (100·9 [95% CI 74·1–137·4]) Day 56- Geometric mean titers (GMTs; MNT_{50}) -(92·5 [95% CI 77·7–110·2]) Seroconversion (based on $PRNT_{50}$) - 92.9% [95% CI 88·2–96·2] Seroconversion (based on MNT_{50}) -88% [95% CI 82.4–92.3]	Solicited local and systemic side-effects in 20·0% (95% CI 14·7–26·5) on days 0-7 and 28-35. No serious adverse events	Utilising previous study(6) the 3 µg + Algel-IMDG & 6µg + Algel-IMDG were selected for phase 2 trial. 2 doses given IM(Day 0,28) The 6 µg + Algel-IMDG group had significantly higher GMTs (p=0·0041). Seroconversion defined as 'a post-vaccination titer at least four times higher than that preceding vaccination.' T-cell responses were Th1-biased.
		190	6 µg + Algel-IMDG group	Day 56- Geometric mean titers (GMTs; $PRNT_{50}$) (197·0 [95% CI 155·6–249·4]) Day 56- Geometric mean titers (GMTs; MNT_{50})-(160.1 [95% CI 135.8–188.8]) Seroconversion (based on $PRNT_{50}$) - (98·3% [95% CI 95·1–99·6]) Seroconversion (based on MNT_{50}) - 96·6% [95% CI 92·8–98·8])	Solicited local and systemic side-effects in 21·1% (95% CI 15·5–27·5) on day 0-7 and 28-35. No serious adverse events	
	Previous phase I trial (6) was subject to **follow-up** at 3 months after 2nd dose (Day 104)		3 µg + Algel-IMDG group	Day 104 GMTs (MNT_{50}) - 39·9 (95% CI 32·0–49·9) Seroconversion (based on MNT_{50}) – 73.5% [95% CI 63.6–81.9]	No new serious (or otherwise) adverse events between days 42-104 from	NAb titers persisted in all participants at day 104 comparable to convalescent sera. T-cell memory response more vivid in 6 µg + Algel-IMDG group. No significant differences in GMTs between days 42 and 104 across all vaccinated groups
			6 µg + Algel-IMDG group	Day 104 GMTs (MNT_{50}) - 69·5 (95% CI 53·7–89·9)		

(Continued)

TABLE 1 Continued

Study	Type of study	Number of participants	Study groups involved	Findings on immunogenicity/efficacy	Findings on safety	Additional comments
				Seroconversion (based on MNT_{50}) – 81·1% [71·4–88·1]		
			6 µg + alum(Algel) group	Day 104 GMTs (MNT_{50}) - 53·3 (95% CI 40·1–71·0) Seroconversion (based on MNT_{50}) – 73·1% [62·9–81·8]		
			Algel only	Day 104 GMTs (MNT_{50}) - 20·7 (95% CI 14·5–29·5)		
Ella et al. (25)	Randomised (phase 3) clinical trial	12221	6 µg + Algel-IMDG group	24 symptomatic COVID-19 cases out of 8471 recipients Efficacy: Any severity COVID-19-77.8% Asymptomatic COVID19- 63·6% Severe COVID-19 (as per FDA definition)-93·4% Against Delta-variant-65.2% Day 56 GMTs (MNT_{50}) – 125.6 Day 56 GMTs (ELISA U/ml): 9742 for S1 protein, 4124 for RBD, 4161 for N protein	1597 adverse events [12·4%] No anaphylaxis/vaccine-related deaths	2 doses (Day 0,28)of 6 µg + Algel-IMDG given . Primary outcome geared to finding efficacy in preventing symptomatic RTPCR +ve COVID-19. Immune responses were found to be independent of age. Lot to lot variations of vaccine batches found insignificant.
		12198	Placebo	106 symptomatic COVID-19 cases out of 8502 recipients Day 56 GMTs (MNT_{50}) – 13.7 Day 56 GMTs (ELISA U/ml): No change from baseline	1597 adverse events [12·4%]	

peak seropositivity of less than 80% (30). Dash et al. similarly reported higher seropositivity rates with Covishield, the IgG titers against Spike protein being three times that seen with Covaxin. However, they also reported a breakthrough infection related fatality with Covishield (32). The superiority of Covishield over BBV152 was again demonstrated by Choudhary et al., which showed several-fold higher elicitation of spike protein IgG by the former vaccine over the latter. The study noted a four-fold reduction in spike protein Ab titers at 6 months after the second dose for Covaxin, while Covishield showed only a two-fold reduction, which was at variance with the COVAT follow-up results. However, Choudhary et al. had a much higher number of vaccinees receiving Covaxin compared to the COVAT study, so could be considered more reliable. Both studies, however, agree on the consistently higher titers of Covishield at all time points. Additionally, in previously unexposed seronegative individuals, an 81.9% seroconversion at 4 weeks after the first dose was observed with Covishield compared to just 16.1% with Covaxin (28). This was also proven in the study by Malhotra et al., which reported poor immunogenicity in individuals partially immunized with BBV152. Unlike Covishield, where antibody titers started peaking quickly after the first dose itself, it required at least two doses for Covaxin to be anywhere near as effective. In participants with prior viral exposure, two doses of BBV152 accorded sufficient protection, with an 87% efficiency against symptomatic reinfection, while a single dose was only 16% effective (43). A questionnaire-based study of health-care workers reported significantly reduced incidence and severity of COVID-19 infection in those receiving two doses of both Covaxin and Covishield compared to a single dose of either vaccine (44). Kumar et al. demonstrated the induction of innate, adaptive immune responses, as well as cytokine and chemokine induction. However, these responses were only observed after

TABLE 2 List of studies on the purified inactivated SARS-CoV-2 vaccine Covaxin.

Study	Type of study	Number of participants	Study groups involved	Findings on immunogenicity/efficacy	Findings on safety	Additional comments
Mohandas et al. (23)	Non-human study	36 Syrian hamsters with 9 in each group	Group I -phosphate-buffered saline (PBS)	IgG negative till virus challenge IgG +ve in all by 14 DPI (OD=0.29) No NAb ($PRNT_{50}$) response till 15 DPI Throat swab Viral gRNA copy number highest post challenge and persisted till 10 DPI	**Not mentioned in study**	3 Doses(Day 0,14,35) given. Vaccinated hamsters had lower weight loss following virus challenge. All vaccinated groups induced IgG2 and the NAb appeared at 3 weeks peaking at 7 weeks All vaccinated groups had normal morphology compared to congestive, fibrotic and haemorrhagic features in group I. No significant elevation of cytokines in vaccinated compared to IL-12 elevation in controls.
			Group II (BBV152C)- 6µg vaccine + Algel	IgG Ab in 3rd week in 2 of 9 (OD=0.285) IgG Ab on day 48 in 9 of 9 (OD=0.55) Throat swab & trachea viral clearance on 7 DPI Lungs viral clearance on day 15 DPI		
			Group III (BBV152A)- 3µg vaccine + Algel-IMDG)	IgG Ab in 3rd week in 8 of 9 (OD=0.42) IgG Ab on day 48 in 9 of 9 (OD=1.2) Highest observed NAb($PRNT_{50}$) (mean=28,810 at 7th week) and post challenge mean=85,623) on 15 DPI Throat swab, lungs & trachea viral clearance on 7 DPI		
			Group IV (BBV152B)- 6µg vaccine + Algel-IMDG	IgG Ab in 3rd week in 8 of 9 (OD=0.62) IgG Ab on day 48 in 9 of 9 (OD=1.32) Throat swab, lungs & trachea viral clearance on 7 DPI		
Yadav et al. (8)	Non-human primate study	20 Rhesus Macaques with 5 in each group	Covaxin 6µg+ Alum	IgG titer 1:1600-1:6400 NAb titer 1:87.4 - 1: 3974 Throat swab -viral clearance on 7 DPI BAL fluid viral clearance on 5 DPI	**No Adverse events noted**	2 dose (day 0,14) study. Necropsy Lung specimens negative for gRNA and sgRNA in vaccinated groups. Radiographic abnormalities resolved by 5 DPI in 2 vaccinated groups other than the 3µg + alum +imidazoquinoline group which showed No clinical or radiographic abnormalities. Resistance to pneumonia on Histopathological examination unlike placebo. Pro-inflammatory cytokines such as IL-6 were lower and anti-inflammatory cytokines such as IL-5 higher in all vaccinated.
			Covaxin 3µg + alum+ imidazoquinoline	Highest IgG titer (1:25600) Highest NAb titers of 1:209 to 1:5,217 Throat swab viral clearance on 7 DPI BAL fluid viral clearance on 5 DPI		
			Covaxin 6µg+ alum+ imidazoquinoline	IgG titer 1:1600-1:6400 NAb titer 1: 29.5 -1: 3403 Throat swab viral clearance on 7 DPI BAL fluid viral clearance on 5 DPI		

(Continued)

10.3389/fimmu.2022.863162

TABLE 2 Continued

Study	Type of study	Number of participants	Study groups involved	Findings on immunogenicity/efficacy	Findings on safety	Additional comments
			Placebo	No NAb and IgG response Throat swab viral clearance not seen even by 7 DPI BAL fluid viral clearance not seen even by 7 DPI		Chest X-ray showed infiltrates, bronchopneumonia, or lobar pneumonia which persisted till 7 DPI.
Ganneru et al. (7)	Pre-clinical study on 3 animal species		BALB/c mice at 1/20th or 1/10th Human single dose + adjuvant (intra-peritoneally)	High Ag Binding and NAb titers($PRNT_{90}$) (100% seroconversion) Day 7 -10^2 titer Day 14 – 10^3 titer Day 21 – 10^4 titer Day 28 – peak titer Adjuvanted (algel/algel-IMDG) formulations elicited high Ab levels targeted against S1 compared to non-adjuvanted and lasted 98 days.	Only local reactogenicity observed which was self resolving	Algel-IMDG found non-mutagenic and well tolerated at test as well as repeat dose in the 3 animal models. The TLR7/8 agonist adjuvant supports Th1-biased Ab responses and has high IgG2a/IgG1 ratio, IFN-γ response compared to algel.
			New Zealand White rabbits	High NAb titers ($PRNT_{90}$ as well as MNT_{50}) comparable to convalescent human sera Day 21- 10^4 titer (100% seroconversion)		
			Wistar rats & Swiss Albino mice		Maximum Tolerated dose (=Human single dose) and repeated dose elicited no ill-effects	
Zare et al. (10)	Cross-sectional study on health workers	503 Health care workers given atleast 1 of 3 different vaccine	Covaxin (42)	None performed	92.9 % had side effects. Injection site pain (83.7%) >Fatigue (41.9%) >headache (27.9%)	Injection site pain was most common in all three vaccines. AZD1222 had highest %age of systemic side-effects. Prevalence rate of complications in Covaxin not significantly different from Sputnik-V and AZD1222. No serious/life-threatening side effects observed in all 3 vaccine groups. Side-effects disappeared by 7 days post-innoculation in all groups.
			Sputnik-V(238)		81.9 % had side-effects. Injection site pain (56.7%) >Muscle pain (41.6%) >Fever & chills (37.4%)	
			AZD1222 (223)		88.8 % had side-effects. Injection site pain (70%) >Fatigue (68.4%) >fever & chills (67.1%)	
Singh et al. (COVAT study) (26)	Cross-sectional study of Health care workers	96 (1st dose) 90 (2nd dose)	Covaxin	Seropositivity after 1st dose- 43.8% GMT's after 1st dose- 16.8 AU/mL. Seropositivity after 2nd dose- 80% GMT's after 2nd dose- 48.3 AU/mL.	31.2% mild-moderate side-effects after 1st dose and 11.1% after 2nd dose. Breakthrough infections in 2.2%. No serious AEFI	People with comorbidity especially Type 2 Diabetes had lower seropositivity in both vaccines. Past history of infection resulted in overall significantly higher seropositivity vis-à-vis unexposed individuals. Females also had 9% higher seropositivity. Covishield had significantly increased seropositivity, NAb titer after 1st dose while Covaxin required 2 doses to achieve significant effect.

(Continued)

10.3389/fimmu.2022.863162

TABLE 2 Continued

Study	Type of study	Number of participants	Study groups involved	Findings on immunogenicity/efficacy	Findings on safety	Additional comments
		456 (1st dose) 425 (2nd dose)	Covishield	Seropositivity after 1st dose- 86.8% GMT's after 1st dose- 62.4 AU/mL. Seropositivity after 2nd dose- 98.1% GMT's after 2nd dose- 129.3 AU/mL.	Higher mild-moderate side-effects 46.7% after 1st dose and 18.1% after 2nd dose. Breakthrough infections in 5.5%. No serious AEFI.	
Singh et al. (COVAT study follow-up) (30)	6-month longitudinal study	74	Covaxin	Anti- spike GMT (AU/ml) (SARS-CoV-2 naïve cohorts) 21 days post 1st dose- 16.17 21 days post 2nd dose- 50.11 3 months post 2nd dose- 50.81 6 months post 2nd dose- 46.27 Anti- spike GMT declined by only 8% at 6 months compared to peak titer. Seropositivity (%) (SARS-CoV-2 naïve cohorts) 21 days post 2nd dose- 77 3 months post 2nd dose- 55.7 6 months post 2nd dose- 37.7	Not mentioned in study	Covaxin showed lower seropositivity and anti-Spike GMT compared to Covishield at all time points but with much less decline from peak titers at 6 months after 2nd dose. Breakthrough infection rates were similar in the 2 vaccines Covishield (54/407, 13.3%) vs Covaxin (10/74, 13.5%).
		407	Covishield	GMT (AU/ml) (SARS-CoV-2 naïve cohorts) 21 days post 1st dose- 61.93 21 days post 2nd dose- 132.88 3 months post 2nd dose- 112.78 6 months post 2nd dose- 73.83 GMT declined by 44% at 6 months compared to peak titer. Seropositivity (%) (SARS-CoV-2 naïve cohorts) 21 days post 2nd dose-98.7 3 months post 2nd dose- 92.6 6 months post 2nd dose- 22.1		
Sharma et al. (29)	Cross-sectional study of Health care workers	168(Atleast 1 dose) 154 (Both doses)	Covaxin	None performed	33 infections of 168 (19.6%) Breakthrough 24 of 154 (15.6%)	History of prior infection with COVID-19 and atleast one vaccine dose was significantly protective of breakthrough infections.
		157(Atleast one dose) 125 (Both doses)	Covishield		24 infections of 157 (15.3%) Breakthrough 13 of 125 (10.4%)	
Dash et al. (32)	Cross-sectional study including breakthrough cases	35	Covaxin	Anti-Spike receptor binding domain IgG Ab - 27 (77.1%) Ab titer- 213.5 AU/ml [interquartile range (IQR)537.5]	Symptomatic-29 (82.9%) Asymptomatic- 6 (17.1%) Hospitalized -3 (8.6%)	Seropositivity in Covishield vaccinees was significantly higher than Covaxin. Among the 27 (breakthrough infection) hospitalised vaccinees, 1 (Covishield recipient) died.
		239	Covishield			

(Continued)

10.3389/fimmu.2022.863162

TABLE 2 Continued

Study	Type of study	Number of participants	Study groups involved	Findings on immunogenicity/efficacy	Findings on safety	Additional comments
				Anti-Spike receptor binding domain IgG Ab - 231 (96.7%) Ab titer- 647.5 AU/ml (IQR: 1645.1),	Symptomatic-199 (83.3%) Asymptomatic – 40 (16.7%) Hospitalized – 24 (10%)	
Kumar et al. (35)	Prospective cohort study of health care workers	44	Covaxin	Increased induction of Type 1,2,17 and pro-inflammatory cytokines (IFN-γ, IL-1a,IL-1b, IL-2, IL-3, TNF-α, IL-4, IL-5,IL-6, IL-7 IL-10, IL-12, IL-13,IL-17A). Reduced synthesis of IL-25, IL-33, GM-CSF, Type 1 interferons. Increased plasma levels of chemokines (CCL4, CXCL1, CXCL2 and CX3CL1). Reduced levels of CXCL10. Significant correlations between IL-2, IL-17A, IL-4, IL-5 and NAb at baseline.	**Not mentioned in study**	The effect of 'Prime boost' Covaxin on cytokine and chemokine profiles was studied at baseline(0) and after 1,2 and 3 months. Raised type 1,17 and pro-inflammatory cytokine levels show 'immune memory induction' while raised type 2 cytokines maybe attributed to vaccine adjuvant. Raised chemokines also show innate immunity induction.
Yadav et al. (39)	Cross-sectional study	17	Covaxin vaccinees(28 days after 2nd dose)	Geometric mean titer (GMT) of serum against B.1- 187.5 (95% CI: 129.3–271.9), Beta- 61.57 (95%CI: 36.34–104.3) Delta - 68.97 (95%CI: 24.72–192.4)	**Not mentioned in study**	Neutralization of sera by covaxin recipients was assessed and compared with sera of recovered patients against Beta and Delta variants.
		20	COVID recovered(5-20 weeks after infection)	GMT of sera against B.1 - 97.8 (95%CI: 61.2–156.2) Beta- 29.6 (95%CI: 13.4–65.0) Delta- 21.2 (95% CI: 6.4–70.1)		
Sapkal et al. (36)	Cross-sectional study	42	Covaxin	GMT of IgG: For S1-Receptor Binding domain protein- 2250 For N Protein- 3099 GMT-Nab by $PRNT_{50}$ (for prototype D614G)- 337.5 GMT by $PRNT_{50}$ (For the B.1.1.28.2 variant)- 175.7	**Not mentioned in study**	IgG levels and NAb activity were assessed and it was concluded that a 2 -dose BBV152 is effective against both B.1.1.28.2 variant and D614G prototype(which was used to develop Covaxin), compared to protection afforded by natural infection.
		Total (n=19) B.1.1.7 (n=2) B.1.351 (n=2) B.1.1.28.2 (n=2) B1 lineage (n=13)	Convalescent sera (15–113 days after positive report).	GMT of IgG: For S1-Receptor Binding domain protein- 794.8 For N Protein- 4627 GMT NAb by $PRNT_{50}$ (for prototype D614G)- 120.1 GMT by $PRNT_{50}$ (For the B.1.1.28.2 variant)- 109.2		
Sapkal et al. (37)	Cross-sectional study		38 vaccine recipients	Nab titers by $PRNT_{50}$ of vaccinee sera had comparable efficacy against UK variant of GR clade (mutant hCoV-19/India/20203522) as well as the hCoV-19/India/2020770 (used for developing Covaxin) belonging to G clade and hCoV- 19/India/2020Q111 belonging to O clade.	**Not mentioned in study**	$PRNT_{50}$ values from the different groups did not show any significant difference (P>0.05).

(Continued)

10.3389/fimmu.2022.863162

TABLE 2 Continued

Study	Type of study	Number of participants	Study groups involved	Findings on immunogenicity/efficacy				Findings on safety	Additional comments
				Median ratio of 50% neutralization- 0.8 hCoV- 19/India/2020770 vs UK variant Median ratio of 50% neutralization- 0.9 hCoV- 19/India/2020Q111					
Yadav et al. (40)	Cross-sectional study involving various categories of Covaxin recipients			GMT of NAb ($PRNT_{50}$)				**Not mentioned in study**	Neutralization was assessed against Delta, Delta AY.1 and B.1.617.3 compared with B.1 variant. NAb titers for BTI group was highest followed by CRV and CNV. In the CNV group, compared to B1, NAb titer against B.1.617.3 was lowest at a 1.88 reduction while Delta showed 1,29 reduction. The CRV and BTI groups also showed a similar pattern of reduction of B.1.617.3>Delta AY.1>Delta, although there were higher fold reductions in neutralization. The role of memory cells could explain the high titers observed in CRV and BTI groups compared to CNV group. Although titers against the new variants were reduced, some protection against severe disease could still be plausible.
		42	COVID-19 naïve vaccinees **(CNV)**	Delta	Delta AY.1	B.1.617.3	B1		
				241.6 (95% CI: 167.8–347.7)	209.1 (95% CI: 146.5–298.3)	165.3 (95% CI: 115.6–236.5)	310.6 (95% CI: 222–434.6)		
		14	COVID-19 recovered and vaccinated **(CRV)**	Delta	Delta AY.1	B.1.617.3	B1		
				328.6 (95% CI: 186.9–577.9)	234.5 (95% CI: 138.7–396.4)	217.8 (95% CI: 136.7–347.1)	820.1 (95% CI: 469–1434)		
		30	Breakthrough infections after vaccination **(BTI)**	Delta	Delta AY.1	B.1.617.3	B1		
				465.6 (95% CI: 213.2–1016)	317.2 (95% CI: 125.5–801.4)	259.7 (95% CI: 157.1–429.4)	896.6 (95% CI: 550.3–1461)		
Kumar et al. (41)	Cross-sectional study involving health care workers	84			SARS-COV-2 IgG proteins (AU/ml)		NAb % inhibition-	**Not mentioned in study**	A single dose of Covaxin administered to previously SARS-COV-2 infected individuals could elicit comparable humoral immune response to that seen in non-exposed individuals administered both doses of the vaccine.
			Vaccinees with no prior infection	Baseline	IgG N- 0.71 IgG S- 0.37		-1.43		
				Month 1	IgG N- 2.4 IgG S- 2.3		9.2		
				Month 2	IgG N- 56.3 IgG S- 86.7		68.9		

(Continued)

10.3389/fimmu.2022.863162

TABLE 2 Continued

Study	Type of study	Number of participants	Study groups involved	Findings on immunogenicity/efficacy				Findings on safety	Additional comments
		30	Vaccinees with prior infection	Baseline	IgG N- 29.3 IgG S- 48.8		74.1		
				Month 1	IgG N- 78.6 IgG S- 167.2		95.8		
				Month 2	IgG N- 95 IgG S- 211		94.5		
Kant et al. (43)	Cross-sectional study involving 98 vaccine recipients	18	Vaccinees given Covishield + Covaxin	GMT S1-RBD ELISA titer	GMT N protein ELISA Titer	IgG (GMT) inactivated SARS-CoV-2 virus	NAb ($PRNT_{50}$) GMT, Against B1/ Alpha/ Beta/ Delta	**Inj. Site Pain** - 11.1% after 1st dose none after 2nd dose **Pyrexia**- 27.7% after 1st dose and 11.1% after 2nd dose **Malaise**- 33.3% after 1st dose and 5.5% after 2nd dose	Pain at injection site was the most common local adverse effect while most common systemic adverse events were pyrexia and malaise. All adverse events in the Covaxin + Covishield group were comparable to either group alone. Covishield vaccinees were found to have the highest titers for GMT S1-RBD. The heterologous group had highest GMT N protein and IgG (GMT) to inactivated virus titer as well as highest levels of NAb (GMT) towards all the 4 variants.
				1866	1145	171.4	**B1**- 539.4 **Alpha**- 396.1 **Beta**- 151 **Delta**- 241.2		
		40	Covishield vaccinees	2260	353.7	111	**B1**- 162 **Alpha**- 122.7 **Beta**- 48.43 **Delta**- 51.99	**Inj. Site pain**- 5% after 1st dose 5% after 2nd dose **Pyrexia**- 20% after 1st dose and 15% after 2nd dose **Malaise**- 5% after 1st dose and 5% after 2nd dose	
		40	Covaxin vaccinees	710	742.4	86	**B1**- 156.6 **Alpha**- 112.4 **Beta**- 52.09 **Delta**- 54.37	**Inj. Site pain** - 7.5% after 1st dose 7.5% after 2nd **Pyrexia**- 30% after 1st dose and 15% after 2nd dose **Malaise**- 32.5% after 1st dose and 15% after 2nd dose	
Basavaraja et al. (27)	Prospective observational study	9292 doses to 5986 vaccinees	Covishield	**Not mentioned in study**				Incidence rate of adverse events was 4.32%. 433 AE (409 expected as per factsheets) 94.22%- associated with immunization of which 78.98% related to vaccine products and 15.24% due to anxiety.	Half (50.9%) vaccinees had a single AE, 34.9% had 2 AE's while 8.6% reported 3 AE's. Most of the AE's followed the 1st dose of vaccination. Covishield vaccinees had mostly fever, injection site tenderness, pain and joint pain muscle aches, while Covaxin recipients had injection site pain, fever and 3 cases had giddiness which was not mentioned in factsheets.

(Continued)

10.3389/fimmu.2022.863162

TABLE 2 Continued

Study	Type of study	Number of participants	Study groups involved	Findings on immunogenicity/efficacy	Findings on safety	Additional comments
		2364 doses to 1749 vaccinees	Covaxin		Incidence rate of adverse events was 0.57%. 12 AE (9 expected as per factsheets) 8 (66.6%)- associated with immunization of which none related to vaccine products and all related to anxiety.	
Choudhary et al. (28)	Longitudinal Cohort study involving Health Care workers	308	Covishield	Highest levels of spike >protein IgG observed in the 12th week (median=1299.5 AU/ml) (IQ:517.9-5019.2) falling to 637.2 AU/ml (IQ: 186.5–3,055.3) after 6 months. In unexposed seronegative individuals, 81.9% had seroconversion at 4 weeks after 1st dose.	Out of 81 breakthrough infections, 37% were Covishield recipients.	Covishield vaccinees had significantly higher IgG Ab compared to Covaxin . There was a 2-fold reduction in spike Ab titers in Covishield while Covaxin vaccinees had a more drastic 4-fold reduction.
		306	Covaxin	Highest levels of spike protein IgG observed in the 12th week (Median= 342.7 AU/ml) (IQ: 76.1–892.8) falling to 95.1 AU/ml (IQ: 36.5–277.2) at 6 months. In unexposed seronegative individuals, 16.1% had seroconversion at 4 weeks after 1st dose.	Out of 81 breakthrough infections, 63% were after Covaxin.	
Desai et al. (38)	Test negative case-control study	1068 matched case-control pairs		Adjusted effectiveness of 2 doses of Covaxin against symptomatic RTPCR positive (tested atleast 2 weeks after 2nd dose) SARS-CoV-2 was 50% (95% CI 33-62) and if testing was at 4 weeks or more, the adjusted effectiveness was 46% (95% CI 22–62). At 6 weeks effectiveness rose to 57% (95% CI 21–76). If participants with prior infection were excluded the adjusted effectiveness was 47% (95% CI 29–61).	**Not mentioned in study**	This study was undertaken at a time of surge in cases during the second wave of COVID in India. The Delta variant was infamous for its immune evasion and might have been responsible for the lower efficacy compared to phase III trials conducted by Bharat Biotech.
Medigeshi et al. (42)	Cross-sectional study	Median duration from 2nd dose of either vaccine- 234 days		GMT of Focus reduction neutralization titer ($FRNT_{50}$) Neutralisation titers above limit of quantification (1:20)Against Omicron	**Not mentioned in study**	Both Covaxin and Covishield vaccinees with no prior infection had a ~26-fold reduction in $FRNT_{50}$ titers against Omicron compared to ancestral variant after 6 months. Those with prior infection had ~57-fold reduction. Significant reduction in neutralizing ability of both vaccines was observed but prior infection was associated with significantly high titers. Anti-nucleocapsid Ab wane in Covaxin vaccinees, however, those with prior infection sustain Ab for longer periods compared to Covishield.
				Ancesrtral / Delta / Omicron		
		20	Only Covaxin	380.4 / 164.7 / 14.3	5 out of 20 samples	
		20	Covaxin + previous infection	806.1 / 260.2 / 14.12	6 out of 20 samples	

(Continued)

10.3389/fimmu.2022.863162

TABLE 2 Continued

Study	Type of study	Number of participants	Study groups involved	Findings on immunogenicity/efficacy	Findings on safety	Additional comments
		20	Only Covishield	379.3 11.9 14.7 5 out o 20 samples		
		20	Covishield + previous infection	1526.2 358.1 26.3 9 out of 20 samples		
Houshmand et al. (31)	Cross-sectional study				**Side-effect intensity/incidence**	
		578	Covishield		98.6 % had atleast one side effect. Highest intensity of almost all side effects	No serious side-effects were reported for BBV152. Adenovirus-vector based vaccines were found to cause higher levels of side-effects attributable to cytokine/chemokine release compared to inactivated vaccines. 73.1% side-effects observed within 24 hours for all vaccines.
		25	Covaxin		100% had atleast 1 side-effect. Local pain in the hand only side-effect of significant intensity.	
		426	GAM-Covid-Vac		93.2% had atleast 1 side-effect. Injection site pain, Fever, muscle pain common.	
		102	BBIP-CorV		87.3% had at least one side effect. Lowest intensity of almost all side effects	
Sapkal et al. (44)		17	CS/CV	S1-RBD IgG Ab titer- 4.13 fold reduction in GMT mean titer ratio of 1st and 6th month Reduction in Ratio of GMT of NAb at 1st and 6th month B.1 (ancestral) Alpha Beta Delta 7.17 6.98 7.19 5.75 Reduction in NAb titers in comparison with B.1 for different VOCs Alpha Beta Delta Omicron 1.28 3.43 1.75 19.16	Not mentioned	Heterologous vaccinees had higher NAb titers despite significant fold reductions in titers 6 months after 2nd dose. Comparison with B.1 ancestral variant revealed that NAb titers were drastically low for omicron variant.
		36	Covishield	S1-RBD IgG Ab titer- 6.8 fold reduction in GMT mean titer ratio of 1st and 6th month Reduction in Ratio of GMT of Nab at 1st and 6th month B.1 (ancestral) Alpha Beta Delta 2.87 3.51 2.76 1.96		

(Continued)

10.3389/fimmu.2022.863162

TABLE 2 Continued

Study	Type of study	Number of participants	Study groups involved	Findings on immunogenicity/efficacy	Findings on safety	Additional comments
				Reduction in NAb titers in comparison with B.1 for different VOCs Alpha: 1.63; Beta: 3.43; Delta: 2.27; Omicron: 23.15		
		35	Covaxin	S1-RBD IgG Ab titer- 4.87 fold reduction in GMT mean titer ratio of 1st and 6th month Reduction in Ratio of GMT of Nab at 1st and 6th month B.1 (ancestral): 3.17; Alpha: 3.72; Beta: 2.61; Delta: 3.36 Reduction in NAb titers in comparison with B.1 for different VOCs Alpha: 1.67; Beta: 2.56; Delta: 2.83; Omicron: 24.21		
Malhotra et al. (33)	Retrospective cohort study involving previously infected HCWs			Estimated vaccine effectiveness against: Reinfection / Symptomatic reinfection / Asymptomatic reinfection		Full vaccination with BBV152 was associated with a good protective effect while partial vaccination was ineffective. Since most of the reinfections occurred during the Delta variant-induced 2nd wave, Covaxin accorded sufficient protection in pre-infected participants.
		1089	Fully vaccinated with Covaxin	86% / 87% / 84%		
		356	Partially vaccinated with Covaxin	12% / 16% / –		
		472	Unvaccinated	– / – / –		

10.3389/fimmu.2022.863162

the second dose and lasted for 3 months, thus explaining the delayed peak of Covaxin action (33).

Response of Covaxin against SARS-CoV-2 variants

Sufficient action of vaccines against newer variants is essential to reduce mortality and control the spread of infection to manageable levels. The ameliorative action of Covaxin against several variants has been tested. A study by Sapkal et al. reported higher GMT of IgG for S1-receptor binding domain protein as well as higher NAb GMT for the B.1.1.28.2 and D614G strains in Covaxin vaccinee sera compared to convalescent sera (35). In another study by Sapkal et al., NAb titers of vaccinee sera had comparable efficacies against GR, G, and O clades of SARS-CoV-2 and could effectively neutralize the Alpha variant (36). Although BBV152 elicited comparatively reduced titers against the Delta and other newer variants, some rudimentary protection was still afforded. Desai et al. undertook their study at the peak of the second wave in India, probably triggered by the evasive Delta variant. They found an adjusted effectiveness against symptomatic infection to be 50% at 2 weeks after the second dose of BBV152, which rose to a somewhat reasonable figure of 57% at 6 weeks. A strong Th1 bias also allayed fears of serious adverse events (40). Ella et al. had reported efficacy of 65.2% against the Delta variant in the phase 3 trials (25). The study by Malhotra et al. conducted during the wave triggered by the Delta variant reported significant effectiveness (86%) of a two-dose Covaxin regimen (43) Yadav et al. observed neutralization of sera by Covaxin recipients in comparison with those of recovered patients and observed significantly higher levels of GMT against ancestral (B.1), Beta and Delta variants in vaccinees in comparison to the unvaccinated suggesting a somewhat ample coverage of these variants by the vaccine (34). In another study by the same author, action of Covaxin against B.1, Delta, Delta AY.1, and 1.617.3 was assessed, and it was inferred that a milder level of protection was nonetheless afforded by the vaccine against the newer variants (37). Higher titers were also observed in vaccinees who had been previously infected compared to vaccinees without any prior exposure. In fact, a significant humoral response was also observed by Kumar et al., who observed that a single dose of BBV152 administered to previously infected individuals had comparable effectiveness to non-exposed vaccinees administered both doses. IgG Ab against Spike proteins in individuals administered a single dose of Covaxin were markedly elevated (28 days after the first dose) at 167.2 AU/ml in recipients with prior viral exposure in comparison to just 2.3 AU/ml in those with no prior infections. However, the difference in titers between the two groups was less significant after two doses. Kumar et al. thus advocated saving on valuable vaccine doses by giving only a single dose of Covaxin to previously infected individuals; instead reserving the two-dose regimen for non-exposed individuals (38).

Response of Covaxin against the B.1.1.529 (Omicron) variant

Covaxin acted poorly against the B.1.1.529 variant and consequently, immune escape appeared widespread. Covishield fared no better. Despite extensive coverage of vaccination campaigns in the Indian subcontinent utilizing both the above vaccines, there were widespread incidences of breakthrough infections and reinfections (Table 2). Recipients of both vaccines with no prior virus exposure had a ~26-fold reduction in neutralization titers ($FRNT_{50}$) against Omicron compared to the ancestral variant, 6 months after the second dose. However, those who had a history of prior exposure to infection had significantly higher titers, albeit these subsided twice as rapidly. Interestingly, Covaxin recipients sustained anti-nucleocapsid antibodies for longer periods as compared to Covishield (41).

Heterologous prime boost vaccination

The study by Kant et al. observing the serendipitous 'mix and match' of Covaxin and Covishield reported the lowest Geometric mean titers (GMT) for both the S1-receptor binding domain antibodies as well as antibodies to the inactivated virus with Covaxin. However, neutralizing antibodies against B1, Alpha, Beta, and Delta were comparable to that observed with Covishield. Interestingly, mixing the two vaccines yielded better results than either vaccine taken alone. The heterologous group reported the highest titers for the N (nucleocapsid) protein and IgG to the inactivated virus. NAb's against the four variants were also significantly higher than that seen in homologous groups. Nonetheless, neutralization of the sera of BBV152 vaccinees measured in geometric mean titer against the B1, Beta, and Delta variants was significantly higher than that seen with sera from recovered patients (39). Sapkal et al. assessed sera of vaccinees who had received heterologous vaccination (first dose Covishield, second dose Covaxin) and despite significant-fold reductions in GMT of NAb 6 months after the second dose, the heterologous group had consistently higher titers compared to the groups receiving homologous vaccination (either Covishield or Covaxin). NAb titers against the Omicron variant were remarkably reduced for both heterologous/homologous vaccination compared to ancestral, Alpha, Beta, and Delta variants. Nonetheless, heterologous vaccination was immunogenically superior to the homologous mode of vaccination (42).

Heterologous prime-boost vaccination was similarly encouraged by other studies which claimed higher inductions of immunogenicity with combinations of vector-based + inactivated vaccines, which suggests great scope for such regimens in tackling newer variants (45).

Conclusion

After a perusal of the studies included in the systematic review, the authors found the safety profile of Covaxin to be satisfactory and comparable with data from other vaccines, most of the complaints being of injection site pain. A study reported milder adverse effect profile of inactivated vaccines such as Covaxin compared to viral-vector-based ones. Although some studies reported slightly more breakthrough infections with the vaccine compared to other candidates, none of the studies reported any serious/severe adverse events or fatalities. Immunogenicity performance of BBV152, albeit higher than the natural immunity of recovered patients, with the added advantage of being Th1-cell biased, was not as competitive as Oxford–AstraZeneca's AZD1222 (Covishield), as the latter consistently showed higher seroconversion rates and NAb titers. Covaxin displayed lower immunogenic parameters at almost all time points after the second dose, with titers usually lagging behind those seen with Covishield. While AZD1222 showed significant immunogenicity after the first dose itself, it required generally two doses of Covaxin to impart sufficient immunity. Previously infected individuals nonetheless showed good results with the administration of a single dose of Covaxin. Individuals with prior viral exposure administered at least two doses of Covaxin had the best results. In all, binding and neutralizing antibody titer values for Covaxin were not very impressive. Although some protection was afforded against strains such as Alpha, Beta, and Delta, it was not substantial. Neither Covaxin nor Covishield could provide sufficient immunity against the Omicron strain. However, a vaccination regimen including both vaccines displayed better immunogenicity, especially against multiple strains. Further experimentation with heterologous boost vaccination may be beneficial in tackling future variants.

Data availability statement

The original contributions presented in the study are included in the article/supplementary material. Further inquiries can be directed to the corresponding author.

Author contributions

Conceptualization, TIA and SM; methodology, validation, TIA and SM; formal analysis, investigation, data curation, writing—original draft preparation, TIA and SM; writing—review and editing, supervision, TIA, SR, SI, JA, KH and SM. All authors have read and agreed to the published version of the manuscript.

Conflict of interest

The authors declare that the research was conducted in the absence of any commercial or financial relationships that could be construed as a potential conflict of interest.

Publisher's note

All claims expressed in this article are solely those of the authors and do not necessarily represent those of their affiliated organizations, or those of the publisher, the editors and the reviewers. Any product that may be evaluated in this article, or claim that may be made by its manufacturer, is not guaranteed or endorsed by the publisher.

References

1. Worldometers.info. *COVID-19 CORONAVIRUS PANDEMIC STATISTICS* (2022). Available at: https://www.worldometers.info/coronavirus/.

2. Kamath P. SC to hear plea for COVID-19 norms violation during kumbh mela, election rallies on may 10. *Republic World* (2021).

3. Ministry of Health and Family Welfare and COWIN. *Vaccination statistics* (2022). Available at: https://dashboard.cowin.gov.in/.

4. Kumar A, Dowling WE, Román RG, Chaudhari A, Gurry C, Le TT, et al. Status report on COVID-19 vaccines development. *Curr Infect Dis Rep* (2021) 23 (6):1–12. doi: 10.1007/s11908-021-00752-3

5. Ganneru B, Jogdand H, Dharam VK, Moluguu NR, Prasad S, Ella KM, et al. Evaluation of safety and immunogenicity of an adjuvanted, TH-1 skewed, whole virion InactivatedSARS-CoV-2 vaccine - BBV152. *BioRxiv Preprint* (2020). doi: 10.1101/2020.09.09.285445

6. Ella R, Vadrevu KM, Jogdand H, Prasad S, Reddy S, Sarangi V, et al. Safety and immunogenicity of an inactivated SARS-CoV-2 vaccine, BBV152: a double-blind, randomised, phase 1 trial. *Lancet Infect Dis* (2021) 21:637–46. doi: 10.1016/S1473-3099(20)30942-7

7. Ganneru B, Jogdand H, Daram VK, Das D, Molugu NR, Prasad SD, et al. Th1 skewed immune response of whole virion inactivated SARS CoV 2 vaccine and its safety evaluation. *ISCIENCE* (2021) 24(4):102298. doi: 10.1016/j.isci.2021.102298

8. Yadav PD, Ella R, Kumar S, Patil DR, Mohandas S, Shete AM, et al. Immunogenicity and protective efficacy of inactivated SARS-CoV-2 vaccine candidate, BBV152 in rhesus macaques. *Nat Commun* (2021) 12(1386):1–11. doi: 10.1038/s41467-021-21639-w

9. Phelamei S. *India's first COVID-19 vaccine 'COVAXIN' by bharat biotech gets DCGI approval for human trials*. Times Now. 30-Jun-2020

10. Zare H, Rezapour H, Mahmoodzadeh S, Fereidouni M. Prevalence of COVID-19 vaccines (Sputnik V , AZD-1222 , and covaxin) side effects among healthcare workers in birjand city , Iran. *Int Immunopharmacol* (2021) 101(Pt B):108351. doi: 10.1016/j.intimp.2021.108351

11. Ks JP, Muthukumaran A, Haridas N, Fernando E, Seshadri J, Kurien AA. Two cases of double-positive antineutrophil cytoplasmic autoantibody and antiglomerular basement membrane disease after BBV152 / covaxin vaccination. *Kidney Int Rep* (2021) 6(12):3090–1. doi: 10.1016/j.ekir.2021.10.004

12. Kar BR, Singh BS, Mohapatra L, Agrawal I. Cutaneous small-vessel vasculitis following COVID-19 vaccine. *J Cosmetic Dermatol* (2021) 20:3382–3. doi: 10.1111/jocd.14452

13. Muhie OA, Adera H, Tsige E, Afework A. Herpes zoster following covaxin receipt. *Int Med Case Rep J* (2021) 14:819–21. doi: 10.2147/IMCRJ.S345288

14. Showkathali R, Yalamanchi R, Narra L, Vinayagamoorthy N, Gunasekaran S, Nayak R, et al. Coronary thrombo-embolic events after covid-19 vaccination- a single centre study. *Indian Heart J* (2022) 74(2):131–34. doi: 10.1016/j.ihj.2022.01.002

15. WHO. *WHO issues emergency use listing for eighth COVID-19 vaccine*. www.who.int (2021). Available at: https://www.who.int/news/item/03-11-2021-who-issues-emergency-use-listing-for-eighth-covid-19-vaccine.

16. *Buenos Aires Province agrees to buy 10 million doses of covaxin vaccine*. Buenos Aires Times (2021). Available at: https://www.batimes.com.ar/news/

argentina/buenos-aires-province-agrees-to-buy-10-million-doses-of-covaxin-vaccine.phtml.

17. *Anvisa allows for limited imports of Sputnik V and covaxin into Brazil*. Mercopress (2021). Available at: https://en.mercopress.com/2021/06/05/anvisa-allows-for-limited-imports-of-sputnik-v-and-covaxin-into-brazil.

18. Tyagi K, Ghosh A, Nair D, Dutta K, Singh P, Ansari IA, et al. Breakthrough COVID19 infections after vaccinations in healthcare and other workers in a chronic care medical facility in new Delhi, India. *Diabetes Metab Syndrome: Clin Res Rev* (2021) 15(3):1007–8. doi: 10.1016/j.dsx.2021.05.001

19. Abhilash KP, Prabhakar, Mathiyalagan P, Krishnaraj VRK, Selvan S, Kanagarajan R, et al. Impact of prior vaccination with covishield TM and covaxin Ò on mortality among symptomatic COVID-19 patients during the second wave of the pandemic in south India during April and may 2021: a cohort study. *Vaccine* (2022) 40(13):2107–13. doi: 10.1016/j.vaccine.2022.02.023

20. Selvaraj P, Muthu S, Jeyaraman N, Prajwal GS, Jeyaraman M. Incidence and severity of SARS-CoV-2 virus post COVID-19 vaccination: A cross-sectional study in India. *Clin Epidemiol Glob Health* (2022) 14:100983. doi: 10.1016/j.cegh.2022.100983

21. Weinberg GA, Szilagyi PG. Vaccine Epidemiology: Efficacy , effectiveness , and the translational research roadmap. *J Infect Dis* (2010) 201(11):1607–10. doi: 10.1086/652404

22. Wells G, Shea B, O'Connell D, Peterson J, Welch V, Losos M, et al. The Newcastle-Ottawa scale (NOS) for assessing the quality if nonrandomized studies in meta-analyses. 2015.

23. Mohandas S, Yadav PD, Shete-Aich A, Abraham P, Vadrevu KM, Sapkal G, et al. Immunogenicity and protective efficacy of BBV152, whole virion inactivated SARS- CoV-2 vaccine candidates in the Syrian hamster model. *ISCIENCE* (2021) 24(2):102054. doi: 10.1016/j.isci.2021.102054

24. Ella R, Reddy S, Jogdand H, Sarangi V, Ganneru B, Prasad S, et al. Safety and immunogenicity of an inactivated SARS-CoV-2 vaccine , BBV152: interim results from a double-blind , randomised , multicentre , phase 2 trial , and 3-month follow-up of a double-blind , randomised phase 1 trial. *Lancet Infect Dis* (2021) 21(7):950–61. doi: 10.1016/S1473-3099(21)00070-0

25. Ella R, Reddy S, Blackwelder W, Potdar V, Yadav P, Sarangi V, et al. Efficacy , safety , and lot-to-lot immunogenicity of an inactivated SARS-CoV-2 vaccine (BBV152): interim results of a randomised , double-blind , controlled , phase 3 trial. *Lancet* (2021) 398(10317):2173–84. doi: 10.1016/S0140-6736(21)02000-6

26. Singh AK, Phatak SR, Singh R, Bhattacharjee K, Singh NK, Gupta A, et al. Antibody response after first and second-dose of ChAdOx1-nCOV (covishield TM Ò) and BBV-152 (covaxin TM Ò) among health care workers in India: The final results of cross-sectional coronavirus vaccine-induced antibody titre (COVAT) study. *Vaccine* (2021) 39(44):6492–509. doi: 10.1016/j.vaccine.2021.09.055

27. Basavaraja CK, Sebastian J, Ravi MD, John SB. Adverse events following COVID-19 vaccination: first 90 days of experience from a tertiary care teaching hospital in south India. *Ther Adv Vaccines Immunother* (2021) 9:1–12. doi: 10.1177/2515135

28. Choudhary HR, Parai D, Dash GC, Kshatri JS, Mishra N, Choudhary PK, et al. Persistence of antibodies against spike glycoprotein of SARS-CoV-2 in healthcare workers post double dose of BBV-152 and AZD1222 vaccines. *Front Med* (2021) 8:778129(778129). doi: 10.3389/fmed.2021.778129

29. Sharma P, Mishra S, Basu S, Kumar R, Tanwar N. Breakthrough infection with severe acute respiratory syndrome coronavirus 2 among healthcare workers in Delhi: A single-institution study. *Cureus* (2021) 13(10):e19070. doi: 10.7759/cureus.19070

30. Singh AK, Phatak SR, Singh R, Bhattacharjee K, Singh NK, Gupta A, et al. Humoral antibody kinetics with ChAdOx1-nCOV (Covishield^{TM}) and BBV-152 (Covaxin^{TM}) vaccine among Indian healthcare workers: A 6- month longitudinal cross-sectional coronavirus vaccine-induced antibody titre (COVAT) study. *Diabetes Metab Syndrome: Clin Res Rev* (2022) 16(2):102424. doi: 10.1016/j.dsx.2022.102424

31. Houshmand B, Keyhan SO, Fallahi HR, Ramezanzade S, Sadeghi E. Vaccine-associated complications: a comparative multicenter evaluation among dental practitioners and dental students — which candidate vaccine is more safe in SARS COV II , gam-COVID-Vac (Sputnik V), ChAdOx1 nCoV-19 (AstraZeneca), BBV152 (covaxin). *Maxillofac Plast Reconstructive Surg* (2022) 44(3). doi: 10.1186/s40902-021-00330-6

32. Dash GC, Subhadra S, Turuk J, Parai D, Rath S, Sabat J, et al. Breakthrough SARS-CoV-2 infections among BBV-152 (COVAXIN®) and AZD1222 (COVISHIELDTM) recipients: Report from the eastern state of India girish. *J Med Virol* (2021), 1–5. doi: 10.1002/jmv.27382

33. Kumar NP, Banurekha VV, GKC P, Nancy A, Padmapriyadarsini C, Mary AS, et al. Prime-boost vaccination with covaxin / BBV152 induces heightened systemic cytokine and chemokine responses. *Front Immunol* (2021) 12:752397 (752397). doi: 10.3389/fimmu.2021.752397

34. Yadav PD, Sapkal GN, Ella R, Sahay RR, Nyayanit DA, Patil DY, et al. Neutralization of beta and delta variant with sera of COVID-19 recovered cases and vaccinees of inactivated COVID-19 vaccine BBV152 / covaxin. *J Travel Med* (2021) 28(7):1–3. doi: 10.1093/jtm/taab104

35. Sapkal G, Ph D, Yadav PD, Ph D, Ella R, Abraham P, et al. Neutralization of VUI b . 1 . 1 . 28 P2 variant with sera of COVID-19 recovered cases and recipients of covaxin an inactivated COVID-19 vaccine. *J Travel Med* (2021) 28(7):1–3. doi: 10.1093/jtm/taab077

36. Sapkal GN, Yadav PD, Ella R, Deshpande GR, Sahay RR, Gupta N, et al. Inactivated COVID-19 vaccine BBV152 / COVAXIN effectively neutralizes recently emerged b . 1 . 1 . 7 variant of SARS-CoV-2. *J Travel Med* (2021) 28 (4):1–3. doi: 10.1093/jtm/taab051

37. Yadav PD, Sahay RR, Sapkal G, Nyayanit D, Shete AM, Deshpande G, et al. Comparable neutralization of SARS-CoV-2 delta AY . 1 and delta with individuals sera vaccinated with BBV152. *Journal of Travel Medicine* 28, no. 8 (2021): taab154. doi: 10.1093/jtm/taab154

38. Kumar NP, Padmapriyadarsini C, Devi KRU, Banurekha VV, Nancy A. Antibody responses to the BBV152 vaccine in individuals previously infected with SARS-CoV-2: A pilot study. *Indian J Med Res* (2021) 153(5–6):671–6. doi: 10.4103/ijmr.ijmr

39. Kant R, Dwivedi G, Zaman K, Sahay RR, Sapkal G, Kaushal H, et al. Immunogenicity and safety of a heterologous prime-boost COVID-19 vaccine schedule: ChAdOx1 vaccine covishield followed by BBV152 covaxin. *J Travel Med* (2021) 28(8):1–4. doi: 10.1093/jtm/taab166

40. Desai D, Khan AR, Soneja M, Mittal A, Naik S, Kodan P, et al. Effectiveness of an inactivated virus-based SARS-CoV-2 vaccine , BBV152 , in India: a test-negative , case-control study. *Lancet Infect Dis* (2020) S1473-3099(21):00674–5. doi: 10.1016/S1473-3099(21)00674-5

41. Medigeshi GR, Batra G, Murugesan DR, Thiruvengadam R, Chattopadhyay S, Das B, et al. Sub-Optimal neutralisation of omicron (B.1.1.529) variant by antibodies induced by vaccine alone or SARS-CoV-2 infection plus vaccine (hybrid immunity) post 6-months. *eBioMedicine* (2022) 78:103938. doi: 10.1016/j.ebiom.2022.103938

42. Sapkal G, Kant R, Dwivedi G, Sahay RR, Yadav PD, Deshpande GR, et al. Immune responses against different variants of SARS-CoV-2 including omicron following 6 months of administration of heterologous prime-boost COVID-19 vaccine. *J Travel Med* (2022), taac033. doi: 10.1093/jtm/taac033

43. Malhotra S, Mani K, Lodha R, Bakhshi S, Mathur VP, Gupta P, et al. SARS-CoV-2 reinfection rate and estimated effectiveness of the inactivated whole virion vaccine BBV152 against reinfection among health care workers in new Delhi, India. *JAMA Netw Open* (2022) 5(1):e2142210–e2142210. doi: 10.1001/jamanetworkopen.2021.42210

44. Parameswaran A, Apsingi S, Eachempati KK, Dannana CS, Jagathkar G, Iyer M, et al. Incidence and severity of COVID-19 infection post-vaccination: a survey among Indian doctors. *Infection* (2022). doi: 10.1007/s15010-022-01758-2

45. Nguyen TT, Quach THT, Tran TM, Phuoc HN, Nguyen HT, Vo TK, Vo GV. Reactogenicity and immunogenicity of heterologous prime-boost immunization with COVID-19 vaccine. *Biomed Pharmacother*. (2022) Mar;147:112650. doi: 10.1016/j.biopha.2022.112650. Epub 2022 Jan 19.

Frontiers in Immunology

Explores novel approaches and diagnoses to treat immune disorders.

The official journal of the International Union of Immunological Societies (IUIS) and the most cited in its field, leading the way for research across basic, translational and clinical immunology.

Discover the latest Research Topics

See more →

Frontiers

Avenue du Tribunal-Fédéral 34
1005 Lausanne, Switzerland
frontiersin.org

Contact us

+41 (0)21 510 17 00
frontiersin.org/about/contact